



HAL
open science

Design and engineering of barrier materials including nano-adsorbents

Xiaoyi Fang

► **To cite this version:**

Xiaoyi Fang. Design and engineering of barrier materials including nano-adsorbents. Food engineering. AgroParisTech, 2013. English. NNT : 2013AGPT0055 . tel-01139146

HAL Id: tel-01139146

<https://pastel.hal.science/tel-01139146>

Submitted on 3 Apr 2015

HAL is a multi-disciplinary open access archive for the deposit and dissemination of scientific research documents, whether they are published or not. The documents may come from teaching and research institutions in France or abroad, or from public or private research centers.

L'archive ouverte pluridisciplinaire **HAL**, est destinée au dépôt et à la diffusion de documents scientifiques de niveau recherche, publiés ou non, émanant des établissements d'enseignement et de recherche français ou étrangers, des laboratoires publics ou privés.



Doctorat ParisTech

THÈSE

pour obtenir le grade de docteur délivré par

L'Institut des Sciences et Industries du Vivant et de l'Environnement (AgroParisTech)

Spécialité : Sciences et Procédés des Aliments et Bioproduits

présentée et soutenue publiquement par

Xiaoyi FANG

13 Septembre 2013

Conception raisonnée de matériaux barrière incorporant des nano-adsorbants

Directeur de thèse : **Violette DUCRUET**
Co-encadrement de la thèse : **Olivier VITRAC**

Jury

M. Stéphane MARAIS,	Professeur, UMR 6270, Université de Rouen	Rapporteur
M. Hendrik MEYER,	Chargé de recherches-HDR, CNRS, Institut Charles Sadron	Rapporteur
M. Eric FAVRE,	Professeur, UMR 7274, ENSIC, Université de Lorraine	Examineur
M. Luc AVEROUS,	Professeur, UMR 7515, ECPM, Université de Strasbourg	Examineur
Mme. Violette DUCRUET,	Ingénieur de recherche-HDR, UMR 1145, INRA	Directrice de Thèse
M. Olivier VITRAC,	Chargé de recherches, UMR 1145, INRA	Co-encadrant

ACKNOWLEDGMENTS

I would like to acknowledge Dr Violette Ducruet, Dr Olivier Vitrac and Dr Sandra Domenek for their continuous guidance, suggestions and encouragements.

I would like to express my friendship to all students, postdocs and technicians helping me in my experiments and discovering the pleasure of France: Cecile Courgneau, Anna Patsioura, Etzael Espino-Perez, Jean-Michael Vauvre, Phuong-Mai Nguyen, Thomas Verroust, Romulo Salazar.

The presented work would not have been possible without the technical assistance of Cedric Plessis in sorption and analytical experiments and without the assistance of Frédéric Jamme at Synchrotron Soleil.

Finally, I would like to thank Région Ile de France for its financial support.

TABLE OF CONTENTS

Chapter 1. Introduction	1
Chapter 2. Literature review	9
2.1 Diffusion in food packaging materials	13
2.1.1 Abstract	16
2.1.2 Introduction	16
2.1.3 The concepts of “generally recognized diffusion models” in legal US and EU systems	18
2.1.4 Some generalities about diffusion	21
2.1.4.1 Mass transfer from and to food packaging materials	21
<i>2.1.4.1.1 Sorption of food constituent into food packaging: first observation of the reality of diffusion</i>	<i>21</i>
<i>2.1.4.1.2 Cross mass transfer in multicomponent food packaging systems</i>	<i>22</i>
<i>2.1.4.1.3 Mass transfer controlled by diffusion in the packaging materials</i>	<i>29</i>
<i>2.1.4.1.4 The concept of functional barrier</i>	<i>31</i>
2.1.4.2 Molecular diffusion	32
<i>2.1.4.2.1 A macroscopic definition</i>	<i>32</i>
<i>2.1.4.2.2 A microscopic definition</i>	<i>33</i>
<i>2.1.4.2.3 Trace diffusion and random walks</i>	<i>35</i>
<i>2.1.4.2.4 Mutual diffusion</i>	<i>36</i>
2.1.4.3 Diffusion in thermoplastic and elastomers	37
2.1.5 Scaling laws and friction models	40
2.1.5.1 Overview	40
<i>2.1.5.1.1 Hydrodynamic theory of diffusion</i>	<i>40</i>
<i>2.1.5.1.2 Theoretical composition laws for diffusants consisting in N repeated patterns</i> 41	
2.1.5.2 Experimental data of diffusion coefficients in solid polymers	44
<i>2.1.5.2.1 Linear substances</i>	<i>44</i>
<i>2.1.5.2.2 Additive type substances</i>	<i>45</i>
<i>2.1.5.2.3 Combined effect of T, Tg and geometry</i>	<i>46</i>
2.1.6 Free-volume theories	48

2.1.6.1	Common assumptions	48
2.1.6.2	Vrentas and Duda theory for rigid solutes	50
2.1.6.3	Extension to flexible solutes	53
2.1.7	Activation models and data	55
2.1.7.1	Apparent effects of temperature and pressure	55
2.1.7.2	Activation energies	58
2.1.7.2.1	<i>Effect of the molecular mass</i>	58
2.1.7.2.2	<i>Polymer effects</i>	59
2.1.7.2.3	<i>Combined solute and polymer effects</i>	60
2.1.8	Alternative models to predict D or to overestimate D	61
2.1.8.1	The justification of alternative models	61
2.1.8.2	Models overestimating D	64
2.1.8.3	Prediction of D based on decision trees and molecular descriptors	70
2.1.9	Conclusions	73
2.1.10	References	75
2.2	Barrier materials	95
2.2.1	Some definitions and choices	95
2.2.2	Non-reactive barrier systems	97
2.2.2.1	Overview	97
2.2.2.2	Common transfer models for passive/active systems	101
2.2.2.2.1	<i>Out-of-equilibrium approaches</i>	101
2.2.2.2.2	<i>Approaches at equilibrium</i>	103
2.2.2.3	Reported experimental performances of passive barrier systems	104
2.2.2.4	New concepts of active systems	105
2.2.3	Reactive barriers	109
2.2.3.1	The concept of sacrificial reagent to increase barrier properties	109
2.2.3.2	Performances of reactive barriers	111
2.3	Conclusions	113
Chapter 3	Objectives and approaches	115
3.1	General objectives	117
3.2	Particular objectives	117

3.3	Approaches followed in this thesis	118
Chapter 4.	Materials and methods	123
4.1	Materials	126
4.1.1	Solutes.....	126
4.1.2	Polymer	128
4.1.3	Nano-adsorbents.....	130
4.1.4	Polymer/nanocomposite film processing and formulation	132
4.1.4.1	Virgin films.....	132
4.1.4.2	Source films	132
4.1.4.3	Nanocomposite film processing	132
4.2	Methods	133
4.2.1	Differential scanning calorimetry (DSC)	135
4.2.2	Polarized optical microscopy.....	135
4.2.3	Measurement of diffusion coefficients.....	135
4.2.3.1	Single film imaging by DUV/fluorescence microspectroscopy	136
4.2.3.1.1	<i>Sample preparation</i>	136
4.2.3.1.2	<i>Theoretical concentration profiles</i>	136
4.2.3.1.3	<i>Data analyzing</i>	137
4.2.3.2	14 films contact method	139
4.2.3.2.1	<i>Sample preparation</i>	139
4.2.3.2.2	<i>Theoretical concentration profiles</i>	139
4.2.3.2.3	<i>Data analyzing</i>	140
Chapter 5.	Results and discussion	143
5.1	Diffusion in bulk polymers	145
5.1.1	Beyond tortuosity: how negative correlations decrease <i>D</i> values with considered time-scale	145
5.1.2	Non-obstacle related effects on <i>D</i>	148
5.1.3	Study and model development	151
5.1.3.1	Abstract	153

5.1.3.2	Introduction	153
5.1.3.3	Theory	155
5.1.3.3.1	<i>Scaling of D with the number of jumping units and temperature for linear solutes</i>	156
5.1.3.3.2	<i>Conventional free-volume theories</i>	160
5.1.3.3.3	<i>Extended free-volume models for aromatic solutes in aliphatic polymers</i>	163
5.1.3.3.4	<i>Modeling of activation terms for oligophenyl solutes</i>	166
5.1.3.4	Experimental section	168
5.1.3.4.1	<i>Materials</i>	168
5.1.3.4.2	<i>Film processing and formulation</i>	169
5.1.3.4.3	<i>Methods</i>	170
5.1.3.5	Results and discussion	172
5.1.3.5.1	<i>Comparison of the scaling of D between linear aliphatic solutes and aromatic solutes</i>	172
5.1.3.5.2	<i>Scaling diffusion coefficients according to Eqs. (5-11), (5-30)-(5-31)</i>	175
5.1.3.5.3	<i>Polymer effects as probed with diphenyl alkanes</i>	177
5.1.3.5.4	<i>Solute activation parameters of oligophenyls</i>	180
5.1.3.5.5	<i>Mechanisms of translation of oligophenyls in aliphatic polymers</i>	183
5.1.3.6	Conclusions	186
5.1.3.7	Author information	188
5.1.3.8	Acknowledgements	188
5.1.3.9	References	188
5.1.4	Possible application for the study of polymer nanocomposites	192
5.2	Characterization and thermodynamic properties of nano-clays	193
5.2.1	Introduction	193
5.2.2	Simulation and experimental study	197
5.2.2.1	Abstract	198
5.2.2.2	Introduction	198
5.2.2.3	Material and method	200
5.2.2.3.1	<i>Materials</i>	200
5.2.2.3.1.1	<i>Nanoclay</i>	200
5.2.2.3.1.2	<i>Probe solutes</i>	201
5.2.2.3.2	<i>Material characterization</i>	201

5.2.2.3.2.1	<i>X-ray diffraction analysis (XRD)</i>	201
5.2.2.3.2.2	<i>Thermogravimetric analysis (TGA)</i>	201
5.2.2.3.2.3	<i>Specific surface area</i>	201
5.2.2.3.3	<i>Sorption properties at infinite dilution</i>	202
5.2.2.3.4	<i>Sorption isotherms of anisole</i>	204
5.2.2.3.5	<i>Molecular modeling strategies</i>	205
5.2.2.3.5.1	<i>Preparation of neat clay crystal structure</i>	205
5.2.2.3.5.2	<i>Preparation of surface modified clays</i>	206
5.2.2.3.5.3	<i>Sorption calculations at diluted state</i>	206
5.2.2.3.5.4	<i>Sorption calculations at concentrated state</i>	207
5.2.2.3.5.5	<i>Sorption properties of organic solutes in surfactants</i>	208
5.2.2.4	Results and Discussion	208
5.2.2.4.1	<i>Experimental characterization of clays</i>	208
5.2.2.4.1.1	<i>Organic composition</i>	208
5.2.2.4.1.2	<i>Gallery structure</i>	211
5.2.2.4.2	<i>Clay atomistic model and its characterization</i>	212
5.2.2.4.3	<i>Sorption properties at infinite dilution</i>	217
5.2.2.4.3.1	<i>Simulated Henry coefficient and isosteric heat of sorption</i>	217
5.2.2.4.3.2	<i>Comparison with experimental adsorption enthalpy</i>	220
5.2.2.4.4	<i>Sorption behavior at concentrated state</i>	225
5.2.2.4.4.1	<i>Simulated isotherms</i>	225
5.2.2.4.4.2	<i>Experimental sorption isotherms</i>	227
5.2.2.4.4.3	<i>Isosteric heats of sorption</i>	231
5.2.2.5	Conclusions	232
5.2.2.6	References	233
5.2.3	Applications for developing polymer nanocomposite systems	237
5.3	Proof of the concepts of barrier materials including nano-adsorbents	239
5.3.1	Introduction	239
5.3.2	Experimental study and interpretation	241
5.3.2.1	Abstract	242
5.3.2.2	Introduction	242
5.3.2.3	Theory of polymer barrier materials	245
5.3.2.3.1	<i>Beyond tortuosity concepts</i>	245

5.3.2.3.2	<i>Reduction of D due to asymmetric barriers to translation: a two states toy model.</i>	247
5.3.2.3.3	<i>Inverse gas chromatography (IGC) as a one-dimensional physical model.</i>	248
5.3.2.3.4	<i>D reduction due to entropic trapping: a first approach</i>	249
5.3.2.4	Materials and methods	251
5.3.2.4.1	<i>Polymer and nano-adsorbents.</i>	251
5.3.2.4.2	<i>Solute probes.</i>	252
5.3.2.4.3	<i>Estimation of $\gamma_{i,MMT}(T)$</i>	252
5.3.2.4.4	<i>Estimation $\gamma_{i,P}(T)$ by a generalized off-lattice Flory-Huggins method</i>	253
5.3.2.4.5	<i>Diffusion coefficient (D) determinations.</i>	253
5.3.2.5	Results and discussion	254
5.3.2.5.1	<i>Effect of crystallite morphology on diffusion coefficients</i>	254
5.3.2.5.2	<i>Partitioning between nanoclays and amorphous regions of PCL and PVA.</i>	254
5.3.2.5.3	<i>Reduction of diffusion coefficients in PCL nanocomposite.</i>	256
5.3.2.5.4	<i>Reduction of diffusion coefficients in PVA nanocomposite.</i>	257
5.3.2.6	Conclusions	261
5.3.2.7	References	261
5.3.3	Does the nano-adsorbent concept work?	266
5.4	Extended results and discussion	269
5.4.1	The concept of increasing dwelling times to lessen D	269
5.4.2	Do we expect a change in the molecular mechanism of diffusion in presence of nano-adsorbents?	272
Chapter 6.	Conclusions and perspectives	275
6.1	Overview	277
6.2	Diffusion of tracers in bulk polymers	278
6.3	A new concept of barrier material: chaotic materials	280
6.4	Outlook	282
Chapter 7.	References	285

LIST OF PUBLICATIONS

Publications included in the thesis

Publication I

X. Fang, and O. Vitrac, (2013). Predicting diffusion coefficients of chemicals in and through packaging materials. Submitted to Crit. Rev. Food. Sci. Nutr.

Publication II

X. Fang, S. Domenek, V. Ducruet, M. Réfrégiers, and O. Vitrac, (2013). Diffusion of Aromatic Solutes in Aliphatic Polymers above Glass Transition Temperature. *Macromolecules*. 46: 874-888.

Publication III

X. Fang, V. Ducruet, and O. Vitrac, (2013). Sorption properties of solutes onto pristine and organo-modified montmorillonites. Submitted to Langmuir.

Publication IV

X. Fang, S. Domenek, and O. Vitrac, (2013). Controlling the molecular interactions to improve the diffusion barrier of biodegradable polymers to organic solutes above Tg. In preparation.

Publications not included

X. Fang, O. Vitrac, S. Domenek, V. Ducruet, (2012). Controlling the molecular interactions to improve the diffusion barrier of biosourced polymers to organic solutes, *Defect and Diffusion Forum*, 323-325, 26.

LIST OF FIGURES

Figure 1-1 Different cases of energy barriers between the matrix and inclusions, $\{l_i\}_{i=1..2}$, $\{E_{ij}\}_{i=1..2}$ are the hop length and the activation energy of diffusion in the inclusions $i=1$ and in the matrix $i=2$. (a) An inclusion with a diffusion coefficient in the inclusions smaller than in the matrix; there is no significant energy barrier between them. (b) An energy barrier E_a for the penetration into inclusion. (c) Partial trapping of particles inside inclusions, the “detrapping” energy is E_t . After Figure 2 of Kalnin and Kotomin (1998)..... 6

Figure 2-1 Microscopic observations in visible light and its molecular interpretation of the sorption of decane in atactic polystyrene at 70 °C (after Morrissey and Vesely (2000)). 22

Figure 2-2 Main mass transfer from, to and cross packaging materials (after Rahman (2007), Vitrac and Hayert (2007a)). 29

Figure 2-3 Concentration profile of migrants (*e.g.* additive) along the thickness of the food-packaging system as detailed in Vitrac and Hayert (2006). When $t=0$, migrants are assumed to be distributed homogeneously in the packaging material so that a uniform concentration profile can be assumed. For $t>0$, mass balance enforces that the surface area below the concentration profile on the food side is equal to complementary surface area between the profiles at $t=0$ and $t>0$ on packaging side. 31

Figure 2-4 Cumulated amount of diffusant (Q_t) crossing a plane sheet of thickness, l_{FB} , with upstream concentration C_I versus dimensionless time $D_{FB}t/l_{FB}^2$. The intercept of tangent line with $Q_t=0$ at $t_{delay}=l_{FB}^2/6D_{FB}$ gives the typical time lag to get a significant permeation across the film. (after Fig. 4.2 in book of Crank (1979)) 32

Figure 2-5 One-dimensional interpretation of molecular diffusion with “eyed” particles a) as populations in contiguous elemental volumes exchanging particles, b) as a local hopping process and c) as mutual diffusion of a bulky additive among connected polymer beads. In the real life (at macroscopic scale), the particles and the direction of jumps are indiscernible. To enable particles counting, the direction of the sight gives here the direction of the next jump. In details, situations in (a) and (b) illustrate the concepts of macroscopic and microscopic mass balance applied implicitly in second and first Fick equations, respectively. 34

Figure 2-6 Simulation of 10 one-dimension random walks starting from a same initial position. The continuous probability Gaussian distributions associated to an infinite number of trajectories are also represented for different times.(see Eqs. (2-6) and (2-7)). 36

Figure 2-7 Schematic representation of multi-scales of the organization of polymer materials (*e.g.* polyethylene). a) chemical structure (Baschnagel *et al.*, 2004), b) intermingled chains (Baschnagel *et al.*, 2004), c) semi-crytalline structure (Queyroy and Monasse, 2012), d) polycrystalline structure (Callister and Rethwisch, 2011), e) heterogeneous materials (Muller-

Plathe, 1991). l_0 : length of a C-C bond, l_p : persistence length, θ : bond angle, ϕ : torsion angle, r_g : gyration radius, d_{ee} : end-to-end distance.....	38
Figure 2-8 Largest polymer displacements versus temperature. T_g is the glass transition temperature, T_m is the melting temperature, (after Paul and Smith (2004)).....	39
Figure 2-9 Scaling of diffusion coefficients in natural rubber and polyvinyl chloride (PVC) with a) molecular mass (M) and b) van-der-Waals volume (V_{vdw}) of diffusant (Berens, 1981).	40
Figure 2-10 Scaling laws associated to the diffusion a-b) of linear n -alkanes (at 40 °C, according to Reynier <i>et al.</i> (2001b), Vitrac <i>et al.</i> (2007)) and c) linear or branched alkanes (between 23 °C and 30 °C, data collected by EU working group SMT-CT98-7513 and published by Begley <i>et al.</i> , (2005), Vitrac <i>et al.</i> , (2006) and available within the EU database hosted on the Safe food packaging portal (INRA, 2011) for low density polyethylene.....	45
Figure 2-11 Scaling laws identified for additive-type molecules in different thermoplastic materials at 298K (Dole <i>et al.</i> , 2006a).	46
Figure 2-12 a, b) Log-log plots of trace diffusion coefficients in polyethylene of linear aliphatic and aromatic solutes. c) The corresponding scaling exponents α versus $T-T_g$ for both linear aliphatic solutes (Koszinowski, 1986; Arnould and Laurence, 1992; Möller and Gevert, 1994; Kwan <i>et al.</i> , 2003; Vitrac <i>et al.</i> , 2007; von Meerwall <i>et al.</i> , 2007) and aromatic solutes (Koszinowski, 1986; Doong and Ho, 1992; Fang <i>et al.</i> , 2013).....	47
Figure 2-13 Distribution of free volumes around a planar and rigid diffusant (fluorene) in high density polyethylene at room temperature pressure as extracted by isobaric and isothermal molecular dynamics simulation. The image is obtained by plotting the projected Connolly surfaces onto the plan defined by the main axes of the diffusant. Only the atoms included in the thickness of the diffusant are considered.	48
Figure 2-14 Interpretation of the translation of additive-type molecules according to the state of the polymer.	58
Figure 2-15 Estimated activation energies between 20 and 40°C in low density polyethylene: a) small molecules $M < 100 \text{ g}\cdot\text{mol}^{-1}$, b) linear alkanes, c) additive molecules with $100 < M < 600 \text{ g}\cdot\text{mol}^{-1}$. Data extracted from the European database of diffusion coefficients (INRA, 2011).	59
Figure 2-16 Van't Hoff diagram of diffusion coefficient of 2',5'-dimethoxy-acetophenone in different polymers at high temperature (near to processing temperature). (after Feigenbaum <i>et al.</i> (2005), Dole <i>et al.</i> (2006a), Dole <i>et al.</i> (2006b)).	60
Figure 2-17 Variation of activation energy for different polymers between 20 and 40°C according to Dole <i>et al.</i> (2006a).	61
Figure 2-18 Estimation of D with molecular weight by both models listed in Table 2-9 and Vitrac model (see section 2.1.8.3) and validation of these models by comparison with data	

collected by the EU project SMT-CT98-7513 (EC, 2002b) and renormalized at 23°C in a) LDPE (345 values), b) HDPE (142 values) and c) PP at 23°C (141 values).....	66
Figure 2-19 Plot of scaling exponents α with molecular weight for different models in Table 2-9 and reported averaged experimental α values in corresponding range of tested molecular weight (after Fang <i>et al.</i> (2013)). Each horizontal segment represents the range of molecular masses used to determine α	67
Figure 2-20 Evaluation of the robustness of the Piringer model for two typical polymers above their T_g : a), c) polypropylene ($T_g=0^\circ\text{C}$) and b), d) polyamide ($T_g=50^\circ\text{C}$). The considered diffusants are aliphatic solutes (<i>e.g.</i> alkanes and alkyl acetates) below the entanglement length. a-b) Comparison between iso- D values (from Fang <i>et al.</i> (2013), see Table 2-6, solid lines) and iso- \check{D} values obtained from Piringer model (see Table 2-9, dashed lines). c,d) Corresponding iso-ratios \check{D}/D where “safe regions” (with overestimations) are depicted in light blue. e) Safe strategies to extend the Piringer model to new polymers in presence of scarce data.....	69
Figure 2-21 Example of automatic classification of Chimmassorb 90 (Vitrac <i>et al.</i> , 2006). The request has been typed online on the Safe Food Packaging Portal (INRA, 2011), which gives in return all substances in the EU database with similar D values.....	72
Figure 2-22 Decision tree for the prediction of diffusion coefficients in LDPE at 23° with different risks of overestimations: 50% or 10% (after Vitrac <i>et al.</i> (2006))......	73
Figure 2-23 The main categories of barrier materials.....	96
Figure 2-24 Overview of existing passive and active systems.....	99
Figure 2-25 Example of outstanding active material: barrier to small molecules such as helium and permeable to larger ones such as water. a) The transport mechanism of water molecular due to “tunneling effect”; b) the permeability of different solute molecules (after Nair <i>et al.</i> (2012))......	100
Figure 2-26 One-dimensional periodic free energy profile including two states: A and P separated by a transition state denoted ‡.....	106
Figure 2-27 The reduction ratio of D by non-reversible and reversible random walks on hexagonal lattices with Poisson distributed dwelling times in two situations: with or without preferential routes. (after Vitrac and Hayert (2007)).....	107
Figure 2-28 a) Excess polymer-air partition coefficient K or “sorption excess” (positive value= chemical affinity for the polymer above the one expected from Eq. (2-29)) versus the volume fraction in particles ϕ_p . b) Reduction of mutual diffusion coefficients with ϕ_p . Subscripts ϕ and B denote effective and bulk properties respectively. Filled and empty symbols represent data obtained with a diameter of 14 nm and 50 nm respectively. The	

theoretical D reduction with impermeable particles (Sangani and Yao, 1988) are plotted with (\times) for particles of diameter 14 nm.	108
Figure 2-29 The concentration profiles of diffusants and reagent in reactive film with thickness, l . The reaction front separated film into diffusion zone, l' , and reaction zone, $l-l'$. C_{10} and C_{20} are the constant diffusants concentration in contact with film and the reagent concentration in reactive film.	110
Figure 4-1 The scheme of the structure of pristine montmorillonites.	130
Figure 4-2 Scheme of sample preparation (A, C=virgin films, B=source film)	136
Figure 4-3 Simulated concentration profiles at cross section of three contact films assembled as in Figure 4-2 with thickness 200 μ m each normalized at a) the interface and b) the center of source layer	136
Figure 4-4 Comparison of theoretical concentration profiles with diffraction patterns (colored curves) and without (black curves) for a) the layer A or C and b) the layer B.	137
Figure 4-5 Example of the collected spectra at each measured position with baseline. Two peaks are related to excitation (<i>i.e.</i> $\lambda=275$ nm) and emission (<i>i.e.</i> $\lambda=280-380$ nm) respectively	137
Figure 4-6 The experimental concentration profiles of biphenyl at 343K (red filled dot) in PP film at a) position C and b) position B fitted with theoretical concentration profiles (colored curves).	138
Figure 4-7 The experimental concentration profile of biphenyl at 343K (red filled dot) in PLA film at position C fitted with theoretical concentration profiles (colored curves).	139
Figure 4-8 Scheme of sample preparation in 14 films contact experiment.	139
Figure 4-9 14 films method involving 2 sources sandwiched among 12 virgin films. Concentration profiles are plotted for different Fourier number. Bars represent the concentration as measured (<i>i.e.</i> averaged over the film thickness) whereas the continuous line represents the continuous profile. All concentration profiles are normalized to yield an overall stack concentration of 2.	140
Figure 4-10 a) Measured profiles after 1 hour of contact (bars), predicted profiles and corresponding 95% confidence intervals are plotted in continuous and dotted lines respectively. All concentrations profiles are normalized to yield an overall stack concentration of 2. b) Least-square fitting criterion between measured and predicted concentration profiles. 95% confidence interval around the minimum is plotted as a red line. c) Details of the minimum region (linear scale of Fourier numbers).	140
Figure 5-1 a) Main homologous series used in this section to probe both free-volume effects and the scaling of D with M . b) Bivariate domain $T \times Tg$ examined in this section	150

Figure 5-2 Log-log plots of trace diffusion coefficients in polyethylene (PE) either with low density (LDPE) or high density (HDPE) of a) linear aliphatic and b) aromatic solutes. D_{ref} was chosen as the diffusion coefficient of the first solute in the considered solute series..... 157

Figure 5-3 Correlations between ζ values as reported in Tables 2 and 3 of³³ and $\ln M/M_0$. Experimentally determined ζ values are plotted as solid symbols and theoretically calculated ones (see Eq. (22) in³³) as empty symbols. The reference solutes are: hexane, methyl acetate and benzene with molecular mass (M_0) of $86 \text{ g}\cdot\text{mol}^{-1}$, $74 \text{ g}\cdot\text{mol}^{-1}$ and $78 \text{ g}\cdot\text{mol}^{-1}$ respectively. 163

Figure 5-4 Scaling exponents of trace diffusion coefficients versus $T-T_g$. Symbols plot determinations of α inferred from experimental D values reported in references enclosed within brackets. α values for oligophenyls measured by this study and those calculated from D values of short linear aliphatic solutes in PVAc³⁴ were not used to fit Eq. (5-18). The classification of solutes as linear aliphatic and aromatic is based on the same one as used in Figure 5-2. 173

Figure 5-5 a) Log-Log plot of trace diffusion coefficients of diphenyl alkanes and b) oligophenyls in various polymers. Symbols are experimental values. Continuous straight lines are scaling relationships fitted according to Eq. (5-11). Dashed lines are values fitted from Eqs. (5-30) and (5-31) for diphenyl alkanes and oligophenyls respectively..... 176

Figure 5-6 Comparison between calculated (with Eqs. (5-30) and (5-31) respectively) and measured diffusion coefficients of a) diphenyl alkanes series and b) oligophenyls series in PLA, PP, PCL(\times) and PVA(\blacktriangle).The continuous lines plot the straight line $y=x$. The corresponding distribution of relative fitting errors values and fitted Gaussian distribution (continuous curve) are plotted within insets. Values in PVA are external validation predictions not used in the fitting procedure. 177

Figure 5-7 Scaling diffusion coefficients of diphenyl alkanes with the number of carbons, N_C , between phenyl rings: a) raw diffusion coefficients measured at 343 K for PLA, 333 K for PP, and 323 K for PCL b) diffusion coefficients relative to biphenyl $D(N_C=0, T, T_g)$. Eq. (5-30) predictions are plotted as continuous lines..... 178

Figure 5-8 Experimental diffusion coefficients of diphenyl alkanes in PLA, PP, PCL (empty symbols) and PVA (filled symbols) versus $T-T_g$ a) raw diffusion coefficients, b) D/D_{solute} . Eq. (5-30) fitted on empty symbols is plotted as continuous lines. Filled symbols are used for external validation purposes..... 180

Figure 5-9 Scaling of diffusion coefficients of oligophenyls with the number of phenyl rings, N_{Ph} , a,c) in PCL and b,d) in PP at different temperatures: a,b) raw diffusion coefficients, c,d)

scaled diffusion coefficients with polymer effects removed. Predictions according to Eq. (5-31) are plotted as continuous lines.	181
Figure 5-10 Normalized van't Hoff plots of oligophenyls a,b) raw diffusion coefficients and c,d) scaled diffusion coefficients with polymer effect removed a,c) in PCL and b,d) in PP. Predictions according to Eq. (5-31) are plotted as continuous lines.	182
Figure 5-11 a,c) Raw and b,d) solute activation energies and diffusion entropy of oligophenyls in PP and PCL versus the number of phenyl rings, N_{Ph} ; e) correlation between solute activation parameters; f) related free barrier energy to diffusion at 298 K.	183
Figure 5-12 a) Comparison of relative solute activation energy (continuous lines, left scale), calculated as $\tau'_{ring}(N_{Ph}) = \tau_{ring}(N_{Ph}) - \tau_{trapped}$ for different p values according to Eqs. (5-32) and (5-33), with experimental values (dotted lines, right scale) reported in Figure 5-11b). The horizontal dashed line represents the average value of Ea_{solute} for studied oligophenyls. b) Comparison of solute entropy (continuous lines, left scale), calculated for different p values according to Eqs. (5-34)-(5-37), with experimental values (dotted line, right scale) reported in Figure 5-11d).	185
Figure 5-13 Interpretation of inverse gas chromatography (IGC) as 1D random walk along a surface energy. The unique assumption is that the number/amount of sorption sites (<i>i.e.</i> the probability of accessibility) is the same for all substances (including for the reference low interacting one) so that the ratio of elution times is a measure of the energy difference $H_{i+adsorbent}^{ex} - RT$. a) Equivalent energy surface. b) Retention times at high and low flow rate (FR). c) Possible interpretation of the right tailing of retention distributions due to a mixed interactions with external/internal accessible surfaces, surfactants or in gas phase.	194
Figure 5-14 a) Detailed description of mass transfer at one adsorption site within the IGC column. The longitudinal direction represents a macroscopic transport along the column, while the transverse direction details the mass balance at molecular scale. b) Corresponding free energy distribution associated to the sorption/desorption jumping processes. According to the transition state theory, ‡ is the transition state whose probability does not depend on the origin of the solute (in gas phase or in adsorbed phase).	203
Figure 5-15 Differential thermal analysis (DTA) curves of a) pristine MMT, b) C18MMT, c) C18OHMMT and d) C6H5MMT. Deconvolved peaks are identified with Roman numbers with corresponding parameters listed in Table 5-6.	209
Figure 5-16 Diffraction spectra of a) MMT, b) C18MMT, c) C6H5MMT and d) C18OHMMT samples. Bragg peaks were fitted as a sum of Gaussian (a, b, d) and Lorentzian curves (c) and baseline. The baseline is fitted with a tangent constrained fourth degree spline polynomials.	211

Figure 5-17 The dspacing distribution calculated according to Bragg’s law. Likeliest values and typical percentiles are reproduced in Table 5-7.	212
Figure 5-18 Illustrations of our atomistic models of MMT: (a) i: overview of periodic unit cell in $2\times 2\times 2$ arrangement with a lattice spacing (d -spacing) in c direction and a significant gap between the two adjacent layers, iii: side view details of the crystal structure with PI symmetry, the elemental crystal pattern is represented in CPK style. iv: the corresponding top view of six tetrahedral silica connected clearly identifiable, (b) Details of the Al octahedral layer with random substitutions by Mg atom. c)-f) Typical side views of pristine MMT (d -spacing= 1.27 nm) and organo-modified MMT (d -spacing=2.2 nm). g)-h) Two typical orientations of one single surfactant molecule: octadecylamine (C18).	213
Figure 5-19 Correlations between surfactant loading and d -spacing as assessed from GCMC simulations.	214
Figure 5-20 Theoretical distributions of surfactant amounts from GCMC simulations (Figure 5-19) integrating the dispersion of d -spacing plotted in Figure 5-16. Mean values and typical percentiles are reproduced in Table 5-8.	215
Figure 5-21 a) Top view of the volume accessible to spherical probes into one typical clay interlayer filled with C18 surfactant to spherical probes (the contact surface for different probe radii are plotted in red color). b) Relationships between volumes and gyration radius of tested solutes. c-d) Accessible volume and surface area according to radius of the considered spherical probe.	216
Figure 5-22 a)-c) The calculated Henry coefficient sampled by one single solute molecule with all clay models at 313 K. The horizontal dashed line separates the theoretical Henry coefficient for an inert ideal gas. d)-f) the isosteric heat calculated in the temperature range from 298 K to 348 K a), d) The effect of surfactant on n -alkanes with equal d -spacing ($d=2.2\text{nm}$), b), e) the effect of d -spacing on n -alkanes in the range of $d=1.27\text{-}2.2\text{nm}$ and c), f) on solute series of heptane, toluene and anisole in the range of $d=1.27\text{-}2.2\text{nm}$	219
Figure 5-23 The corresponding sorption energy (i.e. -isosteric heat) distribution of solute series of heptane, toluene and anisole a)-c) on all clay type with equal d -spacing of 2.2nm and d)-f) on pure MMT with d -spacing ranging from 1.4 to 2.2nm. The averaged energy values are reported in Figure 5-22a)).	220
Figure 5-24 Typical distributions of elution times for n -alkanes ($n=1..6$), toluene and anisole in columns filled with a) pure MMT and b) C18OHMMT samples. Fiited exponentially-modified Gaussians are depicted as thin solid lines and c) the peak shape factor (skewness) of elution profiles as function of the position of the peak mode.	221
Figure 5-25 Effect of flow rate effect on retention times of pentane and hexane. Normalized retention times (see Eq. 4) are plotted as dashed lines.	222

Figure 5-26 The experimentally determined Henry coefficients of pristine MMT compared with simulated ones averaged over the distribution of real d -spacing values (see Figure 5-17). The dashed line represents the straight line. $y=x$. Vertical and horizontal lines represent 95% confidence intervals.....	223
Figure 5-27 Comparisons of isosteric heat of sorption and net values between experimental (IGC) values (open symbols) and simulation ones for a-b) n -alkanes and c) aromatic solutes. Excess in solute-surfactant mixing energies are also represented more general heptane, toluene and anisole (the experimental data are compared with simulation data with two possible interactions: between one solute molecular and clay surface which defined upper boundary above $30 \text{ kJ}\cdot\text{mol}^{-1}$; between solute and surfactant which defined lower boundary below $5 \text{ kJ}\cdot\text{mol}^{-1}$).....	224
Figure 5-28 a) Simulated sorption isotherms of anisole in pure MMT with different d -spacing and b) linear relationship between maximum loading and gap distance.....	226
Figure 5-29 a) Maximum loading as determined from simulated isotherms of clays with a fixed d -spacing of 2.2nm and b) equivalent Henry coefficients K_L as extrapolated from Langmuir equation (see Eq. 14) (solid lines with symbols) compared with K_H values calculated from solute insertion at infinite dilution (see Figure 5-22a)).....	227
Figure 5-30 Experimental sorption isotherms of anisole (open symbols and dashed lines) compared with fitted isotherms relying on BET equation (solid line). Dashed lines are continuous least squares approximates.	228
Figure 5-31 Experimental isosteric heat of sorption vs loading inferred from IGA experiments	231
Figure 5-32 Simulated isosteric heat of sorption versus loading of anisole.....	232
Figure 5-33 Energetic interpretation of $K_{contrast}$ in nano-adsorbent – polymer systems. Excess mixing energies are evaluated for a reference state of the considered solute at liquid state (or equivalent at molten state).....	240
Figure 5-34 One-dimensional periodic free energy profile including two states: MMT and P separated by a transition state denoted ‡.	247
Figure 5-35 (a) Mass transfer description at one adsorption site within the column of IGC. The longitudinal direction represents a macroscopic transport along the column, while the transverse direction details the mass balance at molecular scale. (b) Corresponding free energy distribution in the process of desorption (note that $G_{\Delta} \rightarrow 0$).	249
Figure 5-36 Dynamics of a particle moving randomly within a sphere. (a) Distribution of collision times (reciprocal of a Maxwell-Boltzmann distribution). (b) Velocity correlations for a particular starting position (continuous line) and averaged over all possible starting times	

(dashed line). (c) Velocity correlations averaged all collision intervals. (d) Corresponding $3D(\tau)$ values.	250
Figure 5-37 The diffusion coefficients of PCL films casting a) on a glass surface with and b) on a Teflon surface with close crystallinity degree of 55% and c)-d) the corresponding crystallite morphology in two PCL films. Pictures above depict the size of crystallites by polarized light microscopy (width=100 μm).....	254
Figure 5-38 a) The excess energy of mixing and b) corresponding partitioning coefficient $K_{contrast}$ between organo-modified MMT and amorphous regions of PCL. The symbol of data is coded as xy: x is the index of solute; y is the index of polymer or clay.....	256
Figure 5-39 a) The excess energy of mixing and b) corresponding partitioning coefficient $K_{contrast}$ between pristine MMT and amorphous regions of PVA. The symbol of data is coded as xy: x is the index of solute; y is the index of polymer or clay.....	256
Figure 5-40 Normalized concentration profiles of biphenyl after 20 min of contact time at 298K (a) in pure PCL films with D value of $9.1e^{-13} \text{ m}^2/\text{s}$, (b) in PCL nanocomposite films including 0.5wt % of C18OHMMT with D value of $5.2e^{-13} \text{ m}^2/\text{s}$. The average film thickness is of 40 μm	257
Figure 5-41 Reduction of diffusion coefficients of biphenyl in PCL nanocomposite: a) effect of concentration of nanoclays. b) interpretation according to $K_{contrast}$. Pictures above depict the size of crystallites in PCL and its nanocomposite systems containing 0.5wt% of nanoclays by polarized light microscopy (width=100 μm).....	257
Figure 5-42 Normalized concentration profiles of biphenyl at 343K (a) in pure PVA films with D value of $3.8 \times 10^{-15} \text{ m}^2 \cdot \text{s}^{-1}$, (b) in PVA nanocomposite films including 5wt % of pristine MMT with D value of $3.4 \times 10^{-16} \text{ m}^2 \cdot \text{s}^{-1}$. The average film thickness is of 13 μm	259
Figure 5-43 Molecular dynamics of oligophenylys in vacuum when one or several aromatic rings are blocked randomly: a) internal degrees of freedom, b) corresponding trace of the trajectory of the center-of-mass projected along its main inertia axis.	270
Figure 5-44 a) Extreme configurations leading to a translation of center-of-mass (CM) of quaterphenyl beyond the size of one aromatic ring while keeping the position of end ring fixed. The projections on the main axes represent the same molecule as connected rigid blocks (robot model) The visited distance of CM is represented by an arrow and the ring size by a solid circle centered on CM. b) Sketched fluctuations of mean-square-distance (msd) when one or several rings are alternatively blocked.	270
Figure 5-45 Mean-square-displacement (msd) of the center-of-mass versus time scale, τ , when one single ring is blocked in a) biphenyl, b) <i>p</i> -terphenyl, c) <i>p</i> -quaterphenyl molecules. d) msd value when the ring to be blocked is chosen randomly for all tested solutes. e) Comparison of	

relative solute activation energy (continuous lines, left scale) and calculated for different p_{ring} values as detailed in section 5.1.3.	271
Figure 5-46 Covariances between the displacements of atoms versus time scale, τ , when one single ring is randomly blocked in a) biphenyl, b) <i>p</i> -terphenyl, c) <i>p</i> -quaterphenyl molecules. d) Conformational entropy when 1 to $N_{ph}-1$ ring is randomly blocked as calculated from Eq. (13) in section 5.1.3. e) Comparison of solute entropy (continuous lines, left scale), calculated for different p_{ring} values according to Eqs. (13)-(16) in section 5.1.3 when 1 to $N_{ph}-1$ ring is randomly blocked, and experimental values measured for oligophenyls (dotted line, right scale).....	272
Figure 5-47 Scaling of equivalent transport coefficient (assimilated to D) with molecular mass M in IGC experiments: n-alkanes (circles), toluene and anisole (square). The upper dashed line represents the prediction according to Knudsen scaling.	274
Figure 6-1 Comparison between experimental data of (Janes and Durning, 2013) for particles and Eq.(6-4).....	284

LIST OF TABLES

Table 2-1 List of typical potential substances existing in different materials for food contact purpose.	24
Table 2-2 Main contamination routes of food by materials in direct or indirect contact.....	28
Table 2-3 Scaling law and diffusion mechanisms associated with ideal mixtures ($\Gamma = 1$).	43
Table 2-4 Calculation method of free volume parameters in Eq. (2-22)	51
Table 2-5 ξ and E^* values for 8 diffusant-polymer systems.	52
Table 2-6 Formal equivalences between scaling law of diffusion coefficients and free-volume theory for diffusants based on linearly repeated sub-units (see Figure 2-5) in rubber polymers (Fang <i>et al.</i> , 2013)	53
Table 2-7 Equivalent terms in Eq. (2-24) for two homologous series of aromatic diffusants.	55
Table 2-8 The activation energy and volume responsible for rotation and translation of the additive-type molecule in high density polyethylene at macroscopic and molecular scale. (after Kovarski (1997)).....	56
Table 2-9 Main models to overestimate D values for compliance testing	64
Table 2-10 Available parameter values of main models for different polymers as reported in (Limm and Hollifield, 1996; Begley <i>et al.</i> , 2005; Helmroth <i>et al.</i> , 2005; EC, 2012a)	65
Table 2-11 Main geometric parameters used in CART approaches (Vitrac <i>et al.</i> , 2006) and their physical justifications. Conformers are usually obtained from molecular dynamics simulation to reach representative configurations at the considered temperature.	71
Table 2-12 Values of topological descriptors for six typical molecules as associated to their state of minimum internal energy. The values are ordered as V_{vdw} , ρ , I_z / I_x (see Table 2-11). All molecules were oriented along their main axes (x, y and z); the three main projected surfaces are also depicted.....	71
Table 2-13 Effective TR_{eff} from out-of-equilibrium approaches	102
Table 2-14 Effective D_{eff} from equilibrium approaches	104
Table 2-15 Reported reduction of permeability and D in some typical nanocomposite passive systems	105
Table 2-16 Effective TR_{eff} and D_{eff} in reactive barrier systems (after Table 1 in Yang <i>et al.</i> (2001)).....	111
Table 2-17 Estimated reduction of permeability and D in reactive barrier systems containing reactive flakes (after Table 2 in Yang <i>et al.</i> (2001))	111
Table 3-1 The objectives and corresponding methodologies included in the thesis.....	119
Table 4-1 List of solutes applied in the thesis.....	126

Table 4-2 Information and characterization of applied polymers	129
Table 4-3 The information and chemical structure of four commercial available clays.....	131
Table 4-4 Index of methodologies applied in the thesis.....	134
Table 5-1 Variations of D , which are not affected by the presence of obstacles. D' is the corresponding diffusion coefficient in a nanocomposite material incorporating obstacles. ..	148
Table 5-2 List of studied aromatic solutes	168
Table 5-3 Information and characterization of processed films.....	169
Table 5-4 The detailed information of four tested clays	200
Table 5-5 Information of column dimension and sample filling condition for IGC experiments	202
Table 5-6 Content of tested clays based on the deconvolution of the TGA spectra (peaks are identified with roman numbers in Figure 5-15).	210
Table 5-7 d -spacing values integrating uncertainties over the distributions.....	212
Table 5-8 Comparison of surfactant loading between experimental and calculation.	215
Table 5-9 Comparison of sorption parameters of anisole from IGA experiments and simulations at concentrated and diluted states.	230
Table 5-10 Comparison of recommendations to develop Hybrid MMT-polymer composite systems according to processing and sorption properties.	238
Table 5-11 Polymer-MMT nanocomposite systems used to test the concepts of barrier materials integrating nanoparticles.....	239
Table 5-12 Characteristics of samples prepared. Suppliers: A= Creagif Biopolymères (France); B= Süd Chemie (Germany) and C=Sigma Aldrich (France)	251
Table 5-13 The diffusion coefficients of biphenyl and terphenyl in both PVA film and PVA nanocomposite containing 5wt% of pristine MMT.....	260
Table 5-14 Activation energies of diffusion of p -terphenyl in PVA equilibrated at 28% of relative humidity	261
Table 5-15 Calculated $K_{contrast}$ values versus basal spacing (d) of clay for aromatic solutes.	266
Table 5-16 Reported performances of the different systems.	267

Chapter 1. Introduction

Due to a significant concern for the contamination of food products by substances originating from materials in contact such as packaging materials, INRA (Institut National de la Recherche Agronomique) has collected diffusion coefficients (D) in different polymers (Begley et al., 2005; Cottier et al., 1997; Feigenbaum et al., 2005; Pennarun et al., 2004a; Pennarun et al., 2004b; Pinte et al., 2010; Pinte et al., 2008; Reynier et al., 2001a; Reynier et al., 2001b; Vitrac et al., 2006) as a public mission (Feigenbaum et al., 2002; Nguyen et al., 2013; Vitrac and Hayert, 2007a) and for sanitary survey (Gillet et al., 2009; Vitrac et al., 2007a; Vitrac and Hayert, 2005; Vitrac and Leblanc, 2007). For several decades, the common opinion has been that D values of organic solutes such as additives (e.g. antioxidants, light-stabilizers, plasticizers...), oligomers or non-intentionally added substances (e.g. residues, contaminants, neoformed substances...) were intrinsic properties of polymers and could be only raised in conditions of use due to temperature increase or plasticization. Decreasing D values were thought possible only by changing the design of the packaging assembly (i.e. by inserting a barrier layer between the source and the food) or by blending the barrier material with a higher glass transition temperature (T_g) into the base polymer (Lange and Wyser, 2003). In appearance, diffusion of large and bulky substances in solid thermoplastic polymers suffers a lack of interest from the scientific community. The likely reasons are in two aspects: i) diffusion coefficients of organic substances in solid thermoplastics are spread over several decades requiring long-term measurements or a combination of different techniques at microscopic and macroscopic scales to reach accurate determinations (Goujot and Vitrac, 2013; Moisan, 1980; Roe et al., 1974; Vitrac and Hayert, 2006; Vitrac et al., 2007b); ii) most of the reported works in the literature focused on the transport of gas molecules, mainly oxygen and water (Marais et al., 1999; Métayer et al., 1999; Xu et al., 2001), initially with an intent of understanding diffusion (Bavisi et al., 1996; Bharadwaj and Boyd, 1999; Pavel and Shanks, 2005) and subsequently with an intent of developing new barrier materials (Alexandre et al., 2009; Andrade et al., 2003; Beake et al., 2004; Fang et al., 2005; Hiltner et al., 2005; Liu et al., 2004).

During the last decade, two main trends extended the perspective of barrier materials:

- new biosourced or biodegradable materials, used as mono-materials such as polyesters (Liu et al., 2004; Ray et al., 2003; Shogren, 1997)(Baker et al., 2008) or used in blends with polymers from vegetable (Averous, 2004) or animal (Matet et al., 2013) sources, and requiring optimization in particular to increase their resistance to water;

- the development of nanocomposite systems as a solution to the increasing demand for environmental friendliness and materials with improved barrier properties (Bordes et al., 2009; Bordes et al., 2008; Follain et al., 2013; Katiyar et al., 2011; Lagaron and Lopez-Rubio, 2011; Li et al., 2013; Martucci and Ruseckaite, 2010; Sanchez-Garcia and Lagaron, 2010; Singh et al., 2010; Svagan et al., 2012; Vartiainen et al., 2010; Yu et al., 2006).

Although most of hybrid systems are not yet authorized in the EU due to insufficient migration and toxicological data (Arora and Padua, 2010; Cushen et al., 2013; Espitia et al., 2012; Restuccia et al., 2010; Rhim and Ng, 2007), the concept of nanocomposite materials for food contact is flourishing in the literature. The reviews of (Azeredo, 2009; Hatzigrigoriou and Papaspyrides, 2011) list not only enhanced barrier properties but also novel attributes such as antimicrobial properties (Espitia et al., 2012), oxygen scavenging (Busolo and Lagaron, 2012), enzyme immobilization, and sensor of food storage conditions. The presence of nanoparticles could have also additional benefits by reducing the risk of release of plastic additives (De Abreu et al., 2010).

The reported physical principles of barrier effects in nanocomposites have been reviewed by (Choudalakis and Gotsis, 2009) and comprise: delamination/exfoliation effects, orientation effects, aspect ratio effects, local polymer reordering (*i.e.* T_g shift, densification/dedensification, crystallization-induced). All combined effects were however associated to reductions of permeability lower than one decade and insufficient to transform poor barrier materials into good ones. The work of Merkel et al. (2002a; 2002b; 2003) describes an increase of free-volume around inclusions instead, which tends to increase conversely permeability (Hill, 2006).

The thesis addresses the barrier problem from a different interest i) by focusing on organic molecules instead of gases or water vapor ii) by using modeling as a tool to understand and optimize barrier effects. The initial motivation was to develop new concepts to be used for biodegradable materials (such as polylactide, polycaprolactone), but the work must be envisioned in a broader acceptance of materials incorporating nano-adsorbents to be used as packaging material or as separation membrane. For the first application, the main goals are limiting the sorption of food constituents (*e.g.* lipids or aroma) (Ducruet et al., 2007) in packaging materials or to prevent the leaching of substances (Courgneau et al., 2013). For the second application, it is more prospective but significant results have been recently

discovered by showing that silica beads could block beyond existing theories (Janes and Durning, 2013) in *n*-alkyl acetates in poly(methyl acrylate).

The premises used in this work originate from earlier theoretical works of (Watanabe, 1978) showing that the macroscopic concepts of diffusion and sorption could not be transposed at low scale without significant precaution. In particular, although it is well established that random walks around particles or micro-domains follow well the Smoluchowski equation (von Smoluchowski, 1906) (*i.e.* continuous approach), it is only true after sufficiently many jumps or after a time much longer than a jump itself. In the vicinity of inclusions, the reality may be different and lead to new properties. The main initial application was the description of the escaping time of radicals around traps or quenchers. The results show a well-known result in chromatography: multiplying the number of independent adsorption time increases proportionally the escape/elution time. Such coarse ideas have been generalized in the theoretical work of (Kalnin and Kotomin, 1998) on the generalization of Maxwell-Garnett equation in materials comprising inclusions. The generalization addresses the random walk or trace diffusion of substances in inhomogeneous materials crossing energy barriers as depicted in Figure 1-1. It is shown that significant energy barriers between phases are able to decrease significantly the effective diffusion coefficient regardless the organization of phases and the diffusion coefficient in the continuous phase. Additional proofs on the strong effects of the asymmetry of energy barriers on effective diffusion coefficients can be found in Karayiannis et al. (2001) and (Vitrac and Hayert, 2007b).

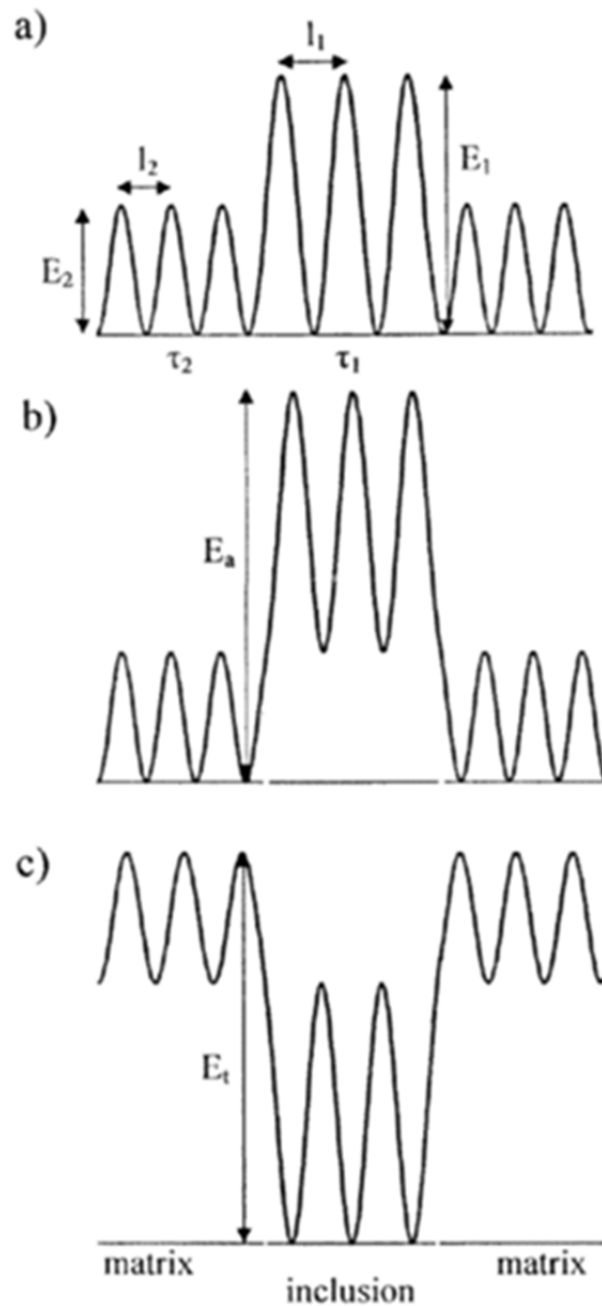


Figure 1-1 Different cases of energy barriers between the matrix and inclusions, $\{l_i\}_{i=1..2}$, $\{E_i\}_{i=1..2}$ are the hop length and the activation energy of diffusion in the inclusions $i=1$ and in the matrix $i=2$. (a) An inclusion with a diffusion coefficient in the inclusions smaller than in the matrix; there is no significant energy barrier between them. (b) An energy barrier E_a for the penetration into inclusion. (c) Partial trapping of particles inside inclusions, the “detrapping” energy is E_t . After Figure 2 of Kalnin and Kotomin (1998).

The thesis explored these phenomena by molecular modeling/simulation and from an experimental point of view. Experiments were used at two stages: to supply reference transport or thermodynamic data to validate calculation methods and theories but also to provide proofs of the concept of diffusion reduction/blocking on real systems. As

recommended in such engineering problems (Xiao et al., 2010), calculations and theories provided support and methods to detect non-conventional effects with particles and means to optimize them by a proper choice of systems and thermodynamic conditions. From previous considerations and because trapping can have both an enthalpic (*i.e.* energetic barrier) or an entropic (*i.e.* correlations) origin, the general approach should be seen as combination of concepts from chromatography and diffusion in amorphous polymers. The document is organized consequently as follows. Section two reviews available theories of diffusion in amorphous polymers and their recent evolutions for systems containing inclusions or not. Emerging concepts for extending free-volume theories of diffusion or to trap reversibly or not organic solutes are particularly illustrated. Section three details the objectives followed and the corresponding experimental or computational strategies. The choices of systems are justified as a balance between feasibility and cognitive needs. The main materials and methods are detailed in section four. Results are presented in section five as independent studies corresponding to the three majors of the thesis: i) to understand enough diffusion in amorphous polymers to detect adsorbent effects, ii) to estimate the energetic barrier on commercially available nano-adsorbents, iii) to probe the concepts on real systems and assessing the remaining distance of progress. Finally the findings are summarized in section six and the concepts are challenged based on the recent results of (Janes and Durning, 2013).

Chapter 2. Literature review

In mass transfer, the concept of barrier materials is a somewhat contentious concept, which has been interpreted differently in different contexts. The notion of barrier is very often related to the macroscopic idea of low permeability (Hansen, 2007), which implies that the reservoir of substance to block is located outside the material. The practical consequence is that the substance needs both i) to be absorbed in the material before diffusing inside and ii) to diffuse along a significantly long period of time so that a steady concentration profile (linear if the diffusion coefficient is uniform) is obtained. Many data have been published for gases (Stern and Fried, 2007) and lead to several prediction attempts. One of this model has been coined by its author Salame (1986) as “Permachor” which has been proposed to extrapolate the permeability of any simple gas in any arbitrary polymer from its permeability in reference polymer at the same temperature (see page 676 in van Krevelen and te Nijenhuis (2009)). In simple words, the approach argues that the relative permeability between two rubber polymers should be independent of the considered substance. Is it true for larger substances? The behavior of a new polymer could be predicted from its barrier performance to one single gas (e.g. helium, oxygen)? As some authors suggest that the approach could also work for large organic substances (Prasad and Brown, 1995), the approach might be highly attractive. But as quoted by van Krevelen page 557 (van Krevelen, 2012), the approach is mainly correlative and does not provides any recommendation to lower the permeability of any new polymer (e.g. composite, semi-crystalline,...) except that permeability decreases as the ratio of cohesive energy density and fractional free volume in the polymer.

Is it possible to transpose similar ideas when the substance is already inside the material as part of its initial composition or if the substance diffuses so slowly that it did not reach opposite side? The answer is no as solubilization and diffusion are closely intricate within the permeability concept. Similarly, the barrier properties of polymer materials are assessed usually with respect to their barrier performances to gas (e.g. oxygen and water vapor). Naive considerations will suggest that a material that is barrier to gas is also a good barrier to larger molecules such as organic substances. This is however only true when the substance does not plasticize the material by contributing to an excess of free volumes. Is the opposite true? That is, do we need a good barrier to gas to limit the diffusion or permeation of larger molecules? If the material is already barrier for one substance, will it be also a good material for a substance with approximately the same specific volume but with different chemical structure and shape? These raised questions do not provide simple answers. Instead of looking for analytical equations, i.e. quantitative relationships, to describe a complicate reality, an alternative could be to use a molecular or theoretical representation of the “barrier effect” as suggested by Goddard Iii et al. (2001) and Kontogeorgis and Folas (2009).

This section reviews extensively the two main topics necessary to understand how energy barriers could be used to modulate effective diffusion coefficients in solid polymers. At first sight, the suggested idea should violate the common belief that sorption and diffusion are macroscopically independent properties. Without prejudging the origin of a possible coupling at microscopic scale, section 2.1 explores theories, data and models of diffusion of organic solutes in rubber polymers from solid to molten states. The expected outcome is a general representation of diffusion and models, which could be used to detect non-standard effects, such as those involving interactions with nano-particles. In particular, it is *a priori* thought that they could be related as specific deviations when a solute or temperature is changed. The concepts of barrier materials are clarified in section 2.2 by considering that a “good barrier” material is a material, which prevents permeation, sorption and desorption phenomena. With this respect, the claimed barrier performance of composite systems, nano or not, are compared with their real ability to reduce robustly diffusion coefficients. The strategies to gain additional selectivity in the blocking of substances are also presented.

2.1 Diffusion in food packaging materials

Article: Predicting diffusion coefficients of chemicals in and through packaging materials

Authors: X. Fang, O. Vitrac

Submitted to: Critical Reviews in Food Science and Nutrition

Predicting diffusion coefficients of chemicals in and through packaging materials

Xiaoyi Fang^{1,2}, Olivier Vitrac^{2,1*}

¹AgroParisTech, UMR 1145 Ingénierie Procédés Aliments, F-91300 Massy, France

²INRA, UMR 1145 Ingénierie Procédés Aliments, F-91300 Massy, France

*E-mail: Olivier.vitrac@agroparistech.fr, Tel.: +33(0)169935063

Predicting diffusion coefficients of chemicals in and through packaging materials

2.1.1 Abstract

Most of the physicochemical properties in polymers such as activity and partition coefficients, diffusion coefficients and their activation with temperature are accessible to direct calculations from first principles. Such predictions are particularly relevant for food packaging as they can be used (1) to demonstrate the compliance or safety of numerous polymer materials and of their constitutive substances (*e.g.* additives, residues...), when they are used: as containers, coatings, sealants, gaskets, printing inks, etc. (2) or to predict the indirect contamination of food by pollutants (*e.g.* from recycled polymers, storage ambiance...) (3) or to assess the plasticization of materials in contact by food constituents (*e.g.* fat matter, aroma...). This review article summarizes the classical and last mechanistic descriptions of diffusion in polymers and discusses the reliability of semi-empirical approaches used for compliance testing both in EU and US. It is concluded that simulation of diffusion in or through polymers is not limited to worst-case assumptions but could also be applied to real cases for risk assessment, designing packaging with low leaching risk or to synthesize plastic additives with low diffusion rates.

Keywords: diffusion, packaging, mathematical modeling, molecular modeling, migration

2.1.2 Introduction

The evolution of our urban lifestyles (takeout food, portioned packaging food, ready-to-eat food or microwaved food...) inevitably leads to a lot of concerns not only of sustainability impacts of packaging (Lewis *et al.*, 2010) but also of packaging food safety involving an increase of the surface area of the materials in contact with food and consequently to a repeated exposure to chemical substances leached by these materials (Delmaar *et al.*, 2005; van Leeuwen and Vermeire, 2007; Halden, 2010). Even if food contact materials are not the only source of exposure, such a chronic exposure starts from the first stages of life: during fetal life with the food ingested by the mother (Ranjit *et al.*, 2010) and baby foods (Muncke, 2011). The exposure related to ubiquitous substances (*i.e.* highly frequent in food) depends on the considered substance or family, its frequency of occurrence, the time and temperature of contact between the food and its packaging (Vitrac and Hayert, 2005, 2007a; Vitrac and Leblanc, 2007; Poças *et al.*, 2010) and in a less extent additional physicochemical factors such as pH and ozone content, which were found significant for the migration of bisphenol A (Mercea, 2009). Calculation methods for assessing consumer exposure of chemicals from

packaging materials have been reviewed by Poças and Hogg (2007). They attract nowadays more and more attention due to the high concern for the contamination of packaged food product by endocrine disruptors (Vandenberg *et al.*, 2009; Wagner and Oehlmann, 2009; Tacker, 2011; Batra, 2011; du Yeon *et al.*, 2012) or cocktail of substances (Muncke, 2009; Zeliger, 2011). As a result, packaging materials are involved in strong scientific controversies propagated by evocative titles or editorials in both magazine and scientific literature such as: "How dangerous is Plastic" in Time Magazine of April 12, 2010 (Walsh, 2010); "...the drinking water left in a hot car can cause breast cancer" in Nature Reviews Endocrinology of May, 2010 (Heath, 2010). Two controversies have found large echoes in the scientific literature: the contamination of drinking water stored in polyethylene terephthalate bottles (Bach *et al.*, 2012) and the role of packaging on the exposure to bisphenol A (Vandenberg *et al.*, 2009; Goetz *et al.*, 2010; Sharpe, 2010; Siva, 2012). Without necessarily similar audience, many surveys tend to incriminate almost all available materials in the market including: plastics (Wittassek and Angerer, 2008; Felix *et al.*, 2008; Guart *et al.*, 2011; Bach *et al.*, 2012; Kappenstein *et al.*, 2012), can coatings (Poole *et al.*, 2004), paper and board (D'Hollander *et al.*, 2010; Vollmer *et al.*, 2011). These experimental studies are macroscopic and usually neglect the physicochemical details and the conditions, where the amounts transferred to the food are significant. Such phenomena have been reviewed by Lau and Wong (2000), Piringer and Baner (2000, 2008), Helmroth *et al.* (2002a), Arvanitoyannis and Bosnea (2004), Poças *et al.* (2008). They all conclude on the key role of diffusion and its activation on migration of organic substances (*e.g.* additives, polymer residues) and mineral substances (*e.g.* catalyst residues) (Fordham *et al.*, 1995; Kawamura *et al.*, 2009; Welle and Franz, 2010; Haldimann *et al.*, 2012). Diffusion mechanisms in solid polymers have been discussed in several reference textbooks (Mehrer, 2010; Neogi, 1996; Stastna and De Kee, 1995; Vieth, 1991) and reviews. They tend however to focus either on the diffusion of gas molecules in polymers (Alexander Stern, 1994; Klopffer and Flaconnèche, 2001) or large molecules in gels (Masaro and Zhu, 1999). Hence, there is a general opinion according to: diffusion coefficients of additive-like molecules could not be predicted accurately (page 156 of Cussler (2009)) or related to the chemical structures of the diffusants (page 135 of Piringer and Baner (2008)). The practical consequence is that migration modeling concepts used to check the compliance of food contact materials or for evaluating consumer exposure to packaging substances rely on models (Helmroth *et al.*, 2002a; Begley *et al.*, 2005) disconnected from the progress gained in the field of Polymer Science or more broadly in Chemical Engineering over the last decade. The question is all the more relevant than it could be expected that the same science might be used to design low migration materials assemblies and to assess the safety of

materials (Vitrac and Hayert, 2007a; Nguyen *et al.*, 2013). For complementary properties, such as partition coefficients (Tehrany and Desobry, 2004) and their activation with temperature, it has been demonstrated that both molecular dynamics (Hess *et al.*, 2008; Hess and van der Vegt, 2008; Özal *et al.*, 2008; Boulougouris, 2010, 2011; De Angelis *et al.*, 2010) and advanced molecular simulation techniques (Gillet *et al.*, 2009a, 2010; Vitrac and Gillet, 2010) enable tailored and accurate estimations of partition coefficients of additive and polymer residues in rubber and glassy polymers (Lipscomb, 1990) without requiring any fitting procedure or experimental data. Similar trends have been obtained for diffusion coefficients, by simulating hundreds of configurations with coarse-grained molecular dynamics (Durand *et al.*, 2010) and by bridging free-volume theories for small and rigid solutes with the theory of flexible solutes in solid polymers (Fang *et al.*, 2013).

This review aims at filling the gap between disciplines to encourage a more critical use of physical models of diffusion rather than empirical approaches to extend the applications where migration modeling can be used for decision making (Brandsch *et al.*, 2002; Arvanitoyannis and Bosnea, 2004; Vergnaud and Rosca, 2006; Vitrac and Hayert, 2007a ; Gillet *et al.*, 2009b). Such contributions could be also thought to be used to assess consumer exposure to arbitrary substances whatever the availability of contamination data and to develop safe materials. In particular, the concepts of homologies which enable to extrapolate the diffusion coefficient of from one molecule to a close one or from a polymer to another one are detailed in depth beyond early attempts by Reynier *et al.* (2001a), Reynier *et al.* (2001b) and Vitrac *et al.* (2006).

2.1.3 The concepts of “generally recognized diffusion models” in legal US and EU systems

US and EU manage the risk of contamination of food by packaging substances by two closely related concepts but with different application modalities: “food contact substance notifications” under the US law and “inert food contact materials” principles in EU regulations.

According to US law, only the regulatory status of the components of a food contact material is tested and not the whole material itself. Under section 409(h)(2)(C) of the Federal Food, Drug, and Cosmetic Act (CFR, 2011) , a “food contact substance” is defined as a special (*i.e.*, indirect (Till *et al.*, 1987)) food additive “intended for use as a component of materials used in manufacturing, packing, packaging, transporting, or holding food if such use is not intended to have any technical effect in such food”. Coatings, plastics, paper, adhesives, as well as colorants, antimicrobials and antioxidants found in packaging fall into this category (Shanklin

and Sánchez, 2005). Any substance, which was not generally considered as safe (GRAS) in food (CFR, 2012a) or in food packaging (CFR, 2012b) and not subjected to any Threshold of Regulation Exemption (CFR, 2012c; Munro *et al.*, 2002), must be listed in the inventory of effective food contact substance (FDA, 2012b), which includes 952 substances at the beginning of 2013 or listed in the CFR parts 174-181. If the substance does not fulfill any of the previous criteria because the substance is not listed and must be used for a different intended use, a notification must be submitted. The notification stepwise process (FDA, 2012a) authorizes diffusion modeling as a substitute of experimental migration testing or to extrapolate the data at a different temperature as soon as a “predictable migration-time behavior (*e.g.* Fickian diffusion)” has been established. An example cited: “migration for two hours of retorting at 121°C can be estimated and added to migration after 238 hours at 40°C”. Without citing it, the reasoning assumes several properties or approximations. Firstly, that the transferred amount is invariant with the product Dt or \sqrt{Dt} (see Eq. 4.18 of Crank’s book (Crank, 1979) and section 2.1.4.1.4), where D is the diffusion coefficient and t is contact time. Secondly, it assumes an Arrhenius behavior over the whole range of temperature between 40°C and 121°C with activation energy of *ca.* 60 kJ·mol⁻¹ ($\approx 8.31 \times 10^{-3} \ln(238/2) / (\frac{1}{273+40} - \frac{1}{273+121})$). Is it true for every polymer? Even if the glass transition temperature is crossed? Even if the material is closer to its melting point/flow threshold than its glass transition temperature? For any migrant regardless its size, geometry and flexibility? Similar extrapolations are used in US system to assess the safety of recycled materials. In this case, surrogates are used to simulate the misuse of materials before recycling (FDA, 2006). They should include: a volatile polar organic substance, a volatile non-polar organic substance, a non-volatile polar organic substance, a non-volatile non-polar organic substance, and a heavy-metal salt. As reported in Appendix 1 of (FDA, 2006), most of the D values used in numeric challenge tests originate also from mathematical models with a goal of extrapolating D values from one molecule to a next one. The safety of packaging for irradiated foods (Paquette Kristina, 2004) and of so-called “functional barriers” (see section 2.1.4.1.4) for both food (FDA, 2006, 2007) and drug (MAPP 5015.5, 2011) applications are supported by very similar arguments.

The EU regulation system uses in a very similar fashion the concept of migration rate or diffusion rate. Article 3 of the EU framework regulation 1935/2004/EC (EC, 2004) defines a so-called “inert packaging” as “manufactured in compliance with good manufacturing practice so that, under normal or foreseeable conditions of use, they do not transfer their constituents to food in quantities which could endanger human health...”. Migration modeling

is a legal concept introduced in EU, initially via the article 14 of the Directive 72/2002/EC (EC, 2002a): “For certain types of plastics the availability of generally recognized diffusion models based on experimental data allows the estimation of the migration level of a substance under certain conditions, therefore avoiding complex, costly and time-consuming testing”. The concept has been reformulated in the Regulation 10/2011/EC: “generally recognized diffusion models based on scientific evidence that are constructed such as to overestimate real migration.” In other words, the estimation of diffusion parameters (*e.g.* diffusion coefficient, activation energies) and partitioning is assumed to be conservative and not the real values. But, How conservative are they? Is it safe to extrapolate the behavior from a small molecule to a large one? From low temperatures to higher temperatures? In EU, the results of the project SMT-CT98-7513(EC, 2002b) and published as a collective work by Begley *et al.* (2005) is usually chosen as reference (Poças *et al.*, 2008), whereas the Food and Drug administration (FDA, 2006) recommends earlier or alternative versions of these models (Baner *et al.*, 1996; Limm and Hollifield, 1996).

The sources of diffusion coefficients and activation energies are scarce and underline the needs of reliable models in absence of a generic database of diffusion coefficients. A bibliometric analysis ([ISI Web of Knowledge v5.9, Thomson Reuters, USA – on Feb 3rd, 2013]) shows that the number of specific studies of diffusion coefficients in polymers is in particularly low regarding the importance of the task (*e.g.* number of substances and polymers): it is usually thought that between 5000 and 8000 different substances would enter into the composition of food contact materials with 885 substances for the sole positive list of additives and monomers for plastics in EU (EC, 2011, 2012a, b). Since 1979, 86 articles have been published in *Macromolecules* – the first journal in Polymer Science by its number citations –with “Diffusion Coefficient” in the title (over a total of 774 with “Diffusion” in the title). The collected effort tended to be reported to less specialized journals such as *Food Additives and Contaminants*, which has reported diffusion coefficient values in 45 articles, since 1990. The concept of “generally recognized diffusion model” is even more difficult to establish. The 90th edition of *CRC Handbook of Chemistry and Physics* (Lide, 2009) reports diffusion coefficients in gases, liquids and semi-conductors but none for polymers. The *Physical Properties of Polymers Handbook* (Mark, 2007) and *The Polymer Data Handbook* (Mark, 1999) report only diffusion coefficients of gases. Only the 4th edition of the *Polymer Handbook* (Brandrup *et al.*, 1999) includes some diffusion coefficients for organic compounds but without inferring any generic rules to extrapolate to other substances and polymers.

2.1.4 Some generalities about diffusion

2.1.4.1 Mass transfer from and to food packaging materials

In most of the cases, the reality of leaching of substances by materials in contact into food cannot be observed by naked eyes. Migrating substances are indeed usually colorless, odorless and tasteless. Even with analytical methods, identifying an unknown chemical among all the food constituents is a cumbersome task (Himmelsbach *et al.*, 2009; Silva *et al.*, 2006; Simal-Gandara *et al.*, 2002). By contrast, the reverse process is easier to highlight. In the everyday life, we shall have already noticed that transparent plastic tableware and containers can be easily tainted by food pigments, or their surface properties can be affected by oily contact. For both transfer from or to food packaging materials, diffusional transport is involved.

2.1.4.1.1 Sorption of food constituent into food packaging: first observation of the reality of diffusion

A change of refraction index associated to the sorption of decane, simulating an oily contact, in polystyrene is presented in Figure 2-1 based on the observations of Morrissey and Vesely (2000) but also described by Feigenbaum *et al.*, (1991). A moving migration front separates an outer region with polystyrene swollen by decane and a dry region, where the polymer remains at glassy state ($T < T_g$ with a glass transition temperature T_g of ca. 95 °C). From a physicochemical point of view, the depicted sorption involves a complex transport mechanism combining the solute concentration gradient and the gradient of elastic stresses as detailed in (Del Nobile *et al.*, 1994; Lipscomb, 1990; Mensitieri *et al.*, 1991; Miller-Chou and Koenig, 2003).

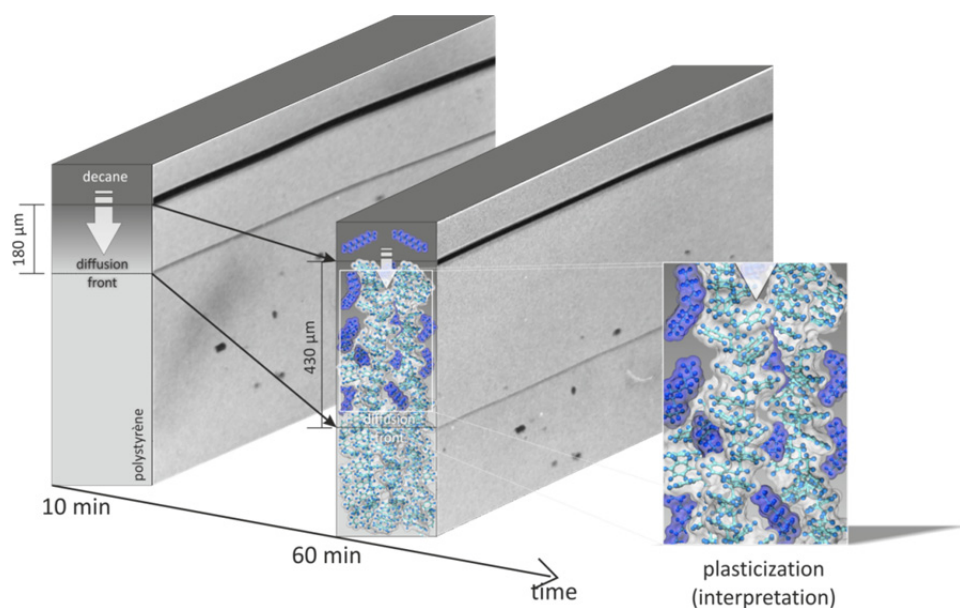


Figure 2-1 Microscopic observations in visible light and its molecular interpretation of the sorption of decane in atactic polystyrene at 70 °C (after Morrissey and Vesely (2000)).

2.1.4.1.2 Cross mass transfer in multicomponent food packaging systems

Main migrants from packaging materials reported in the literature fall into two categories (Brimer and Skaanild, 2011; Crompton, 2007; Deshpande, 2002; Rahman, 2007):

1. Intentionally added substances known as additives to aid processing or end-service (life-time, mechanical properties...), including antioxidants, antiblocking agents, antifungal agents, bactericidal agents, brighteners and whiteners, colorants, expanding agents, impact improvers, ultraviolet protective agents and ultraviolet degradation inhibitors, printing ink adhesives, gas barrier packaging oxygen scavengers, antispit agents, antistatic agents, heat and light stabilizers, melt strength improvers, plasticizers, lubricants and slip agents, pigments, fillers, mold release agents, and fungicides.
2. Polymerization residues, including monomers, oligomers (with a molecular weight of up to 200), catalysts (mainly metallic salts and organic peroxides), solvents, emulsifiers and wetting agents, raw material impurities, plant contaminants, inhibitors, decomposition and side reaction products.

Apart of plasticizers, additives are usually hindered and bulky substances with relatively low diffusion coefficients, well-known primary distribution in packaging assemblies and initial concentrations typically lower than $0.005 \text{ kg}\cdot\text{kg}^{-1}$. Liquid plasticizers (Patrick and Limited, 2005) are by contrast small and low branched molecules used in high concentration (above $0.1 \text{ kg}\cdot\text{kg}^{-1}$) with a much higher migration power. They tend to be ubiquitous not only in cling films but also in printing ink, adhesives, sealing closures, etc. Residues exhibit much broader chemical structures and migration behaviors: polymer degradation products, incomplete cross-linking reaction products, polymerization catalysts and initiators in curing reactions, processing aids such as solvents and surface agents... The occurrence of such substances and their migration routes are far less documented. According to (Deshpande, 2002), the more volatile gaseous monomers, *e.g.* ethylene, propylene, and vinyl chloride, usually decrease in concentration with time, but very low levels may persist in the finished product almost indefinitely. Styrene and acrylonitrile residues are generally the most difficult to remove.

Typical migrants with molecular weight ranging from 100 to $2300 \text{ g}\cdot\text{mol}^{-1}$ are listed in Table 2-1. As detailed in Nguyen *et al.* (2013), recent crises such as those involving printing ink residues arose from an insufficient description and understanding of diffusional transport along the packaging and recycling supply chain. Ink components can be redistributed during

the storage of films before contact (Nguyen *et al.*, 2013) or be present in recycled paper and board fibers and permeate across the primary packaging and contact layers (Biedermann *et al.*, 2011). In simple words, the list of possible contaminants is neither limited to the components of the layer in contact nor to the primary packaging.

Possible migrants which are not in contact with food need to diffuse before contaminating the food. More generally, diffusion is the limiting mechanism as soon as the concentration profile in the any layer (in direct contact or not with food) is not uniform. The identified sources and routes of all transfers are reported in Table 2-2; possible couplings due to cross-transfer are sketched in Figure 2-2 in agreement with the more general discussion found in Vergnaud and Rosca, (2006). Activation of desorption of packaging constituents into food due to plasticization of the contact layer by food constituents (see Figure 2-1) is poorly described the literature and very often referred as “oil extraction” (Helmroth *et al.*, 2002b; Riquet *et al.*, 1998). It is, however, underlined that not only triacylglycerols but many hydrophobic food constituents such as the aroma can also be absorbed in layers in contact (Ducruet *et al.*, 2007).

Table 2-1 List of typical potential substances existing in different materials for food contact purpose.

	<i>Migrants</i>			<i>Source materials (state at ambient temperature 25°C)</i>	<i>In contact with</i>	<i>Refs</i>
	<i>Technical class</i>	<i>Chemical class</i>	<i>M (g · mol⁻¹) & chemical structure</i>			
<i>Additives</i>	Antioxidants	Hindered phenols, Phosphites,	200- 1200/BA	Glassy thermoplastics : PS, PA, PVC, PLA Rubbery thermoplastics : PE, PP	Food and other plastic layer	(Dopico-Garcia <i>et al.</i> , 2003), (Jamshidian <i>et al.</i> , 2012),
	UV stabilizers/UV absorbers	-Benzophenones, Oxanilides, Benzotriazoles -Activated charcoal	200- 2300/LA	- Glassy thermoplastics : PA, PVC, PC -Glassy thermoplastics: PET		(Nerin <i>et al.</i> , 2003b)
	Heat stabilizers	Calcium/zinc stearate or laurate Organotin compounds Tris(nonylphenyl) phosphite Polycarbodiimide	N/A	Glassy thermoplastics: PVC Glassy thermoplastics: PLA		(Adams <i>et al.</i> , 2011) (Al-Malack, 2001) (Yang <i>et al.</i> , 2008a)
	Plasticizers	Phthalic acid esters Epoxidised soybean oil Acetyl tri-n-butyl citrate Di(2-ethylhexyl)adipate Polyester of 1,2-propanediol and/or 1,3- or 1,4-butanediol 12-(Acetoxy)stearic acid 2,3-bis(acetoxy)propyl ester Poly(ethylene glycol)	200- 1000/LA/B	Plasticized thermoplastics: PVC Glassy thermoplastics: PLA		(Fierens <i>et al.</i> , 2012) (Courgneau <i>et al.</i> , 2011)
	Antistatic	N,N-bis(2-hydroxyethyl)alkyl(C8- C18) amine, Amino and quaternary ammonium compounds	<500/L	Glassy thermoplastics : PS Rubbery thermoplastics : PE Glassy thermoplastics: PVC		(Deshpande, 2002), (Metois <i>et al.</i> , 1998), (Barnes <i>et al.</i> , 2007)
	Slip additive and antiblocking agent	Erucamide, oleamide, stearamide	<600/L	Glassy thermoplastics : PS Rubbery thermoplastics : PE		(Barnes <i>et al.</i> , 2007)

				Glassy thermoplastics: PVC		
Residues	Monomers	-Ethylene -BPA -Styrene -Terephthalic acid, ethylene glycol, Bis(2-Hydroxyethyl) terephthalate -Vinyl chloride -Caprolactam -Acrylic acid, 2-ethylhexyl ester -1,4-butanediol - Alpha-methylstyrene - Perfluoromethyl perfluorovinyl ether	60-230/L/LA	-Rubbery thermoplastics :PE - Glassy thermoplastics: PC - Glassy thermoplastics: PS - Glassy thermoplastics: PET - Glassy thermoplastics: PVC - Glassy thermoplastics: PA - PAA or copolymers - PBT, PU - copolymers - fluoropolymers	Food and other plastic layer	(Hoekstra and Simoneau, 2011)
	Catalysts	Antimony trioxide, calcium acetate	N/A	Glassy thermoplastics: PET		(Fordham <i>et al.</i> , 1995) (Pandey and Kim, 2011)
	Cross-linking agents	-Isophorone diisocyanate (IPDI) trimer, -Acrylic polymer -Dicumyl peroxide, triallyl isocyanurate	<800/B	-Rubbery thermoplastics: PEP -Glassy thermoplastics: PVC, PLA		(Jiang <i>et al.</i> , 2009) (Yang <i>et al.</i> , 2008b)
	Processing aids (solvent/surface agents)	- <i>n</i> -alkylbenzenes (<i>n</i> =10..13) -Acrylic polymer	210~340/LA	-Printing inks, lacquers, adhesives -PVC		(Aurela <i>et al.</i> , 2001), (Forrest, 2007)
	Photoinitiators	2-isopropyl thioxanthone 2-ethylhexyl-4-dimethylaminobenzoate 1,3,5-Tris(4-benzoylphenyl) benzene	200~300/BA	Printing inks and lacquers Oxygen scavenging polymer		(Sanches-Silva <i>et al.</i> , 2009), (Forrest, 2007)
	From can coatings	Bisphenol A diglycidyl ether	340/A	Thermoset polymer: epoxy resin, vinylic organosols		(Vera <i>et al.</i> , 2011), (Forrest, 2007)

	From paper and cardboard	Perfluorinated surfactants Mineral oil	<1000	Paper, cardboard		(Trier <i>et al.</i> , 2011)
NIAS	Reaction products	Polymer degradation products	2,2'-Azobis(2-methylpropionitrile), bis(p-methylbenzylidene)sorbitol, tetramethyl butanedinitrile and its hydrolyze acid, 4-methylbenzaldehyde, BADGE	100-400/BA/L	Rubbery thermoplastics: PP Thermoset polymer: epoxy resin, vinylic organosols	(Hakkarainen, 2008)
		Additive degradation products	2,2,6,6-Tetramethylpiperidine, 2,2'-[(3,3'-dichloro[1,1'-biphenyl]-4,4'-diyl)bis(2,1-diazenediyl)]bis[N-(2,5-dimethoxyphenyl)-3-oxo-butanamide	100-200/B	Rubbery thermoplastics	(Alin and Hakkarainen, 2011), (Marqué <i>et al.</i> , 1996), (Gryn'ova <i>et al.</i> , 2012), (Noguerol-Cal <i>et al.</i> , 2010), (Az <i>et al.</i> , 1991)
	Contaminations from recycled materials	Mineral oils (saturated and aromatic hydrocarbons (< <i>n</i> -C28)) BPA, BPF, BADGE, BFDGE	<800/LA	Paper and cardboard	(Vollmer <i>et al.</i> , 2011), (Biedermann <i>et al.</i> , 2013), (Perez-Palacios <i>et al.</i> , 2012)	
		- Volatile, aroma and flavor compounds (limonene, isopropylester of myristic and palmitic acids) -Degradation and secondary reaction products(acetaldehydes, oligomers and diethyleneglicol)	<500/L	Recycled PET, HDPE, PP, PC	(Camacho and Karlsson, 2000), (Nerin <i>et al.</i> , 2003a), (Pennarun <i>et al.</i> , 2004b), (Romao <i>et al.</i> , 2009), (Dutra <i>et al.</i> , 2011)	
Contaminations from adhesives	1,6-dioxacyclododecane-7,12-dione and 1,4,7-trioxacyclotridecane-8,13-dione, Aromatic amines	90-200/BA	Thermoset polymer: PU, CA, Hotmelts	Plastic layer	(Felix <i>et al.</i> , 2012), (Pezo <i>et al.</i> , 2012), (Vera <i>et al.</i> , 2011)	

<i>Active substances</i>	antimicrobials, ethylene oxidation or oxygen scavenging materials	Antimicrobials (caffeine, thymol and carvacrol, citral), Peptides, enzymes, antioxidants (butylated hydroxyanisole (BHA), butylated hydroxytoluene (BHT), propyl gallate (PG), and tert-butylhydroquinone (TBHQ)),	N/A	Glassy thermoplastics: PET, EVOH Rubbery thermoplastics: PP, PE	Food	(Aznar <i>et al.</i> , 2012), (Granda-Restrepo <i>et al.</i> , 2009), (Guillard <i>et al.</i> , 2010), (Peltzer <i>et al.</i> , 2009), (Nichols, 2004), (Buonocore <i>et al.</i> , 2003), (Han, 2003)
<i>Nanocomposites</i>	Nanoreinforcements, antimicrobial nanocomposites, oxygen scavenging nanocomposites, nanoscale enzyme immobilization systems	Clay and silicates, cellulose-based nanoreinforcements, carbon nanotubes, silica, starch nanocrystals, chitin/chitosan nanoparticles, silver, titanium dioxide	N/A	Glassy thermoplastics: PET, PLA, Polyolefin Rubbery thermoplastics: PCL	Food and other plastic layer	(Azeredo, 2009), (Busolo and Lagaron, 2012), (Llorens <i>et al.</i> , 2012), (Solovyov and Goldman, 2007), (Neethirajan and Jayas, 2011), (Smirnova <i>et al.</i> , 2012), (von Goetz <i>et al.</i> , 2013)

Note: BPA: Bisphenol A, BPF: bisphenol F. BADGE: bisphenol A diglycidyl ether, BFDGE: bisphenol F diglycidyl ether. PE: polyethylene, PP: polypropylene, PS: polystyrene, PVC: polyvinyl chloride, PET: polyethylene terephthalate, PC: polycarbonate, PA: polyamide. PEP: polyester-polyurethane, PBT: polybutylene terephthalate, PU: polyurethane. PCL: polycaprolactone. PLA: polylactic acid, EVOH: ethylene-vinyl alcohol copolymer, CA: cyanoacrylate.

L: linear migrants, B: branched migrants, A: aromatic migrants. LA: linear aromatic migrants, BA: branched aromatic migrants.

Table 2-2 Main contamination routes of food by materials in direct or indirect contact

Contamination modes	Description	Examples	Refs
With direct contact with food	Direct contact with the food during packaging, filling, storage, use (i.e. vacuum heating, microwave heating)	Monolayer materials	Goulas <i>et al.</i> (2002), Caner <i>et al.</i> (2004), Berlinet <i>et al.</i> (2008)
Through of layer in contact with food	The substance must pass through one or more materials before coming into contact with the food	Multilayer materials, label, varnishes, decors	Trier <i>et al.</i> (2010), Simal-Gandara <i>et al.</i> (2000), Roduit <i>et al.</i> (2005), Miltz <i>et al.</i> (1997), Marque <i>et al.</i> (1998), Dole <i>et al.</i> (2006a), Feigenbaum <i>et al.</i> (2005)
Contamination of layer in contact with food before conditioning	Putting in contact the inner and outer faces of the packaging (set off phenomenon)	Films rolled, packaging or packaging components stored in stack...	Page and Lacroix (1992), Jung <i>et al.</i> (2010)
Without contact	Contamination via headspace or gas permeation	Ink solvents, flavors, off-flavors, contaminants coming from secondary packaging...	Freire <i>et al.</i> (1998), Sadler <i>et al.</i> (1996), Alin and Hakkarainen (2012), Cao and Corriveau (2008), Tehrany and Desobry (2004), Lorenzini <i>et al.</i> (2010), Nerin <i>et al.</i> (2009), Battelli <i>et al.</i> (2011), Anderson and Castle (2003), Pastorelli <i>et al.</i> (2008), (Linssen <i>et al.</i> , 1998)

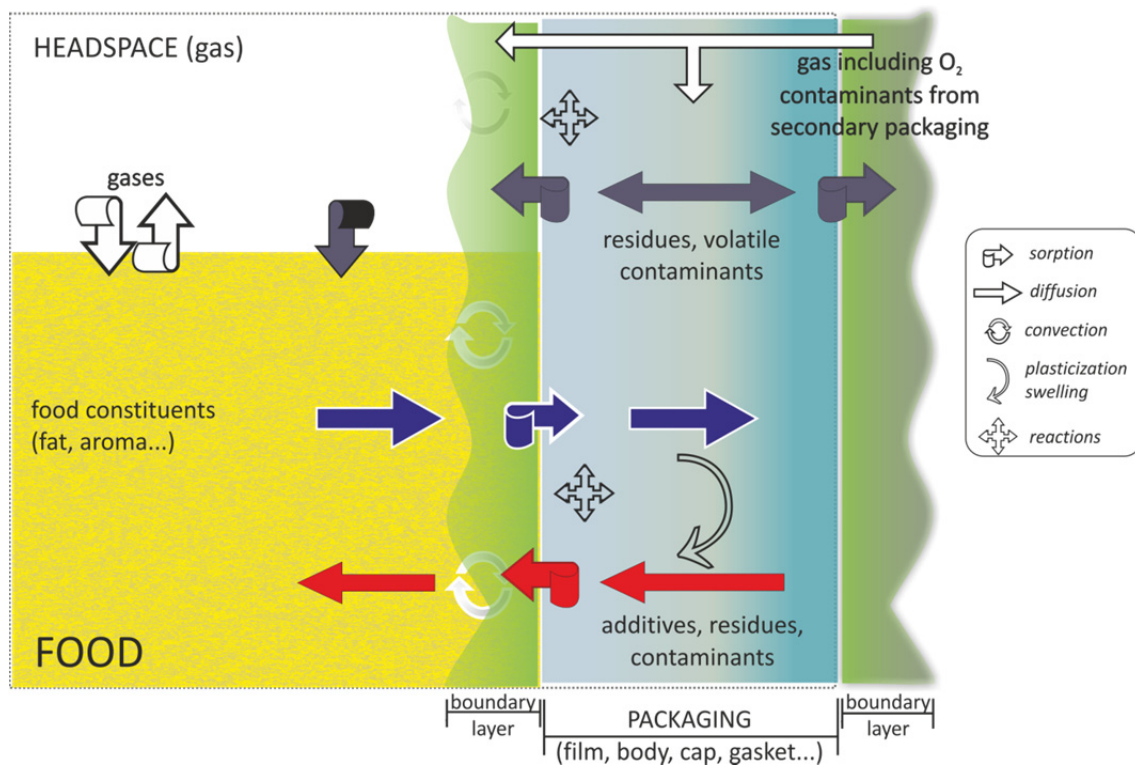


Figure 2-2 Main mass transfer from, to and cross packaging materials (after Rahman (2007), Vitrac and Hayert (2007a)).

2.1.4.1.3 Mass transfer controlled by diffusion in the packaging materials

As reviewed by Wijmans and Baker (1995) “The solution-diffusion model has emerged over the past 20 years as the most widely accepted explanation of transport” in membrane separation and more generally across dense polymers. This model must not be confused with other models, such as the “pore-flow model”, in which migrants are transferred by “pressure-driven convective flow through tiny pores”. This last model applies, for example, for papers and boards but not for plastics and thermosets.

For plastics, the generalization solution-diffusion model is also well accepted for multilayers and multi-materials as justified in Poças *et al.*, (2008); Roduit *et al.*, (2005); Tosa *et al.*, (2008) and in Nguyen *et al.*, (2013); Vitrac and Hayert, (2007a), respectively. For each packaging component, diffusion is controlled by a diffusion coefficient D (S.I. unit $\text{m}^2 \cdot \text{s}^{-1}$). The main assumptions are summarized in Figure 2-3. Between the food and the layer in contact and between packaging components, a partitioning coefficient, as reviewed by Tehrani and Desobry, (2004), controls the distribution of migrants between materials. On food side, mass diffusion combined with advection may also occur. Mass transfer resistances on the food side have been reported both in liquids (Goujot and Vitrac, 2013; Vitrac and Hayert, 2006; Vitrac *et al.*, 2007) and in “solid” food such as meat (Sanches Silva *et al.*, 2010; Sanches Silva *et al.*, 2007) and cheese (Cruz *et al.*, 2008). Concentration profiles of

several chemicals in different food products have been reported during the EU project “Migrosure” (Franz and Simoneau, 2008). The corresponding mathematical modeling of mass transfer through the packaging and food has been formulated almost in its modern form by Reid *et al.*, (1980) and reformulated with several simplifications in several reviews (Helmroth *et al.*, 2002a; Lau and Wong, 2000; Poças *et al.*, 2008) and in more general terms by Rahman (2007) (see Table 40.2). They all acknowledge that the profiles and kinetics fit within the general diffusional and boundary equations discussed earlier by Crank (1979). In the field of food contact materials, the first mathematic models have been described by Reid *et al.* (1980) and subsequently by Chatwin and Katan (1989). The authors showed in particular that the migration process could be satisfactory simplified as a one-dimensional mass transfer problem from a contact material, with a total thickness l_p , to a food system, with a finite volume, denoted V_f . The key features are: i) to keep the real contact surface area, A , between the material and the food and consequently the same dilution ratio Al_p/V_f ; and ii) to reproduce the difference in solute chemical affinity between the food and the plastic in contact with a proper choice of the partition coefficient, $K_{F/P}$. Without increasing significantly the mathematical complexity, a boundary layer approximation can be used to account for the existence of an additional mass transfer resistance on the food side governed by a mass transfer coefficient, h with SI units in $\text{m}\cdot\text{s}^{-1}$ (Reid *et al.*, 1980; Vergnaud, 1998; Vitrac and Hayert, 2005, 2006; Goujot and Vitrac, 2013). Experimental values have been tabulated by (Vitrac *et al.*, 2007) and can be incorporated within a dimensionless mass Biot number: $Bi=hl_p/D$. In the simplest case of monolayer materials with constant and uniform properties, the set of transport and conservation equations corresponding to Figure 2-3 is given by:

$$\left\{ \begin{array}{l} \frac{\partial c_{(x,t)}}{\partial t} = D \frac{\partial^2 c_{(x,t)}}{\partial x^2} \\ j_{|x=l_p}^{(t)} = -D \frac{\partial c}{\partial x} \Big|_{x=l_p}^{(t)} = h \left(K_{F/P} c_{(x=l_p,t)} - c_F \right); \quad \frac{\partial c}{\partial x} \Big|_{j=0}^{t>0} = 0 \\ C_F^{(t)} = C_F^{(t=0)} + \frac{A}{V_F} \int_0^t j_{|x=l_p}^{(\tau)} d\tau \end{array} \right. \quad (2-1)$$

where $c_{(x,t)}$ is the local concentration in packaging layer in contact. For uniform initial concentration profiles, approximate and exact analytical solutions to the set (1) can be found in Sagiv, (2001, 2002); Vitrac and Hayert, (2006); Goujot and Vitrac, (2013). It is important to note that these references use a dimensionless form of Eq. (2-1), involving Bi , a dimensionless time or Fourier number $Fo=Dt/l_p^2$, a dilution ratio $L=Al_p/V_F$

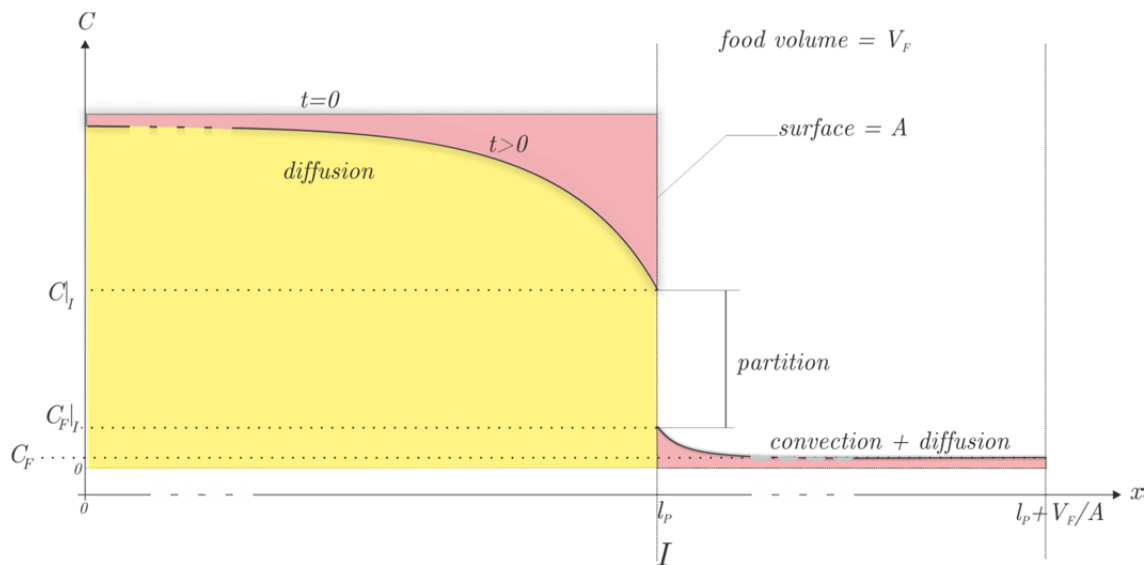


Figure 2-3 Concentration profile of migrants (e.g. additive) along the thickness of the food-packaging system as detailed in Vitrac and Hayert (2006). When $t=0$, migrants are assumed to be distributed homogeneously in the packaging material so that a uniform concentration profile can be assumed. For $t>0$, mass balance enforces that the surface area below the concentration profile on the food side is equal to complementary surface area between the profiles at $t=0$ and $t>0$ on packaging side.

2.1.4.1.4 The concept of functional barrier

The concept of functional barrier is broadly used by the packaging community without clear definition (Widen, 1998). Article 3 of Regulation 10/2011/EC (EC, 2011) defines it as “a barrier consisting of one or more layers of any type of material which ensures that the final material or article complies with Article 3 of Regulation (EC) No 1935/2004”. In more general terms, it could be defined as a barrier layer inducing a significant delay in the permeation of migrants as reproduced in Figure 2-4. When the barrier layer consists of one single layer of thickness l_{FB} and associated with a diffusion coefficient D_{FB} , the delay is given by Eq. of 4.25 in book of Crank (1979):

$$t_{delay} = \frac{l_{FB}^2}{6D_{FB}} \quad (2-2)$$

Glass and aluminum foil are considered absolute barriers and associated to infinite lag time. Polyesters (Bayer, 2002; Pennarun *et al.*, 2004a; Pennarun *et al.*, 2004b), amorphous silicate deposits (Fei *et al.*, 2012) have been proposed as significant functional barriers. Their use including virgin PET has been more particularly suggested for preventing recycled PET to be in direct contact with food (Begley and Hollifield, 1993; Crockett and Sumar, 1996; Triantafyllou *et al.*, 2002; Feigenbaum *et al.*, 2005; Dole *et al.*, 2006b; Cruz *et al.*, 2011).

Polymer materials combining a functional barrier has been also proposed to prevent food contamination by various contact materials, including: irradiated polymers (Sadler *et al.*, 2001), materials incorporating nanoparticles (Alfadul and Elneshwy, 2010), printed materials (Fiselier and Grob, 2012; Johns *et al.*, 2000; Piergiovanni *et al.*, 1999). The extension of transport equations (1) to materials incorporating a functional barrier is given in Laoubi and Vergnaud, (1996).

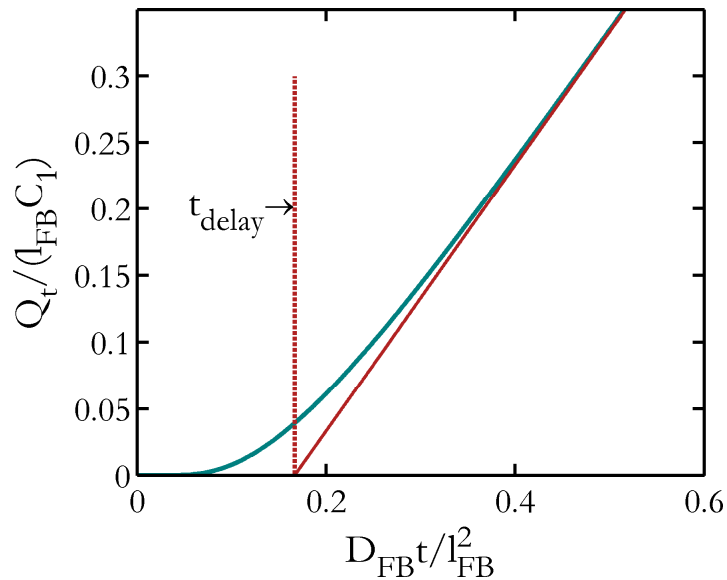


Figure 2-4 Cumulated amount of diffusant (Q_t) crossing a plane sheet of thickness, l_{FB} , with upstream concentration C_1 versus dimensionless time $D_{FB}t/l_{FB}^2$. The intercept of tangent line with $Q_t=0$ at $t_{delay}=l_{FB}^2/6D_{FB}$ gives the typical time lag to get a significant permeation across the film. (after Fig. 4.2 in book of Crank (1979))

2.1.4.2 Molecular diffusion

2.1.4.2.1 A macroscopic definition

The term “diffusion” by itself is the process by which matter is transported from one part of a system to another as a result of random molecular motions of the center-of-mass of molecules (Crank, 1979). The process may cover very different realities: bulk diffusion in gas, liquids or solids, Knudsen diffusion inside pores, surface, surface diffusion, capillary condensation, molecular sieving... (Cussler, 2009; Krishna and Wesselingh, 1997). Molecular diffusion is the general term for a mass transfer in the bulk (*i.e.* far from walls) in absence of external forces and consequently due to the sole effect of the thermal motion of all molecules and atoms. On earth, these conditions are difficult to fulfill in fluids due to some residual advection terms generated by gravity and better verified in solids (Brogioli and Vailati, 2000). Tracer diffusion and self-diffusion are the two special cases of spontaneous mixing of molecules, where diffusion occurs in absence of a significant composition gradient (or

chemical potential gradient). This type of diffusion can be followed using isotopic tracers. The tracer diffusion is usually assumed to be identical to self-diffusion (assuming no significant isotopic effect) and takes place under thermodynamical equilibrium (Masaro and Zhu, 1999). By contrast, mutual diffusion or chemical diffusion occurs in a presence of a concentration gradient or more generally in presence of a chemical potential gradient (Wesselingh and Krishna, 2006). The diffusion coefficients for these two types of diffusion processes are generally different because the diffusion coefficient for chemical diffusion is binary and it includes the effects due to the correlations between the displacements of the different diffusing species (Vignes, 1966).

The apparent paradox associated to a net mass flux along direction x , $J(x)$, in presence of a sparse gradient, is removed by noting that such a flux must be proportional to the difference between the average molar velocity of the considered molecules, u , and of the mass reference frame, u_0 , along x (Wesselingh and Krishna, 2006):

$$J(x) = c(u - u_0) = -D \left. \frac{\partial c}{\partial x} \right|_{(x)} \quad (2-3)$$

The superiority of this representation arises because it is also defined in presence of one single migrant. In this case, u and u_0 are time-averaged instead of population averaged and J is a stokesian flux (Keffer *et al.*, 2004). Although such results may look obvious to many readers, they remain a very active research area (Mu *et al.*, 2009), in particular to express u with the local properties of the polymer bulk or in presence of nanocharges, see some examples in Masaro and Zhu, (1999); Keffer *et al.*, (2004); Choudalakis and Gotsis, (2009); Arora and Padua, (2010); Mu *et al.*, (2010); Spearot *et al.*, (2012); Janes and Durning, (2013). The first concepts emerged with two papers among five that A. Einstein wrote in 1905 identified today as, “the year that changes the face of physics” (Stachel, 2005). As quoted by Einstein himself, the first “paper is a determination of the true sizes of atoms from the diffusion and viscosity of dilute solutions of neutral substances”; the second “proves that, on the assumption of the molecular [kinetic] theory of heat, bodies of the order of magnitude of 1/1000 mm, suspended in liquids, must already perform an observable random movement that is produced by thermal motion”.

2.1.4.2.2 A microscopic definition

Since the works of A. Einstein, the reality of the molecules is not a subject of debate (Psillos, 2011). The description of the random walks of migrants in polymers is exemplified in Figure 2-5 as one-dimensional mass transport. The discrete hopping mechanism but continuous in time is consistent with the kinetic Monte-Carlo simulations proposed in high dimensions by

Vitrac and Hayert (2007a) for diffusants much larger than polymer voids in polymers, such as plastic additives. Below a critical time scale, large comparatively to the vibration of atoms, diffusants appear trapped. Beyond, a sufficient reordering of the whole diffusant-polymer system enables independent displacements of the center-of-mass, denoted CM, of the diffusant. In absence of correlated displacements of CM, the motion is called Brownian (Hanggi and Marchesoni, 2005) and is controlled by the self-similar skewed trajectories. These derivations lead to express the diffusion coefficient, D , as the product of a hopping frequency, $\nu(t)$, and squared hopping length, $l(t)$, (Vitrac and Hayert, 2007a):

$$\lim_{t \rightarrow \infty} D(t) = \lim_{t \rightarrow \infty} \frac{1}{2d} l(t)^2 \nu(t) \quad (2-4)$$

where d is the number of dimensions (*i.e.* d is 3 in 3D). It is very important to note the analogy of Eq. (2-4) and Eq. (2-2) used for functional barriers ($d=3$ in this case as migrants are not confined along a line).

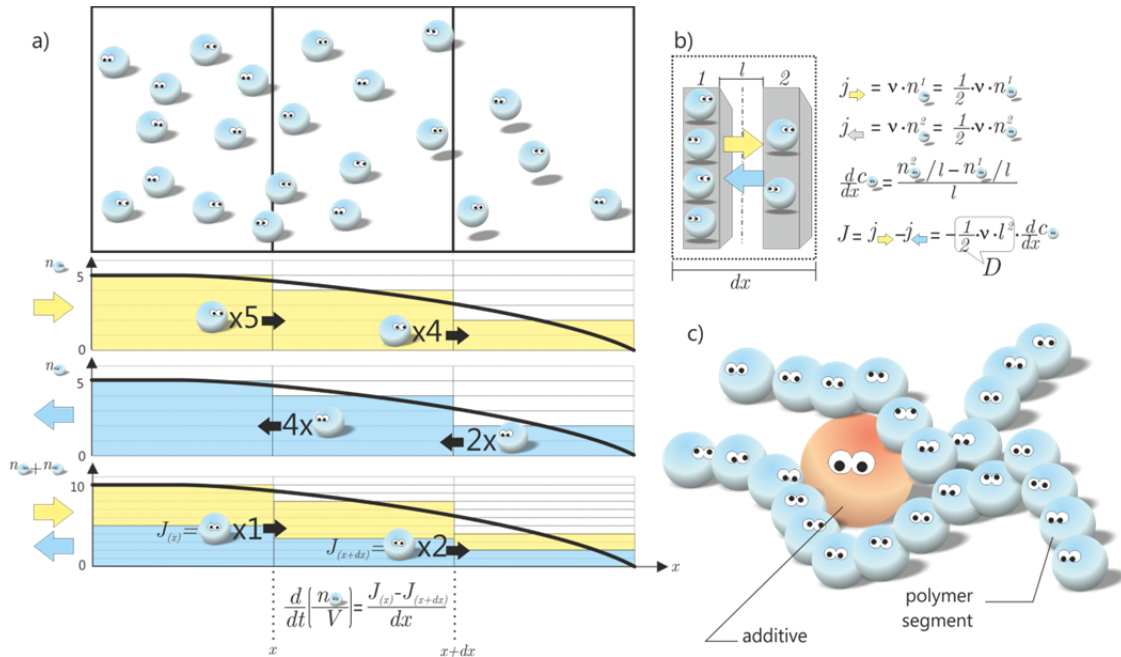


Figure 2-5 One-dimensional interpretation of molecular diffusion with “eyed” particles a) as populations in contiguous elemental volumes exchanging particles, b) as a local hopping process and c) as mutual diffusion of a bulky additive among connected polymer beads. In the real life (at macroscopic scale), the particles and the direction of jumps are indiscernible. To enable particles counting, the direction of the sight gives here the direction of the next jump. In details, situations in (a) and (b) illustrate the concepts of macroscopic and microscopic mass balance applied implicitly in second and first Fick equations, respectively.

2.1.4.2.3 Trace diffusion and random walks

On time scales longer than molecular trapping times, the results of Einstein, Smoluchowsky, Langevin and Perrin (Haw, 2002) enable to relate to the time dependence of the motions of a single additive type substance to Fickian diffusion used in system (1). Einstein turned the macroscopic diffusion problem into a probabilistic description by noting that the evolution of the spatial distribution $p(x,t)$ of a single particle can be predicted by the second equation of Fick (Einstein, 1905b):

$$\frac{\partial p(x,t)}{\partial t} = D \frac{\partial^2 p(x,t)}{\partial x^2} \text{ with } p(x,t=0) = \delta(x) \quad (2-5)$$

where $\delta(x)$ is the delta or Dirac function with $\delta(x=0)=1$ and 0 elsewhere. For an infinite one-dimensional mass transfer problem, multiplying the left hand side of Equation (5) by x^2 and integrating them by parts yields the mean-square-displacement (MSD) of the diffusant:

$$\int_{-\infty}^{+\infty} \frac{\partial p(x,t)}{\partial t} x^2 dx = \frac{\partial}{\partial t} \int_{-\infty}^{+\infty} p(x,t) x^2 dx = \frac{\partial}{\partial t} \langle x^2 \rangle \quad (2-6)$$

By noticing that $\int_{-\infty}^{+\infty} \frac{\partial}{\partial x} \left(x^2 \frac{\partial p(x,t)}{\partial x} \right) dx = \int_{-\infty}^{+\infty} \frac{\partial}{\partial x} (xp(x,t)) dx = 0$ for any odd integrand and that mass balance enforces $\int_{-\infty}^{+\infty} p(x,t) dx = 1$, a similar treatment to the right hand side of Eq. (2-5) leads to a constant:

$$\begin{aligned} \int_{-\infty}^{+\infty} \left(x^2 D \frac{\partial^2 p(x,t)}{\partial x^2} \right) dx &= D \int_{-\infty}^{+\infty} \frac{\partial}{\partial x} \left(x^2 \frac{\partial p(x,t)}{\partial x} \right) dx - D \int_{-\infty}^{+\infty} \left(\frac{\partial x^2}{\partial x} \frac{\partial p(x,t)}{\partial x} \right) dx = 0 - 2D \int_{-\infty}^{+\infty} \left(x \frac{\partial p(x,t)}{\partial x} \right) dx \\ &= -2D \left(\int_{-\infty}^{+\infty} \frac{\partial}{\partial x} (xp(x,t)) dx - \int_{-\infty}^{+\infty} p(x,t) dx \right) = 2D \end{aligned} \quad (2-7)$$

Equating (2-6) and (2-7) demonstrate that the variance of the position of a diffusant centered around of 0 will increase linearly with time as illustrated on simulations depicted in Figure 2-6. This property is used to derive diffusion coefficients in polymers from molecular dynamics simulations including $N_{diffusants}$ according to the generalized Einstein relationship (Durand *et al.*, 2010; Keffer *et al.*, 2004; Li *et al.*, 1997):

$$\begin{aligned}
D &= \frac{1}{6N_{\text{diffusants}}} \lim_{t \rightarrow \infty} \frac{d}{dt} \left\langle \sum_{i=1}^{N_{\text{diffusants}}} \left[r_i^{CM}(t) - r_i^{CM}(0) \right]^2 \right\rangle \\
&= \frac{1}{6N_{\text{diffusants}}} \lim_{t \rightarrow \infty} \frac{d}{dt} \sum_{i=1}^{N_{\text{diffusants}}} g_{CM}(t) \\
&\approx \frac{1}{6N_{\text{diffusants}}} \lim_{t \rightarrow \infty} \frac{g_{CM}(t)}{t}
\end{aligned} \tag{2-8}$$

where $r_i^{CM}(t)$ is the position of the center-of-mass of the i^{th} diffusant. The ensemble averaged operator $\langle \rangle$ is applied to all possible reference positions of CM $r_i^{CM}(0)$. According to Eq. (2-3), it is important to notice that the positions are corrected from a possible drift of the center-of-mass of the whole system.

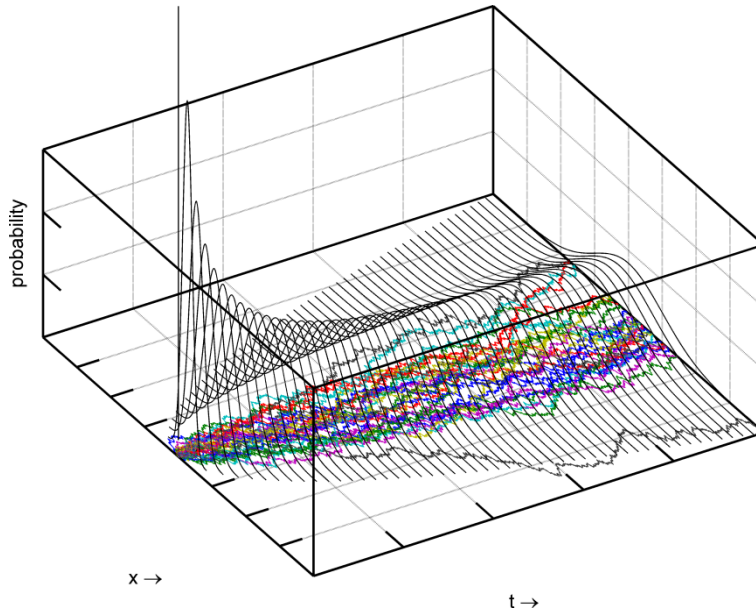


Figure 2-6 Simulation of 10 one-dimension random walks starting from a same initial position. The continuous probability Gaussian distributions associated to an infinite number of trajectories are also represented for different times.(see Eqs. (2-6) and (2-7)).

2.1.4.2.4 Mutual diffusion

When the concentration of diffusant is large (*e.g.* plasticizer or solvent), the flux of diffusant may disturb the local composition of the binary mixture which may in return affect the interactions with surrounding force. In this case, it is preferable to relate the diffusant concentration gradient $\frac{\partial c}{\partial x}$ to its corresponding chemical potential gradient $\frac{\partial \mu}{\partial x}$ (Krishna and Wesselingh, 1997). By expressing chemical potentials in polymers with volume fractions as recommended in Gillet *et al.*, (2009a, 2010) instead of molar fractions, the intuitive approach of Vignes (1966), reviewed by Hsu and Chen, (1998); Nauman and He, (2001), leads to Eqs. (2-9) and (2-10):

$$\frac{\partial \mu}{\partial x} = \frac{\partial \mu}{\partial \phi} \frac{\partial \phi}{\partial x} = RT \frac{\partial \ln(\gamma\phi)}{\partial \phi} \frac{\partial \phi}{\partial x} = \frac{RT}{c} \left[\frac{\partial \ln(\gamma)}{\partial \ln(\phi)} + 1 \right] \frac{\partial c}{\partial x} = \Gamma \frac{RT}{c} \frac{\partial c}{\partial x} \quad (2-9)$$

where γ is the diffusant activity coefficient respectively to its volume fraction ϕ . T is the absolute temperature, R is gas constant, Γ is the thermodynamic factor that controls the deviation from ideality: Γ is a thermodynamic correction factor depending strongly on the local composition and equal to 1 when the polymer-diffusant mixture is ideal, that is when the solute-polymer obeys to Henry's law. Substituting Eq. (2-9) in Eq. (2-3) gives a new definition of the net flux:

$$J(x) = -D_{MS} \frac{c}{RT} \frac{\partial \mu}{\partial x} \Big|_{(x)} = -D\Gamma^{-1} \frac{\partial c}{\partial x} \Big|_{(x)} \quad (2-10)$$

where D_{M-S} is the Maxwell-Stefan diffusivity (Curtiss and Bird, 1996; Krishna and Wesselingh, 1997). Several expressions generalizing $D = \Gamma D_{M-S}$ have been proposed for diffusant-polymer mixtures, they are all derived from Darken equation (Sunderrajan *et al.*, 1996).

As already exemplified in Fig. 2.1, the absorption or the release of substances can modify the relaxation of polymer chains. When mass transfer causes the glass transition to be crossed or approached, major deviations to a Fickian behavior (pure self-similar random walk on several time and length scales) can occur as reported experimentally in Callaghan and Pinder, (1984); Vrentas *et al.*, (1986); Saby-Dubreuil *et al.*, (2001); Dubreuil *et al.*, (2003); Mueller *et al.*, (2012). Consistent descriptions of such transports in technological contexts are proposed by Narasimhan and Peppas (1996).

2.1.4.3 Diffusion in thermoplastic and elastomers

Thermoplastics and elastomers are polymeric materials possibly compounded with additives and charges (Brydson, 1999). Their differences are very subtle: the first one flows in melts when temperature is increased and are used as fibers or containers, whereas elastomer is defined as a polymer which displays rubber-like elasticity (IUPAC, 2007) with primary uses as adhesives or sealants. From a chemical point of view, elastomers are usually polymers cross-linked during a curing step (McKeen, 2008). Such concepts are now extended via physical crosslinking to thermoplastic elastomers (Costa *et al.*, 2010) which combine segments with low glass transition temperature, denoted T_g , and with crystalline segments or rigid segments with high T_g .

Below their melting point at solid state, polymer materials consist of entangled chains, whose organization is not completely random (Crawshaw and Windle, 2003; Lakes, 1993). Fig. 2.7 exemplifies such a hierarchized in high density polyethylene at different scales of observation. The resulting broad dispersion of chain segmental motions in time and space has been investigated by molecular dynamics simulation at atomistic scale (Kotelyanskii and Theodorou, 2004) and coarse-grained scale gathering one or several monomers in one single bead or blob (Vettorel *et al.*, 2007). It usually considered that diffusion in semi-crystalline polymers occurs exclusively in the amorphous phase of the polymer as reviewed by Hedenqvist and Gedde (1996) and experimentally tested by Van Alsten *et al.*, (1995). Although spherulites depicted in Figure 2-7 are argued to be impenetrable, several multi-scale simulations showed that diffusion spreads through defects in spherulites (Mattozzi *et al.*, 2006; Nilsson *et al.*, 2009) and in interphases between crystallites (Zhu *et al.*, 2001). The possible invasion of large crystalline structures by diffusants would explain the apparent homogeneity of diffusion concentration profiles in most of semi-crystalline polymers. As a result, beyond critical time and space scales, diffusion appears homogeneous in space and linear theory of diffusion with a uniform diffusion coefficient (see Eq. (2-1)) is fulfilled.

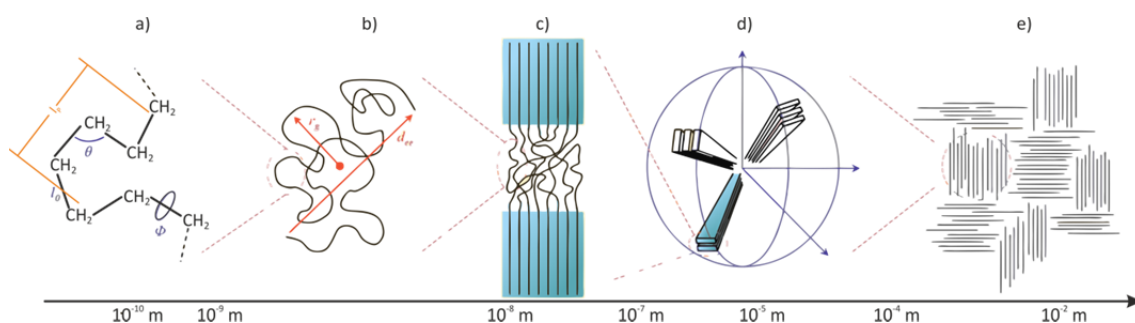


Figure 2-7 Schematic representation of multi-scales of the organization of polymer materials (e.g. polyethylene). a) chemical structure (Baschnagel *et al.*, 2004), b) intermingled chains (Baschnagel *et al.*, 2004), c) semi-crystalline structure (Queyroy and Monasse, 2012), d) polycrystalline structure (Callister and Rethwisch, 2011), e) heterogeneous materials (Muller-Plathe, 1991). l_0 : length of a C-C bond, l_p : persistence length, θ : bond angle, ϕ : torsion angle, r_g : gyration radius, d_{ee} : end-to-end distance.

According to temperature and T_g , the amplitude and frequency of segmental motions can vary in a dramatic extent between rubbery materials ($T > T_g$), with time scales between 10^{-13} s and 10^{-3} s, and glassy materials ($T < T_g$) where they reach 10^3 s and beyond (Barrat *et al.*, 2010). The different cooperative chain segmental displacements from glassy to molten state are sketched in Figure 2-8. As detailed by Baschnagel *et al.*, (2004) from simulations at different

scales and illustrated in Figure 2-14, only crankshaft motions exist below T_g and can contribute to diffusion. Above T_g , local polymer relaxations are combined with large segmental motions between entanglements and restrictions, offering large fluctuations of free volumes (see section 2.1.6). Finally, above the polymer melting point, T_m , the chain can translate along its full length.

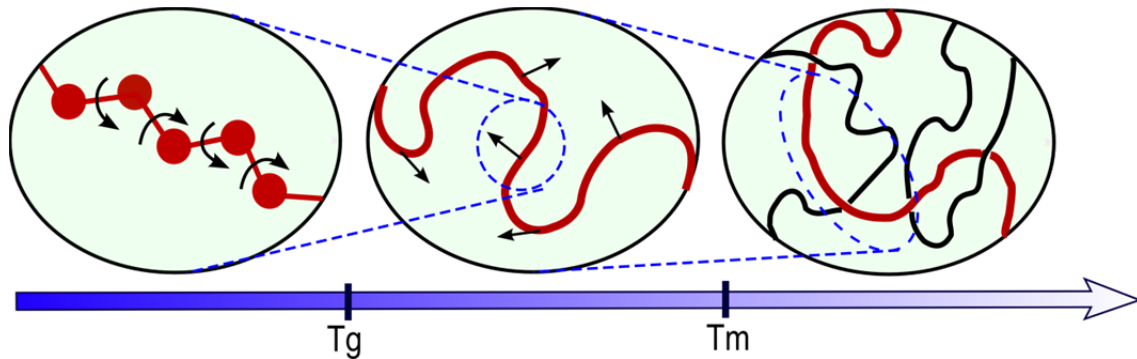


Figure 2-8 Largest polymer displacements versus temperature. T_g is the glass transition temperature, T_m is the melting temperature, (after Paul and Smith (2004)).

Higher densities in glassy materials combined with extremely low renewal rates of free volumes cause diffusion coefficients to be several lower decades in glassy polymers than in rubber ones. Figure 2-9 illustrates the scaling of D for two extreme polymers: natural rubber and glassy polyvinyl chloride (PVC), thought as likely upper and lower envelopes of diffusion coefficients met in plastics and substances with molecular weights (M) lower than $200 \text{ g}\cdot\text{mol}^{-1}$. The ratio of D in rubber to PVC increases exponentially with the volume of the diffusant (see section 2.1.6 for more details) for He ($M=4 \text{ g}\cdot\text{mol}^{-1}$), methane ($M=16 \text{ g}\cdot\text{mol}^{-1}$) and Hexane ($M=86 \text{ g}\cdot\text{mol}^{-1}$) are ca. 10, 10^4 and 10^7 respectively. The difference in translation mechanism between glassy and rubber polymers is further illustrated in Figure 2-14.

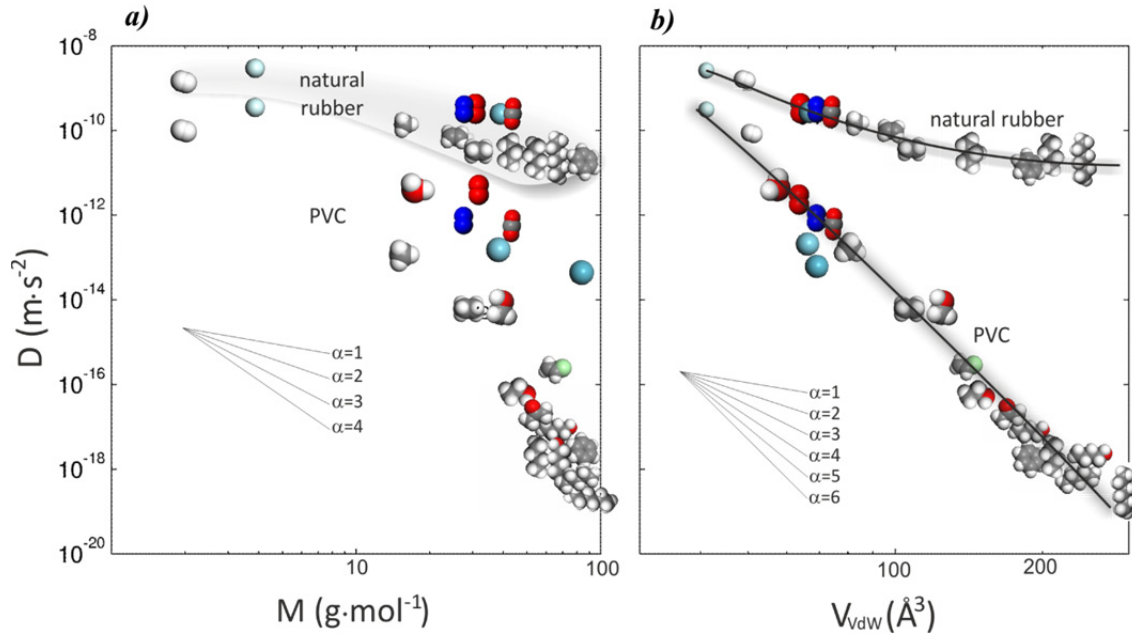


Figure 2-9 Scaling of diffusion coefficients in natural rubber and polyvinyl chloride (PVC) with a) molecular mass (M) and b) van-der-Waals volume (V_{vdw}) of diffusant (Berens, 1981).

2.1.5 Scaling laws and friction models

The molecular weight M is one of the main molecular descriptors to predict an order of magnitude of D . This section presents the main scaling laws $D \propto M^{-\alpha}$ associated to the tracer diffusion or self-diffusion in condensed phases and the polymer matrices. These scaling laws are first introduced from theoretical considerations and compared with experimental values.

2.1.5.1 Overview

2.1.5.1.1 Hydrodynamic theory of diffusion

Firstly Einstein (Einstein, 1905a, b; Einstein and Fürth, 1956) and subsequently Langevin (Langevin, 1908; Lemons and Gythiel, 1997) proposed and extended a likewise interpretation of the Brownian motion. By assuming that acceleration of contribution is short-lived, Einstein showed that the driving force, f , which Langevin showed to be random with white spectrum, should be equated by a drag force proportional to the displacement velocity of the diffusant: $\zeta_0 (u - u_0)$, with ζ_0 a molar friction coefficient. By noting that the work associated to this force is also the work to insert the diffusant in the matrix (Krishna and Wesselingh, 1997), f can be expressed in the form (see Eqs. (2-3) and (2-10)):

$$f = -\frac{\partial \mu_{(x)}}{\partial x} = \zeta_0 (u - u_0) = \zeta_0 \frac{J_{(x)}}{c_{(x)}} = -\zeta_0 \overbrace{\frac{D \Gamma^{-1}}{RT}}^{=1} \frac{\partial \mu_{(x)}}{\partial x} \quad (2-11)$$

By identification, one gets a first mechanistic description of D , known as Einstein relationship:

$$D = \Gamma \frac{RT}{\zeta_0} \quad (2-12)$$

For a spherical substance of radius R_H diffusing in a medium of viscosity η , the Stokes formula with sticks boundary conditions predicts $\zeta_0 = 6\pi\eta R_H$ (6 is replaced by 4 with a slip boundary condition instead (Kirkwood and Riseman, 1948)). For non-spherical substances, R_H is called hydrodynamic radius and its value depends not only on the shape but also mechanism of translation. For instance, for an aromatic ring of diameter R_ϕ , ζ_0 is expected to vary between $\frac{32}{3}\eta R_\phi$ and $16\eta R_\phi$ according to the ring translates edge on (likeliest) or face on (unlikely), respectively. The value averaged over all orientations is $12\eta R_\phi$ (Berg, 1993).

For a flexible substance including N similar heavy atoms or sub-units (*e.g.* methylene group in n -alkanes), so-called blobs, R_H could be thought proportional to the gyration radius $\left(\frac{1}{N} \sum_{i=1}^N (\mathbf{r}_i - \mathbf{r}_{\text{CM}})^2\right)^{1/2}$, where $\{\mathbf{r}_i\}_{i=1..N}$ and \mathbf{r}_{CM} are the position vectors of blobs and of center-of-mass (CM) respectively. The positions depend however on the conformations of the substance so that only the scaling law as: $R_H \propto N^\alpha$ can be easily derived (Yamakawa, 1971), with α depending on the diffusant flexibility. For N compact beads, one expects $\alpha \approx 1/3$ whereas, for a linear and sufficiently long molecule, $1/2$ and $3/5$ are expected in a theta (*i.e.* random coils configurations) and good solvent (*i.e.* stretched configurations), respectively (Teraoka, 2002). It is important to notice that such descriptions prevent α from exceeding a value of 1. The Kirkwood-Riseman theory (Kirkwood and Riseman, 1948) offers further insight by calculating explicitly the total friction coefficient, which simplifies for a bead-spring model as (Pastor and Karplus, 1988):

$$\zeta_t = \eta \frac{6\pi\sigma}{1 + \frac{\sigma}{N} \sum_{i,j=1..N, i \neq j} \langle (\|\mathbf{r}_i - \mathbf{r}_j\|)^{-1} \rangle} N \quad (2-13)$$

where σ is the effective radius of a blob, assumed to be all identical. $\|\mathbf{r}_i - \mathbf{r}_j\|$ is the distance between blobs.

2.1.5.1.2 Theoretical composition laws for diffusants consisting in N repeated patterns

For a linear and flexible solute consisting of N repeated patterns (also called blobs), it is relevant to express D as a scaling law with N or equivalently with M :

$$\frac{D(T)}{D_0(T)} = \left(\frac{M}{M_0} \right)^{-\alpha(T)} \quad (2-14)$$

where M_0 and D_0 are the molecular weight and diffusion coefficients of reference molecule. The values of α for typical mechanisms of diffusion are reported in Table 2-3.

When the displacements of all N blobs are homogenous in time with a growing mean-square-displacement (msd) denoted $g(t)$, the msd of the center-of-mass (CM) is inferred from the covariance of the averaged displacements of all blobs (Fang *et al.*, 2013):

$$g_{CM}(t) = \frac{1}{N^2} \left(\sum_{i=1}^N g(t) + 2 \sum_{i,j:i < j}^N C_{i,j}(t) g(t) \right) = \left(\frac{1}{N} + \frac{2}{N^2} \sum_{i,j:i < j}^N C_{i,j}(t) \right) g(t) \quad (2-15)$$

By neglecting torsional constraints, only the $N-1$ correlations between the displacements of connected blobs are significant and Eq. (2-15) becomes:

$$g_{CM}(t) = \frac{g(t)}{N} + 2 \frac{N-1}{N^2} C_{connect}^{(t)} g(t) \quad (2-16)$$

wherein $C_{connect}^{(t)}$ is the normalized correlation between the displacements of two connected blobs.

Replacing Eq. (2-16) in Eq. (2-8) leads to a definition of D close to the one proposed by Kirkwood and Riseman (1948). In the latter, D is combined to be the sum of two contributions:

- i) A composition law for N blobs equivalent to $\frac{g(t)}{N}$ in Eq. (2-16) and named after Rouse work (Prince E. Rouse, 1953), and corresponding to $\alpha=1$ in Eq. (2-14).
- ii) An additional effect due to weak interactions between blobs generalizing the Derjaguin's approximation between two spherical particles (Derjaguin, 1934).




Replacing ζ_0 in Eq. (2-12) by ζ_t defined in Eq. (2-13), one gets Eq. (2-17) for an ideal system ($I=1$) (Edwards *et al.*, 1981):

$$D = \lim_{t \rightarrow \infty} \frac{g_{CM}(t)}{6t} = D_{rouse} + D_{hydrodynamics} = \frac{RT}{N\zeta_0} + \frac{RT}{6\pi\eta} \frac{\sum_{i,j=1..N, i \neq j} \langle (\mathbf{r}_i - \mathbf{r}_j)^{-1} \rangle}{N^2} \quad (2-17)$$

The concept of hydrodynamic interactions is derived from colloidal theories (Liang *et al.*, 2007) and assume that the linear solute is a collection of colloidal particles diffusing in an incompressible solvent continuum. Such assumption is known to be well verified for polymers in melt or linear diffusants dissolved in a solvent consisting of much smaller molecules (Masaro and Zhu, 1999), but it is questionable for short migrants in interactions

with long and entangled polymer chains where renewal rates of free volumes are much slower. According to Fang *et al.* (2013), long-lived contacts tend to dominate so that the coupling between correlated displacements of blobs can be neglected (*i.e.* no effect of the square dependence) and so that α can be considered equal to unity.

Table 2-3 Scaling law and diffusion mechanisms associated with ideal mixtures ($\Gamma = 1$).

No. of blobs N	Diffusion mechanisms (diffusion regime)	ζ	$D \propto M^{-\alpha}$	α	Ref
1	Molecule consisting of a bead with radius R_H (Stokes-Einstein) in solution 	$6\pi\eta R_H$	$D = \frac{RT}{\zeta_0} \propto \frac{1}{M^{1/2}}$	1/2	(Einstein, 1905b)
$1 < N < 30$	Molecule consisting of N beads (Rouse) in solution 	$N\zeta_0$	$D = \frac{RT}{N\zeta_0} \propto \frac{1}{M}$	1	(Prince E. Rouse, 1953)
$N \gg 30$	Molecule consisting of entangled N beads, which only can translate along its contour (reptation) 	$N\zeta_0$	$D_{tube} = \frac{RT}{N\zeta_0} = \frac{l_{tube}^2}{\tau_{tube}} \propto \frac{N^2}{\tau_{tube}}$ $\tau_{tube} \propto N^3$ $D \propto \frac{R^2}{\tau_{tube}} \propto \frac{N}{N^3} = \frac{1}{N^2}$	2	(De Gennes, 1971) (Doi and Edwards, 1978)
	Reptation with constrained relaxation	N/A	N/A	> 2	(Lodge, 1999) (Bueche, 1968)

R : gyration radius, N : the number of beads in the chain, ζ_0 : the friction coefficient associated to a single bead/blob, and l_{tube} : the length of the reptation tube. τ_{tube} : the retention time in the tube

Scaling of D as $\alpha=1$ (Rouse theory) has been initially proposed in diluted solutions (Prince E. Rouse, 1953), and has been subsequently generalized to concentrated media (Ferry *et al.*, 1955). This theory is the most likely for linear solutes which are not entangled with the polymer. In practice, it is well verified for both self- (*e.g.* *n*-alkane or *n*-alcohols diffusing among other alkanes) and trace diffusion (*e.g.* *n*-alkanes in polyethylene) as soon as the static and dynamic properties of the host can be considered independent from the length of the considered diffusants. For self-diffusion, free volume effects have to be corrected (as the density of the host change with M) to get $\alpha = 1$ (Harmandaris *et al.*, 2002; Meerwall *et al.*, 1998), if not the monomeric friction coefficients, ζ_0 is found to vary with diffusant length (Rhee *et al.*, 1977; Wong *et al.*, 1970). For trace diffusion coefficients, $\alpha=1$ is found in

polyethylene melts without any subsequent correction as the density of the host is constant at constant temperature. Similar results for self and trace D have been systematically investigated by coarse-grained molecular dynamics simulation by Durand *et al.* (2010) with a generic flexible model in the temperature range, 1.3Tg and 4Tg. However, it is emphasized that α values much larger than 1 have been reported by (Kwan *et al.*, 2003; Vitrac *et al.*, 2007) in solid polymers. The breakdown of the Rouse model near T_g has been suggested by Plazek *et al.* (1993) but resisted to correct explanations since recent years.

For large molecules ($N \gg 30$), values greater than 1, ranging between 2 and 2.4 are proposed by reptation theory (Lodge, 1999), but it would be misleading to envision such mechanisms to substances with molecular masses ranging between 10^2 and 10^3 g·mol⁻¹ as their gyration radii are much smaller than the typical entanglement length of polymer segments (Fang *et al.*, 2013). Indeed, reptation mechanisms should be envisioned as a special case of Rouse relaxation where the translational displacements are enabled only along the contour of the molecule. The relaxation of Rouse model in curvilinear frame and its back projected in the laboratory reference frame has been exactly calculated by De Gennes (1971) and is known to be the main factor responsible for an increase of α from 1 to 2 for self-diffusion of polymer chains.

2.1.5.2 Experimental data of diffusion coefficients in solid polymers

Comparatively to diffusion in liquids or polymer melts, diffusion coefficients in solid polymers exhibit a broader range over several decades (Cussler, 2009; Fang *et al.*, 2013; Vitrac *et al.*, 2006), which are associated to a large spectrum of size and shape dependences, but with α values strictly larger than 1.

2.1.5.2.1 Linear substances

In solid polymers, above the glass transition temperature of the polymer but below its melting point (or threshold of flow in the amorphous polymer), it has been proposed that the deviation to Rouse theory (*i.e.* $\alpha > 1$) could be associated to a mixture of short and long-lived contacts with the polymer. For linear solutes, the following scaling of D has been theoretically based on double relaxation mode of blobs displacements:

$$\frac{g_{CM}(t)}{6D_0t} = \frac{1}{\underbrace{\frac{2^N - 1}{2^{N-1} - 1}}_{N^{\Delta\alpha}} N} C(t) \quad (2-18)$$

where $C(t)$ is the cumulated pair correlations between the displacements of all particles in the system to enable the translation of one single blob.

Experimentally, two strategies have been used to assess the deviation of α to unity:

- i) measurement of D values of homologous series in the same conditions (*e.g.* same polymer, same temperature, same method...) applied in Kwan *et al.*, (2003); Vitrac *et al.*, (2007); Fang *et al.*, (2013).
- ii) massive collections of D values of different substances from literatures as applied in (Vitrac *et al.*, 2006).

Both approaches are illustrated in Figure 2-9 and Figure 2-10 respectively. Figure 2-10 provides α value of n -alkanes in low density polyethylene far above T_g . The given experimental data confirm a strong dependence of molecular mass larger than 1 and approximately equal to 2 for linear n -alkanes ($n=12..18$) and non-monotonously increase with the molecular weight. For branched alkanes ($M=10..10^{3.2}$ g·mol⁻¹), the reported α values in Figure 2-10c) vary from 1 to 3.

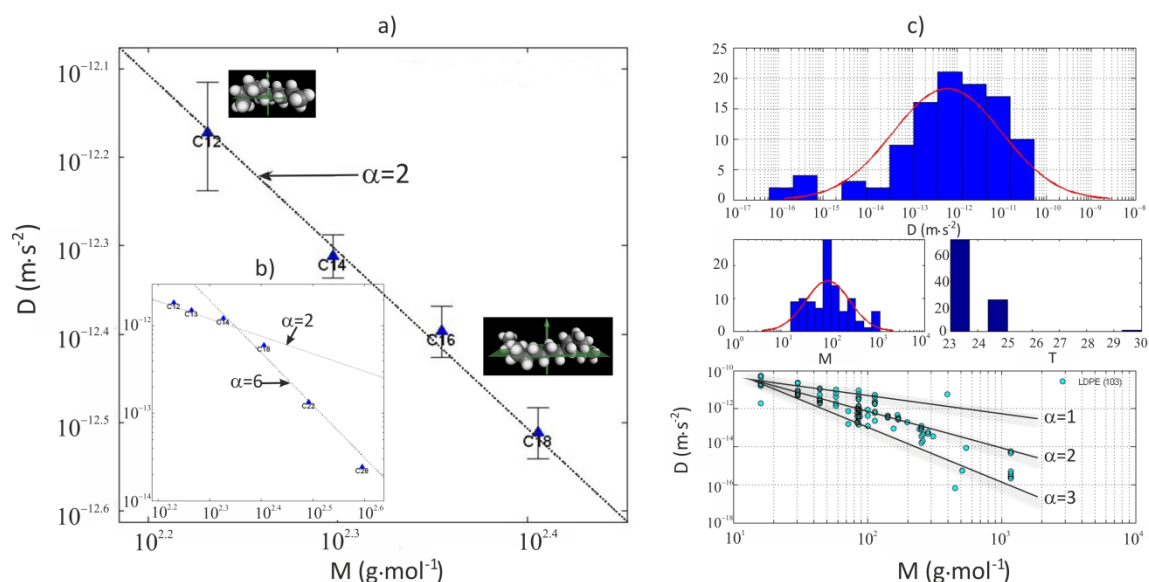


Figure 2-10 Scaling laws associated to the diffusion a-b) of linear n -alkanes (at 40 °C, according to Reynier *et al.* (2001b), Vitrac *et al.* (2007)) and c) linear or branched alkanes (between 23 °C and 30 °C, data collected by EU working group SMT-CT98-7513 and published by Begley *et al.*, (2005), Vitrac *et al.*, (2006) and available within the EU database hosted on the Safe food packaging portal (INRA, 2011) for low density polyethylene.

2.1.5.2.2 Additive type substances

For additive-type molecules, an homologous series of substance is difficult to establish (Hatzigrigoriou *et al.*, 2010; Pinte *et al.*, 2010; Pinte *et al.*, 2008). Scaling of D can be inferred only from the collection on a large set of data of D with M . The reported D values of additive-like molecules varying several decades in both rubbery and glassy states are demonstrated in

Figure 2-11. Scaling exponent α increases again more rapidly with molecular weight in glassy polymer than in rubbery polymer.

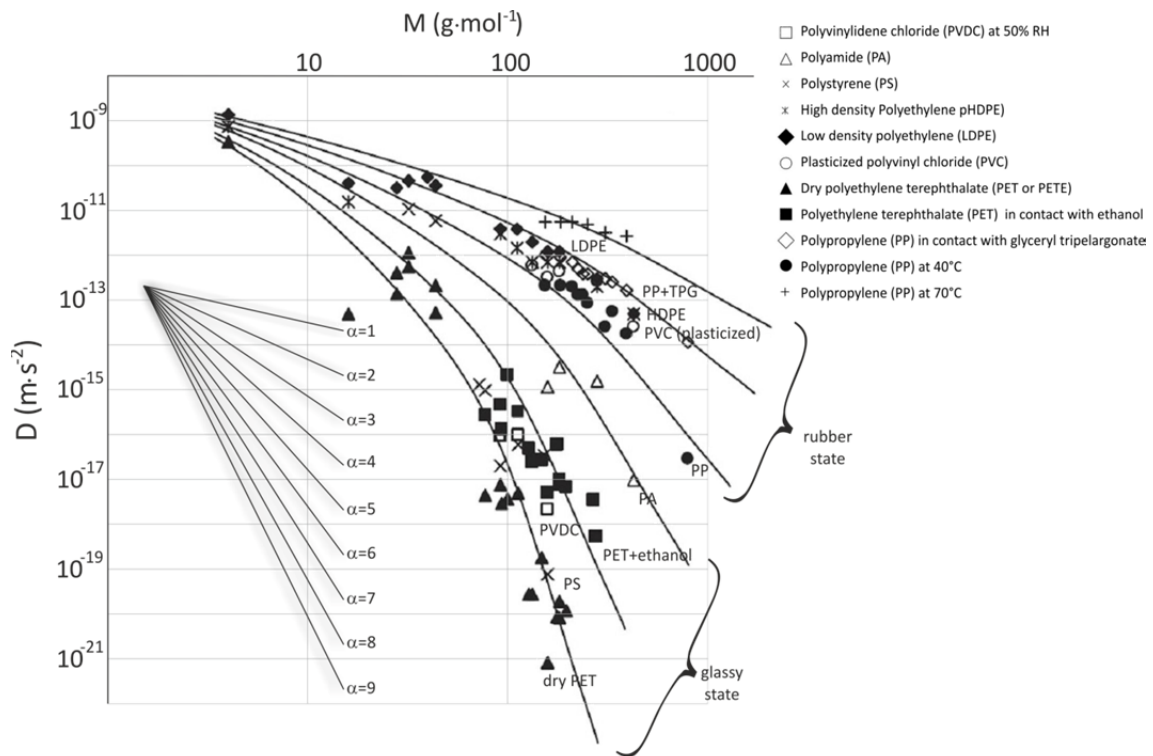


Figure 2-11 Scaling laws identified for additive-type molecules in different thermoplastic materials at 298K (Dole *et al.*, 2006a).

2.1.5.2.3 Combined effect of T , T_g and geometry

Recently, the discrepancy between α values in melts (*e.g.* $\alpha=1$ in polyethylene melt at 453K as shown by von Meerwall *et al.* (2007)) and in solid polymer (Vitrac *et al.*, 2007) has been explained, as the consequence of the temperature dependence of α with polymer density. Indeed thermoplastics are highly thermo-expandable above T_g . For aliphatic polymers above its T_g , plasticized or not, the following T - T_g dependence has been proposed for α :

$$\alpha(T, T_g) = 1 + \Delta\alpha(T - T_g) = 1 + \frac{K_\alpha}{T - T_g + K_\beta} \quad (2-19)$$

where K_α and K_β are temperature-equivalent parameters. K_α is almost constant and K_β depends on the solutes series.

This dependence is illustrated on Figure 2-12 for both linear and aromatic solutes series (Fang *et al.*, 2013). Presented diffusants are almost homologous and gathered in different polymers far above its T_g . For each series, D values are scaled as a power law of M (ranging between 70 and 10^3 g·mol⁻¹), whose exponents are much greater than unity and tend to decrease when temperature is increasing. By fitting collected α values versus T - T_g as described in Eq. (2-19),

Fang *et al.* (2013) gets the scaling of diffusion behaviors of linear and aromatic solutes appear separated by a temperature shift of 91K.

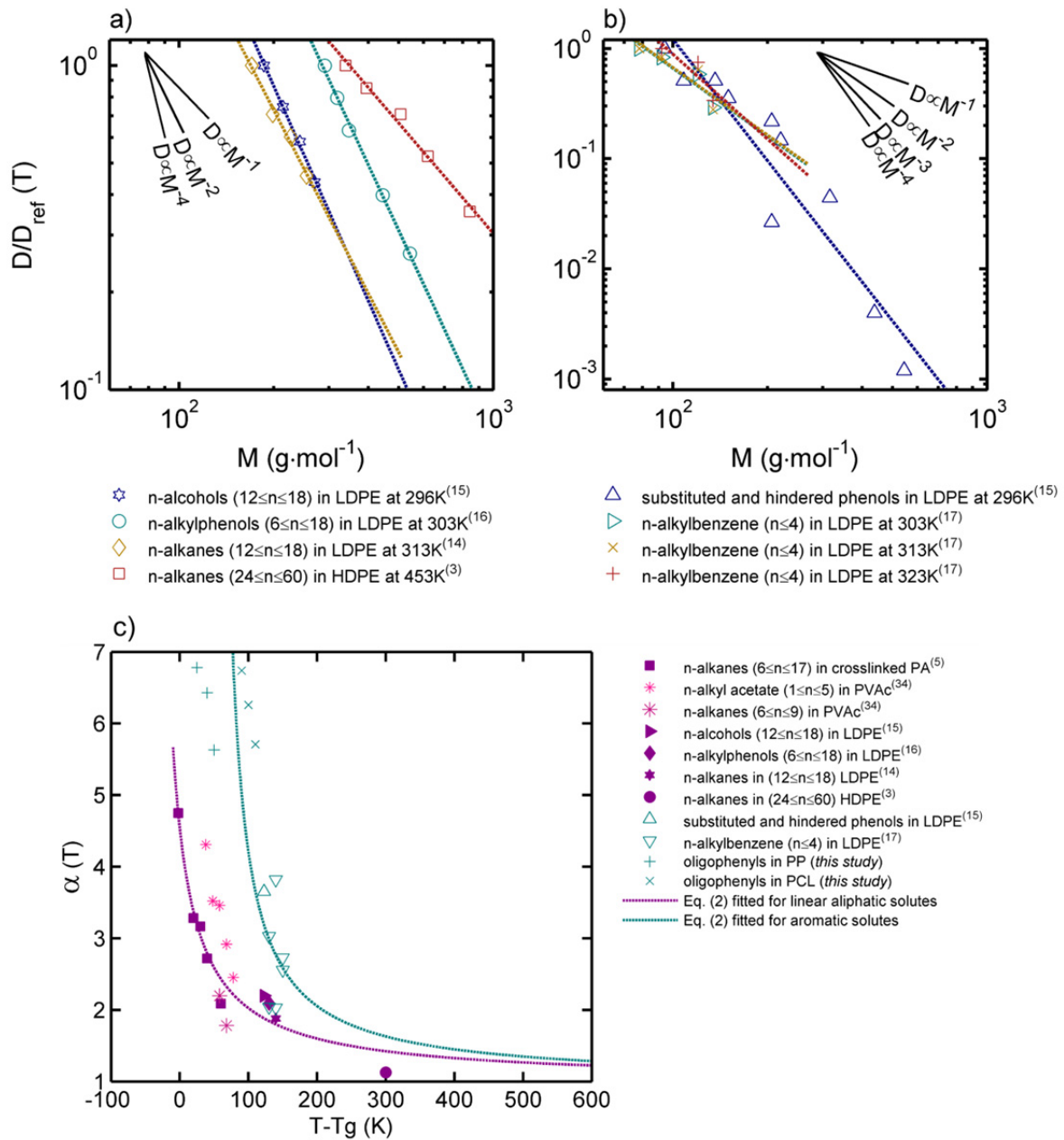


Figure 2-12 a, b) Log-log plots of trace diffusion coefficients in polyethylene of linear aliphatic and aromatic solutes. c) The corresponding scaling exponents α versus $T-T_g$ for both linear aliphatic solutes (Koszinowski, 1986; Arnould and Laurence, 1992; Möller and Gevert, 1994; Kwan *et al.*, 2003; Vitrac *et al.*, 2007; von Meerwall *et al.*, 2007) and aromatic solutes (Koszinowski, 1986; Doong and Ho, 1992; Fang *et al.*, 2013).

2.1.6 Free-volume theories

2.1.6.1 Common assumptions

As quoted by Vrentas and Duda (1977), although the free-volume model of molecular transport is based on an oversimplified view of the detailed molecular processes, there exists a significant amount of evidence that such theories can be used to predict diffusion coefficients in liquids and polymeric materials (Hedenqvist *et al.*, 1996; Jain *et al.*, 1975). Free-volume theories rely on a common assumption that free volumes in amorphous systems can be decomposed between interstitial free volume distributed almost uniformly around the considered substance and discontinuous distribution of holes (*i.e.* pocket of voids) as shown in Figure 2-13 on a cross-section of a simulated polymer including a dissolved rigid aromatic diffusant. The free volume itself can be determined experimentally by positron annihilation lifetime spectroscopy (PALS) (Consolati and Quasso, 2001) or indirectly by following the approach of (Vrentas and Duda, 1977). According to Cohen and Turnbull (1959) and following earlier derivations by Doolittle (1951) for viscosity, it is thought that the redistribution of the energy of the interstitial free volume is so large that only the reorganization of free volume holes can be involved in the translation of diffusants. Both types of voids around diffusants are illustrated in Figure 2-13. In liquids, Frenkel (Frenkel, 1955) describes similarly the transport of holes as a consequence of the displacements of all molecules in the mixture: one molecule occupying the hole next to it while leaving a similar hole at its initial position. The incompressibility of atoms compensates therefore instantaneously any increase in size of a hole by an opposite diminution of another hole.

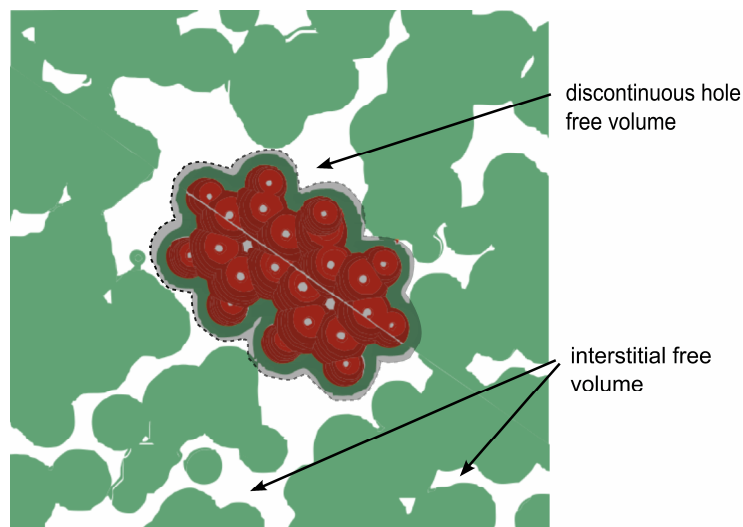


Figure 2-13 Distribution of free volumes around a planar and rigid diffusant (fluorene) in high density polyethylene at room temperature pressure as extracted by isobaric and isothermal molecular dynamics simulation. The image is obtained by plotting the projected Connolly

surfaces onto the plan defined by the main axes of the diffusant. Only the atoms included in the thickness of the diffusant are considered.

The major assumption in Cohen and Turnbull (1959) theory is that the redistribution of holes does not require any change of the energy of the host+diffusant system (*i.e.* no significant free energy barrier to cross). At first sight, one important consequence should be that diffusion in polymers should not be activated by temperature. This conclusion would however be misleading as the static and dynamic properties of the polymers are also affected by temperature. The volume fraction of holes and their renewal rate is indeed higher at higher temperature, so that diffusion appears activated by temperature as the sole consequence of the thermal expansion of the liquid or of the rubber polymer. The interpretation of Cohen and Turnbull (1959) remains in essence statistical. The diffusant translates when any amount of hole free volumes larger than a critical value, denoted \hat{V}^* appears. By noting $D(v)$ the theoretical diffusion coefficient expected for a hole volume v occurring with a probability $p(v)$, the measurable diffusion coefficient is defined as the average over all possibilities of hole volumes larger than \hat{V}^* :

$$D(\hat{V}^*) = \int_{\hat{V}^*}^{+\infty} p(v) D(v) dv \quad (2-20)$$

Equivalently, $p(v)$ must be seen as the limit probability distribution of the number of attempts of moving any atom (Bernouilli trials) before the first translation occurs. As the geometric distribution converges to the exponential one, it comes that $p(v)$ is exponentially distributed and Eq. (2-20) becomes after integration (see Eu (2006) for a detailed demonstration and discussion):

$$D(T) = D_0 \exp\left(-\gamma \hat{V}^* / \hat{V}_{FH}(T)\right) \quad (2-21)$$

where D_0 is a pre-exponential factor proportional to the section of the cage that is related to the geometry of the diffusant itself, γ is an overlap factor (ranged between $\frac{1}{2}$ and 1) introduced because the same free volume is available to more than one diffusant.

$\hat{V}_{FH}(T)$ is the average hole free volume per molecule in the host. As \hat{V}^* is related to the diffusing species and could be thought roughly proportional to the volume of the diffusant. According to Figure 2-9, this approximation is acceptable for short diffusants in elastomers

far above T_g but not in glassy polymers. In the latter, \hat{V}^* is read to be proportional to $6 \ln V_{vdw}$ instead, where V_{vdw} is the Van-der-Waals volume of the diffusing substance.

Additional sophistications are required to explicit the effect of temperature on \hat{V}_{FH} above and below T_g and to enable fractional jumps (translation much smaller than the size of the solute). Finally, the theory of free-volume theory which does not incorporate free energy barrier considerations (see Vitrac and Hayert (2007b)) must be extended to account the mixture of long and short-lived contacts between the solute and the surrounding polymer (Fang *et al.*, 2013).

2.1.6.2 Vrentas and Duda theory for rigid solutes

The Vrentas and Duda model extended iteratively Eq. (2-21) to polymer-solvent mixtures (Eq. (2-22)) through several papers (Vrentas and Duda, 1977; Vrentas *et al.*, 1985a; Vrentas *et al.*, 1985b). The general equation of Vrentas and Duda is more general than Eq. (2-21) and covers mutual diffusion. Since trace diffusion is a special case of mutual diffusion, it can be simplified as Eq. (2-22) for diffusant jumping as a single blob:

$$D = D_0 \exp\left(-\frac{E^*}{RT}\right) \exp\left(-\xi \frac{\gamma \hat{V}_p^*}{\hat{V}_{FH}}\right) \quad (2-22)$$

where $\xi \hat{V}_p^*$ replaces \hat{V}^* in Eq. (2-21). The parameter ξ lumps all diffusant characteristics (volume, geometry,...); it is defined in the original formulation as the ratio of critical molar volume of diffusant jumping unit to critical molar volume of polymer jumping unit. The jumping unit is the elemental fragment of the diffusant or polymer involved in the translation. \hat{V}_p^* is a polymer dependent parameter with a meaning of the specific hole free volume of polymer required for a jump. \hat{V}_{FH} relates to the polymer thermal expansion property defined as the average hole free volume per gram of mixture and γ represents an average overlap factor for the mixture. E^* is an additional activation term corresponding, according to Vrentas and Duda (1977), to the effective energy that a molecule needs to overcome attractive forces. The last version of the theory (Vrentas and Vrentas, 1998; Vrentas *et al.*, 1996) provides a set of rules to calculate practically all parameters in Eq. (2-22). The useful relationships for polymer and diffusant parameters in Eq. (2-22) are gathered in Table 2-4 with key references providing additional details and sophistications.

Table 2-4 Calculation method of free volume parameters in Eq. (2-22)

	<i>Approximation method</i>	<i>Calculation method</i>	<i>ref</i>
\hat{V}_p^*	Molecular simulation (Monte Carlo-type statistics)	$\hat{V}_p^* = \hat{V}_p^0(0)$ where $\hat{V}_p^0(0)$ is the specific volume of equilibrium liquid polymer at 0 K	(Haward, 1970)
E^*	Cohesive energy via solubility coefficients	$E^* = f \left[(\delta - \delta_p)^2 \tilde{V}^0 \right]$ where δ and δ_p are solubility parameter for diffusant and polymer. \tilde{V}^0 are mole volume of diffusant at T	(Hansen, 2007) (van Krevelen and te Nijenhuis, 2009)
γ	William-Landel-Ferry approximation	$\gamma = \hat{V}_p^0(T_g) a \frac{2.303C_1C_2}{\hat{V}_p^0(0)}$ where $\hat{V}_p^0(T_g)$ is specific volume of polymer at T_g , a is thermal expansion coefficient for equilibrium liquid polymer, C_1 and C_2 are WLF constants.	(Kontogeorgis and Folas, 2009)
ξ	Geometrical description of diffusant along the main directions of translation	$\xi = \frac{\xi_L}{1 + \xi_L(1 - A/B)}$ with $\xi_L = \frac{\tilde{V}^0(0)}{\tilde{V}_p^*}$ where B/A is an aspect ratio for the diffusant molecule which is a geometry-based descriptor of molecular shape. $\tilde{V}^0(0)$ is mole volume of equilibrium liquid diffusant at 0 K. \tilde{V}_p^* is critical hole free volume per mole of polymer jumping units required for a jump.	(Vrentas <i>et al.</i> , 1996)
\hat{V}_{FH}	Polymer thermal expansion properties	$\hat{V}_{FH} = \hat{V}_p^0(T_g) \left[f_H^G + a(T - T_g) \right]$ $T \geq T_g$ $\hat{V}_{FH} = \hat{V}_p^0(T_g) \left[f_H^G + (a_g - a_{cg})(T - T_g) \right]$ $T < T_g$ where $\hat{V}_p^0(T_g)$ is specific volume of polymer at T_g . f_H^G is fractional hole free volume of polymer at T_g . a_g and a_{cg} are thermal expansion coefficient for glassy polymer and the sum of the specific occupied volume and the specific interstitial free volume for the glassy polymer respectively.	(Vrentas and Vrentas, 1998)

The whole calculation procedures have been exemplified and tabulated for typical linear and aromatic solutes and different polymers (Vrentas and Vrentas, 1994, 1995; Vrentas *et al.*, 1996). Typical values are listed in Table 2-5.

Table 2-5 ξ and E^* values for 8 diffusant-polymer systems.

<i>diffusant</i>	<i>polymer</i>	<i>B/A</i>	ξ	E^* (kcal/g·mol ⁻¹)	\tilde{V}_P^* (cm ³ /mol)
Methanol	PS	1.251	0.23	-	135
	PMMA		0.19	5.3	135
	PVAC		0.31	3.4	88.8
	PPMS		-	3.1	345
acetone	PS	1.160	-	-	135
	PMMA		0.39	2.8	135
	PVAC		0.60	1.0	88.8
	PPMS		0.15	3.1	345
toluene	PS	1.242	0.56	0	135
	PMMA		0.54	0.21	135
	PVAC		0.75	-0.24	88.8
	PPMS		0.23	4.4	345
ethylbenzene	PS	1.409	0.59	0.61	135
	PMMA		0.54	1.7	135
	PVAC		0.78	-0.11	88.8
	PPMS		0.26	4.4	345

Early versions of free-volume theories (Vrentas and Duda, 1977; Vrentas and Vrentas, 1994) required to fit parameters E^* and ξ from at least two experimental diffusion coefficients and might look empirical or semi-empirical as alternative ones (see section 2.1.8). The presented version of the free-volume theory (Vrentas and Vrentas, 1998) has to be considered, by contrast, as predictive, since all important parameters can be inferred from calculations or properties independent of diffusion ones. For diffusants including repeated patterns or sub-units, it has been shown independently by Fang *et al.* (2013) that properties could be extrapolated from one diffusant (with a molecular mass M_0 and a geometric parameter ξ_0) to a next one in the series from simple rules enabled by the scaling relationship in Eq. (2-19). Indeed, $\xi - \xi_0$ was found well approximated by $0.24 \ln\left(\frac{M}{M_0}\right)$ for all polymers and solute series considered by Vrentas *et al.* (1996). The main analogies and equivalences are listed in Table 2-6. They show in particular that activation energy of linear solutes (*i.e.* aliphatic or aromatic) increases with the logarithm of the molecular mass.

Table 2-6 Formal equivalences between scaling law of diffusion coefficients and free-volume theory for diffusants based on linearly repeated sub-units (see Figure 2-5) in rubber polymers (Fang *et al.*, 2013)

	Scaling law (Eq.(2-19))	Free-volume theory (Eq. (2-22))
Relative diffusant effects	$\ln\left(\frac{M}{M_0}\right)$	$0.24(\xi - \xi_0)$
Scaling exponent $\alpha(T, T_g)$	$1 + \frac{K_\alpha}{T - T_g + K_\beta}$	$0.24 \frac{\gamma}{K_{12}} \frac{\hat{V}_p^*}{K_{22} + T - T_g}$ K_{12}, K_{22} are polymer free-volume parameters.
Relative activation energy $Ea(M, T) - Ea(M_0, T) =$ $Ea(\xi, T) - Ea(\xi_0, T) =$ $\frac{\partial \ln \frac{D(M, T)}{D(M_0, T)}}{\partial 1/T} =$	$K_\alpha \frac{RT^2}{(T - T_g + K_\beta)^2} \ln \frac{M}{M_0}$	$\underbrace{E^*(\xi) - E^*(\xi_0)}_{\rightarrow 0}$ $+ (\xi - \xi_0) \frac{\gamma \bar{V}_p^*}{K_{12}} \frac{RT^2}{(K_{22} + T - T_g)^2}$

At high temperature, free-volume theory predicts $\alpha(T) \rightarrow 0$, However, scaling exponents close to unity in agreement with Rouse theory have been reported for *n*-alkanes including from 8 to 60 carbons in many polymer systems (Chen and Ferry, 1968; Rhee *et al.*, 1977; Von Meerwall and Ferguson, 1979; von Meerwall *et al.*, 2007).

2.1.6.3 Extension to flexible solutes

The last version of the free-volume theory (Vrentas and Vrentas, 1998) does not have adjustable constants if the critical molar volume of polymer jumping units has been determined for the polymer of interest. This quantity is available for common polymers (Table 2-5). This theory assumes however that most of diffusants jump as single units. It is valid for rigid diffusants but questionable for large and flexible diffusants. Also, the average hole free volume associated with polymer and diffusant units are different.

For many diffusants of technological interest which tend to diffuse in a segment-wise manner, several physically driven modifications have been suggested: hybrid model for alkyl phenyl substances (Doong and Ho, 1992), modified free-volume model specifically for plasticizers in PVC (Coughlin *et al.*, 1990, 1991a, b; Mauritz and Storey, 1990; Mauritz *et al.*, 1990), or models for flexible and semi-flexible diffusants that are expected to move in a segmentwise manner (Deppe *et al.*, 1996; Ehlich and Sillescu, 1990). Zielinski (1996) was the first to relate ξ to the Kirkwood and Riseman (1948) theory (see Eq. (2-17)) for flexible diffusants. ξ was therefore related to the root-mean-squared end to end distance of the diffusants so that ξ can

be estimated without diffusion data. Fang *et al.* (2013) followed similar ideas while including trapping effects due to the necessity of concerted displacements of blobs to get a significant translation of the center-of-mass. By following the same approach as used to derive Eq. (2-18) for simplest cases, the diffusion coefficients of many connected blobs was related to the equivalent diffusion coefficients of one single blob $D_{blob}(T, T_g)$:

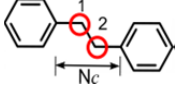
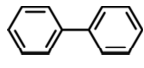
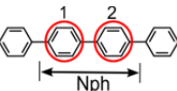
$$D(\text{diffusant}, T, T_g) = \frac{D_{blob}(T, T_g)}{C(\text{diffusant}, T)} \quad (2-23)$$

where $D_{blob}(T, T_g) = \exp\left(-\frac{K_a^{blob}}{K_b + T - T_g}\right)$ with K_a^{blob} and K_b constants are related to free-volume theory. $C(\text{diffusant}, T)$ is a correlation term due to cumulated “trapping” effects with the polymer host. For convenience Eq. (2-23) can be recast for any diffusant chosen as reference and replacing $D_{blob}(T, T_g)$:

$$\frac{D(\text{diffusant}, T, T_g)}{D_0(\text{reference diffusant}, T_{ref})} = D_{excess}^{diffusant}(\text{diffusant}, T) D_{polymer}(T, T_g) \quad (2-24)$$

where $D_0(\text{reference diffusant}, T_{ref})$ is a scaling parameter when diffusant=reference diffusant and $T=T_{ref}$. $D_{polymer}(T, T_g) = \exp\left(-\frac{K_a}{K_b + T - T_g}\right)$ is the free volume contribution and coding for polymer effects via T_g . $D_{excess}^{diffusant}(\text{diffusant}, T)$ is an excess diffusion coefficient when D values are extrapolated from the reference diffusant to any diffusant in the considered series regardless the considered polymer. In particular, it incorporates the effects of temperature on $C(\text{diffusant}, T)$ which cannot be predicted by free-volume theories. The generalized free-volume theory has been extensively tested on two homologous series of aromatic diffusants: diphenyl alkanes and oligophenylys in four different polymers at different temperatures covering from T_g+10 K to T_g+110 K. The main determinations are reported in Table 2-7.

Table 2-7 Equivalent terms in Eq. (2-24) for two homologous series of aromatic diffusants.

	$D_0(\text{reference diffusant}, T_{ref})$	$D_{polymer}(T, T_g)$ $= \exp\left(-\frac{K_a}{K_b + T - T_g}\right)$	$D_{diffusant}^{excess}(\text{diffusant}, T)$
<p>Diphenyl alkanes</p>  <p>N_C: number of carbons between two phenyls</p>	<p>$D_0(\text{biphenyl}, T_{ref})$: D values of biphenyl at T.</p>  <p>$N_C=0, N_{Ph}=2$</p>	<p>$K_a = 600 \text{ K}$ $K_b = 58 \text{ K}$</p>	<p>$\exp\left(-\ln 10 \frac{N_C}{N_{C10}}\right)$</p> <p>$N_{C10}$: number of carbons required to decrease D by 10.</p>
<p>Oligophenyls</p>  <p>N_P: number of phenyl rings between two phenyls</p>	<p>$N_C=0, N_{Ph}=2$</p>		<p>$\exp\left(-\frac{\Delta A_{diffusant}^{excess}(N_{Ph} - 2)}{RT}\right)$</p> <p>$\Delta A_{diffusant}^{excess}(N_{Ph} - 2)$: solute free energy barrier varying with N_{Ph}.</p>

2.1.7 Activation models and data

2.1.7.1 Apparent effects of temperature and pressure

The current review introduced several formal temperature dependences via Einstein relationship (Eq. (2-8)), scaling relationship (Eq. (2-19)), thermal expansion effects (\hat{V}_{FH} expression in Table 2-4), solute specific energy barrier (E^* expression in Table 2-4). None of these effects are captured via the familiar Arrhenius relationship. It is emphasized that the apparent discrepancy occurs because mechanistic theory descriptions cover a range of temperature much larger than the one covered usually experimentally: few tens of Celsius degrees. As a result, the Arrhenius relationship has to be seen as a local approximation of the real behavior around an absolute temperature T_0 and a reference solute with a molecular mass M_0 (or equivalently with a free volume parameter ζ_0):

$$Ea(M_0, T_0) = -R \frac{\partial \ln D(M, T)}{\partial (1/T)} \Bigg|_{M=M_0, T=T_0} = T_0^2 R \frac{\partial \ln D}{\partial T} \Bigg|_{M=M_0, T=T_0} \quad (2-25)$$

Activation volumes are defined similarly and related to the effect of temperature:

$$Va(M_0, T_0) = -RT_0 \left. \frac{\partial \ln D(M, T)}{\partial P} \right|_{M=M_0, T=T_0} \quad (2-26)$$

Activation energies are very important quantities as soon as diffusion coefficients must be extrapolated to a different temperature: *e.g.* from room temperature to oven-heating or sterilization conditions or even to freezing conditions. Contrastingly, the polymers are not significantly compressible so that the values of activation volumes have mainly an interest except for predicting migration under very high pressure (beyond 200 MPa) such as those met in Pascalisation treatments (Dobiáš *et al.*, 2004; Juliano *et al.*, 2010; Lambert *et al.*, 2000; Le-Bail *et al.*, 2006) or to identify the molecular mechanisms of translation.

The activation energies and volumes for translation of paramagnetic probes in high density polyethylene (HDPE) are compared in Table 2-8 with the same quantities at molten state. They confirm the higher energies and activation volumes to induce a diffusant translation rather than to induce a local reorientation. The activation energies in HDPE are of the same order of magnitude as those associated with the relaxations α and $\alpha\beta$ of the polymer (Schmidt-Rohr and Spiess, 1991). For large polycyclic molecules, Ito *et al.* (1987) and Seta *et al.* (1984) showed that activation volume represents only a small fraction of the van-der-Waals volume of the diffusant ranged between 0.05 and 0.2. The fraction is smaller when the diffusant is more flexible. The experimental values of activation volumes validate independently the concept of jumping units smaller than the whole diffusant as found in the last free-volume theories (see section 2.1.6.3).

Table 2-8 The activation energy and volume responsible for rotation and translation of the additive-type molecule in high density polyethylene at macroscopic and molecular scale. (after Kovarski (1997)).

		<i>macroscopic quantities</i>		<i>molecular magnitudes</i>	
		<i>rotation</i>	<i>translation</i>	<i>rotation</i>	<i>translation</i>
		kJ·mol ⁻¹		μs	
Activation energy	solid state ($T > T_g$)	20-50	50-150	$10^{-5} - 1$	> 1
	molten state ($T > T_m$)	10-20	15-40	$10^{-7} - 10^{-5}$	$10^{-6} - 1$
		cm ³ ·mol ⁻¹		Å ³	
Activation volume	solid state ($T > T_g$)	20-70	50-150	30-115	80-250
	Molten state ($T > T_m$)	8-15	13-30	10-25	20-50

According to free-volume theory, the activation energy is expected to increase progressively from rubber to glassy state. The amount of reliable activation energy values tabulated in the

literature is however insufficient to derive a general law. The difficulty to get reliable diffusion coefficients at glassy state arises from non-Fickian kinetics (Chernikov *et al.*, 1990; Geisel *et al.*, 1988) and ageing effects (Ehlich and Sillescu, 1990; Veniaminov and Sillescu, 1999; Zhang and Wang, 1987). By comparing experimental determinations and theories, Tonge and Gilbert (2001b) argued that standard free-volume theories would tend to overestimate D values by neglecting the effect of waiting times before a jump can occur. Hall *et al.* (1999) showed that this effect could be included by assigning a proper value to parameter E^* in Eq. (2-22). In particular, the authors showed that an excess activation energy up to $9 \text{ kJ}\cdot\text{mol}^{-1}$ was required for polar diffusants in a polar matrix.

The mechanisms of translation of additive-type molecules at different temperatures are summarized in Figure 2-14 and compared with the available degree of freedoms in the polymer host. In the molten state ($T > T_m$), the translation of diffusants is enhanced by the translation of the whole polymer chains. In the rubber state ($T_g < T < T_m$), the translation of diffusants depends on local fluctuations of chain contours. In both cases, the activation energy must be envisioned as the consequence of local reorder of chain contours so that the activation energies are expected to increase slowly with the size and rigidity of the diffusant. In the glassy state, no degree of freedom is by contrast available for the polymer to open on a regular basis of free volumes and the translation can only occur occasionally when large reordering of polymer segments occurs. An example of such correlated displacement are the string-like motions of monomers in glassy polymers (Aichele *et al.*, 2003). The energetic barrier of translation must be seen as the consequence of the Poissonian distribution of such collective events as discussed within the framework of the transient state theory in Karayiannis *et al.*, (2001); Vitrac and Hayert, (2007b).

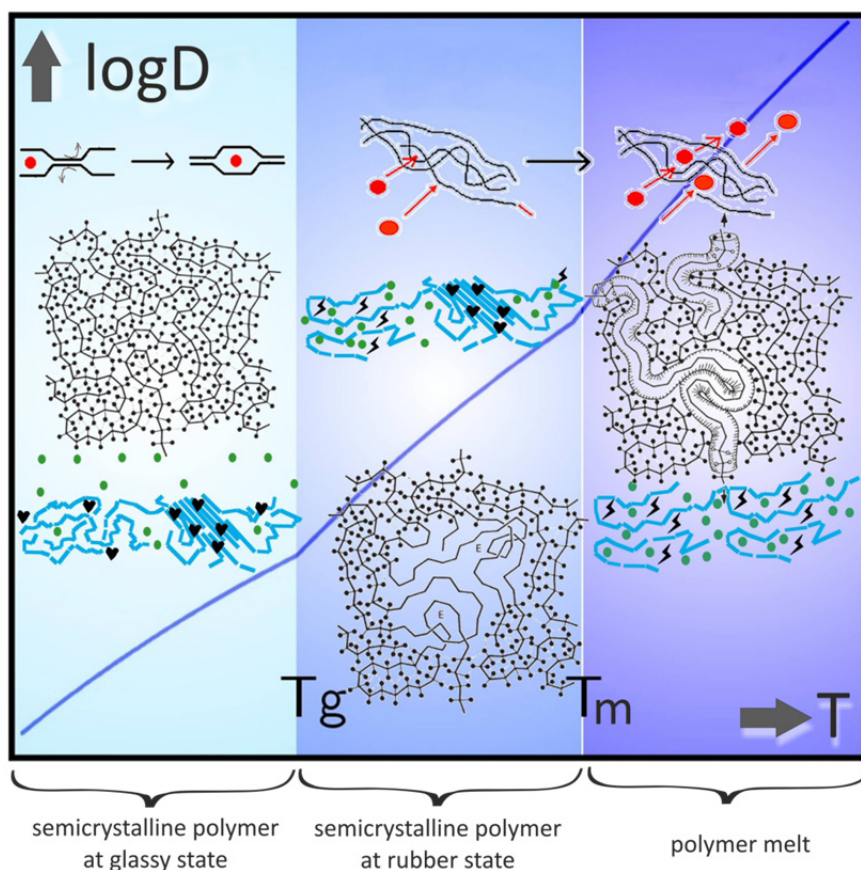


Figure 2-14 Interpretation of the translation of additive-type molecules according to the state of the polymer.

2.1.7.2 Activation energies

2.1.7.2.1 Effect of the molecular mass

The scaling law of diffusion coefficients for diffusants including linearly repeated sub-units (see Table 2-6) predicts a logarithm dependence of activation energy with molecular mass (M). Figure 2-15 plots on a log-log scale the evolution of E_a with M for linear and branched alkanes. The results were calculated from the work of European group SMT-CT98-7513 (EC, 2002b), partly reproduced by Begley *et al.*, (2005); Vitrac *et al.*, (2006) and available in the European database of diffusion coefficients hosted by the Safe-Food-Packaging Portal (INRA, 2011). As the data mixed diffusion coefficients published in peer-reviewed journals, data from migration tests and different kind of polyethylenes, the residual uncertainty is significant. The comparison with M shows however a systematic low dependence of D with M , which tend to confirm the proposed expression of E_a in Table 2-6. In details, volatile molecules ($M < 100 \text{ g}\cdot\text{mol}^{-1}$) have E_a values close to $50 \text{ kJ}\cdot\text{mol}^{-1}$ while the additive molecules have an activation energy comprising between 85 and $100 \text{ kJ}\cdot\text{mol}^{-1}$.

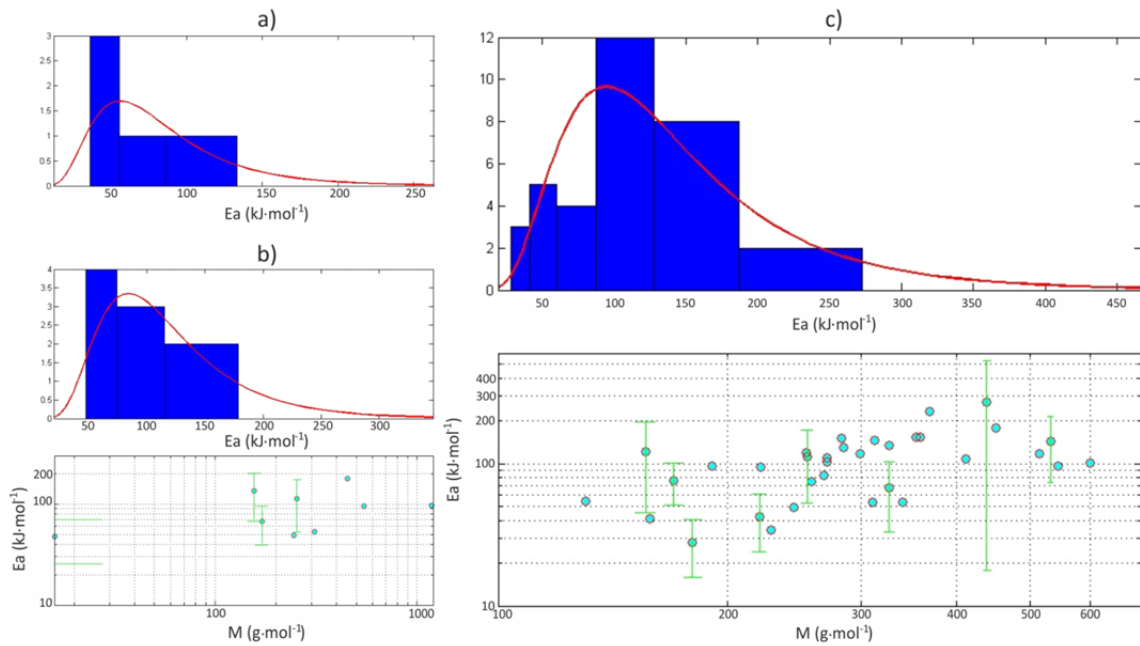


Figure 2-15 Estimated activation energies between 20 and 40°C in low density polyethylene: a) small molecules $M < 100 \text{ g}\cdot\text{mol}^{-1}$, b) linear alkanes, c) additive molecules with $100 < M < 600 \text{ g}\cdot\text{mol}^{-1}$. Data extracted from the European database of diffusion coefficients (INRA, 2011).

2.1.7.2.2 Polymer effects

The effects of the polymer host are analyzed in Figure 2-16 by plotting the Van't Hoff diagrams of a model diffusant (2',5'-dimethoxy-acetophenone) in a broad range of polymers: aliphatic, aromatic, with or without electrostatic interactions... It is emphasized that the data were obtained at or close to molten state with an intent of evaluating the properties of functional barriers of these polymers in co-extrusion conditions (Dole *et al.*, 2006a; Dole *et al.*, 2006b; Feigenbaum *et al.*, 2005). Comparisons between Figure 2-15 and Figure 2-16 show that polymer effects on D are one magnitude lower than solute ones at rubber state. Consistently with Figure 2-12 and Eq. (2-23), D values are lower when $T-T_g$ differences are smaller and apparent activation energies are higher in high T_g polymers. Indeed, high T_g polymers exhibit higher cohesive energies due to specific π - π interactions, polar, H -bonding, which turn to be also very sensitive to temperature. As reported in chapter 7 of Mark (2007) and in chapter 4.4 of van Krevelen and te Nijenhuis (2009), such interactions increase the thermal expansion coefficient with temperature $\alpha(T) = -\frac{1}{\rho} \left(\frac{\partial \rho}{\partial T} \right)_p$ and consequently activate dramatically the renewal rate of free volumes. Several models describing these effects were proposed by Simha and Boyer (1962) and have been incorporated in the Vrentas and Duda free-volume theory (see the expressions of $\hat{V}_{FH}(T)$ beyond and below T_g).

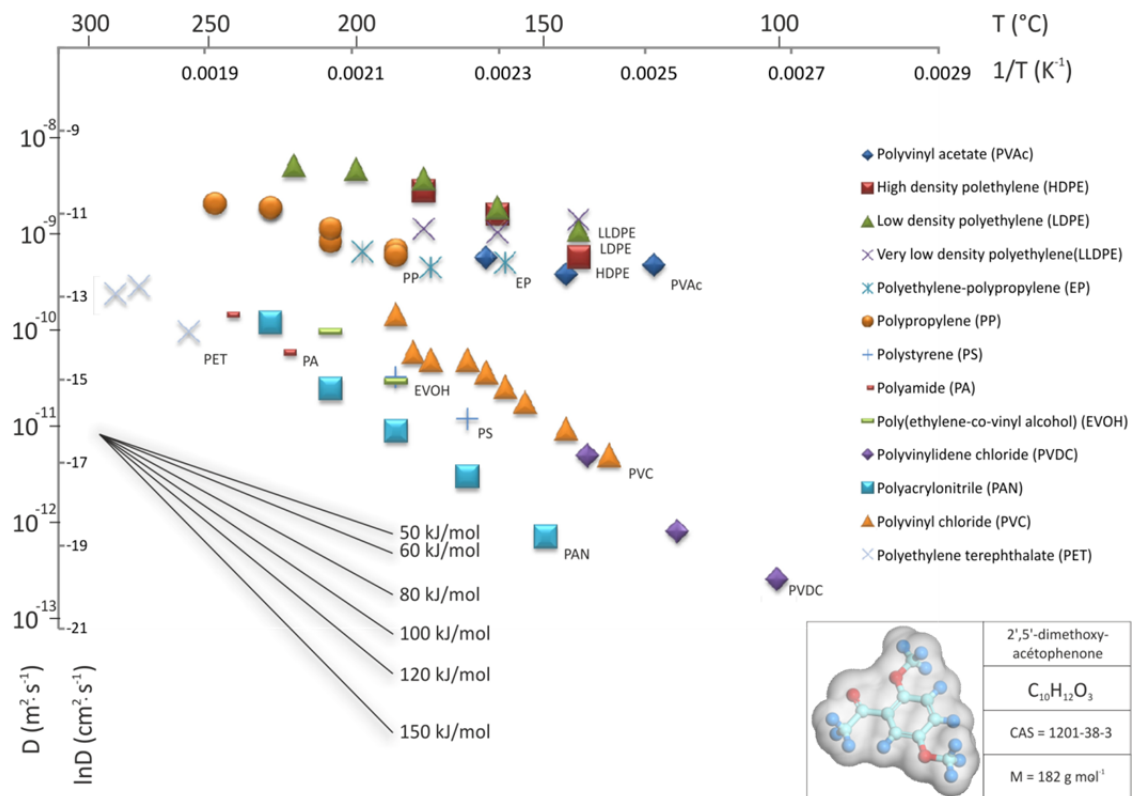


Figure 2-16 Van't Hoff diagram of diffusion coefficient of 2',5'-dimethoxy-acetophenone in different polymers et high temperature (near to processing temperature). (after Feigenbaum *et al.* (2005), Dole *et al.* (2006a), Dole *et al.* (2006b)).

2.1.7.2.3 Combined solute and polymer effects

The activation energies collected around 40°C by Dole *et al.* (2006a) are plotted on a semi-log plot for a broad range of diffusants and polymers. They confirm the previously described trends: activation energies of additive-type substances are higher for larger substances and the activation energies are higher in high T_g polymers. In agreement with the extended free-volume theory proposed by Fang *et al.* (2013), the semi-log plot shows that E_a values tend to be linear with $\ln M$ (see Table 2-6).

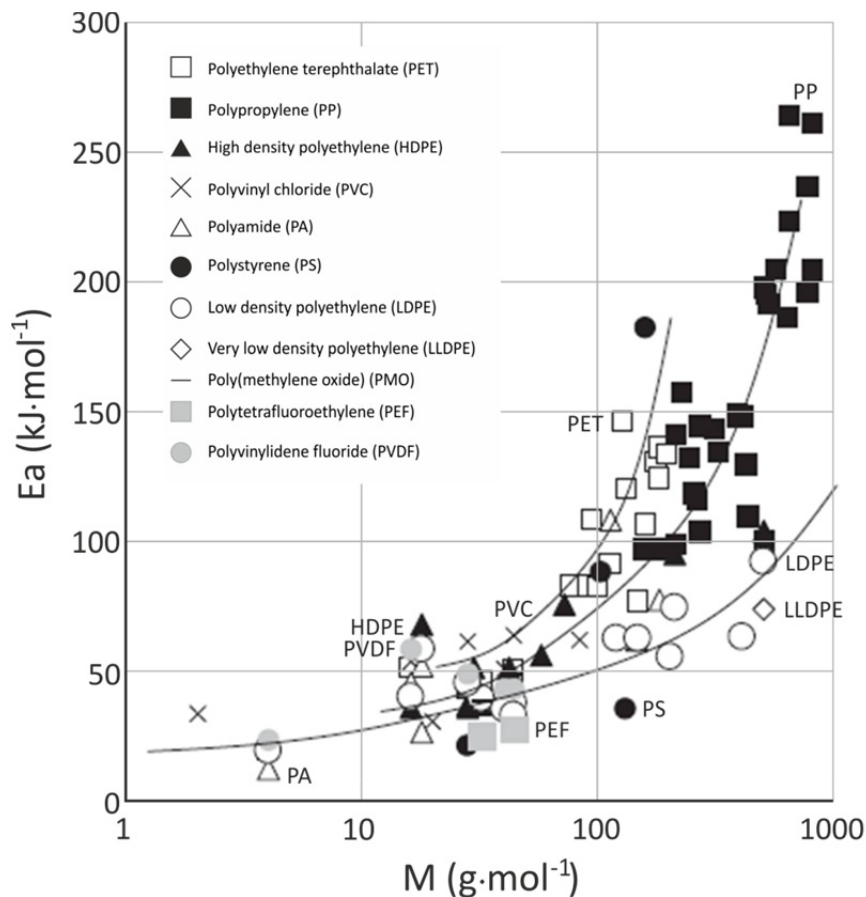


Figure 2-17 Variation of activation energy for different polymers between 20 and 40°C according to Dole *et al.* (2006a).

2.1.8 Alternative models to predict D or to overestimate D

2.1.8.1 The justification of alternative models

Despite necessary adaptations, the polymer science community considers free-volume theories as the most reliable approach to estimate self- and trace diffusion coefficients in polymers as discussed in details in Meerwall *et al.*, (1998); Tonge and Gilbert, (2001a); Harmandaris *et al.*, (2002); Fang *et al.*, (2013). Its range of applicability has been broadly extended during the last four decades from polymer-solvent systems (Narasimhan, 2001) to arbitrary diffusants such as plasticizers (Coughlin *et al.*, 1990, 1991a, b; Mauritz and Storey, 1990; Mauritz *et al.*, 1990) or antioxidants (Boersma, 2003; Boersma *et al.*, 2003a, b), while including glassy polymers (Arnold, 2010; Romdhane *et al.*, 1995). In his literature review of “Models for Diffusion in Polymers”, Mercea (2008) quoted the free-volume theory as “classical approach” but concluded that they do not meet completely the following practical goals to provide enough incentives for the process engineer or the law enforcer: “(i) as simple as possible, (ii) rely on parameters which are well known and easily available, and (iii) at last but not least, the use of the method to predict diffusion processes should not consume more

time and resources than the direct migration/diffusion experiments.” As a result, models so-called “alternative” by opposition with conventional ones (as listed in the review of Masaro and Zhu (1999)) have been sought for the food packaging applications.

The genesis and classification of such alternative models are difficult to reconstruct as they are used almost exclusively by a single scientific community (*i.e.* food packaging) and for a single purpose (*i.e.* compliance testing). The Piringer model, called Piringer “Interaction Model”, is by far the most widely used by this community, which includes also us as authors. It has been firstly proposed by Baner *et al.* (1996) and is recommended by the EU commission for the implementation of diffusion modeling for the estimation of specific migration in support of EU regulation 10/2011/EC (EC, 2012c). The proponents argue that it has theoretical grounds whereas the Food and Drug Administration quotes it as “an empirical correlation based on the molecular weight of the migrant” (FDA, 1999, 2006). Piringer justified firstly his derivations in pages 158-169 of his book “Plastic Packaging Material for Food” (Piringer and Baner, 2000) and extended it in pages 163-193 of its second edition (Piringer and Baner, 2008). The general equation is said to be multipurpose: “a uniform model for predicting diffusion coefficients in gases and condensed phases, including plastic materials” (page 165 of the second edition). The demonstration is difficult to follow and apparently not available in peer-reviewed journals. The general form of equation Piringer (Eq. 6.17 of the second edition) is reshaped in this work to highlight its possible legacy with classical equations (Eq. (2-22)):

$$\begin{aligned} \frac{D}{D_0} &= \exp(w_n - A/A_0 - Ea/RT) \\ &= \underbrace{\exp\left(\frac{Rw_n}{R}\right)}_{\text{entropic contribution}} \underbrace{\exp(-A/A_0) \exp(-Ea/RT)}_{\text{enthalpic contribution}} \end{aligned} \quad (2-27)$$

In its general form, the model can be compared with classical theories to highlight possible similitudes. The exact meaning of the factor w_n , which is entropic by nature (*i.e.* not temperature dependent), is unclear. Based on the calculations of the contribution thermal vibration spectra to the long term translation of the center-of-mass (Fang *et al.*, 2013), the product Rw_n could be associated to the entropy of translation of a reference solute. The authors showed indeed that the translational entropy increases with the number of atoms. The ratio A/A_0 is the ratio of cross section respectively to a reference solute. It could be compared to $\xi-\xi_0$ in classical free-volume theories (*i.e.* Table 2-6). However, w_n , A , A_0 and Ea have only been inferred for the self-diffusion (see Eqs. 6.25-6.27, Fig. 6.3 and Table 6.7 in Piringer and Baner (2008)) and trace-diffusion of n -alkanes in polyethylene (see Eq. 6.28 and Fig. 6.4 in

Piringer and Baner (2008)). In particular, the Eq. (2-27) fails to reproduce the correct scaling of D with M at different temperatures as reported in reference experiments on n -alkanes (Meerwall *et al.*, 1998; von Meerwall *et al.*, 2007). In practice, a simplified version of Eq. (2-27) is preferred instead (see Table 2-9) by using M as the unique descriptor of diffusant effects. Its goal is not to predict D values but to provide overestimates of D . Contrary to free-volume theories (see section 2.1.6 and discussions in Vrentas and Vrentas, (1995, 1998); Vrentas *et al.*, (1996)), the parameters cannot be determined without fitting existing D values. The overestimation concepts have been reviewed by Arvanitoyannis and Bosnea (2004) and have been subjected to several updates in the course of the European project SMT-CT98-7513 (EC, 2002b).

It is worth to notice that concurrent approaches have been proposed during the meanwhile. A very similar empirical equation has been proposed during the EU AIR Research Programme CT94-1025 (Feigenbaum *et al.*, 2002). Based on the same raw data collected during the project SMT-CT98-7513, Helmroth *et al.* (2005) and Vitrac *et al.* (2006) developed different approaches offering the possibility to retrieve either realistic estimates (*i.e.* with half chance to be either an underestimate or an overestimate) or overestimates with an arbitrary “safety margin”. The concepts of D overestimation and “safety margin” on migration (or equivalently C_F) must not be confused. Effects of uncertainties and overestimations on D and other parameters such as partitioning on C_F are particularly discussed in Vitrac and Hayert (2007a). C_F is a monotonously increasing function of D but usually not a linear function of D , so that an overestimation of D is not followed by a similar overestimation of C_F . For diffusion controlled monolayer materials (*e.g.* $Bi > 100$, $Fo < 0.6$), one has $C_F \propto \sqrt{D}$. By following similar considerations, the Helmroth model relies on a stretched exponential (see Table 2-9) and stochastic concepts to overestimate migration rather than simply diffusion coefficients. The probabilistic concept was formally stated and proven simultaneously by Vitrac and Hayert (2005) based on a stochastic resolution of Eq. (2-1). It is however important to note that the introduced law of probability represents the additional safety factor on D we need to consider due the lack of prediction of the considered model. For any model using only M as molecular descriptor, the uncertainty on D is assessed by the distribution of D values of solutes with similar M values in a prescribed polymer at a given T . The model of Vitrac *et al.* (2006) offers an alternative as it includes by contrast enough mechanistic descriptors (see section 2.1.8.3) and proper cross-validation procedures to predict D values to reach prediction errors in the same range as experimental errors.

2.1.8.2 Models overestimating D

Poças *et al.* (2008) and Helmroth *et al.* (2002a) have already reviewed the models, denoted $\check{D}_{(M,T)}$, to overestimate D values. They are reported in Table 2-9 along with their apparent

scaling exponent with M : $\check{\alpha} = -\left. \frac{\partial \ln \check{D}_{(M,T)}}{\partial \ln M} \right|_T$ with corresponding free parameters reported in

Table 2-10. Although all presented models claim to be a generalization of existing mechanistic models, they use simply molecular mass as the unique descriptor of all diffusant effects. In the light of scaling theories (see section 2.1.5), their overestimation features at constant temperature are associated to the consequence of the underestimation of the true dependence of D to M for diffusants larger than a reference diffusant with molecular mass, denoted M_0 :

$$\check{\alpha}(M, T) = -\left. \frac{\partial \ln \check{D}_{(M,T)}}{\partial \ln M} \right|_T \leq -\left. \frac{\partial \ln D_{(M,T)}}{\partial \ln M} \right|_T = \alpha(T, Tg, \text{diffusant series}) \quad \text{for } M \geq M_0 \quad (2-28)$$

Table 2-9 Main models to overestimate D values for compliance testing

$\ln D_{(M,T)} \leq \ln \check{D}_{(M,T)}$	$\check{\alpha} = -\left. \frac{\partial \ln \check{D}_{(M,T)}}{\partial \ln M} \right _T$	Theoretical justifications
Limm model (Limm and Hollifield, 1996):		
$\ln \check{D}_{(M,T)} = \ln D_0 + aM^{\frac{1}{2}} - \frac{bM^{\frac{1}{3}}}{T}$ <p>a and b are adjustable parameters which are specific for each polymer type. See Table 2-10</p>	$-\frac{aM^{1/2}}{2} + \frac{bM^{1/3}}{3T}$	Apparent cross section of diffusant
Helmroth model (Helmroth <i>et al.</i> , 2005):		
$\ln \check{D}_{(M,T)} = \ln D_0 - \left(\frac{M}{M_0} \right)^c + F^{-1}(P 0, S)$ <p>c is polymer dependent parameter. $F^{-1}(P 0, S)$ is the normal inverse distribution with zero mean and standard deviation s. For $P=50\%$ ($F^{-1}(0.5 0, S) = 0$), it gives an estimate and an overestimate for $P>50\%$. See Table 2-10</p>	$c \left(\frac{M}{M_0} \right)^c$	Close to free-volume theories
Piringer model (Begley <i>et al.</i> , 2005; Piringer and Baner, 2000, 2008):		
$\ln \check{D}_{(M,T)} = A'_P - 0.1351M^{2/3} + 0.003M - \frac{\tau + 1045}{RT}$	$0.09007M^{2/3} - 0.003M$	Gas kinetic theory
See Table 2-10		

In the Piringer model, A'_p and τ are polymer dependent parameters. A zero value for τ leads to an apparent activation energy of $87 \text{ kJ}\cdot\text{mol}^{-1}$, which corresponds to a median activation energy in polyolefin matrices (see Figure 2-15, Figure 2-16 and Figure 2-17). τ is corrective activation parameter which depends only on polymer.

Table 2-10 Available parameter values of main models for different polymers as reported in (Limm and Hollifield, 1996; Begley *et al.*, 2005; Helmroth *et al.*, 2005; EC, 2012a)

Polymer	Limm model			Helmroth model			Piringer model	
	$\ln D_0$	a	b	$\ln D_0$	c	s	A'_p	$\tau (K)$
LDPE,LLDPE	4.16	0.555	1140.5	-13.633	0.37	1.3	11	0
HDPE	0.90	0.819	1760.7	-14.144	0.39	N/A	14	1565
PP (homo and random)	- 2.10	0.597	1335.7	-17.779	0.36	2.0	13	1565
PP (rubber)	N/A	N/A	N/A	N/A	N/A	N/A	11	0
PS	N/A	N/A	N/A	N/A	N/A	N/A	0	0
HIPS	N/A	N/A	N/A	N/A	N/A	N/A	1	0
PET	N/A	N/A	N/A	N/A	N/A	N/A	6	1565
PBT	N/A	N/A	N/A	N/A	N/A	N/A	6	1565
PEN	N/A	N/A	N/A	N/A	N/A	N/A	5	1565
PA	N/A	N/A	N/A	N/A	N/A	N/A	2	0
PVC	N/A	N/A	N/A	N/A	N/A	N/A	0	0

LDPE, LLDPE: low density and Linear low-density polyethylene, PP: polypropylene, PS: polystyrene, HIPS: high impact polystyrene, PET: polyethylene terephthalate, PBT: polybutylene terephthalate, PEN: polyethylene naphthalate, PA: polyamide, PVC: polyvinyl chloride.

Contrary to mechanistic models (see Figure 2-12 where α is shown to be a function of the considered chemical series instead), all overestimating models invoke an equivalent scaling exponent $\tilde{\alpha}$ which increases with M . Both Piringer and Helmroth models neglect the strong dependence of the true α with M . Only the model of Limm and Hollifield (1996) takes into account some decrease of $\tilde{\alpha}$ with T but not with $T-T_g$, as predicted by free-volume theory (see Eq. (2-22)). The values of \tilde{D} , calculated according to the three models (see equations and parameters listed in Table 2-9 and Table 2-10) are compared with the 628 D values and collected by the group SMT-CT98-7513 in Figure 2-18. It is important to note that the reported D values cannot be considered as real D values, because there is no standard methods for measuring D , they were derived from different kinds of experiments published or not and arbitrary normalized at 23°C , by assuming an average action energy of $85 \text{ kJ}\cdot\text{mol}^{-1}$ (EC, 2002b). In addition, since all the presented data were used to fit/set the free parameters

involved in the Piringer and Helmroth models, the comparison with reported D values and calculated \bar{D} ones does not constitute an independent validation of these models. With the previous restrictions in mind, the best trade-off between too large overestimations and too large underestimations are obtained from the Piringer model. It underestimates the real D values in 5.2 %, 26.8% and 16.3% of cases, with maximum underestimation factors of 18, 17 and 365 (10 if 365 is considered to be an outlier), for LDPE, HDPE and PP, respectively. When it overestimates results, the overestimation ratio \bar{D}/D is ranged between a factor 1.3 and 193 (5th and 95th percentiles respectively) with an average value of 33 and a maximum value of 1.5×10^3 . If migration is mainly diffusion controlled (*i.e.* $C_F \propto \sqrt{D}$), it would lead to overestimations of C_F by factors 5.7 and 39, respectively.

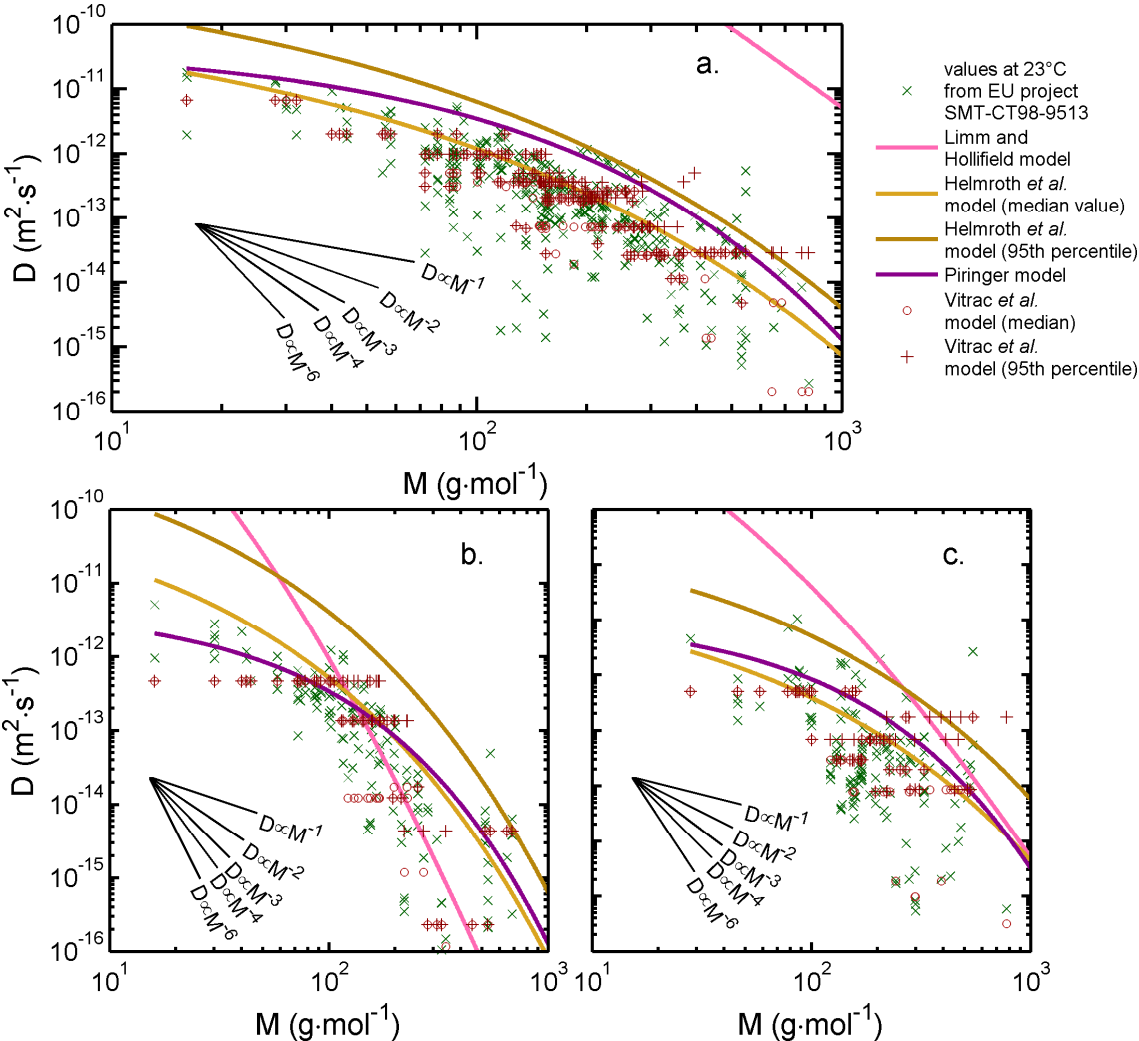


Figure 2-18 Estimation of D with molecular weight by both models listed in Table 2-9 and Vitrac model (see section 2.1.8.3) and validation of these models by comparison with data collected by the EU project SMT-CT98-7513 (EC, 2002b) and renormalized at 23°C in a) LDPE (345 values), b) HDPE (142 values) and c) PP at 23°C (141 values).

The method to derive Ap' and τ values is discussed in a recent European guidance document (EC, 2013). It is proposed to derive Ap' and τ values for unknown polymers based on a small set of data and to use them extrapolate overestimates for a broader range of substances. From Figure 2-18 and Figure 2-19, it is obvious that the intangible dependence of \bar{D} with M cannot fit all polymers and the risk of underestimating D values is large if the reference experimental D values were based on molecules than those targeted by the use of the model. The experimentally determined values of α from Figure 2-12 and theoretical values of $\bar{\alpha}$ calculated from Table 2-9 and Table 2-10 are compared in Figure 2-19 for all three models. All models tend to underestimate true α values far above T_g , in particular in oven-heating and sterilization conditions. As a result, the extrapolation of \bar{D} values to high temperatures might be unsafe in particular if the activation energies for low molecular weight compounds are overestimated.

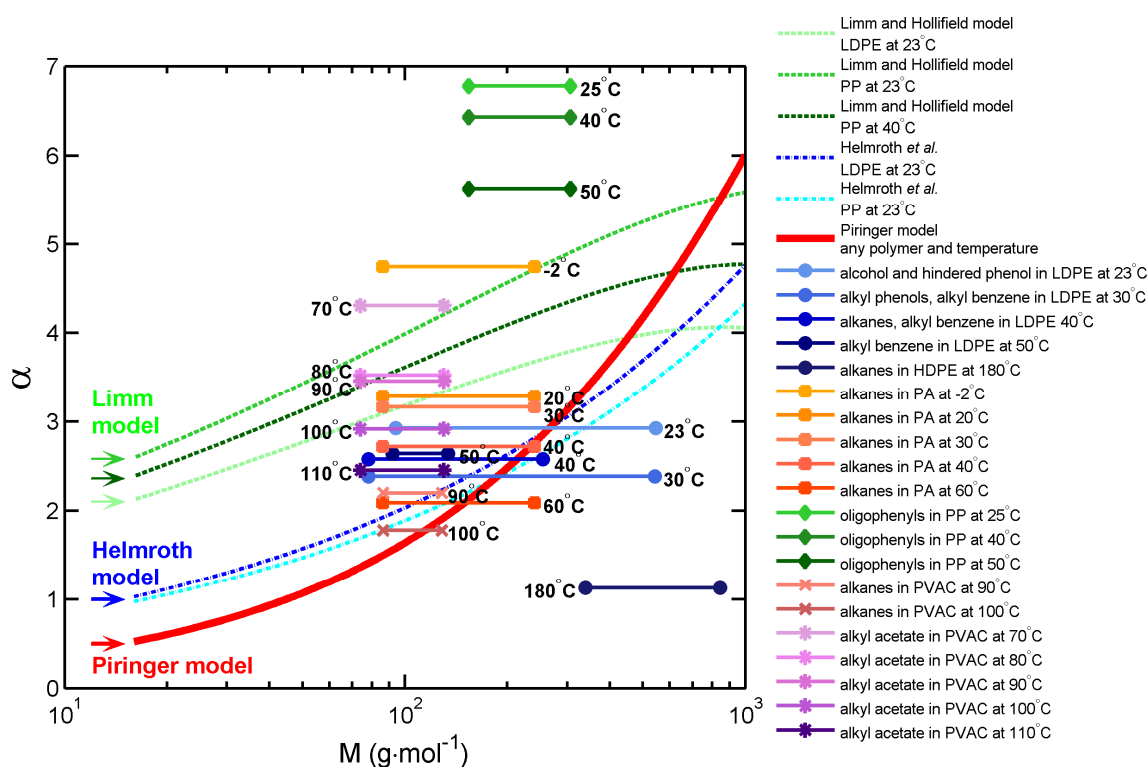


Figure 2-19 Plot of scaling exponents α with molecular weight for different models in Table 2-9 and reported averaged experimental α values in corresponding range of tested molecular weight (after Fang *et al.* (2013)). Each horizontal segment represents the range of molecular masses used to determine α .

The variations of the overestimation ratio offered by the Piringer model in two typical polymers at the rubbery state are reported in Figure 2-20. The reference values (D) were derived from the behaviors of aliphatic solutes and free-volume theory of flexible solutes (Fang *et al.*, 2013). It is noticeable that iso- D values and iso- \bar{D} values are not parallel when

there are plotted versus molecular length/weight and temperature. By itself, the concept of iso- D value or of superposition principles of effects of (M, T, T_g) is a consequence of the proximity of the core free-volume equation (22) and the Williams-Landel-Ferry one. Figure 2-20a) and b) show however that large and small substances with a similar diffusion coefficient at different temperatures according to the free-volume theory (see arrow) are seen with different \check{D} overestimates presenting overestimation ratios varying over several decades. According to ratios \check{D}/D reported in Figure 2-20c) and d), the overestimation is higher for larger substances and at lower temperatures. For volatile compounds or in high-temperature processes (*e.g.* oven-heating, pasteurization, sterilization,...), the ratio of overestimation vanishes exponentially with a significant risk of underestimation. As a result, it is recommended not to use the Piringer model for any purpose independently on the conditions used to set the model parameters. When the parameters need to be assigned for a new polymer or upgraded to include a broader range of conditions, European guidance documents recommend therefore usages of Piringer type diffusion models where extrapolation is likely to be robust (EC, 2012c, 2013). The recommendable directions and extents of extrapolation of \check{D} values from a small set of experimental D values are summarized in Figure 2-20e). As a rule of thumb and because the underestimation region (in red) is mainly located on the left hand-side, extrapolation from small to large molecules would be acceptable for substances belonging to the same category and within a small range of molecular masses (*e.g.* $50 \text{ g}\cdot\text{mol}^{-1}$). When a broader range of substances and conditions are required, reference D values should have to be collected at different temperatures higher than the targeted one and for molecules representatives of the size and shape expected in future applications. Further sophistication would need a better consistency with free-volume theory.

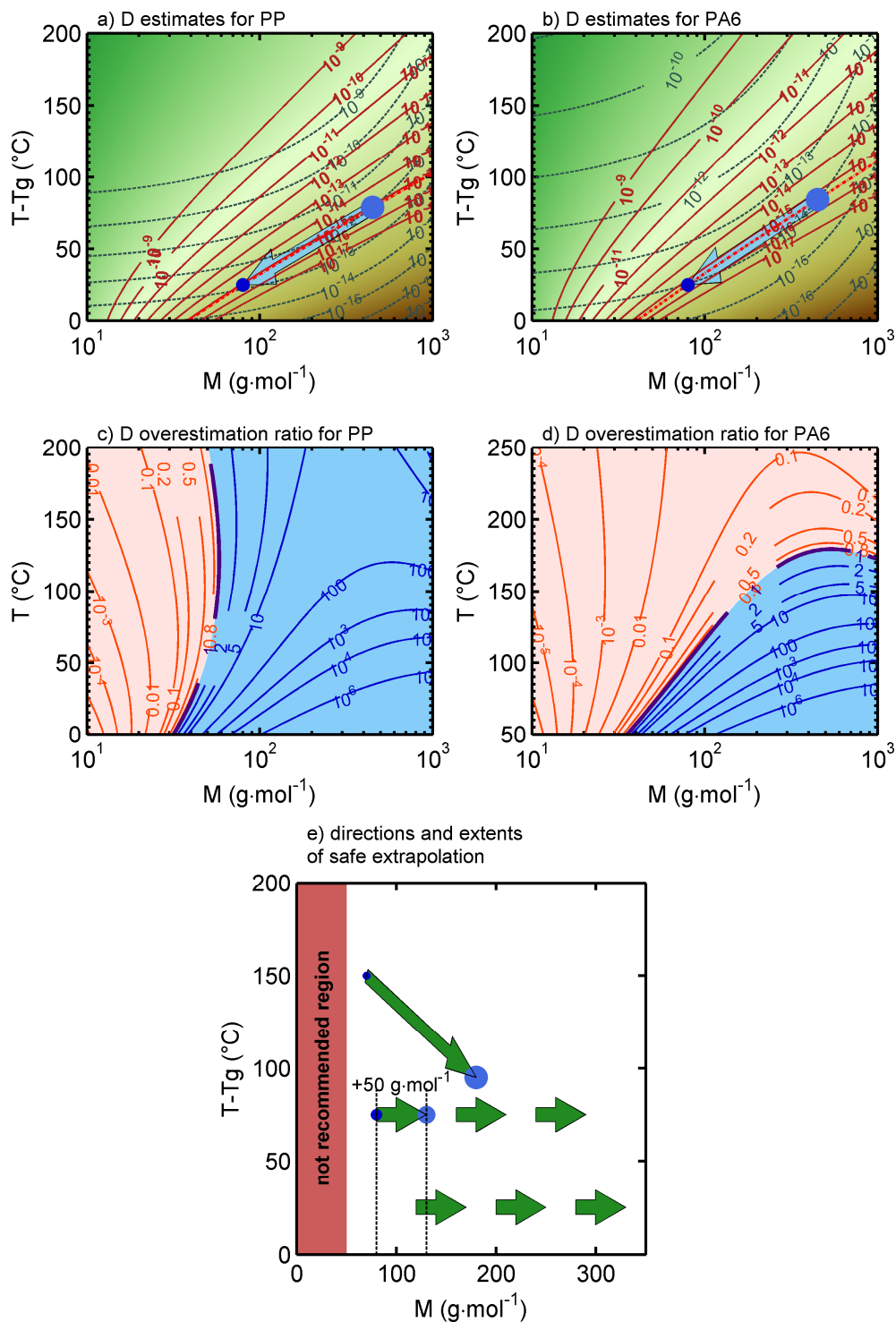


Figure 2-20 Evaluation of the robustness of the Piringer model for two typical polymers above their T_g : a), c) polypropylene ($T_g=0^\circ\text{C}$) and b), d) polyamide ($T_g=50^\circ\text{C}$). The considered diffusants are aliphatic solutes (e.g. alkanes and alkyl acetates) below the entanglement length. a-b) Comparison between iso- D values (from Fang *et al.* (2013), see Table 2-6, solid lines) and iso- \bar{D} values obtained from Piringer model (see Table 2-9, dashed lines). c,d) Corresponding iso-ratios \bar{D}/D where “safe regions” (with overestimations) are depicted in light blue. e) Safe strategies to extend the Piringer model to new polymers in presence of scarce data.

Finally, one may notice that the Piringer model has been also proposed for non-thermoplastic materials such as paper and cardboard (Poças *et al.*, 2011; Störmer, 2010). As these materials are porous with a mass transfer occurring significantly in the gas phase, the general transfer mechanism does not obey to the previous diffusion-dissolution model presented in this review (see section 6.4 from Cussler (2009) for details). Since the detailed mechanisms depend on microscopic details (*e.g.* Knudsen diffusion, capillary condensation, surface diffusion...), they cannot fall within the category of “General recognized diffusion models” (see section 2.1.3). The relative higher importance of the transport through the gas phase will decrease the scaling exponents of effective diffusion coefficients α down to 1/2 or 1/3. Due to a strong risk of underestimation of real D values when it is applied to substances different from tested ones, the usage of the Piringer model or of any free-volume theory should be avoided in these situations.

2.1.8.3 Prediction of D based on decision trees and molecular descriptors

Figure 2-18 showed that diffusion coefficients cannot be explained by a sole molecular descriptor such as molecular mass, M , in particular for large diffusants. For a same M value, the uncertainty can reach three decades (Reynier *et al.*, 2001a). This variability for a same M is associated to coupled displacements of several host segments to reach a translation of large solutes. They cause a significant increase of delays between successive hoppings of diffusant elemental jumping-units. In the framework of generalized free-volume theory, these effects are captured through the prefactor $C(\text{diffusant}, T)$ (see in Eq. (2-23)). Using a different approach, Helmroth *et al.* (2005) proposed to solve the lack of prediction of simple models such as Piringer one by combining a master curve depending only on M with an upper envelope collecting all other effects not related to M . The values of D were assumed log-normal distributed with a standard deviation of $\log \check{D}$, s , as listed in Table 2-9. The integration of an upper confidence interval in the approach offers interesting overestimation capabilities but as in the Piringer model the overestimation ratio remains in essence variable for a same molecular mass and variable with temperature due to a global definition of s and the significant variation of $\frac{\partial \ln D}{\partial \ln M}$ with temperature (see Figure 2-19).

An alternative model was developed by Reynier *et al.* (2001b) and extended significantly by Vitrac *et al.* (2006) based on CART (classification and regression tree) methods. The main advantage of CART is that there are human readable while being able to describe any non-linear behavior (continuous or not). Starting from mechanistic considerations of diffusion close those used in Vrentas and Vrentas (1998), three descriptors (see Table 2-11) have been

proposed to describe *a priori* the diffusion behavior of migrants regardless the considered polymer and temperature: van-der-Waals volume, gyration radius, shape factor. Their values are illustrated in Table 2-12 for typical diffusants. Without fitting, it has been shown that such a classification was able to gather homologous molecules with similar diffusion coefficients. This concept is illustrated on a commercial UV-stabilizer in Figure 2-21. It demonstrates that the diffusant shape and rigidity are the main characteristics controlling the diffusion coefficients rather than the detailed chemistry.

Table 2-11 Main geometric parameters used in CART approaches (Vitrac *et al.*, 2006) and their physical justifications. Conformers are usually obtained from molecular dynamics simulation to reach representative configurations at the considered temperature.

Property	Ensemble average	Associated mechanism
van-der-Waals volume	$\langle V_{vdW} \rangle_{\text{configurations}}$	Scaling law $D \propto M^{-\alpha}$ Activation volume represents a fraction of VdW volum
gyration radius	$\langle \rho \rangle_{\text{configurations}}$	Translation by rotation around a position different than the center of gravity
Shape parameter	$\langle I_z / I_x \rangle_{\text{configurations}}$	Translation in a favour direction (or corollary: a direction of translation is severely disadvantaged)

Table 2-12 Values of topological descriptors for six typical molecules as associated to their state of minimum internal energy. The values are ordered as V_{vdW} , ρ , I_z / I_x (see Table 2-11). All molecules were oriented along their main axes (x, y and z); the three main projected surfaces are also depicted.

β -pinene			Limonene			BHT			Chimassorb 90			Irganox 1076			Irgafos 168		
154	2,5	1,68	158	2,91	4,75	243	3,56	2,65	207	3,9	5,97	593	9,73	22	675	5,72	1,94

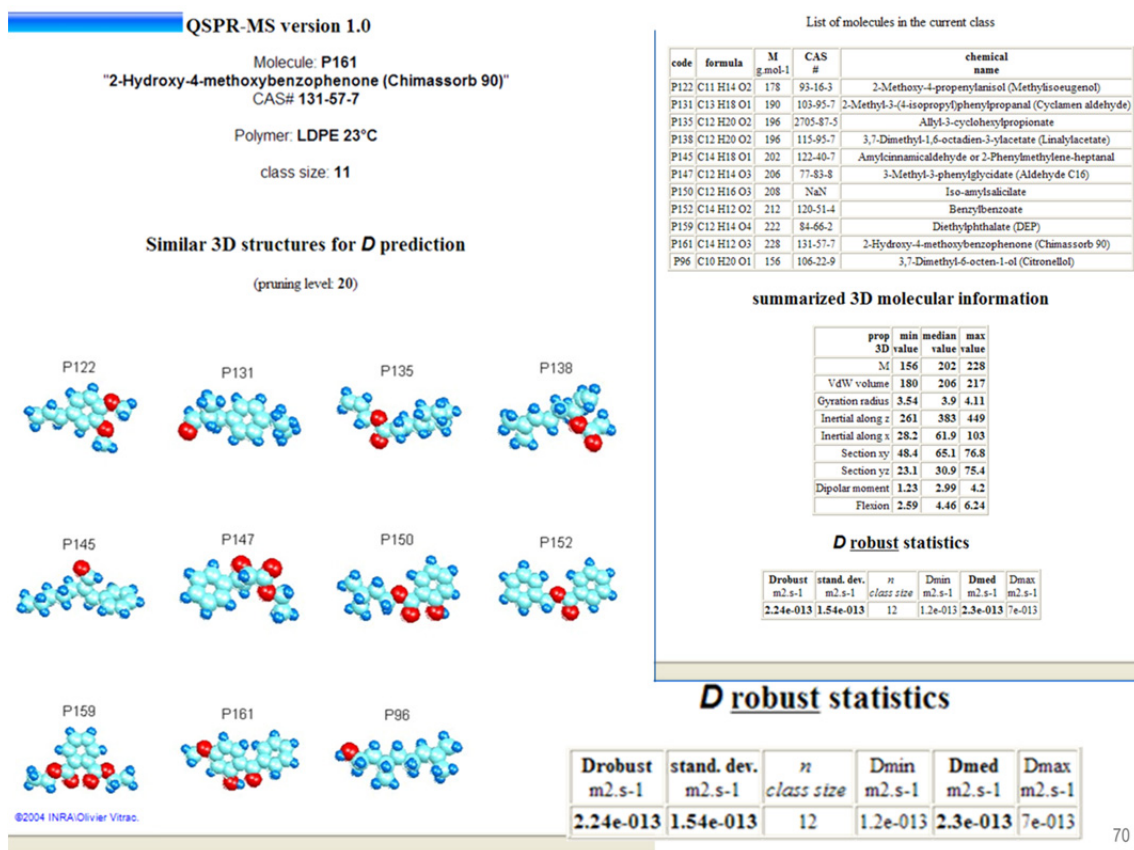


Figure 2-21 Example of automatic classification of Chimassorb 90 (Vitrac *et al.*, 2006). The request has been typed online on the Safe Food Packaging Portal (INRA, 2011), which gives in return all substances in the EU database with similar *D* values.

Regression trees generalize classification trees with an aim of predicting *D* values while keeping similar simplicity (Breiman, 1984). It is a non-linear procedure, belonging to a broad range of machine learning methods, where the mathematical model is coded as a flow chart. Each internal node denotes a test on one of the three considered geometry factors. The last node (leaf) contains an estimate of *D* values: either the median of diffusion coefficients or an upper percentile. The model to predict diffusion coefficients in LDPE is depicted in Figure 2-22. The predictions from pruned and cross-validated trees are plotted in Figure 2-18. Contrary to previous models, the approach was able to keep the variability of original data (tested on 657 *D* values including 267 substances, see Vitrac *et al.* (2006) for details).

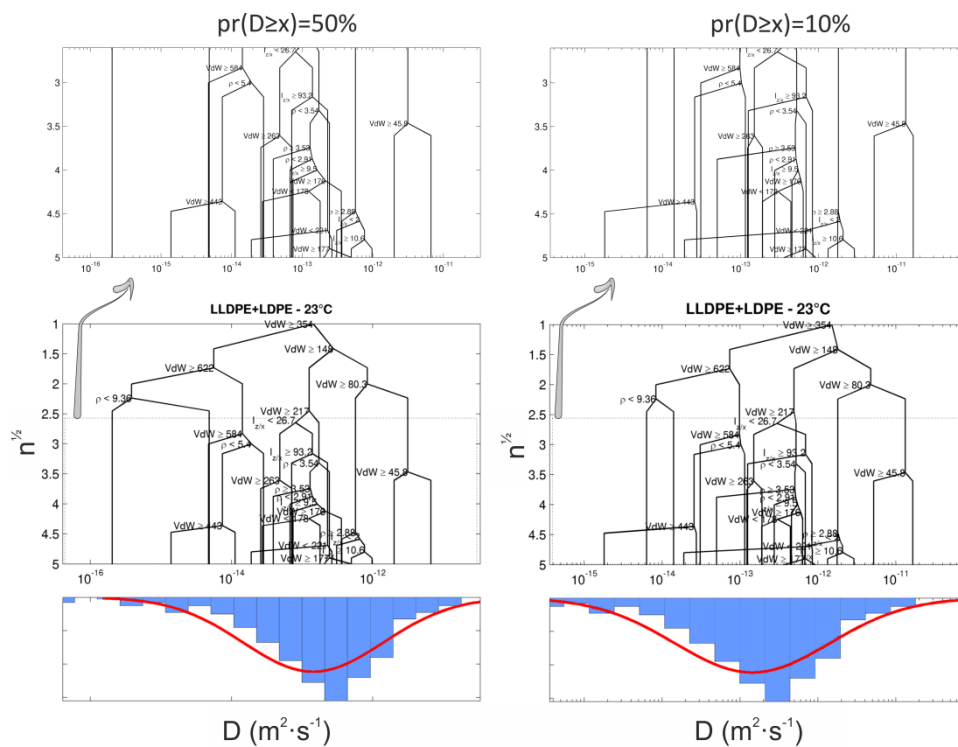


Figure 2-22 Decision tree for the prediction of diffusion coefficients in LDPE at 23°C with different risks of overestimations: 50% or 10% (after Vitrac *et al.* (2006)).

2.1.9 Conclusions

The general discussion initiated by Gillet *et al.* (2009b) on the applicability of mathematical modeling for compliance testing showed that the interest in predictive methods drop dramatically when more than two parameters are unknown: identity of substances, concentration in the materials, diffusion and partition coefficients, external mass transfer resistance. Beyond two unknowns, uncertainty is increasing dramatically so that overestimated values of the migration tend to be systematically over all prescribed thresholds. Substituting point estimates of parameters (without limitations of their number) by their statistical distributions lessens the previous limitations, as demonstrated by Vitrac and Hayert (2005, 2007a) for monolayer and multilayer packaging materials respectively. Without providing additional knowledge, the probabilistic approach combines in various sources of uncertainty and variability, which is more acceptable in particular for risk assessment. Building a mechanistic approach is however more satisfactory as it authorizes modeling as an extrapolation tool to new substances, polymers and conditions (plasticization, temperature). In silico methods are already available for partition coefficients (see introduction) but they start also to be available for diffusion coefficients. As a result, the paradigm of migration modeling may evolve from a prediction in worst-case conditions to real ones with controlled margin of safety. Recently the molecular concepts presented in this review have been integrated in a

research collaborative project SafeFoodPack Design with an aim of developing an engineering approach of “safe” packaging materials (Nguyen *et al.*, 2013). Beyond the concepts optimizing packaging assemblies (*e.g.* with proper functional barriers) and their formulations (*e.g.* substances with lower diffusivities, solubilities and concentrations), intentionally added substances could be also redesigned to minimize the risk of migration for certain usages (*e.g.* sterilization, oven-heating). As a possible illustration, it has been shown that adding a flexible group close to the center of mass of the substances could decrease D by one decade for each 1.3 carbon added (Fang *et al.*, 2013). A list of strategies to reduce the leaching of additives has been itemized by Bart (2006) (see Table 2.19):

- 1) Maximizing solubility or minimize vapor pressure (by adding solubilizing groups, preferring compounds with a low melting point).
- 2) Minimizing volatility and solvent extractability (by adding large substances, preferring oligomeric additives).
- 3) Reducing diffusion (by adding oligomeric additives, polymeric additives).
- 4) Preferring polymer-bound additives (by copolymerization, reactive processing).

Several free and open databases tools and software implement the concepts presented here including: the Safe Food Packaging Portal (databases, real time probabilistic modeling, lectures...) (INRA, 2011), SFPP3 (multilayer modeling) (INRA, 2010), FMECAengine (Vitrac, 2012) (open source implementation of Failure Mode Effects and Criticality Analysis method for packaging and combining chained modeling, sensitivity analysis, migration modeling, expert systems). The end-user should find an incentive by noticing that the present concepts are not limited to thermoplastics but cover any dense polymer matrix cross-linked or not. Technical laboratories are encouraged to integrate the last progress in migration modeling to help the industry to comply with its legal requirements and to implement new integrated food management systems such as ISO 22000.

2.1.10 References

- Adams, W. A., Xu, Y., Little, J. C., Fristachi, A. F., Rice, G. E., and Impellitteri, C. A. (2011). Predicting the migration rate of dialkyl organotin from PVC pipe into water. *Environ Sci Technol.* **45**: 6902-6907.
- Aichele, M., Gebremichael, Y., Starr, F. W., Baschnagel, J., and Glotzer, S. C. (2003). Polymer-specific effects of bulk relaxation and stringlike correlated motion in the dynamics of a supercooled polymer melt. *The Journal of Chemical Physics.* **119**: 5290-5304.
- Al-Malack, M. H. (2001). Migration of lead from unplasticized polyvinyl chloride pipes. *J Hazard Mater.* **82**: 263-274.
- Alexander Stern, S. (1994). Polymers for gas separations: the next decade. *Journal of Membrane Science.* **94**: 1-65.
- Alfadul, S. M., and Elneshwy, A. A. (2010). Use of nanotechnology in food processing, packaging and safety - review. *African Journal of Food, Agriculture, Nutrition and Development.* **10**: 2719-2739.
- Alin, J., and Hakkarainen, M. (2011). Microwave Heating Causes Rapid Degradation of Antioxidants in Polypropylene Packaging, Leading to Greatly Increased Specific Migration to Food Simulants As Shown by ESI-MS and GC-MS. *Journal of Agricultural and Food Chemistry.* **59**: 5418-5427.
- Alin, J., and Hakkarainen, M. (2012). Migration from polycarbonate packaging to food simulants during microwave heating. *Polymer Degradation and Stability.* **97**: 1387-1395.
- Anderson, W. A. C., and Castle, L. (2003). Benzophenone in cartonboard packaging materials and the factors that influence its migration into food. *Food Additives and Contaminants.* **20**: 607-618.
- Arnold, J. C. (2010). A free-volume hole-filling model for the solubility of liquid molecules in glassy polymers 1: Model derivation. *European Polymer Journal.* **46**: 1131-1140.
- Arnould, D., and Laurence, R. L. (1992). Size effects on solvent diffusion in polymers. *Industrial & Engineering Chemistry Research.* **31**: 218-228.
- Arora, A., and Padua, G. W. (2010). Review: nanocomposites in food packaging. *Journal of Food Science.* **75**: R43-R49.
- Arvanitoyannis, I. S., and Bosnea, L. (2004). Migration of substances from food packaging materials to foods. *Critical Reviews in Food Science and Nutrition.* **44**: 63-76.
- Aurela, B., Ohra-aho, T., and Soderhjelm, L. (2001). Migration of alkylbenzenes from packaging into food and Tenax (R). *Packaging Technology and Science.* **14**: 71-77.
- Az, R., Dewald, B., and Schnaitmann, D. (1991). Pigment decomposition in polymers in applications at elevated temperatures. *Dyes and Pigments.* **15**: 1-14.
- Azeredo, H. M. C. d. (2009). Nanocomposites for food packaging applications. *Food Research International.* **42**: 1240-1253.
- Aznar, M., Rodriguez-Lafuente, A., Alfaro, P., and Nerin, C. (2012). UPLC-Q-TOF-MS analysis of non-volatile migrants from new active packaging materials. *Analytical and Bioanalytical Chemistry.* **404**: 1945-1957.
- Bach, C., Dauchy, X., Chagnon, M.-C., and Etienne, S. (2012). Chemical compounds and toxicological assessments of drinking water stored in polyethylene terephthalate (PET) bottles: A source of controversy reviewed. *Water Research.* **46**: 571-583.
- Baner, A., Brandsch, J., Franz, R., and Piringer, O. (1996). The application of a predictive migration model for evaluating the compliance of plastic materials with European food regulations†. *Food Additives and Contaminants.* **13**: 587-601.
- Barnes, K. A., Sinclair, C. R., and Watson, D. H. (2007). Chemical migration and food contact materials. Woodhead.
- Barrat, J.-L., Baschnagel, J., and Lyulin, A. (2010). Molecular dynamics simulations of glassy polymers. *Soft Matter.* **6**: 3430-3446.

- Bart, J. C. J. (2006). *Polymer Additive Analytics. Industrial Practice and Case Studies.* Firenze University Press.
- Baschnagel, J., Wittmer, J. P., and Meyer, H. (2004). Monte Carlo Simulation of Polymers: Coarse-Grained Models. **In:** *Computational Soft Matter: From Synthetic Polymers to Proteins*, pp. 83-140.
- Batra, T. (2011). Endocrine-disrupting carcinogenic plastic contamination in the food chain: a review. *Biosciences, Biotechnology Research Asia*. **8**: 597-601.
- Battelli, G., Limbo, S., Panseri, S., Chiesa, L., Pellegrino, L., Biondi, P. A., and Noni, I. d. (2011). Wrapping films for cheese packaging: qualitative aspects and migration phenomena. *Scienza e Tecnica Lattiero-Casearia*. **62**: 313-326.
- Bayer, F. L. (2002). Polyethylene terephthalate recycling for food-contact applications: testing, safety and technologies: a global perspective. *Food Additives and Contaminants Part a-Chemistry Analysis Control Exposure & Risk Assessment*. **19**: 111-134.
- Begley, T., Castle, L., Feigenbaum, A., Franz, R., Hinrichs, K., Lickly, T., Mercea, P., Milana, M., O'Brien, A., Rebre, S., Rijk, R., and Piringer, O. (2005). Evaluation of migration models that might be used in support of regulations for food-contact plastics. *Food Additives and Contaminants*. **22**: 73-90.
- Begley, T. H., and Hollifield, H. C. (1993). Recycled polymers in food packaging: migration considerations. *Food Technology*. **47**: 109-112.
- Berens, A. R. (1981). Vinyl chloride monomer in PVC: from problem to probe. *Pure Appl. Chem*. **53**: 365-375.
- Berg, H. C. (1993). *Random Walks in Biology.* Princeton University Press.
- Berlinet, C., Brat, P., and Ducruet, V. (2008). Quality of orange juice in barrier packaging material. *Packaging Technology and Science*. **21**: 279-286.
- Biedermann, M., Ingenhoff, J. E., Dima, G., Zurfluh, M., Biedermann-Brem, S., Richter, L., Simat, T., Harling, A., and Grob, K. (2013). Migration of mineral oil from printed paperboard into dry foods: survey of the German market. Part II: advancement of migration during storage. *European Food Research and Technology*. **236**: 459-472.
- Biedermann, M., Uematsu, Y., and Grob, K. (2011). Mineral oil contents in paper and board recycled to paperboard for food packaging. *Packaging Technology and Science*. **24**: 61-73.
- Boersma, A. (2003). Mobility and solubility of antioxidants and oxygen in glassy polymers. I. Concentration and temperature dependence of antioxidant sorption. *Journal of Applied Polymer Science*. **89**: 2163-2178.
- Boersma, A., Cangialosi, D., and Picken, S. J. (2003a). Mobility and solubility of antioxidants and oxygen in glassy polymers II. Influence of physical ageing on antioxidant and oxygen mobility. *Polymer Degradation and Stability*. **79**: 427-438.
- Boersma, A., Cangialosi, D., and Picken, S. J. (2003b). Mobility and solubility of antioxidants and oxygen in glassy polymers. III. Influence of deformation and orientation on oxygen permeability. *Polymer*. **44**: 2463-2471.
- Boulougouris, G. C. (2010). Calculation of the chemical potential beyond the first-order free-energy perturbation: from deletion to reinsertion†. *Journal of Chemical & Engineering Data*. **55**: 4140-4146.
- Boulougouris, G. C. (2011). On the estimation of the free energy, from a single equilibrium statistical ensemble, via particle reinsertion. *The Journal of Physical Chemistry B*. **116**: 997-1006.
- Brandrup, J., Immergut, E. H., and Grulke, E. A. (1999). *Polymer Handbook.* John Wiley & Sons.
- Brandsch, J., Mercea, P., Rüter, M., Tosa, V., and Piringer, O. (2002). Migration modelling as a tool for quality assurance of food packaging. *Food Additives and Contaminants*. **19**: 29-41.
- Breiman, L. (1984). *Classification and Regression Trees.* Wadsworth International Group.

- Brimer, L., and Skaanild, M. T. (2011). Chemical Food Safety. CABI.
- Broglioli, D., and Vailati, A. (2000). Diffusive mass transfer by nonequilibrium fluctuations: Fick's law revisited. *Physical Review E*. **63**: 012105.
- Brydson, J. A. (1999). Plastics Materials. Elsevier Science.
- Bueche, F. (1968). Diffusion of polystyrene in polystyrene: effect of matrix molecular weight. *The Journal of Chemical Physics*. **48**: 1410-1411.
- Buonocore, G. G., Del Nobile, M. A., Panizza, A., Corbo, M. R., and Nicolais, L. (2003). A general approach to describe the antimicrobial agent release from highly swellable films intended for food packaging applications. *Journal of Controlled Release*. **90**: 97-107.
- Busolo, M. A., and Lagaron, J. M. (2012). Oxygen scavenging polyolefin nanocomposite films containing an iron modified kaolinite of interest in active food packaging applications. *Innovative Food Science & Emerging Technologies*. **16**: 211-217.
- Callaghan, P. T., and Pinder, D. N. (1984). Influence of multiple length scales on the behavior of polymer self-diffusion in the semidilute regime. *Macromolecules*. **17**: 431-437.
- Callister, W. D., and Rethwisch, D. G. (2011). Chapter 4. Polymer structures. **In**: Fundamentals of Materials Science and Engineering: An Integrated Approach. Wiley, New York.
- Camacho, W., and Karlsson, S. (2000). Quality-determination of recycled plastic packaging waste by identification of contaminants by CC-MS after microwave assisted extraction (MAE). *Polymer Degradation and Stability*. **71**: 123-134.
- Caner, C., Hernandez, R. J., Pascall, M., Balasubramaniam, V. M., and Harte, B. R. (2004). The effect of high-pressure food processing on the sorption behaviour of selected packaging materials. *Packaging Technology and Science*. **17**: 139-153.
- Cao, X.-L., and Corriveau, J. (2008). Migration of bisphenol A from polycarbonate baby and water bottles into water under severe conditions. *Journal of Agricultural and Food Chemistry*. **56**: 6378-6381.
- CFR (2011). Federal Food, Drug, and Cosmetic Act. **In**: Title 21 - Food and drugs, pp. 109-113. FDA (Ed.), US government Printing Office, Washington D.C.
- CFR (2012a). Part 184 - Direct food substances affirmed as generally recognized as safe. **In**: Title 21. Code of Federal Regulations.
- CFR (2012b). Part 186 - Indirect food substances affirmed as generally recognized as safe. **In**: Title 21. Code of Federal Regulations.
- CFR (2012c). Section 170.39 - Threshold of regulation for substances used in food-contact articles. **In**: Title 21. Code of Federal Regulations.
- Chatwin, P. C., and Katan, L. L. (1989). The role of mathematics and physics in migration predictions. *Packaging Technology and Science*. **2**: 75-84.
- Chen, S. P., and Ferry, J. D. (1968). Erratum-the diffusion of radioactively tagged n-hexadecane and n-dodecane through rubbery polymers. effects of temperature, cross-linking, and chemical structure. *Macromolecules*. **1**: 374-374.
- Chernikov, A. A., Petrovichev, B. A., Rogal'sky, A. V., Sagdeev, R. Z., and Zaslavsky, G. M. (1990). Anomalous transport of streamlines due to their chaos and their spatial topology. *Physics Letters A*. **144**: 127-133.
- Choudalakis, G., and Gotsis, A. D. (2009). Permeability of polymer/clay nanocomposites: A review. *European Polymer Journal*. **45**: 967-984.
- Cohen, M. H., and Turnbull, D. (1959). Molecular transport in liquids and glasses. *The Journal of Chemical Physics*. **31**: 1164-1169.
- Consolati, G., and Quasso, F. (2001). An experimental study of the occupied volume in polyethylene terephthalate. *The Journal of Chemical Physics*. **114**: 2825-2829.
- Costa, F. R., Dutta, N. K., Choudhury, N. R., and Bhowmick, A. K. (2010). Chapter 5. Thermoplastic Elastomers. **In**: Current Topics in Elastomers Research. Bhowmick, A. K. (Ed.), Taylor & Francis.

- Coughlin, C. S., Mauritz, K. A., and Storey, R. F. (1990). A general free volume based theory for the diffusion of large molecules in amorphous polymers above Tg. 3. Theoretical conformational analysis of molecular shape. *Macromolecules*. **23**: 3187-3192.
- Coughlin, C. S., Mauritz, K. A., and Storey, R. F. (1991a). A general free-volume-based theory for the diffusion of large molecules in amorphous polymers above glass temperature. 5. Application to dialkyl adipate plasticizers in poly(vinyl chloride). *Macromolecules*. **24**: 2113-2116.
- Coughlin, C. S., Mauritz, K. A., and Storey, R. F. (1991b). A general free volume based theory for the diffusion of large molecules in amorphous polymers above Tg. 4. Polymer-penetrant interactions. *Macromolecules*. **24**: 1526-1534.
- Courgneau, C., Domenek, S., Guinault, A., Avérous, L., and Ducruet, V. (2011). Analysis of the structure-properties relationships of different multiphase systems based on plasticized poly(lactic acid). *Journal of Polymers and the Environment*. **19**: 362-371.
- Crank, J. (1979). *The Mathematics of Diffusion*. Clarendon Press.
- Crawshaw, J., and Windle, A. H. (2003). Multiscale modelling in polymer science. *Fibre Diffraction Review*. **11**: 52-67.
- Crockett, C., and Sumar, S. (1996). The safe use of recycled and reused plastics in food contact materials. II. *Nutrition and Food Science*: 34-37.
- Crompton, T. R. (2007). *Additive Migration from Plastics Into Foods: A Guide for Analytical Chemists*. Smithers Rapra Technology.
- Cruz, J. M., Sanches Silva, A., Sendón García, R., Franz, R., and Paseiro Losada, P. (2008). Studies of mass transport of model chemicals from packaging into and within cheeses. *Journal of Food Engineering*. **87**: 107-115.
- Cruz, S. A., Oliveira, E. C., de Oliveira, F. C. S., Garcia, P. S., and Kaneko, M. L. Q. A. (2011). Recycled polymers for food contact. *Polimeros-Ciencia E Tecnologia*. **21**: 340-345.
- Curtiss, C. F., and Bird, R. B. (1996). Multicomponent diffusion in polymeric liquids. *Proceedings of the National Academy of Sciences*. **93**: 7440-7445.
- Cussler, E. L. (2009). *Diffusion: Mass Transfer in Fluid Systems*. Cambridge University Press.
- D'Hollander, W., de Voogt, P., De Coen, W., and Bervoets, L. (2010). Perfluorinated substances in human food and other sources of human exposure. *Rev Environ Contam Toxicol*. **208**: 179-215.
- De Angelis, M. G., Boulougouris, G. C., and Theodorou, D. N. (2010). Prediction of Infinite Dilution Benzene Solubility in Linear Polyethylene Melts via the Direct Particle Deletion Method. *The Journal of Physical Chemistry B*. **114**: 6233-6246.
- De Gennes, P. G. (1971). Reptation of a polymer chain in the presence of fixed obstacles. *The Journal of Chemical Physics*. **55**: 572-579.
- Del Nobile, M. A., Mensitieri, G., Netti, P. A., and Nicolais, L. (1994). Anomalous diffusion in poly-ether-ether-ketone. *Chemical Engineering Science*. **49**: 633-644.
- Delmaar, J. E., Park, M. V. D. Z., and van Engelen, J. G. M. (2005) *ConsExpo 4.0-Consumer Exposure and Uptake Models -Program Manual* RIVM report 320104004. National Institute of Public Health and the Environment (RIVM). Bilthoven, The Netherlands.
- Deppe, D. D., Miller, R. D., and Torkelson, J. M. (1996). Small molecule diffusion in a rubbery polymer near Tg: Effects of probe size, shape, and flexibility. *Journal of Polymer Science Part B: Polymer Physics*. **34**: 2987-2997.
- Derjaguin, B. (1934). Untersuchungen über die Reibung und Adhäsion, IV. *Kolloid-Zeitschrift*. **69**: 155-164.
- Deshpande, S. S. (2002). *Handbook of Food Toxicology*. Marcel Dekker, Inc., New-York.
- Dobiáš, J., Voldřich, M., Marek, M., and Chudáčková, K. (2004). Changes of properties of polymer packaging films during high pressure treatment. *Journal of Food Engineering*. **61**: 545-549.

- Doi, M., and Edwards, S. F. (1978). Dynamics of concentrated polymer systems. Part 1.- Brownian motion in the equilibrium state. *Journal of the Chemical Society, Faraday Transactions 2: Molecular and Chemical Physics*. **74**: 1789-1801.
- Dole, P., Feigenbaum, A. E., Cruz, C. D. L., Pastorelli, S., Paseiro, P., Hankemeier, T., Voulzatis, Y., Aucejo, S., Saillard, P., and Papaspyrides, C. (2006a). Typical diffusion behaviour in packaging polymers—application to functional barriers. *Food Additives and Contaminants*. **23**: 202-211.
- Dole, P., Voulzatis, Y., Vitrac, O., Reynier, A., Hankemeier, T., Aucejo, S., and Feigenbaum, A. (2006b). Modelling of migration from multi-layers and functional barriers: Estimation of parameters. *Food Additives and Contaminants*. **23**: 1038-1052.
- Doolittle, A. K. (1951). Studies in Newtonian Flow. I. The Dependence of the Viscosity of Liquids on Temperature. *Journal of Applied Physics*. **22**: 1031-1035.
- Doong, S. J., and Ho, W. S. W. (1992). Diffusion of hydrocarbons in polyethylene. *Industrial & Engineering Chemistry Research*. **31**: 1050-1060.
- Dopico-Garcia, M. S., Lopez-Vilarino, J. M., and Gonzalez-Rodriguez, M. V. (2003). Determination of antioxidant migration levels from low-density polyethylene films into food simulants. *J Chromatogr A*. **1018**: 53-62.
- du Yeon, B., Minji, K., Min Ji, K., Bu Young, J., Myung Chan, C., Seul Min, C., Young Woo, K., Seong Kwang, L., Duck Soo, L., Won, A. J., Seung Jun, K., Youngkwan, L., Hyung Sik, K., and Byung Mu, L. (2012). Human risk assessment of endocrine-disrupting chemicals derived from plastic food containers. *Comprehensive Reviews in Food Science and Food Safety*. **11**: 453-470.
- Dubreuil, A.-C., Doumenc, F., Guerrier, B., and Allain, C. (2003). Mutual diffusion in PMMA/PnBMA copolymer films: influence of the solvent-induced glass transition. *Macromolecules*. **36**: 5157-5164.
- Ducruet, V., Vitrac, O., Saillard, P., Guichard, E., Feigenbaum, A., and Fournier, N. (2007). Sorption of aroma compounds in PET and PVC during the storage of a strawberry syrup. *Food Additives and Contaminants Part a-Chemistry Analysis Control Exposure & Risk Assessment*. **24**: 1306-1317.
- Durand, M., Meyer, H., Benzerara, O., Baschnagel, J., and Vitrac, O. (2010). Molecular dynamics simulations of the chain dynamics in monodisperse oligomer melts and of the oligomer tracer diffusion in an entangled polymer matrix. *Journal of Chemical Physics*. **132**.
- Dutra, C., Pezo, D., Freire, M. T. d. A., Nerín, C., and Reyes, F. G. R. (2011). Determination of volatile organic compounds in recycled polyethylene terephthalate and high-density polyethylene by headspace solid phase microextraction gas chromatography mass spectrometry to evaluate the efficiency of recycling processes. *Journal of Chromatography A*. **1218**: 1319-1330.
- EC (2002a). Commission Directive 2002/72/EC of 6 August 2002 relating to plastic materials and articles intended to come into contact with foodstuffs. *Official Journal of the European Communities*. **L 220**: 18-58.
- EC (2002b) Evaluation of Migration Models to be used under Directive 90/128/EEC. Final report contract SMT4-CT98-7513. European Commission. Brussels.
- EC (2004). Regulation (EC) No 1935/2004 of the European parliament and of the council of 27 October 2004 on materials and articles intended to come into contact with food and repealing Directives 80/590/EEC and 89/109/EEC. *Official Journal of the European Union*. **L 338**: 4-17.
- EC (2011). Commission Regulation (EU) No 10/2011 of 14 January 2011 on plastic materials and articles intended to come into contact with food. *Official Journal of the European Union*. **L 12**: 1-89.

- EC (2012a). Commission Regulation (EU) No 1183/2012 of 30 November 2012 amending and correcting Regulation (EU) No 10/2011 on plastic materials and articles intended to come into contact with food. *Official Journal of the European Union*. **L 338**: 11-15.
- EC (2012b). Corrigendum to Commission Regulation (EU) No 1183/2012 of 30 November 2012 amending and correcting Regulation (EU) No 10/2011 on plastic materials and articles intended to come into contact with food. *Official Journal of the European Union*. **L 349**: 77.
- EC (2012c) Practical guidance document on the implementation of diffusion modelling for the estimation of specific migration in support of Regulation (EU) No 10/2011. Joint Research Centre of the European Commission. Ispra, Italy.
- EC (2013) Estimation of specific migration by generally recognised diffusion models in support of Regulation (EC) No 10/2011. Joint Research Centre of the European Commission. Ispra, Italy.
- Edwards, C. J. C., Rigby, D., and Stepto, R. F. T. (1981). Kirkwood-Riseman interpretation of the diffusion behavior of short polymer chains in dilute solution. *Macromolecules*. **14**: 1808-1812.
- Ehlich, D., and Sillescu, H. (1990). Tracer diffusion at the glass transition. *Macromolecules*. **23**: 1600-1610.
- Einstein, A. (1905a). On the movement of small particles suspended in a stationary liquid demanded by the molecular-kinetic theory of heat. *Annalen der Physik (Leipzig)*. **17**: 549-560.
- Einstein, A. (1905b). Über die von der molekularkinetischen Theorie der Wärme geforderte Bewegung von in ruhenden Flüssigkeiten suspendierten Teilchen. *Annalen der Physik*. **322**: 549-560.
- Einstein, A., and Fürth, R. (1956). Investigations on the Theory of the Brownian Movement. Dover Publications.
- Eu, B. C. (2006). Transport Coefficients of Fluids. Springer London, Limited.
- Fang, X., Domenek, S., Ducruet, V., Réfrégiers, M., and Vitrac, O. (2013). Diffusion of aromatic solutes in aliphatic polymers above glass transition temperature. *Macromolecules*. **46**: 874-888.
- FDA (1999) Guidance for Industry-Preparation of Premarket Notifications for Food Contact Substances: Chemistry Recommendation. FDA. Washington, DC, USA.
- FDA (2006). Guidance for Industry: Use of Recycled Plastics in Food Packaging: Chemistry Considerations. Available: <http://www.fda.gov/food/guidancecomplianceregulatoryinformation/GuidanceDocuments/FoodIngredientsandPackaging/ucm120762.htm>. Date accessed: Feb. 1, 2013.
- FDA (2007). Guidance for Industry: Preparation of Premarket Submissions for Food Contact Substances: Chemistry Recommendations. Available: <http://www.fda.gov/Food/GuidanceComplianceRegulatoryInformation/GuidanceDocuments/FoodIngredientsandPackaging/ucm081818.htm>. Date accessed: Feb. 1, 2013.
- FDA (2012a). Food Ingredients and Packaging Guidance for Industry. Available: <http://www.fda.gov/Food/GuidanceComplianceRegulatoryInformation/GuidanceDocuments/FoodIngredientsandPackaging/#food>. Date accessed: Jan. 4, 2012.
- FDA (2012b). Inventory of Effective Food Contact Substance (FCS) Notifications. Available: <http://www.accessdata.fda.gov/scripts/fcn/fcnNavigation.cfm?filter=&sortColumn=&rp t=fcsListing>. Date accessed: Jan. 4, 2013.
- Fei, F., Chen, Q., Liu, Z., Liu, F., and Solodovnyk, A. (2012). The application of Nano-SiO_x coatings as migration resistance layer by plasma enhanced chemical vapor deposition. *Plasma Chemistry and Plasma Processing*. **32**: 755-766.
- Feigenbaum, A., Dole, P., Aucejo, S., Dainelli, D., Garcia, C. D. L. C., Hankemeier, T., N'Gono, Y., Papaspyrides, C. D., Paseiro, P., Pastorelli, S., Pavlidou, S., Pennarun, P.

- Y., Saillard, P., Vidal, L., Vitrac, O., and Voulzatis, Y. (2005). Functional barriers: properties and evaluation. *Food Additives and Contaminants*. **22**: 956-967.
- Feigenbaum, A., Scholler, D., Bouquant, J., Brigot, G., Ferrier, D., Franz, R., Lillemark, L., Riquet, A. M., Petersen, J. H., Lierop, B. V., and Yagoubi, N. (2002). Safety and quality of food contact materials. Part 1: Evaluation of analytical strategies to introduce migration testing into good manufacturing practice. *Food Additives and Contaminants*. **19**: 184-201.
- Feigenbaum, A. E., Ducruet, V. J., Delpal, S., Wolff, N., Gabel, J. P., and Wittmann, J. C. (1991). Food and packaging interactions: penetration of fatty food simulants into rigid poly(vinyl chloride). *Journal of Agricultural and Food Chemistry*. **39**: 1927-1932.
- Felix, J. S., Isella, F., Bosetti, O., and Nerin, C. (2012). Analytical tools for identification of non-intentionally added substances (NIAS) coming from polyurethane adhesives in multilayer packaging materials and their migration into food simulants. *Analytical and Bioanalytical Chemistry*. **403**: 2869-2882.
- Felix, J. S., Manzoli, J. E., Padula, M., and Monteiro, M. (2008). Plastic packaging with polyamide 6 used for meat foodstuffs and cheese: caprolactam migration and effect of irradiation. A review. *Alimentos e Nutricao*. **19**: 19 (13) 361-370.
- Ferry, J. D., Landel, R. F., and Williams, M. L. (1955). Extensions of the Rouse theory of viscoelastic properties to undiluted linear polymers. *Journal of Applied Physics*. **26**: 359-362.
- Fierens, T., Servaes, K., Van Holderbeke, M., Geerts, L., De Henauw, S., Sioen, I., and Vanermen, G. (2012). Analysis of phthalates in food products and packaging materials sold on the Belgian market. *Food and Chemical Toxicology*. **50**: 2575-2583.
- Fiselier, K., and Grob, K. (2012). Barriers against the migration of mineral oil from paperboard food packaging: experimental determination of breakthrough periods. *Packaging Technology and Science*. **25**: 285-301.
- Fordham, P. J., Gramshaw, J. W., Crews, H. M., and Castle, L. (1995). Element residues in food contact plastics and their migration into food simulants, measured by inductively-coupled plasma-mass spectrometry. *Food Additives and Contaminants*. **12**: 651-669.
- Forrest, J. (2007). Coatings and Inks for Food Contact Materials. Rapra Technology.
- Franz, R., and Simoneau, C. (2008) Final report: Modelling migration from plastics into foodstuffs as a novel and cost efficient tool for estimation of consumer exposure from food contact materials. EU Project QLK1-CT2002-2390. Institute for Health and Consumer Protection Luxembourg.
- Freire, M. T. D., Castle, L., Reyes, F. G. R., and Damant, A. P. (1998). Thermal stability of polyethylene terephthalate food contact materials: formation of volatiles from retail samples and implications for recycling. *Food Additives and Contaminants*. **15**: 473-480.
- Frenkel, J. (1955). Kinetic Theory of Liquids. Dover Publications.
- Geisel, T., Zacherl, A., and Radons, G. (1988). Chaotic diffusion and 1/f-noise of particles in two-dimensional solids. *Zeitschrift für Physik B Condensed Matter*. **71**: 117-127.
- Gillet, G., Vitrac, O., and Desobry, S. (2009a). Prediction of solute partition coefficients between polyolefins and alcohols using a generalized Flory-Huggins approach. *Industrial & Engineering Chemistry Research*. **48**: 5285-5301.
- Gillet, G., Vitrac, O., and Desobry, S. (2010). Prediction of partition coefficients of plastic additives between packaging materials and food simulants. *Industrial & Engineering Chemistry Research*. **49**: 7263-7280.
- Gillet, G., Vitrac, O., Tissier, D., Saillard, P., and Desobry, S. (2009b). Development of decision tools to assess migration from plastic materials in contact with food. *Food Additives and Contaminants Part a-Chemistry Analysis Control Exposure & Risk Assessment*. **26**: 1556-1573.

- Goetz, N. v., Wormuth, M., Scheringer, M., and Hungerbuehler, K. (2010). Bisphenol A: how the most relevant exposure sources contribute to total consumer exposure. *Risk Analysis*. **30**: 473-487.
- Goujot, D., and Vitrac, O. (2013). Extension to nonlinear adsorption isotherms of exact analytical solutions to mass diffusion problems. *Chemical Engineering Science*. **99**: 2-22.
- Goulas, A. E., Riganakos, K. A., Badeka, A., and Kontominas, M. G. (2002). Effect of ionizing radiation on the physicochemical and mechanical properties of commercial monolayer flexible plastics packaging materials. *Food Additives and Contaminants*. **19**: 1190-1199.
- Granda-Restrepo, D. M., Soto-Valdez, H., Peralta, E., Troncoso-Rojas, R., Vallejo-Cordoba, B., Gamez-Meza, N., and Graciano-Verdugo, A. Z. (2009). Migration of alpha-tocopherol from an active multilayer film into whole milk powder. *Food Research International*. **42**: 1396-1402.
- Gryn'ova, G., Ingold, K. U., and Coote, M. L. (2012). New Insights into the Mechanism of Amine/Nitroxide Cycling during the Hindered Amine Light Stabilizer Inhibited Oxidative Degradation of Polymers. *Journal of the American Chemical Society*. **134**: 12979-12988.
- Guart, A., Bono-Blay, F., Borrell, A., and Lacorte, S. (2011). Migration of plasticizersphthalates, bisphenol A and alkylphenols from plastic containers and evaluation of risk. *Food Additives and Contaminants Part a-Chemistry Analysis Control Exposure & Risk Assessment*. **28**: 676-685.
- Guillard, V., Mauricio-Iglesias, M., and Gontard, N. (2010). Effect of Novel Food Processing Methods on Packaging: Structure, Composition, and Migration Properties. *Critical Reviews in Food Science and Nutrition*. **50**: 969-988.
- Hakkarainen, M. (2008). Solid phase microextraction for analysis of polymer degradation products and additives. **In**: *Chromatography for Sustainable Polymeric Materials: Renewable, Degradable and Recyclable*, pp. 23-50. Albertsson, A. C., and Hakkarainen, M. (Eds.), Springer-Verlag Berlin, Berlin.
- Halden, R. U. (2010). Plastics and health risks. **In**: *Annual Review of Public Health*, Vol 31, pp. 179-194. Fielding, J. E., Brownson, R. C., and Green, L. W. (Eds.).
- Haldimann, M., Alt, A., Blanc, A., Brunner, K., Sager, F., and Dudler, V. (2012). Migration of antimony from PET trays into food simulant and food: determination of Arrhenius parameters and comparison of predicted and measured migration data. *Food Additives & Contaminants: Part A*: 1-12.
- Hall, D. B., Hamilton, K. E., Miller, R. D., and Torkelson, J. M. (1999). Translational and rotational diffusion of probe molecules in polymer films near Tg: effect of hydrogen bonding. *Macromolecules*. **32**: 8052-8058.
- Han, J. H. (2003). Chapter 4. Antimicrobial food packaging. **In**: *Novel Food Packaging Techniques*. Ahvenainen, R. (Ed.), CRC Press.
- Hanggi, P., and Marchesoni, F. (2005). Introduction: 100 years of Brownian motion. *Chaos: An Interdisciplinary Journal of Nonlinear Science*. **15**: 026101.
- Hansen, C. M. (2007). *Hansen Solubility Parameters: A User's Handbook*, Second Edition. Taylor & Francis.
- Harmandaris, V. A., Doxastakis, M., Mavrantzas, V. G., and Theodorou, D. N. (2002). Detailed molecular dynamics simulation of the self-diffusion of n-alkane and cis-1,4 polyisoprene oligomer melts. *The Journal of Chemical Physics*. **116**: 436-446.
- Hatzigrigoriou, N. B., Papaspyrides, C. D., Joly, C., and Dole, P. (2010). Effect of migrant Size on diffusion in dry and hydrated polyamide 6. *Journal of Agricultural and Food Chemistry*. **58**: 8667-8673.
- Haw, M. D. (2002). Colloidal suspensions, Brownian motion, molecular reality: a short history. *Journal of Physics: Condensed Matter*. **14**: 7769.

- Haward, R. N. (1970). Occupied volume of liquids and polymers. *Journal of Macromolecular Science, Part C*. **4**: 191-242.
- Heath, V. (2010). The perils of plastic. *Nat Rev Endocrinol*. **6**: 237.
- Hedenqvist, M., Angelstok, A., Edsberg, L., Larsson, P. T., and Gedde, U. W. (1996). Diffusion of small-molecule penetrants in polyethylene: free volume and morphology. *Polymer*. **37**: 2887-2902.
- Hedenqvist, M., and Gedde, U. W. (1996). Diffusion of small-molecule penetrants in semicrystalline polymers. *Progress in Polymer Science*. **21**: 299-333.
- Helmroth, E., Rijk, R., Dekker, M., and Jongen, W. (2002a). Predictive modelling of migration from packaging materials into food products for regulatory purposes. *Trends in Food Science & Technology*. **13**: 102-109.
- Helmroth, E., Varekamp, C., and Dekker, M. (2005). Stochastic modelling of migration from polyolefins. *Journal of the Science of Food and Agriculture*. **85**: 909-916.
- Helmroth, I. E., Dekker, M., and Hankemeier, T. (2002b). Influence of solvent absorption on the migration of Irganox 1076 from LDPE. *Food Additives and Contaminants*. **19**: 176-183.
- Hess, B., Peter, C., Ozal, T., and van der Vegt, N. F. A. (2008). Fast-Growth thermodynamic integration: calculating excess chemical potentials of additive molecules in polymer microstructures. *Macromolecules*. **41**: 2283-2289.
- Hess, B., and van der Vegt, N. F. A. (2008). Predictive modeling of phenol chemical potentials in molten bisphenol A-polycarbonate over a broad temperature range. *Macromolecules*. **41**: 7281-7283.
- Himmelsbach, M., Buchberger, W., and Reingruber, E. (2009). Determination of polymer additives by liquid chromatography coupled with mass spectrometry. A comparison of atmospheric pressure photoionization (APPI), atmospheric pressure chemical ionization (APCI), and electrospray ionization (ESI). *Polymer Degradation and Stability*. **94**: 1213-1219.
- Hoekstra, E. J., and Simoneau, C. (2011). Release of bisphenol A from polycarbonate—a review. *Critical Reviews in Food Science and Nutrition*. **53**: 386-402.
- Hsu, Y.-D., and Chen, Y.-P. (1998). Correlation of the mutual diffusion coefficients of binary liquid mixtures. *Fluid Phase Equilibria*. **152**: 149-168.
- INRA (2010). EU/FP6 Migresives closing conference. Available: http://sfpp3.agroparistech.fr/SFPP3/SFPP3_migresives/. Date accessed: 3, March, 2013.
- INRA (2011). Safe food packaging portal: research server. Available: <http://modmol.agroparistech.fr/>. Date accessed: 18 Feb, 2013.
- Ito, T., Seta, J., and Urakawa, H. (1987). Effects of pressure and solvent on the diffusion of aromatic compounds through polymers. *Colloid and Polymer Science*. **265**: 557-573.
- IUPAC (2007). Compendium of Chemical Terminology, 2nd ed, Vol 79. Blackwell Scientific Publications, Oxford.
- Jain, R. K., Gupta, R. N., and Nanda, V. S. (1975). Crystallinity, relaxational transitions, and free volume in high-density polyethylene. *Journal of Macromolecular Science, Part B*. **11**: 411-417.
- Jamshidian, M., Tehrany, E. A., and Desobry, S. (2012). Release of synthetic phenolic antioxidants from extruded poly lactic acid (PLA) film. *Food Control*. **28**: 445-455.
- Janes, D. W., and Durning, C. J. (2013). Sorption and diffusion of n-alkyl acetates in poly(methyl acrylate)/silica nanocomposites. *Macromolecules*. **46**: 856-866.
- Jiang, C., Driffield, M., Bradley, E. L., Oldring, P. K. T., Cooke, P., Castle, L., and Guthrie, J. T. (2009). Studies of the aging effect on the level of isocyanate residues in polyester-based can coating systems. *Journal of Coatings Technology and Research*. **6**: 437-444.
- Johns, S. M., Jickells, S. M., Read, W. A., and Castle, L. (2000). Studies on functional barriers to migration. 3. Migration of benzophenone and model ink components from

- cartonboard to food during frozen storage and microwave heating. *Packaging Technology and Science*. **13**: 99-104.
- Juliano, P., Koutchma, T., Sui, Q., Barbosa-Cánovas, G., and Sadler, G. (2010). Polymeric-based food packaging for high-pressure processing. *Food Engineering Reviews*. **2**: 274-297.
- Jung, T., Simat, T. J., and Altkofer, W. (2010). Mass transfer ways of ultraviolet printing ink ingredients into foodstuffs. *Food Additives and Contaminants Part a-Chemistry Analysis Control Exposure & Risk Assessment*. **27**: 1040-1049.
- Kappenstein, O., Vieth, B., Luch, A., and Pfaff, K. (2012). Toxicologically relevant phthalates in food. *Exs*. **101**: 87-106.
- Karayiannis, N. C., Mavrantzas, V. G., and Theodorou, D. N. (2001). Diffusion of small molecules in disordered media: study of the effect of kinetic and spatial heterogeneities. *Chemical Engineering Science*. **56**: 2789-2801.
- Kawamura, Y., Mutsuga, M., Yamauchi, T., Ueda, S., and Tanamoto, K. (2009). [Migration tests of cadmium and lead from paint film of baby toys]. *Shokuhin Eiseigaku Zasshi*. **50**: 93-96.
- Keffer, D. J., Edwards, B. J., and Adhangale, P. (2004). Determination of statistically reliable transport diffusivities from molecular dynamics simulation. *Journal of Non-Newtonian Fluid Mechanics*. **120**: 41-53.
- Kirkwood, J. G., and Riseman, J. (1948). The intrinsic viscosities and diffusion constants of flexible macromolecules in solution. *The Journal of Chemical Physics*. **16**: 565-573.
- Klopffer, M. H., and Flaconneche, B. (2001). Transport properties of gases in polymers: Bibliographic review. *Oil & Gas Science and Technology-Revue D Iffp Energies Nouvelles*. **56**: 223-244.
- Kontogeorgis, G. M., and Folas, G. K. (2009). *Thermodynamic Models for Industrial Applications: From Classical and Advanced Mixing Rules to Association Theories*. Wiley.
- Koszinowski, J. (1986). Diffusion and solubility of hydroxy compounds in polyolefines. *Journal of Applied Polymer Science*. **31**: 2711-2720.
- Kotelyanskii, M., and Theodorou, D. N. (2004). *Simulation Methods for Polymers*. Marcel Dekker.
- Kovarski, A. L. (1997). *Molecular Dynamics of Additives in Polymers*. VSP.
- Krishna, R., and Wesselingh, J. A. (1997). The Maxwell-Stefan approach to mass transfer. *Chemical Engineering Science*. **52**: 861-911.
- Kwan, K. S., Subramaniam, C. N. P., and Ward, T. C. (2003). Effect of penetrant size and shape on its transport through a thermoset adhesive: I. n-alkanes. *Polymer*. **44**: 3061-3069.
- Lakes, R. (1993). Materials with structural hierarchy. *Nature*. **361**: 511-515.
- Lambert, Y., Demazeau, G., Largeteau, A., Bouvier, J. M., Laborde-Croubit, S., and Cabannes, M. (2000). Packaging for high-pressure treatments in the food industry. *Packaging Technology and Science*. **13**: 63-71.
- Langevin, P. (1908). Sur la théorie du mouvement brownien. *C. R. Acad. Sci. (Paris)*. **146**: 530-533.
- Laoubi, S., and Vergnaud, J. M. (1996). Theoretical treatment of pollutant transfer in a finite volume of food from a polymer packaging made of a recycled film and a functional barrier. *Food Additives and Contaminants*. **13**: 293-306.
- Lau, O.-W., and Wong, S.-K. (2000). Contamination in food from packaging material. *Journal of Chromatography A*. **882**: 255-270.
- Le-Bail, A., Hamadami, N., and Bahuaud, S. (2006). Effect of high-pressure processing on the mechanical and barrier properties of selected packagings. *Packaging Technology and Science*. **19**: 237-243.

- Lemons, D. S., and Gythiel, A. (1997). Paul Langevin's 1908 paper "On the Theory of Brownian Motion" ["Sur la théorie du mouvement brownien," C. R. Acad. Sci. (Paris) [bold 146], 530--533 (1908)]. *American Journal of Physics*. **65**: 1079-1081.
- Lewis, H., Verghese, K., and Fitzpatrick, L. (2010). Evaluating the sustainability impacts of packaging: the plastic carry bag dilemma. *Packaging Technology and Science*. **23**: 145-160.
- Li, T., Kildsig, D. O., and Park, K. (1997). Computer simulation of molecular diffusion in amorphous polymers. *Journal of Controlled Release*. **48**: 57-66.
- Liang, Y., Hilal, N., Langston, P., and Starov, V. (2007). Interaction forces between colloidal particles in liquid: Theory and experiment. *Advances in Colloid and Interface Science*. **134-135**: 151-166.
- Lide, D. R. (2009). *Handbook of Chemistry and Physics*. CRC Press.
- Limm, W., and Hollifield, H. C. (1996). Modelling of additive diffusion in polyolefins. *Food Additives and Contaminants*. **13**: 949-967.
- Linszen, J. P. H., Rijnen, L., Legger-Huijsman, A., and Roozen, J. P. (1998). Combined GC and sniffing port analysis of volatile compounds in rubber rings mounted on beer bottles. *Food Additives and Contaminants*. **15**: 79-83.
- Lipscomb, G. G. (1990). Unified thermodynamic analysis of sorption in rubbery and glassy materials. *Aiche Journal*. **36**: 1505-1516.
- Llorens, A., Lloret, E., Picouet, P. A., Trbojevich, R., and Fernandez, A. (2012). Metallic-based micro and nanocomposites in food contact materials and active food packaging. *Trends in Food Science & Technology*. **24**: 19-29.
- Lodge, T. P. (1999). Reconciliation of the molecular weight dependence of diffusion and viscosity in entangled polymers. *Physical Review Letters*. **83**: 3218-3221.
- Lorenzini, R., Fiselier, K., Biedermann, M., Barbanera, M., Braschi, I., and Grob, K. (2010). Saturated and aromatic mineral oil hydrocarbons from paperboard food packaging: estimation of long-term migration from contents in the paperboard and data on boxes from the market. *Food Additives and Contaminants Part a-Chemistry Analysis Control Exposure & Risk Assessment*. **27**: 1765-1774.
- MAPP 5015.5, R. (2011). CMC Reviews of Type III DMFs for Packaging Materials. Office of Pharmaceutical Science.
- Mark, J. E. (1999). *Polymer Data Handbook*. Oxford University Press.
- Mark, J. E. (2007). *Physical Properties of Polymer Handbook*. Springer New York.
- Marque, D., Feigenbaum, A., Dainelli, D., and Riquet, A. M. (1998). Safety evaluation of an ionized multilayer plastic film used for vacuum cooking and meat preservation. *Food Additives and Contaminants*. **15**: 831-841.
- Marqué, D., Feigenbaum, A., and Riquet, A. (1996). Repercussions of the ionization of plastic packaging on the compatibility with packaged foodstuffs. *Journal de Chimie Physique et de Physico-Chimie Biologique*. **93**: 165-168.
- Masaro, L., and Zhu, X. X. (1999). Physical models of diffusion for polymer solutions, gels and solids. *Progress in Polymer Science*. **24**: 731-775.
- Mattozzi, A., Serralunga, P., Hedenqvist, M. S., and Gedde, U. W. (2006). Mesoscale modelling of penetrant diffusion in computer-generated polyethylene-spherulite-like structures. *Polymer*. **47**: 5588-5595.
- Mauritz, K. A., and Storey, R. F. (1990). A general free volume based theory for the diffusion of large molecules in amorphous polymers above T_g. 2. Molecular shape dependence. *Macromolecules*. **23**: 2033-2038.
- Mauritz, K. A., Storey, R. F., and George, S. E. (1990). A general free volume-based theory for the diffusion of large molecules in amorphous polymers above the glass temperature. I. Application to di-n-alkyl phthalates in PVC. *Macromolecules*. **23**: 441-450.

- McKeen, L. W. (2008). Effect of Temperature and other Factors on Plastics and Elastomers. Elsevier Science.
- Meerwall, E. v., Beckman, S., Jang, J., and Mattice, W. L. (1998). Diffusion of liquid n-alkanes: Free-volume and density effects. *The Journal of Chemical Physics*. **108**: 4299-4304.
- Mehrer, H. (2010). Diffusion in Solids: Fundamentals, Methods, Materials, Diffusion-Controlled Processes. Springer.
- Mensitieri, G., Apicella, A., Nobile, M. A., and Nicolais, L. (1991). Solvent mixtures sorption in amorphous peek. *Polymer Bulletin*. **27**: 323-330.
- Mercea, P. (2008). Chapter 5 Models for diffusion in polymers. **In**: Plastic Packaging: Interactions with Food and Pharmaceuticals. Piringer, O., and Baner, A. (Eds.), Wiley.
- Mercea, P. (2009). Physicochemical processes involved in migration of bisphenol A from polycarbonate. *Journal of Applied Polymer Science*. **112**: 579-593.
- Metois, P., Scholler, D., Bouquant, J., and Feigenbaum, A. (1998). Alternative test methods to control the compliance of polyolefin food packaging materials with the European Union regulation: the case of aromatic antioxidants and of bis(ethanolamine) antistatics based on H-1-NMR and UV-visible spectrophotometry. *Food Additives and Contaminants*. **15**: 100-111.
- Miller-Chou, B. A., and Koenig, J. L. (2003). A review of polymer dissolution. *Progress in Polymer Science*. **28**: 1223-1270.
- Miltz, J., Ram, A., and Nir, M. M. (1997). Prospects for application of post-consumer used plastics in food packaging. *Food Additives and Contaminants*. **14**: 649-659.
- Möller, K., and Gevert, T. (1994). An FTIR solid-state analysis of the diffusion of hindered phenols in low-density polyethylene (LDPE): The effect of molecular size on the diffusion coefficient. *Journal of Applied Polymer Science*. **51**: 895-903.
- Morrissey, P., and Vesely, D. (2000). Accurate measurement of diffusion rates of small molecules through polymers. *Polymer*. **41**: 1865-1872.
- Mu, M., Clarke, N., Composto, R. J., and Winey, K. I. (2009). Polymer diffusion exhibits a minimum with increasing single-walled carbon nanotube concentration. *Macromolecules*. **42**: 7091-7097.
- Mu, M., Seitz, M. E., Clarke, N., Composto, R. J., and Winey, K. I. (2010). Polymer tracer diffusion exhibits a minimum in nanocomposites containing spherical nanoparticles. *Macromolecules*. **44**: 191-193.
- Mueller, F., Krueger, K.-M., and Sadowski, G. (2012). Non-Fickian diffusion of toluene in polystyrene in the vicinity of the glass-transition temperature. *Macromolecules*. **45**: 926-932.
- Muller-Plathe, F. (1991). Diffusion of penetrants in amorphous polymers: A molecular dynamics study. *The Journal of Chemical Physics*. **94**: 3192-3199.
- Muncke, J. (2009). Exposure to endocrine disrupting compounds via the food chain: Is packaging a relevant source? *Science of The Total Environment*. **407**: 4549-4559.
- Muncke, J. (2011). Endocrine disrupting chemicals and other substances of concern in food contact materials: An updated review of exposure, effect and risk assessment. *The Journal of Steroid Biochemistry and Molecular Biology*. **127**: 118-127.
- Munro, C., Hlywka, J. J., and Kennepohl, E. M. (2002). Risk assessment of packaging materials. *Food Addit Contam*. **19 Suppl**: 3-12.
- Narasimhan, B. (2001). Mathematical models describing polymer dissolution: consequences for drug delivery. *Advanced Drug Delivery Reviews*. **48**: 195-210.
- Narasimhan, B., and Peppas, N. A. (1996). On the importance of chain reptation in models of dissolution of glassy polymers. *Macromolecules*. **29**: 3283-3291.
- Nauman, E. B., and He, D. Q. (2001). Nonlinear diffusion and phase separation. *Chemical Engineering Science*. **56**: 1999-2018.

- Neethirajan, S., and Jayas, D. (2011). Nanotechnology for the food and bioprocessing industries. *Food and Bioprocess Technology*. **4**: 39-47.
- Neogi, P. (1996). Diffusion in Polymers. Marcel Dekker.
- Nerin, C., Albinana, J., Philo, M. R., Castle, L., Raffael, B., and Simoneau, C. (2003a). Evaluation of some screening methods for the analysis of contaminants in recycled polyethylene terephthalate flakes. *Food Additives and Contaminants*. **20**: 668-677.
- Nerin, C., Canellas, E., Aznar, M., and Silcock, P. (2009). Analytical methods for the screening of potential volatile migrants from acrylic-base adhesives used in food-contact materials. *Food Additives and Contaminants Part a-Chemistry Analysis Control Exposure & Risk Assessment*. **26**: 1592-1601.
- Nerin, C., Fernandez, C., Domeno, C., and Salafranca, J. (2003b). Determination of potential migrants in polycarbonate containers used for microwave ovens by high-performance liquid chromatography with ultraviolet and fluorescence detection. *Journal of Agricultural and Food Chemistry*. **51**: 5647-5653.
- Nguyen, P.-M., Goujon, A., Sauvegrain, P., and Vitrac, O. (2013). A computer-aided methodology to design safe food packaging and related systems. *Aiche Journal*: n/a-n/a.
- Nichols, D. (2004). Biocides in Plastics. Rapra.
- Nilsson, F., Gedde, U. W., and Hedenqvist, M. S. (2009). Penetrant diffusion in polyethylene spherulites assessed by a novel off-lattice Monte-Carlo technique. *European Polymer Journal*. **45**: 3409-3417.
- Noguerol-Cal, R., Lopez-Vilarino, J. M., Fernandez-Martinez, G., Gonzalez-Rodriguez, M. V., and Barral-Losada, L. F. (2010). Liquid chromatographic methods to analyze hindered amines light stabilizers (HALS) levels to improve safety in polyolefins. *J Sep Sci*. **33**: 2698-2706.
- Özal, T. A., Peter, C., Hess, B., and van der Vegt, N. F. A. (2008). Modeling solubilities of additives in polymer microstructures: single-step perturbation method based on a soft-cavity reference state. *Macromolecules*. **41**: 5055-5061.
- Page, B. D., and Lacroix, G. M. (1992). Studies into the transfer and migration of phthalate esters from aluminium foil-paper laminates to butter and margarine. *Food Additives and Contaminants*. **9**: 197-212.
- Pandey, S. K., and Kim, K.-H. (2011). An evaluation of volatile compounds released from containers commonly used in circulation of sports beverages. *Ecotoxicology and Environmental Safety*. **74**: 527-532.
- Paquette Kristina, E. (2004). Irradiation of Prepackaged Food: Evolution of the U.S. Food and Drug Administration's Regulation of the Packaging Materials. **In**: Irradiation of Food and Packaging, pp. 182-202. American Chemical Society.
- Pastor, R. W., and Karplus, M. (1988). Parametrization of the friction constant for stochastic simulations of polymers. *The Journal of Physical Chemistry*. **92**: 2636-2641.
- Pastorelli, S., Sanches-Silva, A., Manuel Cruz, J., Simoneau, C., and Paseiro Losada, P. (2008). Study of the migration of benzophenone from printed paperboard packages to cakes through different plastic films. *European Food Research and Technology*. **227**: 1585-1590.
- Patrick, S. G., and Limited, R. T. (2005). Practical Guide to Polyvinyl Chloride. Rapra Technology.
- Paul, W., and Smith, G. D. (2004). Structure and dynamics of amorphous polymers: computer simulations compared to experiment and theory. *Reports on Progress in Physics*. **67**: 1117.
- Peltzer, M., Wagner, J., and Jimenez, A. (2009). Migration study of carvacrol as a natural antioxidant in high-density polyethylene for active packaging. *Food Additives and Contaminants Part a-Chemistry Analysis Control Exposure & Risk Assessment*. **26**: 938-946.

- Pennarun, P. Y., Dole, P., and Feigenbaum, A. (2004a). Functional barriers in PET recycled bottles. Part I. Determination of diffusion coefficients in bioriented PET with and without contact with food simulants. *Journal of Applied Polymer Science*. **92**: 2845-2858.
- Pennarun, P. Y., Ngono, Y., Dole, P., and Feigenbaum, A. (2004b). Functional barriers in PET recycled bottles. Part II. Diffusion of pollutants during processing. *Journal of Applied Polymer Science*. **92**: 2859-2870.
- Perez-Palacios, D., Angel Fernandez-Recio, M., Moreta, C., and Teresa Tena, M. (2012). Determination of bisphenol-type endocrine disrupting compounds in food-contact recycled-paper materials by focused ultrasonic solid-liquid extraction and ultra performance liquid chromatography-high resolution mass spectrometry. *Talanta*. **99**: 167-174.
- Petersen, J. H., and Jensen, L. K. (2010). Phthalates and food-contact materials: enforcing the 2008 European Union plastics legislation. *Food Addit Contam Part A Chem Anal Control Expo Risk Assess*. **27**: 1608-1616.
- Pezo, D., Fedeli, M., Bosetti, O., and Nerin, C. (2012). Aromatic amines from polyurethane adhesives in food packaging: The challenge of identification and pattern recognition using Quadrupole-Time of Flight-Mass Spectrometry(E). *Analytica Chimica Acta*. **756**: 49-59.
- Piergiovanni, L., Fava, P., and Schiraldi, A. (1999). Study of diffusion through LDPE film of Di-n-butyl phthalate. *Food Additives and Contaminants*. **16**: 353-359.
- Pinte, J., Joly, C., Dole, P., and Feigenbaum, A. (2010). Diffusion of homologous model migrants in rubbery polystyrene: molar mass dependence and activation energy of diffusion. *Food Additives & Contaminants: Part A*. **27**: 557-566.
- Pinte, J. r. m., Joly, C., Plé, K., Dole, P., and Feigenbaum, A. (2008). Proposal of a set of model polymer additives designed for confocal FRAP diffusion experiments. *Journal of Agricultural and Food Chemistry*. **56**: 10003-10011.
- Piringer, O. G., and Baner, A. L. (2000). Plastic Packaging Materials for Food: Barrier Function, Mass Transport, Quality Assurance, and Legislation. Wiley-VCH.
- Piringer, O. G., and Baner, A. L. (2008). Plastic Packaging: Interactions with Food and Pharmaceuticals. Wiley.
- Plazek, D. J., Schlosser, E., Schonhals, A., and Ngai, K. L. (1993). Breakdown of the Rouse model for polymers near the glass transition temperature. *The Journal of Chemical Physics*. **98**: 6488-6491.
- Poças, M. d. F., and Hogg, T. (2007). Exposure assessment of chemicals from packaging materials in foods: a review. *Trends in Food Science & Technology*. **18**: 219-230.
- Poças, M. d. F., Oliveira, J. C., Pereira, J. R., Brandsch, R., and Hogg, T. (2011). Modelling migration from paper into a food simulant. *Food Control*. **22**: 303-312.
- Poças, M. F., Oliveira, J. C., Brandsch, R., and Hogg, T. (2010). Feasibility study on the use of probabilistic migration modeling in support of exposure assessment from food contact materials. *Risk Analysis*. **30**: 1052-1061.
- Poças, M. F., Oliveira, J. C., Oliveira, F. A. R., and Hogg, T. (2008). A critical survey of predictive mathematical models for migration from packaging. *Critical Reviews in Food Science and Nutrition*. **48**: 913-928.
- Poole, A., van Herwijnen, P., Weideli, H., Thomas, M. C., Ransbotyn, G., and Vance, C. (2004). Review of the toxicology, human exposure and safety assessment for bisphenol A diglycidylether (BADGE). *Food Additives and Contaminants*. **21**: 905-919.
- Prince E. Rouse, J. (1953). A theory of the linear viscoelastic properties of dilute solutions of coiling polymers. *The Journal of Chemical Physics*. **21**: 1272-1280.
- Psillos, S. (2011). Moving molecules above the scientific horizon: on Perrin's case for realism. *Journal for General Philosophy of Science*. **42**: 339-363.

- Queyroy, S., and Monasse, B. (2012). Effect of the molecular structure of semicrystalline polyethylene on mechanical properties studied by molecular dynamics. *Journal of Applied Polymer Science*. **125**: 4358-4367.
- Rahman, S. (2007). Handbook of Food Preservation, Second Edition. Taylor & Francis.
- Ranjit, N., Siefert, K., and Padmanabhan, V. (2010). Bisphenol-A and disparities in birth outcomes: a review and directions for future research. *J Perinatol*. **30**: 2-9.
- Reid, R. C., Sidman, K. R., Schwope, A. D., and Till, D. E. (1980). Loss of Adjuvants from Polymer Films to Foods Simulants. Effect of the External Phase. *Industrial & Engineering Chemistry Product Research and Development*. **19**: 580-587.
- Reynier, A., Dole, P., and Feigenbaum, A. (2001a). Additive diffusion coefficients in polyolefins. II. Effect of swelling and temperature on the $D = f(M)$ correlation. *Journal of Applied Polymer Science*. **82**: 2434-2443.
- Reynier, A., Dole, P., Humbel, S., and Feigenbaum, A. (2001b). Diffusion coefficients of additives in polymers. I. Correlation with geometric parameters. *Journal of Applied Polymer Science*. **82**: 2422-2433.
- Rhee, C.-K., Ferry, J. D., and Fetters, L. J. (1977). Diffusion of radioactively tagged penetrants through rubbery polymers. II. Dependence on molecular length of penetrant. *Journal of Applied Polymer Science*. **21**: 783-790.
- Riquet, A. M., Wolff, N., Laoubi, S., Vergnaud, J. M., and Feigenbaum, A. (1998). Food and packaging interactions: Determination of the kinetic parameters of olive oil diffusion in polypropylene using concentration profiles. *Food Additives and Contaminants*. **15**: 690-700.
- Roduit, B., Borgeat, C. H., Cavin, S., Fragniere, C., and Dudler, V. (2005). Application of Finite Element Analysis (FEA) for the simulation of release of additives from multilayer polymeric packaging structures. *Food Additives and Contaminants*. **22**: 945-955.
- Romao, W., Spinace, M. A. S., and De Paoli, M. A. (2009). Poly(Ethylene Terephthalate), PET. A Review on the Synthesis Processes, Degradation Mechanisms and its Recycling. *Polimeros-Ciencia E Tecnologia*. **19**: 121-132.
- Romdhane, I. H., Danner, R. P., and Duda, J. L. (1995). Influence of the glass transition on solute diffusion in polymers by inverse gas chromatography. *Industrial & Engineering Chemistry Research*. **34**: 2833-2840.
- Saby-Dubreuil, A. C., Guerrier, B., Allain, C., and Johannsmann, D. (2001). Glass transition induced by solvent desorption for statistical MMA/nBMA copolymers — Influence of copolymer composition. *Polymer*. **42**: 1383-1391.
- Sadler, G., Chappas, W., and Pierce, D. E. (2001). Evaluation of e-beam, gamma- and X-ray treatment on the chemistry and safety of polymers used with pre-packaged irradiated foods: a review. *Food Additives and Contaminants*. **18**: 475-501.
- Sadler, G., Pierce, D., Lawson, A., Suvannunt, D., and Senthil, V. (1996). Evaluating organic compound migration in poly(ethylene terephthalate): A simple test with implications for polymer recycling. *Food Additives and Contaminants*. **13**: 979-989.
- Sagiv, A. (2001). Exact solution of mass diffusion into a finite volume. *Journal of Membrane Science*. **186**: 231-237.
- Sagiv, A. (2002). Theoretical formulation of the diffusion through a slab-theory validation. *Journal of Membrane Science*. **199**: 125-134.
- Sanches-Silva, A., Andre, C., Castanheira, I., Manuel Cruz, J., Pastorelli, S., Simoneau, C., and Paseiro-Losada, P. (2009). Study of the Migration of Photoinitiators Used in Printed Food-Packaging Materials into Food Simulants. *Journal of Agricultural and Food Chemistry*. **57**: 9516-9523.
- Sanches Silva, A., Cruz Freire, J. M., and Paseiro Losada, P. (2010). Study of the diffusion coefficients of diphenylbutadiene and triclosan into and within meat. *European Food Research and Technology*. **230**: 957-964.

- Sanches Silva, A., Cruz, J. M., Sendón Garcí'a, R., Franz, R., and Paseiro Losada, P. (2007). Kinetic migration studies from packaging films into meat products. *Meat Science*. **77**: 238-245.
- Schmidt-Rohr, K., and Spiess, H. W. (1991). Chain diffusion between crystalline and amorphous regions in polyethylene detected by 2D exchange carbon-13 NMR. *Macromolecules*. **24**: 5288-5293.
- Seta, J., Ogino, T., and Ito, T. (1984). Activation volume for the diffusion of disperse dye in nylon 6. *Sen'i Gakkaishi*. **40**: T263-T268.
- Shanklin, A. P., and Sánchez, E. R. (2005). Regulatory report: FDA's Food Contact Substance Notification Program. *In*: Food safety magazine: Building a bridge to global food safety, October/November 2005. Cianci, S. (Ed.).
- Sharpe, R. M. (2010). Is it time to end concerns over the estrogenic effects of bisphenol A? *Toxicological Sciences*. **114**: 1-4.
- Silva, A. S., García, R. S., Cooper, I., Franz, R., and Losada, P. P. (2006). Compilation of analytical methods and guidelines for the determination of selected model migrants from plastic packaging. *Trends in Food Science & Technology*. **17**: 535-546.
- Simal-Gandara, J., Damant, A. P., and Castle, L. (2002). The use of LC-MS in studies of migration from food contact materials: A review of present applications and future possibilities. *Critical Reviews in Analytical Chemistry*. **32**: 47-78.
- Simal-Gandara, J., Sarria-Vidal, M., Koorevaar, A., and Rijk, R. (2000). Tests of potential functional barriers for laminated multilayer food packages. Part I: Low molecular weight permeants. *Food Additives and Contaminants*. **17**: 703-711.
- Simha, R., and Boyer, R. F. (1962). On a general relation involving the glass temperature and coefficients of expansion of polymers. *The Journal of Chemical Physics*. **37**: 1003-1007.
- Siva, N. (2012). Controversy continues over safety of bisphenol A. *The Lancet*. **379**: 1186.
- Smirnova, V. V., Krasnoiarova, O. V., Pridvorova, S. M., Zherdev, A. V., Gmoshinskii, I. V., Kazydub, G. V., Popov, K. I., and Khotimchenko, S. A. (2012). Characterization of silver nanoparticles migration from package materials destined for contact with foods. *Voprosy pitaniia*. **81**: 34-39.
- Solovyov, S., and Goldman, A. (2007). Mass Transport and Reactive Barriers in Packaging: Theory, Applications And Design. DEStech Pub.
- Spearot, D. E., Sudibjo, A., Ullal, V., and Huang, A. (2012). Molecular dynamics simulations of diffusion of O₂ and N₂ penetrants in polydimethylsiloxane-based nanocomposites. *Journal of Engineering Materials and Technology*. **134**: 021013.
- Stachel, J. (2005). Einstein's Miraculous Year: Five Papers That Changed The Face Of Physics. Princeton University Press.
- Stastna, J., and De Kee, D. (1995). Transport Properties in Polymers. Technomic Publishing Company.
- Störmer, A. (2010) Final activity report: Research programme on migration from adhesives in food packaging materials in support of European Legislation and Standardisation. COLL-CT-2006-030309. MIGRESIVES.
- Sunderrajan, S., Hall, C. K., and Freeman, B. D. (1996). Estimation of mutual diffusion coefficients in polymer/penetrant systems using nonequilibrium molecular dynamics simulations. *The Journal of Chemical Physics*. **105**: 1621-1632.
- Tacker, M. (2011). Endocrine disrupting components and packaging. *Ernahrung*. **35**: 308-313.
- Tehrany, E. A., and Desobry, S. (2004). Partition coefficients in food/packaging systems: a review. *Food Additives and Contaminants Part a-Chemistry Analysis Control Exposure & Risk Assessment*. **21**: 1186-1202.
- Teraoka, I. (2002). Polymer Solutions: An Introduction to Physical Properties. Wiley.

- Till, D., Schwöpe, A. D., Ehntholt, D. J., Sidman, K. R., Whelan, R. H., Schwartz, P. S., and Reid, R. C. (1987). Indirect food additive migration from polymeric food packaging materials. *Crit Rev Toxicol.* **18**: 215-243.
- Tonge, M. P., and Gilbert, R. G. (2001a). Testing free volume theory for penetrant diffusion in rubbery polymers. *Polymer.* **42**: 1393-1405.
- Tonge, M. P., and Gilbert, R. G. (2001b). Testing models for penetrant diffusion in glassy polymers. *Polymer.* **42**: 501-513.
- Tosa, V., Kovacs, K., Mercea, P., and Piringer, O. (2008). A finite difference method for modeling migration of impurities in multilayer Systems. *Numerical Analysis and Applied Mathematics.* **1048**: 802-805.
- Triantafyllou, V. I., Karamani, A. G., Akrida-Demertzi, K., and Demertzis, P. G. (2002). Studies on the usability of recycled PET for food packaging applications. *European Food Research and Technology.* **215**: 243-248.
- Trier, X., Granby, K., and Christensen, J. H. (2011). Polyfluorinated surfactants (PFS) in paper and board coatings for food packaging. *Environmental Science and Pollution Research.* **18**: 1108-1120.
- Trier, X., Okholm, B., Foverskov, A., Binderup, M. L., and Petersen, J. H. (2010). Primary aromatic amines (PAAs) in black nylon and other food-contact materials, 2004-2009. *Food Additives and Contaminants Part a-Chemistry Analysis Control Exposure & Risk Assessment.* **27**: 1325-1335.
- Van Alsten, J. G., Lustig, S. R., and Hsiao, B. (1995). Polymer diffusion in semicrystalline polymers. 2. atactic polystyrene-d transport into atactic and isotactic polystyrene. *Macromolecules.* **28**: 3672-3680.
- van Krevelen, D. W., and te Nijenhuis, K. (2009). Properties of Polymers: Their Correlation with Chemical Structure; their Numerical Estimation and Prediction from Additive Group Contributions. Elsevier Science.
- van Leeuwen, C. J., and Vermeire, T. G. (2007). Risk Assessment of Chemicals: An Introduction. Springer.
- Vandenberg, L. N., Maffini, M. V., Sonnenschein, C., Rubin, B. S., and Soto, A. M. (2009). Bisphenol-A and the great divide: a review of controversies in the field of endocrine disruption. *Endocrine Reviews.* **30**: 75-95.
- Veniaminov, A. V., and Sillescu, H. (1999). Polymer and dye probe diffusion in poly(methyl methacrylate) below the glass transition studied by forced rayleigh scattering. *Macromolecules.* **32**: 1828-1837.
- Vera, P., Aznar, M., Mercea, P., and Nerin, C. (2011). Study of hotmelt adhesives used in food packaging multilayer laminates. Evaluation of the main factors affecting migration to food. *Journal of Materials Chemistry.* **21**: 420-431.
- Vergnaud, J. M. (1998). Problems encountered for food safety with polymer packages: chemical exchange, recycling. *Advances in Colloid and Interface Science.* **78**: 267-297.
- Vergnaud, J. M., and Rosca, I. D. (2006). Assessing Food Safety of Polymer Packaging. Rapra Technology.
- Vettorel, T., Meyer, H., Baschnagel, J., and Fuchs, M. (2007). Structural properties of crystallizable polymer melts: Intrachain and interchain correlation functions. *Physical Review E.* **75**.
- Vieth, W. R. (1991). Diffusion in and Through Polymers: Principles and Applications. Carl Hanser GmbH.
- Vignes, A. (1966). Diffusion in binary solutions. variation of diffusion coefficient with composition. *Industrial & Engineering Chemistry Fundamentals.* **5**: 189-199.
- Vitrac, O. (2012). FMECAENGINE: a seamless tool to chain migration simulations and perform related sensitivity analysis. Available. Date accessed:

- Vitrac, O., and Gillet, G. (2010). An Off-Lattice Flory-Huggins approach of the partitioning of bulky solutes between polymers and interacting liquids. *International Journal of Chemical Reactor Engineering*. **8**.
- Vitrac, O., and Hayert, M. (2005). Risk assessment of migration from packaging materials into foodstuffs. *Aiche Journal*. **51**: 1080-1095.
- Vitrac, O., and Hayert, M. (2006). Identification of diffusion transport properties from desorption/sorption kinetics: An analysis based on a new approximation of fick equation during solid-liquid contact. *Industrial & Engineering Chemistry Research*. **45**: 7941-7956.
- Vitrac, O., and Hayert, M. (2007a). Design of safe food packaging under uncertainty. **In**: New trends in chemical engineering research, pp. 251-292. Berton, P. (Ed.), Nova Science Publishers, New York.
- Vitrac, O., and Hayert, M. (2007b). Effect of the distribution of sorption sites on transport diffusivities: A contribution to the transport of medium-weight-molecules in polymeric materials. *Chemical Engineering Science*. **62**: 2503-2521.
- Vitrac, O., and Leblanc, J.-C. (2007). Consumer exposure to substances in plastic packaging. I. Assessment of the contribution of styrene from yogurt pots. *Food Additives and Contaminants*. **24**.
- Vitrac, O., Lezervant, J., and Feigenbaum, A. (2006). Decision trees as applied to the robust estimation of diffusion coefficients in polyolefins. *Journal of Applied Polymer Science*. **101**: 2167-2186.
- Vitrac, O., Mougharbel, A., and Feigenbaum, A. (2007). Interfacial mass transport properties which control the migration of packaging constituents into foodstuffs. *Journal of Food Engineering*. **79**: 1048-1064.
- Vollmer, A., Biedermann, M., Grundboeck, F., Ingenhoff, J.-E., Biedermann-Brem, S., Altkofer, W., and Grob, K. (2011). Migration of mineral oil from printed paperboard into dry foods: survey of the German market. *European Food Research and Technology*. **232**: 175-182.
- von Goetz, N., Fabricius, L., Glaus, R., Weitbrecht, V., Gunther, D., and Hungerbuhler, K. (2013). Migration of silver from commercial plastic food containers and implications for consumer exposure assessment. *Food Addit Contam Part A Chem Anal Control Expo Risk Assess*. **30**: 612-620.
- Von Meerwall, E., and Ferguson, R. D. (1979). Diffusion of hydrocarbons in rubber, measured by the pulsed gradient NMR method. *Journal of Applied Polymer Science*. **23**: 3657-3669.
- von Meerwall, E. D., Lin, H., and Mattice, W. L. (2007). Trace diffusion of alkanes in polyethylene: spin-echo experiment and monte carlo simulation. *Macromolecules*. **40**: 2002-2007.
- Vrentas, J. S., and Duda, J. L. (1977). Diffusion in polymer—solvent systems. I. Reexamination of the free-volume theory. *Journal of Polymer Science: Polymer Physics Edition*. **15**: 403-416.
- Vrentas, J. S., Duda, J. L., and Huang, W. J. (1986). Regions of Fickian diffusion in polymer-solvent systems. *Macromolecules*. **19**: 1718-1724.
- Vrentas, J. S., Duda, J. L., and Ling, H. C. (1985a). Free-volume theories for self-diffusion in polymer-solvent systems. I. Conceptual differences in theories. *Journal of Polymer Science: Polymer Physics Edition*. **23**: 275-288.
- Vrentas, J. S., Duda, J. L., Ling, H. C., and Hou, A. C. (1985b). Free-volume theories for self-diffusion in polymer-solvent systems. II. Predictive capabilities. *Journal of Polymer Science: Polymer Physics Edition*. **23**: 289-304.
- Vrentas, J. S., and Vrentas, C. M. (1994). Solvent self-diffusion in rubbery polymer-solvent systems. *Macromolecules*. **27**: 4684-4690.

- Vrentas, J. S., and Vrentas, C. M. (1995). Determination of free-volume parameters for solvent self-diffusion in polymer-solvent systems. *Macromolecules*. **28**: 4740-4741.
- Vrentas, J. S., and Vrentas, C. M. (1998). Predictive methods for self-diffusion and mutual diffusion coefficients in polymer-solvent systems. *European Polymer Journal*. **34**: 797-803.
- Vrentas, J. S., Vrentas, C. M., and Faridi, N. (1996). Effect of solvent size on solvent self-diffusion in polymer-solvent systems. *Macromolecules*. **29**: 3272-3276.
- Wagner, M., and Oehlmann, J. (2009), Endocrine disruptors in bottles mineral water: total estrogenic burden and migration from plastic bottles, *Environmental Science and Pollution Research*, **16**: 278-286.
- Walsh, B. (2010). How dangerous is plastic? . *Time Magazine* of April 12, 2010, 30-36.
- Welle, F., and Franz, R. (2010). Migration of antimony from PET bottles into beverages: determination of the activation energy of diffusion and migration modelling compared with literature data. *Food Additives & Contaminants: Part A*. **28**: 115-126.
- Wesselingh, J. A., and Krishna, R. (2006). Mass Transfer in Multicomponent Mixtures. VSSD.
- Widen, H. (1998). Recycled plastics for food packaging - a literature review. *SIK Rapport*: 60pp.-60pp.
- Wijmans, J. G., and Baker, R. W. (1995). The solution-diffusion model: a review. *Journal of Membrane Science*. **107**: 1-21.
- Wittassek, M., and Angerer, J. (2008). Phthalates: metabolism and exposure. *Int J Androl*. **31**: 131-138.
- Wong, C.-P., Schrag, J. L., and Ferry, J. D. (1970). Diffusion of radioactively tagged 1,1-diphenylethane and n-hexadecane through rubbery polymers: Dependence on temperature and dilution with solvent. *Journal of Polymer Science Part A-2: Polymer Physics*. **8**: 991-998.
- Yamakawa, H. (1971). Modern Theory of Polymer Solutions. Harper & Row.
- Yang, L., Chen, X., and Jing, X. (2008a). Stabilization of poly(lactic acid) by polycarbodiimide. *Polymer Degradation and Stability*. **93**: 1923-1929.
- Yang, S.-l., Wu, Z.-H., Yang, W., and Yang, M.-B. (2008b). Thermal and mechanical properties of chemical crosslinked polylactide (PLA). *Polymer Testing*. **27**: 957-963.
- Zeliger, H. (2011). Human Toxicology of Chemical Mixtures. Elsevier Science.
- Zhang, J., and Wang, C. H. (1987). Application of the laser-induced holographic relaxation technique to the study of physical aging of an amorphous polymer. *Macromolecules*. **20**: 683-685.
- Zhu, J., Chen, L.-Q., Shen, J., and Tikare, V. (2001). Microstructure dependence of diffusional transport. *Computational Materials Science*. **20**: 37-47.
- Zielinski, J. M. (1996). An alternate interpretation of polymer/solvent jump size units for free-volume diffusion models. *Macromolecules*. **29**: 6044-6047.

2.2 Barrier materials

2.2.1 Some definitions and choices

Over the last decades, plastics have already become the main packaging materials to replace metal, glass, paper, etc. due to their functionality, lightweight, ease of processing and low cost (Arora and Padua, 2010). Barrier materials are required for many applications: plastic reservoirs or containers for chemicals or wastes including oil, products sensitive to corrosion (e.g. electronics), spoilage (food), oxidation (photovoltaic systems, food, drugs, cosmetics...), etc. As discussed in many reviews (Lange and Wyser, 2003; Siracusa, 2012) and monographs (Massey, 2002), permeability is the main limiting property of food packaging materials as it impacts shelf life and sanitary safety of food products. For this sole application, the concept of barrier should be envisioned not only for small penetrants such as gases, water vapor and organic vapor but also for medium-sized penetrants/diffusants including aromas, and flavors from the food in contact and plastic additives from the packaging itself. As mentioned in Brody et al. (2008), “the ideal packaging materials should be inert and resistant to hazards and should not allow molecular transfer from or to packaging materials”.

The definition of a “barrier material” is debatable. According to the Figure 4.2 from Crank’s book ((Crank, 1979), also reproduced in Figure 2-4 of section 2.1.4.1.4), two definitions can be reached:

- by opposition to membrane materials (permeable materials), a good barrier material can be a material with a low permeability to the considered diffusants;
- from a mass transfer point of view, a good barrier material is a material with a low diffusion coefficient and consequently a high lag time when it is exposed to diffusants.

The first concept assumes that the substance is first absorbed, diffuses and subsequently desorbed from the material. It suffers a lack of generality and cannot be applied to all situations (e.g. sorption of plasticizing substances, desorption of substances from the material). Without excluding results aiming to decrease the permeability, this thesis focuses on the second concept. It is preferred because it separates explicitly macroscopic thermodynamic effects due to phase averaging from those related to microscopic effects involving diffusion and all chemical interactions at the scale of diffusants. Indeed, adding inert fillers to any polymer will decrease its permeability without necessarily changing the microscopic details of the transport mechanism or interactions between the diffusant and the polymer. This result, which may be strange for some readers, arises from the definition of

effective permeability, P_{eff} , as the product of an effective diffusion coefficient, D_{eff} , and an effective solubility, S_{eff} . When a volume fraction ϕ of fillers inaccessible to diffusants is incorporated to the polymer (also called blocking effect (Janes and Durning, 2013)), the reduction of S_{eff} comparatively to the solubility in the bulk S_{bulk} is proportional to the reduction of the maximum concentration at equilibrium, hence:

$$S_{eff} = (1 - \phi) S_{eff}^{bulk} \quad (2-29)$$

Most of strategies to reduce D_{eff} deal with “non-reactive” strategies by combining materials, morphologies etc. On the opposite, emerging technologies inspired by catalysis or by biology propose to use technological solutions involving chemical reactions. No strict classifications of strategies have been published and we suggest one in Figure 2-23 to organize the corresponding literature. The distinction between passive and active barriers is somewhat artificial and should be thought as “inert systems” and “systems involving specific chemical interactions”. Reactive systems are similarly split into systems with catalytic activity, where the involved reactant can be regenerated and systems where reactants are irreversibly consumed. The monographies (Crank, 1979; Solovyov and Goldman, 2008) inspired the subsequent discussions. We stress in particular that there is no scientific argument for separating transport properties in nanocomposite materials from mechanisms in other composite materials. Section 2.1 shows that the same “universal” diffusion mechanisms occurred in all thermoplastics and the typical scale starting from where diffusion is pure random walk process (i.e. Brownian displacements) is usually much lower than most of “nano-systems” reported in the literature. Only the interactions between material components or phases (e.g. crystalline lamella) need additional details.

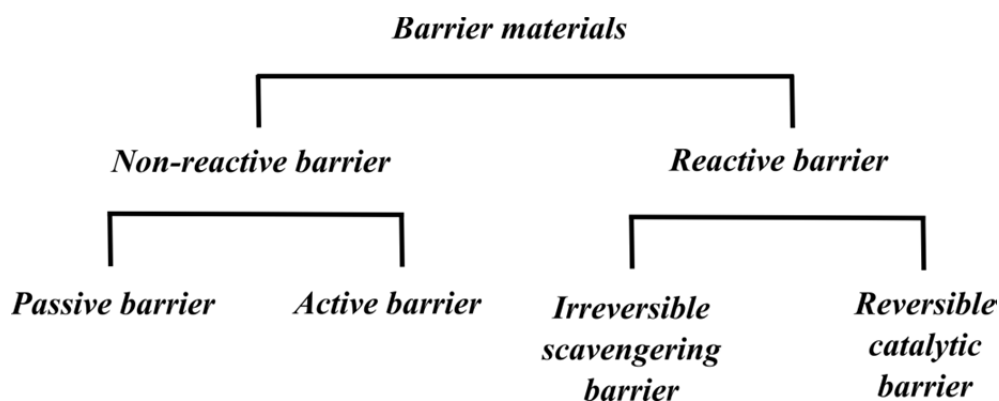


Figure 2-23 The main categories of barrier materials

2.2.2 Non-reactive barrier systems

2.2.2.1 Overview

Figure 2-24 summarizes the different strategies described to improve the barrier properties of thermoplastics and elastomers. Most of the systems rely on an assembling of different materials with different complexities according to the dimension of the arrangement, the orientation effect sought, the sizes of the objects. The distinction between passive and active is artificial but

- some barrier materials have an inert role (clays, crystallites...) and the barrier effect is associated to tortuosity effect;
- some others have an active effect and increase the dwelling time of the diffusant nearby: adsorbent surface, confined layer where diffusion might be slowed down, molecular imprint, solute trapping in specific morphology;
- Some strategies belong to both categories (e.g. specific crystalline morphology with constrained amorphous phase (Hinrichsen et al., 1981)) or to any of them such as parallel association of different materials.

Since last decade, research endeavor tends to focus more on nanocomposites, mainly inorganic-organic systems. They are difficult to define but it is usually accepted that they correspond to materials with at least one dimension in the sub-micro scale (Manias, 2009). A huge number of monographies (Galimberti, 2011; Mai and Yu, 2006; Vilgis and Heinrich, 2009), papers and reviews (Alexandre and Dubois, 2000; Avérous and Pollet, 2011; Lagaron and Lopez-Rubio, 2011; Raquez et al.; Sinha Ray and Okamoto, 2003; Yu et al., 2006) have been published usually with an intent of mechanical reinforcement and less frequently with an intent of improving barrier properties (Messersmith and Giannelis, 1995; Mittal, 2009; Sinha Ray et al., 2003a; Sinha Ray et al., 2003b). From a macroscopic point of view, the contribution of the nano-scale on mass transport may be uncertain. At first sight, solubility is not affected by length scales for a same volume fraction of inert fillers. Diffusion coefficients are more sensitive to the shape factor of fillers than to their minimum length. Finally, small objects are more likely to be oriented randomly so tortuosity effects are expected to be alleviated. However, incorporating nano-fillers instead of larger fillers has been motivated by other considerations. It has been thought that fillers creating strong interactions with polymer chains can affect in return the properties of the amorphous phase of polymer and decrease accordingly diffusion coefficients. Sought effects include:

- a preferable alignment of chains (due to a distance between fillers shorter than the gyration radius of polymer chains) and consequently homogeneously distributed crystallites (Manias, 2009);
- constraining chain relaxation to shift T_g to higher temperatures and consequently reducing accessible free volumes (Olson et al., 1997);

In practice, the consequences on bulk polymer properties and effective permeability are mitigated. The contribution of chain alignment on diffusion anisotropy of penetrants is weak (Chassapis et al., 1996). T_g shifts and variations in free volume of thermoplastics are usually not significant even in the vicinity of the fillers (Muralidharan et al., 2008; Olson et al., 1997) or lead to an increase of permeability (Merkel et al., 2002a, b). In thermoplastics, only crystallite alignment and changes in crystal morphologies have been shown to lessen robustly permeability (Kofinas et al., 1994). This strategy is commonly employed in strain-hardened semi-crystalline polymers for barrier applications (Manias, 2009).

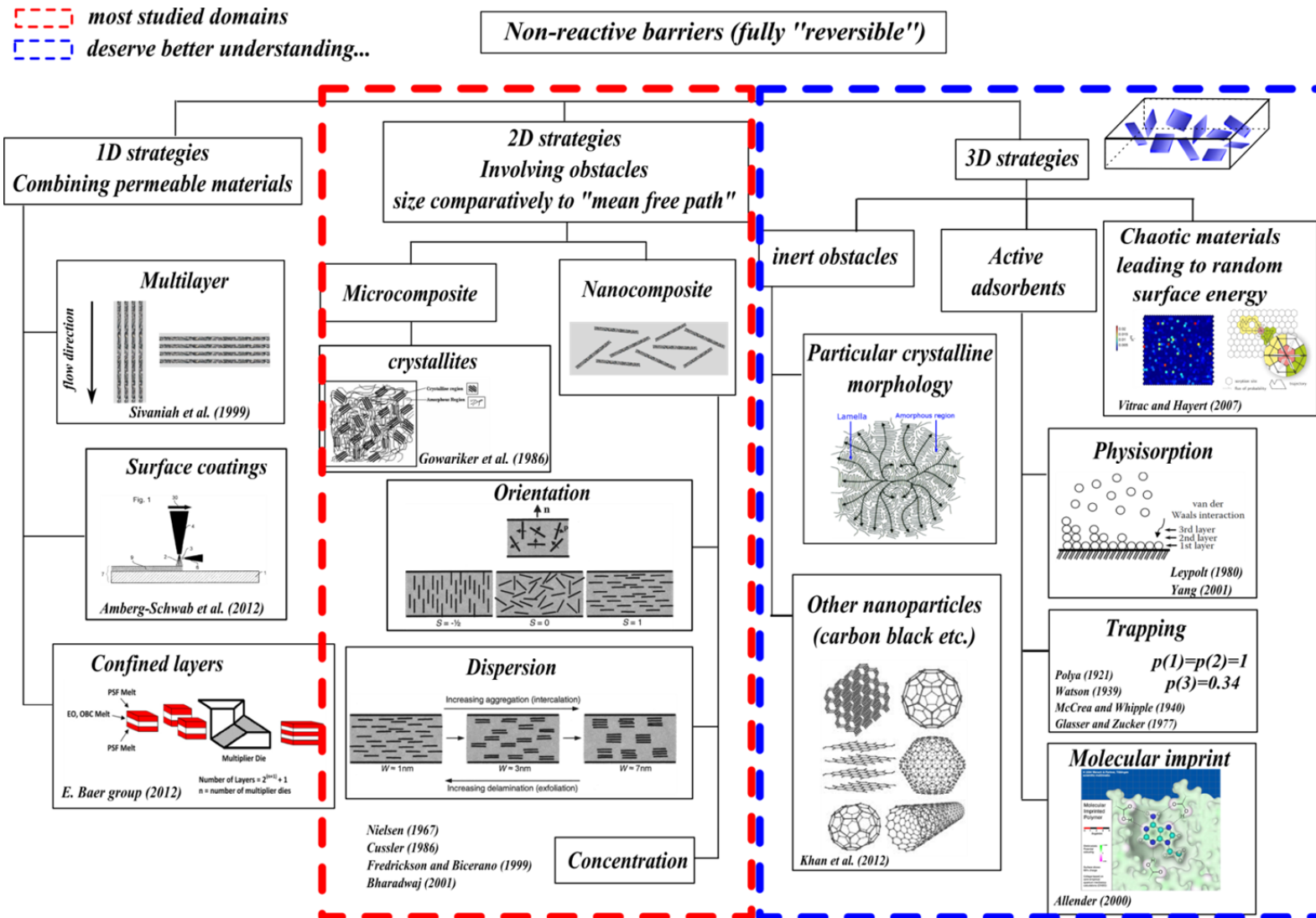


Figure 2-24 Overview of existing passive and active systems

In the thesis, it has been chosen to discuss different classes of strategies regardless the difficulty of processing or assembling of these composite materials and to focus on their theoretical performances instead. Indeed, it is thought that going to first principles on nanocomposite barrier materials may help to revise current practices and to gain new innovation directions. One example is given by the nanocomposite invented by mere happenstance by the group of Nair et al. (2012) where some outstanding results are reproduced in Figure 2-25. The material incorporates nano-channels made in graphene oxide which offers a tunnel transport to large polar molecules (e.g. water, acetone) while being barrier to helium. Potentiality of graphene oxide has been reviewed in Potts et al. (2011).

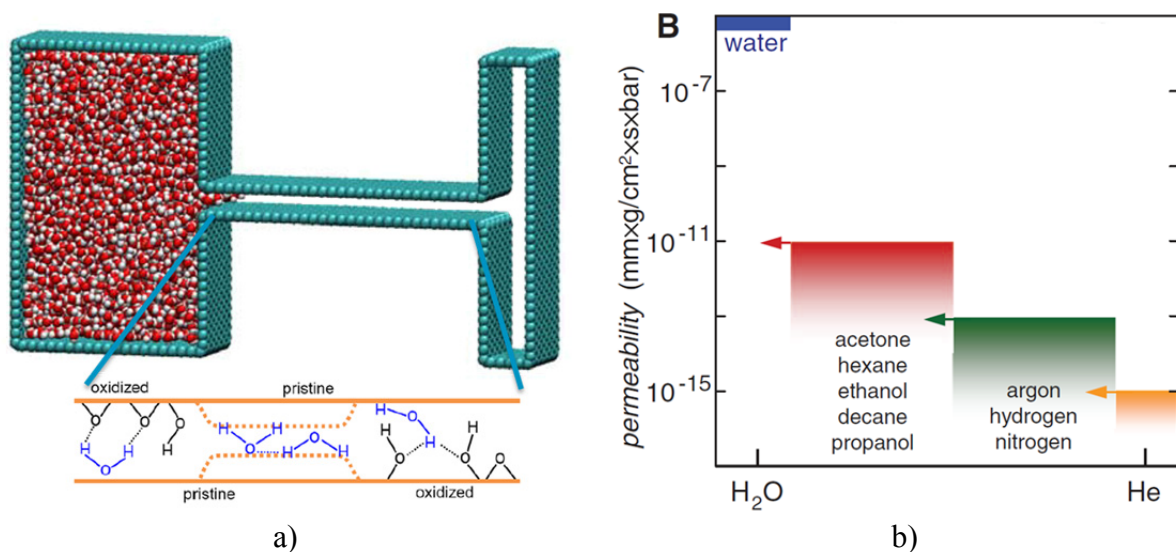


Figure 2-25 Example of outstanding active material: barrier to small molecules such as helium and permeable to larger ones such as water. a) The transport mechanism of water molecular due to “tunneling effect”; b) the permeability of different solute molecules (after Nair *et al.* (2012)).

Concepts associated to active systems are not fully elaborated and remain prospective but are central in the perspective of this thesis. In particular, they highlight a particular role of chaos or disorder on diffusion (Karayiannis et al., 2001; Klages, 2007). Besides foreseen compensation between D_{eff} reduction (*i.e.* controlled by aspect ratio of fillers) and S_{eff} decrease (*i.e.* controlled by fillers loading), Manias (2009) reports for example not so-obvious effects: “Ultimate barrier performance is predicted for those cases where the fillers are arranged in networks. For example, “house-of-cards” type of filler networks would result in a [...] permeability [reduction] by 2 to 4 orders of magnitude compared to the unfilled matrix”. Such effects are beyond “simple” tortuosity effects due to fractal character and strong correlations in the diffusion path of substances. In addition, many results of literature remain not fully interpretable as they do not separate the effects on solubility (at high loading) from those on

diffusion Choudalakis and Gotsis (2009). For example, the reduction of permeability of “H₂O vapor or CO₂ in nanocomposites of the type PE/HDPE-g-MA20/MMT and poly(ε-caprolactone)/mica cannot be predicted by any of the models”.

2.2.2.2 Common transfer models for passive/active systems

Two complementary approaches have been proposed to express effective transport properties in connection with the material structure and the properties of its components or at their interfaces:

- out of equilibrium approaches assuming a constant and unidirectional flux (mainly used for 1D description);
- approaches at equilibrium with no external flux (for systems with arbitrary complexities).

In both strategies, the system is considered at steady state: all properties and concentration profiles are constant with time.

2.2.2.2.1 Out-of-equilibrium approaches

The system to be investigated is subjected to mass flux, J , imposed by a driving force or potential difference Δp , where p is usually a partial pressure (Solovyov and Goldman, 2008):

$$J = -TR_{eq} \Delta p \quad (2-30)$$

where TR_{eq} is an effective transmission rate (or effective mass transfer coefficient) at steady state.

Composition laws for a composite system described by n transmission rates $\{TR_i\}_{i=1..n}$ depend on the organization of phases/components. For laminates, the serial association of mass transfer resistances yields (Eq 3.3.3 in (Solovyov and Goldman, 2008)):

$$TR_{eq}^{-1} = \sum_{i=1}^n TR_i^{-1} \quad (2-31)$$

For more general distributions of phases/components, it has been proposed to volume average transmission rates (Murphy et al., 2011):

$$TR_{eq}^{-1} = \sum_{i=1}^n \phi_i TR_i^{-1} \quad \text{with} \quad \sum_{i=1}^n \phi_i = 1 \quad (2-32)$$

Additional sophistications have been proposed to include shape and orientation effects as listed in Table 2-13. Most of the formula are phenomenological and consider that inserted particles/components are inert obstacles (i.e. $TR=0$). The concepts are useful to describe mass transfer at steady state (i.e. permeation) but not to describe lag times in strong barrier

applications. The relationship between transmission rates and diffusion coefficients is defined only in simple cases, where:

- mass transfer in component, $i=1..n$, occurs along a main direction
- a linear concentration profile can be assumed along the direction of mass transfer,
- sorption isotherm is linear within each component obeying to Henry law (idem for the effective medium),
- the diffusive and thermodynamic properties are uniformly distributed (idem for the effective medium).

These assumptions lead to:

$$TR_{eq} = \frac{D_{eq} S_{eq}}{l_{eq}}, TR_i = \frac{D_i S_i}{l_i} \quad (2-33)$$

where l is the characteristic length scale, S is the solubility.

Table 2-13 Effective TR_{eff} from out-of-equilibrium approaches

Barrier type	TR_{eff}	Corresponding D_{eff}	d	Ref
Multilayer	Eq. (2-33)	$D_{eff} = \frac{\sum l_i}{S_{eff} \sum \frac{l_i}{D_i S_i}}$	1D	(Solovyov and Goldman, 2008)
Composite with plate-like obstacles	$TR_{eff} = \frac{TR_{bulk} (1-\phi)}{1 + \frac{1}{2} \alpha \phi}$	$D_{eff} = \frac{D_{bulk}}{1 + \frac{1}{2} \alpha \phi}$ with assumption : $S_{eff} = S_{bulk} (1-\phi)$	2D	(Nielsen, 1967)
	$TR_{eff} = \frac{TR_{bulk}}{1 + \left(\frac{\pi \alpha \phi}{8(\ln a - \ln 2)} \right)^2}$	$D_{eff} = \frac{D_{bulk}}{(1-\phi)}$ $\times \frac{1}{1 + \left(\frac{\pi \alpha \phi}{8(\ln a - \ln 2)} \right)^2}$ with assumption : $S_{eff} = S_{bulk} (1-\phi)$	2D	(Cussler et al., 1988)
	$TR_{eff} = TR_{bulk} \times \frac{1}{\left[1/(2 + a_1 \kappa x) + 1/(2 + a_2 \kappa x) \right]^2}$	$D_{eff} = \frac{D_{bulk}}{(1-\phi)}$ $\times \frac{1}{\left[1/(2 + a_1 \kappa x) + 1/(2 + a_2 \kappa x) \right]^2}$ with assumption : $S_{eff} = S_{bulk} (1-\phi)$	2D	(Fredrickson and Bicerano, 1999)
	$TR_{eff} = TR_{bulk} \exp \left(- \left(\frac{x}{x_0} \right)^\beta \right)$	$D_{eff} = \frac{D_{bulk} \exp \left(- \left(\frac{x}{x_0} \right)^\beta \right)}{1-\phi}$ with assumption : $S_{eff} = S_{bulk} (1-\phi)$	2D	(Gusev and Lusti, 2001)

	$TR_{eff} = \frac{TR_{bulk} (1-\phi)}{1 + \frac{2}{3} \alpha \phi \left(S + \frac{1}{2} \right)}$	$D_{eff} = \frac{D_{bulk}}{1 + \frac{2}{3} \alpha \phi \left(S + \frac{1}{2} \right)}$ with assumption : $S_{eff} = S_{bulk} (1-\phi)$	2D	(Bharadwaj, 2001)
Composite with spherical obstacles	$TR_{eff} = \frac{TR_{bulk} (1-\phi)}{1 + \frac{\phi}{2}}$	$D_{eff} = \frac{D_{bulk}}{1 + \frac{\phi}{2}}$ with assumption : $S_{eff} = S_{bulk} (1-\phi)$	2D	(Maxwell, 1873)
Composite with cylinder obstacles	$TR_{eff} = \frac{TR_{bulk} (1-\phi)}{1 + \phi}$	$D_{eff} = \frac{D_{bulk}}{1 + \phi}$ with assumption : $S_{eff} = S_{bulk} (1-\phi)$	2D	(Rayleigh, 1892)
Bulk polymer with crystallites	$TR_{eff} = \frac{TR_{amorphous} (1-\phi)}{\tau B}$	$D_{eff} = \frac{D_{amorphous}}{\tau B}$ with assumption : $S_{eff} = S_{bulk} (1-\phi)$	2D	(Vieth, 1991)

TR_{bulk} and $TR_{amorphous}$: the transmission rate of host matrix and that of polymer amorphous respectively. α , ϕ , S : the aspect ratio, the volume fraction and orientation factor of inclusions respectively. x : the product of $\alpha\phi$. $a_1 = (2 - \sqrt{2})/4$, $a_2 = (2 + \sqrt{2})/4$, $\kappa = \pi / (\ln a - \ln 2)$, $\beta = 0.71$, $x_0 = 3.47$. τ : is a factor introduced to account for the reduction of the area available for diffusion. B is a factor which accounts for the reduction in the diffusion of the solute molecules as a result of the decreased chain mobility owing to the presence of the crystallites.

2.2.2.2.2 Approaches at equilibrium

Out-of-equilibrium approaches are insufficient to integrate phenomena occurring on several length scales (fractal media...) or time scales (temporal correlations, first passage times...) or even simple physical phenomena such as: dead volumes, non-linear isotherms. Effective diffusion coefficients are obtained by solving:

$$\nabla \cdot (D_{(x,y,z)} \nabla C) = 0 = D_{eff} \nabla^2 C \quad (2-34)$$

Equalities (2-34) are usually solved along with contact conditions between components/phases/domains via numerical techniques (finite element, finite volume, high order spectral techniques) or by simulating random walks. Both methods, once correctly implemented, are expected to give similar results. Few analytical results have been published (i.e. spherical symmetry) and are reported in Table 2-14.

Table 2-14 Effective D_{eff} from equilibrium approaches

<i>Barrier type</i>	D_{eff}	<i>Ref</i>
Composite with inclusions	$D_{eff} = D_2 \left(\frac{d(D_1 - D_2)\phi}{D_1 + (d-1)D_2 - (D_1 - D_2)\phi} \right)$	(Garnett, 1904)
	$D_{eff} = D_2 k_1 \left(\frac{d(D_1 k - D_2)\phi}{kD_1 + (d-1)D_2 - (kD_1 - D_2)\phi} \right)$	(Kalnin et al., 2002)
Composite with active adsorbents	$D_{eff} = \frac{D_2}{1+k}$	(Leypoldt and Gough, 1980) (Yang and Cussler, 2001; Yang et al., 2001)

D_1 and D_2 are the diffusion coefficients of inclusions and host matrix respectively. d : space dimension, ϕ : the volume fraction of obstacles, k and k_1 are related through the equilibrium concentrations in inclusions ($i=1$) and the matrix ($i=2$) and volume fraction, ϕ .

2.2.2.3 Reported experimental performances of passive barrier systems

The typical performances of passive barrier materials are reported in Table 2-15 for both multilayer and inclusion systems. The performances of multilayer materials are well described with drops of permeability up to 3-4 decades. They found applications from electronic (Murræ, 1988) to food (Lange and Wyser, 2003). Multi-multi-layer systems gave significant permeability reductions to gas up down to two decades. Although their good performance can be compared to multilayer ones, the intrinsic causes are different. As the confinement of polymer chains in layers thicknesses down to nanoscale, the crystallite morphology changes from three-dimensional spherulites to two-dimensional discoids and to “in-plane” lamellar stacks. Down to a certain layer thickness, the polymer layer will form a single crystallite lamellae with large aspect ratio. Consequently the dramatic decrease in gas permeability arises from a reduction of diffusion coefficients due to increased tortuosity of the diffusion pathway of gases (Wang et al., 2009).

The barrier performances of materials relying on inclusions remain by contrast more hypothetical and with less practical applications. Inclusion strategies gave the poorest D reduction with maximum decrease up to a factor two. The reduction is usually used to justify the concept of tortuosity, ξ , as $\xi^2 = D_{bulk} / D_{eff}$ (Shen and Chen, 2007). As confirmed by recent coarse grained simulations (Pryamitsyn et al., 2011), obstruction (*i.e.* filler) effects dominate over the role of polymer interfacial layers. Tortuosity is accordingly seen as increasing with the volume fraction of inclusions/obstacles. In thermoplastics, obstacles can be extraneous particles (*e.g.* nanofillers) or the polymer itself as crystallites are usually inaccessible to penetrants (Jacquelot et al., 2006; Wang et al., 2005). It has been thus shown that 25 nm size

scale discoid crystallites obtained by confined crystallization of poly(ethylene oxide) could lead to tortuosity values up to 100 (Wang et al., 2009).

Table 2-15 Reported reduction of permeability and D in some typical nanocomposite passive systems

<i>Host matrix</i>	<i>Principle</i>	<i>Diffusants</i>	Φ	D_{bulk}/D_{eff}	TR_{bulk}/TR_{eff}	<i>Ref</i>
Poly(butylene succinate)	Inclusions: layered clays	O ₂	<0.05	≤ 2	≤ 2	(Sinha Ray et al., 2003a)
Poly(lactic acid)	Inclusions: layered clay	O ₂ N ₂ CO ₂	<0.004	≤ 2	≤ 2	(Koh et al., 2008) (Chang et al., 2003)
Poly(propylene)	Inclusions: layered clay	O ₂	<0.04	≤ 1.5	≤ 1.5	(Osman et al., 2007)
Polyurethane	Inclusions: layered clay	O ₂	<0.05	≤ 1.7	≤ 1.7	(Osman et al., 2003)
Polyamide 6 (PA)	Inclusions: layered clay	H ₂ O	<0.04	≤ 1.5	N/A	(Abacha et al., 2009)
Polycaprolactone (PCL)	Inclusions: carbon nanotube	O ₂	<0.005	≤ 1.5	≤ 1.5	(Khan et al., 2013)
Chitosan	Inclusions: nanocrystalline cellulose	H ₂ O	<0.1	≤ 1.5	≤ 1.5	(Khan et al., 2012)
Polysulfone (PSF)	Nano-multilayer	O ₂	N/A	N/A	>120	(Murphy et al., 2011)

2.2.2.4 New concepts of active systems

The concepts of effective medium theory for non-inert particles and biphasic have been reviewed in (Sax and Ottino, 1983). They show a strong influence of the percolation threshold and of the coordination number as morphology parameter. The results assume however a similar chemical affinity for both phases. When chemical affinities between both phases are different, the random walk process is modified by additional waiting times due to a significant waiting time between the region with the highest chemical affinity and the region with the lowest chemical affinity. The mean escape time depends both of diffusion coefficients between both phases and on the energetic barrier height (Klages et al., 2008). Combined effects of tortuosity (*i.e.* obstruction effects) and preferred sorption (*i.e.* attraction effects) are discussed in general terms in (Klages, 2007). The principles of accumulation of waiting times to reduce long-term D values is illustrated in the simplest case involving one-dimensional random walk across two periodic wells: one well representing for example the polymer,

denoted P and the second denoted A representing an absorbing phase as depicted in Figure 2-26.

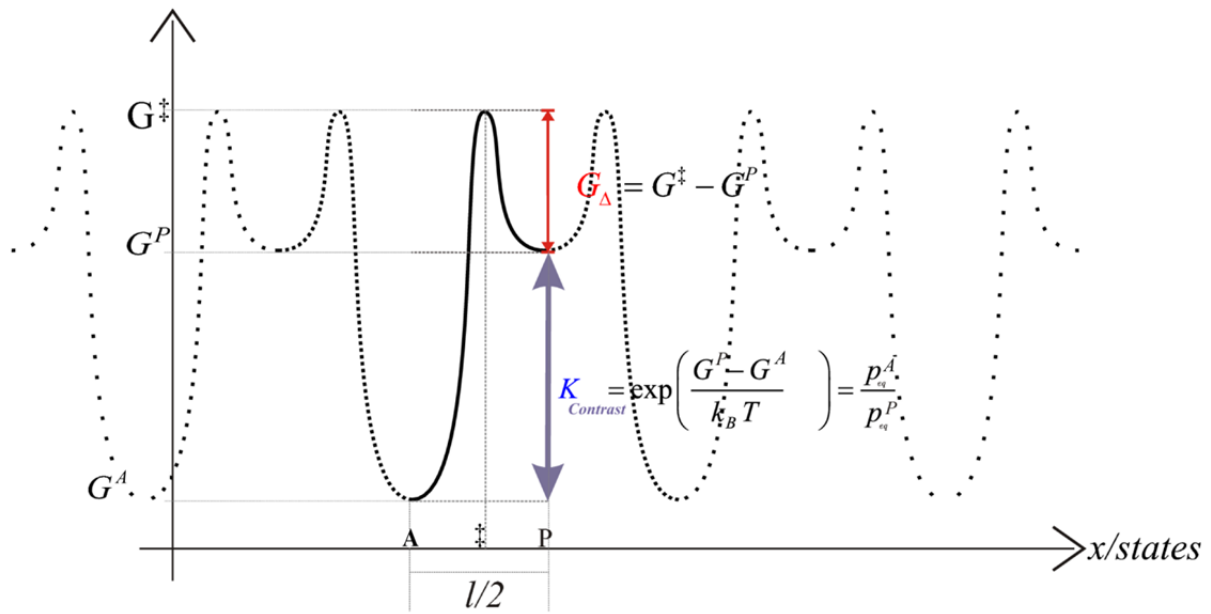


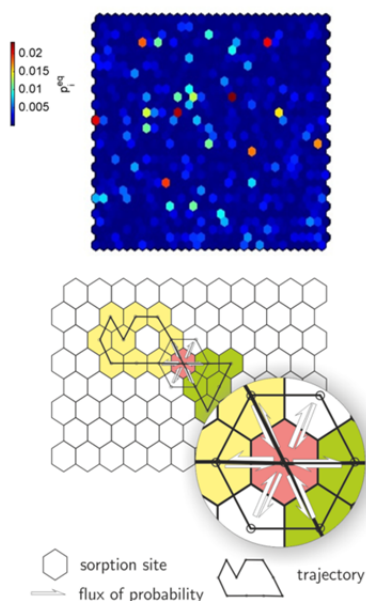
Figure 2-26 One-dimensional periodic free energy profile including two states: A and P separated by a transition state denoted \ddagger .

In the framework of the transition state theory, such a toy model has an analytical solution at thermodynamic equilibrium when $p_{eq}^A k_{A \rightarrow P} = p_{eq}^P k_{P \rightarrow A}$:

$$\begin{aligned}
 2D &= l^2 k_{A \rightarrow P \rightarrow A} \\
 &= \frac{k_0 l^2}{\frac{K}{\exp\left(-\frac{G_\Delta}{RT}\right)} + \frac{1}{\exp\left(-\frac{G_\Delta}{RT}\right)}} = \frac{k_0 l^2}{1 + K_{contrast}} \exp\left(-\frac{G_\Delta}{RT}\right) \\
 &= \frac{D_0}{1 + K_{contrast}} \exp\left(-\frac{G_\Delta}{RT}\right)
 \end{aligned} \tag{2-35}$$

Eq. (2-35) shows that D values decreases theoretically when the partition coefficient between the “MMT” and “polymer”, $K_{contrast}$, increases. In more general cases, reduction of D varies with the arrangement and the dispersion of free energies. Theoretically, by studying the random walk of diffusion on 2D hexagonal lattices, Vitrac and Hayert (2007) found reduction in D from several decades when the dispersion of free energies was increased beyond some threshold while keeping the same average value (see Figure 2-27). Similar results were obtained by Karayiannis et al. (2001).

a) Random walk on hexagonal lattice



b) Reduction in D values with equal average free energy barriers

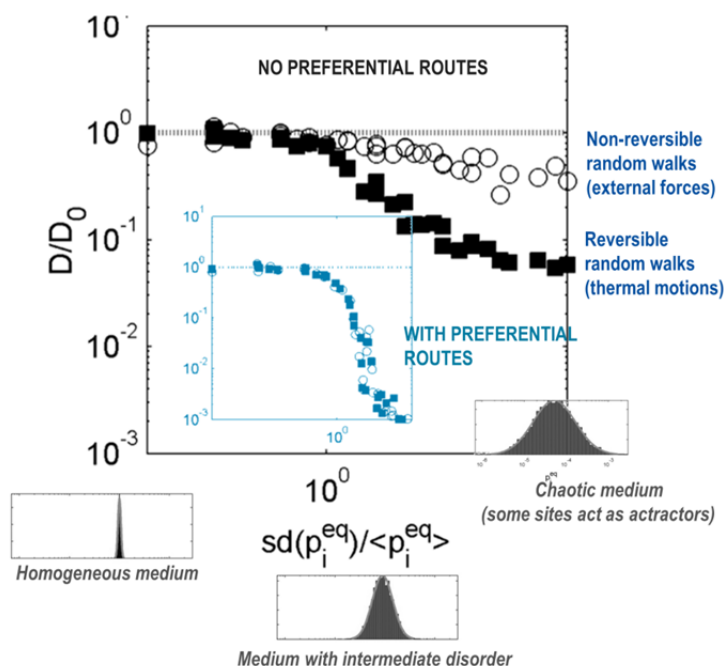


Figure 2-27 The reduction ratio of D by non-reversible and reversible random walks on hexagonal lattices with Poisson distributed dwelling times in two situations: with or without preferential routes. (after Vitrac and Hayert (2007))

Very recent results obtained by (Janes and Durning, 2013) provide unexpected proofs of the concepts followed in the thesis. The authors studied the sorption properties (*i.e.* mutual diffusion coefficient D_{12} and polymer-gas partition coefficient, K) of a homologous series of n -alkyl acetates in poly(methyl acrylate) (PMA) far above its T_g as a function of loading of spherical silica nanoparticles of average diameters 14 and 50 nm. The important decrease in D values results are not fully understood but they found an elegant interpretation within the presented framework of active systems. The results expressed as deviations to bulk properties and averaged over the range of studied concentrations are reproduced in Figure 2-28. They show that the composite system present an excess of affinity comparatively to expectations from Eq. (2-29) and higher D reductions than those expected for inert spherical diameters of similar diameters.

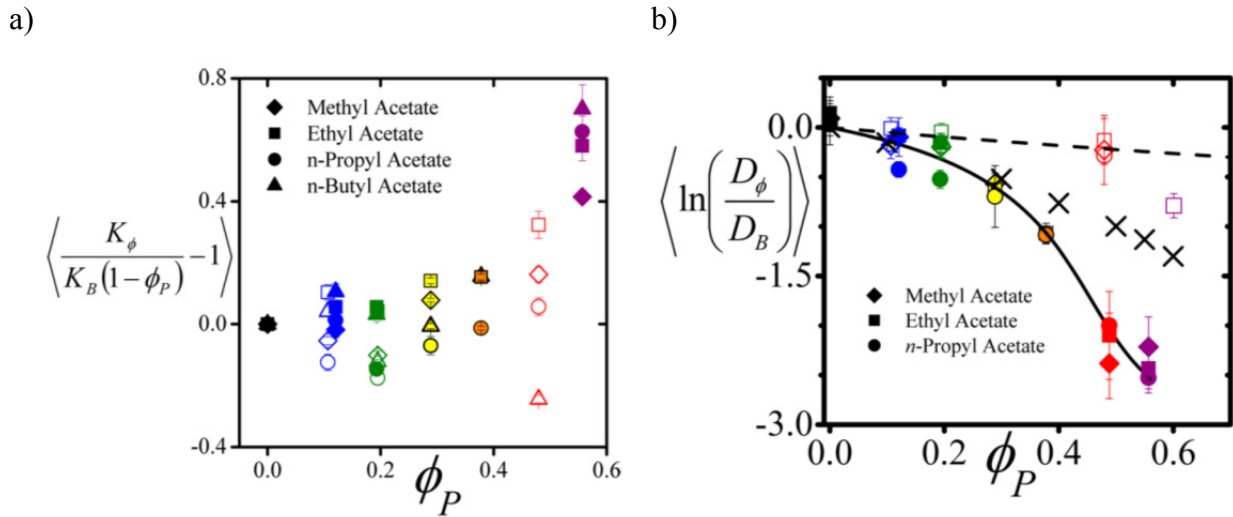


Figure 2-28 a) Excess polymer-air partition coefficient K or “sorption excess” (positive value= chemical affinity for the polymer above the one expected from Eq. (2-29)) versus the volume fraction in particles ϕ_P . b) Reduction of mutual diffusion coefficients with ϕ_P . Subscripts ϕ and B denote effective and bulk properties respectively. Filled and empty symbols represent data obtained with a diameter of 14 nm and 50 nm respectively. The theoretical D reduction with impermeable particles (Sangani and Yao, 1988) are plotted with (\times) for particles of diameter 14 nm.

The authors concluded that “To our knowledge, no theory that assumes the properties of the matrix polymer correspond to that of the unfilled material can adequately describe the suppression of diffusivity observed here for the PNCs [*i.e.* polymer nanocomposites] made with smaller nanoparticles over the whole range of ϕ_P tested”. The authors proposed an interpretation based on the model (Sax and Ottino, 1983). The authors suggest two interpretations:

- i) “Effective “densification” of the PMA due to confinement and strong favorable interactions of polymer segments with the silica surface”;
- ii) “transport is delayed by strong interactions of the diffusant with the silica surface sites, which effectively act as “traps”.”

As acknowledged by the authors themselves, the first interpretation is opposite to the local rarefactions of polymer segments suggested by Merkel et al. (2002b; 2003). This second interpretation could be interpreted through the following reversible “reaction” scheme:



where i is the solute and A the adsorbent particle. $k_{sorption}$ and $k_{desorption}$ are two reaction rates and related to $K_{contrast}$ via:

$$K_{contrast} = \frac{k_{sorption}}{k_{desorption}} \quad (2-37)$$

From similar modeling in catalysis involving physisorption (Leypoldt and Gough, 1980; Yang and Cussler, 2001; Yang et al., 2001), the effective transport equation close to particles become:

$$\frac{\partial C}{\partial t} = \nabla \cdot \left(\frac{D_{bulk}(C)}{1 + K_{contrast}} \nabla C \right) \quad (2-38)$$

Eq. (2-38) yields an effective diffusion coefficient similar to the one obtained with Eq. (2-35). Since the sorption properties in the polymers, the proposed description could be validated or invalidated simply by measuring the adsorption properties of the nanoparticles with the same experimental device.

2.2.3 Reactive barriers

2.2.3.1 The concept of sacrificial reagent to increase barrier properties

According to Yang et al. (2001), a third route to develop barrier films would exist by incorporating chemically reactive groups. The concept has been elaborated further in the third edition of the reference textbook of Cussler (2009), called barrier with sacrificial reagent. It is used in many patents in particular for developing barrier materials to oxygen but the literature remains scarce outside the work of the group of Cussler itself. We present here the interpretation detailed in pages 560-561 of Cussler (2009).

A simple example of coupling between mass transfer and an irreversible reaction is presented in Figure 2-29. Its interest is mainly pedagogical: it demonstrates the reduction of apparent permeability and the increase in lag times based on a simple analytical solution.

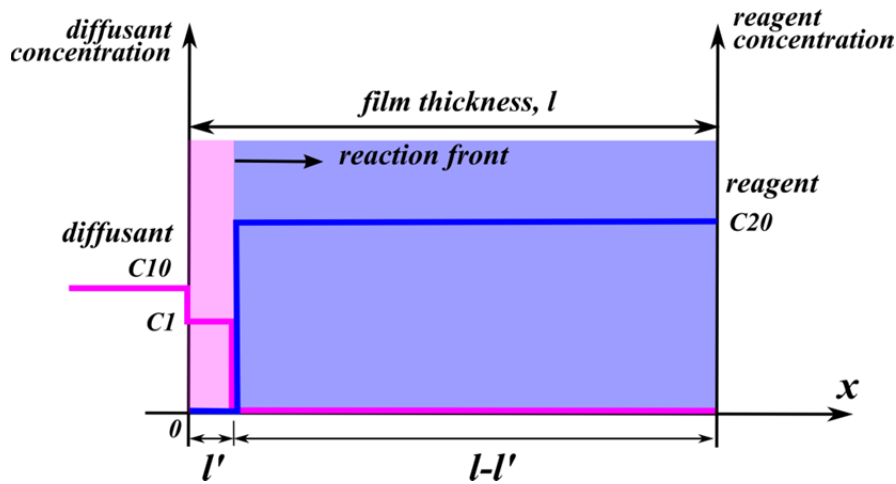
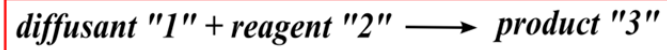


Figure 2-29 The concentration profiles of diffusants and reagent in reactive film with thickness, l . The reaction front separated film into diffusion zone, l' , and reaction zone, $l-l'$. C_{10} and C_{20} are the constant diffusants concentration in contact with film and the reagent concentration in reactive film.

When the reaction front moves slowly, an unsteady-state mass balance can be written assuming reagent is immobile:

$$\frac{d(Al'c_{20})}{dt} = \frac{\nu DSA}{l'}(c_{10} - 0) \quad (2-39)$$

where A is the cross-sectional area, ν is stoichiometric coefficient, the number of moles of reagents consumed by a mole of diffusants. This is subjected to:

$$t = 0 \quad l' = 0 \quad (2-40)$$

By integrating Eq. (2-40) into Eq. (2-39):

$$l' = \left(\frac{2DS_{c_{10}}t}{c_{20}} \right)^{1/2} \quad (2-41)$$

When the reagent is completely exhausted within the reactive film, $l'=l$, the reactive film starts to leak. The lag time is expressed as follows:

$$t_{lag} = \frac{l^2 c_{20}}{2\nu D S c_{10}} \quad (2-42)$$

For more general conditions, we have to refer to reviews (Yang and Cussler, 2001; Yang et al., 2001). Table 2-16 presents theoretical reduction in effective diffusion coefficients and permeability. Most of the results require serial expansions for their demonstration.

Table 2-16 Effective TR_{eff} and D_{eff} in reactive barrier systems (after Table 1 in Yang et al. (2001))

Barrier type	TR_{eff}	Corresponding D_{eff}	d
Nonreactive	$TR_{eff} = TR_{bulk}$	$D_{eff} = \frac{TR_{eff}l}{S_{eff}}$	1D
Reversible reaction yielding a model product	$TR_{eff} = TR_{bulk}(1+K)$	$D_{eff} = \frac{TR_{eff}l}{S_{eff}}$	1D
Reversible reaction yielding an immobile product	$TR_{eff} = TR_{bulk}$	$D_{eff} = \frac{D_{bulk}}{1+K}$	1D
Irreversible reaction yielding an immobile product	$TR_{eff} = TR_{bulk}$	$D_{eff} = D_{bulk} \frac{\nu S_{eff} K c_{10}}{3c_{20}}$	1D

K : the apparent equilibrium constant equals kc_2/k' , k and k' are the forward and reverse reaction rate constants.

2.2.3.2 Performances of reactive barriers

Reactive food packaging materials have been considered for both “barrier packaging” and “intelligent packaging” applications (Brody et al., 2010; López-Rubio et al., 2004). Current applications target mainly an increase of food product shelf life by scavenging oxygen (irreversible reaction), adsorbing carbon dioxide or ethylene, etc. (Brody et al., 2008). The engineering principles of oxygen scavenger has been reviewed by (Yang and Cussler, 2001). The idea consists in adding immobile chemically reactive groups within the film to react with diffusant molecules, by which the lag time could increase about three orders of magnitude. The estimated performances of some specific systems are reported in Table 2-17 with reduction in effective diffusion coefficients (or equivalently increase in lag times) ranging from 300 to 72000.

Table 2-17 Estimated reduction of permeability and D in reactive barrier systems containing reactive flakes (after Table 2 in Yang et al. (2001))

Host matrix	Principle	Diffusants	ϕ	D_{bulk}/D_{eff}	TR_{bulk}/TR_{eff}
Polyvinyl alcohol	Reagent: ZnO	Hydrochloric acid	≈ 0.05	300	8.4
Low density polyethylene	Reagent: linolenic acid	Oxygen	≈ 0.05	72000	10
Polyacrylonitrile	Reagent: linolenic acid	Oxygen	≈ 0.05	-	10
Polyvinylidene chloride	Reagent: linolenic acid	Oxygen	≈ 0.05	-	10
Low density polyethylene	Reagent: CaO	Water†	≈ 0.05	27000	10

Polyacrylonitrile	Reagent: CaO	Water†	≈0.05	-	10
Polyvinylidene chloride	Reagent: CaO	Water†	≈0.05	1680	10

† saturated vapor at 25°C.

2.3 Conclusions

The literature review showed that diffusion in solid polymers is mainly affected by free-volume effects for both gases and organic solutes. Rubber polymers and elastomers offer consequently the poorest barrier properties. Improve their barrier properties by adding nano-fillers has been investigated by many authors but up to now still led to poor barrier improvements. Proven strategies include combining materials in layered structure at microscopic scale (conventional multilayer materials) or at nanoscale (multi-multi layer materials) and materials incorporating scavengers. The first strategy is limited by the compatibility of the layers to be combined (not any material can be used) rather than the second is limited by the availability of reactive systems (they are limited to oxygen and in a less extent to water). The thesis will follow different directions based on the concepts of active or chaotic barriers. The initial idea is that macroscopic diffusion coefficients can be lowered by the coupling of random walk and sorption properties at microscopic scale (note that the coupling is not true at macroscopic scale). In simple words, increasing the dwelling time at molecular scale causes a decrease in mass transport properties. This effect is not new at all since it is known in chromatography as elution time (normal or reverse one). Increasing the chemical affinity for the support/matrix increases the lag time and therefore the apparent diffusion coefficient (note that the correct transport coefficients involve a combination of diffusion and convection). The theoretical reduction of effective D values in condensed media has been proposed in Leypoldt and Gough (1980), Yang et al. (2001) and Vitrac and Hayert (2007) in two different contexts for catalytic reactions with an excess of binding sites and for random walks in polymers, respectively. The authors show that the effect does not depend on the average value of solubility (or equivalently of the free energy) but on the contrast/fluctuations of the free energy. Two systems can be thought to test the proofs of these concepts:

- A system where the second-moment of the free energy of the diffusant-host is high as studied theoretically by Karayiannis et al. (2001);
- A system with at least two states separated by a large partition coefficient (i.e. involving for example an endothermic and an exothermic sorption).

The second solution will be preferred as it could be envisioned that the contrast could be controlled by temperature. For example, the material is barrier or selective at low temperature and permeable at much higher temperature.

Chapter 3. Objectives and approaches

3.1 General objectives

The general objectives of the thesis are to provide experimental proofs and engineering rules for polymer materials barrier to organic solutes and integrating nano-adsorbents. The concepts are tested in the most favorable case, where the original polymer is an aliphatic polymer above its T_g and the nano-adsorbents are organo-modified clays. The reader must be aware that the intent is not to develop a real new barrier composite system but to understand the conditions for which such concept can be effective and could be controlled by changing temperature.

Respectively to the choice of the considered hybrid (*i.e.* organic-inorganic) system, the subject may look not original as many composite systems have been already described in the literature. In our perspective, the originality of the work is in two aspects: i) we address first the barrier properties to organic solutes in the sense of an increase of the lag time to diffusion, whereas most of previous works focus on a reduction of the permeability to gases. ii) the studied system offers the simplest system where sorption is endothermic (polymer) in one phase and exothermic (adsorbent) in the other, so that a strong modulation is expected with temperature. Finally, alumino-silicate clays offers the outstanding properties to be wettable to both polar and apolar compounds (Eltantawy and Arnold, 1972).

3.2 Particular objectives

The new concepts must be separated from other known effects. For example as discussed in section 2.2, incorporating particles is known to create obstacles to diffusion and to modify polymer properties (e.g. crystallinity, morphology and size of crystallites, T_g shift, free-volumes etc.). It could be thought that the sought effects could be detected easily by a D reduction larger than the ones already reported in the literature, which is close to a factor 2. In practice, it is not obvious as a strong effect is expected only if the parameter $K_{contrast}$ is much greater than one. As a result, the main issues are:

- To develop an enough solid theory of diffusion in order to enable to distinguish the effects of tortuosity and orientation from others. At this stage, it is important to note that conventional effects are not affected by a temperature variation whereas $K_{contrast}$ will be. An activation of diffusion with temperature for rubber polymers requires to separate free-volume effects close to T_g from

those far from T_g regardless the considered size of the solutes. In materials incorporating nano-adsorbents, a significant excess of activation energy of D is in particular expected. If the measurements of D are enough accurate and sensitive, it can be thought that this trend could be detected even if the decrease of D is low. For more reliability, an additional and complementary proof will be used. Tortuosity and morphological effects are not expected to affect the scaling of D for different solutes at the same temperature (*i.e.* they are subjected to same topological constraints). The concept considered here relies on the scaling exponent $\alpha(T)$ discussed in section 5.1.3.

- To get a predictive model of $K_{contrast}$, which enables to identify which polymer and surface modifications of clays are optimal for a D reduction. In clear words, do we need to incorporate organo-modified clays in apolar polymers or pristine clays in polar polymers? Do we need to change the conclusions if the solute is polar instead of apolar? Aromatic instead of aliphatic? Behind all these issues, there is a transversal question: From the point of view of organic solutes, is the sorption on montmorillonites a surface phenomenon (adsorption) or a volume phenomenon? In other words, increasing the interlayer distance between clays or covering the surface with surfactants is it an effective direction to increase $K_{contrast}$?
- To test the concepts on real systems where no specific attention was drawn to orientation and exfoliation of the clays. As it is thermodynamically controlled, it should work only by mixing ingredients, at least if the intrinsic properties of the polymer are not significantly altered.

3.3 Approaches followed in this thesis

To meet the different goals and requirements, several approaches (*i.e.* methodological or cognitive) have been developed and tested. They are summarized in Table 3-1. The table is not exhaustive but provides guidance and clue to read the manuscript.

Table 3-1 The objectives and corresponding methodologies included in the thesis.

Objectives	Question type (section)	Approach	Expected results
<p>The representative set of conditions for setting and evaluating the barrier concepts for two test systems: reference systems, nanocomposite systems</p> <p><u>polymer:</u> with variable T_g ($-120^{\circ}\text{C} < T_g < 85^{\circ}\text{C}$)</p> <p><u>homologous solute:</u> Linear (aliphatic or aromatic) solutes branched (aromatic) solutes</p> <p><u>nano-adsorbent:</u> pristine montmorillonites (MMT) three organo-modified ones equipped with different functional group</p> <p>Variable temperature conditions to separate $T-T_g$ effect</p>	<p>Choices (Chapter 4)</p>	<p>Reference systems including polymers and solutes to assess their independent effect on D:</p> <ul style="list-style-type: none"> - Tested virgin films: polylactide, polypropylene, polycaprolactone, polyvinyl alcohol - Source films: formulated polypropylene, polycaprolactone, polyvinyl alcohol - Solutes: <ul style="list-style-type: none"> Linear solutes (literature data) <ul style="list-style-type: none"> - n-alkanes ($n=12..60$) - n-alcohols ($n=12..18$) - n-alkylphenols ($n=6..18$) Branched solutes (literature data/measured ones) <ul style="list-style-type: none"> - n-alkylbenzene ($n \leq 4$) - Substituted and hindered phenols - Diphenylalkanes series - Oligophenyls series <p>Nanocomposite systems to assess nano-adsorbent effect on D Polymer + nano-adsorbents + solute:</p> <ul style="list-style-type: none"> - polycaprolactone + organo-modified clay + biphenyl - polyvinyl alcohol + pristine clay + biphenyl 	<ul style="list-style-type: none"> - Establishment of solution casting method for different polymer and nanocomposite processing - Procedure to formulate source films with uniform concentration profiles. - Formation of stable systems/model for further characterization with repeatable results

$(T_g+10K < T < T_g+110K)$			
Reference methods to assess experimentally diffusion coefficients ranging from $10^{-12} \text{ m}^2 \cdot \text{s}^{-1}$ to $10^{-17} \text{ m}^2 \cdot \text{s}^{-1}$	Methodology (section 5.1.3 & 4.2.3)	<p>Concentration profile methods</p> <ul style="list-style-type: none"> - Low diffusion coefficient (<i>i.e.</i> $< 10^{-14} \text{ m}^2 \cdot \text{s}^{-1}$) → fluorescence microspectroscopy method with synchrotron source - High diffusion coefficient (<i>i.e.</i> $> 10^{-14} \text{ m}^2 \cdot \text{s}^{-1}$) → film stacking method with solvent extraction 	<ul style="list-style-type: none"> - The tested solutes which are naturally fluorescent could adsorb UV and could be detected by fluorescence microspectroscopy and UV spectrophotometer. - Development of two novel methodologies to assess correctly D values for tested D range
Extended free volume theory for flexible and bulk solutes	Cognitive (section 5.1.3)	<ul style="list-style-type: none"> - Scaling law of D for homologous linear solutes - Relationship between scaling law and conventional free-volume theory - Integration of short and long-lived contacts - Integration of effect of oddity of solute jumping units - Integration of activation energy and entropy compensation effects 	<ul style="list-style-type: none"> - Establishment of scaling law of diffusion for linear solutes in aliphatic polymer above T_g - Separation independently polymer effect (<i>i.e.</i> $T-T_g$ effect) and solute effect (<i>i.e.</i> concerted motions)
Calculation of $K_{contrast}$ and its variation with: Temperature, d -spacing, surface coverage, surfactant type	Methodology Cognitive (section 5.2.2)	<ul style="list-style-type: none"> - Characterization of tested clay: XRD, TGA, BET, <i>etc</i> - Reference sorption properties: IGA, IGC <ul style="list-style-type: none"> - At infinite dilution - At high concentration - Molecular simulation <ul style="list-style-type: none"> - Building an atomistic model - Insertion method - Grand canonical simulation method - Discussion for homogenous n-alkanes and aromatic solutes (toluene, anisole), and comparison with their sorption properties on surfactants 	Distinction between adsorption and sorption in the excess of surfactants or in the clay gallery
Proof of the same concepts on typical cases	Cognitive (section 5.2.3)	<p>Many combinations:</p> <ul style="list-style-type: none"> - Apolar clay in apolar polymer - Polar clay in polar polymer - Solutes - Reference $K_{contrast}$ values 	Correlation of D values with $K_{contrast}$ values with effect of temperature

The remaining part of the manuscript is organized as follows. The next chapter (Chapter 4) details the main materials (polymer, substances and clays) used in this study as well as specific methodologies to measure a broad range of D values for homologous solutes in various polymers. Methodologies to process all tested materials (composite or not) are also fully detailed. Details of methodologies, which are more generic are given along the “results and discussion” chapter. Results are presented as independent works on the three main questions:

- Can we get a general theory of diffusion for flexible and rubber solutes in aliphatic polymers? (section 5.1)
- Which physical parameters (*e.g.* basal-spacing, surface coverage, surfactants) are controlling the chemical affinity of pristine and organo-modified montmorillonites (section 5.2)?
- What are the performances of nanoadsorbents on reducing D in typical polymer and contact conditions? (section 5.3)

The directions of optimization of all aforementioned effects are discussed in a specific section (section 5.3.3 and section 5.4). Finally conclusions and recommendations for future works are addressed in Chapter 6.

Chapter 4. Materials and methods

This section provides an exhaustive list of the solutes, polymers and adsorbents used at one stage of this thesis for experiments, simulations or as standard references. The aim is to promote a broad view of tested or examined conditions. In shorts, aliphatic polymers polar or not are well represented above their glass transition temperature (T_g) where they are more permeable to organic solutes. The collection of solutes is significant with one of the largest list of solutes with homologous chemical structures. The reader must not be mistaken, only a fraction of associated diffusion coefficients was measured in the thesis and many data were extracted from an attentive study of literature data starting from years of 60s. Anyway, they were used to build a more general theory of diffusion for bulky and flexible diffusants. The set of tested adsorbents is much smaller and focused on commercially available organo-modified montmorillonites. Only one surfactant including one aromatic ring is less common and was selected to compare the strength of π - π interactions and polar ones between tested solutes and surfactant.

The methodologies were diverse from experimental determinations of raw materials to simulations and mathematical identification of diffusion coefficients. The details of well-known methods are detailed in the sections where the corresponding results are presented. The methods which were significantly developed or modified in this study are presented here. They include mainly practical information:

- to formulate materials with almost incompatible solutes (*i.e.* how to formulate materials with a full list of homologous solutes which start to become less and less soluble?);
- to process nanocomposite materials according to the concepts followed in the thesis;
- to measure reliable diffusion coefficients spread over several decades (10^{-12} - 10^{-17} $\text{m}^2\cdot\text{s}^{-1}$) and activation energies ranging from 40 to 150 $\text{kJ}\cdot\text{mol}^{-1}$.

From our experience, it has been shown that this information was found critical by other research groups to reproduce independently the results presented in this study.

4.1 Materials


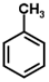
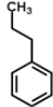
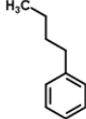
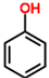
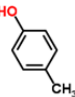
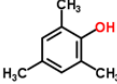
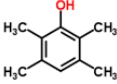
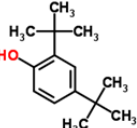
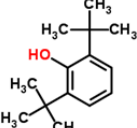
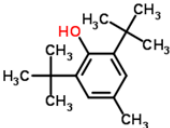
4.1.1 Solutes

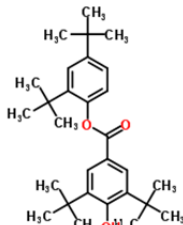
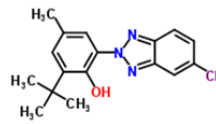
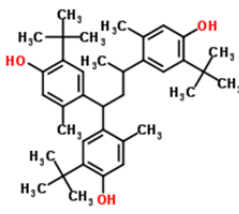
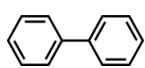
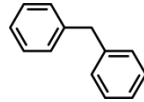
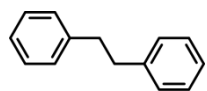
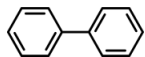
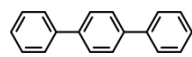
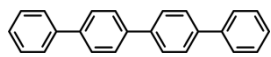
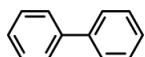
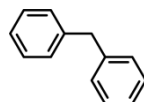
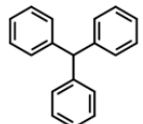
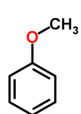
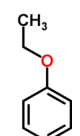
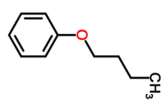
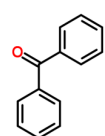
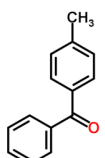
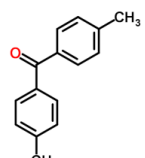
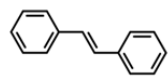
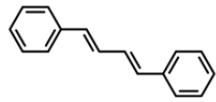
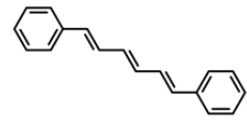
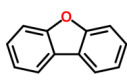
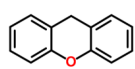
Tested solutes are splitted into three categories according to the studying property:

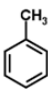
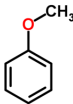
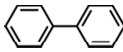
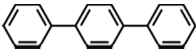
- *Category 1*: to assess the diffusion coefficients of homologous solutes, including mainly a linearly repeated pattern to get reference D values in bulk and corresponding polymers.
- *Category 2*: to assess the sorption properties of solutes onto adsorbents and in polymers to get an estimation of $K_{contrast}$.
- *Category 3*: to assess the D reduction and its likely mechanism on polymer nanocomposite systems.

According to above categories, all tested solutes are listed in Table 4-1.

Table 4-1 List of solutes applied in the thesis

<i>Application</i>	<i>Series</i>	<i>Solutes</i>			
<i>Linear solutes in Category 1†</i>	<i>n</i>-alkanes <i>n</i>-alcohols <i>n</i>-alkylphenols	$n=12..60$ ($M = 170-843 \text{ g}\cdot\text{mol}^{-1}$) $n=12..18$ ($M = 186-270 \text{ g}\cdot\text{mol}^{-1}$) $n=6..18$ ($M = 290-543 \text{ g}\cdot\text{mol}^{-1}$)			
<i>Aromatic solutes in Category 1†</i>	<i>n</i>-alkylbenzene	Benzene	Toluene	Propylbenzene	Butylbenzene
	Structure				
	M ($\text{g}\cdot\text{mol}^{-1}$)	78.1	92.1	120.2	134.2
<i>Aromatic solutes in Category 1†</i>	Substituted and hindered phenols	Phenol	4-Methylphenol	2,4,6-trimethylphenol	Durenol
	Structure				
	M ($\text{g}\cdot\text{mol}^{-1}$)	94.1	108.1	136.2	150.2
<i>Aromatic solutes in Category 1†</i>	Substituted and hindered phenols	2,4-Di- <i>t</i> -butylphenol	2,6-di- <i>t</i> -butylphenol	Butylated hydroxytoluene	
	Structure				
	M ($\text{g}\cdot\text{mol}^{-1}$)	206.3	206.3	220.4	
<i>Aromatic solutes in Category 1†</i>	Substituted and hindered phenols	2,4-Di- <i>t</i> -butylphenyl 3,5-di- <i>t</i> -butyl-4-hydroxybenzoate	2-(5-Chloro-2H-benzotriazol-2-yl)-4-methyl-6-(2-methyl-2-propanyl)phenol	4,4',4''-Butane-1,1,3-triyltris(2- <i>t</i> -butyl-5-methylphenol)	

	Structure			
	M (g·mol ⁻¹)	438.6	315.8	544.8
<i>Aromatic solutes in Category 1</i> [‡]	Diphenyl alkanes	Biphenyl ^a	Diphenylmethane ^b	Bibenzyl ^b
	Structure			
	M (g·mol ⁻¹) N _C =	154.2 0	168.2 1	182.3 2
<i>Aromatic solutes in Category 1</i> [‡]	Oligophenyls	Biphenyl ^a	<i>p</i> -terphenyl ^a	<i>p</i> -quaterphenyl ^a
	structure			
	M (g·mol ⁻¹) N _{Ph} =	154.2 2	230.3 3	306.4 4
<i>Aromatic solutes in Category 1</i> [‡]	Branching phenyl methane	Biphenyl ^a	Diphenylmethane ^a	Triphenylmethane ^a
	structure			
	M (g·mol ⁻¹)	154.2	168.2	244.3
<i>Aromatic solutes in Category 1</i> [‡]	Alkyl phenyl ethers	Anisole ^a	Ethyl phenyl ether ^a	Butyl phenyl ether ^a
	structure			
	M (g·mol ⁻¹)	108.1	122.1	150.2
<i>Aromatic solutes in Category 1</i> [‡]	Substituted benzophenone	Benzophenone ^e ^a	4-methyl benzophenone ^a	4,4'-dimethyl benzophenone ^a
	structure			
	M (g·mol ⁻¹)	182.1	196.2	210.3
<i>Aromatic solutes in Category 1</i> [‡]	Stilbene	Trans-stilbene ^a	Trans,trans-1,4-diphenyl-1,3-butadiene ^a	1,6-diphenyl-1,3,5-hexatriene ^a
	structure			
	M (g·mol ⁻¹)	180.1	206.1	232.1
<i>Aromatic solutes in Category 1</i> [‡]	Various	Dibenzo[b,d]furan ^a	Xanthene ^a	
	structure			
	M (g·mol ⁻¹)	168.2	182.1	
<i>Linear solutes in Category 2</i> [‡]	<i>n</i>-alkanes	n=5..9 (M = 72-128 g·mol ⁻¹)		
<i>Aromatic solutes in</i>	Aromatic solutes	Toluene	Anisole ^a	

Category 2 [‡]	structure		
	M (g·mol ⁻¹)	92.1	108.1
Aromatic solutes in Category 3 [‡]	Aromatic solutes	Biphenyl ^a	<i>p</i> -terphenyl ^a
	structure		
	M (g·mol ⁻¹)	154.2	230.3

[†]: collected diffusion coefficient of solutes reported in literature, [‡] data measured in the thesis.

4.1.2 Polymer

Polymer materials are applied in two systems:

- i) Reference polymers including polyamide (PA), polyethylene (PE), polyvinyl acetate (PVAc), polylactide (PLA), polypropylene (PP), polycaprolactone (PCL) and polyvinyl alcohol (PVA) were applied to investigate diffusion coefficients of organic solutes above T_g .
- ii) In nanocomposite systems, polymer including polycaprolactone (PCL) and polyvinyl alcohol (PVA) were used as host matrix to extract solely effect of nano-adsorbents on diffusion coefficient above T_g .

The detailed information and characterization of applied polymers are listed in Table 4-2. To avoid degradation of PVA which are obliged to be tested at higher temperature due to its high T_g , T_g of PVA was modulated by using it both at dry state and equilibrated at an intermediate relative humidity of 21-28% with 2.4 wt% of water content.

Table 4-2 Information and characterization of applied polymers

Polymer	T _g (°C)	Crystallinity %	Thickness (mm) × width or diameter (mm)	Film processing	Supplier/product reference	Application purpose
Polyamide (PA) †	25	Amorphous	-	-	-	Reference polymer
Polyethylene (PE) with low density (LDPE) or high density (HDPE) †	-100 ~120	Semicrystalline	-	-	-	Reference polymer
Polyvinyl acetate (PVAc) †	32	-	-	-	-	Reference polymer
Poly lactide (PLA) ^a ‡	60	23.6	0.02×600	Extrusion	Treofan (Germany)/ Biophan™	Reference polymer
Polypropylene (PP) ^a ‡	0	55.5	0.2×800	Extrusion blowing	Borealis (Austria)/ HD621CF	Reference polymer
Polycaprolactone (PCL) ^b ‡	-60	50.3	0.01-0.04×200	Solution casting	Creagif Biopolymères (France)/ CAPA 6800	Reference polymer /nanocomposite
Polyvinyl alcohol (PVA) ^c ‡	55 82	50.0	0.01-0.03×200	Solution casting	Sigma-Aldrich (USA)/ Mowiol® 20-98	Reference polymer /nanocomposite

^aFilms were processed at industrial scale and used as received. ^bPCL films with molecular weight of $8 \cdot 10^4 \text{ g} \cdot \text{mol}^{-1}$ were processed at laboratory scale as described in (Marras et al., 2008). ^cThe PVA films with molecular weight of $125000 \text{ g} \cdot \text{mol}^{-1}$ (98.0-98.8 % of hydrolysis degree) were processed at laboratory scale as described in (Otsuka and Suzuki, 2009). *T_g* of PVA were of 82°C and of 55°C, at dry state and when the films were equilibrated at a relative humidity of 21-28% respectively. †: collected diffusion coefficient reported in literature, ‡ data measured in the thesis.

4.1.3 Nano-adsorbents

Pristine montmorillonite and three surface modified ones with different functional cationic surfactants are selected as nano-adsorbents.

Montmorillonite (MMT), is a hydrated alumina-silicate layered clay consisting of an edge-shared octahedral sheet of aluminum hydroxide sandwiched between two silica tetrahedral layers (Olphen, 1964), as depicted in Figure 4-1. The layered crystals, which are approximately 1nm thick with lateral dimensions from 30nm to several microns, are piled parallel to each other and are bonded by local van der Waals and electrostatic forces (Tan et al., 2008). Due to delocalization by negative charges, such as $[\text{SiO}_4]$ replaced by $[\text{AlO}_4]^-$ causing defects in the tetrahedral layer (Heinz and Suter, 2004), $[\text{AlO}_6]$ replaced by $[\text{MgO}_6]^-$ causing defects in the octahedral layer, the imbalance of the surface negative charges is compensated by exchangeable cations (typically Na^+ , K^+ and Ca^{2+}) which are situated in between the charged layers. The charge of the layer is not locally constant as it varies from layer to layer (Alexandre and Dubois, 2000).

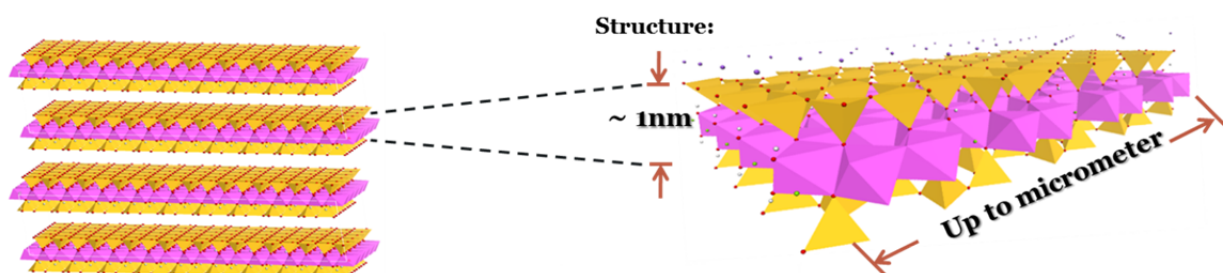
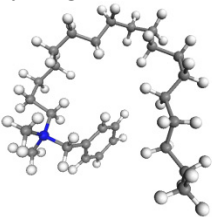
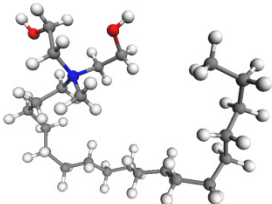
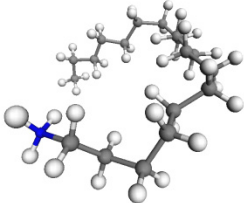


Figure 4-1 The scheme of the structure of pristine montmorillonites.

To render layered hydrophilic MMT miscible with hydrophobic polymer matrices, one must convert the hydrophilic surface to an organophilic one. Generally, this can be done by ion-exchange reactions with cationic surfactants including primary, secondary, tertiary and quaternary alkylammonium or alkylphosphonium cations with or without functional groups. In this study, three cationic surfactants with functional groups (e.g. phenyl ring, OH group) were applied to modify the surface of MMT that are commercial available and listed in Table 4-3. Before usage, all surface modified MMT were dried in a vacuum oven at 80°C for 12 h.

Table 4-3 The information and chemical structure of four commercial available clays

Abbreviation	Chemical composition	Supplier /Product reference
MMT Surfactant: Chemical formula:	Montmorillonite n/a $[\text{Na}_{0.38}\text{K}_{0.01}][\text{Si}_{3.92}\text{Al}_{0.07}\text{O}_8][\text{Al}_{1.45}\text{Mg}_{0.55}\text{O}_2(\text{OH})_2] \cdot 7\text{H}_2\text{O}^\dagger$	Aldrich (France) /682659
C6H5MMT Surfactant: Chemical formula:	Organo-modified montmorillonite Dimethyl, benzyl (hydrogenated tallow) alkyl ammonium‡ 	Rockwood (Germany) /Nanofil [®] 9
C18OHMMT Surfactant: Chemical formula:	Organo-modified montmorillonite Methyl dihydroxyethyl hydrogenated tallow ammonium‡ 	Aldrich (France) /682640
C18MMT Surfactant: Chemical formula:	Organo-modified montmorillonite Octadecylamine 	Aldrich (France) /682616

†: The chemical formula of each clay was determined by the element content measured by combustion for organic compounds and inductively coupled plasma atomic emission spectroscopy (ICP-AES) for inorganic compounds. ‡Tallow is a blend of unsaturated *n*-alkyl groups with an approximate composition: 65wt% of C18, 30wt% of C16, 5wt% of C14 as stated by supplier.

4.1.4 Polymer/nanocomposite film processing and formulation

4.1.4.1 Virgin films

PLA and PP were supplied as films and used as received. PCL and PVA films were processed by solution casting, according to (Marras et al., 2008; Otsuka and Suzuki, 2009) respectively. The PCL solution formed by dissolving 0.28g of PCL powder in 11.5 mL of dichloromethane with final concentration of 2.4 wt% was poured into a glass or a Teflon petri dish with diameter of 10 cm. To control the fast evaporation speed of dichloromethane, the petri dishes were covered by either filter paper or aluminum foil with homogenous pinholes and allowed solvent evaporation at room temperature for at least 12 h. Afterwards PCL films were peeled off from the dish and were dried in an oven at 30 °C for three days to remove residue dichloromethane. The PVA solution was obtained by dissolving 1.67g of PVA powder in 200mL of deionized water. The mixture was heated in an oil bath at 95°C for at least 5h to reach fully dissolution. After cooling down at room temperature, the solution was degassed in a sonicator bath for 10 min. As soon as no bubbles were observed, the solution was poured on a flat glass or plastic surface (ca. ID: 20cm x 20cm) to allow solvent (water) evaporation for at least 3 days. Then the PVA films were peeled off from the surface with the thicknesses ranging from 5 to 35µm. Before use, the films were conditioned under controlled relative humidity for 2 days to reach equilibrium water content.

4.1.4.2 Source films

Films acting as sources of solutes were formulated with each solute either by soaking films in a 0.05 g·ml⁻¹ solute-ethanol solution during a minimal duration of one week at 60°C (e.g. cases of PP, PVA) or by adding the desired solute to the casting solution at a concentration of 0.2 wt% (e.g. case of PCL). Due to the difficulty of absorbing bulky aromatic solutes in PLA films below or close to its *T_g* (to avoid recrystallization), PP films were used as sources instead in PLA contact experiments. All processed films were stored in stack to prevent solute losses and to facilitate the internal homogenization of concentration profiles. The uniformity of concentration profiles in sources was tested over the cross section of microtomed films by fluorescence imaging.

4.1.4.3 Nanocomposite film processing

10 to 50 µm thick of PVA nanocomposites incorporated by pristine MMT, and PCL nanocomposites incorporated by one type of organo-modified MMT (see Table 4-3) were processed by solution casting method described in Marras et al. (2008) and (Gaume et al.,

2012) respectively. For each nanocomposition, clay dispersion (0.1wt%) was obtained by suspension of well-dried clay powder in a corresponding solvent. Both polymer solution and clay suspension were sonicated separately for 30 min at room temperature and subsequently mixed. The mix ratios were calculated based on final concentration of nanoclay in polymer: 0.5 wt% and 5 wt% of organo modified clay in PCL polymer matrix, 0.5 wt% of pristine MMT in PVA polymer matrix. The final mixture was further sonicated for 30 min more and then cast as the same way for virgin films.

4.2 Methods

The methodologies applied in the thesis are detailed in both this section and also in each paper located in Chapter 5. In order to avoid repeated text and also to help the reader, we provided Table 4-4 to index each method.

Table 4-4 Index of methodologies applied in the thesis

<i>Samples</i>	<i>Classification of properties</i>	<i>Physical quantities</i>	<i>Methodologies</i>	<i>Location of method description</i>
Polymer/nanocomposite	Characterization properties	Crystallinity degree	Differential scanning calorimetry (DSC)	Section 4.2.1
Polymer/nanocomposite		Crystallite morphology	Polarized optical microscopy	Section 4.2.2
Nano-adsorbents	Characterization properties	Element content	Chemical analysis (ICP-AES)	Section 5.2.2
		d -spacing	X-ray diffraction analysis (XRD)	Section 5.2.2
		Organic content	Thermogravimetric analysis (TGA)	Section 5.2.2
		Specific surface area	Specific surface area (BET)	Section 5.2.2
Polymer	Thermodynamic properties	Sorption enthalpy (ΔH) /isosteric heat (Q_{is})	Grand Mont-Carlo molecular simulation Intelligent gravimetric analyzer (IGA)	Section 5.2.2
Surfactants		Sorption enthalpy (ΔH) /isosteric heat (Q_{is})	Grand Mont-Carlo molecular simulation	Section 5.2.2
Nano-adsorbents		- Sorption isotherm - Henry coefficients (K_H) - Sorption enthalpy (ΔH) /isosteric heat (Q_{is})	Grand Mont-Carlo molecular simulation Intelligent gravimetric analyzer (IGA) Inverse gas chromatography (IGC)	Section 5.2.2
Polymer/nanocomposite	Mechanical properties	Diffusion coefficients (D)	Solid contact/concentration profile methods - single film imaging by DUV/fluorescence microspectroscopy - 14 films contact method with solvent extraction	Section 5.1.3 Section 5.3.2

4.2.1 Differential scanning calorimetry (DSC)

T_g and crystallinity degree of each polymer reported in Table 4-2 were measured by differential scanning calorimetry (model Q100, TA Instruments, USA) at a heating rate of 10 °C/min within temperature limits adapted to each polymer. The crystallinity degree (χ_c) was calculated from the melting endotherm in the first heating scan

$$\chi_c (\%) = \frac{\Delta H_m - \Delta H_c}{\Delta H_m^{100\%}} \quad (4-1)$$

where ΔH_m and ΔH_c are the experimental melting enthalpy and cold crystallization enthalpy of polymer crystals, respectively. $\Delta H_m^{100\%}$ is the theoretical melting enthalpy of the 100 % crystalline polymer: 93 J·g⁻¹ for PLA (Fischer et al., 1973), 165 J·g⁻¹ for PP (Wunderlich, 1980), 139 J·g⁻¹ for PCL (Crescenzi et al., 1972), 138.6 J·g⁻¹ for PVA (Peppas and Merrill, 1976):

Glass transition temperatures of all polymers except PVA were measured in the second heating scan and taken at the mid-point of the heat capacity step. In the case of both dry and plasticized PVA, T_g values were determined from the first heating scan. Determinations were triplicated.

4.2.2 Polarized optical microscopy

The optical microscopy was performed on an optical microscope (BX51 frame, Olympus, Japan) in which one polarizer and one analyzer are aligned. The images were taken at a magnification of $\times 20$ for each sample.

4.2.3 Measurement of diffusion coefficients

The experimental procedures including sample preparations of two solid contact/concentration profile methods operated at two different length scales are described in Section 5.2.2. Since the data management of two methods was developed in the thesis and also it took a significant amount of time of author to validate and optimize, in this section we provide additional information of data analysis/management and corresponding troubleshooting solutions.

4.2.3.1 Single film imaging by DUV/fluorescence microspectroscopy

4.2.3.1.1 Sample preparation

The scheme of sample preparation is drawn in Figure 4-2. The source film is sandwiched by two virgin films. They are held in a metallic tube. Wood is used at both ends as plugs and the films are maintained in close contact using a screw. All contact layers have the same geometry to guarantee the quality of contact.

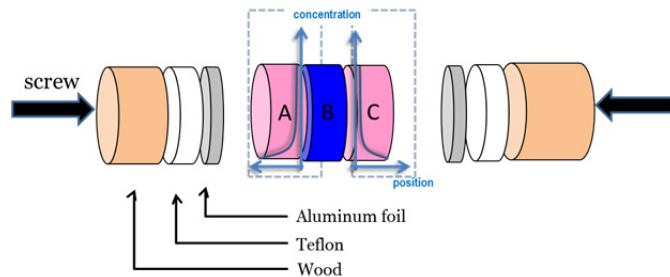


Figure 4-2 Scheme of sample preparation (A, C=virgin films, B=source film)

4.2.3.1.2 Theoretical concentration profiles

Since the diffusion coefficient could be assessed from concentration profiles of both virgin and source film, before the experiments are performed, a series of simulated continuous concentration profiles are prepared by considering geometry, contact time and partitioning of the contact system. According to the expected fitting positions, two series of concentration profiles are prepared either normalized at the interface (*i.e.* position at 200 μm and 400 μm) (see Figure 4-3a) for fitting profiles of layer A and C or normalized at the center of source layer (*i.e.* position at 300 μm) (see Figure 4-3b) for fitting profiles of layer B.

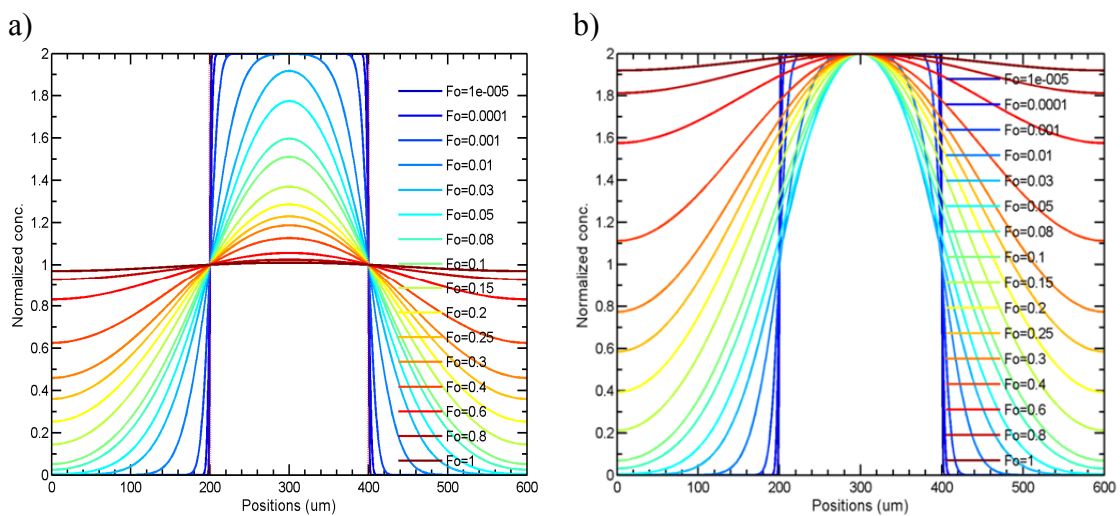


Figure 4-3 Simulated concentration profiles at cross section of three contact films assembled as in Figure 4-2 with thickness 200 μm each normalized at a) the interface and b) the center of source layer

Above theoretical concentration profiles could be used to fit with experimental ones for thick film (i.e. PP film with thickness of 200 μm). In the case of thin film (e.g. PLA film with thickness of 20 μm), the interface diffraction pattern could not be ignored. Mathematically, a diffraction kernel (i.e. Lanczos-windowed sinc) was added into each simulated concentration profile (see Figure 4-4).

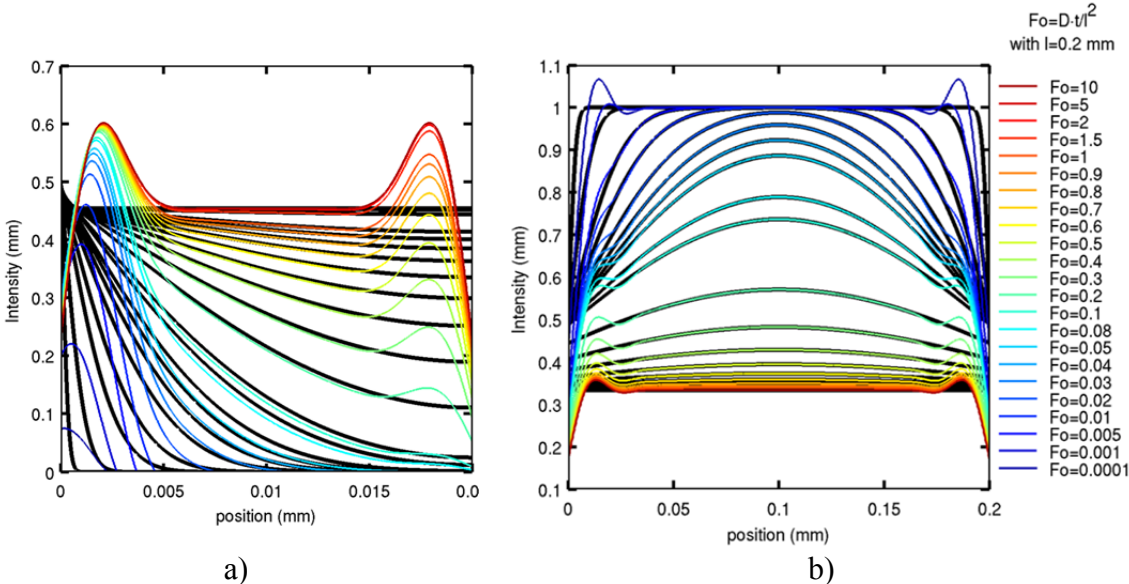


Figure 4-4 Comparison of theoretical concentration profiles with diffraction patterns (colored curves) and without (black curves) for a) the layer A or C and b) the layer B.

4.2.3.1.3 Data analyzing

For each sample, the spectra in the range of wavelength $\lambda=275\text{nm}-550\text{nm}$ are collected along the detected position. Due to the effect of diffraction and sample defect, the baselines are not flat, which could affect the final concentration profiles in a large extent when the emission intensity is low. Therefore, the baselines must be refined (see Figure 4-5)

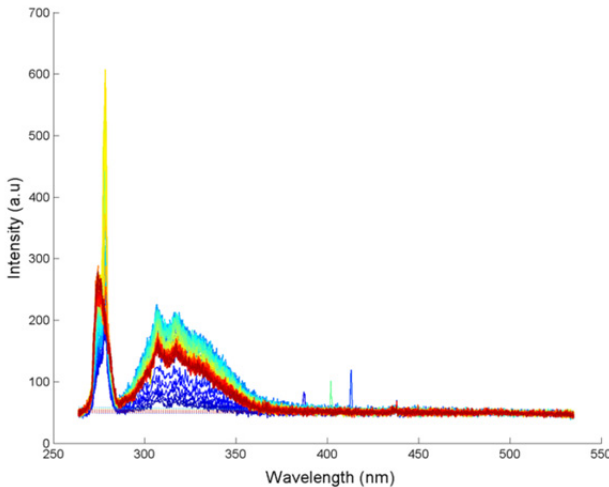


Figure 4-5 Example of the collected spectra at each measured position with baseline. Two peaks are related to excitation (i.e. $\lambda=275\text{nm}$) and emission (i.e. $\lambda=280-380\text{nm}$) respectively

By taking an example of assessing diffusion coefficients of biphenyl in PP films and PLA films at 343 K, D values are extracted by fitting the experimental concentration profiles with the theoretical ones. The raw data and its fitting for PP film at position C and B and for PLA film at position C are plotted in Figure 4-6 and Figure 4-7 respectively. It is worth to notice that the starting fitting point (*i.e.* interface location) is very critical on the fitting quality and on the extracted Fourier number. For PP layer at position A or C, the starting fitting point is the maximum at the peak of the concentration profiles. For layer B, the starting fitting point could be obscured as soon as the maximum intensity is not a plateau.

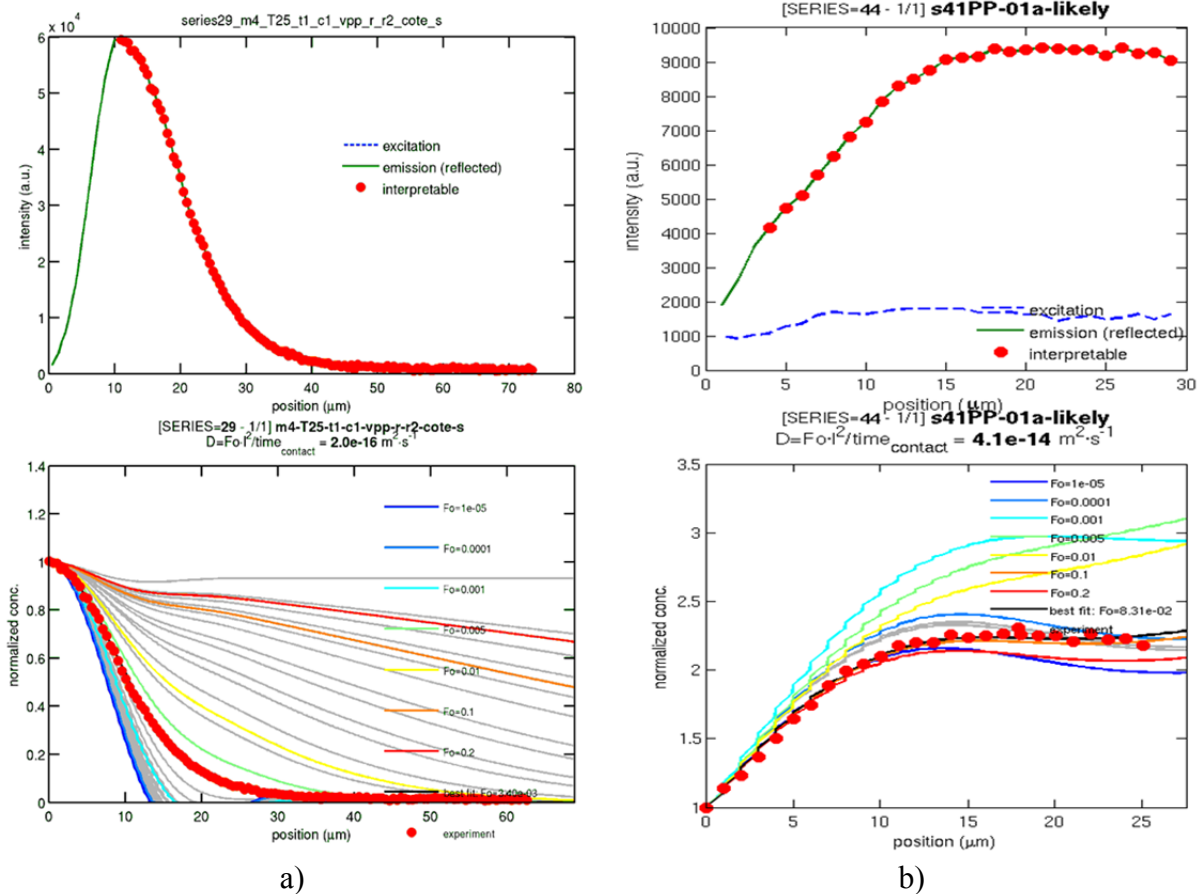


Figure 4-6 The experimental concentration profiles of biphenyl at 343K (red filled dot) in PP film at a) position C and b) position B fitted with theoretical concentration profiles (colored curves).

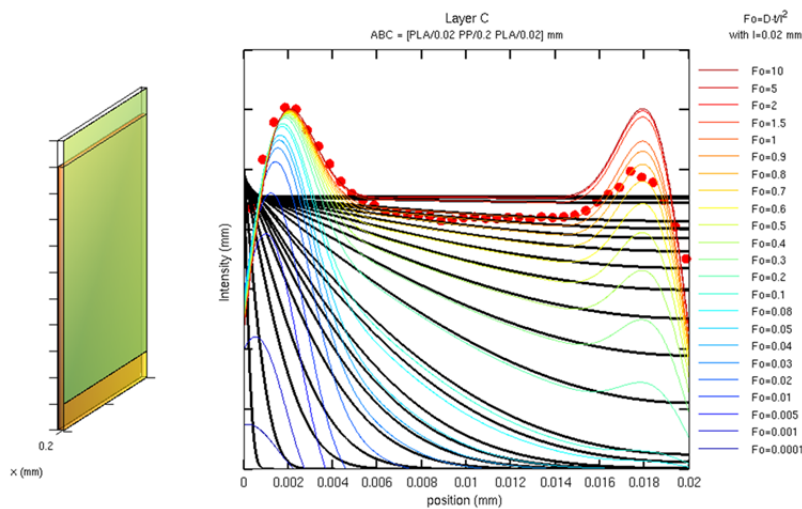


Figure 4-7 The experimental concentration profile of biphenyl at 343K (red filled dot) in PLA film at position C fitted with theoretical concentration profiles (colored curves).

4.2.3.2 14 films contact method

4.2.3.2.1 Sample preparation

The scheme of sample preparation is provided in Figure 4-8.

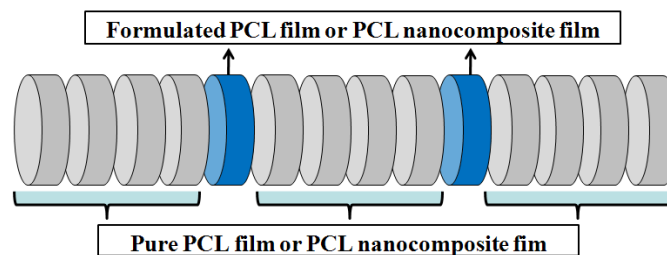


Figure 4-8 Scheme of sample preparation in 14 films contact experiment

4.2.3.2.2 Theoretical concentration profiles

14 films contact method is derived from Roe tests in which the high dilution induced by the dispersion of small amount of substance in a large volume of polymer. The dilution problem can be circumvented by inserting two sources instead of a single one. Optimal assembling involves two sources and a total of 14 films (see Figure 4-9).

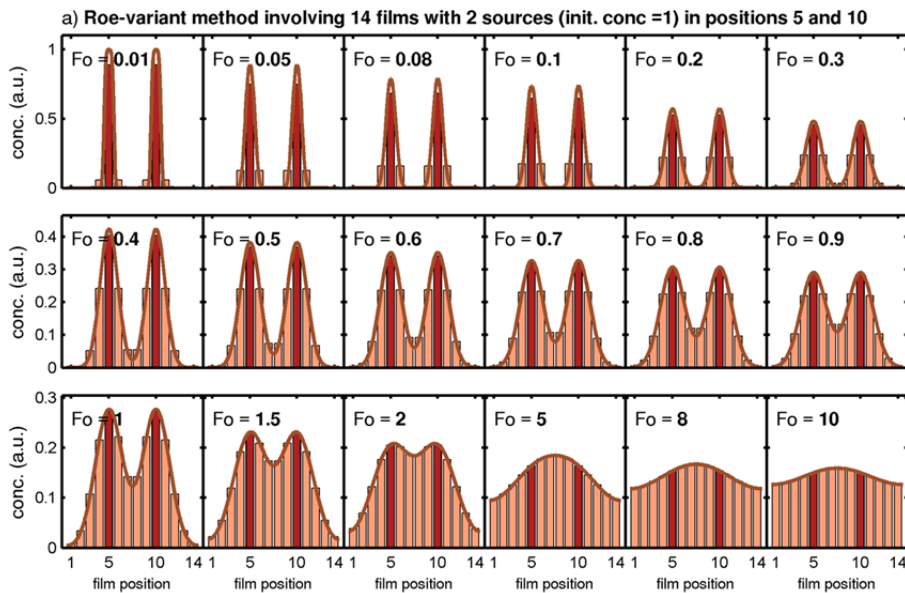


Figure 4-9 14 films method involving 2 sources sandwiched among 12 virgin films. Concentration profiles are plotted for different Fourier number. Bars represent the concentration as measured (*i.e.* averaged over the film thickness) whereas the continuous line represents the continuous profile. All concentration profiles are normalized to yield an overall stack concentration of 2.

4.2.3.2.3 Data analyzing

An example of the 14 film method (sources in positions 5 and 10) applied to the determination of the diffusion coefficient of biphenyl in polycaprolactone at 296 K is shown in Figure 4-10.

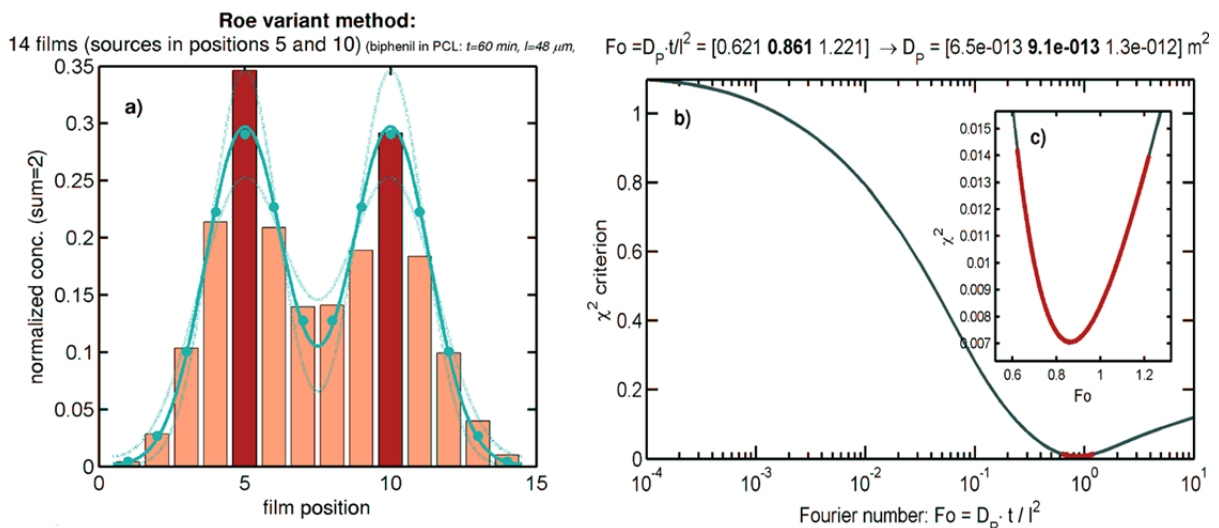


Figure 4-10 a) Measured profiles after 1 hour of contact (bars), predicted profiles and corresponding 95% confidence intervals are plotted in continuous and dotted lines respectively. All concentrations profiles are normalized to yield an overall stack concentration of 2. b) Least-square fitting criterion between measured and predicted concentration profiles.

95% confidence interval around the minimum is plotted as a red line. c) Details of the minimum region (linear scale of Fourier numbers).

Chapter 5. Results and discussion

5.1 Diffusion in bulk polymers

As first description, nanocomposite effects in polymers are very often described from collisional theory and tortuosity concepts used in porous or mesoporous media (see section 2.2). It is usually thought that inserting obstacles (*e.g.* particles, crystallites) decreases the mean free path as considered in Knudsen diffusion theory (Shen and Chen, 2007). This concept does not hold for diffusion in polymers because the average ballistic length of the center-of-mass (CM) before a collision occurs is much smaller than the gyration radius of any organic solute which is larger than $50 \text{ g}\cdot\text{mol}^{-1}$. Indeed, viscous/friction forces are dominating over inertia and external forces (*e.g.* pressure gradient). In this perspective, tortuosity effects must be thought as a consequence of the local polymer structure and renewal rates of free volumes, and assessed from the decrease of the second moment of the position of CM (*i.e.* variance or mean square displacement) instead of its first moment (*i.e.* average distance crossed after a given amount of time). In other words, the trajectory of organic substances in solid polymers appears skewed due to the random displacements regardless the “real” obstacles met. In addition, as random walks are not oriented, the concept of orientations of obstacles holds only through the notions of diffusion anisotropy. This first part introduces theoretical results, which will be used to analyze in time and in space the effects of “normal diffusion” (in this section) from those related to interactions with obstacles/adsorbents (section 5.3). For concision, only diffusion at infinite dilution, also known as trace or tracer diffusion, is addressed.

5.1.1 Beyond tortuosity: how negative correlations decrease D values with considered time-scale

On long time scales, the mean distance covered by a tracer is always zero even if tracer CM drifts slowly away from the origin according to the generalized Einstein relation (5-1). The displacement of CM is said to be second order stationary and its mean square displacement (msd) increases linearly with time lag t :

$$\frac{d}{dt} \left\langle \mathbf{r}_{\text{CM}}(\tau, t) \mathbf{r}_{\text{CM}}(\tau, t)^T \right\rangle_{\text{all } \tau} = 2\mathbf{D}(t) \quad (5-1)$$

where T stands for transpose, $\mathbf{r}_{\text{CM}}(t, \tau)$ is the displacement vector (3 by 1 matrix in an arbitrary Cartesian system) relative to its average value, $\langle \mathbf{r}_{\text{CM}}(\tau, t) \rangle_{\text{all } t} = 0$, and relative to the displacement of the CM of the whole polymer host+diffusant system, denoted O. By noting

\mathbf{x}_O and \mathbf{x}_{CM} the position vectors of O and CM respectively, the displacement between times τ and $\tau+t$, $\mathbf{r}_{CM}(t, \tau)$ is defined as:

$$\mathbf{r}_{CM}(\tau, t) = \mathbf{x}_{CM}(\tau + t) - \mathbf{x}_{CM}(\tau) - (\mathbf{x}_O(\tau + t) - \mathbf{x}_O(\tau)) \quad (5-2)$$

Because the probability of reaching any starting point is lower than 1 according to Pólya's random walk constant, the operator $\langle \rangle_{all\tau}$ in Eq. (5-1) averages the mean square displacement over all possible starting times τ and it assumes that the transition probability associated to each displacement is translationally invariant. $\mathbf{D}(t)$ is a symmetric positive-semidefinite diffusion matrix. Its eigenstructure codes for the main directions of molecular diffusion at time scale τ . When all diagonal terms are strictly positive, the unique Cholesky decomposition of $\mathbf{D}(t)$ is:

$$\mathbf{D}(t) = \mathbf{B}(t)\mathbf{\Lambda}(t)^{1/2} \left(\mathbf{B}(t)\mathbf{\Lambda}(t)^{1/2} \right)^T \quad (5-3)$$

where $\mathbf{\Lambda}(t)$ is a diagonal matrix of eigenvalues and where the columns of $\mathbf{B}(t)$ are the corresponding unit eigenvectors. Hence, displacements at the scale τ are expected to fluctuate at a random rate $d\mathbf{r}_G(t, \tau)/dt$ equal to $\mathbf{B}(t)\mathbf{\Lambda}(t)^{1/2} \mathbf{X}$, where \mathbf{X} is a random vector, whose components are standard normal variates. When displacements are isotropic, all diagonal terms of $\mathbf{\Lambda}(t)$ are equal to a same scalar value, denoted $D(t)$. The value of $D(t)$ is given by the derivative of the total mean square displacement operator of CM, denoted $msd_{CM}(t)$, with t . The latter is conveniently defined as the expectation a quadratic form (or equivalently as the squared Frobenius norm of $\langle \mathbf{r}_G(\tau, t)\mathbf{r}_G(\tau, t)^T \rangle_{all\tau}$):

$$\begin{aligned} msd_{CM}(t) &= \left\langle \mathbf{r}_{CM}(\tau, t)^T \mathbf{r}_{CM}(\tau, t) \right\rangle_{all\tau} \\ &= \text{tr} \left[\left\langle \mathbf{r}_{CM}(\tau, t)\mathbf{r}_{CM}(\tau, t)^T \right\rangle_{all\tau} \right] + \left\langle \mathbf{r}_{CM}(\tau, t)^T \right\rangle_{all\tau} \left\langle \mathbf{r}_{CM}(\tau, t) \right\rangle_{all\tau} \end{aligned} \quad (5-4)$$

As the distance $msd_{CM}(t)$ and the trace operator do not depend on the orientation of the reference frame, Eq. (5-1) becomes in the orthonormal basis defined by the columns of $\mathbf{B}(t)$:

$$\frac{d}{dt} msd_{CM}(t) = \text{tr} \left[\frac{d}{dt} \left\langle \mathbf{r}_{CM}(\tau, t)\mathbf{r}_{CM}(\tau, t)^T \right\rangle_{all\tau} \right] = 2 \text{tr}(\mathbf{D}(t)) = 2 \text{tr}(\mathbf{\Lambda}(t)) = 6D(t) \quad (5-5)$$

The well-known result in Eq. (5-5) will be generalized to the $3N$ by $3N$ atomic displacement correlation matrix associated to N heavy atoms belonging to a same diffusant in section 5.2. At the long term time limit corresponding to the frequency $f=1/t=0$, the macroscopic translational diffusion coefficient is accordingly defined as:

$$D(f=0) = \frac{1}{6} \lim_{t \rightarrow \infty} \frac{d}{dt} \text{msd}_{\text{CM}}(t) \quad (5-6)$$

The scaling relationship of $\text{msd}_{\text{CM}}(t)$ with t is of significant concern because it determines the convergence rate towards the asymptotic regime of diffusion, where corresponding to a diffusion coefficient independent of the time scale considered. It is obtained when the spectrum of the fluctuations of the operator $d\text{msd}_{\text{CM}}(t)/dt$ is completely sampled (continuous spectrum corresponding to white noise). The convergence is only rapid if translational events are independent and homogeneously distributed over time. When displacements are controlled by energetic barriers; the frequencies of crossing the barrier in both directions are asymmetric and strong variations in the autocorrelation functions are expected with t along with complex frequency dependence. The corresponding colored-random walk is better described as a Poisson process, where n displacements associated to time lag t are expected to occur during nt under stationary condition. The corresponding msd is given by the composition law of n possible dependent displacements:

$$\begin{aligned} \text{msd}_{\text{CM}}(nt) &= \sum_{0 \leq i, j \leq n-1} \text{tr} \left[\left\langle \mathbf{r}_{\text{CM}}(\tau, t + i\tau) \mathbf{r}_{\text{CM}}(\tau, t + j\tau)^T \right\rangle_{\text{all } \tau} \right] \\ &= \text{msd}_{\text{CM}}(t) \left[n + 2 \sum_{1 \leq k \leq n-1} (n-k) \langle \cos \theta_{\text{CM}}^k(t) \rangle_{\text{all } \tau} \right] \geq 0 \end{aligned} \quad (5-7)$$

where $\langle \cos \theta_{\text{CM}}^k(\tau) \rangle_{\text{all } t} = \frac{\text{tr} \left[\left\langle \mathbf{r}_{\text{CM}}(\tau, t) \mathbf{r}_{\text{CM}}(\tau, \tau + kt)^T \right\rangle_{\text{all } \tau} \right]}{\text{tr} \left[\left\langle \mathbf{r}_{\text{CM}}(\tau, t) \mathbf{r}_{\text{CM}}(\tau, t)^T \right\rangle_{\text{all } \tau} \right]}$ is the correlation coefficient of order

k between displacements occurring during t and separated by a time lag kt . By setting n to a low value, e.g. $n=2$, the expected damping of $\langle \cos \theta_{\text{CM}}^k(t) \rangle_{\text{all } \tau}$ with k can be neglected and all correlation coefficients can be assumed homogeneous and equal to $\langle \cos \theta_{\text{CM}}(t) \rangle_{\text{all } t}$ so that Eq. (5-7) becomes:

$$\text{msd}_{\text{CM}}(nt) \stackrel{n \rightarrow 2}{=} n \text{msd}_{\text{CM}}(t) \left[1 + 2(n-1) \langle \cos \theta_{\text{CM}}(t) \rangle_{\text{all } \tau} \right] \quad (5-8)$$

Without making any assumption of the spectrum of fluctuations of $\text{msd}_{\text{CM}}(t)$ or $d\text{msd}_{\text{CM}}(t)/dt$, Eq. (5-8) is particularly useful to calculate the cumulated growth of $\ln \text{msd}_{\text{CM}}(t)$ with $\ln t$ for any $t=n^k t_0$:

$$\ln \text{msd}_{\text{CM}}(n^k t_0) - \ln \text{msd}_{\text{CM}}(t_0) = \ln n^k t_0 - \ln t_0 + \sum_{i=0}^{k-1} \ln \left[1 + (n-1) \langle \cos \theta_{\text{CM}}(n^i t_0) \rangle_{\text{all } \tau} \right] \quad (5-9)$$

For $n=2$ and by assuming that $\ln \text{msd}_{\text{CM}}(t)$ is continuously differentiable with $\ln \tau$, the cumulated correlated displacements between t_0 and t are found proportional to the deviation to the unitary scaling slope as:

$$\frac{1}{k \ln 2} \sum_{i=0}^{k-1} \ln \left[1 + \langle \cos \theta_{\text{CM}}(2^i t_0) \rangle_T \right] = \int_{t_0}^{2^k t_0} \left(\frac{d \ln \text{msd}_{\text{CM}}(t)}{d \ln t} - 1 \right) dt \stackrel{\text{for sufficiently large } t \gg t_0}{\approx} \ln \frac{D(t)}{D(t_0)} \quad (5-10)$$

When displacements are independent at scales t_0 and t (*i.e.* $D(t) \approx \text{msd}_{\text{CM}}(t)/6t$), approximation setup in Eq. (5-10) generalizes to several time scales the expression $D(t)/D(t_0) = \xi^2$ used to define tortuosity. In the bulk polymer or in contact with nanoparticles, strong interactions with polymer host segments (long-lived contacts) may lead to negatively-correlated displacements (*i.e.* which tend to be balanced each other out). Cumulated correlation coefficient between displacements on long terms is expected to cause a major deviation to fluctuations of $d \text{msd}_{\text{CM}}(t)/dt$ to white noise (with constant spectra). According to Langevin theory of diffusion, it represents the spectrum of the mean force acting on CM and in this case it is not random.

5.1.2 Non-obstacle related effects on D

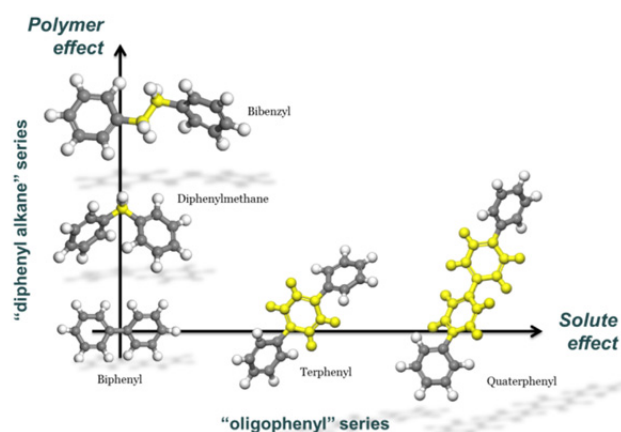
Both obstacles and combinations of spatial and temporal (*e.g.* trapping, confinement) effects may cause a significant reduction of D with time scale. By considering that D is also a function of T, T_g, M (see section 2.1) and by noting $D'(T, T_g, M)$ its corresponding value in a material incorporating obstacles, Table 5-1 describes expected scaling or equalities due to “pure” inert obstacle effects. The only assumption is that obstacles are “felt” by all diffusants whatever their structure, the considered temperature and polymer glass transition temperature.

Table 5-1 Variations of D , which are not affected by the presence of obstacles. D' is the corresponding diffusion coefficient in a nanocomposite material incorporating obstacles.

Non obstacle effects	Expected equalities	Possible interpretation when a significant deviation to equality is detected
Effect of a shift of the glass transition temperature (see section 5.1.3)	$\left. \frac{\partial \ln D(t)}{\partial T_g} \right _{M,T} \approx \left. \frac{\partial \ln D'(t)}{\partial T_g} \right _{M,T}$	Nano-fillers modify locally polymer relaxation and in return diffusion
Effect of temperature	$\left. \frac{\partial \ln D(t)}{\partial 1/T} \right _{M,T_g} \approx \left. \frac{\partial \ln D'(t)}{\partial 1/T} \right _{M,T_g}$	A specific interaction with nano-fillers is detected and it is activated by temperature
Effect of molecular size for linear solutes (see section 5.1.3)	$\left. \frac{\partial \ln D(t)}{\partial \ln M} \right _{T_g,T} \approx \left. \frac{\partial \ln D'(t)}{\partial \ln M} \right _{T_g,T}$	Nanofillers modify the mechanism of translation of solutes.

In the thesis, it has been thought that getting a general free-volume theory (FVT) for solutes including repeated patterns could be used to detect and probe - through its deviations - the nature of interactions with nano-fillers or nano-adsorbents. The conventional Vrentas and Duda FVT theory has been tested to assess the scaling proposed in Table 5-1 on aliphatic polymers above their T_g . The approach used both carefully sectioned literature data (*e.g.* homologous substances, same method, and different temperatures) and dedicated experiments summarized in Figure 5-1. The main originality consisted in studying linear diffusants based on a same rigid pattern (*i.e.* aromatic ring) or blob. As detailed in section 4.1.1 many variants have been studied with different numbers of blobs, distances between blobs, rigidity of bonds between bonds, hybrid molecules including aliphatic segments. This section focuses on the most extensively studied series in 4 polymers and at 3 to 4 temperatures each: diphenyl alkanes and oligophenyls. The first series is particularly interesting as it offers almost similar van-der-Waals volumes (only the exclusion volume changed), it was used to probe robustly polymer effects with the same number of blobs. The second one, sharing biphenyl as common diffusant, is used to test existing diffusion scaling theories with molecular mass (*e.g.* Rouse theory and related ones). The range $T-T_g$ covered 10K to 110K, which is almost commensurable to the application range of most rubber polymers. Finally, it is very important to stress that all reported diffusion coefficients were measured at infinite dilution without any risk of plasticization or modification of free volumes. In particular, this work contrasts significantly with experimental determinations of D carried out mainly during the last three decades from mass uptake or spin-echo NMR experiments at high concentration. Indeed, the extrapolation down to infinite dilution requires using existing FVT to correct the shift of T_g due to plasticization. The methodology used here does not require these corrections.

a)



b)

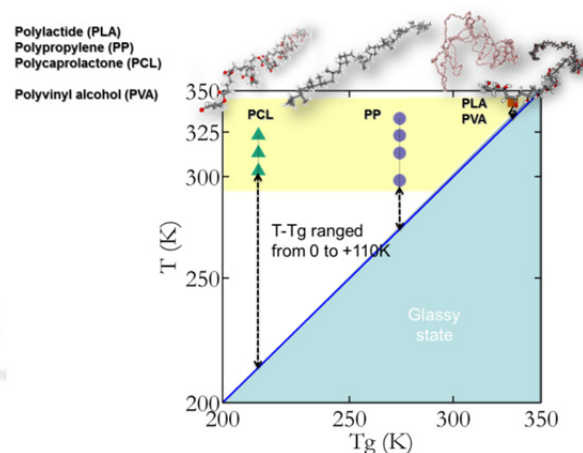


Figure 5-1 a) Main homologous series used in this section to probe both free-volume effects and the scaling of D with M . b) Bivariate domain $T \times Tg$ examined in this section

5.1.3 Study and model development

Publication II

Title: Diffusion of Aromatic Solutes in Aliphatic Polymers above Glass Transition Temperature. <i>Macromolecules</i>

Authors: X. Fang, S. Domenek, V. Ducruet, M. Réfrégiers, and O. Vitrac

Published in: <i>Macromolecules</i> . 46: 874-888 (2013)

Diffusion of aromatic solutes in aliphatic polymers above glass transition temperature

Xiaoyi Fang², Sandra Domenek², Violette Ducruet¹, Matthieu Refregiers³, Olivier Vitrac^{1*}

¹INRA, UMR 1145 Ingénierie Procédés Aliments, F-91300 Massy, France

²AgroParisTech, UMR 1145 Ingénierie Procédés Aliments, F-91300 Massy, France

³Synchrotron SOLEIL, l'Orme des Merisiers, F-91192 Gif-sur-Yvette, France

5.1.3.1 Abstract

The paper presents a harmonized description of the diffusion of solutes with repeated aromatic jumping units (JU) in entangled aliphatic polymers above their T_g . It is shown that the trace diffusion coefficients, D , are scaled with the number of JU or equivalently with solute molecular mass, M , as $M^{-1}M^{-K_\alpha/(T-T_g+K_\beta)}$, where K_α and K_β are temperature-equivalent parameters related to Williams-Landel-Ferry (WLF) ones. The scaling of diffusion behaviors of linear aliphatic and aromatic solutes appear separated by a temperature shift, K_β , of *ca.* 91 K. The effects of the number of JU and the distance between two JU were specifically probed in several aliphatic polymers (polypropylene, polylactide and polycaprolactone) at different temperatures above T_g with two homologous solute series: short oligophenyls and diphenyl alkanes. An extended free-volume theory for many JU was accordingly inferred to account for the observed statistical independence between the fluctuations of the free volumes probed by each JU and the probability of the collective displacement of the center-of-mass of the solute. Outstanding properties of short oligophenyls series provided further insight on the underlying molecular mechanism of translation. Their activation energies grow differently according to the number of phenyl rings, N_{Ph} , being odd or even. Constrained molecular dynamics demonstrated that such a parity effect could be remarkably reproduced when the translation of each JU (*i.e.* phenyl ring) was randomly controlled by a combination of short and long-lived contacts.

Keywords: diffusion, aromatic molecules, aliphatic polymers, scaling exponents, free volume, activation energy, molecular dynamics

5.1.3.2 Introduction

No general diffusion model is available to predict the broad range of trace diffusion coefficients (D) of organic solutes such as oligomers, additives, residues, contaminants or

degradation products in polymer materials at solid state, which corresponds to their conditions of service. By analyzing D values in polyolefins, a strong dependence of D values has been highlighted for several categories of organic solutes: resembling the polymer (*e.g.* linear or branched solutes) or not (*e.g.* aromatic molecules, hindered antioxidants)¹. The exponents, α , scaling D with molecular mass (M) as $D \propto M^\alpha$, were found strictly greater than 1 and typically above 2, which reflects variations of D over several decades with only small change of M , between 10^2 and 10^3 g·mol⁻¹ for most of the molecules of technological interest such as antioxidants, UV stabilizers, plasticizers,... Those variations were related mainly to three geometric factors: molecular volume, shape factor and gyration radius. D values reported by Berens² suggest that mass/volume dependence is even greater when below the polymer glass transition temperature (T_g). On the opposite, in melts, scaling exponents for homologous alkane series in polyethylene were experimentally assessed close to 1 in agreement with the Rouse theory³. Molecular dynamics simulations of generic polydisperse systems above T_g found also exponents of 1 for a wide range of thermodynamical conditions⁴. The absence of temperature effect on α was, however, not verified experimentally. Thus, Kwan *et al.*⁵ reported a strong effect of temperature on α values – with α falling from 4.7 to 2.1 between 23°C and 85°C – for *n*-alkanes dispersed in a lightly cross-linked amorphous polyamide, suggesting a continuous but sharp evolution from T_g to higher temperatures and without a significant contribution of the possible crystalline phase.

Such a high mass dependence, with α values varying between 2⁶ and 3⁷ have also been reported for the self-diffusion of entangled polymer chains subjected to reptation and strong reptation translation mechanisms respectively, with intermediate values close to 2.4 when reptation is combined with a constraint release mechanism⁸. The formal analogy is, nevertheless, of a limited use for solutes with molecular masses ranging between 10^2 and 10^3 g·mol⁻¹, as their gyration radii are much smaller than the typical entanglement length of polymer segments. For organic solutes larger than voids between polymer segments and smaller than entanglement length, only a partial and local coupling between the reorientation and local relaxation modes of the polymer can be expected⁹. It was thus shown that aromatic molecules remain non-oriented in the amorphous phase of polyethylene when the material was stretched uniaxially^{10, 11}, whereas anisotropic diffusion of toluene was observed in compressed natural rubber¹².

The main goal of this study is to provide a consistent description of molecular diffusion mechanisms of aromatic solutes mimicking molecules of technological interest in linear polymers and to provide a polymer-independent description of the strong dependence of D with M at any temperature greater than T_g . In a first approximation, such solutes can be

described as the repetition of rigid jumping units subjected to independent displacements on short time scales. An extended version of free-volume theory is accordingly introduced to account for the weak coupling between polymer relaxation, controlling the fast displacements of each jumping unit, and the collective reorientation and translation of the whole solute. It was validated on two independent homologous series of solutes. The first series of diphenyl alkanes with close size was used to probe polymer effects (*i.e.* independent motions of jumping units) at a similar reference temperature. The second series, short linear oligophenyls, probed specifically solute-related effects (*i.e.* the collective motions of repeated jumping units) and their activation by temperature. As both series started with a common first molecule, biphenyl, entropic effects could be reliably scaled for both series.

This paper is organized as follows. Scaling laws for linear aliphatic and aromatic solutes in aliphatic polymers are discussed in section two in the framework of a coarse-grained theory of diffusion of solutes consisting in a linearly repeated jumping units or blobs. The existence of at least two correlation time scales between the displacements of jumping units and surrounding host particles is used to justify the major deviation to the Rouse theory¹³ and to conventional free-volume theories in dense entangled aliphatic polymers (*i.e.* far below their melting points). An extended free-volume theory is proposed based on a formal separation of thermal expansion effects acting on the displacements of each jumping unit, so called “host effect”, and barrier effects, so called “guest effects”. A simple theory of activation barriers for the diffusion of oligophenyls is accordingly proposed. Section three reports the methodologies used to determine trace diffusion coefficients, ranged between $10^{-17} \text{ m}^2 \cdot \text{s}^{-1}$ and $10^{-12} \text{ m}^2 \cdot \text{s}^{-1}$, in three different polymers: polypropylene (PP), polycaprolactone (PCL) and polylactide (PLA) for both homologous solute series. A fourth polymer, plasticized and unplasticized polyvinyl alcohol (PVA), was used as external validation for arbitrary polymers above T_g . The proposed free-volume theory is tested against experimental in section four. The scaling of activation energies and entropies of oligophenyls is discussed according to results obtained in constrained molecular dynamics simulation. The likely mechanism of translation of aromatic molecules in linear polymers above T_g and its consequence on solute mass dependence is finally proposed in the last section.

5.1.3.3 Theory

This section discusses the possible causes responsible for the deviation of solutes larger than voids to existing diffusion theories in linear polymers at solid state. By relying on the diffusion properties of solutes including linearly repeated jumping units (or also called blobs),

two major arguments are proposed: i) the increase in polymer density with decreasing temperature down to T_g affects the individual displacements of each jumping unit, ii) and the resulting displacement of the center-of-mass (CM) is strongly affected by the heterogeneous dynamics of individual jumping unit.

5.1.3.3.1 *Scaling of D with the number of jumping units and temperature for linear solutes*

The strong slowdown of D values with M (respectively the number of jumping units in solutes with linearly repeated patterns) is major characteristic of organic solutes in polymers at solid state (e.g. semi-crystalline polymers or polymers below their flow thresholds). Published values are scarce, mainly due to the necessity to work with homologous structure series and a wide range of D values. Scaling of D in polyethylene far above its T_g is reported in Figure 5-1 for two solute series artificially split into two categories : i) linear aliphatic solutes (Figure 5-2a), including linear n -alkanes ($n=12..60$)^{3, 14}, n -alcohols ($n=12..18$)¹⁵ and esterified phenols containing a 3(3,5-di-tert-butyl-4-hydroxyphenyl) head and a long n -alkyl tail ($n=6..18$)¹⁶, and ii) aromatic solutes (Figure 5-2b), including n -alkylbenzene containing short n -alkyl chains ($n=0..4$)¹⁷, substituted and hindered phenols ($M= 94-545 \text{ g}\cdot\text{mol}^{-1}$)¹⁵, respectively. For each series, D values are scaled as a power law of M (ranging between 70 and $10^3 \text{ g}\cdot\text{mol}^{-1}$), whose exponents are much greater than unity and tend to decrease when temperature is increasing. α values assessed up to 4 or 5 constitute a major deviation to the Rouse theory that predicts values close to unity instead. According to the Rouse theory, unitary values are related to a purely single chain relaxation with a uniform friction factor and without any chain end effects¹³. Trace diffusion coefficients of n -alkanes in polyethylene melts³ suggest that α values close to unity should be recovered far from T_g . In agreement with experimental results and free-volume theories, we propose a scaling exponent deviation to the Rouse theory, denoted $\Delta\alpha$, which depends mainly on the temperature difference $T-T_g$:

$$\frac{D(M, T)}{D(M_0, T)} = \left(\frac{M}{M_0} \right)^{-\alpha(T-T_g)} \propto M^{-1} M^{-\Delta\alpha(T-T_g)} \quad (5-11)$$

where M_0 is the molecular weight of a reference molecule in the considered series of molecules with linearly repeated patterns.

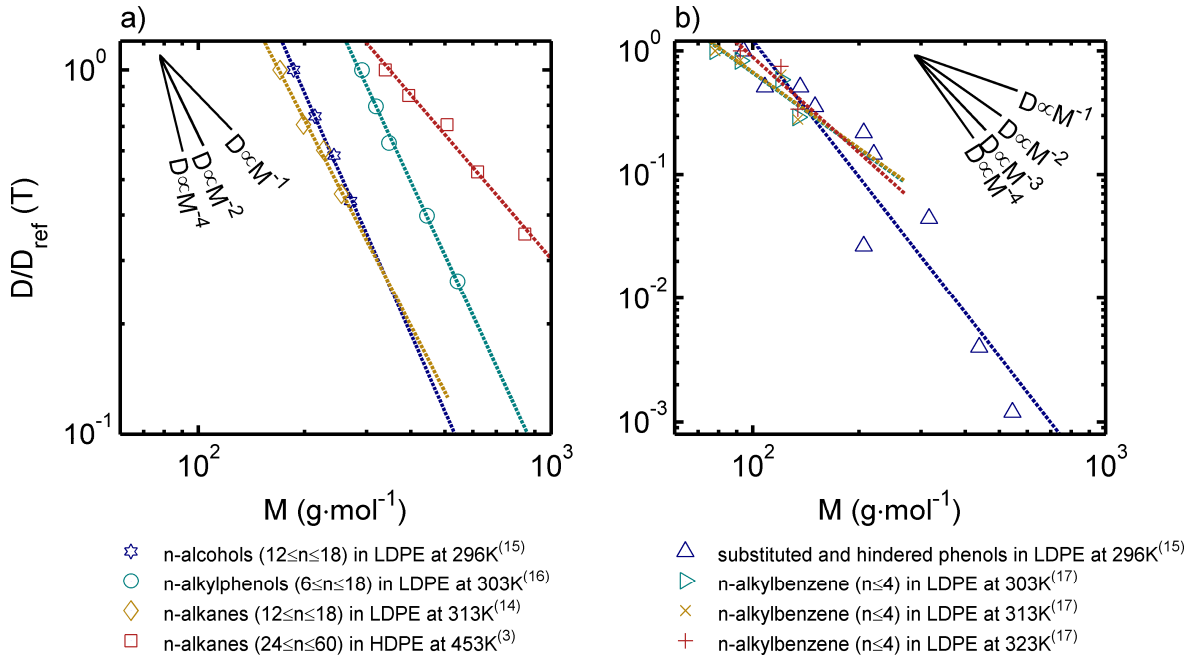


Figure 5-2 Log-log plots of trace diffusion coefficients in polyethylene (PE) either with low density (LDPE) or high density (HDPE) of a) linear aliphatic and b) aromatic solutes. D_{ref} was chosen as the diffusion coefficient of the first solute in the considered solute series.

For solutes consisting in a small number of linearly repeated jumping units or blobs, N , the deviation to the Rouse theory close to T_g can be thought as the consequence of irregular jumping unit displacements with time. To justify this argument, we adopt the coarse-grained model of Herman *et al.*¹⁸⁻²¹ initially proposed to describe the dynamics of flexible linear chains in the melt. Similarly, by neglecting end-effects, we assume that the mean-square-displacement of a single jumping unit increases with time as:

$$g(t) = 6D_{blob}(t)t \quad (5-12)$$

where $D_{blob}(t)$ is the time-dependent diffusion coefficient of a blob/jumping unit. For any solute with identical jumping units indexed $i=1..N$, D_{blob} is assumed to decrease with the amount of cumulated pair correlations between the displacements of jumping unit i , denoted $\Delta \mathbf{r}_i(t)$, and the displacements of all particles within the system (*i.e.* including host and solute), denoted $\Delta \mathbf{r}_j(t)$, as:

$$D_{blob}(t) = \frac{D_0}{\sum_{\text{all } j \text{ including } i} \frac{\langle \Delta \mathbf{r}_i(t) \cdot \Delta \mathbf{r}_j(t) \rangle}{\langle \Delta \mathbf{r}_i(t)^2 \rangle}} = \frac{D_0}{\sum_{\text{all } j \text{ including } i} C_{i,j}(t)} = \frac{D_0}{C(t)} \quad (5-13)$$

where D_0 is a scaling constant. In this simplified description, jumping units have a similar spherical shape and volume regardless the detailed chemical structure of the solute and host polymer chains. An increasing $C(t)$ with time leads to a sub-diffusive regime. The mean-

square-displacement of the center-of-mass (CM) is accordingly given by the covariance of the averaged displacements of all jumping units:

$$g_{CM}(t) = \frac{1}{N^2} \left(\sum_{i=1}^N g(t) + 2 \sum_{i,j:i < j}^N C_{i,j}(t) g(t) \right) = \left(\frac{1}{N} + \frac{2}{N^2} \sum_{i,j:i < j}^N C_{i,j}(t) \right) g(t) \quad (5-14)$$

For a linear and flexible solute and by neglecting torsional constraints, only the $N-1$ correlations between the displacements of connected jumping units are significant. Eq. (5-14) becomes accordingly:

$$g_{CM}(t) = \frac{g(t)}{N} + 2 \frac{N-1}{N^2} C_{connect}^{(t)} g(t) \quad (5-15)$$

wherein $C_{connect}^{(t)}$ is the normalized correlation between the displacements of two connected jumping units. Incorporating Eqs. (5-12) and (5-13) yields finally:

$$g_{CM}(t) = \frac{1}{N} \left(\frac{1}{C(t)} + 2 \left(1 - \frac{1}{N} \right) \frac{C_{connect}^{(t)}}{C(t)} \right) 6D_0 t \xrightarrow{C_{connect}^{(t)} \ll C(t)} \frac{1}{N} \frac{6D_0 t}{C(t)} \quad (5-16)$$

By assuming that $C_{connect}^{(t)}$ is small comparatively to correlations with the displacements of host polymer segments in a dense system, the mean-square-displacement of CM and consequently the tracer diffusion coefficient, $D = \lim_{t \rightarrow \infty} g_{CM}(t)/6t$, is scaled as $1/N$, in agreement with the Rouse theory¹³.

In presence of strong coupling between the lateral displacements of solute jumping units and host particles (*e.g.* large jumping units), the translation of each connected jumping unit is expected to be highly heterogeneous and controlled by a combination of short and long-lived dynamic contacts as discussed in general terms in²² and²³. In the followings, we will assume the simplest case where two relaxation modes resulting of many body interactions can be independently applied to each jumping unit: $C(t)$ and $C_{trapped}^{(t)}$, with respective probabilities $1-p$ and p . $C_{trapped}^{(t)} \gg C(t)$ is the total correlation when a jumping unit is almost “blocked” or significantly hindered by host segments. From this simplified description, g_{CM} is governed by the superposition of all possible partitions between “trapped” (*i.e.* long-lived contacts with host) and “untrapped” (*i.e.* short-lived contacts with host) jumping units. By assuming that $g(t)$ still obey to Eqs. (5-12) and (5-13), Eq. (5-16) is replaced by:

$$\begin{aligned}
\frac{g_{CM}(t)}{6D_0t} &= \frac{\overbrace{(1-p)^N \frac{1}{NC(t)}}^{\text{all jumping units translate according to } C(t)} + \sum_{j=1}^N \overbrace{\binom{N}{j} p^j \left(\frac{N-j}{N^2 C(t)} + \frac{j}{N^2 C_{trapped}^{(t)}} \right)}^{\substack{N-j \text{ jumping units translate according to } C(t) \\ j \text{ jumping units translate according to } C_{trapped}^{(t)}}}}{(1-p)^N + \sum_{j=1}^N \binom{N}{j} p^j} \\
&\xrightarrow[\substack{p \rightarrow 1 \\ C_{trapped}^{(t)} \gg C(t)}]{} \frac{N(2^{N-1}-1)}{2^N-1} \frac{1}{N^2 C(t)} = \frac{1}{\underbrace{\frac{2^N-1}{2^{N-1}-1}}_{N^{\Delta\alpha}}} \frac{1}{N} C(t)
\end{aligned} \tag{5-17}$$

wherein $\binom{N}{j}$ is the number of combinations to choose exactly j jumping units among N with long-lived contacts (governed by $C_{trapped}^{(t)}$) and p^j is the related probability by assuming that j jumping units are blocked independently.

Eq. (5-17) stresses that a higher dependence to N ($\alpha > 1$), and therefore to M , is expected for small N (typically lower than 5) as soon as $p \rightarrow 1$ and while several populations of contacts between jumping units and surrounding coexists. Considering only two populations provides a rough scaling of D with the number of jumping units, but its main interest is to highlight that the scaling with N or M would be the result of the heterogeneous dynamics of the coupling between the fluctuations of free volume (*i.e.* associated to the displacements of a single jumping unit) and collective displacements of many jumping units.

As the value p is related to the probability to find a free volume close to each jumping unit, we propose to test against experimental values a phenomenological temperature superposition model where the temperature shift factor $\Delta\alpha$ is a function of the reciprocal fractional free volume in the polymer, written as for any $T > Tg - K_\beta$:

$$\alpha(T - Tg) = 1 + \Delta\alpha(T - Tg) = 1 + \frac{K_\alpha}{T - Tg + K_\beta} \tag{5-18}$$

where K_α and K_β are parameters that can be fitted from experimental α values or derived from existing free-volume theory. K_α acts as a scaling constant and K_β is a constant related to the size of the solute jumping unit. It is important to note that Eq. (5-18) is a special form of the Williams-Landel-Ferry (WLF) equation²⁴ applied to the scaling relationship in Eq. (5-11). Indeed, by chosen Tg as reference temperature as suggested by Ehlich *et al.*²⁵ and Deppe *et al.*²⁶, Eqs. (5-11) and (5-18) yield :

$$\begin{aligned}
-\ln a_T(M, T) + \ln a_T(M_0, T) &= \ln \frac{D(M, T)}{D(M, Tg)} - \ln \frac{D(M_0, T)}{D(M_0, Tg)} \\
&= (\alpha(Tg) - \alpha(T)) \ln \frac{M}{M_0} = \frac{K_\alpha}{K_\beta} \frac{T - Tg}{T - Tg + K_\beta} \ln \frac{M}{M_0} \quad (5-19)
\end{aligned}$$

which can be identified as a sum of two temperature shifts obeying to standard WLF equation: $-\ln a_T(M, T) = \frac{C_1(M)(T - Tg)}{C_2 + T - Tg}$, with $C_1(M) - C_1(M_0) = \frac{K_\alpha}{K_\beta} \ln \frac{M}{M_0}$ and $C_2 = |K_\beta|$.

It should be noticed that the absolute value of K_β keeps the consistency $D(T) > D(Tg)$ for any $T > Tg - K_\beta$. More rigorously, a temperature greater than $Tg - K_\beta$ should be chosen instead of Tg .

When applied to a broad range of temperatures, Eq. (5-19) implies a significant deviation of activation of diffusion from Arrhenius' law and a log-dependence of the apparent activation energy, denoted Ea , with M :

$$Ea(M, T) = -R \frac{\partial \ln D(M, T)}{\partial 1/T} = Ea(M_0, T) + K_\alpha \frac{RT^2}{(T - Tg + K_\beta)^2} \ln \frac{M}{M_0} \quad (5-20)$$

Similar deviations to Arrhenius behavior was already proposed by Deppe *et al* (see Eq. (7) in²⁶) for aromatic solutes in rubbery poly(isobutyl methacrylate) near its Tg . An Arrhenius behavior is expected to occur only when $T \gg Tg - K_\beta$. A similar log-type scaling of Ea with M is consistently inferred for n -alkanes in low-density polyethylene from activation energies reported in¹⁵, with values of 57, 66 and 107 kJ·mol⁻¹ for dodecane, octadecane and dotriacontane respectively. From D values collected in¹⁷, the same trend is also drawn for n -alkylbenzene in polyethylene. As discussed in²⁵, the dependence of WLF parameter C_1 to $\ln M$ could be related either to a stronger coupling with matrix mobility or to an increase in the volume of the solute jumping unit.

5.1.3.3.2 Conventional free-volume theories

Free-volume theories argue that the translation of the center-of-mass (CM) of the solute is controlled in time by the redistribution of voids around the solute due to thermal fluctuations. However, early models derived from viscosity theories²⁷, such as the one proposed by Cohen and Turbull²⁸, tend to underestimate the mass dependence by assuming that the whole solute translates as a single jumping unit, which yields a scaling exponent α close to 1. Theories modified by the Vrentas and Duda model^{29, 30} for polymer-solvent mixtures incorporate two additional features: i) an internal energy change is required to initiate a translation of CM and

ii) an increase in free volume due to polymer thermal expansion. The corresponding self-diffusion coefficient of the solute indexed 1 within the polymer indexed 2 is given by Eqs (11)-(13):

$$D_1 = \bar{D}_0 \exp\left(-\frac{E^*}{RT}\right) \exp\left(-\frac{\omega_1 \bar{V}_1^* + \omega_2 \xi \bar{V}_2^*}{\hat{V}_{FH} / \gamma}\right) \quad (5-21)$$

$$E^* = E_P - E_S \quad (5-22)$$

$$\frac{\hat{V}_{FH}}{\gamma} = \omega_1 \frac{K_{11}(K_{21} + T - Tg_1)}{\gamma_1} + \omega_2 \frac{K_{12}(K_{22} + T - Tg_2)}{\gamma_2} \quad (5-23)$$

where ω_1 and ω_2 are the mass fractions in species 1 (solute with glass transition temperature Tg_1) and 2 (polymer with glass transition temperature Tg_2) respectively. \bar{D}_0 is a scaling constant. E^* is the effective energy barrier per mole to overcome attractive forces and defined as a balance between the barrier in dilute state ($\omega_1 \rightarrow 0$), E_P , and in pure solvent ($\omega_1 \rightarrow 1$), E_S . \bar{V}_1^* and \bar{V}_2^* are the specific hole free volume of solute and polymer required for a jump respectively. \hat{V}_{FH}/γ is the effective (including overlaps) average hole free volume per unit of mass of mixture. $\xi = V_S^*/Vm^*$ lumps all solute geometric effects at infinite dilution. It is conventionally interpreted as the ratio of the critical molar volumes of the solute, V_S^* , and polymer segment jumping units, Vm^* . V_S^* has a simple geometric interpretation for rigid solutes as extensively discussed in³¹. $\{\gamma_i\}_{i=1,2}$, $\{K_{ii}\}_{i=1,2}$, $\{K_{ij}\}_{i \neq j; i=1,2; j=1,2}$, are parameters that account for overlapping factors, free-volume parameters and of their interactions respectively. At diluted state ($\omega_1 \rightarrow 0$), which is of technological interest for most of the additives and polymer residues, Eqs. (11)-(13) can be recast in a simpler model relatively to a reference solute with a ratio of critical molar volumes $\xi_0 = V_{S_0}^*/Vm^*$:

$$\frac{D_1(\xi, T)}{D_1(\xi_0, T)} = \exp\left(-\frac{E^*(\xi) - E^*(\xi_0)}{RT}\right) \exp\left(-(\xi - \xi_0) \frac{\gamma_2}{K_{12}} \frac{\bar{V}_2^*}{K_{22} + T - Tg_2}\right) \quad (5-24)$$

As Eq. (5-18), Eq. (5-24) is also related to the WLF equation, with an additional temperature-related translation term induced by the energy barrier E^* :

$$\begin{aligned}
-\ln a_T(M, T) + \ln a_T(M_0, T) = & -\frac{E^*(\xi) - E^*(\xi_0)}{R} \left(\frac{1}{T} - \frac{1}{Tg_2} \right) \\
& + (\xi - \xi_0) \frac{\gamma_2 \bar{V}_2^*}{K_{12} K_{22}} \frac{T - Tg_2}{K_{22} + T - Tg_2}
\end{aligned} \quad (5-25)$$

When $E^*=0$, Eqs. (5-25) and (5-19) are equivalent with $(\xi - \xi_0) \frac{\gamma_2 \bar{V}_2^*}{K_{12}} = K_\alpha \ln \frac{M}{M_0}$ and $K_{22} = |K_\beta|$. The difference in activation energies between a solute and a reference one in the same series is consequently proportional to the difference of $\xi - \xi_0$:

$$\begin{aligned}
Ea(\xi, T) - Ea(\xi_0, T) = & E^*(\xi) - E^*(\xi_0) + (\xi - \xi_0) \frac{\gamma_2 \bar{V}_2^*}{K_{12}} \frac{RT^2}{(K_{22} + T - Tg_2)^2} \\
\approx & (\xi - \xi_0) \frac{\gamma_2 \bar{V}_2^*}{K_{12}} \frac{RT^2}{(K_{22} + T - Tg_2)^2}
\end{aligned} \quad (5-26)$$

According to Vrentas *et al.*³², $E^*(\xi)$ is related to the variation of internal energy when a solute is introduced at infinite dilution in the polymer and its contribution is assumed to be negligible in the vicinity of Tg for any solute with good solubility in the polymer.

All solute-related effects are gathered in Eqs. (5-24)-(5-26) into a single dimensionless parameter, ξ (see³² for detailed discussion). For a given polymer, they lead to express the decrease of $\ln D$ for a homologous series of solutes (*e.g.* with increasing length) as a similar increase of Ea . The solute effect on D is therefore purely enthalpic and vanishes at high temperature. A crude comparison between apparent activation energies of D associated to Eq. (5-20) and Eq. (5-26) lead to $\xi - \xi_0 \propto \ln M/M_0$. As the free-volume theory was initially designed for polymer-solvent mixtures, only ξ values for short homologous solutes have been reported in the literature. Figure 5-3 correlates experimental and theoretical estimations of ξ from Vrentas *et al.*³³ with $\ln M/M_0$ for linear and aromatic solutes in polyvinyl acetate ($Tg=305$ K). Experimental values were obtained by Arnould and Laurence³⁴ for $T-Tg$ values ranging between 28 K and 78 K and M values ranging from 74 g·mol⁻¹ to 130 g·mol⁻¹. The comparisons verify a same linear model for short linear and aromatic solutes: $\xi(M) - \xi_0(M_0) \approx 0.24 \ln(M/M_0)$, where ξ_0 is a constant which depends on the considered reference solute and series. Such a correlation combined with Eqs. (5-11) and (5-24) yield the following approximation of $\alpha(T)$ based on free-volume theory:

$$\alpha(T) \approx 0.24 \frac{\gamma_2}{K_{12}} \frac{\bar{V}_2^*}{K_{22} + T - Tg_2} \quad (5-27)$$

Close to T_g , this description is particularly attractive for linearly repeated solutes because ζ_0 could be estimated from simple molecular descriptors^{31, 33} and extrapolated to larger molecules. For temperatures not too far from T_g , the correlation would elucidate the paradox discussed in³⁵: ζ would vary with M for short alkanes and not for large ones. According to correlations depicted in Figure 5-3, the logarithm dependence with M will lower the effect of M for large solutes: the variation of ζ is twice more larger from C6 to C10 (+4 carbons) than from C14 to C18 (+4 carbons). At high temperature, conventional free-volume theory suffers however a lack of generality as $\alpha(T) \rightarrow 0$. Scaling exponents close to unity in agreement with Rouse theory have been indeed reported for n -alkanes including from 8 to 60 carbons in many systems, comprising polyethylene melts³ and elastomers³⁶⁻³⁸.

In the remainder of the paper, we drop the indices 1 and 2, and Tg_2 is replaced by Tg .

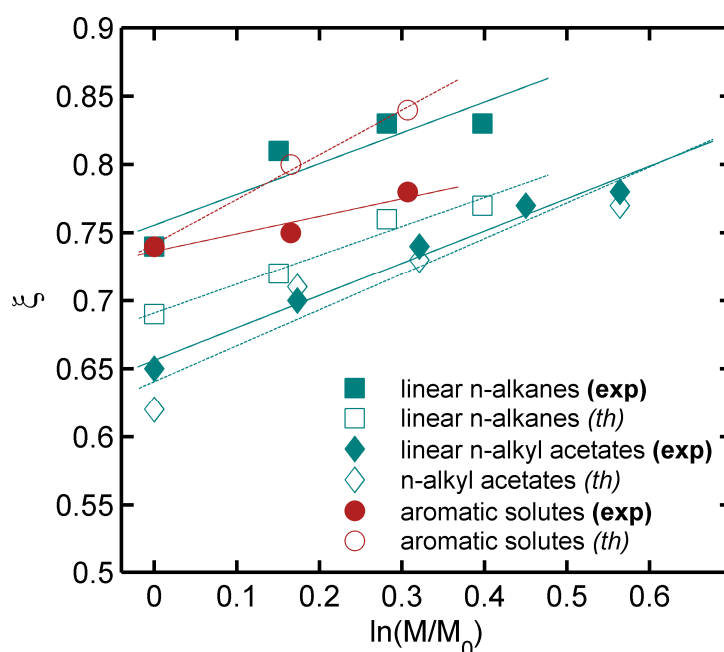


Figure 5-3 Correlations between ζ values as reported in Tables 2 and 3 of³³ and $\ln M/M_0$. Experimentally determined ζ values are plotted as solid symbols and theoretically calculated ones (see Eq. (22) in³³) as empty symbols. The reference solutes are: hexane, methyl acetate and benzene with molecular mass (M_0) of $86 \text{ g}\cdot\text{mol}^{-1}$, $74 \text{ g}\cdot\text{mol}^{-1}$ and $78 \text{ g}\cdot\text{mol}^{-1}$ respectively.

5.1.3.3.3 Extended free-volume models for aromatic solutes in aliphatic polymers

For larger solutes, the necessity of extending conventional free-volume theories has been discussed by many authors: either in general terms in³⁹ or specifically for plasticizers in PVC⁴⁰⁻⁴⁴ or for flexible and semi-flexible solutes that are expected to move in a segmentwise manner^{25, 26}. Indeed, translation of additive-type solutes invoke apparent activation energies much greater than values reported for solvents in rubber polymers, ranging typically from 50

to $150 \text{ kJ}\cdot\text{mol}^{-1}$ ^{9, 45}. As such values are close to the activation energies of polymer relaxations, it is thought that large or bulky solutes involve the same cooperative motions of polymer segments as observed in viscous flow^{36, 46, 47}. In addition, though the activation volumes of translational diffusion of additive-type molecules are significant, ranging from 80 to 250 \AA^3 , they remain significantly smaller than the solute itself⁴⁸. As a result, a piece-wise translation based on the translation of elemental blobs (see section 2.1) appears more likely. In this work, we advance another argument to justify a proper extension for solutes with intermediate molecular mass. For a same polymer and a series of solutes based on repeated patterns, free-volume theories assume that the decrease of $\ln D$ with M is due to a similar increase in Ea (see Eqs. (5-24) or (5-26)). In our experiments, it was found that that Ea did not vary monotonously with M , whereas the decrease of $\ln D$ did. Our interpretation is that the conventional free-volume theory designed for rigid solutes assumes that the translation of the solute center-of-mass (CM) and polymer relaxation are simultaneous and interrelated phenomena at rubbery state: one translation of polymer segments causing necessarily the translation of solute CM regardless the size of the solute. For large solutes either bulky or flexible, the possible absence of exact match between the shape of free volumes freed by the polymer and the shape of elemental jumping units should promote a delay (*i.e.* long-lived contacts) between the effective translation of the jumping unit and unconcerted motions of polymer segments. This last assumption is particularly very likely in the light of experimental results showing that aromatic solutes remained non-oriented with aliphatic polymer segments^{10, 11}.

In this work, we extend free-volume theory to aromatic solutes including N_{ph} phenyl rings by assuming that the translation of each phenyl ring, controlled by $D_{blob}(T, Tg)$, obeys to free-volume theory on short-time scales whereas the translation of many jumping units on long-time scales follows relationships similar to Eq. (5-16) or (5-17), controlled by a total correlation term $C(solute, T)$. As the toxicity of benzene hinders a direct measurement of effective free-volume parameters $\{K_a^{blob} = \xi_{benzene} \gamma_2 \bar{V}_2^* / K_{12}, K_b = K_{22}\}$ with this probe molecular, diffusion coefficients were rescaled with respect to an arbitrary reference solute instead:

$$\begin{aligned}
D(\text{solute}, T, T_g) &= \frac{D_{blob}(T, T_g)}{C(\text{solute}, T)} = \frac{1}{C(\text{solute}, T)} \exp\left(-\frac{K_a^{blob}}{K_b + T - T_g}\right) \\
&= \frac{C(\text{reference}_{solute}, T)}{C(\text{solute}, T)} D(\text{reference}_{solute}, T, T_g)
\end{aligned} \tag{5-28}$$

For a reference solute, chosen as the closest to benzene (e.g. biphenyl) in the studied series, $D(\text{reference}_{solute}, T, T_g)$ can be related to $D_{blob}(T, T_g)$ via Eq. (5-24). By noticing that $E^*(\text{benzene}) \approx 0$ (it is zero for toluene according to³⁰), Eq. (5-28) is finally recast as the product of two independent contributions: one due the solute and one due to the polymer:

$$\begin{aligned}
D(\text{solute}, T, T_g) &= D_{solute}(\text{solute}, T) \cdot D_{polymer}(T, T_g) \\
&= \frac{C(\text{reference}_{solute}, T)}{C(\text{solute}, T)} \exp\left(\frac{-E^*(\text{reference}_{solute})}{RT}\right) \cdot \exp\left(-\left(\frac{\xi_{solute}^{reference}}{\xi_{benzene}} - 1\right) \frac{K_a^{blob}}{K_b + T - T_g}\right) D_{blob}(T, T_g) \\
&= D_{solute}(\text{solute}, T) \exp\left(-\frac{K_a}{K_b + T - T_g}\right) \quad \text{with} \quad Ka = \frac{\xi_{solute}^{reference}}{\xi_{benzene}} K_a^{blob}
\end{aligned} \tag{5-29}$$

Although initial considerations are different, Eq. (5-29) resembles Eq. (9) used in¹⁷ to describe the diffusion of *n*-alkylbenzene in polyethylene via a hybrid model. The solute series chosen in this study enabled to test two effects: the contribution of the distance between two jumping units (diphenyl alkanes series) and the contribution of the number of repeated jumping units (oligophenyls series).

By assuming that the probability of concerted motions between two jumping units decreases exponentially with the distance between two jumping units, Eq. (5-29) was written for diphenyl alkanes according to the number of carbons between two phenyl rings, N_C , (from 0 to 2), as:

$$\frac{D(N_C, T, T_g)}{D_{solute}(N_C = 0, T)} = \exp\left(-\ln 10 \frac{N_C}{N_{C_{10}}}\right) \exp\left(-\frac{K_a}{K_b + T - T_g}\right) \tag{5-30}$$

where $N_{C_{10}}$ is the number of carbons required to decrease D by 10. The first exponential in Eq. (5-30) emphasizes that increasing the distance between two phenyl rings (higher N_C) strengthens considerably $C(t)$ (and possibly $C_{trapped}$). In particular, the polymer host is thought to fill the space between two phenyl rings as the consequence of a reduction of the solute excluded volume. As the number of phenyl rings are the same in diphenyl alkanes, Eq. (5-30) offered an opportunity to assess with a good accuracy of polymer host effects by fitting K_a

and K_b on D values obtained in different polymers (*i.e.* with different T_g) and at a similar reference temperature.

Polymer coupling effect, $C(\text{solute}, T)$, was related to a solute free energy barrier varying with N_{Ph} : $\Delta A_{\text{solute}}(N_{Ph}) = E_{a_{\text{solute}}}(N_{Ph}) - TS_{\text{solute}}(N_{Ph})$, where $E_{a_{\text{solute}}}$, and S_{solute} are the solute translation activation energy and entropy respectively. In the canonical ensemble, ΔA_{solute} is the Helmholtz free energy associated to the probability to find a significant translation of CM when all phenyl rings are subjected to correlated displacements with the surroundings. As in Eq. (5-30), Eq. (5-29) was written relatively to biphenyl as:

$$\frac{D(T, T_g, N_{Ph})}{D_0 \exp\left(\frac{-\Delta A_{\text{solute}}(N_{Ph} = 2)}{RT}\right)} = \exp\left(\frac{-\Delta A_{\text{solute excess}}(N_{Ph} - 2)}{RT}\right) \exp\left(-\frac{K_a}{K_b + T - T_g}\right) \quad (5-31)$$

with $\Delta A_{\text{solute}}(N_{Ph}) = \Delta A_{\text{solute}}(N_{Ph} = 2) + \Delta A_{\text{solute excess}}(N_{Ph} - 2)$ for $N_{Ph} \geq 2$ and $\Delta A_{\text{solute excess}}(N_{Ph} - 2) = 0$ for $N_{Ph} = 2$.

5.1.3.3.4 Modeling of activation terms for oligophenyl solutes

The assumption of $\Delta A_{\text{solute}}(N_{Ph})$ controlled by a partitioning of the correlation with the displacements of surrounding jumping units as $C(t)$ and $C_{\text{trapped}}(t)$, with probabilities $1-p$ and p respectively, was tested by constrained molecular dynamics for the simplest scenario: $C_{\text{trapped}}(t) \rightarrow \infty$ and $C(t) > 0$. The advantage of this scenario is that it can be simulated directly molecular dynamics simulation on isolated molecules by assuming that one or several rings have their positions fixed.

$E_{a_{\text{solute}}}$ and S_{solute} versus N_{Ph} were calculated respectively in order to enable a comparison with experimental values. $E_{a_{\text{solute}}}$ was defined according to the typical temperature-dependent translational time of CM, $\tau_{\text{ring}}(N_{Ph}) \propto \exp(E_{a_{\text{solute}}}(N_{Ph})/RT)$, to cross a distance equal to the diameter of a phenyl ring ϕ_{ring} when 0 to N_{Ph} rings are blocked. As in Eq. (5-17), $\tau_{\text{ring}}(N_{Ph})$ is obtained by averaging over all possible configurations to block phenyl rings:

$$\begin{aligned}
\tau_{ring}(N_{Ph}) &= \frac{(1-p)^{N_{Ph}} \tau_0(N_{Ph}) + \sum_{j=1}^{N_{Ph}} p^j \sum_{k=1}^{\binom{N_{Ph}}{j}} \tau(j,k)}{(1-p)^{N_{Ph}} + \sum_{j=1}^{N_{Ph}} \binom{N_{Ph}}{j} p^j} \\
&\approx \frac{\sum_{j=1}^{N_{Ph}-1} p^j \sum_{k=1}^{\binom{N_{Ph}}{j}} \tau(j,k)}{(1-p)^{N_{Ph}} + \sum_{j=1}^{N_{Ph}} \binom{N_{Ph}}{j} p^j} + \tau_{trapped}
\end{aligned} \tag{5-32}$$

where $\tau(j,k)$ is set the minimum time to induce a displacement of CM equal to \varnothing_{ring} with exactly j rings blocked within the k^{th} configuration chosen among the $\binom{N_{Ph}}{j}$ possibilities:

$$\tau(j,k) = \min \left(\frac{\varnothing_{ring}^2}{\langle \Delta \mathbf{r}_{CM}(t) \rangle_{j,k}^2 / t} \right) \text{ for } 1 \leq j \leq N_{Ph} - 1 \tag{5-33}$$

The special cases, where no ring is blocked and where all rings are blocked, were associated to τ_0 and $\tau(N_{Ph}, 1)$ respectively. $\tau(N_{Ph}, 1)$ was expected to be large but finite, so that it can be set to a constant $\tau_{trapped}$. Beyond $\tau(j,k)$, CM is likely to displace to a distance larger than one ring so that a different combination of trapped and untrapped rings is expected to occur.

According to Eqs. (5-32) and (5-33), translation of CM occurs mainly as a sequence of macrostates where 1.. $N_{Ph}-1$ rings are randomly blocked. The transition from one macrostate to the next one occurs at the fastest rate enabled by the dynamics of the CM when the solute is subjected to topological constraints.

The translational entropy, S_{solute} , which measures the number of microstates associated to a macrostate was calculated analytically according to the same framework but at atomistic scale. All possible displacements of atoms were described as the superposition of $3N_A-6$ quantum harmonic oscillators, with N_A the number of heavy atoms (*i.e.* carbons for tested molecules) in the considered solute. Absolute entropies were calculated according to Eq. (5-34), as justified in⁴⁹:

$$S_{conformational} = k_B \sum_{i=1}^{3N_A-6} \frac{\hbar \omega_i / k_B T}{\exp(\hbar \omega_i / k_B T) - 1} - \ln(1 - \exp(-\hbar \omega_i / k_B T)) \tag{5-34}$$

where the quasiharmonic frequencies $\omega_i = \sqrt{k_B T / \lambda_i}$ were calculated from the eigenvalues, λ_i , of the covariance matrix of the fluctuations of atom positions:

$$\sigma_{i_1, i_2} = \left\langle \left(r_{i_1} - \langle r_{i_1} \rangle \right) \left(r_{i_2} - \langle r_{i_2} \rangle \right) \right\rangle \quad (5-35)$$

where i_1 and i_2 are carbon coordinate indices chosen among $1 \dots 3N_A$.

The translational entropy was calculated by the entropy difference when the position of CM was fixed or not, as described in⁵⁰:

$$S(j, k) = S_{\text{conformational}}(j, k) - S_{\text{conformational}}^{\text{fixed CM}}(j, k) \quad (5-36)$$

Finally, S_{solute} was obtained by averaging over all possibilities to block any combination of phenyl rings in the solute:

$$S_{\text{solute}}(N_{Ph}) = \frac{(1-p)^{N_{Ph}} S_0(N_{Ph}) + \sum_{j=1}^{N_{Ph}} p^j \sum_{k=1}^{\binom{N_{Ph}}{j}} S(j, k)}{(1-p)^{N_{Ph}} + \sum_{j=1}^{N_{Ph}} \binom{N_{Ph}}{j} p^j} \quad (5-37)$$

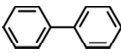
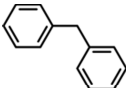
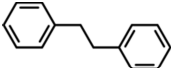
where $S(N_{Ph}, 1) = 0$ due to the absence of available degree of freedoms. $S_0(N_{Ph})$ is the entropy when no phenyl ring is blocked.

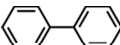
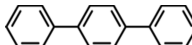
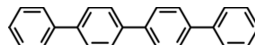
5.1.3.4 Experimental section

5.1.3.4.1 Materials

Table 5-2 and Table 5-3 list the studied aromatic solutes and polymers respectively. The two tested series included phenyl rings as elemental jumping units and shared biphenyl as common molecule. In details, the diphenyl alkanes series enabled to assess the effect of the distance between two elemental jumping units for different $T-T_g$ values while keeping T close to a same reference temperature. By contrast, the oligophenyls series was used to assess the effect of the number of jumping units and the effect of collective barriers ($E_{a\text{solute}}$, S_{solute}) by shifting both T and T_g values.

Table 5-2 List of studied aromatic solutes

Series	Solutes		
Diphenyl alkanes	biphenyl ^a	Diphenylmethane ^b	Bibenzyl ^b
Structure			
M (g·mol ⁻¹)	154.2	168.2	182.3
N _{C=}	0	1	2

Oligophenyls	biphenyl ^a	<i>p</i> -terphenyl ^a	<i>p</i> -quaterphenyl ^a
structure			
M (g·mol ⁻¹)	154.2	230.3	306.4
N _{Ph} =	2	3	4

^asupplied by Sigma-Aldrich Chemistry (Germany) with purity of 99.5 %. ^bsupplied by Acros Organics (France) with purity of 99 %.

Effects of *T-Tg* ranging from 10 K to 110 K on solute diffusion coefficients were investigated in four different polymer hosts above their respective *Tg*, including: polylactide (PLA), polypropylene (PP), polycaprolactone (PCL) and polyvinyl alcohol (PVA). *Tg* of PVA was modulated by using it both at dry state and equilibrated at an intermediate relative humidity of 21% with 2.4 wt% of water content. *K_a* and *K_b* values used in Eqs. (5-30) and (5-31) were exclusively fitted on *D* values of diphenyl alkanes obtained in PLA, PP and PCL at 343 K, 333 K and 323 K respectively. PVA data were used exclusively for external validation purposes.

Table 5-3 Information and characterization of processed films

Polymer	<i>Tg</i> (°C)	Crytallinity %	Thickness (mm) × width or diameter (mm)	Film processing	Supplier/product reference
Polylactide (PLA) ^a	60	23.6	0.02×600	Extrusion	Treofan (Germany)/ Biophan™
Polypropylene (PP) ^a	0	55.5	0.2×800	Extrusion blowing	Borealis (Austria)/ HD621CF
Polycaprolactone (PCL) ^b	-60	50.3	0.01-0.04×200	Solution casting	Creagif Biopolymères (France)/ CAPA 6800
Polyvinyl alcohol (PVA) ^c	55 82	50.0	0.01-0.03×200	Solution casting	Sigma-Aldrich (USA)/ Mowiol® 20-98

^aFilms were processed at industrial scale and used as received. ^bPCL films with molecular weight of 8·10⁴ g·mol⁻¹ were processed at laboratory scale as described in⁵¹. ^cMolecular weight of PVA is 125000 g·mol⁻¹ with 98.0-98.8 % of hydrolysis degree. *Tg* of PVA films were of 82°C and of 55°C, at dry state and when the films were equilibrated at a relative humidity of 21% respectively. All films were processed at laboratory scale as described in⁵².

5.1.3.4.2 Film processing and formulation

PLA and PP were supplied as films and used as received. PCL and PVA films were processed by solution casting, according to^{51,52} respectively. PCL dissolved in dichloromethane with

concentration of 2.4 wt% was poured into a glass petri dish. After 24 h of evaporation at room temperature, PCL films were peeled off from the dish and dried in an oven at 30 °C for three days. PVA films were formed by applying the similar process by using deionized water as solvent with PVA concentration of 2 wt%. The evaporation of water took at least three days. Then, the films were conditioned under controlled relative humidity.

T_g and crystallinity degree of each polymer were measured by differential scanning calorimetry (model Q100, TA Instruments, USA) at a heating rate of 10 °C/min within temperature limits adapted to each polymer. The crystallinity degree was calculated from the melting endotherm in the first heating scan with the help of the theoretical melting enthalpy of the 100 % crystalline polymer: 93 J·g⁻¹ for PLA⁵³, 165 J·g⁻¹ for PP⁵⁴, 139 J·g⁻¹ for PCL⁵⁵, 138.6 J·g⁻¹ for PVA⁵⁶. Glass transition temperatures of all polymers except PVA were measured in the second heating scan and taken at the mid-point of the heat capacity step. In the case of both dry and plasticized PVA, T_g values were determined from the first heating scan. Determinations were triplicated.

5.1.3.4.3 Methods

Diffusion coefficient determination

According to expected values of diffusion coefficients, roughly below and above 10⁻¹⁴ m²·s⁻¹, two complementary solid-contact methods operating at two different length scales were used to reach contact times shorter than two weeks. It was checked that both methods gave similar diffusion coefficients for the solute common to both series: biphenyl. Films acting as sources of solutes were formulated with each solute either by soaking films in a 0.05 g·ml⁻¹ solute-ethanol solution during a minimal duration of one week at 60°C (cases of PP, PVA) or by adding the desired solute to the casting solution at a concentration of 0.2 wt% (case of PCL). Due to the difficulty of absorbing bulky aromatic solutes in PLA films below or close to its T_g (to avoid recrystallization), PP films were used as sources instead in PLA experiments. All processed films were stored stacked to prevent solute losses and to facilitate the internal homogenization of concentration profiles. The uniformity of concentration profiles in sources was tested over the cross section of microtomed films by fluorescence imaging.

A modified method originally proposed by⁵⁷ was used for high diffusion coefficients (above 10⁻¹⁴ m²·s⁻¹, *i.e.* mainly in a temperature range of T_g+90 K and T_g+110 K). It consisted in stacking twelve virgin films with two source films formulated with the considered solute. Theoretically, by positioning sources in positions 5 and 10 in a stack consisting of 14 films

with approximately the same thickness, the solute concentration profile evolve with diffusion time from a bimodal one to a monomodal one (with one single maximum located between films 7 and 8). The variations in shape of the profile combined with the variations in concentration improved dramatically the comparison with the corresponding theoretical profiles expressed in function of the dimensionless position x/l and dimensionless time $Fo=Dt/l^2$, where x is the position and l the average film thickness. In our experiment, films cut as disks were folded in aluminum foil and inserted in a copper cylinder of a same diameter. The cylinder was closed by two Teflon disks and the whole stack was packed with pressure by a screw system. Such conditions ensured good contact between films without mass transfer resistance and impervious conditions at both ends of the stack and on its lateral surface. After contact time at a constant temperature, solute concentration in each film was measured after solvent extraction in double beam UV/VIS spectrophotometer (model UVIKON 933, KONTRON Instruments, France). Extraction solvents were dichloromethane for PP and PCL, and deionized water for PVA. D values were retrieved by fitting numerically dimensionless theoretical concentration profiles (including the real geometry of each film) to measured concentration profiles. When several contact times or stack geometries were used for the same solute, D was defined as the regression slope of Fo versus x/l^2 .

For low diffusion coefficients, similar principles but at microscopic scale were used to reach similar contact times. A source film was sandwiched between two virgin films during a prescribed time. Diffusion was stopped by quenching films in liquid nitrogen, The concentration profile along the section of each film was subsequently determined, after microtoming (model LKB 2218 HistoRange, LKB-Produkter AB, Sweden) with cutting thickness of 15 μm , by deep-UV fluorescence microspectroscopy on an inverted microscope (model IX71, Olympus, Japan) in epi-configuration mode. A synchrotron source with a specific excitation wavelength ranging from 275 nm to 295 nm was used according to the tested solute (DISCO beamline, synchrotron Soleil, France). Bi-dimensional fluorescence emission spectra were acquired with a spectral resolution of 0.5 nm between 280 nm and 480 nm (LSM 710, Zeiss, Germany), and a spatial resolution of 0.5 or 1 μm . Concentrations were inferred from the surface area between the spectrum and the baseline. D values were identified similarly by a fitting procedure with a numerical model incorporating partitioning effects when required. Three to five concentration profiles along the same section were used in the fitting procedure.

All experiments were triplicated or duplicated. All numerical models relied on finite volume difference scheme taking into account the real thickness of each film and a solver optimized for diffusion problems and distributed as an open-source project⁵⁸.

Constrained molecular dynamics simulation

Displacements of solute atoms available in constrained oligophenyls solutes were studied regardless the polymer host by constrained molecular dynamics. Starting from a random configuration, explicit constraints were applied by fixing the positions of all atoms of one or several phenyl rings. Long-term molecular dynamics simulations of isolated molecules subjected to such constraints were performed in the NVT ensemble at 298 K under vacuum boundary conditions using a Nosé-Hoover thermostat. For covalent and non-covalent interactions, COMPASS forcefield⁵⁹ was employed without any cutoff and dynamic simulations were conducted with Discover program (Accelrys, USA). Mean-square displacements of the center-of-mass and covariances of atom displacements were averaged over several initial configurations.

5.1.3.5 Results and discussion

5.1.3.5.1 Comparison of the scaling of D between linear aliphatic solutes and aromatic solutes

The assumption of the scaling exponent α following the temperature dependence as proposed in Eq. (5-18) is tested in Figure 5-4 for α values inferred from diffusion coefficients collected at different temperatures on a semi-crystalline polyethylene (PE)^{3, 14-17} and amorphous polyamide, based upon poly-(ϵ -caprolactam) lightly cross-linked with diglycidyl ether of bisphenol A⁵. It is important to notice that reported α values are associated to diffusion coefficients measured only within the same study (with the same polymer and the same measurement protocol) and for solutes larger than 70 g·mol⁻¹. T_g values involved in Eq. (5-18) were either the reported ones or derived from the host polymer mass. As applied in Figure 5-2, solute series were categorized as linear aliphatic and aromatic solutes. The “linear aliphatic” series merged linear n -alkanes, n -alcohols and esterified phenols with long n -alkyl chains ($n=6..18$) whereas the “aromatic” series combined short n -alkylbenzenes ($n=0..4$), substituted and hindered phenols ($M= 94-545$ g·mol⁻¹). Values of α generated by this study for oligophenyls and reported for short linear aliphatic solutes in polyvinyl acetate (PVAc)³⁴ were excluded from the fitting procedure and included only a posteriori as external validation of Eq. (5-18).

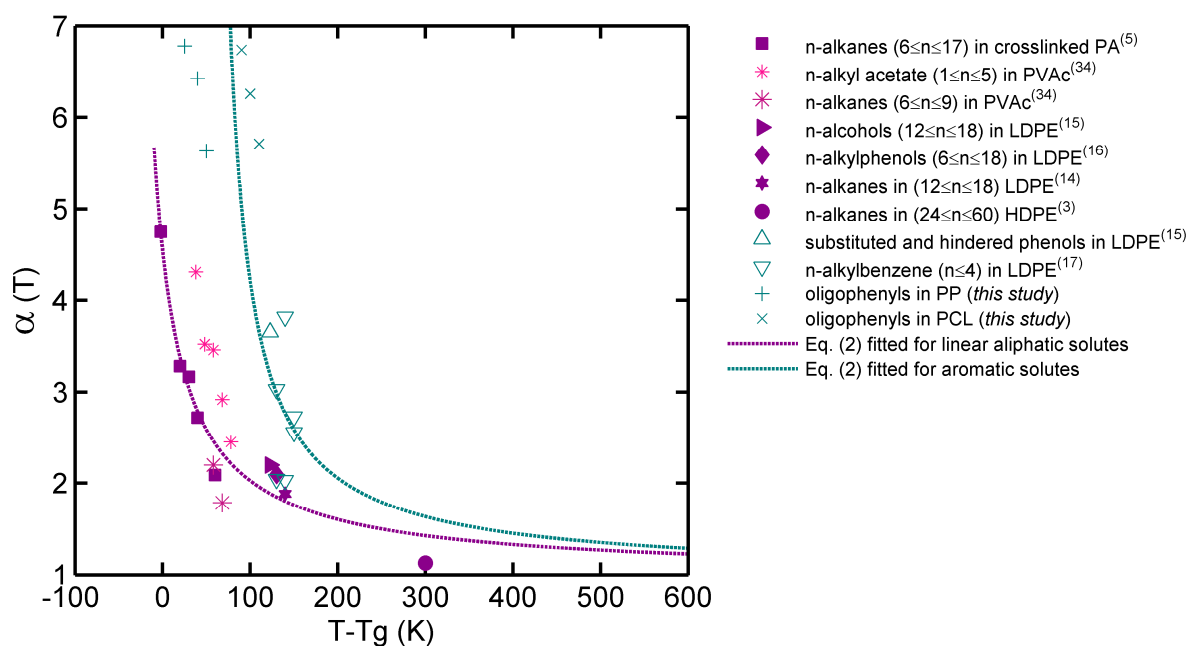


Figure 5-4 Scaling exponents of trace diffusion coefficients versus $T-T_g$. Symbols plot determinations of α inferred from experimental D values reported in references enclosed within brackets. α values for oligophenyls measured by this study and those calculated from D values of short linear aliphatic solutes in PVAc³⁴ were not used to fit Eq. (5-18). The classification of solutes as linear aliphatic and aromatic is based on the same one as used in Figure 5-2.

Eq. (5-18) fitted well α values of both linear aliphatic solutes and aromatic solutes and also offers a continuous reconciliation between the diffusion behavior in solids and melts. Master curves looked homothetic with a positive temperature shift of 91 K from linear aliphatic solutes to aromatic solutes, corresponding to a K_β value of 40 K and -51 K respectively. The approximation derived from Eqs. (5-19) and (5-25): $K_\beta^{\text{aliphatic solutes}} \approx \left| K_\beta^{\text{aromatic solutes}} \right| \approx K_{22} = C_2$, was well verified. For comparison, a value of 50 K is reported for K_{22} in³⁰, when polystyrene is probed with toluene and ethylbenzene as molecular probe. Based on the viscoelastic response of polymer systems, the WLF constant C_2 is quoted for linear homopolymers between 30 K and 70 K^{60, 61}. Predictions of Eq. (5-18) were also in good agreement with the values of the two independent sets of data. Scaling exponents α inferred from diffusion coefficients in PVAc³⁴ of short linear aliphatic solutes, including n -alkyl acetates ($n=1..5$) and n -alkanes ($n=6..9$), were shown to be broadly spanned from 1.6 to 4.5 as foreseen by Eq. (5-18) applied to linear aliphatic solutes. Free-volume parameters proposed in³⁰ for this series of molecules and by using Eq. (5-27) lead to similar conclusions. The predictions for aromatic solutes were even more remarkable, as Eq. (5-18) was able to predict the scaling exponents for oligophenyls close to T_g , as reported in this study in PP and PCL (see section 4.2),

whereas no value has been already published. Eq. (5-18) predicts that α decreases rapidly to finally converge to 1 far from T_g . At high temperature, a unitary coefficient α , as predicted by the Rouse theory¹³, has been found in different polymers^{3,36-38} for linear aliphatic solutes, but it has not still been described for aromatic solutes. The generalization to aromatic solutes is however very likely in the light of the comparison of the ratios of diffusion coefficient of radio-labeled 1,1-diphenyl ethane to the one of radio-labeled *n*-dodecane or *n*-hexadecane as reported in⁶² and³⁶ in various rubber polymers for large $T-T_g$ values, plasticized or not. The ratios found slightly above 1 were interpreted as higher friction factors. As depicted in Figure 5-4, they prove in particular that exponents α of aromatic solutes tend to be above those of *n*-alkanes solutes while converging to the same universal unity value in aliphatic polymers and by extension in elastomers and thermosets far above their T_g . At intermediate temperatures (in semi-crystalline or below the flow threshold of the polymer), α values increase dramatically when the temperature is decreasing, with literature values reported up to 4.7⁵. The very large α values obtained in this study for oligophenylys would demonstrate the existence of friction factors even larger than previously reported ones.

As no existing theory holds for exponents α larger than 1 and solutes that are non-entangled with polymer segments, some analogies with the scaling of self-diffusion in monodisperse systems are first discussed. In monodisperse mixtures of non-entangled *n*-alkanes ($M=114-844 \text{ g}\cdot\text{mol}^{-1}$), scaling exponents were described to decrease almost linearly from 2.72 to 1.85 when temperature was increasing from 303 K to 443 K^{63, 64}. T_g of corresponding liquid *n*-alkanes are expected to be lower than polyethylene (theoretically 200 K for an infinitely long polyethylene⁶⁵), with values ranged between 51 K and 186 K (according to the equation of Fox and Loshaek⁶⁶ and parameters fitted in^{67, 68}). According to Figure 5-4, self-diffusion could be envisioned equivalently as trace diffusion in a host with a very low T_g . In a small range of temperatures centered around a reference temperature θ , the linear decrease of $\alpha(T)$ is particularly granted by the asymptotic behavior of Eq. (5-18) towards the melt region. When $T \gg \max(0, T_g - K_\beta)$, Eq. (5-18) is indeed approximated by $\alpha(T) \approx 1 + K_\alpha / (T - T_g) \approx \alpha(\theta) - K_\alpha (T - \theta) / (T - T_g)^2$. The absence of effect of K_β far from T_g suggests that only thermal expansion effects of the polymer host dominate. They are controlled by the value of K_α , which was found very similar for both linear and aromatic solutes, 144 K and 156 K respectively. Similar arguments were used to explain the thermal dependence on α in non-entangled monodisperse systems^{63, 64}. They may be nevertheless approximate because not only the static properties (*i.e.* density, free volumes distribution... of

the polymer) are affected by the host molecular mass but also the dynamic ones (*i.e.* T_g is increasing with M)^{3,4}.

Near T_g , the variation of static polymer effects cannot be invoked alone to justify the large values of α . We related phenomenologically this additional effect in Eq. (5-18) to a guest parameter, formally $-K_\beta$, which can be envisioned as a critical temperature deviation to T_g to translate an elemental jumping unit. For solutes consisting in the repetition of a similar jumping unit, K_β was thought to be constant: positive when the jumping unit resembles polymer segments and can easily accommodate the fluctuations of the contour of polymer segments; and negative otherwise. The concepts of accommodation between a bulky guest molecule (*e.g.* aromatic fluorescent dye) and host aliphatic chains have been studied in low molecular weight alkanes⁶⁸. Coarse grained simulation of molecular dynamics of spherical solutes larger than the polymer beads⁴⁶ confirmed further the proposed description involving both polymer static and dynamic effect: trace diffusion coefficients were found scaled as a power law of the volume of the bead with a scaling exponent increasing from 0.8 to 1.43 when the stiffness of the polymer host increased.

5.1.3.5.2 *Scaling diffusion coefficients according to Eqs. (5-11), (5-30)-(5-31)*

Phenomenological scaling of D with M at different temperatures for both tested aromatic solute series is depicted in Figure 5-5 along with the predictions according to Eqs. (5-30) and (5-31). One important goal is to demonstrate that the temperature shift factor associated to D depends on some solute contributions and that proposed equations prolong naturally the conventional Williams-Landel-Ferry model (see Eqs. (5-19) and (5-25)). To test the proposed free-volume theory, the following fitting procedure was applied. Polymer related parameters, K_a and K_b , were exclusively fitted from the D values of diphenyl alkanes series at constant temperature (*i.e.* from D values obtained in different polymers with different T_g). The determined values of K_a and K_b values were directly applied to each oligophenyl solute to extract $Ea_{solute}(N_{Ph})$ and $S_{solute}(N_{Ph})$. External validation was finally achieved by predicting D values of biphenyl in plasticized and unplasticized PVA, where the experimental D values of PVA were evidently not included in the fitting procedure.

Figure 5-5 shows the very strong mass dependence on D values for both diphenyl alkanes and oligophenyls, with α decreasing with increasing temperature from 24 to 20 (95% confidence interval ∓ 4.5), and from 5.3 to 4.3 (95% confidence interval ∓ 1.6), respectively. Such values were far from values previously reported for aromatic solutes (see Figure 5-4) and varied in a small extent with tested temperatures and considered polymers. As depicted in

Figure 5-6, Eqs. (5-30) and (5-31) fitted well the broad distribution of D over five decades for all tested polymers, with a fitting error distributed normally and in the range of experimental errors. Predictions of D values of biphenyl in an external polymer (PVA) by Eq. (5-30) were also in good agreement with experimental data for both dry and plasticized PVA. The predictions for dry and plasticized PVA confirmed the temperature-humidity induced plasticization superposition assessed with fluorescent diffusion probes in polyamide⁶⁹. Such preliminary comparisons between experimental values and model ones justify globally the separation of the polymer and solute contributions for aromatic solutes in aliphatic polymers. Both effects are analyzed separately hereafter.

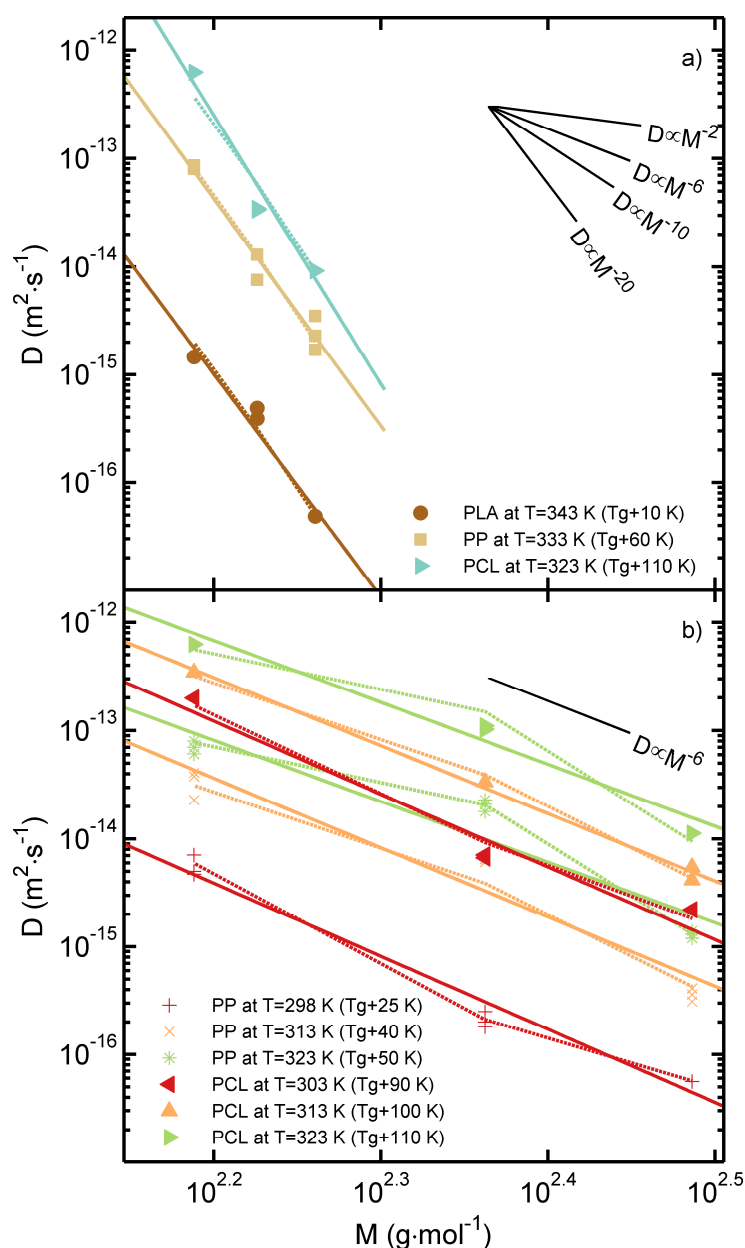


Figure 5-5 a) Log-Log plot of trace diffusion coefficients of diphenyl alkanes and b) oligophenyls in various polymers. Symbols are experimental values. Continuous straight lines

are scaling relationships fitted according to Eq. (5-11). Dashed lines are values fitted from Eqs. (5-30) and (5-31) for diphenyl alkanes and oligophenyls respectively.

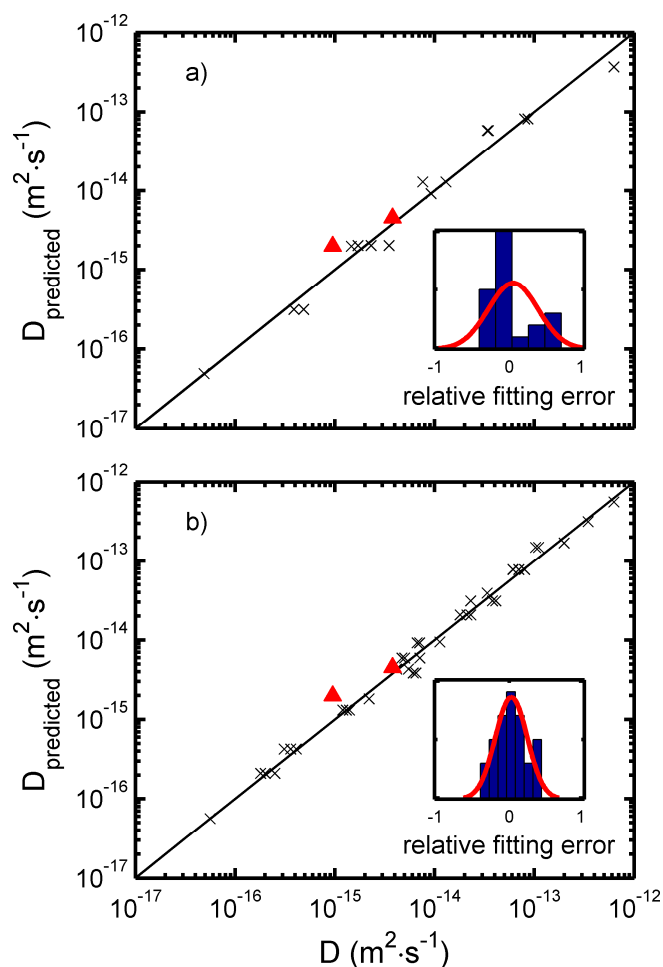


Figure 5-6 Comparison between calculated (with Eqs. (5-30) and (5-31) respectively) and measured diffusion coefficients of a) diphenyl alkanes series and b) oligophenyls series in PLA, PP, PCL(\times) and PVA(\blacktriangle). The continuous lines plot the straight line $y=x$. The corresponding distribution of relative fitting errors values and fitted Gaussian distribution (continuous curve) are plotted within insets. Values in PVA are external validation predictions not used in the fitting procedure.

5.1.3.5.3 Polymer effects as probed with diphenyl alkanes

Diphenyl alkanes series presented several remarkable features to probe polymer effects. Firstly, solutes corresponding to a small range of N_C values (here 0, 1, 2) are of similar size so that they are probing almost the same size of free volume pockets. Secondly, increasing the distance between phenyl rings enabled to assess the effect of expected higher correlations with the surroundings, $C(t)$. Finally, the large spread of diffusion coefficients with N_C improved the accuracy on polymer parameter estimates, K_a and K_b , used in Eqs. (5-30) and (5-31).

By noting $D_{polymer}(T, Tg) = \exp\left(-\frac{K_a}{K_b + T - Tg}\right)$, Figure 5-7 plots both the scaling of D and the solute contribution, defined as $D/D_{polymer}$, versus the number of carbon atoms, N_C , at a constant temperature. The inferred scaling did not depend on the considered polymer and was associated to a $N_{C_{10}}$ value of 1.3 in Eq. (5-30), which implies that D decreases 10-folds when 1.3 carbons is added between the two phenyl rings.

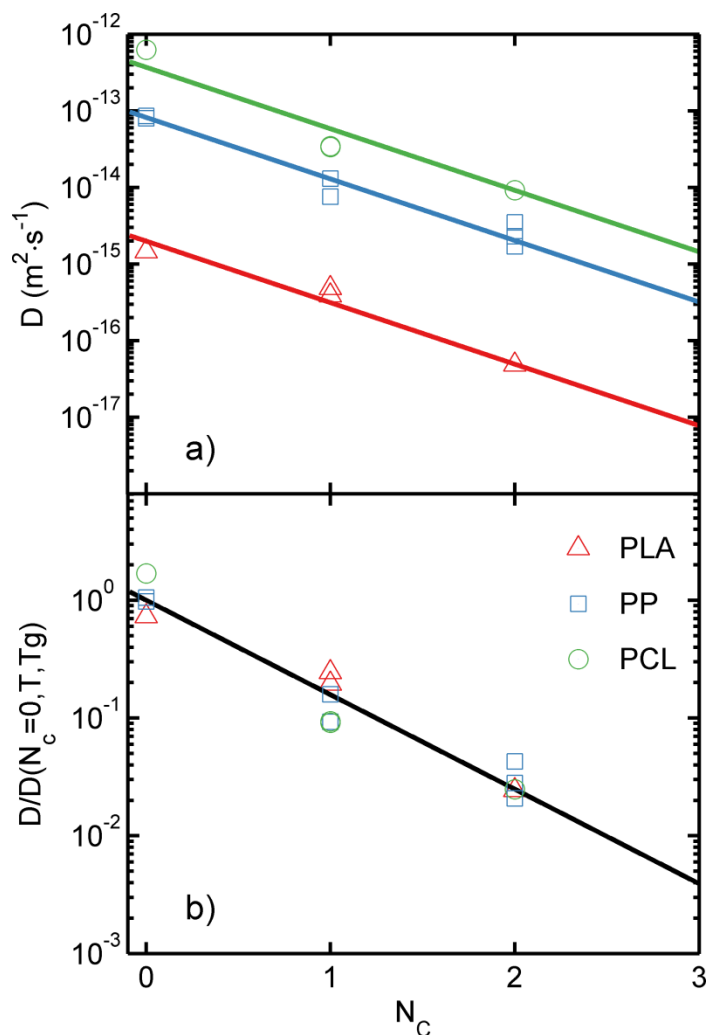


Figure 5-7 Scaling diffusion coefficients of diphenyl alkanes with the number of carbons, N_C , between phenyl rings: a) raw diffusion coefficients measured at 343 K for PLA, 333 K for PP, and 323 K for PCL b) diffusion coefficients relative to biphenyl $D(N_C=0, T, Tg)$. Eq. (5-30) predictions are plotted as continuous lines.

The corresponding polymer contribution was assessed as D/D_{solute} with $D_{solute}(N_C, T) = D_{solute}(N_C = 0, T) \exp\left(-\ln 10 \frac{N_C}{N_{C_{10}}}\right)$. D and D/D_{solute} in polymers used for fitting (PLA, PP, PCL) and validation (PVA) are plotted versus $T - Tg$ in Figure 5-8a) and b)

respectively. Results showed accordingly an evolution of D/D_{solute} that was independent of the considered solute and where polymer effects were finally reduced to an effect of the distance to T_g . Values of K_a and K_b were found equal to 600 K and 58 K respectively, and predicted independently with an acceptable accuracy of the D values of biphenyl in both dry and plasticized PVA. The estimated value of K_b is of the same magnitude order as the value of 50 K for the polymer-related parameter K_{22} reported in³⁰. As quoted in⁴⁰, such ranges of K_b were assumed to be generic for linear homopolymers and therefore also valid for oligophenyls series too. According to Eqs. (5-19) and (5-25), it could be thought that $\{K_a, K_b\}$ (*i.e.* fitted on our diphenyl alkanes data) and $\{K_\alpha, |K_\beta|\}$ (*i.e.* fitted exclusively from literature data on different aromatic solutes) might be also related together. However, it is expected to be true only if no additional energy barrier exists. In our study, it is very likely for a solute comprising only one single jumping unit. In other words, only the value of $K_a^{blob} = \frac{\xi_{benzene}}{\xi_{biphenyl}} K_a$ (associated to benzene, see Eq. (5-29)) can be compared to $K_\alpha \ln M_{benzene}$. By using “universal” values for WLF constants⁷⁰, one derives an estimate of $\xi_{biphenyl}$ of 0.65 via $C_1 = K_a / (\xi_{biphenyl} K_b) \approx 16$; and from Figure 5-3, we infer an approximate value of $\xi_{benzene}$ as $\xi_{biphenyl} - 0.24 \ln 2 \approx 0.48$. Finally, we get $K_a^{blob} \approx (0.48/0.65)600 \approx 445$ K, which must be compared to $K_\alpha \ln M_{benzene} \approx 150 \ln 78 \approx 654$ K. The magnitude orders are comparable and the observed discrepancy is a result of combined uncertainties on K_α (α values from literature are scares and noisy) and ξ values. In addition, by taking an upper value of 18⁶¹ for C_1 would have lead to $K_a^{blob} \approx 501$ K. The agreement between K_b and $|K_\beta|$ is even more convincing with values of 58 K and 51 K, respectively.

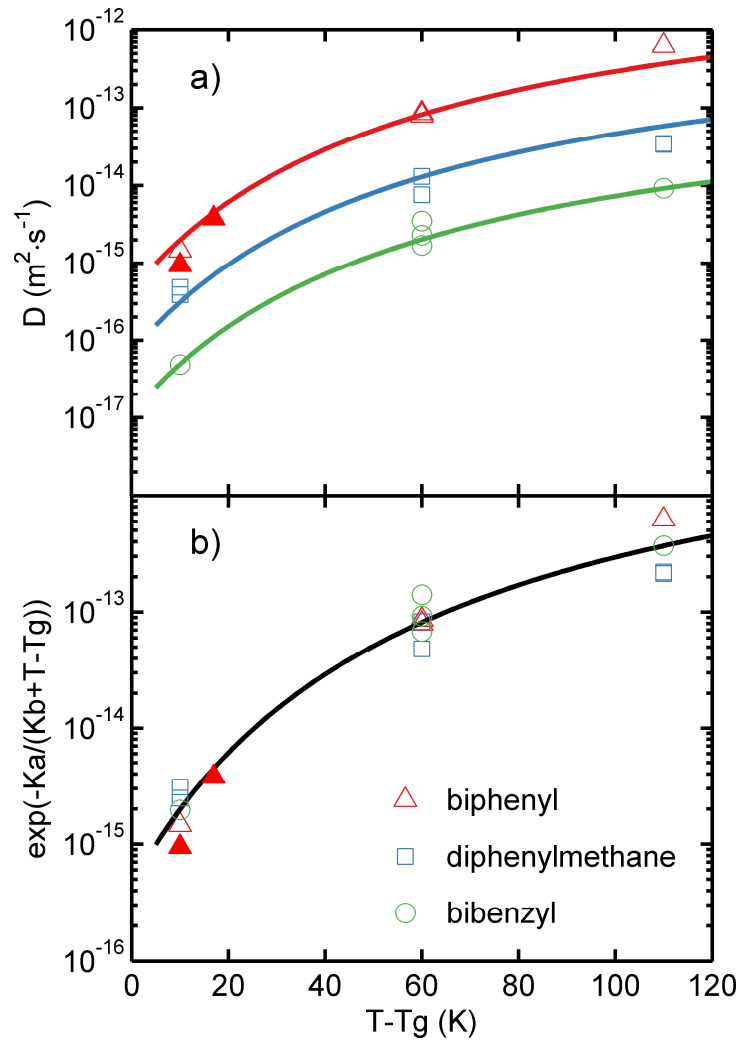


Figure 5-8 Experimental diffusion coefficients of diphenyl alkanes in PLA, PP, PCL (empty symbols) and PVA (filled symbols) versus $T - T_g$ a) raw diffusion coefficients, b) D/D_{solute} . Eq. (5-30) fitted on empty symbols is plotted as continuous lines. Filled symbols are used for external validation purposes.

5.1.3.5.4 Solute activation parameters of oligophenyls

Diffusion coefficients of oligophenyls exhibited much a lower dependence with molecular mass, which was associated in Eq. (5-31) to a free energy barrier, which is also a function of the number of phenyl rings. Figure 5-9 plots the dependence of D (Figure 5-9a) and b)) and of D scaled by the polymer exponential factor, $\exp\left(-\frac{K_a}{K_b + T - T_g}\right)$, (Figure 5-9c) and d)) versus the number of phenyl rings, N_{Ph} . Whatever the considered temperature and tested polymer, the exponential decrease of D with N_{Ph} was non-regular, suggesting a non-monotonous variation of the energy barrier to translation with N_{Ph} . The trend is confirmed by plotting both D and D scaled by polymer effects on a van't Hoff plot in Figure 5-10. While a

significant deviation to an Arrhenius behavior was observed on raw diffusion coefficients in polymers close to their T_g as shown in Figure 5-10a) and b), a pure Arrhenius behavior was recovered by contrast once the effects of density were corrected. It was particularly interesting to notice that the slope of the van't Hoff plot was systematically much higher for *p*-terphenyl than those of the former and following solutes in the series.

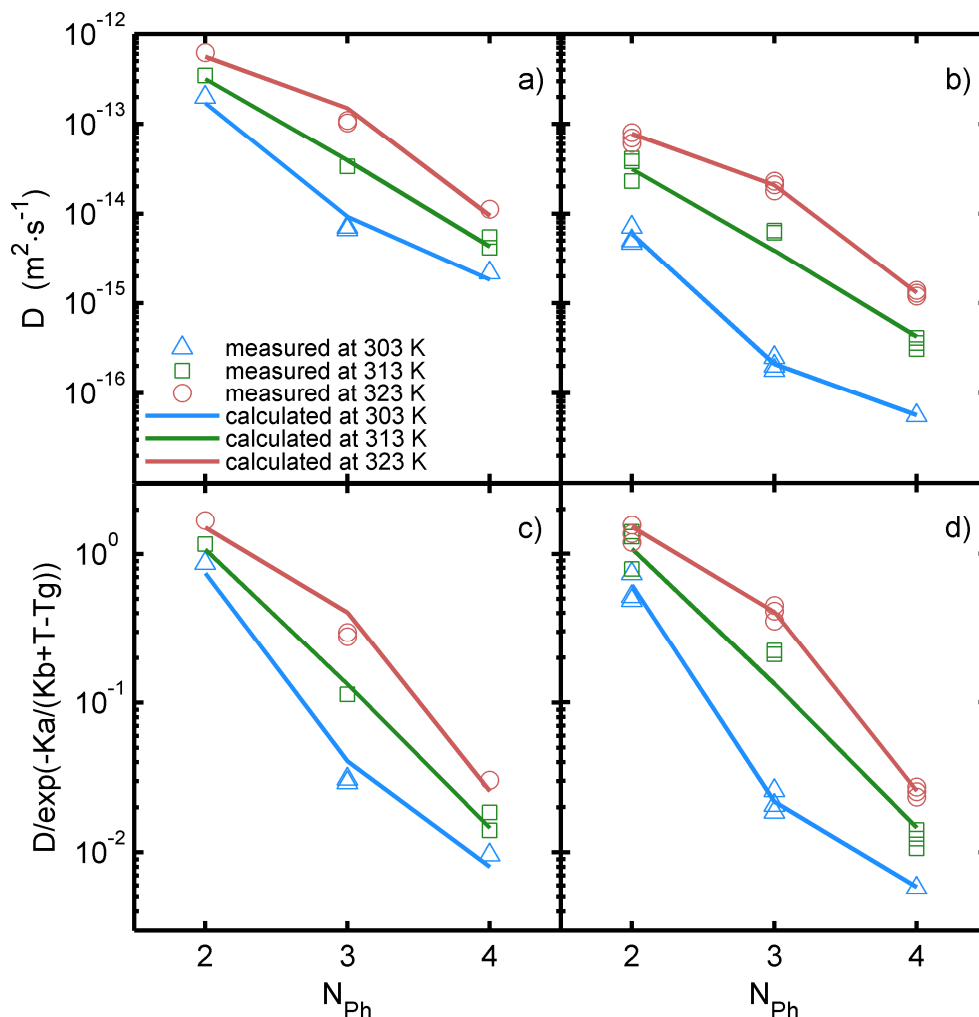


Figure 5-9 Scaling of diffusion coefficients of oligophenylys with the number of phenyl rings, N_{Ph} , a,c) in PCL and b,d) in PP at different temperatures: a,b) raw diffusion coefficients, c,d) scaled diffusion coefficients with polymer effects removed. Predictions according to Eq. (5-31) are plotted as continuous lines.

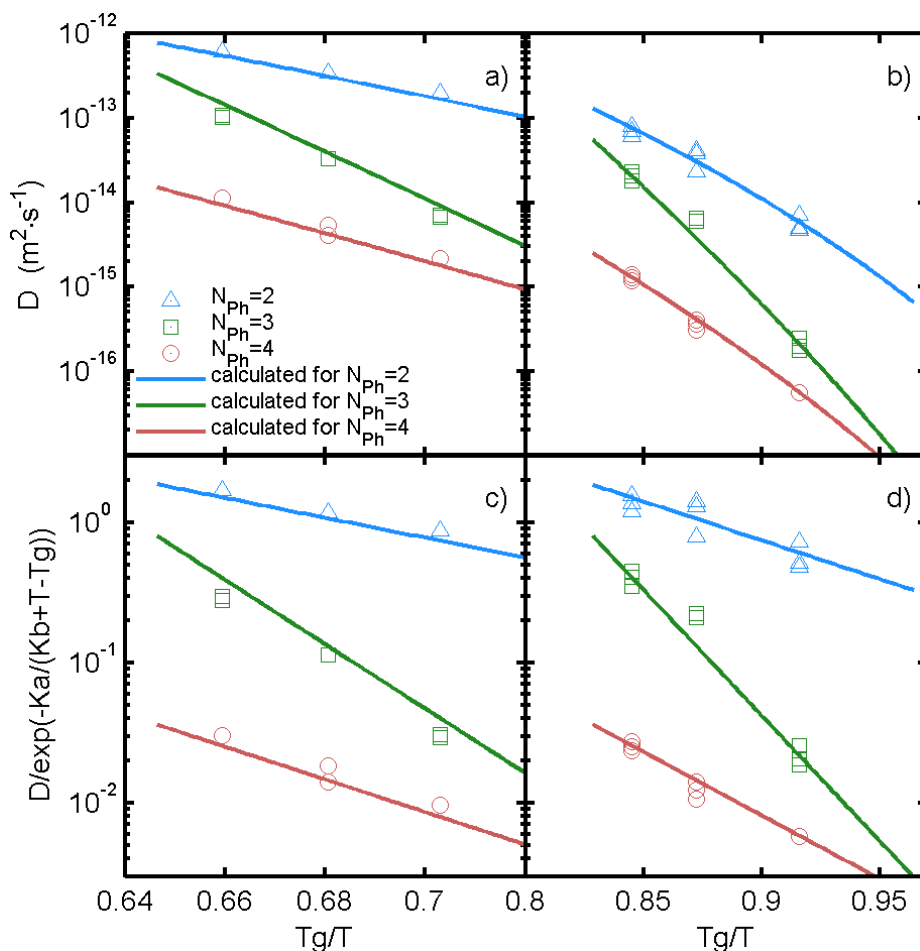


Figure 5-10 Normalized van't Hoff plots of oligophenyls a,b) raw diffusion coefficients and c,d) scaled diffusion coefficients with polymer effect removed a,c) in PCL and b,d) in PP. Predictions according to Eq. (5-31) are plotted as continuous lines.

The non-monotonous variations of solute activation energies, $E_{a,solute}$, and entropies, S_{solute} , are specifically captured in Figure 5-11b) and d). Raw activation values, as estimated from Figure 5-10a) and b), are also given in Figure 5-11a) and c). Regardless polymer effects were included or not, activation parameters exhibited systematically a hat shape with a maximum for $N_{ph}=3$. Such non-monotonous variations appeared for both tested polymers (PP and PCL) with apparent activation energies and entropies of PP shifted from PCL ones by approximately $35 \text{ kJ}\cdot\text{mol}^{-1}$ and $95 \text{ J}\cdot\text{mol}^{-1}\cdot\text{K}^{-1}$, respectively. PP and PCL activation values were exactly reconciled once polymer effects were removed by Eq. (5-31). It is worth to notice that the reconciliation was obtained by removing the polymer contribution, whereas it was inferred independently from the D values of diphenyl alkanes. Since both enthalpy and entropy exhibited similar shape, an apparent position correlation between both quantities was found as plotted in Figure 5-11e). Enthalpy-entropy compensation is often considered to be a statistical artifact due to correlations between errors on each estimate and because entropy must be extrapolated to infinite temperature. As polymer effects were removed in our case, it

could however be thought that the extrapolation of solute effects regardless the true physical state of the polymer at an infinite temperature can have a reasonable meaning. Such kind of discussions can be found in⁷¹. The corresponding internal free energy barriers at 298 K required to induce a translation of oligophenyls are represented in Figure 5-11f). As activation energy and entropy contribute with opposite signs to the free energy barrier, free energy was found monotonous with N_{Ph} .

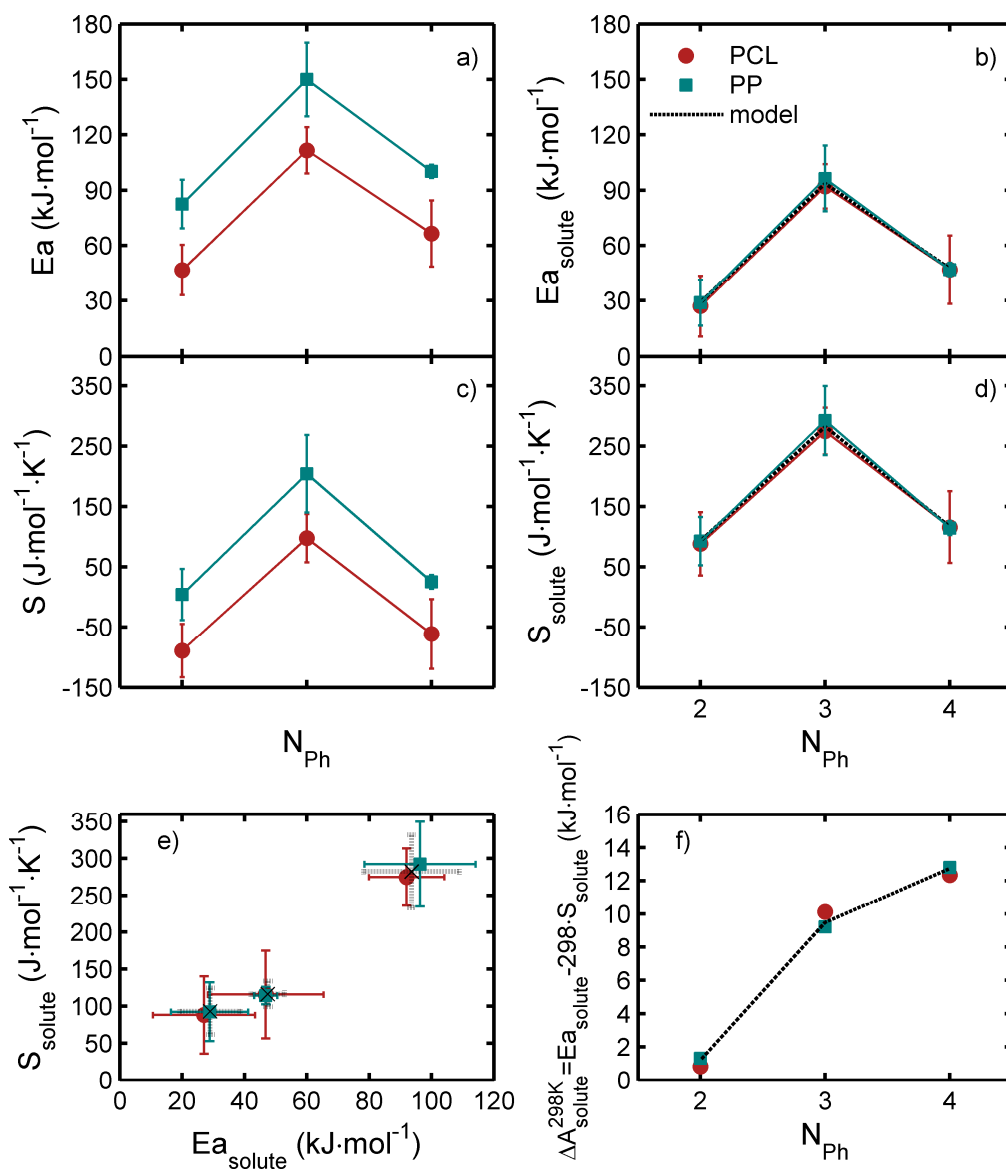


Figure 5-11 a,c) Raw and b,d) solute activation energies and diffusion entropy of oligophenyls in PP and PCL versus the number of phenyl rings, N_{Ph} ; e) correlation between solute activation parameters; f) related free barrier energy to diffusion at 298 K.

5.1.3.5.5 Mechanisms of translation of oligophenyls in aliphatic polymers

Diffusion of large organic solutes in polymer hosts cannot be directly studied by molecular dynamics close to their T_g at atomistic scale. Our experimental results highlighted however

two noticeable properties to derive tractable simulations and to gain further insights on the translation mechanisms of linear aromatic molecules in rubber polymers:

- The displacements of each jumping unit (*i.e.* “polymer effects” in the text) and “solute effects” (*i.e.* collective displacements of jumping units) on D are separable;
- Activation energies associated to the displacement of several jumping units vary with the parity of the number of jumping units. Such a feature can be directly tested by simulation.

The main idea was to test whether two correlation modes between the displacements of phenyl rings and surrounding atoms could explain the effect of the parity of N_{ph} on activation terms. Since neither the partitions between both modes nor the correlation times are known, our strategy consisted in studying the translation of CM in constrained long-term molecular dynamics (10 ns or more), where the positions of one or several phenyl rings (*i.e.* jumping units) are kept fixed, under vacuum boundary conditions (*i.e.* without polymer host). The minimum times to enable a translation of CM longer than a phenyl ring diameter (*i.e.* length of one jumping unit) and the related translational entropy were analyzed according to Eqs. (5-32) and (5-37) respectively and finally compared to their experimentally inferred counterparts: $E_{a,solute}$ and S_{solute} . By fixing *a priori* different values to p , it was in particular possible to assess which value could reproduce a non-monotonous variation with the number of jumping units.

The results obtained by averaging over a wide range of initial configurations are plotted in Figure 5-12 and compared to experimental values reported in Figure 5-11. The typical “hat shape” of activation energies was particularly reproduced without significant bias with $RT\ln(\tau_{ring}-\tau_{trapped})$ calculated from Eqs. (5-32) and (5-33) when $p \rightarrow 1$ (Figure 5-12a)). S_{solute} values derived from Eqs. (5-34)-(5-37) led also approximately to the similar trend when $p \rightarrow 1$ (Figure 5-12b)). The theoretical translational entropy underestimated however systematically the real one due to the loss of fluctuations information caused by the fixed positions of some phenyl rings. It is worth to notice that the reported “hat-shape” of activation terms could not be predicted with the simple coarse-grained theory supported either in Eq. (5-15) or in Eq. (5-17) because they assume that the displacements of all phenyl rings are equivalent. In reality, the gyration radius and mean-square-displacement of oligophenyls are dramatically affected by the combination of phenyl rings that are fixed. Among all tested oligophenyls ($N_{ph}=2, 3, 4$), p -terphenyl is the one that offers the highest ratio of possibilities to reduce dramatically the fluctuations of CM and other atoms. Particularly efficient configurations (*i.e.* five over the 2^3 possibilities): blocking the central ring alone or blocking randomly two or three rings. Such effects could not be captured by a generic flexible model that assume a

uniform relaxation model along the chain (see Eq. (5-13)) or uniform covariances between connected jumping units (see Eq. (5-14)) and were consequently better reproduced by atomistic simulations. It is particularly noticeable that increasing p in simulations induced enthalpy-entropy compensation as experimentally assessed so that the partitioning between short and long-lived contacts could be proposed as the main cause of the phenomenon. Corollary, the suggested high value of p (*i.e.* at least one jumping unit has long-lived contacts with surrounding host) does not depend on the length of studied solutes and could be general for all linear aromatic solutes within aliphatic polymers.

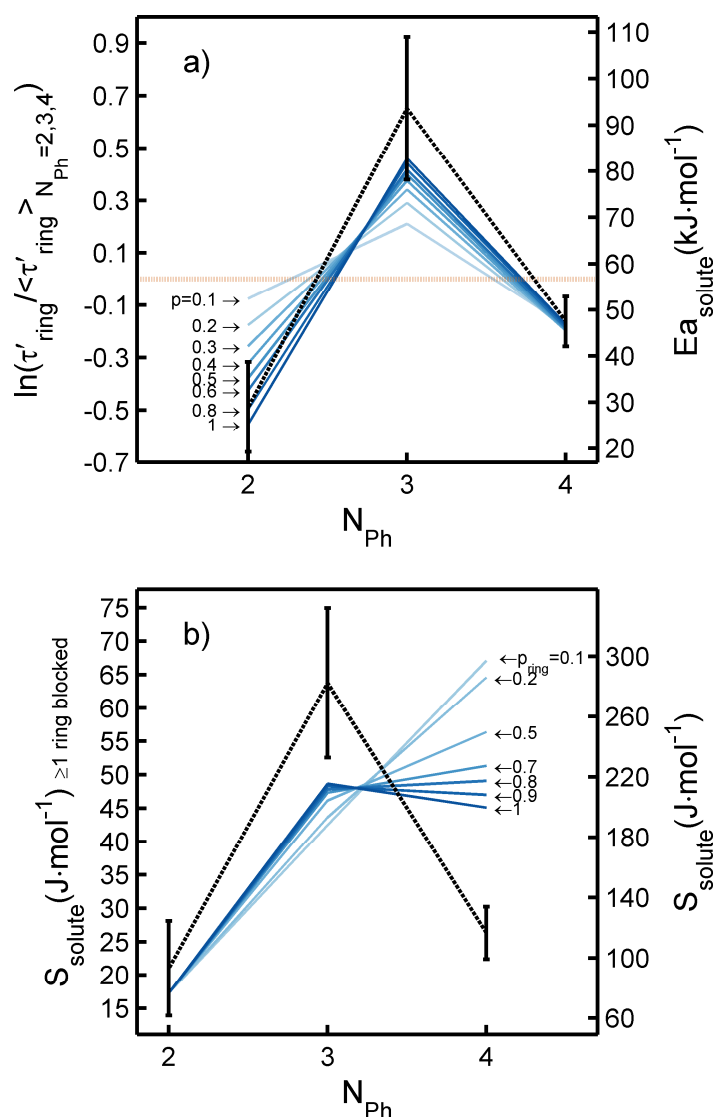


Figure 5-12 a) Comparison of relative solute activation energy (continuous lines, left scale), calculated as $\tau'_{ring}(N_{Ph}) = \tau_{ring}(N_{Ph}) - \tau_{trapped}$ for different p values according to Eqs. (5-32) and (5-33), with experimental values (dotted lines, right scale) reported in Figure 5-11b). The horizontal dashed line represents the average value of Ea_{solute} for studied oligophenylys. b) Comparison of solute entropy (continuous lines, left scale), calculated for different p values

according to Eqs. (5-34)-(5-37), with experimental values (dotted line, right scale) reported in Figure 5-11d).

5.1.3.6 Conclusions

The presented work introduces several invariant scaling relationships for the trace diffusion coefficients (D) of homologous bulky solutes in thermoplastic polymers above their T_g and presents a first molecular interpretation of corresponding translation mechanisms. D values over five decades were measured for two homologous series of short aromatic solutes, diphenyl alkanes and oligophenyls, in different polymers and at various temperatures, T . The collected values completed the available picture from literature by integrating D values for low $T-T_g$ values. The analysis of the scaling with molecular mass, as $D \propto M^{\alpha(T-T_g)}$, shows that aromatic solutes have a parallel behavior to linear aliphatic solutes but shifted by *ca.* +91 K. The proposed scaling is notably able to reconcile α values experimentally assessed in melts³ and in solids. It could be thought that the temperature shift would include the behavior all organic solutes larger than voids, with left and right bounds set by linear aliphatic and aromatic solutes respectively. However, α values derived for diphenyl alkanes showed that aromatic solutes including a flexible segment between two phenyl rings were associated to a much larger temperature shift. Such dramatic effect of the solute chemical structure was found independent of the considered aliphatic polymer and associated only to the size and type of the solute jumping unit. It would explain both the logarithm dependence of the apparent activation energy with molecular mass and the additional deviation to the Arrhenius behavior close to T_g , as specifically discussed in⁴. Because the specific volume of polymers is also a function of $T-T_g$, a modification of the distribution of free volume in the polymer must be also invoked, as already suggested for the self-diffusion of non-entangled *n*-alkanes⁶³. Near T_g , the proposed scaling exhibits a close proximity with the last version of the free-volume theory of Vrentas and Duda³¹ by noting that the variation of ζ is proportional to the logarithm of M for an homologous series of linear solutes. As a result, the concept of temperature shift in WLF equation (*i.e.* $T-T_g$ shift) can be generalized also with solute geometry considerations: a large solute can have the same D value as a smaller one but at a much higher temperature. Changing the jumping unit would add an additional temperature shift as observed for α values between aromatic and aliphatic solutes.

Conventional free-volume theories assume that solute effects are purely enthalpic (*i.e.* they tend to vanish at high temperature). For flexible solutes including bulky jumping units, it is proposed that the free volume fluctuations of polymer host segments control the short-range

translation of each individual jumping unit but with a broad distribution of related time scales. Consequently, the displacements of many jumping units appear to be controlled by the possibility to get concerted displacements between jumping units. Polymer and solute related effects have been separated by rescaling the diffusion coefficients with the diffusion coefficient of a reference solute at a reference temperature. The variation of this reference D value in different polymers was associated to static polymer effects and expressed as a single exponential term, $\exp(-K_a/(T-Tg+K_b))$. It was verified thus that the values of 600 K and 58 K, proposed for K_a and K_b respectively, enabled the extrapolation of known diffusion coefficients from one aliphatic polymer to another one (*e.g.* unplasticized to plasticized, apolar to polar). The extrapolation of D to a different number of jumping units or to a different temperature than the reference one required to account for a specific free energy, so-called solute free energy barrier. Solute effects were found to follow an Arrhenius' law for oligophenyls including from two to four phenyl rings. Related activation energies and entropies were, however, highlighted to vary non-monotonously with M .

This outstanding effect of the parity of the number of ring was used to assess, via constrained molecular dynamics simulations, the probability of phenyl rings (jumping units) to behave as anchors in the translation mechanisms of aromatic solutes. It is argued that, though the polymer at rubbery state does not control the reorientation frequency of the entire molecule (*i.e.* each phenyl ring is displacing independently while being limited by the connectivity of rings), it tends to hinder the reorientation of individual phenyl rings. Our simulations show that constraining randomly one or several phenyl rings slows down the mean-square-displacement of the center-of-mass (CM) of solutes in a different way according to the number of rings, N_{Ph} , being odd or even. For example, when $N_{Ph}=3$, it is twice more likely to block a ring at one end than in the middle; so that the slowdown is stronger than for $N_{Ph}=2$ or 4. As our interpretation matched remarkably the relative energies experimentally determined on oligophenyls series, it is thought that the proposed anchor effect of phenyl rings is universal in aliphatic polymers at least between $Tg+51$ K and $Tg+150$ K, where α was estimated to be much larger than unity (as shown in Figure 5-4). In addition, enthalpy-entropy compensation is shown to occur so that the solute-related free energy barrier is a monotonous function of the number of jumping units, whereas related entropy and related activation energy are not.

Presented results should find applications in many domains where diffusion coefficients of aromatic molecules and polymer residues are particularly critical: contamination by substances leached from polymer materials, loss of additives during physical ageing of polymers, reactivities in polymers in processing and use conditions. In particular, reported

results open the way to design of substances with low diffusion coefficients with an odd number of rings and/or with flexible segments close to CM. The behavior of branched aromatic molecules will be presented in a companion paper.

5.1.3.7 Author information

Corresponding Author

*E-mail olivier.vitrac@agroparistech.fr

Tel. +33 (0)169935063

Notes

The authors declare no competing financial interest.

5.1.3.8 Acknowledgements

The first authors would like to acknowledge the support of the PhD grant from Région Île-de-France. We also gratefully thank Dr. Frédéric Jamme for his technical assistance. This work was supported by the DISCO beamline of the synchrotron Soleil (Proposal 20100909).

5.1.3.9 References

- (1) Vitrac, O.; Lézervant, J.; Feigenbaum, A. *Journal of Applied Polymer Science* **2006**, *101*, (4), 2167-2186.
- (2) Berens, A. R. *Pure Appl. Chem.* **1981**, *53*, (2), 365-375.
- (3) von Meerwall, E. D.; Lin, H.; Mattice, W. L. *Macromolecules* **2007**, *40*, (6), 2002-2007.
- (4) Durand, M.; Meyer, H.; Benzerara, O.; Baschnagel, J.; Vitrac, O. *The Journal of Chemical Physics* **2010**, *132*, (19), 194902.
- (5) Kwan, K. S.; Subramaniam, C. N. P.; Ward, T. C. *Polymer* **2003**, *44*, (10), 3061-3069.
- (6) Gennes, P. G. d. *The Journal of Chemical Physics* **1971**, *55*, (2), 572-579.
- (7) Bueche, F. *The Journal of Chemical Physics* **1968**, *48*, (3), 1410-1411.
- (8) Lodge, T. P. *Physical Review Letters* **1999**, *83*, (16), 3218-3221.
- (9) Quijada-Garrido, I.; Barrales-Rienda, J. M.; Frutos, G. *Macromolecules* **1996**, *29*, (22), 7164-7176.
- (10) Phillips, P. J. *Chemical Reviews* **1990**, *90*, (2), 425-436.

- (11) Wirtz, A. C.; Hofmann, C.; Groenen, E. J. J. *ChemPhysChem* **2011**, *12*, (8), 1519-1528.
- (12) Fechete, R.; Demco, D. E.; Blümich, B. *Macromolecules* **2003**, *36*, (19), 7155-7157.
- (13) Rouse, J. P. E. *The Journal of Chemical Physics* **1953**, *21*, (7), 1272-1280.
- (14) Vitrac, O.; Mougharbel, A.; Feigenbaum, A. *Journal of Food Engineering* **2007**, *79*, (3), 1048-1064.
- (15) Koszinowski, J. *Journal of Applied Polymer Science* **1986**, *31*, (8), 2711-2720.
- (16) Möller, K.; Gevert, T. *Journal of Applied Polymer Science* **1994**, *51*, (5), 895-903.
- (17) Doong, S. J.; Ho, W. S. W. *Industrial & Engineering Chemistry Research* **1992**, *31*, (4), 1050-1060.
- (18) Herman, M. F.; Tong, P. *Macromolecules* **1993**, *26*, (15), 3733-3737.
- (19) Herman, M. F. *The Journal of Chemical Physics* **1995**, *103*, (10), 4324-4332.
- (20) Herman, M. F.; Panajotova, B.; Lorenz, K. T. *The Journal of Chemical Physics* **1996**, *105*, (3), 1153-1161.
- (21) Herman, M. F.; Panajotova, B.; Lorenz, K. T. *The Journal of Chemical Physics* **1996**, *105*, (3), 1162-1174.
- (22) Gniewek, P.; Kolinski, A. *The Journal of Chemical Physics* **2011**, *134*, (5), 056101.
- (23) Skolnick, J.; Yaris, R.; Kolinski, A. *The Journal of Chemical Physics* **1988**, *88*, (2), 1407-1417.
- (24) Williams, M. L.; Landel, R. F.; Ferry, J. D. *Journal of the American Chemical Society* **1955**, *77*, (14), 3701-3707.
- (25) Ehlich, D.; Sillescu, H. *Macromolecules* **1990**, *23*, (6), 1600-1610.
- (26) Deppe, D. D.; Miller, R. D.; Torkelson, J. M. *Journal of Polymer Science Part B: Polymer Physics* **1996**, *34*, (17), 2987-2997.
- (27) Doolittle, A. K. *Journal of Applied Physics* **1951**, *22*, (8), 1031-1035.
- (28) Cohen, M. H.; Turnbull, D. *The Journal of Chemical Physics* **1959**, *31*, (5), 1164-1169.
- (29) Vrentas, J. S.; Duda, J. L. *Journal of Polymer Science: Polymer Physics Edition* **1977**, *15*, (3), 403-416.
- (30) Vrentas, J. S.; Vrentas, C. M. *Macromolecules* **1994**, *27*, (17), 4684-4690.
- (31) Vrentas, J. S.; Vrentas, C. M. *European Polymer Journal* **1998**, *34*, (5-6), 797-803.
- (32) Vrentas, J. S.; Duda, J. L.; Ling, H. C. *Journal of Polymer Science: Polymer Physics Edition* **1985**, *23*, (2), 275-288.
- (33) Vrentas, J. S.; Vrentas, C. M.; Faridi, N. *Macromolecules* **1996**, *29*, (9), 3272-3276.

- (34) Arnould, D.; Laurence, R. L. *Industrial & Engineering Chemistry Research* **1992**, *31*, (1), 218-228.
- (35) Vrentas, J. S.; Vrentas, C. M. *Journal of Polymer Science Part B: Polymer Physics* **1993**, *31*, (1), 69-76.
- (36) Chen, S. P.; Ferry, J. D. *Macromolecules* **1968**, *1*, (4), 374-374.
- (37) Von Meerwall, E.; Ferguson, R. D. *Journal of Applied Polymer Science* **1979**, *23*, (12), 3657-3669.
- (38) Rhee, C.-K.; Ferry, J. D.; Fetters, L. J. *Journal of Applied Polymer Science* **1977**, *21*, (3), 783-790.
- (39) Vrentas, J. S.; Duda, J. L.; Ling, H. C.; Hou, A. C. *Journal of Polymer Science: Polymer Physics Edition* **1985**, *23*, (2), 289-304.
- (40) Mauritz, K. A.; Storey, R. F.; George, S. E. *Macromolecules* **1990**, *23*, (2), 441-450.
- (41) Mauritz, K. A.; Storey, R. F. *Macromolecules* **1990**, *23*, (7), 2033-2038.
- (42) Coughlin, C. S.; Mauritz, K. A.; Storey, R. F. *Macromolecules* **1990**, *23*, (12), 3187-3192.
- (43) Coughlin, C. S.; Mauritz, K. A.; Storey, R. F. *Macromolecules* **1991**, *24*, (7), 1526-1534.
- (44) Coughlin, C. S.; Mauritz, K. A.; Storey, R. F. *Macromolecules* **1991**, *24*, (8), 2113-2116.
- (45) Hayashi, H.; Matsuzawa, S. *Journal of Applied Polymer Science* **1992**, *46*, (3), 499-505.
- (46) Budzien, J.; McCoy, J. D.; Rottach, D.; Curro, J. G. *Polymer* **2004**, *45*, (11), 3923-3932.
- (47) Solunov, C. A. *Journal of Physics: Condensed Matter* **2002**, *14*, (31), 7297.
- (48) Kovarskiĭ, A. L., *Molecular Dynamics of Additives in Polymers*. VSP: 1997.
- (49) Andricioaei, I.; Karplus, M. *The Journal of Chemical Physics* **2001**, *115*, (14), 6289-6292.
- (50) Schafer, H.; Mark, A. E.; Gunsteren, W. F. v. *The Journal of Chemical Physics* **2000**, *113*, (18), 7809-7817.
- (51) Marras, S. I.; Kladi, K. P.; Tsivintzelis, I.; Zuburtikudis, I.; Panayiotou, C. *Acta Biomaterialia* **2008**, *4*, (3), 756-765.
- (52) Otsuka, E.; Suzuki, A. *Journal of Applied Polymer Science* **2009**, *114*, (1), 10-16.
- (53) Fischer, E. W.; Sterzel, H. J.; Wegner, G. *Colloid & Polymer Science* **1973**, *251*, (11), 980-990.
- (54) Wunderlich, B., *Macromolecular physics*. Academic Press: 1980.

- (55) Crescenzi, V.; Manzini, G.; Calzolari, G.; Borri, C. *European Polymer Journal* **1972**, *8*, (3), 449-463.
- (56) Peppas, N. A.; Merrill, E. W. *Journal of Applied Polymer Science* **1976**, *20*, (6), 1457-1465.
- (57) Roe, R.-J.; Bair, H. E.; Gieniewski, C. *Journal of Applied Polymer Science* **1974**, *18*, (3), 843-856.
- (58) Vitrac, O. FMECA engine: software developed in the framework of the project SafeFoodPack Design <https://github.com/ovitrac/FMECAengine> (July 17, 2012),
- (59) Sun, H. *The Journal of Physical Chemistry B* **1998**, *102*, (38), 7338-7364.
- (60) Ngai, K. L.; Plazek, D. J., Temperature Dependence of the Viscoelastic Response of Polymer Systems. In *Physical Properties of Polymer Handbook*, 2 ed.; Mark, J. E., Ed. Springer New York: 2007; p 455.
- (61) Strobl, G. R., *The Physics of Polymers: Concepts for Understanding Their Structures and Behavior*. Springer-Verlag: 1997.
- (62) Wong, C.-P.; Schrag, J. L.; Ferry, J. D. *Journal of Polymer Science Part A-2: Polymer Physics* **1970**, *8*, (6), 991-998.
- (63) von Meerwall, E.; Beckman, S.; Jang, J.; Mattice, W. L. *The Journal of Chemical Physics* **1998**, *108*, (10), 4299-4304.
- (64) Harmandaris, V. A.; Doxastakis, M.; Mavrantzas, V. G.; Theodorou, D. N. *The Journal of Chemical Physics* **2002**, *116*, (1), 436-446.
- (65) Miller, A. A. *Journal of Polymer Science Part A-2: Polymer Physics* **1968**, *6*, (1), 249-257.
- (66) Fox, T. G.; Loshaek, S. *Journal of Polymer Science* **1955**, *15*, (80), 371-390.
- (67) Waheed, N.; Ko, M.; Rutledge, G., Atomistic Simulation of Polymer Melt Crystallization by Molecular Dynamics. In *Progress in Understanding of Polymer Crystallization*, Reiter, G.; Strobl, G., Eds. Springer: Berlin, Heidelberg, 2007; Vol. 714, pp 457-480.
- (68) Park, H. S.; Chang, T.; Lee, S. H. *The Journal of Chemical Physics* **2000**, *113*, (13), 5502-5510.
- (69) Hatzigrigoriou, N. B.; Vouyiouka, S. N.; Joly, C.; Dole, P.; Papaspyrides, C. D. *Journal of Applied Polymer Science* **2012**, *125*, (4), 2814-2823.
- (70) Angell, C. A. *Polymer* **1997**, *38*, (26), 6261-6266.
- (71) Starikov, E. B.; Nordén, B. *The Journal of Physical Chemistry B* **2007**, *111*, (51), 14431-14435.

5.1.4 Possible application for the study of polymer nanocomposites

Without being exhaustive, the presented study offers a broad view of the behaviors of linear or low-branched organic solutes (*e.g.* aliphatic, aromatic or a combination) in arbitrary polymers above T_g . Within the general goal of developing new concepts for polymer nanocomposite systems, the proposed FVT provides a new tool to detect and analyze deviation to bulk polymer behaviors as shown in Table 5-1. In particular, the possible increase in dwelling times (attraction around particles) should be quantifiable as an additional activation term:

$$-R \frac{\partial \ln D}{\partial 1/T} = Ea_{FV} + Ea_{solute} + \left(H_{i+polymer}^{ex} - H_{i+adsorbent}^{ex} \right) \quad (5-38)$$

where Ea_{FV} and Ea_{solute} are activation terms related to polymer (*i.e.* free-volume) and solute (*i.e.* due to long-lived polymer-solute contacts). The last term represents, $H_{i+polymer}^{ex} - H_{i+adsorbent}^{ex}$, the difference in excess mixing enthalpies between adsorbed and absorbed states and it is an estimate of the activation of $K_{contrast}$ by temperature (see section 5.3).

5.2 Characterization and thermodynamic properties of nano-clays

5.2.1 Introduction

Free-volume theories (FVT) of rubber polymers show that increasing D values can be easily realized by lowering T_g , for example by adding plasticizers. However, no clear strategy is proposed for the reverse process. Increasing E^* could be envisioned but its degree of freedom for diffusing guest and not for the polymer host. We adopt here a different point of view. There is a well-known application, where the effective transport property is essentially controlled by thermodynamic considerations. In the thesis, inverse gas chromatography (IGC) using filled columns with adsorbents allowed to estimate interaction energies at infinite dilution between solutes and nano-adsorbents. IGC offers also an intuitive approach of chaotic materials with low effective diffusion coefficients or more consistently with increased lag time. The analogy between lag time (*i.e.* waiting time) and transport properties has been presented in Figure 2-4. In the special case of chromatography, the lag time is called elution time or retention time. FVT cannot explain the observed behaviors, the column is usually filled with a partly porous/mesoporous media (in our case montmorillonites), the free volume is therefore large but retention times are dramatically activated by temperature. According to FVT, temperature is sensitive, on the contrary, significantly only close to T_g and almost zero far from T_g , which is in disagreement with IGC type results.

The phenomena occurring during a typical IGC experiment are sketched in Figure 5-13. As in nanocomposite material, the feature of interest is that the excess of lag time comparatively to a reference solute which has no interacting with station phase giving the reference lag time when the underlying transport is controlled only by advection (*i.e.* mass flow rate). The Gaussian shape possibly is convolved with a decaying exponential of the measured response, which is a consequence of a lateral dispersion of the transport or/and a consequence of fluctuations in the strength of interactions. It is quite obvious that replacing the gas carrier by a continuous cohesive phase (*e.g.* polymer) should not change the ratios of elution times (*i.e.* comparatively to the non-interacting reference) while $H_{i+polymer}^{ex} - H_{i+adsorbent}^{ex}$ remains close to the result with a perfect gas $RT - H_{i+adsorbent}^{ex}$.

$$K_{g/MMT}(T) = \frac{C_g}{C_s} = \frac{K_H}{RT} = \exp\left(\frac{\Delta G}{RT}\right) = \frac{t_R^{ref}(T)}{t_R(T) - t_R^{ref}(T)} = \frac{1}{t_R^*(T)}$$

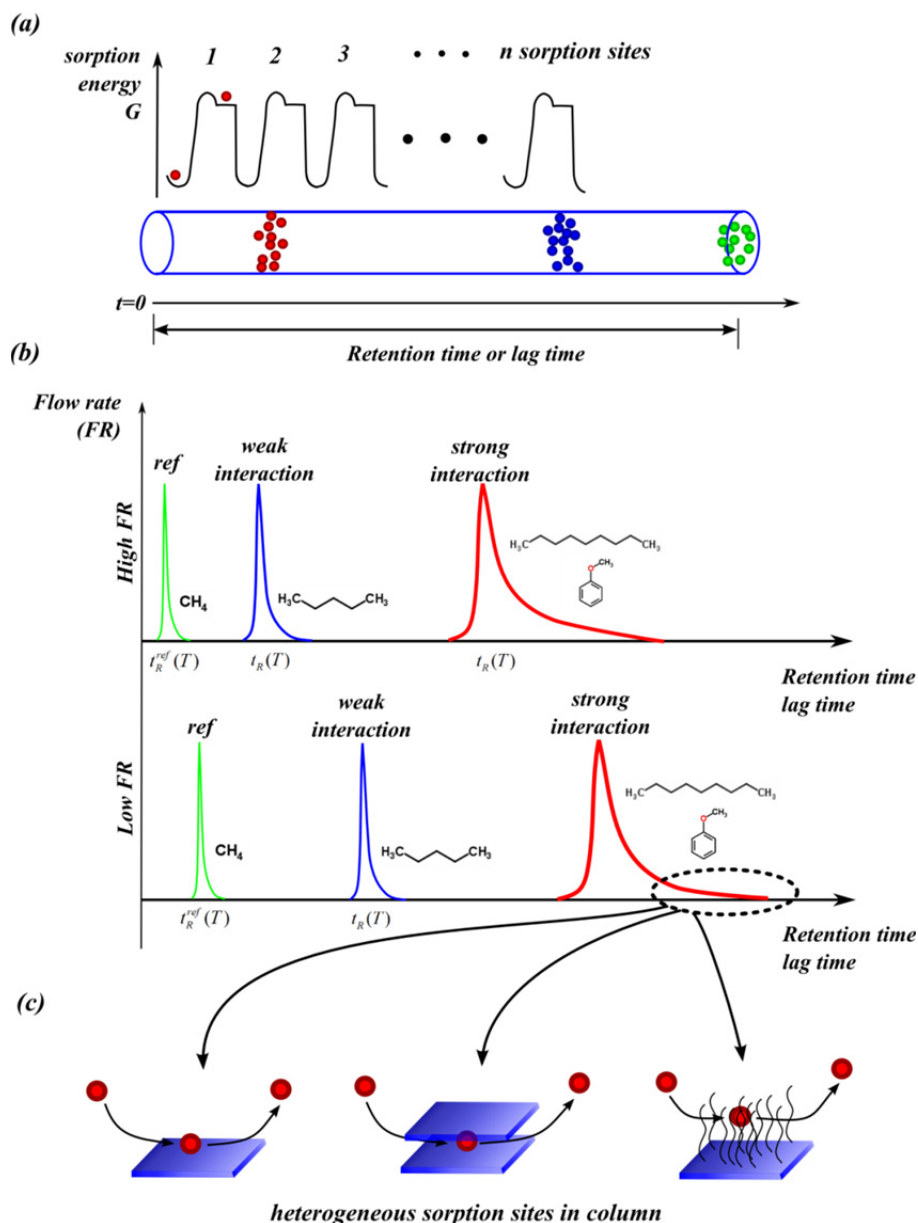


Figure 5-13 Interpretation of inverse gas chromatography (IGC) as 1D random walk along a surface energy. The unique assumption is that the number/amount of sorption sites (*i.e.* the probability of accessibility) is the same for all substances (including for the reference low interacting one) so that the ratio of elution times is a measure of the energy difference $H_{i+adsorbent}^{ex} - RT$. a) Equivalent energy surface. b) Retention times at high and low flow rate (FR). c) Possible interpretation of the right tailing of retention distributions due to a mixed interactions with external/internal accessible surfaces, surfactants or in gas phase.

It would have been desirable to assess sorption properties with the same homologous solutes as those reported in Figure 5-1a). According to Clausius-Clapeyron relationship, vapor pressures/retention times decrease/increase exponentially with isosteric heat of sorption and

therefore with probe size, aromaticity and hydrogen bonding. Since results were highly reproducible and interpretable for sufficiently long IGC columns with low flow rates of nitrogen, only short diffusants were accessible to measurements in the temperature range compatible with material usage (*i.e.* from 40°C to 140°C). They included: linear alkanes shorter than C9 and aromatic molecules including one single ring: toluene and anisole. For longer retention times, IGC experiments were completed with gravimetric sorption experiments but provided results at higher concentrations.

It is worth to notice that our intent differs significantly from published thermodynamic studies aiming mainly at optimizing the dispersion properties of montmorillonites (MMT) in polymers. Previous studies focused therefore on the surface energies of MMT in processing conditions using organic solutes to mimic polymer segments in order to improve compatibility and dispersion of both (Picard et al., 2007). In this study, the intent is to estimate excess “condensation energies” of organic solutes onto pristine and commercial organo-modified MMT, envisioned as model adsorbents. A practical consequence is that potentials were expressed with respect to the amorphous condensed state of the considered solute (*i.e.* liquid or molten state). Sorption will be therefore exothermic, if the heat of sorption is greater than the vaporization heat. Regarding to the assumption that nanocomposite materials are barrier to apolar or low polar substances, good adsorption properties were expected mainly close to room temperature and when van-der-Waals interactions were exacerbated by hybrid inorganic-organic interactions (pristine MMT) or π - π interactions (*i.e.* with aromatic surfactants). In ideal case $H_{i+adsorbent}^{ex}$ should be significantly negative (*i.e.* exothermic mixture respectively to liquid state) due to enough attractive forces. The special contribution of hydrogen-bonding was studied on a single solute, anisole, on the different tested montmorillonites including one modified with a polar surfactant. Molecular modeling and experiments proposed extrapolation of tested conditions to arbitrary substances, basal spacing and to assess whether chemical modifications induced (*i.e.* more polar, aromatic groups) on commercial MMT could be also available for sorption of organic solutes. Indeed, they are mainly used for a different purpose: to reinforce the surfactant intercalation.

5.2.2 Simulation and experimental study

Publication III

Title: Sorption properties of solutes onto pristine and organo-modified montmorillonites
Authors: X. Fang, V. Ducruet, and O. Vitrac
Submitted to: Langmuir

Sorption properties of solutes onto pristine and organo-modified montmorillonites

Xiaoyi Fang^{1,2}, Violette Ducruet^{2,1}, Olivier Vitrac^{2,1*}

¹*AgroParisTech, UMR 1145 Ingénierie Procédés Aliments, F-91300 Massy, France*

²*INRA, UMR 1145 Ingénierie Procédés Aliments, F-91300 Massy, France*

5.2.2.1 Abstract

Sorption of organic solutes onto montmorillonites (MMT) is usually described as a surface phenomenon. This work studied by molecular simulation and experimental approach the sorption of typical aliphatic and aromatic solutes on different commercially available MMT: pristine and organo-modified by apolar, polar and aromatic quaternary alkylammonium surfactants. Respectively to the liquid reference state of tested solutes, only pristine MMT presented significantly exothermic sorption and consequently strong capacities to absorb organic at low temperature. The sorption process is described in three stages with concentration: preferable adsorption onto the clay surface, slightly intercalation and clay swelling. For organo-modified MMT, only the two last stages have been experimentally identified with a preferred sorption in the excess of surfactants. The residual specificity of organo-modified MMTs is controlled by the lateral groups of surfactants: van-der-Waals interactions, π - π interactions, hydrogen bonding. For applications in polymer nanocomposites, current practices seeking surfactant intercalation and clay exfoliation by polymer segments are not favorable to increase their barrier properties (*e.g.* packaging/reservoir applications), their selectivity (*e.g.* membrane used in separation application) or their controlled-release capacity. This study reports the effects of main parameters such as basal spacing, temperature, solute probe and surfactant type to optimize the sorption properties of MMT to organic solutes (*e.g.* active substances, pollutants/contaminants,...).

5.2.2.2 Introduction

Montmorillonites (MMT) are aluminosilicate materials organized as clays. Adsorption of organic solutes onto MMT finds different applications in pesticide adsorption, wastewater purification, therapeutic and cosmetic applications (Khan, 1975; Park et al., 2013; Rodríguez, 2003; Wypych and Satyanarayana, 2004), where the adsorption properties of MMT are mainly studied in aqueous solutions. The properties are particularly noticeable as they present favorable interactions with both water (*i.e.* hydrophilic behavior) and apolar organic

compounds (*i.e.* organophilic behavior). In particular, their wettability can be inverted according to the sought final goal. One typical example is the extraction and recovery of oil by injecting water at high-pressure (Eltantawy and Arnold, 1972). For polymer applications, it is common to do the reverse process by replacing adsorbed water in pristine MMT, a naturally hydrated aluminosilicate layered clay, by organic cationic surfactants. This outstanding feature arises from defects in the edge-shared octahedral sheet of aluminum hydroxide sandwiched between two silica tetrahedral layers (Olphen, 1964): few $[\text{SiO}_4]$ sites are replaced by $[\text{AlO}_4]^-$ in the tetrahedral layer, $[\text{AlO}_6]$ replaced by $[\text{MgO}_6]^-$ in the octahedral layer, which creates a local accumulation of negative charges naturally compensated by exchangeable cations such as Na^+ , K^+ and Ca^{2+} (Heinz and Suter, 2004b). Once the cations are replaced by ion-exchange reactions with large cationic surfactants, including primary, secondary, tertiary and quaternary alkylammonium or alkylphosphonium cations with or without functional groups, organo-modified MMT become dispersible in hydrophobic polymer melts (Dennis et al., 2001). When they are oriented in parallel to lamination or drawing direction, exfoliated structures find applications in nanocomposite systems to improve the diffusion barrier to gases of thermoplastics (Chang et al., 2003; Khan et al., 2013; Koh et al., 2008; Osman et al., 2003; Osman et al., 2007; Sinha Ray et al., 2003). In this application, the barrier performance is the sole consequence of the favorable shape factor of the structure: 1nm thick with lateral dimensions from 30nm to several microns (Tan et al., 2008). The possible interactions with organic solutes of these materials have been far less studied. They are particular incentives for two main technological applications: i) describing the interactions of nanocomposite packaging materials with their organic packaged content and ii) developing selective barrier materials to organic compounds, whose selectivity can be modulated by changing temperature. The first concern is associated to the risk assessment of these materials (Luetzow, 2012) for food contact or cosmetic applications in EU (EC, 2011; EFSA, 2011) and in US (FDA, 2012a, b) . The second concern is motivated by the substitution of the “passive” barrier paradigm by the “active barrier” one where MMT are considered as nano-adsorbent instead of passive obstacles. Such concepts have been explored in purification applications by proposing MMT as a substitute of activated carbon (Park et al., 2011). For material applications, the use of organo-clays instead of neat MMT solves the issue of their miscibility with the polymer but it is expected to lower the sorption potential of MMT. Indeed, the excess of surfactant is expected to reduce the surface area accessible to small solutes and to increase the basal spacing of MMT and therefore the possibilities of strong retention (Koh and Dixon, 2001).

The present paper aims at developing an atomistic interpretation of the sorption of short organic solutes (aliphatic or aromatic) in commercially available MMT organo-modified or not. In particular, the effects of adsorption and trapping are separated and analyzed according to temperature, basal spacing and surfactant loading. Two behaviors are reported and compared with experiments: sorption properties at infinite dilution and concentrated state.

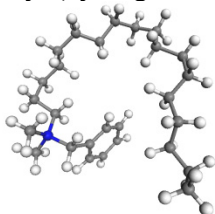
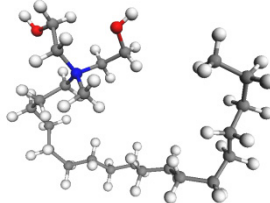
5.2.2.3 Material and method

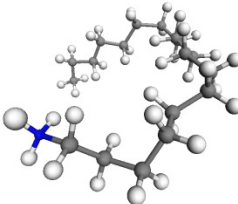
5.2.2.3.1 Materials

5.2.2.3.1.1 Nanoclay

In this study, four commercially available clays including pristine MMT and organo-modified ones containing different cationic surfactants are tested as listed in Table 5-4. The elemental content of each clay was determined by combustion for organic compounds and inductively coupled plasma atomic emission spectroscopy (ICP-AES) for inorganic compounds.

Table 5-4 The detailed information of four tested clays

Abbreviation	Chemical composition	Supplier /Product reference
MMT	Montmorillonite	Aldrich (France) /682659
Chemical formula:	$[\text{Na}_{0.38}\text{K}_{0.01}][\text{Si}_{3.92}\text{Al}_{0.07}\text{O}_8][\text{Al}_{1.45}\text{Mg}_{0.55}\text{O}_2(\text{OH})_2] \cdot 7\text{H}_2\text{O}$	
Surfactant:	N/A	
C6H5MMT	Organo-modified montmorillonite	
Chemical formula:	$[\text{Na}_{0.11}\text{K}_{0.02}][\text{Si}_{3.92}\text{Al}_{0.08}\text{O}_8][\text{Al}_{1.35}\text{Mg}_{0.22}\text{O}_2(\text{OH})_2] \cdot \text{C}_{13.47}\text{H}_{12.77}\text{N}_{0.47}$	
Surfactant:	Dimethyl, benzyl (hydrogenated tallow) alkyl ammonium*  Mw: 376.8	Rockwood (Germany) /Nanofil [®] 9
C18OHMMT	Organo-modified montmorillonite	
Chemical formula:	$[\text{Na}_{0.01}\text{K}_{0.004}][\text{Si}_{3.92}\text{Al}_{0.09}\text{O}_8][\text{Al}_{1.52}\text{Mg}_{0.23}\text{O}_2(\text{OH})_2] \cdot \text{C}_{6.99}\text{H}_{12.70}(\text{OH})_{2.89}\text{N}_{0.31}$	
Surfactant:	Methyl dihydroxyethyl hydrogenated tallow ammonium*  Mw: 360.5	Aldrich (France) /682640

C18MMT	Organo-modified montmorillonite	
Chemical formula:	$[\text{Na}_{0.01}\text{K}_{0.02}][\text{Si}_{3.92}\text{Al}_{0.09}\text{O}_8][\text{Al}_{1.58}\text{Mg}_{0.32}\text{O}_2(\text{OH})_2] \cdot \text{C}_{9.65}\text{H}_{20.01}\text{N}_{0.53}$	
Surfactant:	<p>Octadecylamine</p>  <p>Mw: 270.5</p>	<p>Aldrich (France) /682616</p>

*Tallow is a blend of unsaturated *n*-alkyl groups with an approximate composition: 65wt% of C18, 30wt% of C16, 5wt% of C14 as stated by supplier.

5.2.2.3.1.2 Probe solutes

Similar solute probes were chosen for experiments and molecular calculations. They include a homologous series of volatile *n*-alkanes from C5 to C9 and two aromatic compounds: toluene and anisole (*i.e.* methoxybenzene). All substances were supplied by Sigma-Aldrich (Germany) with HPLC grade.

5.2.2.3.2 Material characterization

5.2.2.3.2.1 X-ray diffraction analysis (XRD)

The structure of nanoclays was investigated by X-ray diffraction (XRD) analysis using a X'Pert diffractometer (PANalytical, Netherlands) with Ni-filtered Cu K α radiation ($\lambda=0.154$ nm) and operated at 40 kV/40 mA. The diffraction intensity was scanned with scattering angle 2θ varying at $0.01^\circ \cdot \text{min}^{-1}$ in the range of $1-11^\circ$. The basal spacing d (so called d -spacing in the rest of paper) of the nanoclay crystal lattice is calculated from Bragg's law:

$$2d \sin \theta = n\lambda \quad (5-39)$$

where n is an integer determined by the order given.

5.2.2.3.2.2 Thermogravimetric analysis (TGA)

The compositions of nanoclay samples were determined by thermogravimetric analyzer (TGA) (model Q500, TA Instruments, USA) with ramp at $10 \text{ K} \cdot \text{min}^{-1}$ from 30 to 900°C under nitrogen at a flow rate of $50 \text{ ml} \cdot \text{min}^{-1}$.

5.2.2.3.2.3 Specific surface area

The specific surface area of nanoclay was determined by nitrogen adsorption (*i.e.* BET approach at 77K (Brunauer et al., 1938)) using surface area measurement analyzer (model

ASAP 2000, Micromeritics, France). The specific surface area was determined by fitting with BET equation in the range of activities from 0.05 to 0.35 while assuming cross section area of one nitrogen molecule is equal to 16.2 \AA^2 (Aylmore et al., 1970).

5.2.2.3.3 Sorption properties at infinite dilution

Inverse gas chromatography measurements were carried out at infinite dilution by using a Carlo Erba 6000 Vega II gas chromatograph equipped with a flame ionization detection (FID) system. The clay samples were packed into glass columns (120 mm×4 mm ID), which were deactivated with dimethyldichlorosilane before use (Boutboul et al., 2002). The mass of the stationary phase was ranged from 0.6 g to 2.0 g according to the density of the clay (see Table 5-5). For each MMT, three columns were prepared independently and all measurements were triplicated on each column. Elution of each solute was operated in isothermal conditions at temperature ranging from 40°C to 140°C with 20°C intervals with dry nitrogen as gas carrier. The injector and detector temperatures were maintained at 220 and 250°C, respectively. A flow rate of dry nitrogen as gas carrier at 5 ml·min was applied for tested organo-modified MMT but a higher flow rate of 20mL/min was used for pristine MMT to compensate much longer retention times. The possible effect of flow rate was tested between 5 mL·min⁻¹ and 20 mL·min⁻¹. To meet adsorption at infinite dilution, all probe solutes were injected in splitless mode with a Hamilton syringe (Supelco, Bellefonte, PA, USA). The injection volume was of 0.05 µl. Data were detected and collected by the Borwin 1.2 data acquisition software (version 1.2, Thermo Fisher Scientific Inc, USA). All injections were triplicated. For a same column, retention time variations were lower than 1% between repetitions.

Table 5-5 Information of column dimension and sample filling condition for IGC experiments

MMT type	Length (mm)	Internal diameter (mm)	Net weight (g)	Density in column (g·cm ⁻³)
MMT	118	4	1.94	1.31
C6H5MMT	118	4	0.65	0.44
C18OHMMT	118	4	0.97	0.65
C18MMT	117	4	0.90	0.62

Raw elution profiles were fitted by exponentially modified Gaussian (EMG) distributions which describe the elution process as a convolution of a Gaussian, $G(t)$ and exponential random processes, $E(t)$ (Dyson, 1998). By noting μ and σ the average and standard-deviation of $G(t)$ and τ the exponential decay of $E(t)$, one gets:

$$\begin{aligned}
F(t) &= G(t) \otimes E(t) \\
&= h \exp\left(\frac{-(\mu-t)^2}{2\sigma^2}\right) \left(\frac{\sigma}{\tau} \sqrt{\frac{\pi}{2}} \operatorname{erfc}\left(\frac{1}{\sqrt{2}}\left(\frac{\mu-t}{\sigma} - \frac{\sigma}{\tau}\right)\right)\right)
\end{aligned} \tag{5-40}$$

where $\operatorname{erfc}()$ is the complementary error function. Parameters μ , σ and τ were fitted using the optimized method described by Kalambet et al. (2011).

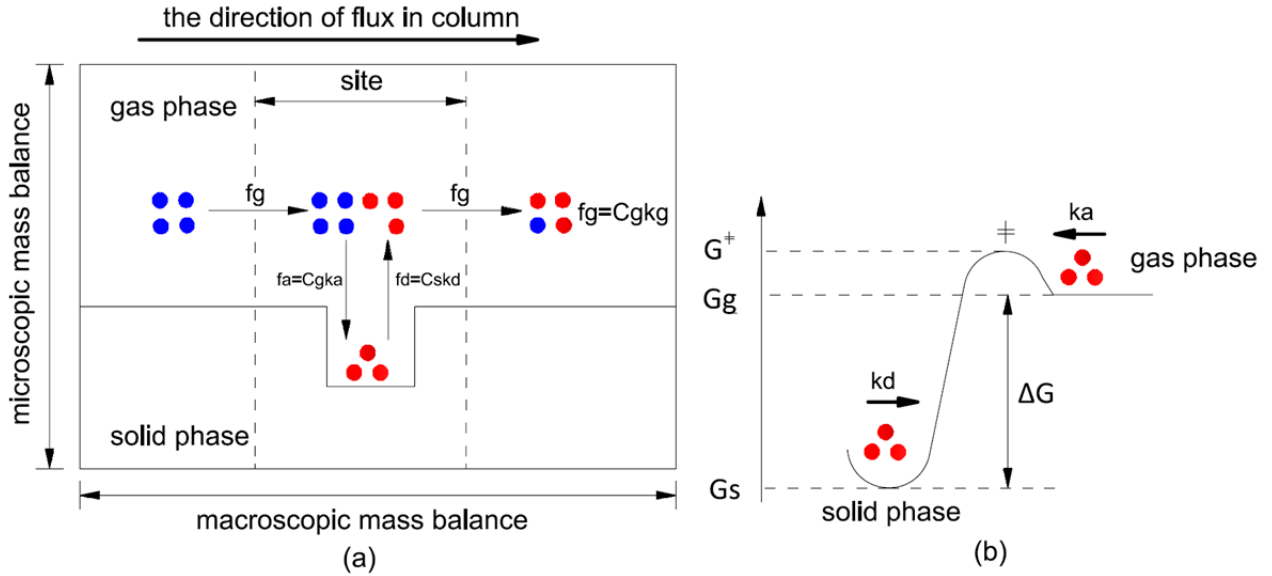


Figure 5-14 a) Detailed description of mass transfer at one adsorption site within the IGC column. The longitudinal direction represents a macroscopic transport along the column, while the transverse direction details the mass balance at molecular scale. b) Corresponding free energy distribution associated to the sorption/desorption jumping processes. According to the transition state theory, \ddagger is the transition state whose probability does not depend on the origin of the solute (in gas phase or in adsorbed phase).

The thermodynamic interpretation as partition coefficient between the gas carrier and MMT, $K_{g/MMT}(T)$, requires a microscopic model of the sorption process. The successive sorption/desorption of solutes was assumed to be a Poisson process, where each individual sorption event is described as a jumping process governed by frequencies k_g , k_a and k_d and corresponding mass fluxes, f_g , f_a and f_d in gas, adsorbed and desorbed phases as detailed in Figure 5-14. By noticing that the micro-reversibility (*i.e.* condition of local thermodynamic equilibrium) enforces $f_a=f_d$, the effective retention time t_R^{site} is averaged inferred by averaging dwelling times over adsorbed and non-adsorbed populations:

$$t_R^{site} = \frac{1}{k_g} \frac{c_g k_g}{c_g (k_g + k_a)} + \left(\frac{1}{k_d} + \frac{1}{k_g}\right) \frac{c_g k_a}{c_g (k_g + k_a)} = \frac{1}{k_g + k_a} \left(1 + \frac{k_a}{k_d} + \frac{k_a}{k_g}\right) \tag{5-41}$$

Finally, by noticing that inequalities $k_g \gg k_a$ and $k_g \gg k_d$ hold between a solid and gas carrier, the total retention time for a column including N sorption sites becomes:

$$t_R = \sum_{i=1}^N t_R^{site} = \frac{N}{k_g} \left(1 + \frac{k_a}{k_d} \right) = t_R^{ref} \left(1 + \frac{k_a}{k_d} \right) = t_R^{ref} \left(1 + \frac{\exp\left(-\frac{G_g - G^\ddagger}{RT}\right)}{\exp\left(-\frac{G_s - G^\ddagger}{RT}\right)} \right) = t_R^{ref} \left(1 + \exp\left(-\frac{\overbrace{G_g - G_s}^{\Delta G}}{RT}\right) \right) \quad (5-42)$$

where T is temperature in K, R is the gas constant; t_R^{ref} is the retention time for a solute non-interacting with the surface but possibly subjected to tortuosity effects in the column. In this study, methane was chosen as reference solute.

From the different definitions of $K_{g/MMT}(T)$, Eq. (5-42) yields to practical definitions of the Henry coefficient, $K_H = p/C_s$, where p as the solute partial pressure, C_s is solute mass uptake per volume of pristine MMT:

$$K_{g/MMT}(T) = \frac{C_g}{C_s} = \frac{K_H}{RT} = \exp\left(\frac{\Delta G}{RT}\right) = \frac{t_R^{ref}(T)}{t_R(T) - t_R^{ref}(T)} = \frac{1}{t_R^*(T)} \quad (5-43)$$

with $\Delta G = H_g - H_s - T(S_g - S_s)$, where $\{H\}_{i=g,s}$ and $\{S\}_{i=g,s}$ are the enthalpy and entropy associated to the gas phase “g” and adsorbed state “s”. The isosteric heat of sorption at diluted state is given accordingly by:

$$Q_{st} = H_g - H_s = -R \frac{\partial \ln t_R^*}{\partial 1/T} - RT \quad (5-44)$$

In details, Eq. (5-44) assumes that adsorbed solutes are in equilibrium with a large gas reservoir and that adsorption remains exclusively a surface phenomenon. This assumption may be too restrictive as MMT can be stacked and trap air volume where solutes remain in interactions with the surface. The transition from a surface to volume sorption in cavities is expected to cause an additional variation of ΔS , broadening and tailing of elution times. These factors could not be assessed experimentally due to additional artifacts common in chromatography: restricted/Knudsen diffusion, eddy effects, dead volume... In practice, the parameter μ was chosen to assess t_R and the same number of sites was assumed to be accessible to the test and reference solutes.

5.2.2.3.4 Sorption isotherms of anisole

Adsorption isotherms of anisole onto MMT were determined using a vacuum balance method with increasing activities (p/p_0) from 0.05 to 0.90. Adsorbed amounts on ca. 60 mg of MMT

were weighed using an microbalance (Intelligent Gravimetric Analyzer, model IGA-100, Hiden Isochema, UK) with a resolution of 0.2 μg . Buoyancy corrections were applied when required (mainly at higher pressure) from calibration and blank experiments with inert materials (for components of the measurement chamber and counterweight area). To maximize solute adsorption capacity, all clays were degassed under strong vacuum (10^{-4} Pa) at the test temperature for at least 2 days until to reach a constant weight. The sample was maintained at the set temperature $\pm 0.2^\circ\text{C}$ via a PID-controlled circulating water bath. Regardless a possible different behavior of anisole inside the clay interlayer (*i.e.* confinement) and at the external surface, all measured isotherms were fitted with the BET equation:

$$m_{\text{loading}} = \frac{m_B C_B (p/p_0)}{(1 - p/p_0)(1 + (C_B - 1)(p/p_0))} \quad (5-45)$$

where m_B is the monolayer capacity per gram or per volume of pristine MMT and $RT \ln C_B$ is the theoretical excess of sorption energy of the multilayer comparatively to the bulk. p is the total pressure in the chamber and p_0 is the saturation pressure.

When $p \rightarrow 0$ (*i.e.* at zero surface coverage), an estimation of the Henry coefficient can be derived from Eq.(5-45):

$$K_B = \frac{p_0}{C_B m_B} \quad (5-46)$$

Corresponding isosteric heats of sorption, Q_{st} were calculated from the Clausius-Clapeyron relationship and a polynomial approximant of $p=f(m)$:

$$Q_{st}(m) = -R \left. \frac{\partial \ln p}{\partial 1/T} \right|_m \quad (5-47)$$

5.2.2.3.5 Molecular modeling strategies

5.2.2.3.5.1 Preparation of neat clay crystal structure

We employed Materials Studio modeling environment (MS, version 6.x) to build crystal structure of clay and sample interaction energies. Additional codes and scripting features (*e.g.* topology modifications, space filling methods, forcefield assignment...) were obtained using the in-house library Molecular Studio bridging MS and Matlab (Mathworks, USA). The clay atomistic model (*ca.* 24×10^3 atoms for two periodic clays) was referred to experimental results of XRD for interlayer spacing (d -spacing) and ICP-AES for their relative composition.

The cell unit of a periodic clay was assembled with the MS crystal builder module using the atomic coordinates proposed by (Tsipursky and Drits, 1984) and the lattice parameters:

$a=5.20 \text{ \AA}$, $b=9.20 \text{ \AA}$, $c=14.0 \text{ \AA}$, $\alpha=90^\circ$, $\beta=99^\circ$, $\gamma=90^\circ$ (Mering and Oberlin, 1967). Atomic charges were assigned based on the measurements of (Heinz et al., 2005; Heinz and Suter, 2004a) with an accuracy of roughly $\pm 0.1e$. To minimize cutoff effects in the translational direction, a typical large cell possessing totally: 1248 of hydrogen atoms, 7488 of oxygen atoms, 250 of magnesium atoms, 998 of aluminum atoms and 2496 of silica atoms was built with *P1* symmetry (i.e. only translational periodic) based on a $24 \times 13 \times 1$ arrangement of cell units and finally gave an overall system size of $a=124.8 \text{ \AA}$, $b=119.6 \text{ \AA}$, $c=14.0 \text{ \AA}$. Different *d*-spacing could be achieved by changing the value of parameter *c* in our simulations. A realistic density and distribution of charge defects in crystal was achieved by replacing randomly some internal aluminum atoms by magnesium to match the chemical formula of a real MMT $[\text{Na}_{0.38}\text{K}_{0.01}][\text{Si}_{3.92}\text{Al}_{0.07}\text{O}_8][\text{Al}_{1.45}\text{Mg}_{0.55}\text{O}_2(\text{OH})_2] \cdot 7\text{H}_2\text{O}$ with cation exchange capacity (CEC) of 110. The final structure reached the following formula of $[\text{Si}_4\text{O}_8][\text{Al}_{1.6}\text{Mg}_{0.4}\text{O}_2(\text{OH})_2]$ with an average CEC of 108. In details, 20 % of $[\text{AlO}_6]$ were replaced by $[\text{MgO}_6]$ with the following neighbor table of Al atoms: 41 % had three Al atoms as neighbors; 44% had two Al atoms and one Mg atom; 13% had one Al atom and two Mg atoms; and 2% of Al atoms were surrounded by three Mg atoms (see Figure 5-18). The final net charge of the Al octahedral layer reached $-249.2e$ and was assumed to be representative of the entire clay crystal.

5.2.2.3.5.2 Preparation of surface modified clays

Organo-modified clay structures were prepared with sorption program by loading a maximum number of surfactants sampled from a set of 2×10^4 conformers generated during a long-term molecular dynamics ($>10 \text{ ns}$). The maximum loading value was estimated from TGA experiments. In agreement with XRD results on commercial organo-modified MMT, an interlayer spacing of 2.2 nm was assigned for all organo-modified MMTs. A satisfactory saturation of the interlayer spacing was achieved using a space-filling method based on the metropolis Monte Carlo sampling (Metropolis et al., 1953) and COMPASS forcefield. Each insertion was followed by a short molecular dynamics under constant volume/constant temperature (NVT) while keeping the MMT crystal rigid.

5.2.2.3.5.3 Sorption calculations at diluted state

Henry coefficients and isosteric heats were calculated using the Widom test particle method (Widom, 1963) at fixed loading: one single solute (with random conformer) was inserted at random position in the adsorbent framework. The Henry coefficient was sampled by brute force Monte Carlo sampling as (Bezus et al., 1978; June et al., 1990):

$$K_H = \frac{RT}{\exp\left[\frac{\mu_{intra}}{RT}\right] \left\langle \exp\left[-\frac{u_m}{RT}\right] \right\rangle_u} \approx \frac{RT \left\langle \exp\left[-\frac{u_{intra}}{RT}\right] \right\rangle_u}{\left\langle \exp\left[-\frac{u_m}{RT}\right] \right\rangle_u} \quad (5-48)$$

where μ_{intra} is intramolecular chemical potential sampled as (Frenkel and Smit, 2001):

$$\exp\left[\frac{\mu_{intra}}{RT}\right] \approx \left\langle \exp\left[-\frac{u_{intra}}{RT}\right] \right\rangle_u \quad (5-49)$$

which was estimated as the exponential average of intramolecular energy over the trajectory of conformations; u_m is the molar total energy of the configuration m . It is worth to notice that the algorithm sampled all possible positions in contact with the clay surface or not (*i.e.* in the gap).

The isosteric heat of sorption was derived in two different ways according to sorption was considered a cavity filling or a surface interaction process. In the first case, it was defined from the difference in internal energies between the gas reservoir $U_g \approx \langle u_i \rangle_g$ and in the adsorbed phase $U_s \approx \langle u_{i+MMT} \rangle - \langle u \rangle_{MMT}$:

$$\hat{Q}_{st} = H_g - H_s = PV + U_g - U_s = RT + \underbrace{\langle u_i \rangle_g}_{=0} - (\langle u_{i+MMT} \rangle - \langle u \rangle_{MMT}) \quad (5-50)$$

In Eq. (5-50), the solute in the reservoir is assumed to behave as an ideal gas, so that $PV=RT$ and $\langle u_i \rangle_g = 0$. In addition, the internal degrees of freedom of the solute are assumed to be unaffected by the sorption process so that the solute intramolecular energies remains equal, $\langle u_{i+MMT} \rangle$ and $\langle u_{MMT} \rangle$ are the averaged energy of the clays with and without gas. Since $H_g > H_s$, this energy difference is mainly negative. By noticing that the insertion method sampled both “adsorbed” and “confined/intercalated” states, with a partitioning which was independent of the temperature, a more reliable estimate of Q_{st} was achieved with $\hat{Q}_{st} = R \partial \ln K_H / \partial (1/T)$.

5.2.2.3.5.4 Sorption calculations at concentrated state

Adsorption at higher concentration was investigated via the Grand Canonical Monte Carlo (GCMC) simulation method (Bezus et al., 1978; June et al., 1990). By contrast with real adsorption experiments, the reservoir and adsorbent were not in direct physical contact; but the Monte Carlo procedure guaranteed that the adsorbates have an equal temperature and chemical potential in both the reservoir and in the adsorbent framework. As for the Widom insertion method, the solute conformers were considered to be rigid and only rigid body

translations and reorientations were authorized. All calculations were carried out with a cutoff radius of 1.25 nm. The swelling of the clays was not considered (their atom positions were fixed) and the calculated sorption isotherm was compared with Langmuir equation:

$$m = m_L \frac{KP}{1 + KP} \quad (5-51)$$

where m_L is the maximum loading per gram or volume of adsorbent framework at saturation and K is the Langmuir equilibrium constant. Their combination provides an additional estimate of the Henry constant at infinite dilution:

$$K_L = \frac{1}{Km_L} \approx K_H \quad (5-52)$$

5.2.2.3.5.5 Sorption properties of organic solutes in surfactants

On commercial organo-modified MMT, tested solutes were also expected to absorb in the excess of surfactants. This effect was investigated by calculating excess chemical potentials and mixing energies using the methodology described in (Gillet et al., 2009, 2010; Vitrac, 2010).

5.2.2.4 Results and Discussion

5.2.2.4.1 Experimental characterization of clays

The chemical composition and basal spacing are the main inputs for the development of atomistic models, which match the composition and structure of commercially available pristine MMT and chemically modified ones.

5.2.2.4.1.1 Organic composition

The organic compositions of clays were determined by thermal decompositions (*i.e.* TGA) under nitrogen atmosphere. The results expressed as rate of weight loss are summarized in Figure 5-15. The corresponding peaks were deconvolved as a sum of Gaussian curves using a separable nonlinear least-square method. The detailed interpretation of main peaks is reported in Table 5-6. The first peak below 150°C was present in in all samples and very significant in pristine MMT. It was associated to the residual free water adsorbed on MMT. The organic content of organo-modified clay samples started to decompose from 170°C and desorbed from surface in two major organic fractions as discussed by Corres et al. (2013). The first fraction appears for temperatures below 350°C (see peaks (ii)+(iii) in Figure 5-15) as a result of the decomposition of the excess of alkylammonium halide, which has not been eliminated after the cationic exchange reaction (Filippi et al., 2011). The decomposition temperatures are

known to be lower than those observed with pure surfactants due to a possible catalytic role of MMT (Bellucci et al., 2007; Xie et al., 2001). The second fraction rises from 400 °C to 450 °C (*i.e.* peak (iv)+(v) in Figure 5-15) and is associated with the decomposition of surfactants undergoing an exchange reaction in the clay gallery. The decomposition was delayed due the clay layer structure, which hindered the diffusion of volatile products (Monticelli et al., 2007). The decomposition above 500°C (*i.e.* peak (vi) in Figure 5-15) is produced by dehydroxylation of aluminosilicate (Mackenzie and Society, 1957). Table 5-6 shows the presence of an excess of surfactant which were not adsorbed with the surface. The excess is partly significant for the clay type: C6H5MMT.

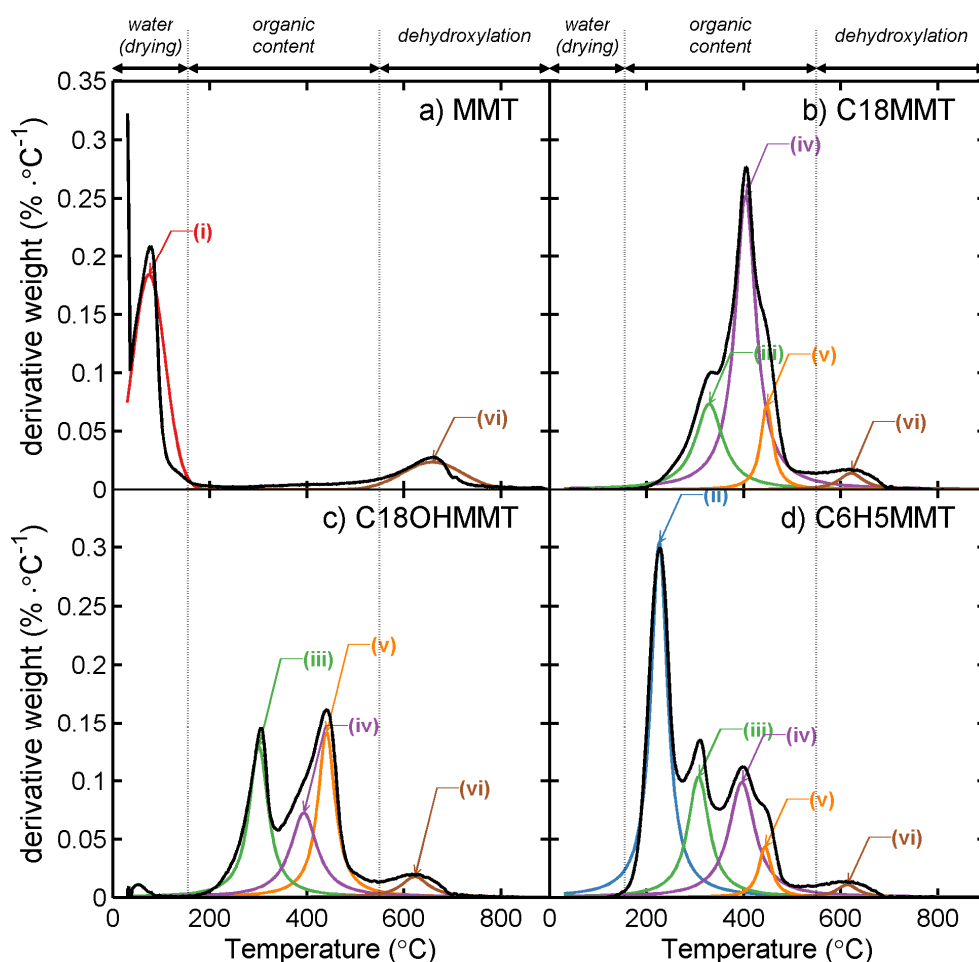


Figure 5-15 Differential thermal analysis (DTA) curves of a) pristine MMT, b) C18MMT, c) C18OHMMT and d) C6H5MMT. Deconvolved peaks are identified with Roman numbers with corresponding parameters listed in Table 5-6.

Table 5-6 Content of tested clays based on the deconvolution of the TGA spectra (peaks are identified with roman numbers in Figure 5-15).

MMT type	Peaks and their approximate temperature range						Estimates		
	peak (i) <150°C	peak (ii) at 226°C	peak (iii) at 300- 330°C	peak (iv) at 400°C	peak (v) at 440- 450°C	peak (vi) at >500°C	excess surfactant content (ii)+(iii)	surfactant content at surface of MMT (iv)+(v)	total organic content (ii)+(iii)+(iv)+ (v)
MMT	14.4%	-	-	-	-	5.3%	0%	0%	0%
C18MMT	0.5%	-	5.5%	18.7%	5.2%	1.1%	5.5%	23.9%	29.4%
C18OHMMT	1.4%	-	9.5%	5.5%	10.0%	1.3%	9.5%	15.6%	25.1%
C6H5MMT	0.2%	20.3%	6.8%	6.8%	2.9%	0.8%	27.0%	9.6%	36.6%

5.2.2.4.1.2 Gallery structure

The basal spacing of our tested MMT was assessed at the maximum of the Bragg diffraction intensities. The diffraction peaks were fitted as a sum of Gaussian or Lorentzian above the spectrum baseline (see Figure 5-16). Such mathematical treatments enabled to get the width of the Bragg reflection. This width is a consequence of incoherent scattering associated to the finite thickness of clays (James, 1948), of the lack of specific orientation of clays and of possible variations in basal spacing due to different arrangements of alkylammonium cations as monomolecular, bimolecular or pseudo tri molecular layers (Lagaly et al., 2013). A distribution of the likely d -spacing of tested MMT was achieved by applying Bragg's law to the support of the last deconvoluted peak (see Figure 5-17). Pristine MMT showed a d -spacing of 1.35 nm with a 95% confidence interval varying from 0.9 and 2 nm. Organo-modified MMT exhibited narrower distributions with between 2 and 2.3 nm. The differences between distribution averages and modes are collected in Table 5-7. It is worth to notice that only C6H5MMT exhibited a bimodal distribution suggesting clays are organized in a lamellar structure involving three clays or more.

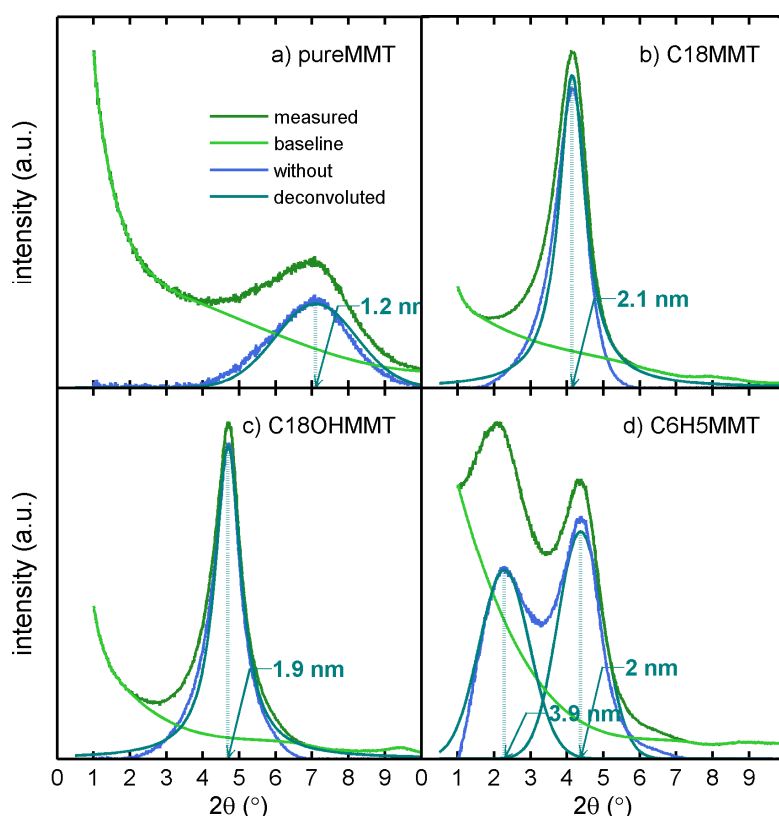


Figure 5-16 Diffraction spectra of a) MMT, b) C18MMT, c) C6H5MMT and d) C18OHMMT samples. Bragg peaks were fitted as a sum of Gaussian (a, b, d) and Lorentzian curves (c) and baseline. The baseline is fitted with a tangent constrained fourth degree spline polynomials.

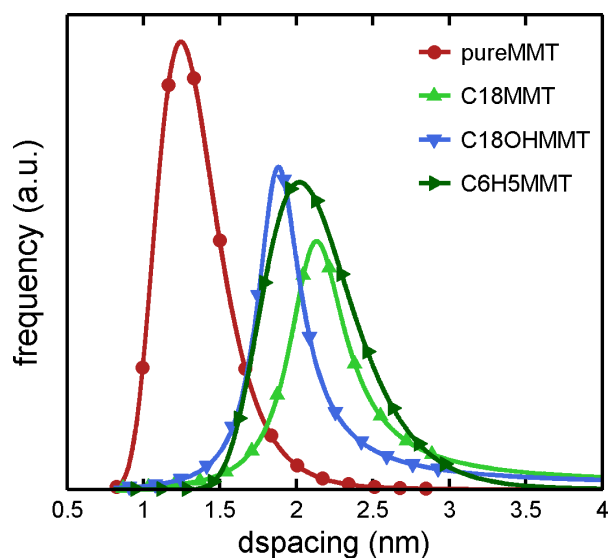


Figure 5-17 The dspacing distribution calculated according to Bragg's law. Likeliest values and typical percentiles are reproduced in Table 5-7.

Table 5-7 *d*-spacing values integrating uncertainties over the distributions

<i>MMT type</i>	<i>d-spacing at peak (nm)</i>	<i>averaged d-spacing (nm) †</i>
MMT	1.27	1.35 [0.98 1.31 1.98]
C18MMT	2.13	2.26 [1.53 2.20 3.28]
C18OHMMT	1.88	2.03 [1.39 1.94 3.19]
C6H5MMT	2.02	2.15 [1.62 2.11 2.97]

†[2.5%, 50%, 97.5%] percentile values (see Figure 5-17)

5.2.2.4.2 Clay atomistic model and its characterization

The clay structure is presented in Figure 5-18 with periodic boundary conditions not only in the plane of the clay (*PI* symmetry) but also perpendicularly. This construction enables to describe an infinite stacking at minimum cost by setting the size of the periodic-cell to the desired *d*-spacing value. The surfactant/solute is therefore in contact with both sides on the same clay. The assumption may appear restrictive as the same substitutions of Al atoms by Mg ones appear on both for the first clay and its mirror copy. Detailed calculations show that averaged configurations (with solutes at different positions) were unaffected by the repetitions of the charges. When electrostatic interactions were significant, a systematic verification was carried out with an aperiodic system along the vertical direction. The simulated surfaces were sufficiently large to include all considered adsorbates. With a typical *d*-spacing of 2.2 nm, surfactants on organo-modified MMT appear organized as a combination of bilayers (aligned

molecules with head and tail configurations, see Figure 5-18h) and of pseudo-bilayers (with molecules contacting twice the surfaces, see Figure 5-18g). It is worth to notice that no typical orientation (*e.g.* such as liquid-crystal) was detected for surfactants.

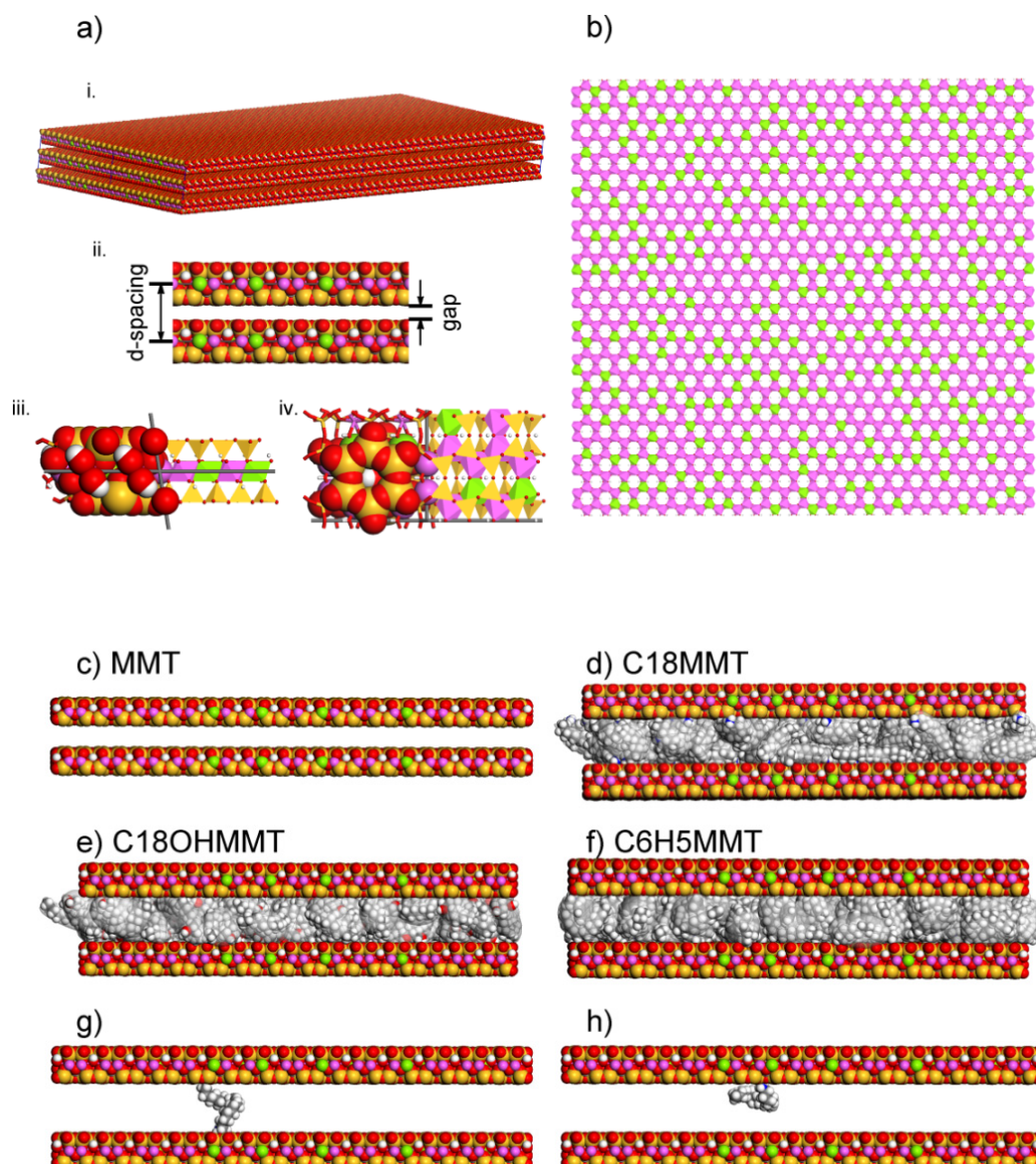


Figure 5-18 Illustrations of our atomistic models of MMT: (a) i: overview of periodic unit cell in $2 \times 2 \times 2$ arrangement with a lattice spacing (d -spacing) in c direction and a significant gap between the two adjacent layers, iii: side view details of the crystal structure with PI symmetry, the elemental crystal pattern is represented in CPK style. iv: the corresponding top view of six tetrahedral silica connected clearly identifiable, (b) Details of the Al octahedral layer with random substitutions by Mg atom. c)-f) Typical side views of pristine MMT (d -spacing= 1.27 nm) and organo-modified MMT (d -spacing=2.2 nm). g)-h) Two typical orientations of one single surfactant molecule: octadecylamine (C18).

The maximum surfactant loading achievable in our simulations versus d -spacing is reported in Figure 5-19. For values larger than 1.5 nm (for gaps larger than pristine MMT one), master

curves were found linear with d -spacing. Hence, it confirms the space filling role of surfactants. Branched or aromatic surfactants (C18OHMMT and C6H5MMT), having a higher steric volume, created higher free volumes.

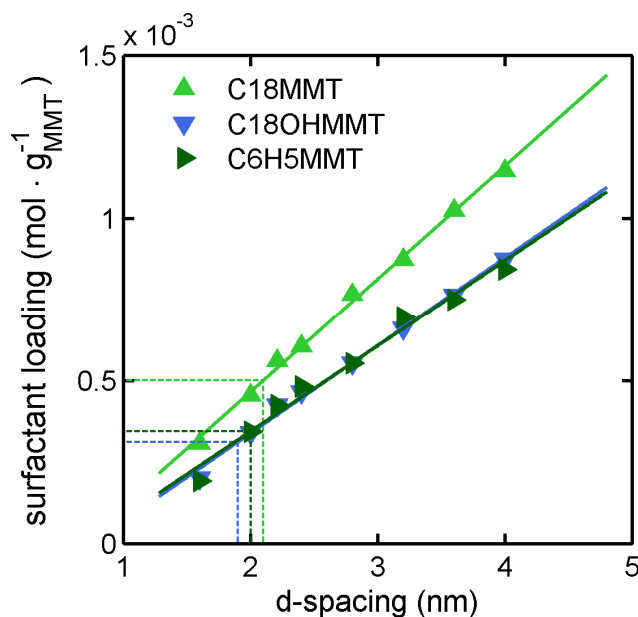


Figure 5-19 Correlations between surfactant loading and d -spacing as assessed from GCMC simulations.

The correlations between d -spacing and surfactant loading were used to estimate the distributions of loading when d -spacing values are distributed as shown in Figure 5-17. Averaged values and typical percentiles are listed in Table 5-6 and compared with the experimental loading inferred from the integration of TGA peaks (iv) and (v) in Figure 5-15 (see Table 5-6). An exact match was found for C6H5MMT and a significant underestimation was found for C18MMT and C18OHMMT by factors 2.2 and 1.4 respectively. The discrepancy for these two MMTs was associated to their different organizations mainly as pair of clays instead as well organized thick stacks (see their X-ray diffraction spectra in Figure 5-16). Thin systems expose much more free surfaces unit amount of clay, where surfactants are not limited by the accessible volume between two clay layers.

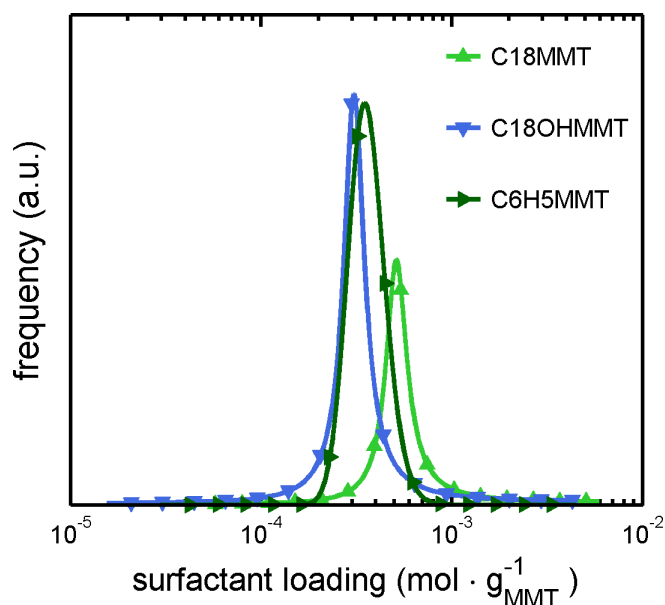


Figure 5-20 Theoretical distributions of surfactant amounts from GCMC simulations (Figure 5-19) integrating the dispersion of d -spacing plotted in Figure 5-16. Mean values and typical percentiles are reproduced in Table 5-8.

Table 5-8 Comparison of surfactant loading between experimental and calculation.

MMT type	Surfactant loading ($\text{mol} \cdot \text{g}^{-1}_{\text{MMT}}$) calculated from		Ratios Mc/ Ms
	TGA peaks (iv)-(v) (Mc)	Simulated results at $d=2.2\text{nm}$ (Ms)	
C18MMT	1.26×10^{-3}	5.62×10^{-4} [4.7×10^{-4} , 6.1×10^{-4} , 8.6×10^{-4}] †	2.2 [2.7, 2.1, 1.5] †
C18OHMMT	5.87×10^{-4}	4.24×10^{-4} [2.8×10^{-4} , 3.7×10^{-4} , 5.2×10^{-4}] †	1.4 [2.1, 1.6, 1.1] †
C6H5MMT	4.05×10^{-4}	4.24×10^{-4} [3.0×10^{-4} , 3.7×10^{-4} , 4.1×10^{-4}] †	1.0 [1.4, 1.1, 1.0] †

† [2.5%, 50%, 97.5%] percentiles with real distribution (see Figure 5-20)

From our GCMC simulations, Figure 5-18 gives an impression of a dense coverage of the surface of MMT at equilibrium. As a result, industrial practices which offers ever higher coverage or saturation may be thought hindering subsequent sorption by organic solutes by two entropic effects: i) reduction of the accessible surface area of MMTs and ii) by promoting interactions with surfactants instead of MMTs. These effects were globally investigated by studying the accessible free-volume properties for spherical probes with different gyration radius. The results are plotted in Figure 5-21 and compared with the gyration radius and volumes of the considered solutes in this study. The corresponding accessible free volume of space-filling models decreased linearly with probe radius up to toluene size but decreased non-linearly for larger solutes. Although this geometric and static approach neglects the

swelling of the clay, it suggested a rapid saturation of organo-modified MMT when they are used as adsorbents. And this effect will be enforced in well stacked clay with large surface.

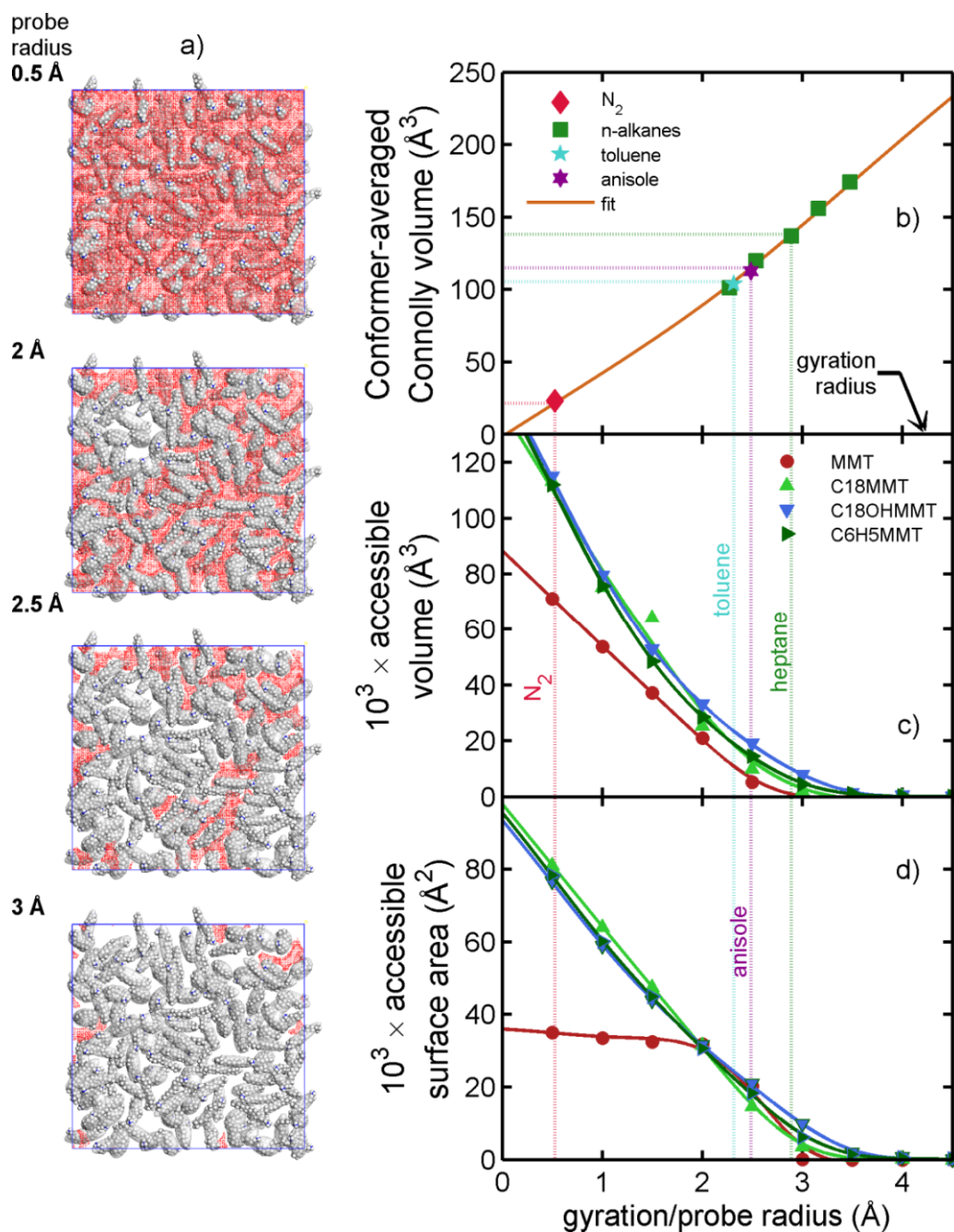


Figure 5-21 a) Top view of the volume accessible to spherical probes into one typical clay interlayer filled with C18 surfactant to spherical probes (the contact surface for different probe radii are plotted in red color). b) Relationships between volumes and gyration radius of tested solutes. c-d) Accessible volume and surface area according to radius of the considered spherical probe.

5.2.2.4.3 Sorption properties at infinite dilution

5.2.2.4.3.1 Simulated Henry coefficient and isosteric heat of sorption

Henry coefficients, K_H , and isosteric heat of sorption, Q_{st} , obtained from particle insertions at different temperatures are plotted in Figure 5-22. For each considered solute, the presented results compile Monte Carlo simulations with Widom test particle (Widom, 1963) insertions each from an initial set of 10^4 conformers. Although adsorbates, surfactants and MMT were considered rigid, the large set of conformers enabled to integrate all interactions: inside the framework (*i.e.* MMT and surfactants), intramolecular and intermolecular ones. The only assumption was that the distributions of conformers were same at adsorbed/gas state. As expected from accessibility considerations depicted in Figure 5-21, K_H values appeared noisier in organo-modified MMT and especially for larger solutes. The low convergence of averaged energies was associated to fluctuating contact numbers with MMT surface in crowded environments. Corresponding distribution of adsorbed energies are shown in Figure 5-23. They were mono-modal but very broad and centered on a low negative average at large d -spacing values. The shape was the consequence of the simultaneous sampling of adsorbed states with highly negative energy values and intercalated states with positive ones. Incorporating directly these raw values at constant temperature in Eq. (5-50) led to strongly underestimated Q_{st} values. Since the shape of the distribution was un-affected by temperature (for a same set of conformers), the Clausius-Clapeyron relationship was used instead to derive reliable Q_{st} values from simulations obtained at different temperatures (*i.e.* ranging from 298K to 348K). These results are plotted in Figure 5-22d)-f).

Changing d -spacing affected strongly the distributions of energies (see Figure 5-23d)-f)) and K_H values (Figure 5-22a)-c)) but in a less extent Q_{st} values. These results confirmed that the partition between adsorbed and intercalated solutes was mainly controlled by entropic considerations rather than by enthalpic ones. In details, the interpretation is more subtle as lower d -spacing values reduced the amount of intercalated solutes while decreasing the average distance between the solute and the surface. By assuming that the interactions between the polar or aromatic solute and the pristine clay surface were Coulombic, a correlation between Q_{st} and the reciprocal square gap distance is proposed in Figure 5-22f). For aromatic solutes, Q_{st} increased monotonically until to reach a constant value. For aliphatic solutes, it reaches a maximum value before decreasing. The different behavior for aliphatic solutes was associated to the preferential selection of stretched and planar (no out-of-plane atoms) conformers in confined spaces (*i.e.* for d -spacing values below 1.35 nm). For higher d -spacing above 1.4 nm, the gap between clays must be envisioned as a small gas reservoir, where the interactions walls-solutes remain strong but where the solute can explore a broad

configuration (by translation or rotation) and conformational space. These properties cause a dramatic entropic increase of K_H values while keeping interaction energy levels close. For very large d -spacing value, K_H is finally expected to reach the theoretical value of an ideal gas: RT . From Figure 5-22c) at a constant temperature, K_H was found exponentially scaled respectively to a reference d -spacing d_0 as:

$$\frac{K_H(d)}{K_H(d_0)} = \frac{RT \exp\left(-(\delta/d)^2\right)}{RT \exp\left(-(\delta/d_0)^2\right)} = \exp\left(-(\delta/d)^2 + (\delta/d_0)^2\right) \quad (5-53)$$

where δ is a fitting parameter which is almost independent of the considered solute, with a likely value of 6.13 (95% confidence interval is 5.95 to 6.46).

For a same d -spacing of 2.2 nm, aliphatic solutes exhibited a slightly higher chemical affinity (*i.e.* lower K_H value) for organo-modified MMTs than for pure MMT. Best affinity was obtained with C6H5MMT. When the real d -spacing of pure MMT (*ca.* 1.3 nm) was used instead, the results were conversely opposite, confirming that pristine MMT was by far the best adsorbent for all organic solutes. Simulations showed therefore that intercalating surfactants between clays, which causes a d -spacing increase from 1.35 to 2.2 nm, reduce dramatically the benefits on interactions between organic substances and aluminosilicates respectively to two aspects.

- From an energetic point of view, large spaces prevent the selection of conformers which maximize the interactions with the surface of the clays. Accordingly isosteric heat of anisole decreases from 120 $\text{kJ}\cdot\text{mol}^{-1}$ down to 60 $\text{kJ}\cdot\text{mol}^{-1}$ as a sole consequence of a d -spacing increase from 1.35 nm to 2.2 nm (Figure 5-22f)). In the meanwhile, the new interactions due to surfactants compensate the loss of attractive forces only by 20 – 25 $\text{kJ}\cdot\text{mol}^{-1}$ (Figure 5-22d)). The conclusions were not modified by changing the type of surfactants.
- From an entropic point of view, increasing d -spacing (*e.g.* with or without surfactants) expands the accessible configurational space to solutes. In absence of surfactants, it is so large that too few numbers of configurations contribute to have a high number of “contacts” with the surface. In details, the exploration of the configurational space in large gaps is also associated to energy barriers but they are so low comparatively to interaction energies with clays that they are captured in the entropic contribution (*i.e.* temperature independent).

From a technological point of view, the sorption affinity can be changed either with temperature or by updating d-spacing.

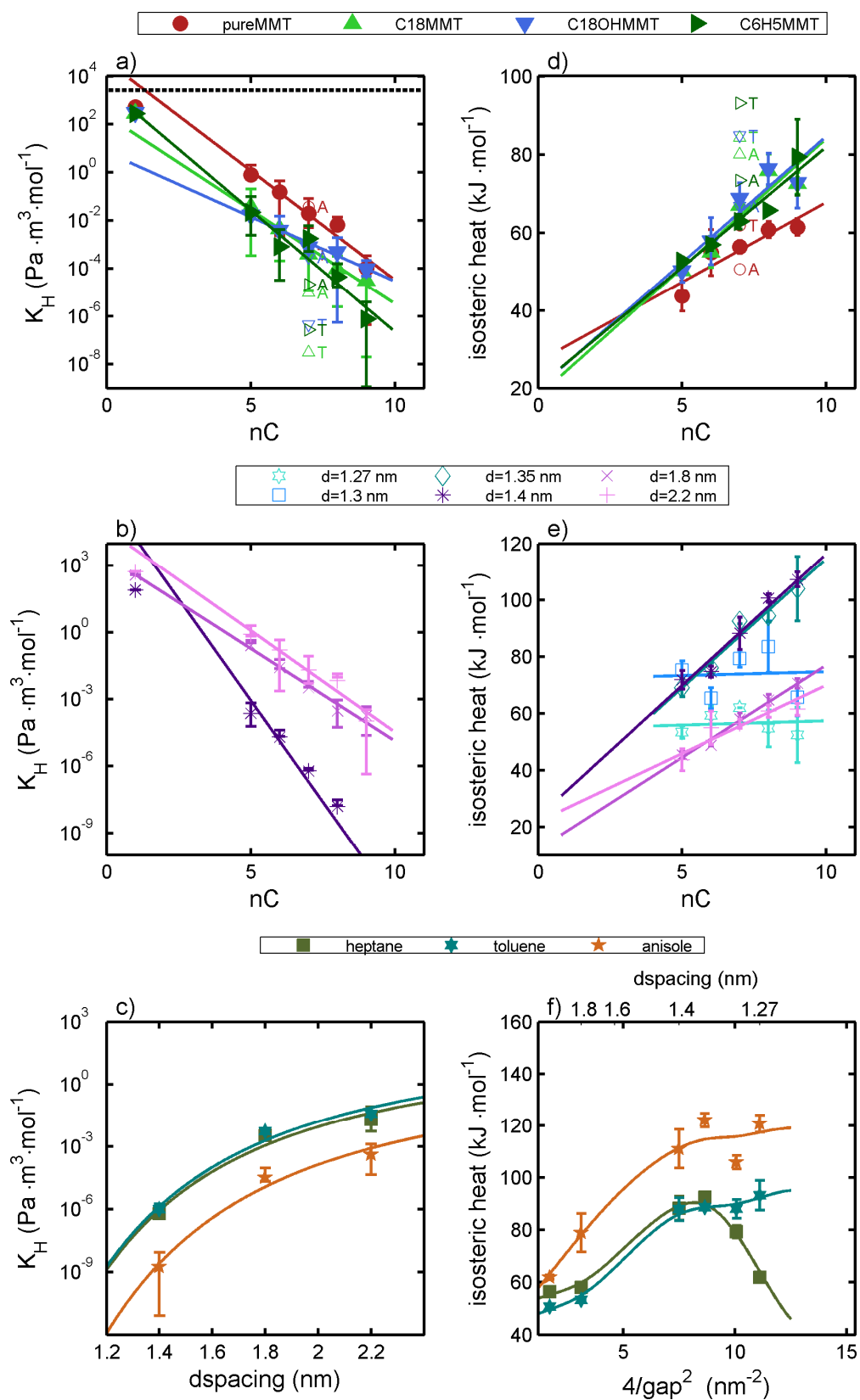


Figure 5-22 a)-c) The calculated Henry coefficient sampled by one single solute molecule with all clay models at 313 K. The horizontal dashed line separates the theoretical Henry coefficient for an inert ideal gas. d)-f) the isosteric heat calculated in the temperature range

from 298 K to 348 K a), d) The effect of surfactant on *n*-alkanes with equal *d*-spacing (*d*=2.2nm), b), e) the effect of *d*-spacing on *n*-alkanes in the range of *d*=1.27-2.2nm and c), f) on solute series of heptane, toluene and anisole in the range of *d*=1.27-2.2nm

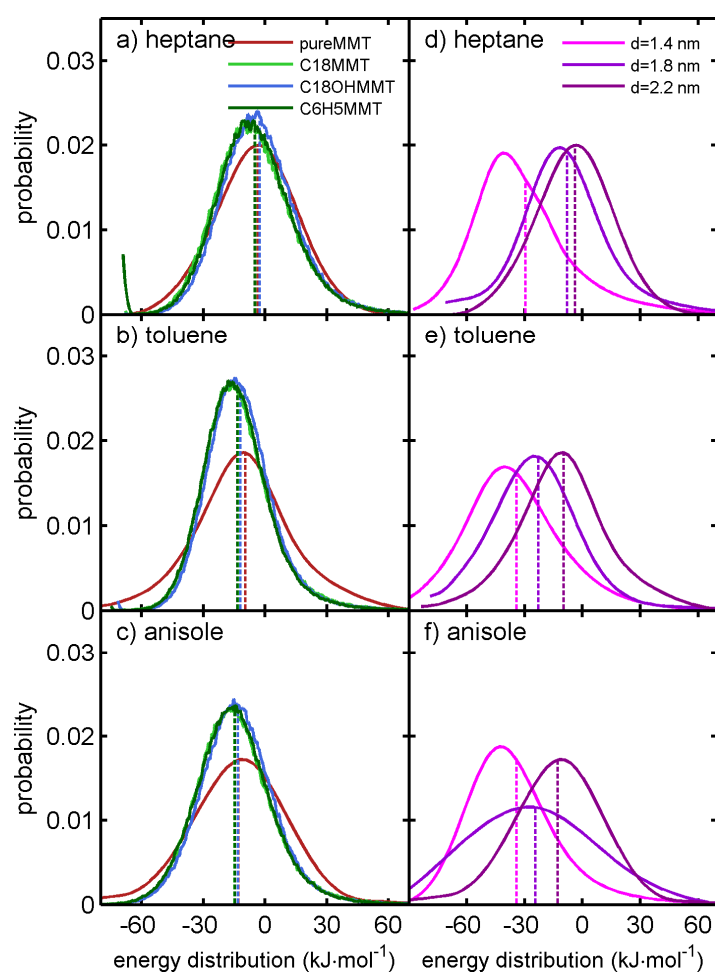


Figure 5-23 The corresponding sorption energy (i.e. -isosteric heat) distribution of solute series of heptane, toluene and anisole a)-c) on all clay type with equal *d*-spacing of 2.2nm and d)-f) on pure MMT with *d*-spacing ranging from 1.4 to 2.2nm. The averaged energy values are reported in Figure 5-22a)).

5.2.2.4.3.2 Comparison with experimental adsorption enthalpy

Simulated isosteric Q_{st} values were compared with experimental ones obtained on commercially available MMTs. The reference values were obtained from IGC experiments from similar solutes. As calculations showed that K_H value of methane was close to the value for ideal gas RT , so it was chosen as reference (i.e. non-interacting) solute in all determinations. Typical elution times are plotted in Figure 5-24 on a log-scale as well as their fit as exponentially modified Gaussian. On pristine MMT, only elution times up to hexane were practically measurable even at high temperatures of 120°C. For larger alkanes and

aromatic solutes, retention times were out of reach even using higher flow rates (*i.e.* $\approx 20\text{ml}\cdot\text{min}$). The absence effect of flow rate on normalized retention times, t_R (see Eq. (5-42)) is plotted in Figure 5-25. It confirms that t_R is mainly controlled by thermodynamics considerations allowing a determination of K_H via Eq. (5-43).

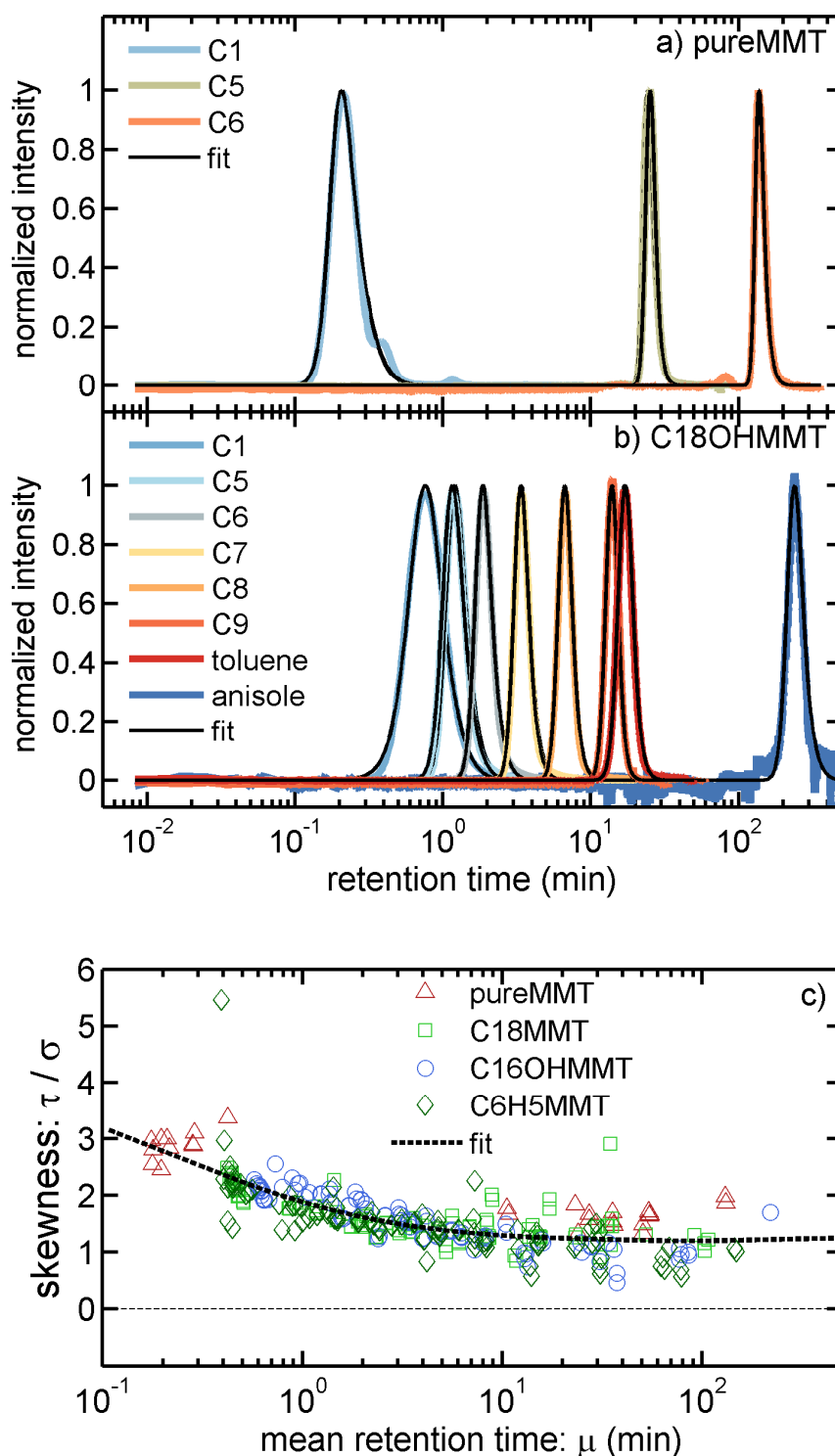


Figure 5-24 Typical distributions of elution times for n -alkanes ($n=1..6$), toluene and anisole in columns filled with a) pure MMT and b) C18OHMMT samples. Fitted exponentially-modified Gaussians are depicted as thin solid lines and c) the peak shape factor (skewness) of elution profiles as function of the position of the peak mode.

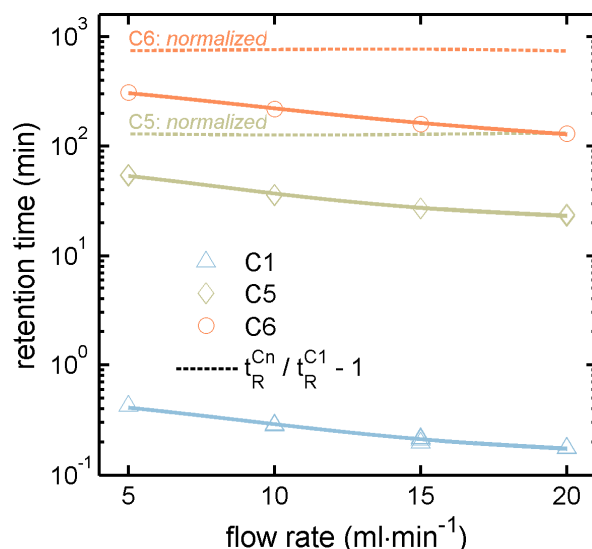


Figure 5-25 Effect of flow rate effect on retention times of pentane and hexane. Normalized retention times (see Eq. 4) are plotted as dashed lines.

The experimental K_H values and simulated ones are compared in Figure 5-26 for pristine MMT. They were in very good agreement when simulated K_H were averaged over the real distribution of d -spacing as determined from XRD experiments (see Figure 5-27). By comparing with the effect of d -spacing values on K_H as reported in Figure 5-22b), it is worth to notice that the largest d -spacing contributed to the most to the final K_H value as predicted from Eq. (5-53). For pristine MMT, d -spacing varied significantly between 1 nm and 2.2 nm (Figure 5-17) but basal-spacing over 1.27 were accessible to insertion. In details, confidence intervals plotted in Figure 5-26 represent the final uncertainty on K_H due to sampling errors and to the broad distribution of d -spacing values (each distribution included both uncertainty and variability in XRD determinations as discussed in 3.2.2).

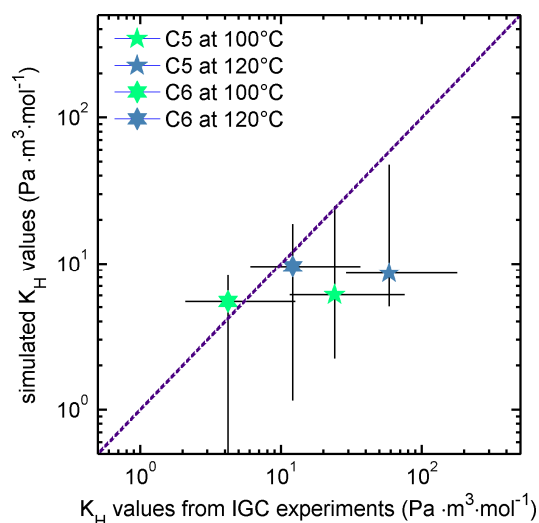


Figure 5-26 The experimentally determined Henry coefficients of pristine MMT compared with simulated ones averaged over the distribution of real d -spacing values (see Figure 5-17). The dashed line represents the straight line, $y=x$. Vertical and horizontal lines represent 95% confidence intervals

By opposition with results of Figure 5-26, crude comparisons between simulated and experimental K_H values yield poor agreements for commercial organo-modified MMT. As reported in Figure 5-27, experimental Q_{st} values were found close to the latent heat of vaporization heat of pure solutes, ΔH_v , without presenting a significant net heat of adsorption $q_{st} = Q_{st} - \Delta H_v$. Our experimental methodology to determine K_H values was not incriminated as our experimental Q_{st} and q_{st} values for pristine MMT matched both the values reported by Keldsen et al. (1994) (Figure 5-27a)) and the simulated values for d -spacing ranging between 1.27 and 1.35 nm (Figure 5-27b)). An alternative interpretation of the sorption at infinite dilution of linear alkanes and aromatic solutes was tested by considering that solutes were mainly in interaction with surfactants without possible contact with MMT surface. This assumption was particularly consistent with the excess of surfactants as determined from TGA experiments (see Figure 5-15 and Table 5-6). It was tested by calculating excess mixing energy of each solute with the different surfactants from pair contact energies. Corresponding values are reported in Figure 5-27b)-c). Since the mixing was expected to be mainly endothermic respectively to pure compounds, excess energies were mainly negative or close to zero. They reproduced well the magnitude orders and the trend with the number of carbons for alkanes. Only the values for anisole were underestimated. This minor deviation was associated to the poor reliability of the contact energy method for molecules involving significant hydrogen-bonding (not all configurations are likely).

From the different analyses, it was hinted that the high surface coverage of organo-modified MMT lessened dramatically their chemical affinity for organic solutes. This effect was partly detected by simulation with a decrease of about 25-40 $\text{kJ}\cdot\text{mol}^{-1}$. It could be thought the absence of full agreement between experiments and simulations for organo-modified MMT could result of the lowest saturation of clays in our simulations (see Table 5-8). It is however unlikely since the discrepancy was not depending on the type of surfactants and on the surface loading deviation (*i.e.* high for C18MMT and not significant for C6H5MMT). In addition, the lower skewness of elution times (Figure 5-24c)) with organo-modified MMTs tended to confirm a sorption process in a homogeneous phase different from the broad process found with pristine MMT. It was therefore thought that the residual affinity at infinite dilution with commercial organo-modified MMT was mainly due to preferential interactions between

solutes and the surfactants in excess, hindering the accessibility of solutes to MMT surface (see Figure 5-18). In this perspective, polar or aromatic surfactants gave accordingly a slightly higher affinity for polar and aromatic solutes respectively.

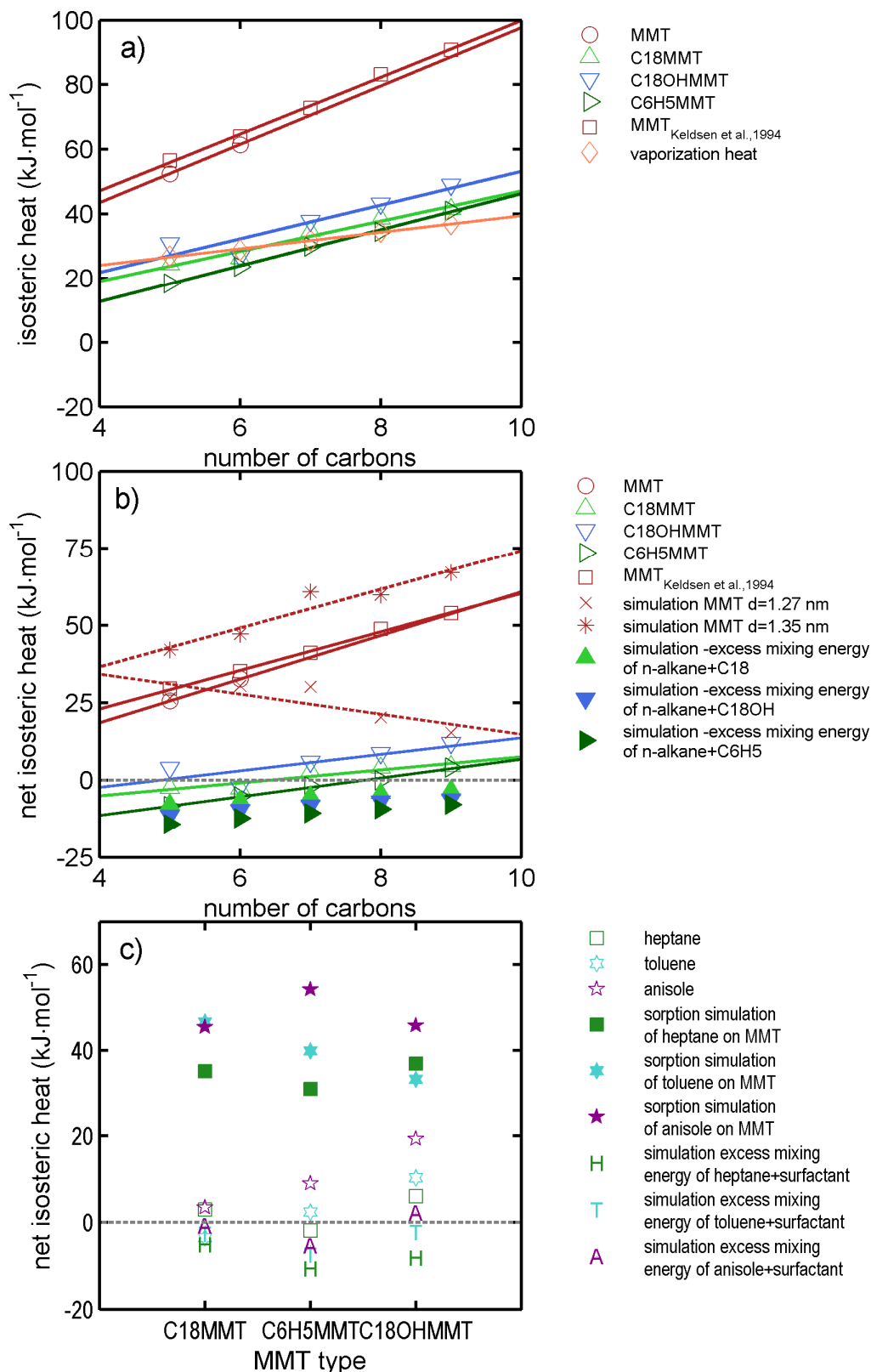


Figure 5-27 Comparisons of isosteric heat of sorption and net values between experimental (IGC) values (open symbols) and simulation ones for a-b) *n*-alkanes and c) aromatic solutes. Excess in solute-surfactant mixing energies are also represented more general heptane,

toluene and anisole (the experimental data are compared with simulation data with two possible interactions: between one solute molecular and clay surface which defined upper boundary above $30 \text{ kJ}\cdot\text{mol}^{-1}$; between solute and surfactant which defined lower boundary below $5 \text{ kJ}\cdot\text{mol}^{-1}$).

5.2.2.4.4 Sorption behavior at concentrated state

Increasing the solute concentration offered the possibility to elucidate surface accessibility and competitive sorption issues in both simulated and tested MMTs. One informative quantity is the saturation amount. It is worth to notice that simulations and experiments differed however with some respects: simulation considered that d -spacing was fixed whereas swelling could occur in sorption experiments with increasing loading. Corresponding isotherms were fitted independently as Langmuir isotherms (see Eq. (5-51)) for different d -spacing and BET ones (see Eq. (5-45)) in presence of swelling, respectively.

5.2.2.4.4.1 Simulated isotherms

Simulated sorption isotherms, depicted in Figure 5-28, showed that saturation amounts m_L increased with d -spacing in pristine MMT. The adsorbed amount was found proportional to the gap distance and function of the gyration radius of the considered solute (see Figure 5-21). From the saturation point of view, sorption was not anymore a surface phenomenon but a space filling one.

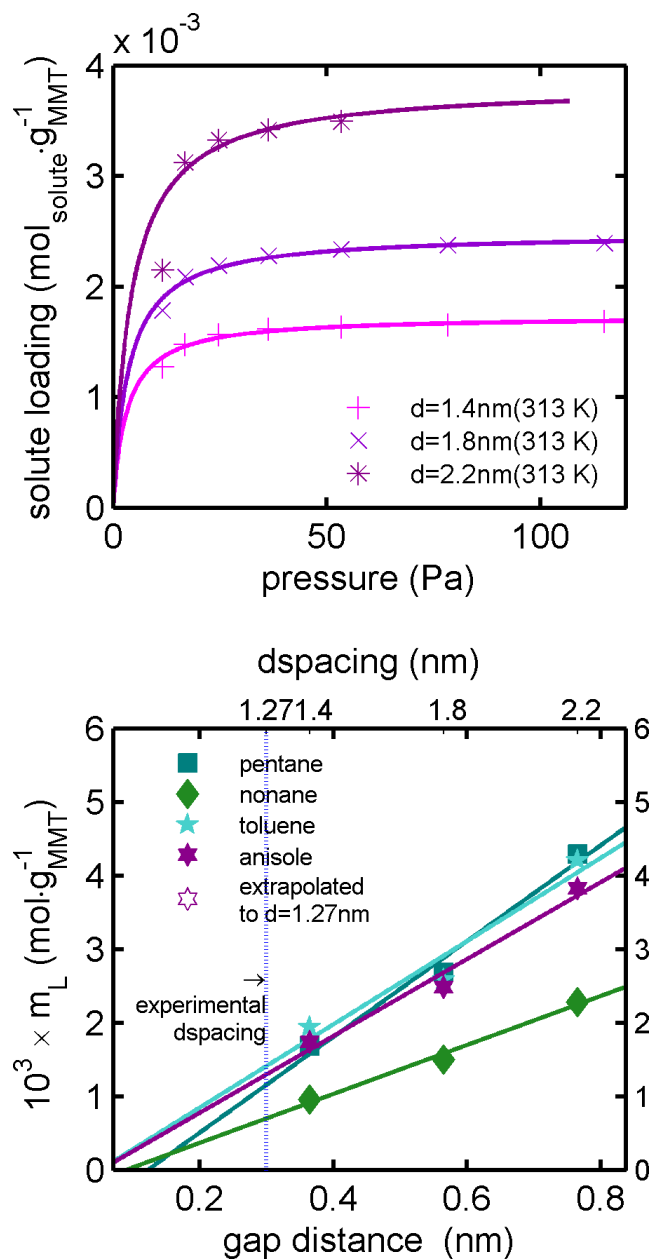


Figure 5-28 a) Simulated sorption isotherms of anisole in pure MMT with different d -spacing and b) linear relationship between maximum loading and gap distance.

Maximum loading capacities for pristine and organo-modified MMTs are compared in Figure 5-29 for all considered solutes and a fixed d -spacing of 2.2 nm. Saturation amounts were twice lower for organo-modified MMT. By using fitted Langmuir isotherms, it was possible to compare the estimate Henry coefficients calculated at infinite dilution K_H and at higher concentrations and so-called K_L (see Eq. (5-52)). K_L and K_H were very close for pristine MMT but in ratios varying from 10 to 10³ in organo-modified MMTs. The higher values of K_L confirmed the rapid loss of chemical affinity of organo-modified MMTs as soon as the concentration in solutes increased. This sorption behavior has to be envisioned as a double

sorption process where the clay surface is first saturated (controlled by a coefficient K_H) followed by a saturation of the gap between the clays (controlled by the clay K_L).

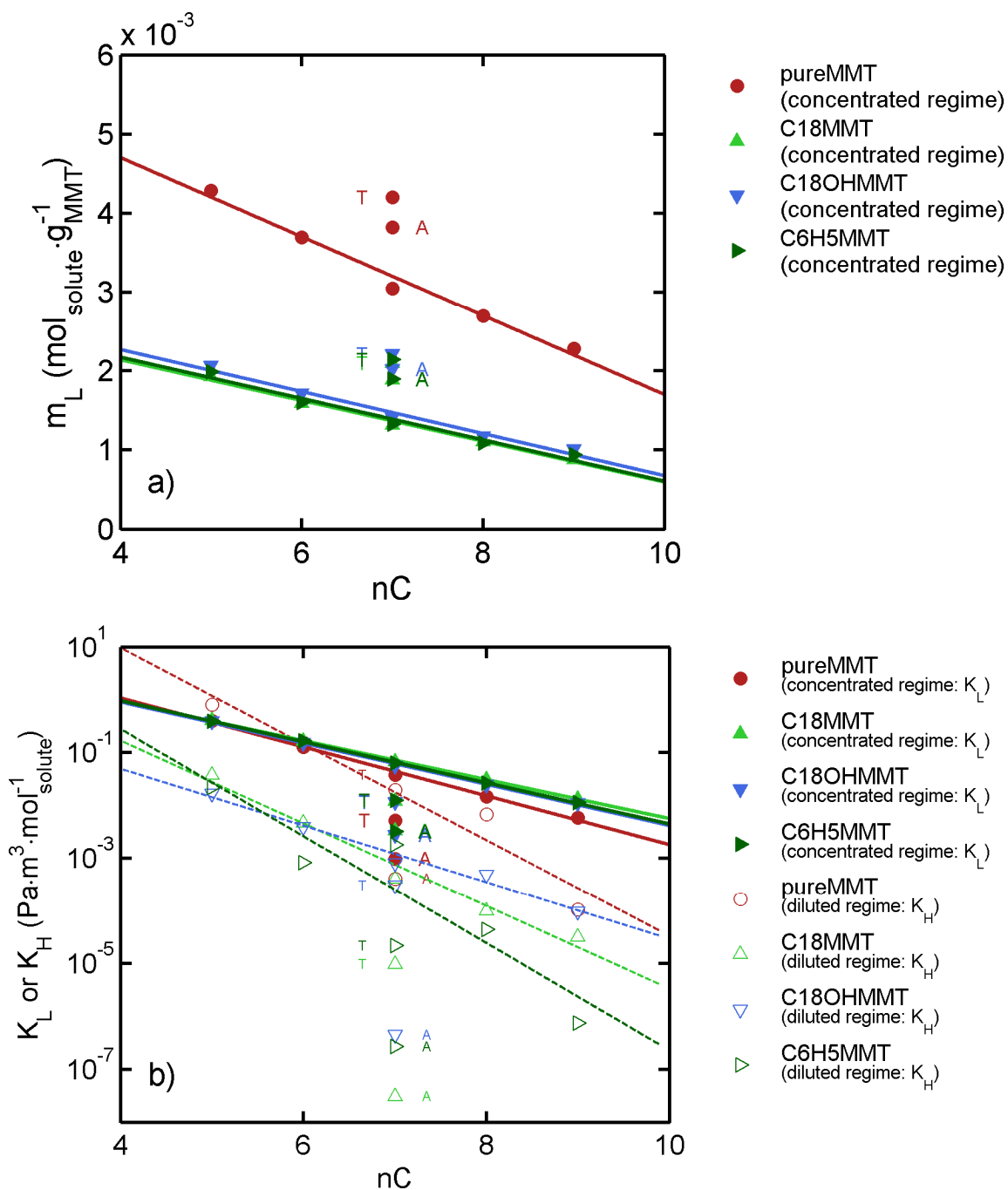


Figure 5-29 a) Maximum loading as determined from simulated isotherms of clays with a fixed d -spacing of 2.2nm and b) equivalent Henry coefficients K_L as extrapolated from Langmuir equation (see Eq. 14) (solid lines with symbols) compared with K_H values calculated from solute insertion at infinite dilution (see Figure 5-22a)).

5.2.2.4.4.2 Experimental sorption isotherms

Simulations with constant d -spacing described sorption of organic solutes in organo-modified MMT as poor efficient process due to steric effect which prevents the solute to access to the

surface, where sorption is highly exothermic. Experimental isotherms at higher concentration (*i.e.* at partial pressures 10 times higher) of anisole (see Figure 5-30) showed a subsequent different sorption behavior highly favored by lower temperatures. The “S” shape of the isotherms was associated to a strong swelling of MMTs. The loadings of anisole were five to six times higher for organo-modified MMTs than for pristine one due to its larger *d*-spacing combined with swelling effect and significantly higher for polar (C18OHMMT) and apolar (C6H5MMT) MMTs.

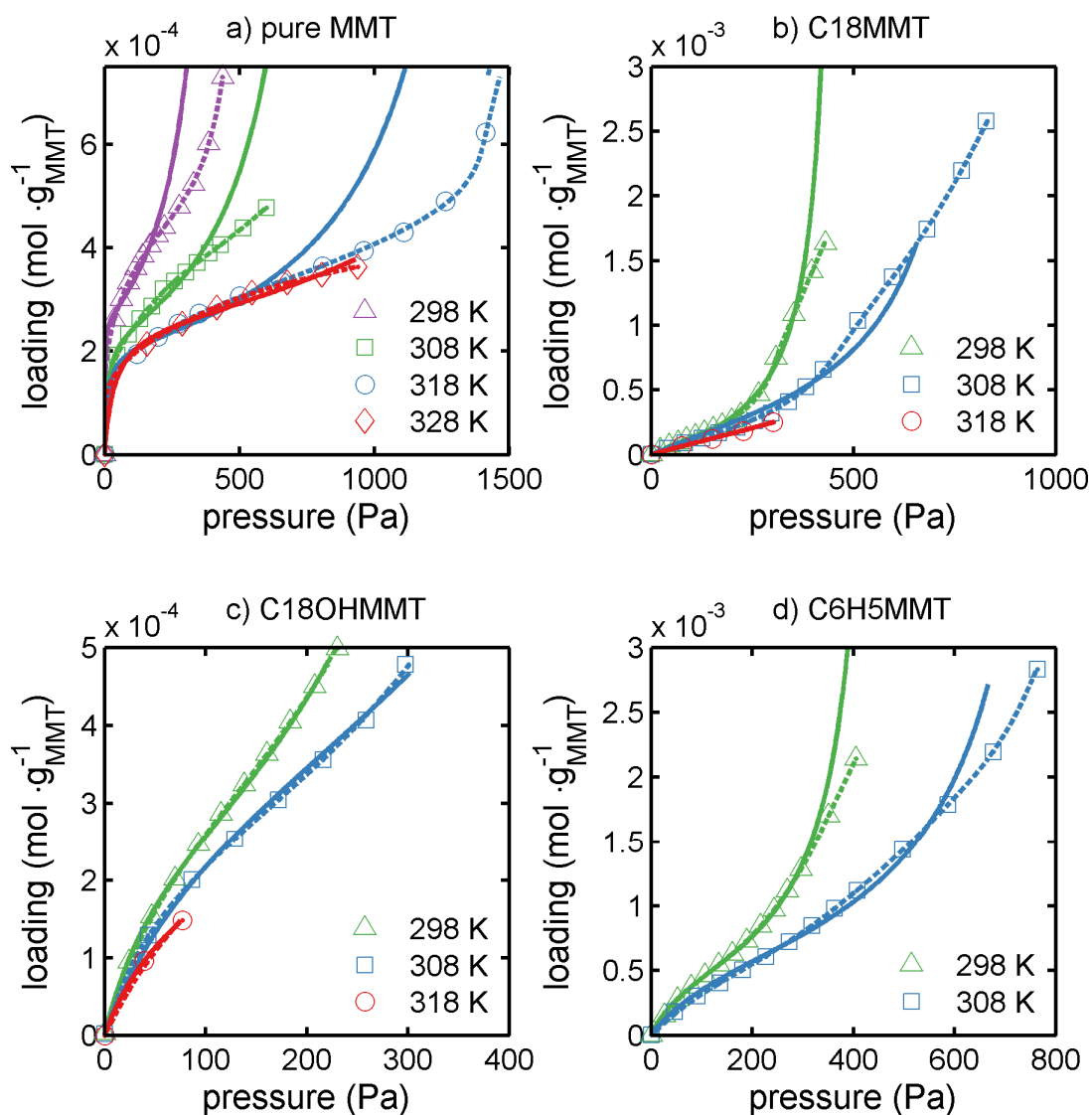


Figure 5-30 Experimental sorption isotherms of anisole (open symbols and dashed lines) compared with fitted isotherms relying on BET equation (solid line). Dashed lines are continuous least squares approximates.

The different sorption behaviors of anisole on MMT were properly described by the BET equation, while swelling was not too high (typically for activities lower than 0.5). Corresponding BET parameters (mainly K_B and m_B) are listed in Table 5-9 along comparable simulated values K_L , K_H and m_L . The following inequalities were obtained for the parameters

describing the behaviors at infinite dilution $K_H \ll K_L \ll K_B$, showing lower interactions with MMT when the concentration in solute is increasing from zero. At higher concentrations, the ratio m_L/m_B was also greater than 1, close to a factor 2 in pristine MMT and 5 in organo-modified ones. Such values suggested that swelling occurred after 1/2 and 1/5 of the gap spaces are filled respectively. According to BET theory, $RT \ln C_B$ represents the difference in energy between the monolayer and the subsequent layers. It is significant only in pristine MMT $12.6 \pm 3 \text{ kJ} \cdot \text{mol}^{-1}$ and almost negligible in organo-modified MMT. In addition, the low variation of K_B with temperature in organo-modified MMTs confirmed weakest interactions between the first adsorbed layer and the substrate and therefore its entropic control.

Table 5-9 Comparison of sorption parameters of anisole from IGA experiments and simulations at concentrated and diluted states.

Clay	Temperature (K)	<i>IGA experiment (with swelling)</i>				<i>Simulation with constant d-spacing</i>		
		BET parameters				Langmuir parameters		Henry coefficient
		$10^4 \times m_B$ (mol·g ⁻¹)	K_B^\dagger (Pa·g·mol ⁻¹)	C_B	$RT \ln C_B$ (kJ·mol ⁻¹)	$10^4 \times m_L$ (mol·g ⁻¹)	K_L^\dagger (Pa·g·mol ⁻¹)	K_H^\dagger (Pa·g·mol ⁻¹)
pure MMT	298	2.6	5.14×10^3	348.4	14.5	-	-	-
	308	2.3	4.59×10^4	81.0	11.2	-	-	-
	313	-	-	-	-	4.7 (d=1.27 nm)	1.83×10^3 (d=1.4nm)	3.2×10^{-3} (d=1.4nm)
	318	2.1	5.44×10^4	137.5	13.0	-	-	-
	328	2.5	1.38×10^5	76.3	11.8	-	-	-
C18MMT	298	3.3	1.03×10^6	1.4	0.8	-	-	-
	308	4.4	7.81×10^5	2.5	2.3	-	-	-
	313	-	-	-	-	19 (d=2.2nm)	3.85×10^3 (d=2.2nm)	3.57×10^{-2} (d=2.2nm)
	318	5.4	1.18×10^6	2.4	2.3	-	-	-
C18OHMMT	298	2.4	1.85×10^5	8.8	5.4	-	-	-
	308	3.2	2.86×10^5	8.1	5.4	-	-	-
	313	-	-	-	-	20 (d=2.2nm)	3.17×10^3 (d=2.2nm)	5.13×10^{-1} (d=2.2nm)
	318	2.3	2.86×10^5	19.2	7.8	-	-	-
C6H5MMT	298	6.1	1.20×10^5	7.6	5.0	-	-	-
	308	7.6	1.91×10^5	7.0	5.0	-	-	-
	313	-	-	-	-	19 (d=2.2nm)	3.64×10^3 (d=2.2nm)	3.10×10^{-1} (d=2.2nm)

$^\dagger K_H$, K_L and K_B are expressed relatively to the mass of pristine MMT instead of its volume.

5.2.2.4.4.3 Isotheric heats of sorption

Isosteric sorption energies (Q_{st}) of anisole on tested MMTs have been extracted from IGA experiments in a small range of temperature to reduce free-volume effects (thermal expansion). Results plotted in Figure 5-31 showed a high Q_{st} value in pristine MMT decreasing rapidly with loading down to the vaporization of heat of anisole (ΔH_v). Organo-modified MMT exhibited by contrast negative net heat of sorptions ($Q_{st} < \Delta H_v$). Only C6H5MMT offered slightly higher interactions compared with other organo-modified MMTs, the trend is consistent with simulated net isosteric heat for anisole plotted in Figure 5-27c). By keeping constant d -spacing, simulated results (see Figure 5-32) reproduced similar Q_{st} magnitude orders in pristine MMT above $100 \text{ kJ}\cdot\text{mol}^{-1}$ with the difference that the simulated values are increasing with loading at constant d -spacing (*i.e.* due to the increase of number of contact in a confined space). As reported in Figure 5-22f), increasing d -spacing lowered significantly Q_{st} values so that swelling should be the first cause of Q_{st} drop with loading. As already noticed at infinite dilution for organo-modified MMT, simulation yielded to higher Q_{st} values than experimental ones (see Figure 5-27c)), but consistently significantly lower than values obtained with pristine MMT. This argument was used to hypothesize an easier access for the solute molecule to the surfactant brush phase rather than clay surface in organo-modified MMT. The results at higher concentration would confirm independently this interpretation. Apart polar surfactants, all other surfactants would lead to a positive energy of mixing and consequently a negative q_{st} value.

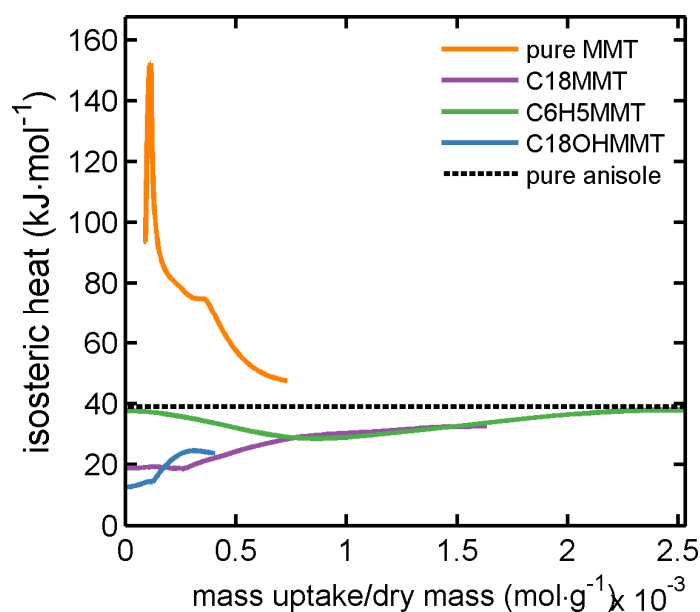


Figure 5-31 Experimental isosteric heat of sorption vs loading inferred from IGA experiments

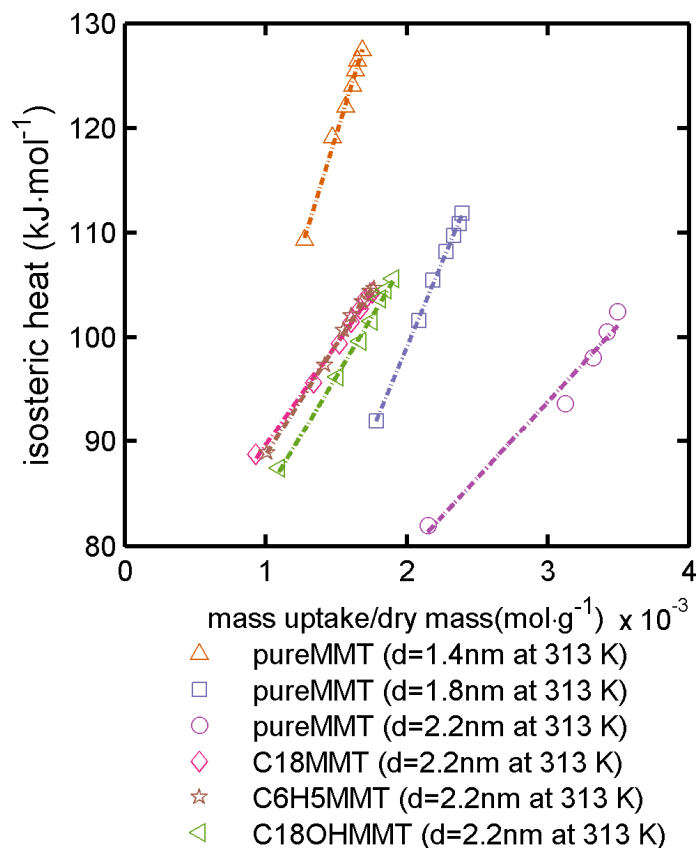


Figure 5-32 Simulated isosteric heat of sorption versus loading of anisole.

5.2.2.5 Conclusions

The study reports measured and simulated Henry coefficients, sorption isotherms and isosteric heat for aliphatic and aromatic volatile solutes in commercially available montmorillonite (MMT). Simulation enabled us to study systematically the effect of basal spacing (d) and solute concentration in pristine MMT. For this case, solutes are intercalated between the clays according to the following general model at infinite dilution:

$$\begin{aligned}
 k_{i,MMT}^{(T,d)} &= k_{i,MMT}^{(T_0,d)} \exp\left(\frac{Q_{st}(d)}{RT} \left(\frac{1}{T_0} - \frac{1}{T}\right)\right) \\
 &\approx RT \left\langle \exp\left(-(\delta/d)^2\right) \right\rangle \exp\left(\frac{\langle Q_{st}(d) \rangle}{RT} \left(\frac{1}{T_0} - \frac{1}{T}\right)\right)
 \end{aligned}
 \tag{5-54}$$

where δ is a scaling constant to be fitted and controlling the entropic contribution (*i.e.* temperature independent) on Henry coefficients. The likely value was found independent of tested solutes and varied between 6 nm and 6.4 nm. $\langle \rangle$ is the average operator over the distribution of real d -spacing values as assessed from XRD determinations. It describes a strong increase of the configurational (*i.e.* conformational, positional/rotational) entropy when d -spacing is increasing. $Q_{st}(d)$ is also a function of d due to the reduction of the number of contacts between solutes and MMT surface. When d is decreasing, Q_{st} increases rapidly up to

same asymptotic value until the gap becomes too small to insert any solute molecule. For flexible solutes, low gaps promote stretched conformers so that Q_{st} are lower in compact clays.

In pristine MMT, entropic effects tend to dominate for d -spacing values larger than 1.8nm. Tested organo-modified MMT offered d -spacing values around 2.2 nm. For this d -spacing value, simulations showed that chemical affinities were higher for organo-modified clays than for pristine ones. Contrary to intuition, experimental net isosteric heat of sorption were found in opposite sign between pristine and organo-modified ones. The correct interpretation of negative values with organo-modified ones was inferred from complementary calculations of mixing energies in pure surfactants. The mixture was assessed significantly endothermic and confirming unambiguously the inaccessibility of the surface of organo-modified MMT. Since this intercalation was possible in simulation but not in our IGC experiment, it was finally concluded that commercially MMT were saturated with excess of surfactants. Such an interpretation was confirmed with TGA experiments. At higher solute concentrations, IGA experiments showed a strong swelling of clays due to the intercalation of solutes while keeping sorption energies close to values found in pure surfactants. As a result, organo-modified MMT appeared as poor adsorbent of organic solutes.

Such results will find applications in packaging and separation technologies where MMT are used to induce barrier effects or to trap organic solutes. Regardless their ability to be dispersed in the considered medium, pristine MMT or slightly organo-modified MMT are highly preferable to saturated ones. Further studies are particularly required to establish the relationship between the basal spacing of MMT and their selectivity to bulky solutes in various temperature and relative humidity conditions.

5.2.2.6 References

- Aylmore, L. A. G., Sills, I. D., and Quirk, J. P. (1970). Surface Area of Homoionic Illite and Montmorillonite Clay Minerals as Measured by the Sorption of Nitrogen and Carbon Dioxide. *Clays and Clay Minerals*. **18**: 91-96.
- Bellucci, F., Camino, G., Frache, A., and Sarra, A. (2007). Catalytic charring–volatilization competition in organoclay nanocomposites. *Polymer Degradation and Stability*. **92**: 425-436.
- Bezus, A. G., Kiselev, A. V., Lopatkin, A. A., and Du, P. Q. (1978). Molecular statistical calculation of the thermodynamic adsorption characteristics of zeolites using the atom-atom approximation. Part 1.-Adsorption of methane by zeolite NaX. *Journal of the Chemical Society, Faraday Transactions 2: Molecular and Chemical Physics*. **74**: 367-379.
- Boutboul, A., Lenfant, F., Giampaoli, P., Feigenbaum, A., and Ducruet, V. (2002). Use of inverse gas chromatography to determine thermodynamic parameters of aroma–starch interactions. *Journal of Chromatography A*. **969**: 9-16.

- Brunauer, S., Emmett, P. H., and Teller, E. (1938). Adsorption of Gases in Multimolecular Layers. *Journal of the American Chemical Society*. **60**: 309-319.
- Chang, J.-H., An, Y. U., and Sur, G. S. (2003). Poly(lactic acid) nanocomposites with various organoclays. I. Thermomechanical properties, morphology, and gas permeability. *Journal of Polymer Science Part B: Polymer Physics*. **41**: 94-103.
- Corres, M. A., Zubitur, M., Cortazar, M., and Mugica, A. (2013). Thermal decomposition of phenoxy/clay nanocomposites: Effect of organoclay microstructure. *Polymer Degradation and Stability*. **98**: 818-828.
- Dennis, H. R., Hunter, D. L., Chang, D., Kim, S., White, J. L., Cho, J. W., and Paul, D. R. (2001). Effect of melt processing conditions on the extent of exfoliation in organoclay-based nanocomposites. *Polymer*. **42**: 9513-9522.
- Dyson, N. A. (1998). Chromatographic Integration Methods. Royal Soc of Chemistry.
- EC (2011). RECOMMENDATIONS: COMMISSION RECOMMENDATION of 18 October 2011 on the definition of nanomaterial (2011/696/EU). *Official Journal of the European Union*. **L 275**: 38-40.
- EFSA (2011). SCIENTIFIC OPINION: Guidance on the risk assessment of the application of nanoscience and nanotechnologies in the food and feed chain. *EFSA Journal*. **9**: 2140.
- Eltantawy, I. M., and Arnold, P. W. (1972). Adsorption of n-Alkanes by Wyoming Montmorillonite. *nature physical science*. **237**: 123-125.
- FDA (2012a). Draft Guidance for Industry: Assessing the Effects of Significant Manufacturing Process Changes, Including Emerging Technologies, on the Safety and Regulatory Status of Food Ingredients and Food Contact Substances, Including Food Ingredients that are Color Additives. FDA, Washington, DC, USA.
- FDA (2012b). Guidance for Industry Safety of Nanomaterials in Cosmetic Products. FDA, Washington, DC, USA.
- Filippi, S., Paci, M., Polacco, G., Dintcheva, N. T., and Magagnini, P. (2011). On the interlayer spacing collapse of Cloisite® 30B organoclay. *Polymer Degradation and Stability*. **96**: 823-832.
- Frenkel, D., and Smit, B. (2001). Understanding Molecular Simulation: From Algorithms to Applications. Elsevier Science.
- Gillet, G., Vitrac, O., and Desobry, S. p. (2009). Prediction of Solute Partition Coefficients between Polyolefins and Alcohols Using a Generalized Flory–Huggins Approach. *Industrial & Engineering Chemistry Research*. **48**: 5285-5301.
- Gillet, G., Vitrac, O., and Desobry, S. p. (2010). Prediction of Partition Coefficients of Plastic Additives between Packaging Materials and Food Simulants. *Industrial & Engineering Chemistry Research*. **49**: 7263-7280.
- Heinz, H., Koerner, H., Anderson, K. L., Vaia, R. A., and Farmer, B. L. (2005). Force Field for Mica-Type Silicates and Dynamics of Octadecylammonium Chains Grafted to Montmorillonite. *Chemistry of Materials*. **17**: 5658-5669.
- Heinz, H., and Suter, U. W. (2004a). Atomic Charges for Classical Simulations of Polar Systems. *The Journal of Physical Chemistry B*. **108**: 18341-18352.
- Heinz, H., and Suter, U. W. (2004b). Surface structure of organoclays. *Angewandte Chemie-International Edition*. **43**: 2239-2243.
- James, R. W. (1948). The Optical Principles of the Diffraction of X-rays. G. Bell and Sons.
- June, R. L., Bell, A. T., and Theodorou, D. N. (1990). Molecular dynamics study of methane and xenon in silicalite. *The Journal of Physical Chemistry*. **94**: 8232-8240.
- Kalambet, Y., Kozmin, Y., Mikhailova, K., Nagaev, I., and Tikhonov, P. (2011). Reconstruction of chromatographic peaks using the exponentially modified Gaussian function. *Journal of Chemometrics*. **25**: 352-356.
- Keldsen, G. L., Nicholas, J. B., Carrado, K. A., and Winans, R. E. (1994). Molecular modeling of the enthalpies of adsorption of hydrocarbons on smectite clay. *The Journal of Physical Chemistry*. **98**: 279-284.

- Khan, R. A., Dussault, D., Salmieri, S., Safrany, A., and Lacroix, M. (2013). Mechanical and barrier properties of carbon nanotube reinforced PCL-based composite films: Effect of gamma radiation. *Journal of Applied Polymer Science*. **127**: 3962-3969.
- Khan, S. U. (1975). Soil Organic Matter. Elsevier Science.
- Koh, H. C., Park, J. S., Jeong, M. A., Hwang, H. Y., Hong, Y. T., Ha, S. Y., and Nam, S. Y. (2008). Preparation and gas permeation properties of biodegradable polymer/layered silicate nanocomposite membranes. *Desalination*. **233**: 201-209.
- Koh, S.-M., and Dixon, J. B. (2001). Preparation and application of organo-minerals as sorbents of phenol, benzene and toluene. *Applied Clay Science*. **18**: 111-122.
- Lagaly, G., Ogawa, M., and Dekany, I. (2013). Chapter 10.3 Clay Mineral-Organic Interactions. **In**: Handbook of Clay Science, pp. 309-377. Bergaya, F., and Lagaly, G. (Eds.), Elsevier Science.
- Luetzow, M. (2012). State of the art on the initiatives and activities relevant to risk assessment and risk management of nanotechnologies in the food and agriculture sectors. Takeuchi, M., and Fukushima, K. (Eds.)FAO & WHO.
- Mackenzie, R. C., and Society, M. (1957). The differential thermal investigation of clays. Mineralogical Society (Clay Minerals Group).
- Mering, J., and Oberlin, A. (1967). Electron-Optical Study of Smectites. *Clays and Clay Minerals*. **15**: 3-25.
- Metropolis, N., Rosenbluth, A. W., Rosenbluth, M. N., Teller, A. H., and Teller, E. (1953). Equation of State Calculations by Fast Computing Machines. *The Journal of Chemical Physics*. **21**: 1087-1092.
- Monticelli, O., Musina, Z., Frache, A., Bellucci, F., Camino, G., and Russo, S. (2007). Influence of compatibilizer degradation on formation and properties of PA6/organoclay nanocomposites. *Polymer Degradation and Stability*. **92**: 370-378.
- Olphen, H. V. (1964). An Introduction to Clay Colloid Chemistry. *Soil Science*. **97**: 290.
- Osman, M. A., Mittal, V., Morbidelli, M., and Suter, U. W. (2003). Polyurethane Adhesive Nanocomposites as Gas Permeation Barrier. *Macromolecules*. **36**: 9851-9858.
- Osman, M. A., Mittal, V., and Suter, U. W. (2007). Poly(propylene)-Layered Silicate Nanocomposites: Gas Permeation Properties and Clay Exfoliation. *Macromolecular Chemistry and Physics*. **208**: 68-75.
- Park, Y., Ayoko, G. A., and Frost, R. L. (2011). Application of organoclays for the adsorption of recalcitrant organic molecules from aqueous media. *Journal of Colloid and Interface Science*. **354**: 292-305.
- Park, Y., Ayoko, G. A., Kurdi, R., Horváth, E., Kristóf, J., and Frost, R. L. (2013). Adsorption of phenolic compounds by organoclays: Implications for the removal of organic pollutants from aqueous media. *Journal of Colloid and Interface Science*. **406**: 196-208.
- Rodríguez, J. L. P. (2003). Applied Study of Cultural Heritage and Clays. Consejo Superior de Investigaciones Científicas.
- Sinha Ray, S., Okamoto, K., and Okamoto, M. (2003). Structure–Property Relationship in Biodegradable Poly(butylene succinate)/Layered Silicate Nanocomposites. *Macromolecules*. **36**: 2355-2367.
- Tan, W., Zhang, Y., Szeto, Y.-s., and Liao, L. (2008). A novel method to prepare chitosan/montmorillonite nanocomposites in the presence of hydroxy-aluminum oligomeric cations. *Composites Science and Technology*. **68**: 2917-2921.
- Tsipursky, S. I., and Drits, V. A. (1984). The distribution of octahedral cations in the 2:1 layers of dioctahedral smectites studied by oblique-texture electron diffraction. *Clay Minerals*. **19**: 177-193.
- Vitrac, O. a. G., Guillaume (2010). An Off-Lattice Flory-Huggins Approach of the Partitioning of Bulky Solutes between Polymers and Interacting Liquids. *International Journal of Chemical Reactor Engineering*. **8**.

- Widom, B. (1963). Some Topics in the Theory of Fluids. *The Journal of Chemical Physics*. **39**: 2808-2812.
- Wypych, F., and Satyanarayana, K. G. (2004). *Clay Surfaces: Fundamentals and Applications*. Elsevier Science.
- Xie, W., Gao, Z., Pan, W.-P., Hunter, D., Singh, A., and Vaia, R. (2001). Thermal Degradation Chemistry of Alkyl Quaternary Ammonium Montmorillonite. *Chemistry of Materials*. **13**: 2979-2990.

5.2.3 Applications for developing polymer nanocomposite systems

This work presented a significant collection of both experimental and simulated thermodynamic data of interactions between organic solutes and clays: isosteric heat of sorption from IGC determinations; sorption isotherm and isosteric heat from IGA experiments; Henry coefficients, sorption isotherm and isosteric heat from simulations. The most important factor is basal spacing which controls the entropic contribution on excess chemical-potentials. It was studied systematically mainly by simulation as it was not possible at infinite dilution of solute to change the arrangement of clays in commercial MMT. However, the comparison between pristine and organo-modified MMT at low and high solute concentrations (IGA experiments) offered possibilities to assess swelling effects and the competition between adsorbing substances.

It is worth to notice that no enthalpy-entropy compensation was revealed with sorption/adsorption, whereas it was very significant for the diffusion in bulk polymers. On one hand, it is shown that increasing d -spacing from a critical value (*i.e.* 2.2nm) does not change in a large extent net isosteric heat of sorption in good agreement with previous descriptions in the literature. On the other hand, Henry coefficients increase dramatically with d -spacing due to a lower entropy loss by condensation of vapors, which is associated to poorer conversions of free rotational and rotational degrees of freedom in surrounding gas into bound displacements onto the surface. In simple words, envisioning the gap between clays as a small gas reservoir lowers dramatically the affinity of solute vapors for the clays thought as a volume phase. In nanocomposite, the gap may be filled by polymer segments, surfactants or a combination of both. In commercially organo-modified MMTs, the excess of surfactants damages the enthalpy balance by lowering the favorable interactions with the clay+surfactant mixture. Calculations of excess mixing energies between tested solutes and considered surfactants demonstrate clearly that solute+surfactant energies dominate in organo-modified MMT.

With our goal of developing a barrier material using clays as nanoadsorbents, the picture of the best polymer-clay composite system gained by this study was expected to differ significantly from the commonly accepted strategies with similar systems. The discrepancies are highlighted in Table 5-10.

Table 5-10 Comparison of recommendations to develop Hybrid MMT-polymer composite systems according to processing and sorption properties.

	Conventional recommendations for nanocomposite systems	Recommendations issued from this study
Best MMT	Organo-modified MMT to facilitate dispersion in polymer	Pristine MMT to facilitate the accessibility to the clay surface
Optimal basal spacing of the clays dispersed in the polymer	Significant or total exfoliation (i.e. large basal spacing)	Partial intercalation with low basal spacing
Surface coverage of clays	Large surface coverage by surfactants or polymer segments	Maximizing free surface
Recommended surfactant	Polar ones	Non-polar or aromatic ones

5.3 Proof of the concepts of barrier materials including nano-adsorbents

5.3.1 Introduction

The strong deviations between conventional recommendations and those of this work suggested that accessible materials for testing the nano-adsorbent concepts would be significantly suboptimal. In particular, it was clear that the objectives of processability and affinity were significantly antagonist. By considering that full clay exfoliation and orientation were not necessary (particles do not require to be sheared), solution casting was the best commendable process for testing the concepts on simple nanocomposite systems. Two systems at both ends of proposed recommendations were chosen to test the proposed concepts of barrier materials, as reported in Table 5-11.

Table 5-11 Polymer-MMT nanocomposite systems used to test the concepts of barrier materials integrating nanoparticles

Systems	Test conditions	PRO	CON
SYSTEM 1: a low polar polyester containing organo-modified MMT	Polycaprolactone (PCL) $T = 298 \text{ K}$	Easy to process	Large crystallites affected strongly by the presence of nucleating agents
SYSTEM 2: a water-soluble polymer containing pristine MMT	plasticized polyvinyl alcohol (PVA) $T = 338\text{-}368 \text{ K}$	Easy to process, small crystallites (transparent materials)	Highly sensitive to relative humidity and consequently strong aging effect

Even if it is not essential in this study, it deserves to note that both polymers are biodegradable and are considered as poor barriers to organic substances in tested conditions. Reference materials were the same polymers without clays.

Barrier properties were tested against apolar and low polar substances used in sections 5.2.2 and 5.3.2 at infinite dilution and at different temperatures. The possible barrier improvements associated to the sole sorption effects should be envisioned as an effect of $K_{contrast}$ as defined in sections 5.2.2 and 5.3.2. The enthalpic interpretation of $K_{contrast}$ as a difference in excess mixing energies is illustrated in Figure 5-33. Best results are expected, when mixing is endothermic in one compartment and exothermic in the other, such as apolar

substance in nanocomposite systems including pristine MMT and polar polymer (see system 2 in Table 5-11).

$$K_{P/MMT}(T) = \exp\left(\frac{\Delta G}{RT}\right) = \exp\left(\frac{H_P - H_{MMT} - T(S_P - S_{MMT})}{RT}\right) = \underbrace{K_{P/MMT}^{enthalpy}(T)}_{\text{to be maximized...}} K_{P/MMT}^{entropy}$$

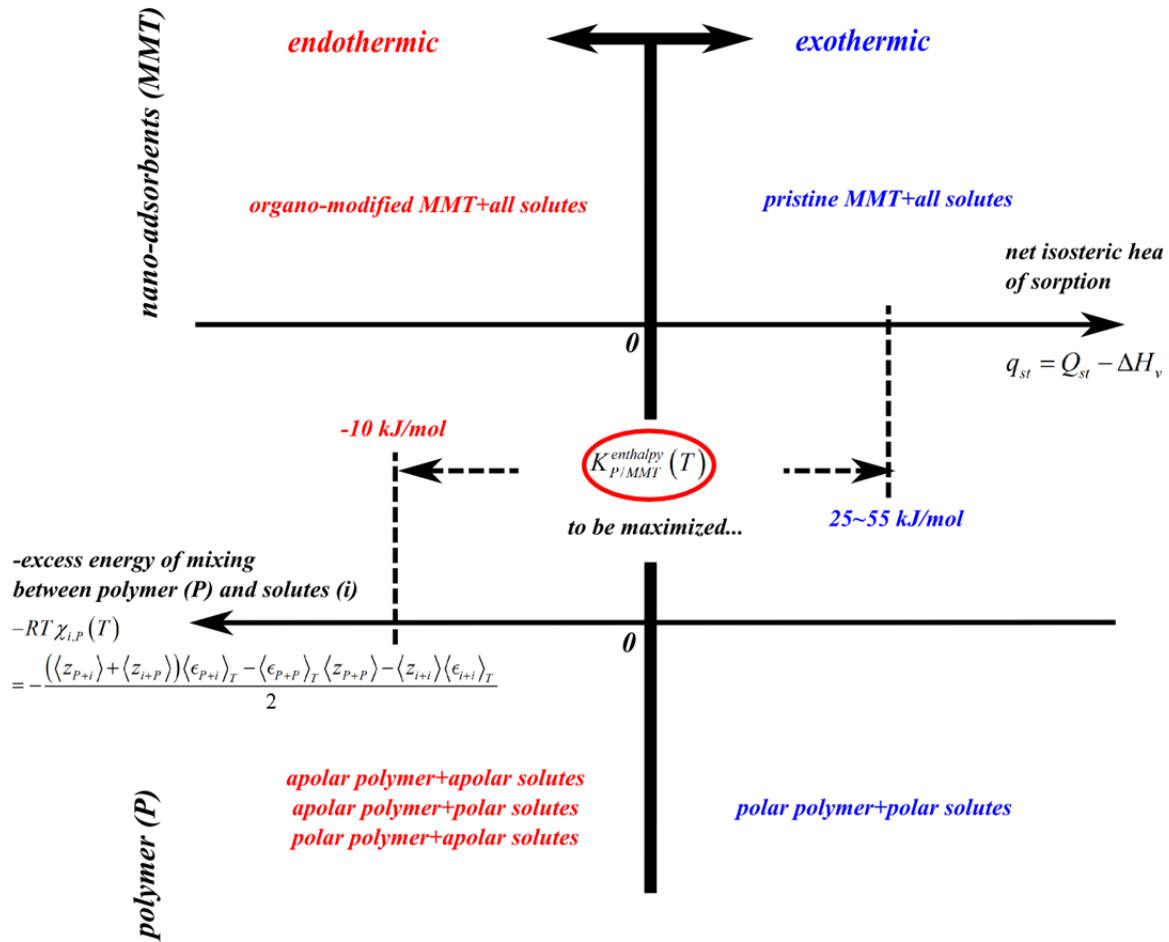


Figure 5-33 Energetic interpretation of $K_{contrast}$ in nano-adsorbent – polymer systems. Excess mixing energies are evaluated for a reference state of the considered solute at liquid state (or equivalent at molten state).

5.3.2 Experimental study and interpretation

Publication IV

Title: Controlling the molecular interactions to improve the diffusion barrier of biodegradable polymers to organic solutes above T _g
Authors: X. Fang, S. Domenek, and O. Vitrac
Submitted to: In preparation

Controlling the molecular interactions to improve the diffusion barrier of biodegradable polymers to organic solutes above Tg

Xiaoyi Fang^{1,2}, Sandra Domenek^{1,2}, Violette Ducruet^{2,1}, Olivier Vitrac^{2,1*}

¹AgroParisTech, UMR 1145 Ingénierie Procédés Aliments, F-91300 Massy, France

²INRA, UMR 1145 Ingénierie Procédés Aliments, F-91300 Massy, France

5.3.2.1 Abstract

The study presents a new concept of nanocomposite and selective barrier material, which can be combined together with conventional effects of obstruction. Its implementation found applications for biodegradable polymers but other application in synthetic ones and membrane technology could be also envisioned. It consists in dispersing nano-adsorbents optimized for the penetrant to be blocked. Contrary to the common thinking, it is demonstrated that sorption properties and diffusion coefficients could be combined at microscopic scale to induce a diffusion process with heterogeneous dynamics and consequently lower diffusion coefficients (D). D reductions are scaled as $1/(1+K_{contrast}(T))$, where $K_{contrast}(T)$ is the effective partition coefficient of solute between the adsorbents and the polymer. In the case of positive excess chemical potential in favor of the nano-adsorbents, $K_{contrast}(T)$ can be controlled by temperature. The barrier concepts were experimentally probed on two aromatic solutes (*i.e.* biphenyl and *p*-terphenyl) in two extreme systems involving the solution casted polymers incorporated by montmorillonites (MMT) as nano-adsorbents: system 1 is organo-modified MMT in polycaprolactone (PCL), system 2 is pristine MMT in polyvinyl alcohol (PVA). Only system 2 showed a strong D reduction up to one decade. Since the D reduction was found varying with temperature and basal spacing of MMT, the solute molecule trapping was controlled by both enthalpy and entropy effects.

5.3.2.2 Introduction

Environmental issues encourage the use of biodegradable or biosourced polymers¹ and their nanocomposite versions to reach appropriate performances²⁻⁷ for food contact applications. Currently available biodegradable polymers rely mainly on polyesters, which exhibit limited resistance to water (*e.g.* coming from food or from the storage ambiance) and to organic substances such as those originating from food products (*e.g.* aroma, fat)^{6,8-11}. It is worth to notice that these drawbacks occur also with different extents in synthetic polymers¹². Similarly, environment-friendly materials or not tend to leach their organic content with molecular weight lower than 10^3 g·mol⁻¹ as a consequence of local phase separation^{13,14} or

diffusion of non-covalently bounded substances such as additives, oligomers and residues¹⁵. Due to a multiplication of crises involving packaging materials¹⁶⁻²¹, innovations in materials, which lead to lower migration and/or food contamination should be also encouraged^{22,23}. Without underestimating that nanocomposite systems may have their own safety issues due to their nanoform or residue content²⁴, nanocomposite materials offer good opportunities to block not only water and oxygen but also organic substances in particular in rubber materials with high intrinsic permeabilities. One may note also that such developments found earlier applications in hybrid membrane technologies²⁵.

Most of the literature reports that barrier effects due to nanoparticles have been associated to obstacle effects possibly combined with nucleating effects affecting crystal growth and morphology^{7,26-32} with performances, which do not exceed a factor five reduction³³⁻³⁵. Insufficient orientation or density of obstacles are usually the main arguments advanced for the low barrier enhancement achieved in most applications. By considering platelets (*i.e.* nematic phase) as inclusions perpendicular to main fluxes,³⁶ hypothesized from a large set of detailed finite-element simulations that the permeability reduction should be scaled as a stretched exponential, such as $P/P_0 = \exp\left(-(x/3.47)^{0.71}\right)$, where x is the product of platelet aspect ratio by their volume fraction. As a result, gaining reductions lower than 0.1 based on sole obstacle effects would require x values larger than 11.2 that is for example for perfectly oriented clays: an aspect ratio of 500 for a volume fraction of 0.023. Any deviation of previous parameters to nominal values or orientation is expected to damage irreversibly the barrier properties so that the interest of such applications can be really challenged³⁷. The situation appears all the more complicated that free-volume measurements showed evidences of an enhancement of the transport of penetrants around particles due to dedensification of the polymer nearby^{38,39}.

Technological alternatives are scarce but they can be categorized into reactive systems or active systems. The first one has been reviewed by^{40,41} and consists in using a chemical reaction to block/scavenge irreversibly the penetrant. As discussed in⁴², there are limited to gas scavenging applications (oxygen, carbon dioxide, ethylene) for packaging applications. Active barrier systems have not been theorized yet for barrier materials but the concept is well established in catalysis involving physisorption⁴³, which can be also seen as an extension of reactive systems where the reaction is reversible^{40,41}. The mass conservation in the conventional solubilization-diffusion model^{44,45} is modified to integrate partitioning effects between⁴⁶ the continuous phase and the “active” surface of the catalyst:

$$\left\{ \begin{array}{l} \frac{\partial C}{\partial t} = \nabla \cdot \left(\frac{D_0(C)}{1 + K_{contrast}} \nabla C \right) \\ \text{with } K_{contrast} = \frac{k_{sorption}}{k_{desorption}} \\ s + A \xrightarrow{k_{sorption}} [sA] \xrightarrow{k_{desorption}} s + A \end{array} \right. \quad (5-55)$$

where C is the concentration, D_0 is the concentration in the bulk polymer, $K_{contrast}$ is the equilibrium constant or equivalently the partition coefficient between adsorbed/absorbed penetrants and “free” ones. In the equivalent reaction scheme, A is the adsorbent and s is the diffusing solute. The generalization of Eq. (5-55) to inclusions, where absorption replaces adsorption can be found in ⁴⁷. All models predict a strong decrease of effective diffusion coefficient, $D_{eff}=D_0/(1+K_{contrast})$ in Eq. (5-55), as soon as the chemical affinity is stronger for the dispersed phase/inclusion than for the continuous polymer phase. As the trapping effect is controlled by thermodynamics, it presents several advantages over pure obstacle effects: it does not depend on the orientation of particles and may be very effective at very low concentration; the blocking effect could be modulated by changing the temperature (e.g. the effect disappears when temperature is increasing when sA mixing energies are significantly exothermic); the blocking may be very effective for one solute and not for another. Without excluding other effects, substantial experimental proofs of the presented concept has been recently supplied by the dramatic blocking of n -alkyl acetates in poly(methyl acrylate) by spherical small silica particles ⁴⁸.

The general goal of this work is to propose a technological route to design new barrier materials including specifically optimized nano-adsorbents and ore generally called “chaotic materials” as they aim to hinder diffusion by modifying microscopically the energy surface onto which solutes translate. In this work, we called “barrier material” a system which induces a significant lag time to diffusion. The consequences about effective sorption are not considered in this work as it has been shown by kinetic Monte-Carlo simulations that D reductions were a consequence of the fluctuations of the energy barriers opposed to the diffusion and not of the average solubility ^{49,50}. We propose to explore the concepts experimentally and theoretically to block the diffusion of organic substances in rubber polymers at infinite dilution. The exploration of such phenomena is currently possible to the development of tailored methods for calculating excess chemical potentials in polymers ⁵¹⁻⁵³ and at the surface of nanoparticles such as clays ⁵⁴. It is important to note that thermodynamically-controlled blocking effects can be easily separated from obstruction ones by comparing the barrier performances at different temperatures or for a homologous series of

solutes. Indeed, the excess of activation energies or additional mass dependence could be compared and analyzed from extended free-volume theories or scaling relationships⁵⁴⁻⁵⁶.

The paper is organized in five sections. Through different theoretical examples, section two extends the common concept of tortuosity to the more general one of spatial and time correlations. In particular, that diffusion hindering due to spatial heterogeneities or heterogeneous dynamics can be combined together and cumulated to reach stronger diffusion blocking. Section three presents the systems considered in this work and the methodologies used to assess $K_{contrast}$ on real systems. Two extreme hybrid systems were considered to assess the barrier properties to apolar or low polar diffusants (*n*-alkanes, a short series of oligophenyls, methoxybenzene). The first system was an apolar polymer polycaprolactone (PCL) incorporating organo-modified montmorillonites (MMT) by casting. The second system consisted in pristine MMT mixed also by casting with a polar polymer polyvinyl alcohol (PVA). Besides their differences in polarities, the tested polymers exhibit different sensitivity to nucleation due to the incorporation of nanoparticles. The last section summarizes the findings and proposes additional optimization directions.

5.3.2.3 Theory of polymer barrier materials

The considerations described in this section were motivated by the observations of Watanabe⁵⁷, which state that macroscopic concepts of diffusion and sorption could not be transposed at low scale without significant precaution. Although it is well established that random walks around particles follow well the Smoluchowski equation, the continuous approach is only true after sufficiently many jumps or after a time much longer than a jump itself. In the vicinity of inclusions, the reality may be different and may lead to new properties. Detailed theoretical considerations can be found in reference text book of Klages⁵⁸ or in the general modeling of⁵⁹. In simple words, heterogeneities in space (obstacles) induce tortuosity effects (oppose to the growth of the mean-square-displacement of the diffusant) whereas fluctuations of interactions with the host environment cause heterogeneous dynamics and therefore additional dwelling times between hopping events.

5.3.2.3.1 Beyond tortuosity concepts.

According to literature, two effects independent of polymer chemical structure are known to impart D in solids: tortuosity⁶⁰ and local distribution of free energies^{50,58}. Tortuosity is a

qualitative concept derived from porous media and defined as the scaling coefficient ξ^2 between a medium without obstacle, D_0 , and with obstacles D :

$$\xi^2 = D_0/D \geq 1 \quad (5-56)$$

As reviewed in ⁶⁰, tortuosity increased with the volume fraction of obstacles. In thermoplastics, obstacles can be extraneous particles (e.g. nanofillers) or the polymer itself as crystallites are usually inaccessible to penetrants. It has been thus shown that 25 nm size scale discoid crystallites obtained by confined crystallization of poly(ethylene oxide) lead to τ^2 values up to 100 ⁶¹. This work examines an approach that could lead theoretically to similar D reduction as shown by Kinetic Monte-Carlo simulations ⁵⁰ by introducing strong fluctuations of the chemical affinity within the polymer matrix. The presence of attractors introduces correlation in diffusants trajectories that lower diffusion coefficients between times scales t_0 and $t=2^k t_0$, where k is a positive integer. Indeed, the effect of additional zigzags in the random walk of diffusants must be envisioned as negative correlations impeding the mean square displacements, $\left\langle \mathbf{r}(\tau, 2^k t_0) \cdot \mathbf{r}(\tau, 2^k t_0) \right\rangle_{\text{all } \tau}$:

$$\begin{aligned} \left\langle \mathbf{r}(\tau, 2^k t_0) \cdot \mathbf{r}(\tau, 2^k t_0) \right\rangle_{\text{all } t} &= 2 \left\langle \mathbf{r}(\tau, 2^{k-1} t_0) \cdot \mathbf{r}(\tau, 2^{k-1} t_0) \right\rangle_{\text{all } \tau} (1 + \cos \theta_{k-1}) \\ &= 2^k \left\langle \mathbf{r}(\tau, t_0) \cdot \mathbf{r}(\tau, t_0) \right\rangle_{\text{all } \tau} \prod_{i=0}^{k-1} (1 + \cos \theta_i) \end{aligned} \quad (5-57)$$

where $\mathbf{r}(\tau, 2^k t_0)$ is the displacement at time τ during the time lag (also-called diffusion time) $t = 2^k t_0$; $\cos \theta_i$ is the averaged angle between displacements observed at time scale $2^i \tau$. Operators $\left\langle \right\rangle_{\text{all } \tau}$ and \cdot denote ensemble average over all possible starting times and scalar product. By noticing for sufficiently large i that $D(2^i t_0) \simeq \frac{1}{6} \left\langle \mathbf{r}(\tau, 2^i t_0) \cdot \mathbf{r}(\tau, 2^i t_0) \right\rangle / 2^i t_0$, one gets finally:

$$\frac{1}{k \ln 2} \sum_{i=0}^{k-1} \ln(1 + \cos \theta_i) = \int_{t_0}^{2^k t_0} \left(\frac{d \ln \left\langle \mathbf{r}(\tau, t) \cdot \mathbf{r}(\tau, t) \right\rangle_{\text{all } \tau}}{d \ln \tau} - 1 \right) d\tau \simeq \ln \frac{D(t = 2^k t_0)}{D(t_0)} \quad (5-58)$$

where $\mathbf{r}(t, \tau)$ is the displacement vector between t and $t+\tau$, $\cos \theta_i$ is the averaged angle between displacements observed at time scale $2^i \tau$.

Similarities between Eqs. (5-56) and (5-58) show that tortuosity can be interpreted as correlated motions (with negative correlations). In addition, Eq. (5-58) highlights that

tortuosity (obstruction) and attraction (preferred sorption) effects can be combined together in chaotic materials on several time scales by accumulating correlations on a log-time scale (conditions of pink noise) to reduce macroscopic (long-term) D values.

5.3.2.3.2 Reduction of D due to asymmetric barriers to translation: a two states toy model.

From previous considerations, obstacles are special cases of regions separated by infinite energy barriers. An interesting alternative is to assess transport when accessible regions are separated by an asymmetric barrier as it could be envisioned between a polymer, denoted P, and nano-adsorbents, denoted as MMT. The corresponding one-dimensional periodic free energy profile is depicted in Figure 5-34. In the framework of the transition state theory, such a toy model has an analytical solution at thermodynamic equilibrium when

$$p_{eq}^{MMT} k_{MMT \rightarrow P} = p_{eq}^P k_{P \rightarrow MMT} :$$

$$2D = l^2 k_{MMT \rightarrow P \rightarrow MMT} = \frac{k_0 l^2}{\frac{K}{\exp\left(-\frac{G_\Delta}{RT}\right)} + \frac{1}{\exp\left(-\frac{G_\Delta}{RT}\right)}} = \frac{k_0 l^2}{1 + K_{contrast}} \exp\left(-\frac{G_\Delta}{RT}\right) = \frac{D_0}{1 + K_{contrast}} \exp\left(-\frac{G_\Delta}{RT}\right) \quad (5-59)$$

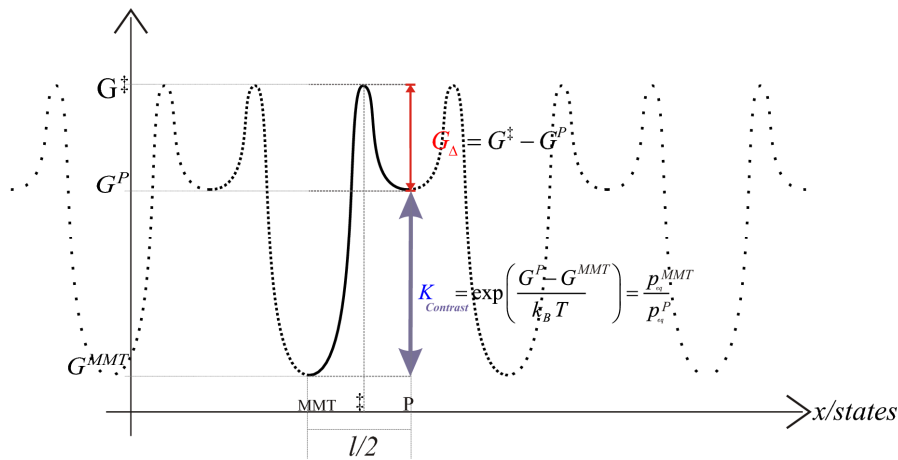


Figure 5-34 One-dimensional periodic free energy profile including two states: MMT and P separated by a transition state denoted ‡.

For a given solute i , Eq. (5-59) predicts in particular a strong reduction of macroscopic D according to the partitioning of i between MMT and P:

$$K_{i,contrast}(T) = \frac{C_{i,MMT}}{C_{i,P}} = \frac{K_{i,P}}{\langle K_{i,MMT} \rangle_{dspacing}} = \exp\left(\frac{\mu_{i,P}^{ex} - \mu_{i,MMT}^{ex}}{RT}\right) = \frac{\gamma_{i,P}(T)}{\gamma_{i,MMT}(T)} \quad (5-60)$$

ratio of concentrations

difference in excess chemical potentials

ratio of activity coefficients

where C and K is solute concentration and its henry coefficients in polymer (P) or clay (MMT). μ and γ are excess chemical potential and the activity coefficients with same notation as C .

$K_{contrast}$ could be written also by extrapolate from a volatile solute, $K_{i,contrast}^{volatile}(T)$, to a non-volatile one, $K_{i,contrast}^{non-volatile}(T)$:

$$K_{i,contrast}^{non-volatile}(T) = K_{i,contrast}^{volatile}(T) \exp\left(\frac{\Delta H^{non-volatile} - \Delta H^{volatile}}{RT}\right) \quad (5-61)$$

where ΔH is the difference of excess energy of mixing between P and MMT for non-volatile or volatile solute.

5.3.2.3.3 Inverse gas chromatography (IGC) as a one-dimensional physical model.

By accepting to replace the polymer P by a carrier gas ($G_A \rightarrow 0$), the situation described in Figure 5-34 is almost fulfilled in inverse gas chromatography (IGC) in steady state, as shown in Figure 5-35. The residence time of each solute at any sorption site depends strongly whether it interacts or not with the solid in the column. The whole process is described as a jumping process with frequencies k_g , k_a and k_d and corresponding mass fluxes, f_g , f_a and f_d . The micro-reversibility at the scale of the adsorption site (condition of local thermodynamic equilibrium) enforces $f_a = f_d$. The effective residence time is averaged between dwelling times of adsorbed and non-adsorbed populations as:

$$t_R^{site} = \frac{1}{k_g} \frac{c_g k_g}{c_g (k_g + k_a)} + \left(\frac{1}{k_d} + \frac{1}{k_g}\right) \frac{c_g k_a}{c_g (k_g + k_a)} = \frac{1}{k_g + k_a} \left(1 + \frac{k_a}{k_d} + \frac{k_a}{k_g}\right) \quad (5-62)$$

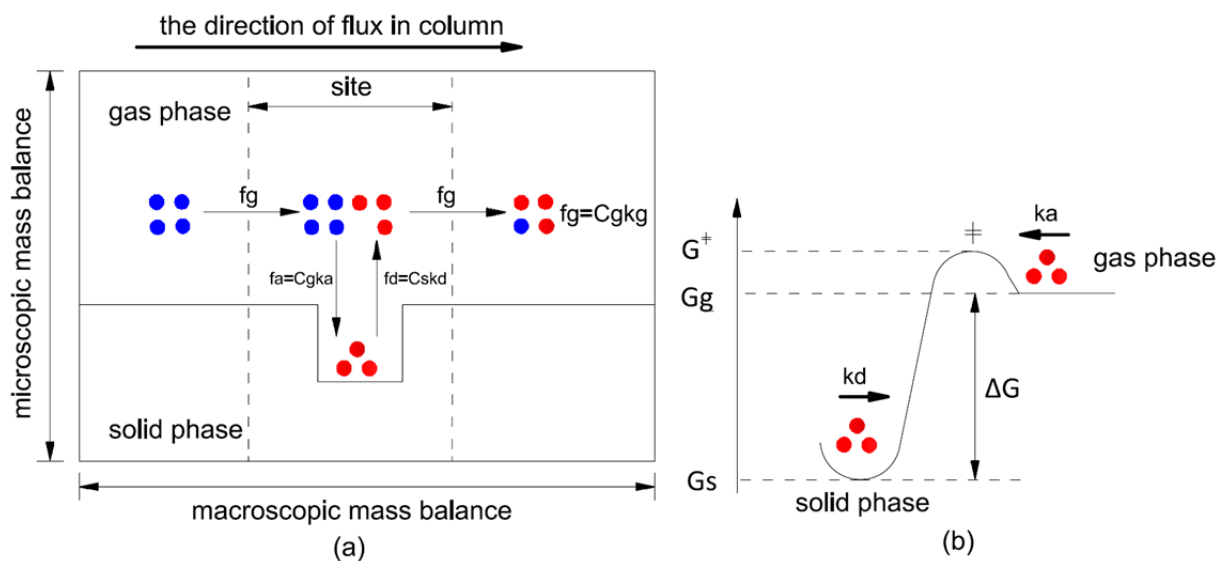


Figure 5-35 (a) Mass transfer description at one adsorption site within the column of IGC. The longitudinal direction represents a macroscopic transport along the column, while the transverse direction details the mass balance at molecular scale. (b) Corresponding free energy distribution in the process of desorption (note that $G_{\Delta} \rightarrow 0$).

By noticing that $k_g \gg k_a$, $k_g \gg k_d$ hold between a solid and gas carrier, the total retention time in column including N sorption sites becomes:

$$t_R = \sum_{i=1}^N t_R^{site} = \frac{N}{k_g} \left(1 + \frac{k_a}{k_d} \right) = t_R^{ref} \left(1 + \frac{k_a}{k_d} \right) \quad (5-63)$$

with t_R^{ref} being the residence time for a solute non-interacting with the surface but possibly subjected to tortuosity effects in the column. Additional arrangements enable to infer $\gamma_{i,MMT}(T)$ (required in Eq. (5-60)) from the definition of the partitioning of solute i between the gas phase and the solid:

$$K_{i,g/MMT}(T) = \exp\left(\frac{G_g - G_{MMT}}{RT}\right) = \frac{\gamma_{i,MMT}}{\gamma_{i,g}} = \frac{P_i^{sat} V_i}{RT} \gamma_{i,MMT} = \frac{t_R^{ref}(T)}{t_R(T) - t_R^{ref}(T)} = \frac{1}{t_R^*(T)} \quad (5-64)$$

where P_i^{sat} and V_i being respectively the saturation vapor pressure and the molar volume of the solute i . As shown in Eq. (5-60), Eq. (5-64) predicts strong increase of normalized retention times $t_R^*(T)$ when the chemical affinity increases for the solid.

5.3.2.3.4 *D reduction due to entropic trapping: a first approach*

Entropic trapping can be envisioned when the molecule gets temporarily sorbed in a large cavity, where it can maximize its conformational entropy. In this case there is no energy barrier but the reverse desorption process is affected by low probability to get a favorable conformation/configuration which authorizes an escape. The resulting heterogeneous Poissonian dynamics may affect significantly random walks as analyzed in ⁶². Such effects can be appraised via the Green-Kubo relation:

$$\frac{d}{dt} \langle \mathbf{r}(\tau, t) \cdot \mathbf{r}(\tau, t) \rangle_{all t} = 2 \int_0^t \left\langle \frac{d\mathbf{r}}{d\tau}(\tau + \kappa) \cdot \frac{d\mathbf{r}}{d\tau}(\tau) \right\rangle_{all \tau} d\kappa = 2 \int_0^t \langle \mathbf{v}(\tau + \kappa) \cdot \mathbf{v}(\tau) \rangle_{all \tau} d\kappa = 6D(t) \quad (5-65)$$

When diffusant velocity correlation obeys to a linear damping law with a time constant t_0 , $D(t)$ increases as $D(0)(1 - \exp(-t/t_0))$. In presence of trapping, the variation is opposite and D is found decreasing. Following the same ideas of ⁶³, one convenient picture is to think about a

point particle undergoing a true random walk (non-correlated motions) within an empty sphere (geometrical constraints). The particle is expected to collide periodically with the wall so that velocity will appear opposite as depicted in Figure 5-36b). In practice no starting time needs to be privileged (stationary condition) and the time interval between two collisions is consequently given by the ratio between the sphere diameter and the particle velocity. For a true random walk, impinging times obeys to the reciprocal Maxwell-Boltzmann distribution depicted in Figure 5-36a). The corresponding velocity correlation functions and D variations are plotted in Figure 5-36c) and d) respectively. It is worth to notice that the limit D value goes down to zero for a perfectly trapped molecule. As molecules are non-permanently trapped in IGC, the effect of dragging (as performed in IGC) is also represented by introducing an asymmetric trapping (periods with positive correlations are 5% longer than with negative correlations). In the latter case, the variation of D is non-monotonous and dragging dominates long-term transport.

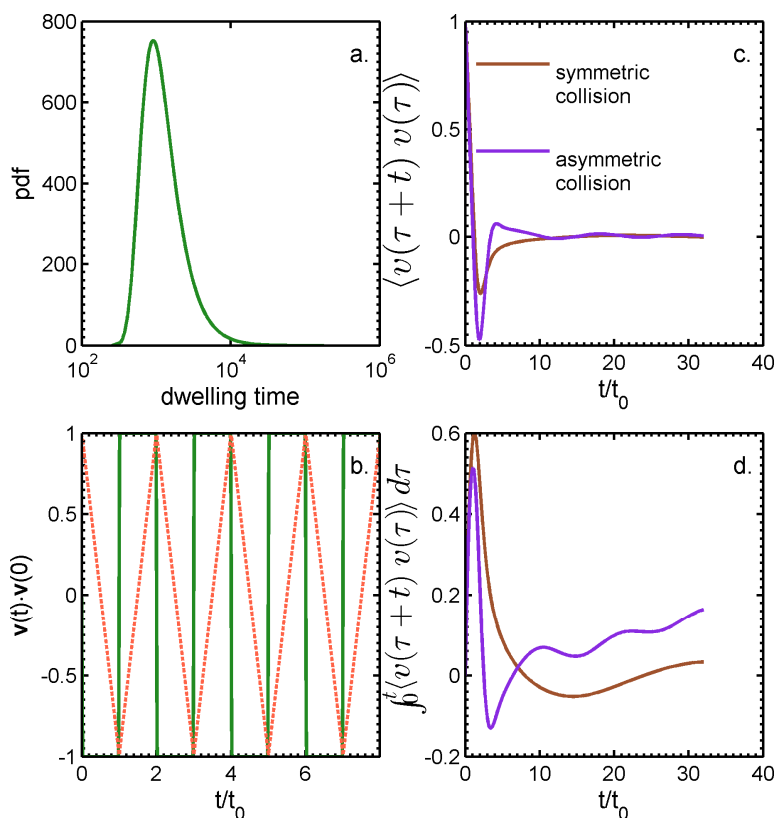


Figure 5-36 Dynamics of a particle moving randomly within a sphere. (a) Distribution of collision times (reciprocal of a Maxwell-Boltzmann distribution). (b) Velocity correlations for a particular starting position (continuous line) and averaged over all possible starting times (dashed line). (c) Velocity correlations averaged all collision intervals. (d) Corresponding $3D(\tau)$ values.

Concepts of correlations used in Eq. (5-58) can be also transposed to Eq. (5-65) by noticing that the friction coefficient ξ appearing in the Einstein scaling of diffusion $D = \Gamma \frac{RT}{\xi}$ accepts an interpretation as a memory function in Langevin equation, where R is the ideal constant gas, T the absolute temperature and Γ a thermodynamic correction factor. Indeed, one gets:

$$\frac{d}{dt} \left\langle \mathbf{v}(\tau + \kappa) \cdot \mathbf{v}(\tau) \right\rangle_{\text{all } \tau} = - \int_0^t \xi(t - \kappa) \left\langle \mathbf{v}(\tau + \kappa) \cdot \mathbf{v}(\tau) \right\rangle_{\text{all } \tau} d\kappa \quad (5-66)$$

5.3.2.4 Materials and methods

5.3.2.4.1 Polymer and nano-adsorbents.

10 to 50 μm thick of PCL and PVA films and their nanocomposite including one type of montmorillonites (MMT) (concentrations ranging from 0.5 to 5%wt) were processed by solution casting as described in ^{64,65} respectively. The characterizations of tested samples are listed in Table 5-12.

Table 5-12 Characteristics of samples prepared. Suppliers: A= Creagif Biopolymères (France); B= Süd Chemie (Germany) and C=Sigma Aldrich (France)

	<i>sample</i>	<i>T_g</i> (°C)	<i>Crystallinity</i> %	<i>type of clay</i> (<i>clay content</i>)	<i>type of surfactant at</i> <i>clay surface</i>	<i>Polymer</i> <i>/MMT</i> <i>suppliers</i>
Apolar polymer + apolar adsorbents	PCL	-60	55	N/A	N/A	A
	PCL+C6H5MMT	-60	49	C6H5MMT (0.5~5wt%)	dimethyl, benzyl(hydrogenated tallow)alkyl ammonium	A/B
	PCL+C18OHMMT	-60	48	C18OHMMT (0.5~5wt%)	methyl dihydroxyethyl hydrogenated tallow ammonium	A/C
	PCL+C18MMT	-60	48	C18MMT (0.5~5wt%)	octadecylamine	A/C
polar polymer + polar adsorbents	PVA	55 82	50	N/A	N/A	C
	PVA+MMT	55 82	50	MMT (5wt%)	N/A	C/C

T_g of PVA were of 82°C and of 55°C, at dry state and when the films were equilibrated at a relative humidity of 28% respectively.

5.3.2.4.2 Solute probes

The thermodynamic properties of polymer and nano-adsorbents are tested by a homologous series of volatile *n*-alkanes from C5 to C9 and two aromatic compounds: toluene and anisole (*i.e.* methoxybenzene). The diffusion coefficients in polymer and nanocomposite systems are measured by aromatic solutes including biphenyl and *p*-terphenyl. All substances were supplied by Sigma-Aldrich (Germany) with HPLC grade.

5.3.2.4.3 Estimation of $\gamma_{i,MMT}(T)$

IGC was combined with Eq. (5-64) to derive activity coefficients for volatile solutes: *n*-alkanes (from pentane to nonane), toluene and anisole (see Eq. (5-67)) in pristine and organo-modified MMT. Deactivated glass columns filled with each type of MMT were placed in a Carlo Erba 6000 Vega II gas chromatograph with nitrogen as gas carrier. Retention times were measured at temperatures ranging between 313 and 413 K by means of a flame ionization detector subsequently to an injection of 0.02 μl of pure solute with a nitrogen gas flow rate of 5-20 $\text{ml}\cdot\text{min}^{-1}$.

$$\gamma_{i,MMT} = \frac{RT}{t_R^*(T)P_i^{sat}(T)V_i} \quad (5-67)$$

Since experimental values could be obtained at different temperatures from those used for the determination of diffusion coefficients, an extrapolation was carried out by using the net isosteric heat of sorption: $q_{i,st} = -R \partial \ln \gamma_{i,MMT} / \partial (1/T) \Big|_{\text{infinite dilution}} - \Delta H_{i,vap}$, where $\Delta H_{i,vap}$ is the latent heat of vaporization of the solute *i*. q_{st} is expected to be positive in presence of an excess of attractive forces on MMT surface in comparison to the pure liquid state of the solute.

For non-volatile solutes such as biphenyl and *p*-terphenyl, the activity coefficients could not be determined by IGC experiments. The values were estimated from molecular simulations using the same particle insertion method and clay gallery as detailed in⁵⁴. Activity coefficients in pristine MMT were extracted from the estimations of Henry coefficients at the desired temperature averaged over the distribution of basal spacing (*d*) of MMT reported in⁵⁴ as:

$$\gamma_{i,MMT} = \frac{\langle K_H \rangle_{spacing}}{P_i^{sat}(T)V_i} \quad (5-68)$$

As discussed by⁵⁴, the calculated Henry coefficients for the same solutes at a certain temperature could vary significantly with the basal spacing (denoted as *d*-spacing in the rest of the paper). According to the XRD determination of basal spacing distribution in Fig. 4 of⁵⁴,

d -spacing ranging from 1.2 to 2.2nm were used to calculate K_H for pristine MMT dispersed in dry PVA. For the case of highly intercalated MMT in wet PVA, the reported values close to 2.2nm^{66,67} were chosen.

5.3.2.4.4 Estimation $\gamma_{i,P}(T)$ by a generalized off-lattice Flory-Huggins method

Activity coefficients of tested solutes in amorphous regions of PCL and PVA were calculated from Boltzmann-averaged pair energy contacts, denoted, $\langle \epsilon_{A+B} \rangle_T$, and from averaged number of neighbors in contact, $\langle z_{A+B} \rangle$ ⁵¹⁻⁵³:

$$\gamma_{i,P}(T) = \exp(1 + \chi_{i,P}(T)) = \exp\left(1 + \frac{(\langle z_{P+i} \rangle + \langle z_{i+P} \rangle) \langle \epsilon_{P+i} \rangle_T - \langle \epsilon_{P+P} \rangle_T \langle z_{P+P} \rangle - \langle z_{i+i} \rangle \langle \epsilon_{i+i} \rangle_T}{2RT}\right) \quad (5-69)$$

Sampling was performed from a set of 10^4 conformers generated by molecular dynamics. Polymers were replaced oligomers with non-contact tail and head atoms. The number of monomers was chosen to minimize the sampling bias: $\langle z_{P+i} \rangle \langle \epsilon_{P+i} \rangle_T - \langle z_{i+P} \rangle \langle \epsilon_{P+i} \rangle_T$.

5.3.2.4.5 Diffusion coefficient (D) determinations.

D values of aromatic solutes, biphenyl and p-terphenyl, were obtained by using a modified Roe⁶⁸ method involving 12 virgin films and two source films in positions 5 and 10. Depending on the solubility of probe solutes in casting solvent, the source films were either formulated by directly dissolving probe solutes in polymer solution with concentration of 0.2wt% or by soaking virgin films in a 0.05g·ml⁻¹ solute-ethanol solution during a minimal duration of one week at 60°C. After contact times ranging between 20 min to several days according to the diffusion coefficients, the bulk concentration in each film was measured by UV absorption subsequently to a complete film dissolution in dichloromethane. D values were identified by fitting simulated profiles to experimental ones. Our simulations relied on the 1D resolution of a diffusion equation for impervious boundary conditions by a finite-volume method.

The values of D determined at temperature T were compared to $1/(1+K_{contrast}(T))$ by approximating $K_{contrast}$ for solute i and a basal d -spacing d from Eqs. (5-68)-(5-69) as:

$$K_{i,contrast}^{(T,d)} = \frac{\gamma_{i,P}}{\gamma_{i,MMT}^{(T_0,d)} \exp\left(\frac{q_{i,st}}{RT} \left(\frac{1}{T_0} - \frac{1}{T}\right)\right)} \approx \frac{\exp(1 + \chi_{i,P})}{\langle \gamma_{i,MMT}^{(T,d)} \rangle_{all d}} \quad (5-70)$$

Eq. (5-70) highlights that $K_{contrast}$ is increasing with decreasing of temperature if $q_{i,st}$ value is positive.

5.3.2.5 Results and discussion

5.3.2.5.1 Effect of crystallite morphology on diffusion coefficients

Since the pioneering work of⁶⁹ crystallites in semicrystalline polymers are known to decrease diffusion coefficients by increasing tortuosity in the polymer matrix. In order to separate the solely “nano” effect from it induced changes in crystalline morphology on diffusion coefficients, PCL films were casted on both glass and Teflon surface with controlled solvent vaporization speed to form different size of crystallite while keeping the crystallinity degree constant⁷⁰ (see Table 5-12). As shown in Figure 5-37, the maximum reduction of diffusion coefficients in PCL films could reach 2.33 times by increasing the size of crystallites from less than 1 μm to 25 μm . To prove efficiency of nano-adsorbents on D reduction, this factor needs therefore to be taken into account.

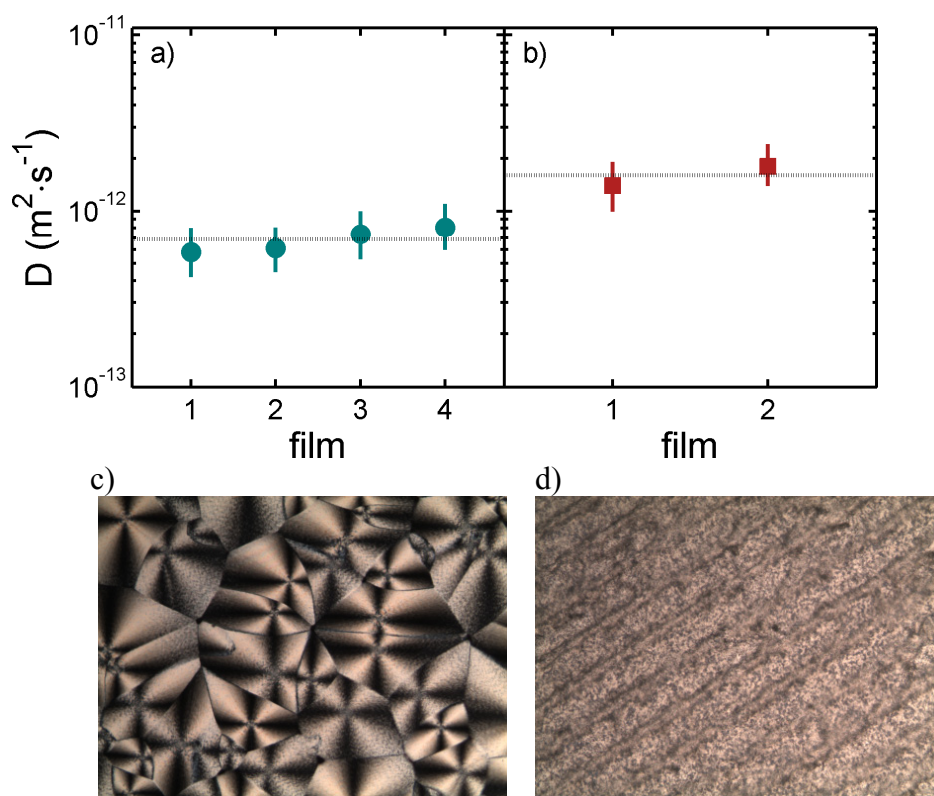


Figure 5-37 The diffusion coefficients of PCL films casting a) on a glass surface with and b) on a Teflon surface with close crystallinity degree of 55% and c)-d) the corresponding crystallite morphology in two PCL films. Pictures above depict the size of crystallites by polarized light microscopy (width=100 μm).

5.3.2.5.2 Partitioning between nanoclays and amorphous regions of PCL and PVA.

According to Eqs (5-59), (5-60) and (5-61), an improvement of barrier properties can be expected only if the chemical affinity is significant for a solute at the surface of nanoclays

than that in amorphous regions of the polymer. In another words, the value of $K_{contrast}$ has to be much higher than 1 to realize a significant reduction of D . Figure 5-38 and Figure 5-39 summarize both experimental and simulation values and show that the sorption of both polar and apolar solute in polymers including PCL and PVA are endothermic without varying significantly with solute size. In simple words, energy is required to create a cavity that enables the sorption of an organic solute. By contrast, adsorption becomes slightly exothermic at the surface of organo-modified MMT with the increasing solute size and is significant at the surface of pristine MMT due to favorable chemical interactions.

It has been reported in several papers that the pristine MMT possess much higher surface energy compared with organo-modified ones^{71,72}, which has been applied in nanocomposite systems to help polymer chains penetrate into clay gallery and form a good exfoliation and dispersion. However, even the adsorption mechanisms and models between organic solutes and clay surface are well explained and discussed in⁷³, very few experimental data of excess energy of mixing of homologous series of solutes on clay surface are reported..

Based on our experimental observations, it is worth to notice that the attractive interactions tended to be higher for the pair of pristine MMT with increasing size of solute or solute with phenyl rings (*e.g.* toluene). Consequently the $K_{contrast}$ calculated from Eq. (5-60) is significant in PVA nanocomposite systems containing pristine MMT as nano-adsorbents, which makes this system more promising for D reduction. As the interactions between solutes and clay surface are dominated by van-der-Waals forces, partitioning in favor of pristine MMT decreases dramatically when temperature increases (see Figure 5-39b)), which reduces $K_{contrast}$ values. In contrast, low $K_{contrast}$ (*i.e.* ≤ 1) in PCL nanocomposite systems were observed for all tested solutes, which implies that the tortuosity effect would dominates the reduction of D values.

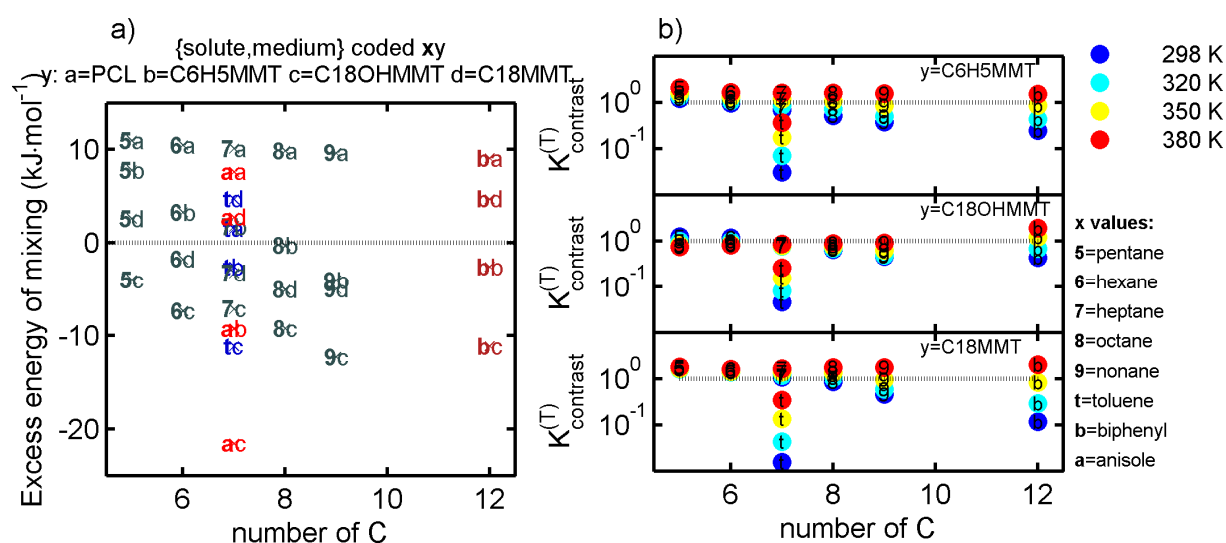


Figure 5-38 a) The excess energy of mixing and b) corresponding partitioning coefficient $K_{contrast}$ between organo-modified MMT and amorphous regions of PCL. The symbol of data is coded as xy: x is the index of solute; y is the index of polymer or clay.

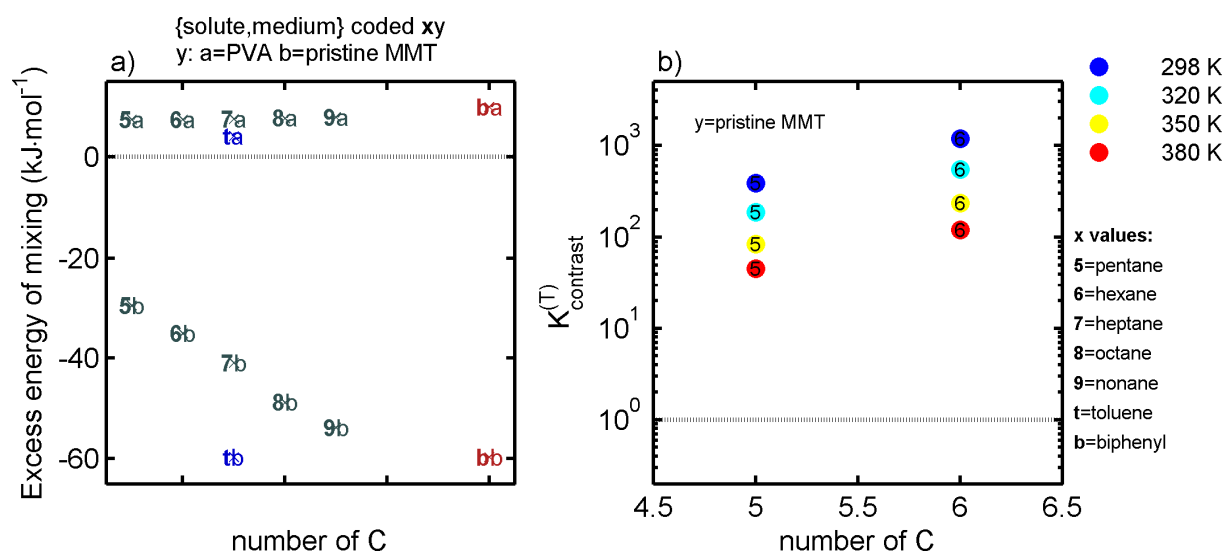


Figure 5-39 a) The excess energy of mixing and b) corresponding partitioning coefficient $K_{contrast}$ between pristine MMT and amorphous regions of PVA. The symbol of data is coded as xy: x is the index of solute; y is the index of polymer or clay.

5.3.2.5.3 Reduction of diffusion coefficients in PCL nanocomposite.

According to Eq. (5-59) and Figure 5-38b), there is no preferable chemical affinity between tested solutes with increasing size and organo-modified MMT. Accordingly the changes of diffusion coefficients of a solute such as biphenyl in PCL nanocomposite should only be associated to the tortuosity effect created by nanoclays. The experiments proof of reduction of diffusion coefficients (see Figure 5-40) with nanoclay concentration are depicted in Figure 5-41. A maximum D reduction of a factor 0.6 was obtained in PCL nanocomposite containing a low concentration of nanoclay (i.e. 0.5 wt%) and it was vanished at higher concentration (i.e. 5wt%). By considering the nucleating agent effect of nanoclay on the crystalline morphology in PCL (see Figure 5-41), D reduction would be expected higher but not less than a factor of 0.3 in low filled nanocomposite systems. The factor is calculated based on the ratio provided by Figure 5-37. For highly filled nanocomposites, a higher tortuosity effect is expected according to tortuosity models^{25,74-76}, which is in opposite with our experimental observations. The similar phenomena is also reported by Alexandre, Langevin, Médéric, Aubry, Couderc, Nguyen, Saiter, Marais⁷⁰ for the water vapor diffusing in polyamide 12/montmorillonite nanocomposite containing more than 3% of nanoclay. The existence of more aggregation in both intercalated and exfoliated structures would favor the solute

diffusion along a new pathway consisting in a percolation path through the clay-polymer interfacial zones as in the conventional composite systems including micro-sized obstacles.

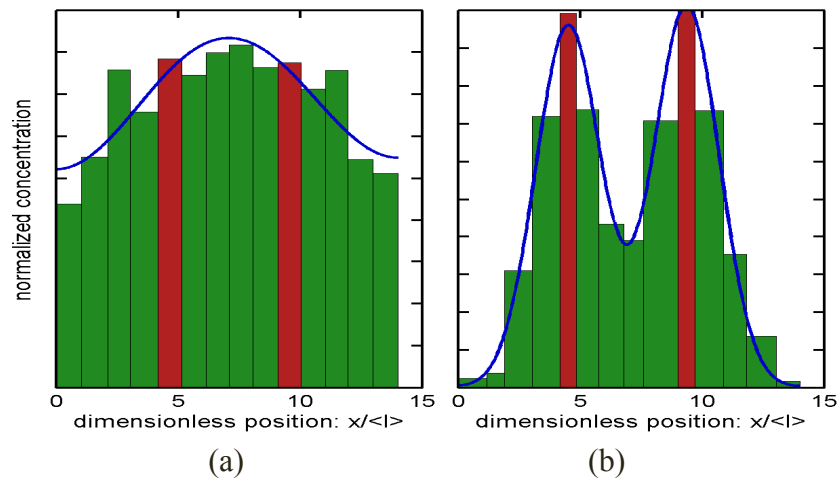


Figure 5-40 Normalized concentration profiles of biphenyl after 20 min of contact time at 298K (a) in pure PCL films with D value of $9.1 \times 10^{-13} \text{ m}^2/\text{s}$, (b) in PCL nanocomposite films including 0.5wt % of C18OHMMT with D value of $5.2 \times 10^{-13} \text{ m}^2/\text{s}$. The average film thickness is of $40 \text{ }\mu\text{m}$.

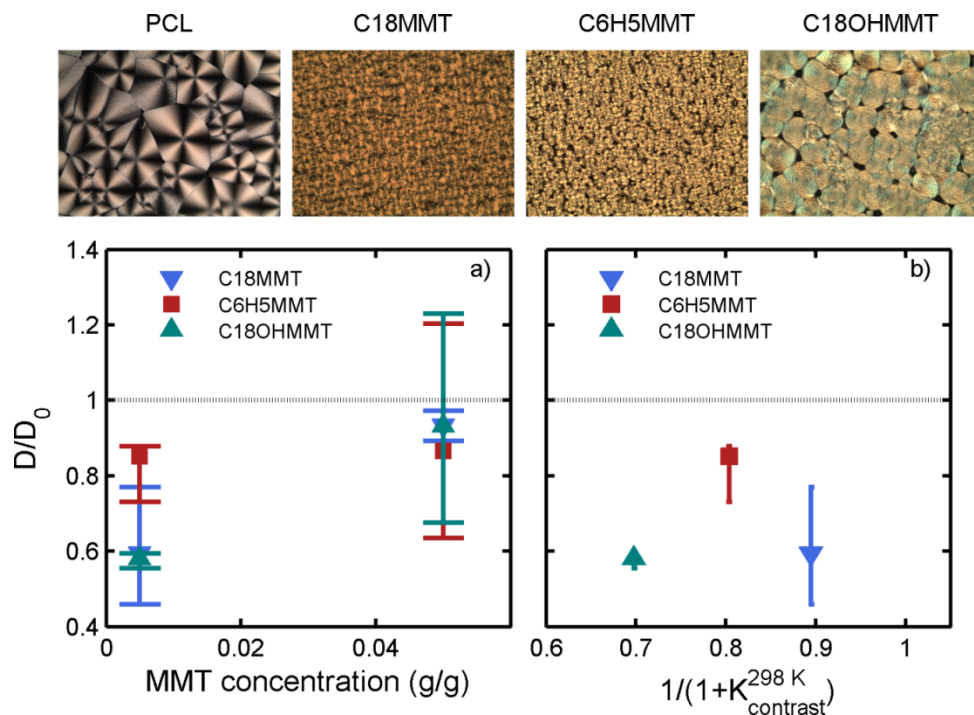


Figure 5-41 Reduction of diffusion coefficients of biphenyl in PCL nanocomposite: a) effect of concentration of nanoclays. b) interpretation according to $K_{contrast}$. Pictures above depict the size of crystallites in PCL and its nanocomposite systems containing 0.5wt% of nanoclays by polarized light microscopy (width= $100 \text{ }\mu\text{m}$).

5.3.2.5.4 Reduction of diffusion coefficients in PVA nanocomposite.

Typical experimental and fitted profiles obtained with PVA containing pristine MMT or not are presented in Figure 5-42. They showed a very significant slowdown of diffusion in

nanocomposite material in wet PVA. The corresponding D reductions are reported in Table 5-13. D reduction reached values down to 0.1-0.29 for both biphenyl and p -terphenyl in PVA nanocomposite films containing 5wt% of pristine MMT and conditioned at relative water humidity of 28%. Since a similar T_g was determined for nanocomposite and neat PVA, it was inferred that the observed D reduction could be associated to a similar increase in $K_{contrast}$. Calculations showed indeed a very significant enhancement of $K_{contrast}$ with values much greater than 1 in PVA as shown in Figure 5-39b) for short n -alkanes. As concluded in⁵⁴ that d -spacing of MMT dominates the Henry coefficients which used to calculate $K_{contrast}$ in the paper, the effect of film processing (*i.e.* solvent casting) and polymer state on changing d -spacing, *ca.* the swelling or intercalation effect on pristine MMT by solvent or polymer chain, must be taken into account. As a result, $K_{contrast}$ are calculated depending on sample state of PVA nanocomposites.

The calculations were carried out at d -spacing of 2.2nm as reported in similar conditions^{66,67} for wet PVA nanocomposites. Such conditions enabled the insertion of both solutes p -terphenyl and biphenyl using a particle insertion method. Although uncertainty was important, they confirmed similar improvements of $K_{contrast}$ for aromatic solutes too, as reported in Table 5-13. The values of $1/(1+K_{contrast})$ were in particular significantly correlated with assessed D drops (see the theoretical correlation in Eq. (5-59)). The thermodynamic control on D reduction was demonstrated by the suppression of the blocking effect when the temperature increased 30°C.

The previous conclusions and performances were however not reproduced in dry PVA. The results showed by contrast a slightly increase of diffusion coefficients in PVA nanocomposite systems. The vanished MMT effect may be associated to difficult intercalation of solute molecules into MMT interlayer due to the reduction of the basal spacing in polymer at dry state, where it is expected to match the one achieved in dry pristine MMT. Simulations confirmed that intercalations of biphenyl and p -terphenyl could not be achieved with a low d -spacing.

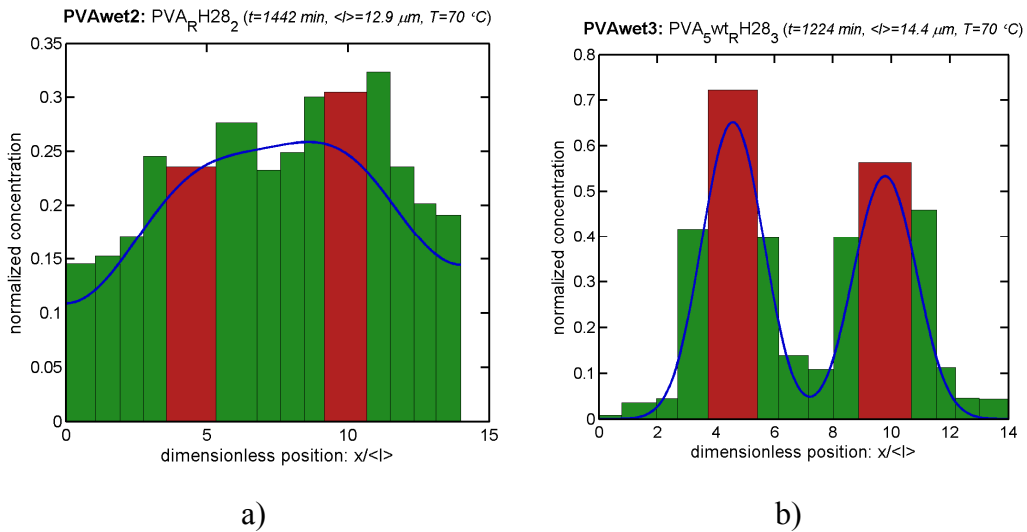


Figure 5-42 Normalized concentration profiles of biphenyl at 343K (a) in pure PVA films with D value of $3.8 \times 10^{-15} \text{ m}^2 \cdot \text{s}^{-1}$, (b) in PVA nanocomposite films including 5wt % of pristine MMT with D value of $3.4 \times 10^{-16} \text{ m}^2 \cdot \text{s}^{-1}$. The average film thickness is of $13 \mu\text{m}$.

Calculations of apparent activation energies and solute related activation energies as detailed in⁵⁶ confirmed an excess of activation by temperature which could not be associated to free-volume effects in the polymer. Values listed in Table 5-14 shows an excess of *ca.* $20 \text{ kJ} \cdot \text{mol}^{-1}$ in favor of MMT. The values remain lower than the theoretical values expected from Figure 5-39 (40 to $60 \text{ kJ} \cdot \text{mol}^{-1}$) but remain compatible with an assumption of a reduction of D due to $K_{contrast}$.

Table 5-13 The diffusion coefficients of biphenyl and terphenyl in both PVA film and PVA nanocomposite containing 5wt% of pristine MMT.

Sample condition	Solute	T-Tg (°C)	D_{PVA} ($m^2 \cdot s^{-1}$)		$D_{PVAnanocomposite}$ ($m^2 \cdot s^{-1}$) with $\phi=1wt\%$		$D_{PVAnanocomposite}$ ($m^2 \cdot s^{-1}$) with $\phi=5wt\%$		Maximum reduction ratio $\frac{D_{PVAnanocomposites}}{D_{PVA}}$	$K_{contrast}^{(T)}$ ‡	$\frac{1}{1 + K_{contrast}^{(T)}}$ ‡
			T (°C)	values	T (°C)	values	T (°C)	values			
Dry state	biphenyl	-	70	8.9×10^{-17} 5.7×10^{-17} 7.3×10^{-17}	-	-	70	1.4×10^{-16} 1.0×10^{-16}	1.64	-	-
	biphenyl	-	95	9.9×10^{-16}	-	-	95	2.1×10^{-15}	2.12	-	-
Wet state†	biphenyl	15	70	3.8×10^{-15} 1.5×10^{-15} 9.1×10^{-16} 7.6×10^{-16}	70	1.2×10^{-15}	70	3.4×10^{-16} 8.0×10^{-16} 1.8×10^{-16} 1.4×10^{-16}	0.1	1.7-8.6	0.1-0.5
	p-terphenyl	10	65	1.8×10^{-17}	-	-	65	5.3×10^{-18}	0.29	1.35-5.0	0.16 - 0.4
		40	95	3.2×10^{-16}	-	-	95	1.6×10^{-16}	0.48	0.2-2.3	0.3-0.8

† Relative humidity of 28%, ‡ $K_{contrast}$ were calculated based on simulated Henry coefficient of solute on pristine MMT with d -spacing at 2.2 nm as reported in^{66,67}.

Table 5-14 Activation energies of diffusion of *p*-terphenyl in PVA equilibrated at 28% of relative humidity

	PVA	PVA nanocomposite
Apparent activation energy	$99 \pm 7 \text{ kJ}\cdot\text{mol}^{-1}$	$112 \pm 9 \text{ kJ}\cdot\text{mol}^{-1}$
Solute activation energy ($E_{a_{\text{solute}}}$) [†]	$5 \pm 3 \text{ kJ}\cdot\text{mol}^{-1}$	$23 \pm 6 \text{ kJ}\cdot\text{mol}^{-1}$

[†] $E_{a_{\text{solute}}}$ is the apparent activation energy when the contribution of the polymer thermal expansion is removed from D values: $D/\exp\left(-K_a/(T - T_g + K_b)\right)$ as discussed in⁵⁶.

5.3.2.6 Conclusions

The current study introduces new concepts of nanocomposite barrier materials for organic solutes based on nano-adsorbents dispersed in a polymer matrix. The obvious advantage is that it works at low concentration in combination with conventional obstruction effects but regardless the shape and orientation of particles. Such effects could be therefore obtained instead of extrusion film processing by using solution casting processes. The corresponding scaling of D reduction is proportional to $1/(1+K_{\text{contrast}})$ and can exceed one decade as soon as K_{contrast} is greater than 10. The concepts could be transposed from inverse gas chromatography concepts where lag times (or reciprocal diffusion coefficients) replace elution times. The difficulties are however significant. It is expected to work only if the solute chemical potential contrast is significant between the polymer and nano-adsorbents. Hybrid systems involving inorganic systems such as pristine aluminosilicates (MMT) are best candidates due to the strength of van-der-Waals interactions or polar interactions. These conditions ensure a net exothermic sorption in favor of MMT. In other words, K_{contrast} increases with increasing temperature and vanishes at high temperatures. Experimentally, the concept has been proven only with a polar polymer containing pristine MMT partially swollen by water to ensure sufficient basal spacing for trapping large bulky solutes such as biphenyl and *p*-terphenyl. Additional verifications are required to confirm results for a broader range of polymers and adsorbents systems. In particular, excess activation energies are required to be determined.

5.3.2.7 References

1. Han JH. *Innovations in food packaging: Introduction to modified atmosphere packaging*: Elsevier Academic; 2005.
2. Raquez J-M, Habibi Y, Murariu M, Dubois P. "Polylactide (PLA)-based nanocomposites". *Progress in Polymer Science*. (0).
3. Sinha Ray S, Okamoto M. Polymer/layered silicate nanocomposites: a review from preparation to processing. *Progress in Polymer Science*. 2003;28(11):1539-1641.
4. Yu L, Dean K, Li L. Polymer blends and composites from renewable resources. *Progress in Polymer Science*. 2006;31(6):576-602.

5. Alexandre M, Dubois P. Polymer-layered silicate nanocomposites: preparation, properties and uses of a new class of materials. *Mat Sci Eng R*. Jun 15 2000;28(1-2):1-63.
6. Lagaron JM, Lopez-Rubio A. Nanotechnology for bioplastics: opportunities, challenges and strategies. *Trends in Food Science & Technology*. 2011;22(11):611-617.
7. Avérous L, Pollet E. Biorenewable nanocomposites. *MRS Bulletin*. 2011;36:703-710.
8. Domb AJ, Kost J, Wiseman DM. *Handbook of biodegradable polymers*: Harwood Academic Publishers; 1997.
9. Johnson RM, Mwaikambo LY, Tucker N. *Biopolymers*: Rapra Technology; 2003.
10. Letcher TM. *Thermodynamics, solubility and environmental issues*: Elsevier; 2007.
11. Salazar R, Domenek S, Courgneau C, Ducruet V. Plasticization of poly(lactide) by sorption of volatile organic compounds at low concentration. *Polymer Degradation and Stability*. 2012;97(10):1871-1880.
12. Ducruet V, Vitrac O, Saillard P, Guichard E, Feigenbaum A, Fournier N. Sorption of aroma compounds in PET and PVC during the storage of a strawberry syrup. *Food additives and contaminants*. Nov 2007;24(11):1306-1317.
13. Courgneau C, Vitrac O, Ducruet V, Riquet A-M. Local demixion in plasticized polylactide probed by electron spin resonance. *Journal of Magnetic Resonance*. 2013;233(0):37-48.
14. Dury-Brun C, Lequin S, Chalier P, Desobry S, Voilley A. Tracer Aroma Compound Transfer from a Solid and Complex-Flavored Food Matrix Packed in Treated Papers or Plastic Packaging Film. *Journal of Agricultural and Food Chemistry*. 2007/02/01 2007;55(4):1411-1417.
15. Vitrac O, Hayert M. Risk assessment of migration from packaging materials into foodstuffs. *Aiche Journal*. 2005;51(4):1080-1095.
16. Poças MdF, Oliveira JC, Pereira JR, Brandsch R, Hogg T. Modelling migration from paper into a food simulant. *Food Control*. 2011;22(2):303-312.
17. Dupakova Z, Klaudivsova K, Votavova L, Dobias J, Voldrich M. Migration of Printing ink Constituents from Packaging into Food Simulants. *Czech Journal of Food Sciences*. 2009 2009;27:S429-S429.
18. Biedermann M, Ingenhoff JE, Dima G, et al. Migration of mineral oil from printed paperboard into dry foods: survey of the German market. Part II: advancement of migration during storage. *European Food Research and Technology*. 2013 2013;236(3):459-472.
19. Kappenstein O, Vieth B, Luch A, Pfaff K. Toxicologically relevant phthalates in food. *Exs*. 2012 2012;101:87-106.
20. Perez-Palacios D, Angel Fernandez-Recio M, Moreta C, Teresa Tena M. Determination of bisphenol-type endocrine disrupting compounds in food-contact recycled-paper materials by focused ultrasonic solid-liquid extraction and ultra performance liquid chromatography-high resolution mass spectrometry. *Talanta*. Sep 15 2012;99:167-174.
21. Pennarun PY, Ngonu Y, Dole P, Feigenbaum A. Functional barriers in PET recycled bottles. Part II. Diffusion of pollutants during processing. *Journal of Applied Polymer Science*. Jun 5 2004;92(5):2859-2870.
22. Nguyen P-M, Goujon A, Sauvegrain P, Vitrac O. A computer-aided methodology to design safe food packaging and related systems. *Aiche Journal*. 2013:n/a-n/a.
23. Vitrac O, Hayert M. Design of safe food packaging under uncertainty. In: Berton P, ed. *New trends in chemical engineering research*. New York: Nova Science Publishers; 2007:251-292.
24. Arora A, Padua GW. Review: Nanocomposites in Food Packaging. *Journal of Food Science*. Jan-Feb 2010;75(1):R43-R49.

25. Cussler EL, Hughes SE, Ward III WJ, Aris R. Barrier membranes. *Journal of Membrane Science*. 1988;38(2):161-174.
26. Sinha Ray S, Okamoto K, Okamoto M. Structure–Property Relationship in Biodegradable Poly(butylene succinate)/Layered Silicate Nanocomposites. *Macromolecules*. 2003/04/01 2003;36(7):2355-2367.
27. Sinha Ray S, Yamada K, Okamoto M, Fujimoto Y, Ogami A, Ueda K. New polylactide/layered silicate nanocomposites. 5. Designing of materials with desired properties. *Polymer*. 2003;44(21):6633-6646.
28. Yampolskii Y, Pinnau I, Freeman BD. *Materials science of membranes for gas and vapor separation: prediction of gas permeation parameters of polymers*: Wiley; 2006.
29. Sperling LH. *Introduction to physical polymer science: concentrated solutions, phase separation behavior, and diffusion*: Wiley-Interscience; 2006.
30. Bicerano J. *Prediction of polymer properties: transport of small penetrant molecules*: Marcel Dekker; 2002.
31. Mark JE. *Physical properties of polymers handbook: permeability of polymers to gases and vapors*: Springer; 2007.
32. Hegde RR, Spruiell JE, Bhat GS. Different crystallization mechanisms in polypropylene-nanoclay nanocomposite with different weight percentage of nanoclay additives. *Journal of Materials Research*. May 2012;27(10):1360-1371.
33. Jacquelot E, Espuche E, Gérard JF, Duchet J, Mazabraud P. Morphology and gas barrier properties of polyethylene-based nanocomposites. *Journal of Polymer Science Part B: Polymer Physics*. 2006;44(2):431-440.
34. Wang ZF, Wang B, Qi N, Zhang HF, Zhang LQ. Influence of fillers on free volume and gas barrier properties in styrene-butadiene rubber studied by positrons. *Polymer*. 2005;46(3):719-724.
35. Gorrasi G, Tortora M, Vittoria V, Kaempfer D, Mülhaupt R. Transport properties of organic vapors in nanocomposites of organophilic layered silicate and syndiotactic polypropylene. *Polymer*. 2003;44(13):3679-3685.
36. Gusev AA, Lusti HR. Rational Design of Nanocomposites for Barrier Applications. *Advanced Materials*. 2001;13(21):1641-1643.
37. Xiao J, Huang Y, Manke CW. Computational Design of Polymer Nanocomposite Coatings: A Multiscale Hierarchical Approach for Barrier Property Prediction. *Industrial & Engineering Chemistry Research*. 2010/09/01 2010;49(17):7718-7727.
38. Merkel TC, Freeman BD, Spontak RJ, et al. Sorption, transport, and structural evidence for enhanced free volume in poly(4-methyl-2-pentyne)/fumed silica nanocomposite membranes. *Chemistry of Materials*. Jan 2003;15(1):109-123.
39. Merkel TC, Freeman BD, Spontak RJ, et al. Ultraporous, Reverse-Selective Nanocomposite Membranes. *Science*. April 19, 2002 2002;296(5567):519-522.
40. Yang C, Cussler EL. Oxygen barriers that use free radical chemistry. *AIChE Journal*. 2001;47(12):2725-2732.
41. Yang C, Nuxoll EE, Cussler EL. Reactive barrier films. *AIChE Journal*. 2001;47(2):295-302.
42. Solovyov S, Goldman A. *Mass Transport and Reactive Barriers in Packaging: Theory, Applications And Design*: Destech Publications Incorporated; 2008.
43. Cussler EL. *Diffusion: Mass Transfer in Fluid Systems*: Cambridge University Press; 2009.
44. Vitrac O, Hayert M. Identification of diffusion transport properties from desorption/sorption kinetics: An analysis based on a new approximation of Fick equation during solid-liquid contact. *Industrial & Engineering Chemistry Research*. Nov 2006;45(23):7941-7956.

45. Goujot D, Vitrac O. Extension to nonlinear adsorption isotherms of exact analytical solutions to mass diffusion problems. *Chemical Engineering Science*. 2013;99(0):2-22.
46. Leyboldt JK, Gough DA. Penetrant time lag in a diffusion-reaction system. Comments. *The Journal of Physical Chemistry*. 1980/05/01 1980;84(9):1058-1059.
47. Kalnin JR, Kotomin E. Modified Maxwell-Garnett equation for the effective transport coefficients in inhomogeneous media. *Journal of Physics A: Mathematical and General*. 1998;31(35):7227.
48. Janes DW, Durning CJ. Sorption and Diffusion of n-Alkyl Acetates in Poly(methyl acrylate)/Silica Nanocomposites. *Macromolecules*. Feb 2013;46(3):856-866.
49. Karayiannis NC, Mavrantzas VG, Theodorou DN. Diffusion of small molecules in disordered media: study of the effect of kinetic and spatial heterogeneities. *Chemical Engineering Science*. 2001;56(8):2789-2801.
50. Vitrac O, Hayert M. Effect of the distribution of sorption sites on transport diffusivities: A contribution to the transport of medium-weight-molecules in polymeric materials. *Chemical Engineering Science*. 2007;62(9):2503-2521.
51. Gillet G, Vitrac O, Desobry Sp. Prediction of Solute Partition Coefficients between Polyolefins and Alcohols Using a Generalized Flory–Huggins Approach. *Industrial & Engineering Chemistry Research*. 2009;48(11):5285-5301.
52. Gillet G, Vitrac O, Desobry Sp. Prediction of Partition Coefficients of Plastic Additives between Packaging Materials and Food Simulants. *Industrial & Engineering Chemistry Research*. 2010;49(16):7263-7280.
53. Vitrac OaG, Guillaume. An Off-Lattice Flory-Huggins Approach of the Partitioning of Bulky Solutes between Polymers and Interacting Liquids. *Int. J. Chem. React. Eng.* 2010;8.
54. Fang X, Vitrac O. Sorption properties of solutes onto pure and organo-modified montmorillonites. *submitted to Langmuir*. 2013.
55. Durand M, Meyer H, Benzerara O, Baschnagel J, Vitrac O. Molecular dynamics simulations of the chain dynamics in monodisperse oligomer melts and of the oligomer tracer diffusion in an entangled polymer matrix. *J. Chem. Phys.* May 2010;132(19).
56. Fang X, Domenek S, Ducruet V, Réfrégiers M, Vitrac O. Diffusion of Aromatic Solutes in Aliphatic Polymers above Glass Transition Temperature. *Macromolecules*. 2013/02/12 2013;46(3):874-888.
57. Watanabe H. Escape probability of a random walker on a lattice doped with absorbers. *The Journal of Chemical Physics*. 1978;69(11):4872-4875.
58. Klages R. *Microscopic chaos, fractals and transport in nonequilibrium statistical mechanics*: World Scientific; 2007.
59. Anta JA, Mora-Sero I, Dittrich T, Bisquert J. Interpretation of diffusion coefficients in nanostructured materials from random walk numerical simulation. *Physical Chemistry Chemical Physics*. 2008;10(30):4478-4485.
60. Shen L, Chen Z. Critical review of the impact of tortuosity on diffusion. *Chemical Engineering Science*. 2007;62(14):3748-3755.
61. Wang H, Keum JK, Hiltner A, Baer E. Confined Crystallization of PEO in Nanolayered Films Impacting Structure and Oxygen Permeability. *Macromolecules*. 2009;42(18):7055-7066.
62. Kundu K, Phillips P. Hopping transport on site-disordered d-dimensional lattices. *Physical Review A*. 1987;35(2):857-865.
63. Rottach DR, Tillman PA, McCoy JD, Plimpton SJ, Curro JG. The diffusion of simple penetrants in tangent site polymer melts. *The Journal of Chemical Physics*. 1999;111(21):9822-9831.

64. Marras SI, Kladi KP, Tsivintzelis I, Zuburtikudis I, Panayiotou C. Biodegradable polymer nanocomposites: The role of nanoclays on the thermomechanical characteristics and the electrospun fibrous structure. *Acta Biomaterialia*. 2008;4(3):756-765.
65. Otsuka E, Suzuki A. A simple method to obtain a swollen PVA gel crosslinked by hydrogen bonds. *Journal of Applied Polymer Science*. 2009;114(1):10-16.
66. Sapalidis AA, Katsaros FK, Kanellopoulos NK. PVA / Montmorillonite Nanocomposites: Development and Properties. In: Cuppoletti J, ed. *Nanocomposites and Polymers with Analytical Methods*: InTech; 2011.
67. Strawhecker KE, Manias E. Structure and Properties of Poly(vinyl alcohol)/Na+ Montmorillonite Nanocomposites. *Chemistry of Materials*. 2000/10/01 2000;12(10):2943-2949.
68. Roe R-J, Bair HE, Gieniewski C. Solubility and diffusion coefficient of antioxidants in polyethylene. *Journal of Applied Polymer Science*. 1974;18(3):843-856.
69. Michaels AS, Bixler HJ. Solubility of gases in polyethylene. *Journal of Polymer Science*. 1961;50(154):393-412.
70. Alexandre B, Langevin D, Médéric P, et al. Water barrier properties of polyamide 12/montmorillonite nanocomposite membranes: Structure and volume fraction effects. *Journal of Membrane Science*. 2009;328(1-2):186-204.
71. Nam PH, Fujimori A, Masuko T. The dispersion behavior of clay particles in poly(L-lactide)/organo-modified montmorillonite hybrid systems. *Journal of Applied Polymer Science*. 2004;93(6):2711-2720.
72. Tiwari RR, Khilar KC, Natarajan U. Synthesis and characterization of novel organo-montmorillonites. *Applied Clay Science*. 2008;38(3-4):203-208.
73. Calvet R. Adsorption of Organic-Chemicals in Soils. *Environ. Health Perspect*. Nov 1989;83:145-177.
74. Nielsen LE. Models for the Permeability of Filled Polymer Systems. *Journal of Macromolecular Science: Part A - Chemistry*. 1967/08/01 1967;1(5):929-942.
75. Fredrickson GH, Bicerano J. Barrier properties of oriented disk composites. *The Journal of Chemical Physics*. 1999;110(4):2181-2188.
76. Bharadwaj RK. Modeling the Barrier Properties of Polymer-Layered Silicate Nanocomposites. *Macromolecules*. 2001/12/01 2001;34(26):9189-9192.

5.3.3 Does the nano-adsorbent concept work?

It would not be appropriate and comprehensive to conclude only on cases where a strong reduction of D was observed even if reductions were comparable to performances or better than those reported in the literature. The elements of demonstrations are summarized here after:

- Significant D reductions were observed only in conditions where they were expected to occur: *i.e.* when variations of mixing energies are of opposite sign.
- D reduction was correlated to an increase of $K_{contrast}$ (reported in Table 5-15). $K_{contrast}$ is dominated by the relative basal spacing of MMT to the size of diffusant molecule.
- D reduction was correlated to the number of adsorption sites provided by the amount of adsorbents.
- Increasing temperature lessen dramatically barrier effect as expected according to the dependence on $K_{contrast}$.

Table 5-15 Calculated $K_{contrast}$ values versus basal spacing (d) of clay for aromatic solutes

Solute	$K_{contrast}$ d=1.4nm	$K_{contrast}$ d=2.2nm
Toluene	$3.1 \times 10^6 - 6.7 \times 10^6$	67 – 263
Biphenyl	$1.9 \times 10^5 - 8.3 \times 10^5$	1.7 – 8.2
<i>p</i> -terphenyl	-	0.27 – 5

The best D reductions are reported in Table 5-16. It is worth to notice that they were obtained without using the strategies known to be efficient in the literature (Choudalakis and Gotsis, 2009):

- No “forced” exfoliation of clays (exfoliation is however very likely in PVA based systems).
- No calendaring: no specific orientation of crystallites or clays.
- Low concentration of nanoclays.
- D reductions are stronger than those reported in the literature due to the sole tortuosity effect (Sinha Ray et al., 2003).

Table 5-16 Reported performances of the different systems.

MMT-polymer system	Best D reduction (conditions)	Corresponding $K_{contrast}$ values
System 1: PCL based	$\frac{D_{PCLnanocomposites}}{D_{PCL}} = 0.6$ (T= 313K, $\phi=0.5\text{wt}\%$, solute=biphenyl)	≤ 1
System 2: PVA based	$\frac{D_{PVAnanocomposites}}{D_{PVA}} = 0.1$ (T= 343K, $\phi=5\text{wt}\%$, solute=biphenyl)	8.2

From the presented results, it seems reasonable to assume that the barrier effect is obtained due to an excess of chemical affinity for the incorporated particles. In the logic of the design and to optimize the barrier properties or the selectivity of materials, estimating or predicting $K_{contrast}$ and its dependence with temperature without processing the material was also a significant concern. The success appears more mitigated due to a lack of accuracy in the prediction of the D reduction. The properties in the polymer were not an issue comparatively to the strong variation and uncertainty on the determination of the excess chemical potentials at the surface of clays. Two approaches have been tested on commercial MMT: the experimental approach based on IGC or IGA experiments and molecular simulations. The main drawbacks of experimental approaches are that they require temperatures higher than the ones met in conditions of use for low volatile substances and they are carried out clays with an average d -spacing which may be dramatically different from the one achieved once the clays are dispersed in the polymer (*i.e.* swelling or exfoliation). Conversely, simulations can explore a much larger range of temperature and d -spacing. They are remarkably efficient to predict the excess enthalpic contribution but remain very rough to calculate efficiently the excess entropy contribution in large cavities or for large solutes. Current conclusions need to be consolidated by integrating experimental determinations of d -spacing in our simulations.

5.4 Extended results and discussion

Several results have been collected during the thesis, which were not included in the papers submitted for publication. All the results were not fully interpreted but they are presented in this section when they provide either a further understanding or when they consolidate or extend previous conclusions.

5.4.1 The concept of increasing dwelling times to lessen D

The conventional concept of tortuosity used in nanocomposite materials has been advantageously replaced by the concept of space-time correlations, which fits better the diffusion mechanism. Spatial and temporal evolutions are indeed strongly intricate together in random-walk problems. In heterogeneous systems incorporating nano-adsorbents, modifying sorption properties locally induces dynamical heterogeneities and some displacements appeared consequently correlated in time. Standard tortuosity would have conversely generated correlations in space but both phenomena can be described by the same Eq.(5-10). From certain point of view, the specific solute barrier effect identified in section 5.1.3, where each ring or blob remains in contact with the polymer is also some kind of specific local sorption. Indeed, the escape rate of each blob follows an exponential scaling with the noise intensity, as also noticed in IGC experiments (see section 5.2.2). It has been shown to be also true for sorption within clay cavities but without reproducing the same mass dependence (see section 5.1.3).

An interpretation of the trapping of a random combination of aromatic rings on oligophenyl diffusant series is illustrated in Figure 5-43. Figure 5-43b) demonstrates that the mobility of the center-of-mass (CM) decreases with the number of blocked rings. The effect is all the stronger than the rings are closer to CM.

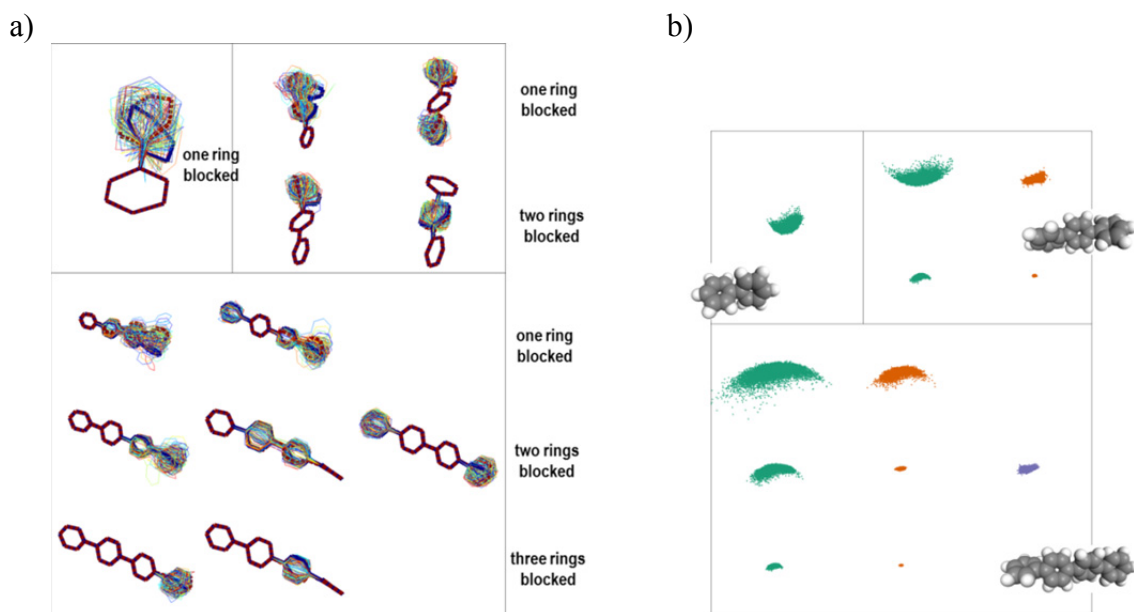


Figure 5-43 Molecular dynamics of oligophenyls in vacuum when one or several aromatic rings are blocked randomly: a) internal degrees of freedom, b) corresponding trace of the trajectory of the center-of-mass projected along its main inertia axis.

In bulk polymers, the alternative blocking of aromatic rings has been proposed to explain both:

- the excess of activation energy of organic solutes comparatively to Vrentas and Duda free volume theories;
- the strong scaling of D with the number of rings.

The corresponding envisioned growth of the mean-square distance of CM is sketched in Figure 5-44b) for quaterphenyl.

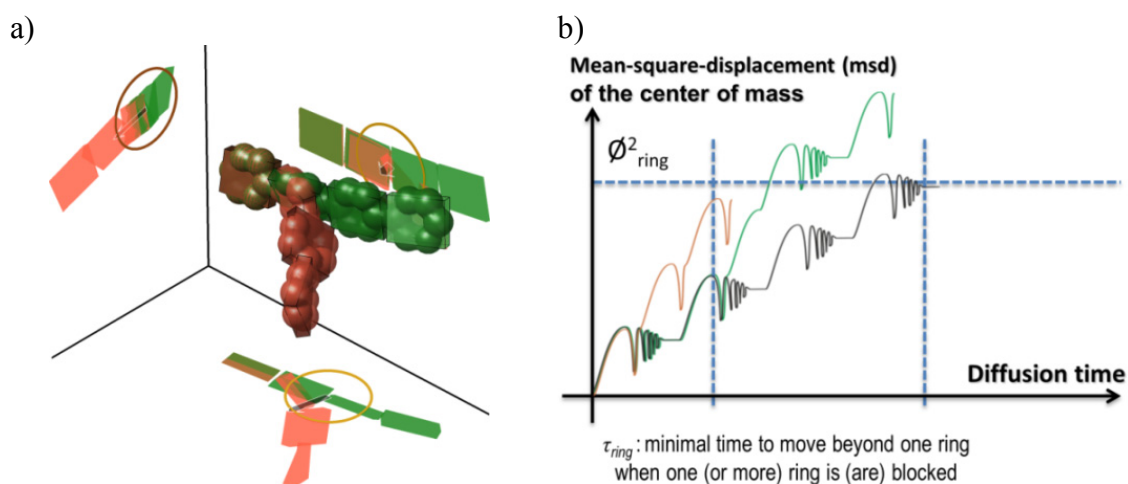


Figure 5-44 a) Extreme configurations leading to a translation of center-of-mass (CM) of quaterphenyl beyond the size of one aromatic ring while keeping the position of end ring fixed. The projections on the main axes represent the same molecule as connected rigid blocks (robot model) The visited distance of CM is represented by an arrow and the ring size

by a solid circle centered on CM. b) Sketched fluctuations of mean-square-distance (msd) when one or several rings are alternatively blocked.

The trajectory should be envisioned in a statistical sense as a random combination of all possible translation mechanisms: with no ring blocked, with one, two rings... blocked. The multiplication of possible combinations of sticky events (*e.g.* long-lived contacts with host) has two major consequences: an increase of the total trapping time (and accordingly activation energy) for larger solutes and a similar increase of translational entropy. These effects are detailed specifically in Figure 5-45 and Figure 5-46 respectively for oligophenyl solutes and compared with global values diphenyl alkanes. It is in particular shown that increasing the distance between two aromatic rings (*i.e.* “making the equivalent bond more flexible”) causes a higher independence of their displacements and made more unlikely the existence of concerted motions.

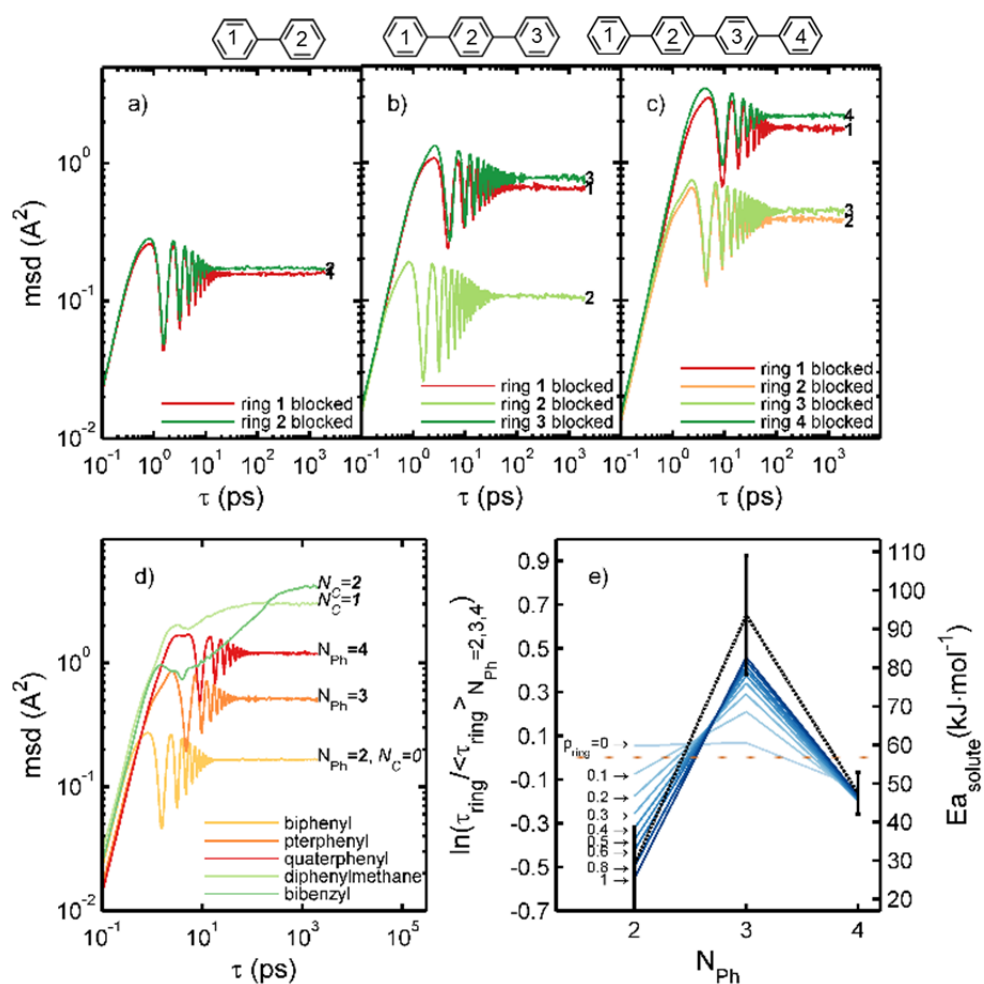


Figure 5-45 Mean-square-displacement (msd) of the center-of-mass versus time scale, τ , when one single ring is blocked in a) biphenyl, b) *p*-terphenyl, c) *p*-quaterphenyl molecules. d) msd value when the ring to be blocked is chosen randomly for all tested solutes. e) Comparison of relative solute activation energy (continuous lines, left scale) and calculated for different p_{ring} values as detailed in section 5.1.3.

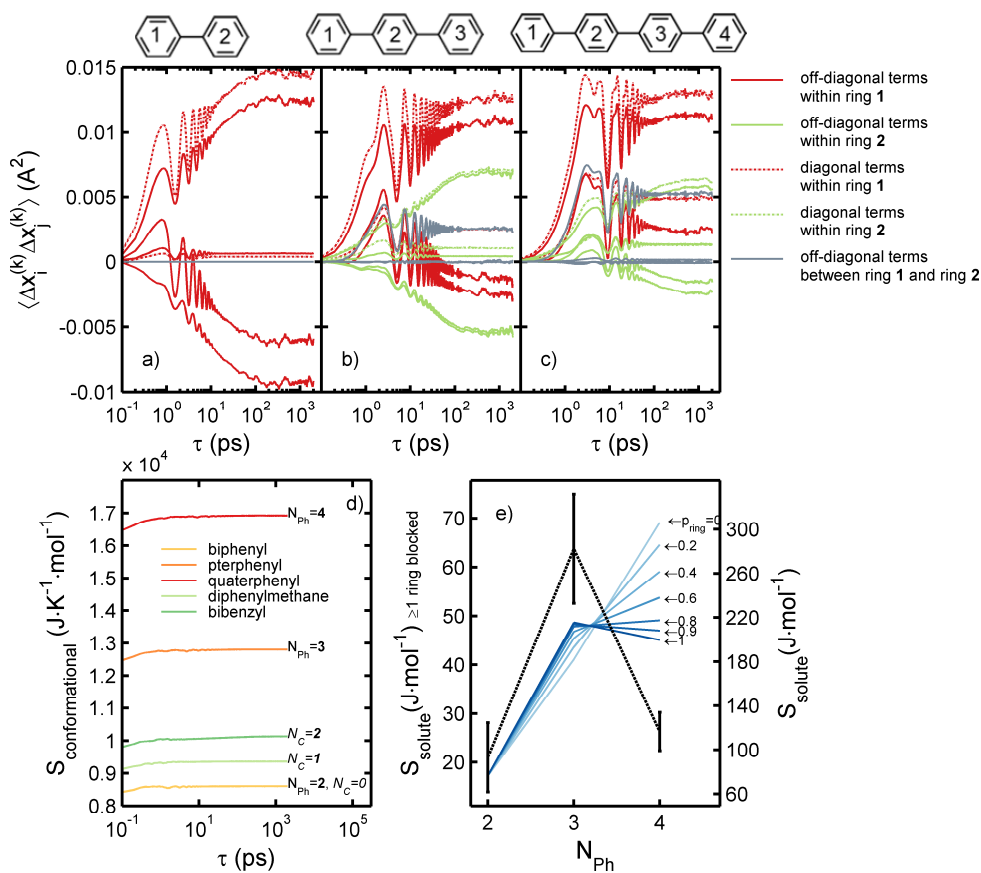


Figure 5-46 Covariances between the displacements of atoms versus time scale, τ , when one single ring is randomly blocked in a) biphenyl, b) *p*-terphenyl, c) *p*-quaterphenyl molecules. d) Conformational entropy when 1 to $N_{\text{Ph}}-1$ ring is randomly blocked as calculated from Eq. (13) in section 5.1.3. e) Comparison of solute entropy (continuous lines, left scale), calculated for different p_{ring} values according to Eqs. (13)-(16) in section 5.1.3 when 1 to $N_{\text{Ph}}-1$ ring is randomly blocked, and experimental values measured for oligophenylys (dotted line, right scale).

5.4.2 Do we expect a change in the molecular mechanism of diffusion in presence of nano-adsorbents?

It could be thought that a selective trapping of aromatic rings could occur not only in the bulk but also at the surface of MMT and could cause also an additional reduction of D . This effect has not been seen as a similar decrease has been assessed for biphenyl and terphenyl on the best system 2. As first sight, the absence of dependence of D reduction on N could be opposed to the proposed sorption theory of diffusion blocking (see Table 5-1). The presented results are however scarce (2 substances) and modifications in the mechanism of translation can be expected to be detectable only if the following conditions are fulfilled:

- the frequency and lifetime of contacts with MMT are large enough to dominate the mechanism of translation;

- both substances have the same accessibility to the basal spacing;
- the sticky effect remains independent between rings.

For rigid and stiff bulky solutes such as biphenyl and terphenyl, the fulfillment of the two last conditions remains highly uncertain. The main doubt remains on the real accessibility of large solutes to the clay: do they have a full access to the basal spacing or to only external parts?

From a conceptual point of view, if IGC experiments are thought as an equivalent physical model of active barrier materials, some of previous discussions can be tested and in particular the effect on mass dependence. In IGC experiments, the Knudsen regime of diffusion could be thought as first approximation (walls/clays are here considered as inert) of an equivalent diffusion coefficient with M once the advection contribution is removed:

$$D_{Knudsen} = \frac{\lambda u}{3} = \frac{\lambda}{3} \sqrt{\frac{2k_B T}{M}} \propto M^{-\frac{1}{2}} \quad (5-71)$$

where λ is the mean free path and u is the molecular velocity as derived from kinetic theory of gases.

Experimental scaling based on the reciprocal retention time (thought as reciprocal lag-time) yielded to a very strong mass dependence higher than those known in common theories of diffusion with a scaling exponent close to 6 as large as the one noticed in bulk for oligophenyls in amorphous polymers (see section 5.1.3). The analogy is fortuitous but illustrates the possible strong effect of dwelling times for alleviate D values or to increase the selectivity of diffusion. These effects are particularly well captured through Eq. (5-10) once we integrate the amount of correlations depending on the number of contacts with the surface.

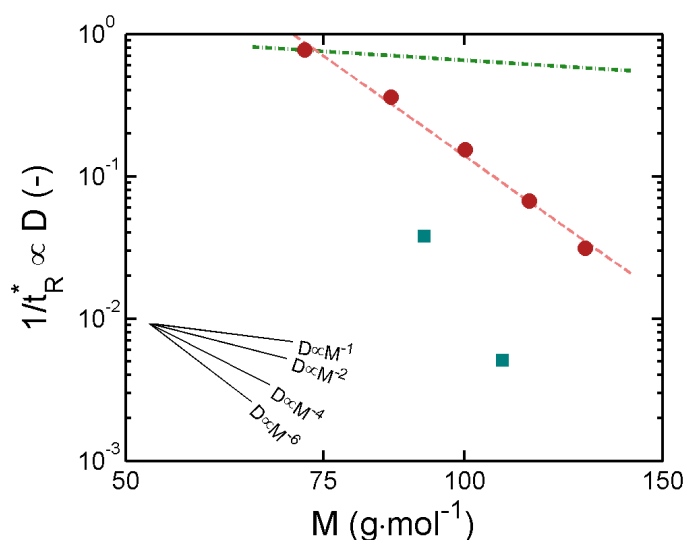


Figure 5-47 Scaling of equivalent transport coefficient (assimilated to D) with molecular mass M in IGC experiments: n-alkanes (circles), toluene and anisole (square). The upper dashed line represents the prediction according to Knudsen scaling.

Chapter 6. Conclusions and perspectives

6.1 Overview

The thesis adopted the following definition of barrier materials: “a barrier material is a material of thickness l leading to a significant lag-time, $t_{lag} = l^2/6D$, when it is exposed to one or several penetrant(s)”. The research endeavor was mainly a contribution to the understanding of relationships between the microscopic mechanisms of translation of organic solutes in solid polymers (*i.e.* in conditions of use) and related macroscopic diffusion coefficients D . One important application sought from the beginning was the development of a new concept of barrier material, which could be used broadly to an arbitrary polymer and in particular to new biodegradable polymer, to improve their resistance to organic substances (*e.g.* lipids, aroma...) or to prevent the leaching of their additives in particular in food. Due to the difficulty to measure D values for a broad range solute sizes in common bio-based polyesters at glassy state. The effort was reoriented on aliphatic rubber polymers, plasticized or not (*e.g.* PCL, PLA, PP, PVA). The concept of barrier material relied on a non-conventional idea of barrier to diffusion from Karayiannis et al. (2001) and Vitrac and Hayert (2007). Based on Kinetic Monte-Carlo simulations, both papers argued that D would decrease as a consequence of heterogeneities in space and time. Such D reductions are expected with a similar average sorption and deviated from the common semi-empirical definitions of tortuosity (Shen and Chen, 2007). To make the concept more tangible, two guiding ideas emerged rapidly:

- by noticing that elution times are analogous to lag-times, IGC experiments highlight the physical principles to decrease D ;
- polymer nanocomposite materials incorporate usually inert obstacles, which can be advantageously replaced by proper active surfaces to induce significant physisorption.

Without available experimental proofs from literature to support directly our concept, it was very important to recognize that our concept only could be validated if the desired effect could be separated from conventional ones such as polymer reordering or conventional “tortuosity” effects. A general strategy based on a solid theory of diffusion in thermoplastics was therefore required to separate unequivocally “bulk” effects from “chaotic” ones. The best proof should be advocated as follows: “the new system is able to modify the apparent activation energy of diffusion coefficients of a homologous series of diffusants”. This tool needed to be developed but it was not sufficient to alleviate the main difficulty: how to design such systems? It was decided to rely on commercial nano-clays, whose modalities of incorporation in polymers by dispersion have been sufficiently described. It was also clear

that such system: polymer + nano-particles + solutes would operate only in certain conditions of temperature and when the solute would “prefer” the clay surfaces more than the bulk polymer. Excess chemical potentials needed therefore to be optimized, calculated or experimentally determined.

To elaborate further these ideas without any guarantee of results, the research effort was broken into four independent tasks being presented as four separated publications. It includes a quite extensive review of predictive models being able to relate D values or its activation (by temperature or plasticization effects) to polymer properties and solute chemical structure (see section 2.1). The review shows, as expected, a strong confusion or disagreement between models used for risk assessment by the food packaging communities and those used by the polymer science community to assess the resistance of materials to solvent. The first ones tend to overestimate real D values for large solutes based on properties of small solutes, whereas second ones were initially designed to handle small and rather rigid solutes. In absence of a large consensus about a generic model, we proposed to extend existing free-volume theories to large flexible solutes (see section 5.1). The initial review was very useful with this respect as we could extract from the literature almost five independent homologous series of solutes at different temperatures to assess the effect of $T-T_g$ on the scaling of diffusion with solute size or length. The remaining extensions and sophistications were supplied by the data generated during this thesis, with homologous substances absorbing in UV range and fluorescent. Regardless of the ability or not to get a processable material, a neutral comparison of the chemical interactions between solute and polymer and between solute and clay was required. Only the second type of interactions was not explicitly considered in the literature. Indeed, the comparison should rely on several representative substances, while taking the pure state of the solute as reference chemical potential (see section 5.2). The main difficulty was to account for entropic effects as the arrangement and surface modification was also expected to affect chemical potentials. Finally, the assessment of some real materials designed according to a tradeoff between laboratory capabilities, commercial availabilities of chemical solutions and our calculations were carried out (see section 5.3). The results obtained on each of this important topic are summarized hereafter with an emphasis of helping those, who would like to develop further part or the whole of the concepts illustrated in this thesis.

6.2 Diffusion of tracers in bulk polymers

Trace diffusion (also called self-diffusion at infinite dilution) is the phenomenological description relating the net fluxes to the Brownian motions (*i.e.* uncorrelated and skewed

displacements) of penetrants in the polymer in absence of external driving forces. D is the scaling coefficient between the averaged square visited/crossed distance and diffusion time. Its scalar value carries all the detailed information on the “accidents” at molecular scale when the trajectory of solute center-of-mass (CM) is not self-similar and still contains correlated displacements. Beyond the time scale of vibration of atoms, persistent negative correlations (sub-diffusive regime) between the displacements of CM are responsible for a significant lowering of D values from microscopic scales up to macroscopic ones, where displacements appear independent. These correlations or apparent trapping have multiple origins: i) some concerted motions of parts of the penetrant molecule are required to enable a significant translation of CM on the long term, ii) some favorable fluctuations of polymer free volumes are required to accommodate the whole or a fraction of the penetrant. When the penetrant hops are controlled by energetic barriers, the frequencies of crossing the barrier in both directions are asymmetric and strong variations in the autocorrelation functions are additionally expected with diffusion time.

Organic solutes with molecular weights lower than $10^3 \text{ g} \cdot \text{mol}^{-1}$ exhibit the broadest scaling of D values over ten decades and the richest diversity of translation mechanism (Hall et al., 1999; Vitrac et al., 2006). Only few detailed mechanisms are understood and they still fail to be captured within a single theory. The smallest solutes can be considered rigid and translate according to a “red sea mechanism”. By taking into account their effective cross-sections, the last version of the free-volume theory (FVT) of Vrentas and Duda (Vrentas and Vrentas, 1998; Vrentas et al., 1996) provides acceptable predictions for small solutes in both rubber and glassy polymers. For larger and flexible solutes, it is not possible to consider anymore that the scaling of D is a pure enthalpic process (*i.e.* with geometric effects vanishing at high temperature). Such solutes can be envisioned conversely as connected jumping units (JU), obeying individually to FVT, but whose CM displacements involve concerted motions of several JUs. We developed such a theory to explain the scaling of D values with the length or molecular mass, M , of linear solutes as: $D/D_0 = (M/M_0)^{-\alpha(T-T_g)}$, where the difference $T-T_g$ is the distance to the glass transition temperature. By studying systematically the effect of the number of JU, the distance between JU and the branching of JU, it has been shown that adding flexible and symmetry properties around CM causes a dramatic decrease (of one decade or more) of D values while keeping approximately the same M value. Such considerations could open the design of additives with limited leaching during material service time.

6.3 A new concept of barrier material: chaotic materials

Until recently, little choice was available to reduce D in a given polymer. Indeed, the renewal rate of free volumes in the host matrix is the main controlling parameter and remains fundamentally an intrinsic property of the polymer itself. Only significant change of crystallinity degree can strongly affect D values of gas molecules (Kanehashi et al., 2010). More encouraging results have been obtained by the group of Baer (Arabeche et al., 2012; Langhe et al., 2012; Murphy et al., 2011) in confined polymer layers. Alternatives aiming at decreasing D by increasing tortuosity in polymers are challenged by the following Pólya result in 3D: “the probability to returns to the origin is lower than 1 (0.34 in infinite space)”. In other words, random walks enable each solute to visit every defect and only obstacles exhibiting large surfaces perpendicular to main flux (*e.g.* undamaged exfoliated and oriented clays) can hinder significantly their diffusion. Following an early idea of (Watanabe, 1978), we investigated theoretically and experimentally a different approach by modifying the surface energies onto which the solute is moving, such concept is a so-called chaotic material (*i.e.* with attractive regions). By noticing that the solubilization of most organic solutes in polymers is endothermic whereas it is an exothermic process at the surface of most nano-clays, adding alumino-silicate based nano-adsorbents was shown to lead to comparable D reduction without requiring large exfoliation ratio or any orientation effect.

By noticing that D should scale as $1/\left(1 + K_{i,contrast}^{(T,d)}\right)$, an optimization approach of barrier effects has been proposed based on an estimate of the partition coefficient between the montmorillonites (MMT) and the polymer, $K_{i,contrast}^{(T,d)}$:

$$\begin{aligned}
 K_{i,contrast}^{(T,d)} &= \frac{C_{i,MMT}}{C_{i,P}} = \frac{k_{i,P}^{(T)}}{k_{i,MMT}^{(T,d)}} = \frac{\bar{V}_i P_{i,sat}^{(T)} \exp(1 + \chi_{i,P})}{k_{i,MMT}^{(T_0,d)} \exp\left(\frac{Q_{st}(d)}{RT} \left(\frac{1}{T_0} - \frac{1}{T}\right)\right)} \\
 &= \frac{\bar{V}_i P_{i,sat}^{(T_0)}}{k_{i,MMT}^{(T_0,d)}} \exp\left(1 + \chi_{i,P} - \frac{q_{st}(d)}{RT} \left(\frac{1}{T_0} - \frac{1}{T}\right)\right) = K_{i,contrast}^{(T_0,d)} \exp\left(-\frac{q_{st}(d)}{RT} \left(\frac{1}{T_0} - \frac{1}{T}\right)\right) \\
 &\approx \frac{\bar{V}_i P_{i,sat}^{(T_0)}}{RT \left\langle \exp\left(-(\delta/d)^2\right) \right\rangle} \exp\left(1 + \chi_{i,P} - \frac{\langle q_{st}(d) \rangle}{RT} \left(\frac{1}{T_0} - \frac{1}{T}\right)\right) \\
 &\approx \underbrace{\frac{K_{i,contrast}^{(T_0,d \rightarrow \infty)}}{1 - \left\langle \exp\left(-(\delta/d)^2\right) \right\rangle}}_{\text{entropy contribution}} \underbrace{\exp\left(-\frac{\langle q_{st}(d) \rangle}{RT} \left(\frac{1}{T_0} - \frac{1}{T}\right)\right)}_{\text{enthalpy contribution}}
 \end{aligned} \tag{6-1}$$

where $\{C_{i,k}\}_{k=MMT,P}$ and $\{k_{i,k}\}_{k=MMT,P}$ are the solute concentration and the Henry coefficient in phase k . Q_{st} and q_{st} are the isosteric and net isosteric heat of sorption. $\chi_{i,P}$ is the Flory-Huggins coefficient in the polymer. All parameters can be determined either from independent

experiments or molecular simulations, including Grand Canonical Molecular Simulations. Both approaches were used in this work on MMT whereas a generalized Flory-Huggins simulations (Gillet et al., 2009, 2010; Vitrac and Gillet, 2010) was preferred to estimate $\chi_{i,p}$. $\langle \rangle$ stands for values averaged over the distribution of basal spacing as determined by XRD experiments. δ is a constant to be fitted from experiments or from simulations.

Equation (6-1) shows that $K_{contrast}$ is highly dependent of temperature and decreases rapidly with temperature when $q_{st} > 0$ (*i.e.* exothermic mixing). Besides, it shows that sorption onto MMT should be considered as a sorption process in volume and not only at the surface when the basal spacing is lower than a critical value (e.g. 2.2 nm for our tested MMT). The contribution of adsorption onto the surface of clays dominates the temperature dependence (*i.e.* exponential term so-called “enthalpy contribution”), whereas the pre-exponential factor depends strongly on the basal spacing of the considered clays, d . Indeed, the dependence q_{st} with d was found weak beyond some critical d -spacing for rigid adsorbates. For flexible adsorbates, the values of q_{st} are modified by the preferential selection of stretched conformers which can intercalate between the clays. Increasing d -spacing causes conversely a dramatic increase of the sorption entropy over several decades while keeping the adsorbates under the strong influence of the surface van-der-Waals potential (and electrostatic potential for polar adsorbates) when d -spacing is lower than 2.5 nm. Beyond, the thermodynamic potential dominates and excess chemical potentials approach the ones obtained in a gas phase. Covering the surface with quaternary ammonium surfactants alleviates sorption of organic solutes by both increasing the basal spacing and reducing the accessibility to surface. As a result, using commercially available organo-modified MMT with a large excess of surfactants instead of pristine ones solves processing issues but is unfavorable to increase $K_{contrast}$. Optimal results could be obtained with non-exfoliated pristine MMT in polar polymers and preserving significant cavities, where solutes could remain significantly trapped. The proof of this concept was shown by turning PVA into a significant barrier material to aromatic solutes (*i.e.* biphenyl and p-terphenyl) by the direct incorporation of pristine MMT in PVA during a casting step in water as solvent. It is worth to notice that the $K_{contrast}$ would be even much higher up to 10^5 if the pristine MMT could keep its basal spacing after processing. It was also well verified that a temperature increase was able to remove the effect. It was ever not possible to demonstrate an increase of $K_{contrast}$ with adsorbent size as p-terphenyl as the increase in isosteric heat of sorption was compensated by opposed loss of accessibility to smaller gaps.

6.4 Outlook

The theoretical, simulation and experimental work open a methodology to develop materials with a good selectivity to organic substances. One important contribution is to emphasize on hybrid systems where particles and inclusions exhibit positive net isosteric heat of sorption (*i.e.* exothermic mixing) for organic diffusants to be blocked. The selectivity of such systems can be modified easily by changing the temperature: decreasing temperature raises the selectivity and increasing temperature to suppress it. Such materials could be therefore used in separation techniques such as large scale chromatography with filled columns, membrane separation (nano-filtration, pervaporation...). It has been shown in mesoporous systems (*e.g.* stacked clays) that additional selectivity could be also gained by entropic trapping in cavities where the diffusant remains in interaction with the cavity's walls. In this case, the effects are not controlled anymore by temperature and the selectivity is provided by the flexibility and shape of the diffusants. In this perspective, nanoparticles or cluster of nanoparticles with incurved surfaces or internal cavities (*e.g.* tubes...) might improve the observed effects.

Besides technological considerations, one significant contribution of this work is to provide a flexible framework to probe, analyze and optimize blocking effects due to significant interactions with dispersed nanoparticles. This capacity is illustrated hereafter. The effect of concentration in nano-adsorbents was not studied specifically in the thesis as the extent of the accessible surface to large tested solutes could not be determined accurately. It has been thought and verified that a significant barrier effect could be achieved at very low concentration. Strong effects of particle concentration have been found conversely by (Janes and Durning, 2013). The reported results described a blocking effect of *n*-alkyl acetates onto spherical silica beads dispersed in rubber poly(methyl acrylate), which works significantly at high volume fraction in particles, denoted Φ_P . The authors supplied both reductions of effective diffusion coefficients D_{eff}/D_0 and also variations of effective solubility/Henry coefficients due to the incorporation of particles, which enable a reinterpretation of presented data. By considering that a fraction $\alpha \leq 1$ of particle volume is accessible to solutes, the effective Henry coefficient of the nanocomposite system, k_{eff} , is:

$$k_{eff}(k_P) = \left(\alpha \frac{\phi_P}{k_P} + \frac{(1-\phi_P)}{k_{PMA}} \right)^{-1} \quad (6-2)$$

where k_{PMA} and k_P are the Henry coefficients of the polymer and of the active surface, respectively. The case of inert particles corresponds to $k_P \rightarrow \infty$ and $k_{eff} = (1-\Phi_P)k_{PMA}$. In Figure 5 of (Janes and Durning, 2013), results are expressed as excess of chemical affinity

comparatively to inert beads $k_{eff}(k_P \rightarrow \infty)/k_{eff} - 1$. These values can be used to calculate an estimate of $\alpha K_{contrast}$:

$$K_{contrast} = \frac{k_{PMA}}{k_P} = \frac{1}{\alpha} \left(\frac{k_{eff}(k_P \rightarrow \infty)}{k_{eff}(k_P)} - 1 \right) \frac{1 - \phi_P}{\phi_P} \quad (6-3)$$

When applied to all experimental values collected by authors for different Φ_P values up to 0.6, Eq. (6-3) leads to $\alpha K_{contrast}$ of 0.45 ± 0.05 independent of Φ_P . By assuming that the blocking effect due to $K_{contrast}$ is proportional to two effects combined:

- Increase in the fractional time in contact with the active surface, proportional to $\alpha \frac{\phi_P}{1 - \phi_P}$ as discussed in (Kalnin and Kotomin, 1998);
- Increase in the physical obstruction, that is $\frac{\phi_P}{2}$ from Maxwell results for diluted impermeable spheres ((Masaro and Zhu, 1999)) and extended as to higher concentrations $\frac{\phi_P}{2(1 - \phi_P)}$.

As both spatial and temporal heterogeneities are strongly intricate (e.g. the collision causing the sticky event), the quadratic terms appear as a cumulated correlation (i.e. product of equivalent tortuosity factors) as explained in section 5.1.1 and also appear in the recent models (Minelli et al., 2011).

$$\frac{D_{eff}}{D_0} = \frac{1}{1 + \frac{\alpha}{2} \left(\frac{\phi_P}{1 - \phi_P} \right)^2 K_{contrast}} \quad (6-4)$$

The comparison between experimental results and Eq. (6-4) led to an estimate of α ranging between $1.7 \cdot 10^{-2}$ and $2.9 \cdot 10^{-2}$, which is compatible with a realistic adsorbing layer of 0.2-0.4 nm thick. The comparison is plotted in Figure 6-1 for beads of diameter 14 nm.

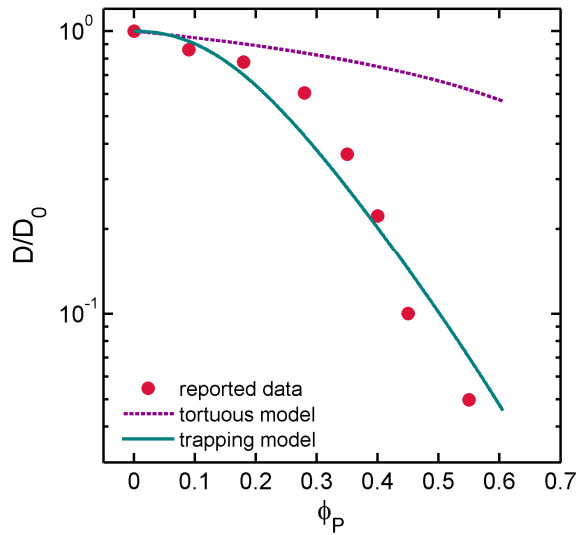


Figure 6-1 Comparison between experimental data of (Janes and Durning, 2013) for particles and Eq.(6-4).

Additional theory and experimental verification appears highly desirable to validate and extend presented concepts for more general active particles or reactive systems.

Chapter 7. References

- Abacha, N., Kubouchi, M. K., and Sakai, T. (2009). Diffusion behavior of water in polyamide 6 organoclay nanocomposites. *eXPRESS Polymer Letters*. **3**: 245-255.
- Adams, W. A., Xu, Y., Little, J. C., Fristachi, A. F., Rice, G. E., and Impellitteri, C. A. (2011). Predicting the migration rate of dialkyl organotin from PVC pipe into water. *Environ Sci Technol*. **45**: 6902-6907.
- Aichele, M., Gebremichael, Y., Starr, F. W., Baschnagel, J., and Glotzer, S. C. (2003). Polymer-specific effects of bulk relaxation and stringlike correlated motion in the dynamics of a supercooled polymer melt. *The Journal of Chemical Physics*. **119**: 5290-5304.
- Al-Malack, M. H. (2001). Migration of lead from unplasticized polyvinyl chloride pipes. *J Hazard Mater*. **82**: 263-274.
- Alexander Stern, S. (1994). Polymers for gas separations: the next decade. *Journal of Membrane Science*. **94**: 1-65.
- Alexandre, B., Langevin, D., Mederic, P., Aubry, T., Couderc, H., Nguyen, Q. T., Saiter, A., and Marais, S. (2009a). Water barrier properties of polyamide 12/montmorillonite nanocomposite membranes: Structure and volume fraction effects. *Journal of Membrane Science*. **328**: 186-204.
- Alexandre, B., Langevin, D., Médéric, P., Aubry, T., Couderc, H., Nguyen, Q. T., Saiter, A., and Marais, S. (2009b). Water barrier properties of polyamide 12/montmorillonite nanocomposite membranes: Structure and volume fraction effects. *Journal of Membrane Science*. **328**: 186-204.
- Alexandre, M., and Dubois, P. (2000). Polymer-layered silicate nanocomposites: preparation, properties and uses of a new class of materials. *Materials Science & Engineering R-Reports*. **28**: 1-63.
- Alfadul, S. M., and Elneshwy, A. A. (2010). Use of nanotechnology in food processing, packaging and safety - review. *African Journal of Food, Agriculture, Nutrition and Development*. **10**: 2719-2739.
- Alin, J., and Hakkarainen, M. (2011). Microwave Heating Causes Rapid Degradation of Antioxidants in Polypropylene Packaging, Leading to Greatly Increased Specific Migration to Food Simulants As Shown by ESI-MS and GC-MS. *Journal of Agricultural and Food Chemistry*. **59**: 5418-5427.
- Alin, J., and Hakkarainen, M. (2012). Migration from polycarbonate packaging to food simulants during microwave heating. *Polymer Degradation and Stability*. **97**: 1387-1395.
- Anderson, W. A. C., and Castle, L. (2003). Benzophenone in cartonboard packaging materials and the factors that influence its migration into food. *Food Additives and Contaminants*. **20**: 607-618.
- Andrade, G. S., Collard, D. M., Schiraldi, D. A., Hu, Y. S., Baer, E., and Hiltner, A. (2003). Oxygen barrier properties of PET copolymers containing bis(2-hydroxyethyl) hydroquinones. *Journal of Applied Polymer Science*. **89**: 934-942.
- Andricioaei, I., and Karplus, M. (2001). On the calculation of entropy from covariance matrices of the atomic fluctuations. *The Journal of Chemical Physics*. **115**: 6289-6292.
- Angell, C. A. (1997). Why $C_1 = 16-17$ in the WLF equation is physical—and the fragility of polymers. *Polymer*. **38**: 6261-6266.
- Anta, J. A., Mora-Sero, I., Dittrich, T., and Bisquert, J. (2008). Interpretation of diffusion coefficients in nanostructured materials from random walk numerical simulation. *Physical Chemistry Chemical Physics*. **10**: 4478-4485.
- Arabeche, K., Delbreilh, L., Adhikari, R., Michler, G. H., Hiltner, A., Baer, E., and Saiter, J.-M. (2012). Study of the cooperativity at the glass transition temperature in PC/PMMA multilayered films: Influence of thickness reduction from macro- to nanoscale. *Polymer*. **53**: 1355 - 1361.
- Arnold, J. C. (2010). A free-volume hole-filling model for the solubility of liquid molecules in glassy polymers 1: Model derivation. *European Polymer Journal*. **46**: 1131-1140.

- Arnould, D., and Laurence, R. L. (1992). Size effects on solvent diffusion in polymers. *Industrial & Engineering Chemistry Research*. **31**: 218-228.
- Arora, A., and Padua, G. W. (2010). Review: Nanocomposites in Food Packaging. *Journal of Food Science*. **75**: R43-R49.
- Arvanitoyannis, I. S., and Bosnea, L. (2004). Migration of substances from food packaging materials to foods. *Critical Reviews in Food Science and Nutrition*. **44**: 63-76.
- Aurela, B., Ohra-aho, T., and Soderhjelm, L. (2001). Migration of alkylbenzenes from packaging into food and Tenax (R). *Packaging Technology and Science*. **14**: 71-77.
- Averous, L. (2004). Biodegradable multiphase systems based on plasticized starch: A review. *Journal of Macromolecular Science-Polymer Reviews*. **C44**: 231-274.
- Avérous, L., and Pollet, E. (2011). Biorenewable nanocomposites. *MRS Bulletin*. **36**: 703-710.
- Aylmore, L. A. G., Sills, I. D., and Quirk, J. P. (1970). Surface Area of Homoionic Illite and Montmorillonite Clay Minerals as Measured by the Sorption of Nitrogen and Carbon Dioxide. *Clays and Clay Minerals*. **18**: 91-96.
- Az, R., Dewald, B., and Schnaitmann, D. (1991). Pigment decomposition in polymers in applications at elevated temperatures. *Dyes and Pigments*. **15**: 1-14.
- Azeredo, H. M. C. d. (2009). Nanocomposites for food packaging applications. *Food Research International*. **42**: 1240-1253.
- Aznar, M., Rodriguez-Lafuente, A., Alfaro, P., and Nerin, C. (2012). UPLC-Q-TOF-MS analysis of non-volatile migrants from new active packaging materials. *Analytical and Bioanalytical Chemistry*. **404**: 1945-1957.
- Bach, C., Dauchy, X., Chagnon, M.-C., and Etienne, S. (2012). Chemical compounds and toxicological assessments of drinking water stored in polyethylene terephthalate (PET) bottles: A source of controversy reviewed. *Water Research*. **46**: 571-583.
- Baker, G. L., Vogel, E. B., and Smith, M. R. (2008). Glass transitions in polylactides. *Polymer Reviews*. **48**: 64-84.
- Baner, A., Brandsch, J., Franz, R., and Piringer, O. (1996). The application of a predictive migration model for evaluating the compliance of plastic materials with European food regulations†. *Food Additives and Contaminants*. **13**: 587-601.
- Barnes, K. A., Sinclair, C. R., and Watson, D. H. (2007). Chemical migration and food contact materials. Woodhead.
- Barrat, J.-L., Baschnagel, J., and Lyulin, A. (2010). Molecular dynamics simulations of glassy polymers. *Soft Matter*. **6**: 3430-3446.
- Bart, J. C. J. (2006). Polymer Additive Analytics. Industrial Practice and Case Studies. Firenze University Press.
- Baschnagel, J., Wittmer, J. P., and Meyer, H. (2004). Monte Carlo Simulation of Polymers: Coarse-Grained Models. **In**: Computational Soft Matter: From Synthetic Polymers to Proteins, pp. 83-140.
- Batra, T. (2011). Endocrine-disrupting carcinogenic plastic contamination in the food chain: a review. *Biosciences, Biotechnology Research Asia*. **8**: 597-601.
- Battelli, G., Limbo, S., Panseri, S., Chiesa, L., Pellegrino, L., Biondi, P. A., and Noni, I. d. (2011). Wrapping films for cheese packaging: qualitative aspects and migration phenomena. *Scienza e Tecnica Lattiero-Casearia*. **62**: 313-326.
- Bavisi, B. H., Pritchard, G., and Ghotra, J. S. (1996). Measuring and reducing moisture penetration through thick laminates. *Advances in Polymer Technology*. **15**: 223-235.
- Bayer, F. L. (2002). Polyethylene terephthalate recycling for food-contact applications: testing, safety and technologies: a global perspective. *Food Additives and Contaminants Part a-Chemistry Analysis Control Exposure & Risk Assessment*. **19**: 111-134.
- Beake, B. D., Shipway, P. H., and Leggett, G. J. (2004). Influence of mechanical properties on the nanowear of uniaxially oriented poly(ethylene terephthalate) film. *Wear*. **256**: 118-125.

- Begley, T., Castle, L., Feigenbaum, A., Franz, R., Hinrichs, K., Lickly, T., Mercea, P., Milana, M., O'Brien, A., Rebre, S., Rijk, R., and Piringer, O. (2005). Evaluation of migration models that might be used in support of regulations for food-contact plastics. *Food Additives and Contaminants*. **22**: 73-90.
- Bellucci, F., Camino, G., Frache, A., and Sarra, A. (2007). Catalytic charring–volatilization competition in organoclay nanocomposites. *Polymer Degradation and Stability*. **92**: 425-436.
- Berens, A. R. (1981). Vinyl chloride monomer in PVC: from problem to probe. *Pure Appl. Chem*. **53**: 365-375.
- Berg, H. C. (1993). *Random Walks in Biology*. Princeton University Press.
- Berlinet, C., Brat, P., and Ducruet, V. (2008). Quality of orange juice in barrier packaging material. *Packaging Technology and Science*. **21**: 279-286.
- Bezus, A. G., Kiselev, A. V., Lopatkin, A. A., and Du, P. Q. (1978). Molecular statistical calculation of the thermodynamic adsorption characteristics of zeolites using the atom-atom approximation. Part 1.-Adsorption of methane by zeolite NaX. *Journal of the Chemical Society, Faraday Transactions 2: Molecular and Chemical Physics*. **74**: 367-379.
- Bharadwaj, R. K. (2001). Modeling the Barrier Properties of Polymer-Layered Silicate Nanocomposites. *Macromolecules*. **34**: 9189-9192.
- Bharadwaj, R. K., and Boyd, R. H. (1999). Small molecule penetrant diffusion in aromatic polyesters: a molecular dynamics simulation study. *Polymer*. **40**: 4229-4236.
- Bicerano, J. (2002). *Prediction of polymer properties: transport of small penetrant molecules*. Marcel Dekker.
- Biedermann, M., Ingenhoff, J. E., Dima, G., Zurfluh, M., Biedermann-Brem, S., Richter, L., Simat, T., Harling, A., and Grob, K. (2013). Migration of mineral oil from printed paperboard into dry foods: survey of the German market. Part II: advancement of migration during storage. *European Food Research and Technology*. **236**: 459-472.
- Biedermann, M., Uematsu, Y., and Grob, K. (2011). Mineral oil contents in paper and board recycled to paperboard for food packaging. *Packaging Technology and Science*. **24**: 61-73.
- Boersma, A. (2003). Mobility and solubility of antioxidants and oxygen in glassy polymers. I. Concentration and temperature dependence of antioxidant sorption. *Journal of Applied Polymer Science*. **89**: 2163-2178.
- Boersma, A., Cangialosi, D., and Picken, S. J. (2003a). Mobility and solubility of antioxidants and oxygen in glassy polymers II. Influence of physical ageing on antioxidant and oxygen mobility. *Polymer Degradation and Stability*. **79**: 427-438.
- Boersma, A., Cangialosi, D., and Picken, S. J. (2003b). Mobility and solubility of antioxidants and oxygen in glassy polymers. III. Influence of deformation and orientation on oxygen permeability. *Polymer*. **44**: 2463-2471.
- Bordes, P., Pollet, E., and Avérous, L. (2009). Nano-biocomposites: Biodegradable polyester/nanoclay systems. *Progress in Polymer Science*. **34**: 125-155.
- Bordes, P., Pollet, E., Bourbigot, S., and Averous, L. (2008). Structure and properties of PHA/clay nano-biocomposites prepared by melt intercalation. *Macromolecular Chemistry and Physics*. **209**: 1473-1484.
- Boulougouris, G. C. (2010). Calculation of the Chemical Potential beyond the First-Order Free-Energy Perturbation: From Deletion to Reinsertion†. *Journal of Chemical & Engineering Data*. **55**: 4140-4146.
- Boulougouris, G. C. (2011). On the Estimation of the Free Energy, From a Single Equilibrium Statistical Ensemble, via Particle Reinsertion. *The Journal of Physical Chemistry B*. **116**: 997-1006.
- Boutboul, A., Lenfant, F., Giampaoli, P., Feigenbaum, A., and Ducruet, V. (2002). Use of inverse gas chromatography to determine thermodynamic parameters of aroma–starch interactions. *Journal of Chromatography A*. **969**: 9-16.

- Brandrup, J., Immergut, E. H., and Grulke, E. A. (1999). *Polymer Handbook*. John Wiley & Sons.
- Brandsch, J., Mercea, P., Rüter, M., Tosa, V., and Piringer, O. (2002). Migration modelling as a tool for quality assurance of food packaging. *Food Additives and Contaminants*. **19**: 29-41.
- Brauer, B., and Funke, T. (2012). Applied Science - Full Papers presented exclusively for You Determination of potentially endocrine Substances in Mineral Water and Plastic Migrates by SBSE-GC-MS. *Deutsche Lebensmittel-Rundschau*. **108**: 21-+.
- Breiman, L. (1984). Classification and regression trees. Wadsworth International Group.
- Brimer, L., and Skaanild, M. T. (2011). *Chemical Food Safety*. CABI.
- Brody, A. L., Bugusu, B., Han, J. H., Sand, C. K., and McHugh, T. H. (2008). Scientific Status Summary: Innovative food packaging solutions. *Journal of Food Science*. **73**: R107-R116.
- Brody, A. L., Strupinsky, E. P., and Kline, L. R. (2010). *Active Packaging for Food Applications*. Taylor & Francis.
- Broglioli, D., and Vailati, A. (2000). Diffusive mass transfer by nonequilibrium fluctuations: Fick's law revisited. *Physical Review E*. **63**: 012105.
- Brunauer, S., Emmett, P. H., and Teller, E. (1938). Adsorption of Gases in Multimolecular Layers. *Journal of the American Chemical Society*. **60**: 309-319.
- Brydson, J. A. (1999). *Plastics Materials*. Elsevier Science.
- Budzien, J., McCoy, J. D., Rottach, D., and Curro, J. G. (2004). Effects of chain stiffness and penetrant size on penetrant diffusion in simple polymers: deduced relations from simulation and PRISM theory. *Polymer*. **45**: 3923-3932.
- Bueche, F. (1968). Diffusion of Polystyrene in Polystyrene: Effect of Matrix Molecular Weight. *The Journal of Chemical Physics*. **48**: 1410-1411.
- Buonocore, G. G., Del Nobile, M. A., Panizza, A., Corbo, M. R., and Nicolais, L. (2003). A general approach to describe the antimicrobial agent release from highly swellable films intended for food packaging applications. *Journal of Controlled Release*. **90**: 97-107.
- Busolo, M. A., and Lagaron, J. M. (2012). Oxygen scavenging polyolefin nanocomposite films containing an iron modified kaolinite of interest in active food packaging applications. *Innovative Food Science & Emerging Technologies*. **16**: 211-217.
- Callaghan, P. T., and Pinder, D. N. (1984). Influence of multiple length scales on the behavior of polymer self-diffusion in the semidilute regime. *Macromolecules*. **17**: 431-437.
- Callister, W. D., and Rethwisch, D. G. (2011). Chapter 4. Polymer structures. **In**: *Fundamentals of Materials Science and Engineering: An Integrated Approach*. Wiley, New York.
- Calvet, R. (1989). Adsorption of Organic-Chemicals in Soils. *Environmental Health Perspectives*. **83**: 145-177.
- Camacho, W., and Karlsson, S. (2000). Quality-determination of recycled plastic packaging waste by identification of contaminants by CC-MS after microwave assisted extraction (MAE). *Polymer Degradation and Stability*. **71**: 123-134.
- Caner, C., Hernandez, R. J., Pascall, M., Balasubramaniam, V. M., and Harte, B. R. (2004). The effect of high-pressure food processing on the sorption behaviour of selected packaging materials. *Packaging Technology and Science*. **17**: 139-153.
- Cao, X.-L., and Corriveau, J. (2008). Migration of bisphenol A from polycarbonate baby and water bottles into water under severe conditions. *Journal of Agricultural and Food Chemistry*. **56**: 6378-6381.
- CFR (2011). Federal Food, Drug, and Cosmetic Act. **In**: Title 21 - Food and drugs, pp. 109-113. FDA (Ed.), US government Printing Office, Washington D.C.
- CFR (2012a). Part 184 - Direct food substances affirmed as generally recognized as safe. **In**: Title 21. Code of Federal Regulations.

- CFR (2012b). Part 186 - Indirect food substances affirmed as generally recognized as safe. **In:** Title 21. Code of Federal Regulations.
- CFR (2012c). Section 170.39 - Threshold of regulation for substances used in food-contact articles. **In:** Title 21. Code of Federal Regulations.
- Chang, J.-H., An, Y. U., and Sur, G. S. (2003). Poly(lactic acid) nanocomposites with various organoclays. I. Thermomechanical properties, morphology, and gas permeability. *Journal of Polymer Science Part B: Polymer Physics*. **41**: 94-103.
- Chassapis, C. S., Petrou, J. K., Petropoulos, J. H., and Theodorou, D. N. (1996). Analysis of Computed Trajectories of Penetrant Micromolecules in a Simulated Polymeric Material. *Macromolecules*. **29**: 3615-3624.
- Chatwin, P. C., and Katan, L. L. (1989). The role of mathematics and physics in migration predictions. *Packaging Technology and Science*. **2**: 75-84.
- Chen, S. P., and Ferry, J. D. (1968). Erratum-The Diffusion of Radioactively Tagged n-hexadecane and n-dodecane through Rubbery Polymers. Effects of Temperature, Cross-linking, and Chemical Structure. *Macromolecules*. **1**: 374-374.
- Chernikov, A. A., Petrovichev, B. A., Rogal'sky, A. V., Sagdeev, R. Z., and Zaslavsky, G. M. (1990). Anomalous transport of streamlines due to their chaos and their spatial topology. *Physics Letters A*. **144**: 127-133.
- Choudalakis, G., and Gotsis, A. D. (2009). Permeability of polymer/clay nanocomposites: A review. *European Polymer Journal*. **45**: 967-984.
- Cohen, M. H., and Turnbull, D. (1959). Molecular Transport in Liquids and Glasses. *The Journal of Chemical Physics*. **31**: 1164-1169.
- Consolati, G., and Quasso, F. (2001). An experimental study of the occupied volume in polyethylene terephthalate. *The Journal of Chemical Physics*. **114**: 2825-2829.
- Corres, M. A., Zubitur, M., Cortazar, M., and Mugica, A. (2013). Thermal decomposition of phenoxy/clay nanocomposites: Effect of organoclay microstructure. *Polymer Degradation and Stability*. **98**: 818-828.
- Costa, F. R., Dutta, N. K., Choudhury, N. R., and Bhowmick, A. K. (2010). Chapter 5. Thermoplastic Elastomers. **In:** Current Topics in Elastomers Research. Bhowmick, A. K. (Ed.), Taylor & Francis.
- Cottier, S., Riquet, A. M., Feigenbaum, A., and Mortreuil, P. (1997). Change of the structure of a can coating during contact with food simulants: an ESR study. *Polymer International*. **43**: 353-358.
- Coughlin, C. S., Mauritz, K. A., and Storey, R. F. (1990). A general free volume based theory for the diffusion of large molecules in amorphous polymers above T_g. 3. Theoretical conformational analysis of molecular shape. *Macromolecules*. **23**: 3187-3192.
- Coughlin, C. S., Mauritz, K. A., and Storey, R. F. (1991a). A general free-volume-based theory for the diffusion of large molecules in amorphous polymers above glass temperature. 5. Application to dialkyl adipate plasticizers in poly(vinyl chloride). *Macromolecules*. **24**: 2113-2116.
- Coughlin, C. S., Mauritz, K. A., and Storey, R. F. (1991b). A general free volume based theory for the diffusion of large molecules in amorphous polymers above T_g. 4. Polymer-penetrant interactions. *Macromolecules*. **24**: 1526-1534.
- Courgneau, C., Domenek, S., Guinault, A., Avérous, L., and Ducruet, V. (2011). Analysis of the Structure-Properties Relationships of Different Multiphase Systems Based on Plasticized Poly(Lactic Acid). *Journal of Polymers and the Environment*. **19**: 362-371.
- Courgneau, C., Vitrac, O., Ducruet, V., and Riquet, A.-M. (2013). Local demixion in plasticized polylactide probed by electron spin resonance. *Journal of Magnetic Resonance*. **233**: 37-48.
- Crank, J. (1979). The Mathematics of Diffusion. Clarendon Press.
- Crawshaw, J., and Windle, A. H. (2003). Multiscale modelling in polymer science. *Fibre Diffraction Review*. **11**: 52-67.

- Crescenzi, V., Manzini, G., Calzolari, G., and Borri, C. (1972). Thermodynamics of fusion of poly- β -propiolactone and poly- ϵ -caprolactone. comparative analysis of the melting of aliphatic polylactone and polyester chains. *European Polymer Journal*. **8**: 449-463.
- Crockett, C., and Sumar, S. (1996). The safe use of recycled and reused plastics in food contact materials. II. *Nutrition and Food Science*: 34-37.
- Crompton, T. R. (2007). Additive Migration from Plastics Into Foods: A Guide for Analytical Chemists. Smithers Rapra Technology.
- Cruz, J. M., Sanches Silva, A., Sendón García, R., Franz, R., and Paseiro Losada, P. (2008). Studies of mass transport of model chemicals from packaging into and within cheeses. *Journal of Food Engineering*. **87**: 107-115.
- Cruz, S. A., Oliveira, E. C., de Oliveira, F. C. S., Garcia, P. S., and Kaneko, M. L. Q. A. (2011). Recycled Polymers for Food Contact. *Polimeros-Ciencia E Tecnologia*. **21**: 340-345.
- Curtiss, C. F., and Bird, R. B. (1996). Multicomponent diffusion in polymeric liquids. *Proceedings of the National Academy of Sciences*. **93**: 7440-7445.
- Cushen, M., Kerry, J., Morris, M., Cruz-Romero, M., and Cummins, E. (2013). Migration and exposure assessment of silver from a PVC nanocomposite. *Food Chemistry*. **139**: 389-397.
- Cussler, E. L. (2009). Diffusion: Mass Transfer in Fluid Systems. Cambridge University Press.
- Cussler, E. L., Hughes, S. E., Ward Iii, W. J., and Aris, R. (1988). Barrier membranes. *Journal of Membrane Science*. **38**: 161-174.
- D'Hollander, W., de Voogt, P., De Coen, W., and Bervoets, L. (2010). Perfluorinated substances in human food and other sources of human exposure. *Rev Environ Contam Toxicol*. **208**: 179-215.
- De Abreu, D. A. P., Cruz, J. M., Angulo, I., and Losada, P. P. (2010). Mass Transport Studies of Different Additives in Polyamide and Exfoliated Nanocomposite Polyamide Films for Food Industry. *Packaging Technology and Science*. **23**: 59-68.
- De Angelis, M. G., Boulougouris, G. C., and Theodorou, D. N. (2010). Prediction of Infinite Dilution Benzene Solubility in Linear Polyethylene Melts via the Direct Particle Deletion Method. *The Journal of Physical Chemistry B*. **114**: 6233-6246.
- De Gennes, P. G. (1971). Reptation of a Polymer Chain in the Presence of Fixed Obstacles. *The Journal of Chemical Physics*. **55**: 572-579.
- Del Nobile, M. A., Mensitieri, G., Netti, P. A., and Nicolais, L. (1994). Anomalous diffusion in poly-ether-ether-ketone. *Chemical Engineering Science*. **49**: 633-644.
- Delmaar, J. E., Park, M. V. D. Z., and van Engelen, J. G. M. (2005). ConsExpo 4.0-Consumer Exposure and Uptake Models -Program Manual National Institute of Public Health and the Environment (RIVM), Bilthoven, The Netherlands.
- Deppe, D. D., Miller, R. D., and Torkelson, J. M. (1996). Small molecule diffusion in a rubbery polymer near T_g: Effects of probe size, shape, and flexibility. *Journal of Polymer Science Part B: Polymer Physics*. **34**: 2987-2997.
- Derjaguin, B. (1934). Untersuchungen über die Reibung und Adhäsion, IV. *Kolloid-Zeitschrift*. **69**: 155-164.
- Deshpande, S. S. (2002). Handbook of Food Toxicology. Marcel Dekker, Inc., New-York.
- Dobiáš, J., Voldřich, M., Marek, M., and Chudáčková, K. (2004). Changes of properties of polymer packaging films during high pressure treatment. *Journal of Food Engineering*. **61**: 545-549.
- Doi, M., and Edwards, S. F. (1978). Dynamics of concentrated polymer systems. Part 1.- Brownian motion in the equilibrium state. *Journal of the Chemical Society, Faraday Transactions 2: Molecular and Chemical Physics*. **74**: 1789-1801.
- Dole, P., Feigenbaum, A. E., Cruz, C. D. L., Pastorelli, S., Paseiro, P., Hankemeier, T., Voulzatis, Y., Aucejo, S., Saillard, P., and Papispyrides, C. (2006a). Typical diffusion

- behaviour in packaging polymers – application to functional barriers. *Food Additives and Contaminants*. **23**: 202-211.
- Dole, P., Voulzatis, Y., Vitrac, O., Reynier, A., Hankemeier, T., Aucejo, S., and Feigenbaum, A. (2006b). Modelling of migration from multi-layers and functional barriers: Estimation of parameters. *Food Additives and Contaminants*. **23**: 1038-1052.
- Domb, A. J., Kost, J., and Wiseman, D. M. (1997). Handbook of biodegradable polymers. Harwood Academic Publishers.
- Doolittle, A. K. (1951). Studies in Newtonian Flow. I. The Dependence of the Viscosity of Liquids on Temperature. *Journal of Applied Physics*. **22**: 1031-1035.
- Doong, S. J., and Ho, W. S. W. (1992). Diffusion of hydrocarbons in polyethylene. *Industrial & Engineering Chemistry Research*. **31**: 1050-1060.
- Dopico-Garcia, M. S., Lopez-Vilarino, J. M., and Gonzalez-Rodriguez, M. V. (2003). Determination of antioxidant migration levels from low-density polyethylene films into food simulants. *J Chromatogr A*. **1018**: 53-62.
- Du Yeon, B., Minji, K., Min Ji, K., Bu Young, J., Myung Chan, C., Seul Min, C., Young Woo, K., Seong Kwang, L., Duck Soo, L., Won, A. J., Seung Jun, K., Youngkwan, L., Hyung Sik, K., and Byung Mu, L. (2012). Human risk assessment of endocrine-disrupting chemicals derived from plastic food containers. *Comprehensive Reviews in Food Science and Food Safety*. **11**: 453-470.
- Dubreuil, A.-C., Doumenc, F., Guerrier, B., and Allain, C. (2003). Mutual Diffusion in PMMA/PnBMA Copolymer Films: Influence of the Solvent-Induced Glass Transition. *Macromolecules*. **36**: 5157-5164.
- Ducruet, V., Vitrac, O., Saillard, P., Guichard, E., Feigenbaum, A., and Fournier, N. (2007). Sorption of aroma compounds in PET and PVC during the storage of a strawberry syrup. *Food Addit Contam*. **24**: 1306-1317.
- Dupakova, Z., Klaudivsova, K., Votavova, L., Dobias, J., and Voldrich, M. (2009). Migration of Printing ink Constituents from Packaging into Food Simulants. *Czech Journal of Food Sciences*. **27**: S429-S429.
- Durand, M., Meyer, H., Benzerara, O., Baschnagel, J., and Vitrac, O. (2010). Molecular dynamics simulations of the chain dynamics in monodisperse oligomer melts and of the oligomer tracer diffusion in an entangled polymer matrix. *Journal of Chemical Physics*. **132**.
- Dury-Brun, C., Lequin, S., Chalier, P., Desobry, S., and Voilley, A. (2007). Tracer Aroma Compound Transfer from a Solid and Complex-Flavored Food Matrix Packed in Treated Papers or Plastic Packaging Film. *Journal of Agricultural and Food Chemistry*. **55**: 1411-1417.
- Dutra, C., Pezo, D., Freire, M. T. d. A., Nerín, C., and Reyes, F. G. R. (2011). Determination of volatile organic compounds in recycled polyethylene terephthalate and high-density polyethylene by headspace solid phase microextraction gas chromatography mass spectrometry to evaluate the efficiency of recycling processes. *Journal of Chromatography A*. **1218**: 1319-1330.
- Dyson, N. A. (1998). Chromatographic Integration Methods. Royal Soc of Chemistry.
- EC (2002a). COMMISSION DIRECTIVE 2002/72/EC of 6 August 2002 relating to plastic materials and articles intended to come into contact with foodstuffs. *Official Journal of the European Communities*. **L 220**: 18-58.
- EC (2002b). Evaluation of Migration Models to be used under Directive 90/128/EEC. Hinrichs, K., and Piringer, O. (Eds.), European Commission, Brussels.
- EC (2004). Regulation (EC) No 1935/2004 of the European parliament and of the council of 27 October 2004 on materials and articles intended to come into contact with food and repealing Directives 80/590/EEC and 89/109/EEC. *Official Journal of the European Union*. **L 338**: 4-17.

- EC (2011a). COMMISSION REGULATION (EU) No 10/2011 of 14 January 2011 on plastic materials and articles intended to come into contact with food. *Official Journal of the European Union*. **L 12**: 1-89.
- EC (2011b). RECOMMENDATIONS: COMMISSION RECOMMENDATION of 18 October 2011 on the definition of nanomaterial (2011/696/EU). *Official Journal of the European Union*. **L 275**: 38-40.
- EC (2012a). COMMISSION REGULATION (EU) No 1183/2012 of 30 November 2012 amending and correcting Regulation (EU) No 10/2011 on plastic materials and articles intended to come into contact with food. *Official Journal of the European Union*. **L 338**: 11-15.
- EC (2012b). Corrigendum to Commission Regulation (EU) No 1183/2012 of 30 November 2012 amending and correcting Regulation (EU) No 10/2011 on plastic materials and articles intended to come into contact with food. *Official Journal of the European Union*. **L 349**: 77.
- EC (2012c). Practical guidance document on the implementation of diffusion modelling for the estimation of specific migration in support of Regulation (EU) No 10/2011. Hoekstra, E. J. (Ed.), Joint Research Centre of the European Commission, Ispra, Italy.
- EC (2013). Estimation of specific migration by generally recognised diffusion models in support of Regulation (EC) No 10/2011. Hoekstra, E. J. (Ed.), Joint Research Centre of the European Commission, Ispra, Italy.
- Edwards, C. J. C., Rigby, D., and Stepto, R. F. T. (1981). Kirkwood-Riseman Interpretation of the Diffusion Behavior of Short Polymer Chains in Dilute Solution. *Macromolecules*. **14**: 1808-1812.
- EFSA (2011). SCIENTIFIC OPINION: Guidance on the risk assessment of the application of nanoscience and nanotechnologies in the food and feed chain. *EFSA Journal*. **9**: 2140.
- Ehlich, D., and Sillescu, H. (1990). Tracer diffusion at the glass transition. *Macromolecules*. **23**: 1600-1610.
- Einstein, A. (1905a). On the movement of small particles suspended in a stationary liquid demanded by the molecular-kinetic theory of heat. *Annalen der Physik (Leipzig)*. **17**: 549-560.
- Einstein, A. (1905b). Über die von der molekularkinetischen Theorie der Wärme geforderte Bewegung von in ruhenden Flüssigkeiten suspendierten Teilchen. *Annalen der Physik*. **322**: 549-560.
- Einstein, A., and Fürth, R. (1956). Investigations on the Theory of the Brownian Movement. Dover Publications.
- Eltantawy, I. M., and Arnold, P. W. (1972). Adsorption of n-Alkanes by Wyoming Montmorillonite. *nature physical science*. **237**: 123-125.
- Espitia, P. J. P., Soares, N. D. F., Coimbra, J. S. D., de Andrade, N. J., Cruz, R. S., and Medeiros, E. A. A. (2012). Zinc Oxide Nanoparticles: Synthesis, Antimicrobial Activity and Food Packaging Applications. *Food and Bioprocess Technology*. **5**: 1447-1464.
- Eu, B. C. (2006). Transport Coefficients of Fluids. Springer London, Limited.
- Fang, J. M., Fowler, P. A., Escrig, C., Gonzalez, R., Costa, J. A., and Chamudis, L. (2005). Development of biodegradable laminate films derived from naturally occurring carbohydrate polymers. *Carbohydrate Polymers*. **60**: 39-42.
- Fang, X., Domenek, S., Ducruet, V., Réfrégiers, M., and Vitrac, O. (2013). Diffusion of Aromatic Solutes in Aliphatic Polymers above Glass Transition Temperature. *Macromolecules*. **46**: 874-888.
- Fang, X., and Vitrac, O. (2013). Sorption properties of solutes onto pure and organo-modified montmorillonites. *submitted to Langmuir*.
- FDA (1999). Guidance for Industry-Preparation of Premarket Notifications for Food Contact Substances: Chemistry Recommendation. FDA, Washington, DC, USA.

- FDA (2006). Guidance for Industry: Use of Recycled Plastics in Food Packaging: Chemistry Considerations. **In:** Guidance, Compliance & Regulatory Information. CFSAN (Ed.), U.S. Food and Drug Administration, College Park, MD, U.S.A.
- FDA (2007). Guidance for Industry: Preparation of Premarket Submissions for Food Contact Substances: Chemistry Recommendations. **In:** Guidance, Compliance & Regulatory Information. CFSAN (Ed.), U.S. Food and Drug Administration, College Park, MD, U.S.A.
- FDA (2012a). Draft Guidance for Industry: Assessing the Effects of Significant Manufacturing Process Changes, Including Emerging Technologies, on the Safety and Regulatory Status of Food Ingredients and Food Contact Substances, Including Food Ingredients that are Color Additives. FDA, Washington, DC, USA.
- FDA (2012b). Food Ingredients and Packaging Guidance for Industry. FDA.
- FDA (2012c). Guidance for Industry Safety of Nanomaterials in Cosmetic Products. FDA, Washington, DC, USA.
- FDA (2012d). Inventory of Effective Food Contact Substance (FCS) Notifications. F.D.A.
- Fechete, R., Demco, D. E., and Blümich, B. (2003). Self-Diffusion Anisotropy of Small Penetrants in Compressed Elastomers. *Macromolecules*. **36**: 7155-7157.
- Fei, F., Chen, Q., Liu, Z., Liu, F., and Solodovnyk, A. (2012). The Application of Nano-SiO_x Coatings as Migration Resistance Layer by Plasma Enhanced Chemical Vapor Deposition. *Plasma Chemistry and Plasma Processing*. **32**: 755-766.
- Feigenbaum, A., Dole, P., Aucejo, S., Dainelli, D., Garcia, C. D. L. C., Hankemeier, T., N'Gono, Y., Papaspyrides, C. D., Paseiro, P., Pastorelli, S., Pavlidou, S., Pennarun, P. Y., Saillard, P., Vidal, L., Vitrac, O., and Voulzatis, Y. (2005). Functional barriers: Properties and evaluation. *Food Additives and Contaminants*. **22**: 956-967.
- Feigenbaum, A., Scholler, D., Bouquant, J., Brigot, G., Ferrier, D., Franz, R., Lillemark, L., Riquet, A. M., Petersen, J. H., Lierop, B. V., and Yagoubi, N. (2002). Safety and quality of food contact materials. Part 1: Evaluation of analytical strategies to introduce migration testing into good manufacturing practice. *Food Additives and Contaminants*. **19**: 184-201.
- Feigenbaum, A. E., Ducruet, V. J., Delpal, S., Wolff, N., Gabel, J. P., and Wittmann, J. C. (1991). Food and packaging interactions: penetration of fatty food simulants into rigid poly(vinyl chloride). *Journal of Agricultural and Food Chemistry*. **39**: 1927-1932.
- Felix, J. S., Isella, F., Bosetti, O., and Nerin, C. (2012). Analytical tools for identification of non-intentionally added substances (NIAS) coming from polyurethane adhesives in multilayer packaging materials and their migration into food simulants. *Analytical and Bioanalytical Chemistry*. **403**: 2869-2882.
- Felix, J. S., Manzoli, J. E., Padula, M., and Monteiro, M. (2008). Plastic packaging with polyamide 6 used for meat foodstuffs and cheese: caprolactam migration and effect of irradiation. A review. *Alimentos e Nutricao*. **19**: 19 (13) 361-370.
- Ferry, J. D., Landel, R. F., and Williams, M. L. (1955). Extensions of the Rouse Theory of Viscoelastic Properties to Undiluted Linear Polymers. *Journal of Applied Physics*. **26**: 359-362.
- Fierens, T., Servaes, K., Van Holderbeke, M., Geerts, L., De Henauw, S., Sioen, I., and Vanermen, G. (2012). Analysis of phthalates in food products and packaging materials sold on the Belgian market. *Food and Chemical Toxicology*. **50**: 2575-2583.
- Filippi, S., Paci, M., Polacco, G., Dintcheva, N. T., and Magagnini, P. (2011). On the interlayer spacing collapse of Cloisite® 30B organoclay. *Polymer Degradation and Stability*. **96**: 823-832.
- Fischer, E. W., Sterzel, H. J., and Wegner, G. (1973). Investigation of the structure of solution grown crystals of lactide copolymers by means of chemical reactions. *Colloid & Polymer Science*. **251**: 980-990.

- Fiselier, K., and Grob, K. (2012). Barriers against the Migration of Mineral Oil from Paperboard Food Packaging: Experimental Determination of Breakthrough Periods. *Packaging Technology and Science*. **25**: 285-301.
- Follain, N., Belbekhouche, S., Bras, J., Siqueira, G., Marais, S., and Dufresne, A. (2013). Water transport properties of bio-nanocomposites reinforced by *Luffa cylindrica* cellulose nanocrystals. *Journal of Membrane Science*. **427**: 218-229.
- Fordham, P. J., Gramshaw, J. W., Crews, H. M., and Castle, L. (1995). Element residues in food contact plastics and their migration into food simulants, measured by inductively-coupled plasma-mass spectrometry. *Food Additives and Contaminants*. **12**: 651-669.
- Forrest, J. (2007). Coatings and Inks for Food Contact Materials. Rapra Technology.
- Fox, T. G., and Loshaek, S. (1955). Influence of molecular weight and degree of crosslinking on the specific volume and glass temperature of polymers. *Journal of Polymer Science*. **15**: 371-390.
- Franz, R., and Simoneau, C. (2008). FINAL REPORT: Modelling migration from plastics into foodstuffs as a novel and cost efficient tool for estimation of consumer exposure from food contact materials. pp. 1-55. Institute for Health and Consumer Protection Luxembourg.
- Fredrickson, G. H., and Bicerano, J. (1999). Barrier properties of oriented disk composites. *The Journal of Chemical Physics*. **110**: 2181-2188.
- Freire, M. T. D., Castle, L., Reyes, F. G. R., and Damant, A. P. (1998). Thermal stability of polyethylene terephthalate food contact materials: formation of volatiles from retail samples and implications for recycling. *Food Additives and Contaminants*. **15**: 473-480.
- Frenkel, D., and Smit, B. (2001). Understanding Molecular Simulation: From Algorithms to Applications. Elsevier Science.
- Frenkel, J. (1955). Kinetic theory of liquids. Dover Publications.
- Galimberti, M. (2011). Rubber-Clay Nanocomposites: Science, Technology, and Applications. Wiley.
- Garnett, J. C. M. (1904). Colours in Metal Glasses and in Metallic Films. *Philosophical Transactions of the Royal Society of London. Series A, Containing Papers of a Mathematical or Physical Character*. **203**: 385-420.
- Gaume, J., Rivaton, A., Thérias, S., and Gardette, J.-L. (2012). Influence of nanoclays on the photochemical behaviour of poly(vinyl alcohol). *Polymer Degradation and Stability*. **97**: 488-495.
- Geisel, T., Zacherl, A., and Radons, G. (1988). Chaotic diffusion and 1/f-noise of particles in two-dimensional solids. *Zeitschrift für Physik B Condensed Matter*. **71**: 117-127.
- Genies, P. G. d. (1971). Reptation of a Polymer Chain in the Presence of Fixed Obstacles. *The Journal of Chemical Physics*. **55**: 572-579.
- Gillet, G., Vitrac, O., and Desobry, S. (2009a). Prediction of Solute Partition Coefficients between Polyolefins and Alcohols Using a Generalized Flory-Huggins Approach. *Industrial & Engineering Chemistry Research*. **48**: 5285-5301.
- Gillet, G., Vitrac, O., and Desobry, S. (2010a). Prediction of Partition Coefficients of Plastic Additives between Packaging Materials and Food Simulants. *Industrial & Engineering Chemistry Research*. **49**: 7263-7280.
- Gillet, G., Vitrac, O., Tissier, D., Saillard, P., and Desobry, S. (2009d). Development of decision tools to assess migration from plastic materials in contact with food. *Food Additives and Contaminants Part a-Chemistry Analysis Control Exposure & Risk Assessment*. **26**: 1556-1573.
- Gniewek, P., and Kolinski, A. (2011). Note: A simple picture of subdiffusive polymer motion from stochastic simulations. *The Journal of Chemical Physics*. **134**: 056101.
- Goetz, N. v., Wormuth, M., Scheringer, M., and Hungerbuehler, K. (2010). Bisphenol A: how the most relevant exposure sources contribute to total consumer exposure. *Risk Analysis*. **30**: 473-487.

- Gorrasi, G., Tortora, M., Vittoria, V., Kaempfer, D., and Mülhaupt, R. (2003). Transport properties of organic vapors in nanocomposites of organophilic layered silicate and syndiotactic polypropylene. *Polymer*. **44**: 3679-3685.
- Goujot, D., and Vitrac, O. (2013). Extension to nonlinear adsorption isotherms of exact analytical solutions to mass diffusion problems. *Chemical Engineering Science*. **99**: 2-22.
- Goulas, A. E., Riganakos, K. A., Badeka, A., and Kontominas, M. G. (2002). Effect of ionizing radiation on the physicochemical and mechanical properties of commercial monolayer flexible plastics packaging materials. *Food Additives and Contaminants*. **19**: 1190-1199.
- Granda-Restrepo, D. M., Soto-Valdez, H., Peralta, E., Troncoso-Rojas, R., Vallejo-Cordoba, B., Gamez-Meza, N., and Graciano-Verdugo, A. Z. (2009). Migration of alpha-tocopherol from an active multilayer film into whole milk powder. *Food Research International*. **42**: 1396-1402.
- Gryn'ova, G., Ingold, K. U., and Coote, M. L. (2012). New Insights into the Mechanism of Amine/Nitroxide Cycling during the Hindered Amine Light Stabilizer Inhibited Oxidative Degradation of Polymers. *Journal of the American Chemical Society*. **134**: 12979-12988.
- Guart, A., Bono-Blay, F., Borrell, A., and Lacorte, S. (2011). Migration of plasticizersphthalates, bisphenol A and alkylphenols from plastic containers and evaluation of risk. *Food Additives and Contaminants Part a-Chemistry Analysis Control Exposure & Risk Assessment*. **28**: 676-685.
- Gusev, A. A., and Lusti, H. R. (2001). Rational Design of Nanocomposites for Barrier Applications. *Advanced Materials*. **13**: 1641-1643.
- Hakkarainen, M. (2008). Solid phase microextraction for analysis of polymer degradation products and additives. **In**: *Chromatography for Sustainable Polymeric Materials: Renewable, Degradable and Recyclable*, pp. 23-50. Albertsson, A. C., and Hakkarainen, M. (Eds.), Springer-Verlag Berlin, Berlin.
- Halden, R. U. (2010). Plastics and Health Risks. **In**: *Annual Review of Public Health*, Vol 31, pp. 179-194. Fielding, J. E., Brownson, R. C., and Green, L. W. (Eds.).
- Haldimann, M., Alt, A., Blanc, A., Brunner, K., Sager, F., and Dudler, V. (2012). Migration of antimony from PET trays into food simulant and food: determination of Arrhenius parameters and comparison of predicted and measured migration data. *Food Additives & Contaminants: Part A*: 1-12.
- Hall, D. B., Hamilton, K. E., Miller, R. D., and Torkelson, J. M. (1999a). Translational and Rotational Diffusion of Probe Molecules in Polymer Films near T_g: Effect of Hydrogen Bonding. *Macromolecules*. **32**: 8052-8058.
- Han, J. H. (2003). Chapter 4. Antimicrobial food packaging. **In**: *Novel Food Packaging Techniques*. Ahvenainen, R. (Ed.), CRC Press.
- Han, J. H. (2005). *Innovations in food packaging: Introduction to modified atmosphere packaging*. Elsevier Academic.
- Hanggi, P., and Marchesoni, F. (2005). Introduction: 100 years of Brownian motion. *Chaos: An Interdisciplinary Journal of Nonlinear Science*. **15**: 026101.
- Hansen, C. M. (2007). *Hansen Solubility Parameters: A User's Handbook*, Second Edition. Taylor & Francis.
- Harmandaris, V. A., Doxastakis, M., Mavrantzas, V. G., and Theodorou, D. N. (2002). Detailed molecular dynamics simulation of the self-diffusion of n-alkane and cis-1,4 polyisoprene oligomer melts. *The Journal of Chemical Physics*. **116**: 436-446.
- Hatzigrigoriou, N. B., and Papaspyrides, C. D. (2011). Nanotechnology in Plastic Food-Contact Materials. *Journal of Applied Polymer Science*. **122**: 3720-3739.
- Hatzigrigoriou, N. B., Papaspyrides, C. D., Joly, C., and Dole, P. (2010). Effect of Migrant Size on Diffusion in Dry and Hydrated Polyamide 6. *Journal of Agricultural and Food Chemistry*. **58**: 8667-8673.

- Hatzigrigoriou, N. B., Vouyiouka, S. N., Joly, C., Dole, P., and Papaspyrides, C. D. (2012). Temperature-humidity superposition in diffusion phenomena through polyamidic materials. *Journal of Applied Polymer Science*. **125**: 2814-2823.
- Haw, M. D. (2002). Colloidal suspensions, Brownian motion, molecular reality: a short history. *Journal of Physics: Condensed Matter*. **14**: 7769.
- Haward, R. N. (1970). Occupied Volume of Liquids and Polymers. *Journal of Macromolecular Science, Part C*. **4**: 191-242.
- Hayashi, H., and Matsuzawa, S. (1992). Concentration distribution of antioxidant additive BHT in polypropylene after heating. *Journal of Applied Polymer Science*. **46**: 499-505.
- Heath, V. (2010). The perils of plastic. *Nat Rev Endocrinol*. **6**: 237.
- Hedenqvist, M., Angelstok, A., Edsberg, L., Larsson, P. T., and Gedde, U. W. (1996). Diffusion of small-molecule penetrants in polyethylene: free volume and morphology. *Polymer*. **37**: 2887-2902.
- Hedenqvist, M., and Gedde, U. W. (1996). Diffusion of small-molecule penetrants in semicrystalline polymers. *Progress in Polymer Science*. **21**: 299-333.
- Hegde, R. R., Spruiell, J. E., and Bhat, G. S. (2012). Different crystallization mechanisms in polypropylene-nanoclay nanocomposite with different weight percentage of nanoclay additives. *Journal of Materials Research*. **27**: 1360-1371.
- Heinz, H., Koerner, H., Anderson, K. L., Vaia, R. A., and Farmer, B. L. (2005). Force Field for Mica-Type Silicates and Dynamics of Octadecylammonium Chains Grafted to Montmorillonite. *Chemistry of Materials*. **17**: 5658-5669.
- Heinz, H., and Suter, U. W. (2004a). Atomic Charges for Classical Simulations of Polar Systems. *The Journal of Physical Chemistry B*. **108**: 18341-18352.
- Heinz, H., and Suter, U. W. (2004b). Surface structure of organoclays. *Angewandte Chemie-International Edition*. **43**: 2239-2243.
- Helmroth, E., Rijk, R., Dekker, M., and Jongen, W. (2002a). Predictive modelling of migration from packaging materials into food products for regulatory purposes. *Trends in Food Science & Technology*. **13**: 102-109.
- Helmroth, E., Varekamp, C., and Dekker, M. (2005). Stochastic modelling of migration from polyolefins. *Journal of the Science of Food and Agriculture*. **85**: 909-916.
- Helmroth, I. E., Dekker, M., and Hankemeier, T. (2002b). Influence of solvent absorption on the migration of Irganox 1076 from LDPE. *Food Additives and Contaminants*. **19**: 176-183.
- Herman, M. F. (1995). The role of correlated many chain motions in linear chain polymer melts. *The Journal of Chemical Physics*. **103**: 4324-4332.
- Herman, M. F., Panajotova, B., and Lorenz, K. T. (1996a). A quantitative theory of linear chain polymer dynamics in the melt. I. General scaling behavior. *The Journal of Chemical Physics*. **105**: 1153-1161.
- Herman, M. F., Panajotova, B., and Lorenz, K. T. (1996b). A quantitative theory of linear chain polymer dynamics in the melt. II. Comparison with simulation data. *The Journal of Chemical Physics*. **105**: 1162-1174.
- Herman, M. F., and Tong, P. (1993). Scaling analysis of multichain cooperative motions in the lateral motion model for polymer melts. *Macromolecules*. **26**: 3733-3737.
- Hess, B., Peter, C., Ozal, T., and van der Vegt, N. F. A. (2008). Fast-Growth Thermodynamic Integration: Calculating Excess Chemical Potentials of Additive Molecules in Polymer Microstructures. *Macromolecules*. **41**: 2283-2289.
- Hess, B., and van der Vegt, N. F. A. (2008). Predictive Modeling of Phenol Chemical Potentials in Molten Bisphenol A-Polycarbonate over a Broad Temperature Range. *Macromolecules*. **41**: 7281-7283.
- Hill, R. J. (2006). Diffusive Permeability and Selectivity of Nanocomposite Membranes. *Industrial & Engineering Chemistry Research*. **45**: 6890-6898.

- Hiltner, A., Liu, R. Y. F., Hu, Y. S., and Baer, E. (2005). Oxygen transport as a solid-state structure probe for polymeric materials: A review. *Journal of Polymer Science Part B-Polymer Physics*. **43**: 1047-1063.
- Himmelsbach, M., Buchberger, W., and Reingruber, E. (2009). Determination of polymer additives by liquid chromatography coupled with mass spectrometry. A comparison of atmospheric pressure photoionization (APPI), atmospheric pressure chemical ionization (APCI), and electrospray ionization (ESI). *Polymer Degradation and Stability*. **94**: 1213-1219.
- Hinrichsen, G., Eberhardt, A., Lippe, U., and Springer, H. (1981). Orientation mechanisms during biaxial drawing of polymer films. *Colloid and Polymer Science*. **259**: 73-79.
- Hoekstra, E. J., and Simoneau, C. (2011). Release of Bisphenol A from Polycarbonate—A Review. *Critical Reviews in Food Science and Nutrition*. **53**: 386-402.
- Hsu, Y.-D., and Chen, Y.-P. (1998). Correlation of the mutual diffusion coefficients of binary liquid mixtures. *Fluid Phase Equilibria*. **152**: 149-168.
- INRA (2010). EU/FP6 Migresives closing conference. http://sfpp3.agroparistech.fr/SFPP3/SFPP3_migresives/.
- INRA (2011). SAFE FOOD PAKCAGING PORTAL: research server. <http://modmol.agroparistech.fr/>.
- Ito, T., Seta, J., and Urakawa, H. (1987). Effects of pressure and solvent on the diffusion of aromatic compounds through polymers. *Colloid and Polymer Science*. **265**: 557-573.
- IUPAC (2007). Compendium of Chemical Terminology, 2nd ed, Vol 79. Blackwell Scientific Publications, Oxford.
- Jacquelot, E., Espuche, E., Gérard, J. F., Duchet, J., and Mazabraud, P. (2006). Morphology and gas barrier properties of polyethylene-based nanocomposites. *Journal of Polymer Science Part B: Polymer Physics*. **44**: 431-440.
- Jain, R. K., Gupta, R. N., and Nanda, V. S. (1975). Crystallinity, relaxational transitions, and free volume in high-density polyethylene. *Journal of Macromolecular Science, Part B*. **11**: 411-417.
- James, R. W. (1948). *The Optical Principles of the Diffraction of X-rays*. G. Bell and Sons.
- Jamshidian, M., Tehrani, E. A., and Desobry, S. (2012). Release of synthetic phenolic antioxidants from extruded poly lactic acid (PLA) film. *Food Control*. **28**: 445-455.
- Janes, D. W., and Durning, C. J. (2013). Sorption and Diffusion of n-Alkyl Acetates in Poly(methyl acrylate)/Silica Nanocomposites. *Macromolecules*. **46**: 856-866.
- Jiang, C., Driffield, M., Bradley, E. L., Oldring, P. K. T., Cooke, P., Castle, L., and Guthrie, J. T. (2009). Studies of the aging effect on the level of isocyanate residues in polyester-based can coating systems. *Journal of Coatings Technology and Research*. **6**: 437-444.
- Johns, S. M., Jickells, S. M., Read, W. A., and Castle, L. (2000). Studies on functional barriers to migration. 3. Migration of benzophenone and model ink components from cartonboard to food during frozen storage and microwave heating. *Packaging Technology and Science*. **13**: 99-104.
- Johnson, R. M., Mwaikambo, L. Y., and Tucker, N. (2003). *Biopolymers*. Rapra Technology.
- Juliano, P., Koutchma, T., Sui, Q., Barbosa-Cánovas, G., and Sadler, G. (2010). Polymeric-Based Food Packaging for High-Pressure Processing. *Food Engineering Reviews*. **2**: 274-297.
- June, R. L., Bell, A. T., and Theodorou, D. N. (1990). Molecular dynamics study of methane and xenon in silicalite. *The Journal of Physical Chemistry*. **94**: 8232-8240.
- Jung, T., Simat, T. J., and Altkofer, W. (2010). Mass transfer ways of ultraviolet printing ink ingredients into foodstuffs. *Food Additives and Contaminants Part a-Chemistry Analysis Control Exposure & Risk Assessment*. **27**: 1040-1049.
- Kalambet, Y., Kozmin, Y., Mikhailova, K., Nagaev, I., and Tikhonov, P. (2011). Reconstruction of chromatographic peaks using the exponentially modified Gaussian function. *Journal of Chemometrics*. **25**: 352-356.

- Kalnin, J. R., and Kotomin, E. (1998). Modified Maxwell-Garnett equation for the effective transport coefficients in inhomogeneous media. *Journal of Physics A: Mathematical and General*. **31**: 7227.
- Kalnin, J. R., Kotomin, E. A., and Maier, J. (2002). Calculations of the effective diffusion coefficient for inhomogeneous media. *Journal of Physics and Chemistry of Solids*. **63**: 449-456.
- Kanehashi, S., Kusakabe, A., Sato, S., and Nagai, K. (2010). Analysis of permeability; solubility and diffusivity of carbon dioxide; oxygen; and nitrogen in crystalline and liquid crystalline polymers. *Journal of Membrane Science*. **365**: 40-51.
- Kappenstein, O., Vieth, B., Luch, A., and Pfaff, K. (2012). Toxicologically relevant phthalates in food. *Exs*. **101**: 87-106.
- Karayiannis, N. C., Mavrantzas, V. G., and Theodorou, D. N. (2001). Diffusion of small molecules in disordered media: study of the effect of kinetic and spatial heterogeneities. *Chemical Engineering Science*. **56**: 2789-2801.
- Katiyar, V., Gerds, N., Koch, C. B., Risbo, J., Hansen, H. C. B., and Plackett, D. (2011). Melt Processing of Poly(L-Lactic Acid) in the Presence of Organomodified Anionic or Cationic Clays. *Journal of Applied Polymer Science*. **122**: 112-125.
- Kawamura, Y., Mutsuga, M., Yamauchi, T., Ueda, S., and Tanamoto, K. (2009). [Migration tests of cadmium and lead from paint film of baby toys]. *Shokuhin Eiseigaku Zasshi*. **50**: 93-96.
- Keffer, D. J., Edwards, B. J., and Adhangale, P. (2004). Determination of statistically reliable transport diffusivities from molecular dynamics simulation. *Journal of Non-Newtonian Fluid Mechanics*. **120**: 41-53.
- Keldsen, G. L., Nicholas, J. B., Carrado, K. A., and Winans, R. E. (1994). Molecular modeling of the enthalpies of adsorption of hydrocarbons on smectite clay. *The Journal of Physical Chemistry*. **98**: 279-284.
- Khan, A., Khan, R. A., Salmieri, S., Le Tien, C., Riedl, B., Bouchard, J., Chauve, G., Tan, V., Kamal, M. R., and Lacroix, M. (2012). Mechanical and barrier properties of nanocrystalline cellulose reinforced chitosan based nanocomposite films. *Carbohydrate Polymers*. **90**: 1601-1608.
- Khan, R. A., Dussault, D., Salmieri, S., Safrany, A., and Lacroix, M. (2013). Mechanical and barrier properties of carbon nanotube reinforced PCL-based composite films: Effect of gamma radiation. *Journal of Applied Polymer Science*. **127**: 3962-3969.
- Khan, S. U. (1975). *Soil Organic Matter*. Elsevier Science.
- Kirkwood, J. G., and Riseman, J. (1948). The Intrinsic Viscosities and Diffusion Constants of Flexible Macromolecules in Solution. *The Journal of Chemical Physics*. **16**: 565-573.
- Klages, R. (2007). *Microscopic chaos, fractals and transport in nonequilibrium statistical mechanics*. World Scientific.
- Klages, R., Radons, G., and Sokolov, I. M. (2008). *Anomalous Transport: Foundations and Applications*. Wiley.
- Klopffer, M. H., and Flaconneche, B. (2001). Transport properties of gases in polymers: Bibliographic review. *Oil & Gas Science and Technology-Revue D Ifp Energies Nouvelles*. **56**: 223-244.
- Kofinas, P., Cohen, R. E., and Halasa, A. F. (1994). Gas permeability of polyethylene/poly(ethylene-propylene) semicrystalline diblock copolymers. *Polymer*. **35**: 1229-1235.
- Koh, H. C., Park, J. S., Jeong, M. A., Hwang, H. Y., Hong, Y. T., Ha, S. Y., and Nam, S. Y. (2008). Preparation and gas permeation properties of biodegradable polymer/layered silicate nanocomposite membranes. *Desalination*. **233**: 201-209.
- Kontogeorgis, G. M., and Folas, G. K. (2009). *Thermodynamic Models for Industrial Applications: From Classical and Advanced Mixing Rules to Association Theories*. Wiley.

- Koszinowski, J. (1986). Diffusion and solubility of hydroxy compounds in polyolefines. *Journal of Applied Polymer Science*. **31**: 2711-2720.
- Kotelyanskii, M., and Theodorou, D. N. (2004). Simulation Methods for Polymers. Marcel Dekker.
- Kovarski, A. L. (1997). Molecular Dynamics of Additives in Polymers. VSP.
- Krishna, R., and Wesselingh, J. A. (1997). The Maxwell-Stefan approach to mass transfer. *Chemical Engineering Science*. **52**: 861-911.
- Kundu, K., and Phillips, P. (1987). Hopping transport on site-disordered d-dimensional lattices. *Physical Review A*. **35**: 857-865.
- Kwan, K. S., Subramaniam, C. N. P., and Ward, T. C. (2003). Effect of penetrant size and shape on its transport through a thermoset adhesive: I. n-alkanes. *Polymer*. **44**: 3061-3069.
- Lagaly, G., Ogawa, M., and Dekany, I. (2013). Chapter 10.3 Clay Mineral-Organic Interactions. In: Handbook of Clay Science, pp. 309-377. Bergaya, F., and Lagaly, G. (Eds.), Elsevier Science.
- Lagaron, J. M., and Lopez-Rubio, A. (2011). Nanotechnology for bioplastics: opportunities, challenges and strategies. *Trends in Food Science & Technology*. **22**: 611-617.
- Lakes, R. (1993). Materials with Structural Hierarchy. *Nature*. **361**: 511-515.
- Lambert, Y., Demazeau, G., Largeteau, A., Bouvier, J. M., Laborde-Croubit, S., and Cabannes, M. (2000). Packaging for high-pressure treatments in the food industry. *Packaging Technology and Science*. **13**: 63-71.
- Lange, J., and Wyser, Y. (2003). Recent innovations in barrier technologies for plastic packaging—a review. *Packaging Technology and Science*. **16**: 149-158.
- Langevin, P. (1908). Sur la théorie du mouvement brownien. *C. R. Acad. Sci. (Paris)*. **146**: 530-533.
- Langhe, D. S., Murphy, T. M., Shaver, A., LaPorte, C., Freeman, B. D., Paul, D. R., and Baer, E. (2012). Structural relaxation of polystyrene in nanolayer confinement. *Polymer*. **53**: 1925 - 1931.
- Laoubi, S., and Vergnaud, J. M. (1996). Theoretical treatment of pollutant transfer in a finite volume of food from a polymer packaging made of a recycled film and a functional barrier. *Food Additives and Contaminants*. **13**: 293-306.
- Lau, O.-W., and Wong, S.-K. (2000). Contamination in food from packaging material. *Journal of Chromatography A*. **882**: 255-270.
- Le-Bail, A., Hamadami, N., and Bahuau, S. (2006). Effect of high-pressure processing on the mechanical and barrier properties of selected packagings. *Packaging Technology and Science*. **19**: 237-243.
- Lemons, D. S., and Gythiel, A. (1997). Paul Langevin's 1908 paper "On the Theory of Brownian Motion" ["Sur la théorie du mouvement brownien," *C. R. Acad. Sci. (Paris)* [bold 146], 530--533 (1908)]. *American Journal of Physics*. **65**: 1079-1081.
- Letcher, T. M. (2007). Thermodynamics, solubility and environmental issues. Elsevier.
- Lewis, H., Verghese, K., and Fitzpatrick, L. (2010). Evaluating the Sustainability Impacts of Packaging: the Plastic Carry Bag Dilemma. *Packaging Technology and Science*. **23**: 145-160.
- Leypoldt, J. K., and Gough, D. A. (1980). Penetrant time lag in a diffusion-reaction system. Comments. *The Journal of Physical Chemistry*. **84**: 1058-1059.
- Li, T., Kildsig, D. O., and Park, K. (1997). Computer simulation of molecular diffusion in amorphous polymers. *Journal of Controlled Release*. **48**: 57-66.
- Li, Y., Ren, P. G., Zhang, Q., Shen, T. T., Ci, J. H., and Fang, C. Q. (2013). Properties of Poly(Lactic Acid)/Organo-Montmorillonite Nanocomposites Prepared by Solution Intercalation. *Journal of Macromolecular Science Part B-Physics*. **52**: 1041-1055.
- Liang, Y., Hilal, N., Langston, P., and Starov, V. (2007). Interaction forces between colloidal particles in liquid: Theory and experiment. *Advances in Colloid and Interface Science*. **134-135**: 151-166.

- Lide, D. R. (2009). Handbook of Chemistry and Physics. CRC Press.
- Limm, W., and Hollifield, H. C. (1996). Modelling of additive diffusion in polyolefins. *Food Additives and Contaminants*. **13**: 949-967.
- Linssen, J. P. H., Rijnen, L., Legger-Huijsman, A., and Roozen, J. P. (1998). Combined GC and sniffing port analysis of volatile compounds in rubber rings mounted on beer bottles. *Food Additives and Contaminants*. **15**: 79-83.
- Lipscomb, G. G. (1990). Unified thermodynamic analysis of sorption in rubbery and glassy materials. *Aiche Journal*. **36**: 1505-1516.
- Liu, R. Y. F., Bernal-Lara, T. E., Hiltner, A., and Baer, E. (2004). Interphase materials by forced assembly of glassy polymers. *Macromolecules*. **37**: 6972-6979.
- Llorens, A., Lloret, E., Picouet, P. A., Trbojevich, R., and Fernandez, A. (2012). Metallic-based micro and nanocomposites in food contact materials and active food packaging. *Trends in Food Science & Technology*. **24**: 19-29.
- Lodge, T. P. (1999). Reconciliation of the Molecular Weight Dependence of Diffusion and Viscosity in Entangled Polymers. *Physical Review Letters*. **83**: 3218-3221.
- López-Rubio, A., Almenar, E., Hernandez-Muñoz, P., Lagarón, J. M., Catalá, R., and Gavara, R. (2004). Overview of Active Polymer-Based Packaging Technologies for Food Applications. *Food Reviews International*. **20**: 357-387.
- Lorenzini, R., Fiselier, K., Biedermann, M., Barbanera, M., Braschi, I., and Grob, K. (2010). Saturated and aromatic mineral oil hydrocarbons from paperboard food packaging: estimation of long-term migration from contents in the paperboard and data on boxes from the market. *Food Additives and Contaminants Part a-Chemistry Analysis Control Exposure & Risk Assessment*. **27**: 1765-1774.
- Luetzow, M. (2012). State of the art on the initiatives and activities relevant to risk assessment and risk management of nanotechnologies in the food and agriculture sectors. Takeuchi, M., and Fukushima, K. (Eds.)FAO & WHO.
- Mackenzie, R. C., and Society, M. (1957). The differential thermal investigation of clays. Mineralogical Society (Clay Minerals Group).
- Mai, Y. W., and Yu, Z. Z. (2006). Polymer Nanocomposites. CRC Press.
- Manias, E. (2009). Polymer Nanocomposite Technology, Fundamentals of Barrier. **In**: TAPPI-2009: Flexible Packaging, Nanotechnology Symposium Book, pp. 1-6.
- MAPP 5015.5, R. (2011). CMC Reviews of Type III DMFs for Packaging Materials. Office of Pharmaceutical Science.
- Marais, S., Metayer, M., and Labbe, M. (1999). Water diffusion and permeability in unsaturated polyester resin films characterized by measurements performed with a water-specific permeameter: Analysis of the transient permeation. *Journal of Applied Polymer Science*. **74**: 3380-3395.
- Mark, J. E. (1999). Polymer Data Handbook. Oxford University Press.
- Mark, J. E. (2007a). Physical Properties of Polymer Handbook. Springer New York.
- Mark, J. E. (2007b). Physical properties of polymers handbook: permeability of polymers to gases and vapors. Springer.
- Marque, D., Feigenbaum, A., Dainelli, D., and Riquet, A. M. (1998). Safety evaluation of an ionized multilayer plastic film used for vacuum cooking and meat preservation. *Food Additives and Contaminants*. **15**: 831-841.
- Marqué, D., Feigenbaum, A., and Riquet, A. (1996). Repercussions of the ionization of plastic packaging on the compatibility with packaged foodstuffs. *Journal de Chimie Physique et de Physico-Chimie Biologique*. **93**: 165-168.
- Marras, S. I., Kladi, K. P., Tsivintzelis, I., Zuburtikudis, I., and Panayiotou, C. (2008). Biodegradable polymer nanocomposites: The role of nanoclays on the thermomechanical characteristics and the electrospun fibrous structure. *Acta Biomaterialia*. **4**: 756-765.

- Martucci, J. F., and Ruseckaite, R. A. (2010). Three-Layer Sheets Based on Gelatin and Poly(lactic acid), Part 1: Preparation and Properties. *Journal of Applied Polymer Science*. **118**: 3102-3110.
- Masaro, L., and Zhu, X. X. (1999). Physical models of diffusion for polymer solutions, gels and solids. *Progress in Polymer Science*. **24**: 731-775.
- Massey, L. K. (2002). Permeability Properties of Plastics and Elastomers, 2nd Ed.: A Guide to Packaging and Barrier Materials. Elsevier Science.
- Matet, M., Heuzey, M. C., Pollet, E., Aji, A., and Averous, L. (2013). Innovative thermoplastic chitosan obtained by thermo-mechanical mixing with polyol plasticizers. *Carbohydrate Polymers*. **95**: 241-251.
- Mattozzi, A., Serralunga, P., Hedenqvist, M. S., and Gedde, U. W. (2006). Mesoscale modelling of penetrant diffusion in computer-generated polyethylene-spherulite-like structures. *Polymer*. **47**: 5588-5595.
- Mauritz, K. A., and Storey, R. F. (1990). A general free volume based theory for the diffusion of large molecules in amorphous polymers above T_g. 2. Molecular shape dependence. *Macromolecules*. **23**: 2033-2038.
- Mauritz, K. A., Storey, R. F., and George, S. E. (1990). A general free volume-based theory for the diffusion of large molecules in amorphous polymers above the glass temperature. I. Application to di-n-alkyl phthalates in PVC. *Macromolecules*. **23**: 441-450.
- Maxwell, J. C. (1873). Treatise on Electricity and Magnetism. Clarendon Press, London, Oxford.
- McKeen, L. W. (2008). Effect of Temperature and other Factors on Plastics and Elastomers. Elsevier Science.
- Meerwall, E. v., Beckman, S., Jang, J., and Mattice, W. L. (1998). Diffusion of liquid n-alkanes: Free-volume and density effects. *The Journal of Chemical Physics*. **108**: 4299-4304.
- Mehrer, H. (2010). Diffusion in Solids: Fundamentals, Methods, Materials, Diffusion-Controlled Processes. Springer.
- Mensitieri, G., Apicella, A., Nobile, M. A., and Nicolais, L. (1991). Solvent mixtures sorption in amorphous peek. *Polymer Bulletin*. **27**: 323-330.
- Mercea, P. (2008). Chapter 5 Models for diffusion in polymers. **In**: Plastic Packaging: Interactions with Food and Pharmaceuticals. Pinger, O., and Baner, A. (Eds.), Wiley.
- Mercea, P. (2009). Physicochemical Processes Involved in Migration of Bisphenol A from Polycarbonate. *Journal of Applied Polymer Science*. **112**: 579-593.
- Mering, J., and Oberlin, A. (1967). Electron-Optical Study of Smectites. *Clays and Clay Minerals*. **15**: 3-25.
- Merkel, T. C., Freeman, B. D., Spontak, R. J., He, Z., Pinnau, I., Meakin, P., and Hill, A. J. (2002a). Sorption, Transport, and Structural Evidence for Enhanced Free Volume in Poly(4-methyl-2-pentyne)/Fumed Silica Nanocomposite Membranes. *Chemistry of Materials*. **15**: 109-123.
- Merkel, T. C., Freeman, B. D., Spontak, R. J., He, Z., Pinnau, I., Meakin, P., and Hill, A. J. (2002b). Ultrapermable, Reverse-Selective Nanocomposite Membranes. *Science*. **296**: 519-522.
- Merkel, T. C., He, Z. J., Pinnau, I., Freeman, B. D., Meakin, P., and Hill, A. J. (2003). Effect of nanoparticles on gas sorption and transport in poly(1-trimethylsilyl-1-propyne). *Macromolecules*. **36**: 6844-6855.
- Messersmith, P. B., and Giannelis, E. P. (1995). Synthesis and barrier properties of poly(ϵ -caprolactone)-layered silicate nanocomposites. *Journal of Polymer Science Part A: Polymer Chemistry*. **33**: 1047-1057.
- Métayer, M., Labbé, M., Marais, S., Langevin, D., Chappay, C., Dreux, F., Brainville, M., and Belliard, P. (1999). Diffusion of water through various polymer films: a new high performance method of characterization. *Polymer Testing*. **18**: 533-549.

- Metois, P., Scholler, D., Bouquant, J., and Feigenbaum, A. (1998). Alternative test methods to control the compliance of polyolefin food packaging materials with the European Union regulation: the case of aromatic antioxidants and of bis(ethanolamine) antistatics based on H-1-NMR and UV-visible spectrophotometry. *Food Additives and Contaminants*. **15**: 100-111.
- Metropolis, N., Rosenbluth, A. W., Rosenbluth, M. N., Teller, A. H., and Teller, E. (1953). Equation of State Calculations by Fast Computing Machines. *The Journal of Chemical Physics*. **21**: 1087-1092.
- Michaels, A. S., and Bixler, H. J. (1961). Solubility of gases in polyethylene. *Journal of Polymer Science*. **50**: 393-412.
- Miller-Chou, B. A., and Koenig, J. L. (2003). A review of polymer dissolution. *Progress in Polymer Science*. **28**: 1223-1270.
- Miller, A. A. (1968). Kinetic interpretation of the glass transition: Glass temperatures of n-alkane liquids and polyethylene. *Journal of Polymer Science Part A-2: Polymer Physics*. **6**: 249-257.
- Miltz, J., Ram, A., and Nir, M. M. (1997). Prospects for application of post-consumer used plastics in food packaging. *Food Additives and Contaminants*. **14**: 649-659.
- Minelli, M., Baschetti, M. G., and Doghieri, F. (2011). A comprehensive model for mass transport properties in nanocomposites. *Journal of Membrane Science*. **381**: 10-20.
- Mittal, V. (2009). Barrier Properties of Polymer Clay Nanocomposites. Nova Science Publishers, Incorporated.
- Moisan, J. Y. (1980). Diffusion des additifs du polyethylene—I: Influence de la nature du diffusant. *European Polymer Journal*. **16**: 979-987.
- Möller, K., and Gevert, T. (1994). An FTIR solid-state analysis of the diffusion of hindered phenols in low-density polyethylene (LDPE): The effect of molecular size on the diffusion coefficient. *Journal of Applied Polymer Science*. **51**: 895-903.
- Monticelli, O., Musina, Z., Frache, A., Bellucci, F., Camino, G., and Russo, S. (2007). Influence of compatibilizer degradation on formation and properties of PA6/organoclay nanocomposites. *Polymer Degradation and Stability*. **92**: 370-378.
- Morrissey, P., and Vesely, D. (2000). Accurate measurement of diffusion rates of small molecules through polymers. *Polymer*. **41**: 1865-1872.
- Mu, M., Clarke, N., Composto, R. J., and Winey, K. I. (2009). Polymer Diffusion Exhibits a Minimum with Increasing Single-Walled Carbon Nanotube Concentration. *Macromolecules*. **42**: 7091-7097.
- Mu, M., Seitz, M. E., Clarke, N., Composto, R. J., and Winey, K. I. (2010). Polymer Tracer Diffusion Exhibits a Minimum in Nanocomposites Containing Spherical Nanoparticles. *Macromolecules*. **44**: 191-193.
- Mueller, F., Krueger, K.-M., and Sadowski, G. (2012). Non-Fickian Diffusion of Toluene in Polystyrene in the Vicinity of the Glass-Transition Temperature. *Macromolecules*. **45**: 926-932.
- Muller-Plathe, F. (1991). Diffusion of penetrants in amorphous polymers: A molecular dynamics study. *The Journal of Chemical Physics*. **94**: 3192-3199.
- Muncke, J. (2009). Exposure to endocrine disrupting compounds via the food chain: Is packaging a relevant source? *Science of The Total Environment*. **407**: 4549-4559.
- Muncke, J. (2011). Endocrine disrupting chemicals and other substances of concern in food contact materials: An updated review of exposure, effect and risk assessment. *The Journal of Steroid Biochemistry and Molecular Biology*. **127**: 118-127.
- Munro, C., Hlywka, J. J., and Kennepohl, E. M. (2002). Risk assessment of packaging materials. *Food Addit Contam*. **19 Suppl**: 3-12.
- Muralidharan, M. N., Kumar, S. A., and Thomas, S. (2008). Morphology and transport characteristics of poly(ethylene-co-vinyl acetate)/clay nanocomposites. *Journal of Membrane Science*. **315**: 147-154.

- Murphy, T. M., Langhe, D. S., Ponting, M., Baer, E., Freeman, B. D., and Paul, D. R. (2011). Physical aging of layered glassy polymer films via gas permeability tracking. *Polymer*. **52**: 6117 - 6125.
- Murrae, J. B. (1988). Polymers for Electronic and Photonic Applications. **In**: Electronic and Photonic Applications of Polymers, pp. 1-73. American Chemical Society.
- Nair, R. R., Wu, H. A., Jayaram, P. N., Grigorieva, I. V., and Geim, A. K. (2012). Unimpeded Permeation of Water Through Helium-Leak-Tight Graphene-Based Membranes. *Science*. **335**: 442-444.
- Nam, P. H., Fujimori, A., and Masuko, T. (2004). The dispersion behavior of clay particles in poly(L-lactide)/organo-modified montmorillonite hybrid systems. *Journal of Applied Polymer Science*. **93**: 2711-2720.
- Narasimhan, B. (2001). Mathematical models describing polymer dissolution: consequences for drug delivery. *Advanced Drug Delivery Reviews*. **48**: 195-210.
- Narasimhan, B., and Peppas, N. A. (1996). On the Importance of Chain Reptation in Models of Dissolution of Glassy Polymers. *Macromolecules*. **29**: 3283-3291.
- Nauman, E. B., and He, D. Q. (2001). Nonlinear diffusion and phase separation. *Chemical Engineering Science*. **56**: 1999-2018.
- Neethirajan, S., and Jayas, D. (2011). Nanotechnology for the Food and Bioprocessing Industries. *Food and Bioprocess Technology*. **4**: 39-47.
- Neogi, P. (1996). Diffusion in Polymers. Marcel Dekker.
- Nerin, C., Albinana, J., Philo, M. R., Castle, L., Raffael, B., and Simoneau, C. (2003a). Evaluation of some screening methods for the analysis of contaminants in recycled polyethylene terephthalate flakes. *Food Additives and Contaminants*. **20**: 668-677.
- Nerin, C., Canellas, E., Aznar, M., and Silcock, P. (2009). Analytical methods for the screening of potential volatile migrants from acrylic-base adhesives used in food-contact materials. *Food Additives and Contaminants Part a-Chemistry Analysis Control Exposure & Risk Assessment*. **26**: 1592-1601.
- Nerin, C., Fernandez, C., Domeno, C., and Salafranca, J. (2003b). Determination of potential migrants in polycarbonate containers used for microwave ovens by high-performance liquid chromatography with ultraviolet and fluorescence detection. *Journal of Agricultural and Food Chemistry*. **51**: 5647-5653.
- Ngai, K. L., and Plazek, D. J. (2007). Temperature Dependence of the Viscoelastic Response of Polymer Systems. **In**: Physical Properties of Polymer Handbook, p. 455. Mark, J. E. (Ed.), Springer New York.
- Nguyen, P.-M., Goujon, A., Sauvegrain, P., and Vitrac, O. (2013). A computer-aided methodology to design safe food packaging and related systems. *Aiche Journal*: n/a-n/a.
- Nichols, D. (2004). Biocides in Plastics. Rapra.
- Nielsen, L. E. (1967). Models for the Permeability of Filled Polymer Systems. *Journal of Macromolecular Science: Part A - Chemistry*. **1**: 929-942.
- Nilsson, F., Gedde, U. W., and Hedenqvist, M. S. (2009). Penetrant diffusion in polyethylene spherulites assessed by a novel off-lattice Monte-Carlo technique. *European Polymer Journal*. **45**: 3409-3417.
- Noguerol-Cal, R., Lopez-Vilarino, J. M., Fernandez-Martinez, G., Gonzalez-Rodriguez, M. V., and Barral-Losada, L. F. (2010). Liquid chromatographic methods to analyze hindered amines light stabilizers (HALS) levels to improve safety in polyolefins. *J Sep Sci*. **33**: 2698-2706.
- Olphen, H. V. (1964). An Introduction to Clay Colloid Chemistry. *Soil Science*. **97**: 290.
- Olson, B. G., Peng, Z. L., Srithawatpong, R., McGervey, J. D., Ishida, H., Jamieson, A. M., Manias, E., and Giannelis, E. P. (1997). Free Volume in Layered Organosilicate-Polystyrene Nanocomposites. **In**: Materials Science Forum, pp. 336-340.
- Osman, M. A., Mittal, V., Morbidelli, M., and Suter, U. W. (2003). Polyurethane Adhesive Nanocomposites as Gas Permeation Barrier. *Macromolecules*. **36**: 9851-9858.

- Osman, M. A., Mittal, V., and Suter, U. W. (2007). Poly(propylene)-Layered Silicate Nanocomposites: Gas Permeation Properties and Clay Exfoliation. *Macromolecular Chemistry and Physics*. **208**: 68-75.
- Otsuka, E., and Suzuki, A. (2009). A simple method to obtain a swollen PVA gel crosslinked by hydrogen bonds. *Journal of Applied Polymer Science*. **114**: 10-16.
- Özal, T. A., Peter, C., Hess, B., and van der Vegt, N. F. A. (2008). Modeling Solubilities of Additives in Polymer Microstructures: Single-Step Perturbation Method Based on a Soft-Cavity Reference State. *Macromolecules*. **41**: 5055-5061.
- Page, B. D., and Lacroix, G. M. (1992). Studies into the transfer and migration of phthalate esters from aluminium foil-paper laminates to butter and margarine. *Food Additives and Contaminants*. **9**: 197-212.
- Pandey, S. K., and Kim, K.-H. (2011). An evaluation of volatile compounds released from containers commonly used in circulation of sports beverages. *Ecotoxicology and Environmental Safety*. **74**: 527-532.
- Paquette Kristina, E. (2004). Irradiation of Prepackaged Food: Evolution of the U.S. Food and Drug Administration's Regulation of the Packaging Materials. **In**: Irradiation of Food and Packaging, pp. 182-202. American Chemical Society.
- Park, H. S., Chang, T., and Lee, S. H. (2000). Diffusion of small probe molecule in oligomers. *The Journal of Chemical Physics*. **113**: 5502-5510.
- Park, Y., Ayoko, G. A., and Frost, R. L. (2011). Application of organoclays for the adsorption of recalcitrant organic molecules from aqueous media. *Journal of Colloid and Interface Science*. **354**: 292-305.
- Pastor, R. W., and Karplus, M. (1988). Parametrization of the friction constant for stochastic simulations of polymers. *The Journal of Physical Chemistry*. **92**: 2636-2641.
- Pastorelli, S., Sanches-Silva, A., Manuel Cruz, J., Simoneau, C., and Paseiro Losada, P. (2008). Study of the migration of benzophenone from printed paperboard packages to cakes through different plastic films. *European Food Research and Technology*. **227**: 1585-1590.
- Patrick, S. G., and Limited, R. T. (2005). Practical Guide to Polyvinyl Chloride. Rapra Technology.
- Pavel, D., and Shanks, R. (2005). Molecular dynamics simulation of diffusion of O₂ and CO₂ in blends of amorphous poly(ethylene terephthalate) and related polyesters. *Polymer*. **46**: 6135-6147.
- Peltzer, M., Wagner, J., and Jimenez, A. (2009). Migration study of carvacrol as a natural antioxidant in high-density polyethylene for active packaging. *Food Additives and Contaminants Part a-Chemistry Analysis Control Exposure & Risk Assessment*. **26**: 938-946.
- Pennarun, P. Y., Dole, P., and Feigenbaum, A. (2004a). Functional barriers in PET recycled bottles. Part I. Determination of diffusion coefficients in bioriented PET with and without contact with food simulants. *Journal of Applied Polymer Science*. **92**: 2845-2858.
- Pennarun, P. Y., Ngono, Y., Dole, P., and Feigenbaum, A. (2004b). Functional barriers in PET recycled bottles. Part II. Diffusion of pollutants during processing. *Journal of Applied Polymer Science*. **92**: 2859-2870.
- Peppas, N. A., and Merrill, E. W. (1976). Differential scanning calorimetry of crystallized PVA hydrogels. *Journal of Applied Polymer Science*. **20**: 1457-1465.
- Perez-Palacios, D., Angel Fernandez-Recio, M., Moreta, C., and Teresa Tena, M. (2012). Determination of bisphenol-type endocrine disrupting compounds in food-contact recycled-paper materials by focused ultrasonic solid-liquid extraction and ultra performance liquid chromatography-high resolution mass spectrometry. *Talanta*. **99**: 167-174.

- Petersen, J. H., and Jensen, L. K. (2010). Phthalates and food-contact materials: enforcing the 2008 European Union plastics legislation. *Food Addit Contam Part A Chem Anal Control Expo Risk Assess.* **27**: 1608-1616.
- Pezo, D., Fedeli, M., Bosetti, O., and Nerin, C. (2012). Aromatic amines from polyurethane adhesives in food packaging: The challenge of identification and pattern recognition using Quadrupole-Time of Flight-Mass Spectrometry(E). *Analytica Chimica Acta.* **756**: 49-59.
- Phillips, P. J. (1990). Mechanism of orientation of aromatic molecules by stretched polyethylene. *Chemical Reviews.* **90**: 425-436.
- Picard, E., Gauthier, H., Gérard, J. F., and Espuche, E. (2007). Influence of the intercalated cations on the surface energy of montmorillonites: Consequences for the morphology and gas barrier properties of polyethylene/montmorillonites nanocomposites. *Journal of Colloid and Interface Science.* **307**: 364-376.
- Piergiovanni, L., Fava, P., and Schiraldi, A. (1999). Study of diffusion through LDPE film of Di-n-butyl phthalate. *Food Additives and Contaminants.* **16**: 353-359.
- Pinte, J., Joly, C., Dole, P., and Feigenbaum, A. (2010). Diffusion of homologous model migrants in rubbery polystyrene: molar mass dependence and activation energy of diffusion. *Food Additives & Contaminants: Part A.* **27**: 557-566.
- Pinte, J. r. m., Joly, C., Plé, K., Dole, P., and Feigenbaum, A. (2008). Proposal of a Set of Model Polymer Additives Designed for Confocal FRAP Diffusion Experiments. *Journal of Agricultural and Food Chemistry.* **56**: 10003-10011.
- Piringer, O. G., and Baner, A. L. (2000). Plastic packaging materials for food: barrier function, mass transport, quality assurance, and legislation. Wiley-VCH.
- Piringer, O. G., and Baner, A. L. (2008). Plastic Packaging: Interactions with Food and Pharmaceuticals. Wiley.
- Plazek, D. J., Schlosser, E., Schonhals, A., and Ngai, K. L. (1993). Breakdown of the Rouse model for polymers near the glass transition temperature. *The Journal of Chemical Physics.* **98**: 6488-6491.
- Poças, M. d. F., and Hogg, T. (2007). Exposure assessment of chemicals from packaging materials in foods: a review. *Trends in Food Science & Technology.* **18**: 219-230.
- Poças, M. d. F., Oliveira, J. C., Pereira, J. R., Brandsch, R., and Hogg, T. (2011). Modelling migration from paper into a food simulant. *Food Control.* **22**: 303-312.
- Poças, M. F., Oliveira, J. C., Brandsch, R., and Hogg, T. (2010). Feasibility Study on the Use of Probabilistic Migration Modeling in Support of Exposure Assessment from Food Contact Materials. *Risk Analysis.* **30**: 1052-1061.
- Poças, M. F., Oliveira, J. C., Oliveira, F. A. R., and Hogg, T. (2008). A Critical Survey of Predictive Mathematical Models for Migration from Packaging. *Critical Reviews in Food Science and Nutrition.* **48**: 913-928.
- Poole, A., van Herwijnen, P., Weideli, H., Thomas, M. C., Ransbotyn, G., and Vance, C. (2004). Review of the toxicology, human exposure and safety assessment for bisphenol A diglycidylether (BADGE). *Food Additives and Contaminants.* **21**: 905-919.
- Potts, J. R., Dreyer, D. R., Bielawski, C. W., and Ruoff, R. S. (2011). Graphene-based polymer nanocomposites. *Polymer.* **52**: 5-25.
- Prince E. Rouse, J. (1953). A Theory of the Linear Viscoelastic Properties of Dilute Solutions of Coiling Polymers. *The Journal of Chemical Physics.* **21**: 1272-1280.
- Pryamitsyn, V., Hanson, B., and Ganesan, V. (2011). Coarse-Grained Simulations of Penetrant Transport in Polymer Nanocomposites. *Macromolecules.* **44**: 9839-9851.
- Psillos, S. (2011). Moving Molecules Above the Scientific Horizon: On Perrin's Case for Realism. *Journal for General Philosophy of Science.* **42**: 339-363.
- Queyroy, S., and Monasse, B. (2012). Effect of the molecular structure of semicrystalline polyethylene on mechanical properties studied by molecular dynamics. *Journal of Applied Polymer Science.* **125**: 4358-4367.

- Quijada-Garrido, I., Barrales-Rienda, J. M., and Frutos, G. (1996). Diffusion of Erucamide (13-cis-Docosamide) in Isotactic Polypropylene†. *Macromolecules*. **29**: 7164-7176.
- Rahman, S. (2007). Handbook of Food Preservation, Second Edition. Taylor & Francis.
- Ranjit, N., Siefert, K., and Padmanabhan, V. (2010). Bisphenol-A and disparities in birth outcomes: a review and directions for future research. *J Perinatol*. **30**: 2-9.
- Raquez, J.-M., Habibi, Y., Murariu, M., and Dubois, P. "Polylactide (PLA)-based nanocomposites". *Progress in Polymer Science*.
- Ray, S. S., Okamoto, K., and Okamoto, M. (2003). Structure-property relationship in biodegradable poly(butylene succinate)/layered silicate nanocomposites. *Macromolecules*. **36**: 2355-2367.
- Rayleigh, L. (1892). LVI. On the influence of obstacles arranged in rectangular order upon the properties of a medium. *Philosophical Magazine Series 5*. **34**: 481-502.
- Reiter, G., and Strobl, G. R. (2007). Progress in Understanding of Polymer Crystallization. Springer.
- Restuccia, D., Spizzirri, U. G., Parisi, O. I., Cirillo, G., Curcio, M., Iemma, F., Puoci, F., Vinci, G., and Picci, N. (2010). New EU regulation aspects and global market of active and intelligent packaging for food industry applications. *Food Control*. **21**: 1425-1435.
- Reynier, A., Dole, P., and Feigenbaum, A. (2001a). Additive diffusion coefficients in polyolefins. II. Effect of swelling and temperature on the $D = f(M)$ correlation. *Journal of Applied Polymer Science*. **82**: 2434-2443.
- Reynier, A., Dole, P., Humbel, S., and Feigenbaum, A. (2001b). Diffusion coefficients of additives in polymers. I. Correlation with geometric parameters. *Journal of Applied Polymer Science*. **82**: 2422-2433.
- Rhee, C.-K., Ferry, J. D., and Fetters, L. J. (1977). Diffusion of radioactively tagged penetrants through rubbery polymers. II. Dependence on molecular length of penetrant. *Journal of Applied Polymer Science*. **21**: 783-790.
- Rhim, J.-W., and Ng, P. K. W. (2007). Natural Biopolymer-Based Nanocomposite Films for Packaging Applications. *Critical Reviews in Food Science and Nutrition*. **47**: 411-433.
- Riquet, A. M., Wolff, N., Laoubi, S., Vergnaud, J. M., and Feigenbaum, A. (1998). Food and packaging interactions: Determination of the kinetic parameters of olive oil diffusion in polypropylene using concentration profiles. *Food Additives and Contaminants*. **15**: 690-700.
- Rodríguez, J. L. P. (2003). Applied Study of Cultural Heritage and Clays. Consejo Superior de Investigaciones Científicas.
- Roduit, B., Borgeat, C. H., Cavin, S., Fragniere, C., and Dudler, V. (2005). Application of Finite Element Analysis (FEA) for the simulation of release of additives from multilayer polymeric packaging structures. *Food Additives and Contaminants*. **22**: 945-955.
- Roe, R.-J., Bair, H. E., and Gieniewski, C. (1974). Solubility and diffusion coefficient of antioxidants in polyethylene. *Journal of Applied Polymer Science*. **18**: 843-856.
- Romao, W., Spinace, M. A. S., and De Paoli, M. A. (2009). Poly(Ethylene Terephthalate), PET. A Review on the Synthesis Processes, Degradation Mechanisms and its Recycling. *Polimeros-Ciencia E Tecnologia*. **19**: 121-132.
- Romdhane, I. H., Danner, R. P., and Duda, J. L. (1995). Influence of the Glass Transition on Solute Diffusion in Polymers by Inverse Gas Chromatography. *Industrial & Engineering Chemistry Research*. **34**: 2833-2840.
- Rottach, D. R., Tillman, P. A., McCoy, J. D., Plimpton, S. J., and Curro, J. G. (1999). The diffusion of simple penetrants in tangent site polymer melts. *The Journal of Chemical Physics*. **111**: 9822-9831.
- Rouse, J. P. E. (1953). A Theory of the Linear Viscoelastic Properties of Dilute Solutions of Coiling Polymers. *The Journal of Chemical Physics*. **21**: 1272-1280.

- Saby-Dubreuil, A. C., Guerrier, B., Allain, C., and Johannsmann, D. (2001). Glass transition induced by solvent desorption for statistical MMA/nBMA copolymers — Influence of copolymer composition. *Polymer*. **42**: 1383-1391.
- Sadler, G., Chappas, W., and Pierce, D. E. (2001). Evaluation of e-beam, gamma- and X-ray treatment on the chemistry and safety of polymers used with pre-packaged irradiated foods: a review. *Food Additives and Contaminants*. **18**: 475-501.
- Sadler, G., Pierce, D., Lawson, A., Suvannunt, D., and Senthil, V. (1996). Evaluating organic compound migration in poly(ethylene terephthalate): A simple test with implications for polymer recycling. *Food Additives and Contaminants*. **13**: 979-989.
- Sagiv, A. (2001). Exact solution of mass diffusion into a finite volume. *Journal of Membrane Science*. **186**: 231-237.
- Sagiv, A. (2002). Theoretical formulation of the diffusion through a slab-theory validation. *Journal of Membrane Science*. **199**: 125-134.
- Salazar, R., Domenech, S., Courgneau, C., and Ducruet, V. (2012). Plasticization of poly(lactide) by sorption of volatile organic compounds at low concentration. *Polymer Degradation and Stability*. **97**: 1871-1880.
- Sanches-Silva, A., Andre, C., Castanheira, I., Manuel Cruz, J., Pastorelli, S., Simoneau, C., and Paseiro-Losada, P. (2009). Study of the Migration of Photoinitiators Used in Printed Food-Packaging Materials into Food Simulants. *Journal of Agricultural and Food Chemistry*. **57**: 9516-9523.
- Sanches Silva, A., Cruz Freire, J. M., and Paseiro Losada, P. (2010). Study of the diffusion coefficients of diphenylbutadiene and triclosan into and within meat. *European Food Research and Technology*. **230**: 957-964.
- Sanches Silva, A., Cruz, J. M., Sendón Garcí'a, R., Franz, R., and Paseiro Losada, P. (2007). Kinetic migration studies from packaging films into meat products. *Meat Science*. **77**: 238-245.
- Sanchez-Garcia, M., and Lagaron, J. (2010). On the use of plant cellulose nanowhiskers to enhance the barrier properties of polylactic acid. *Cellulose*. **17**: 987-1004.
- Sangani, A. S., and Yao, C. (1988). Bulk thermal conductivity of composites with spherical inclusions. *Journal of Applied Physics*. **63**: 1334-1341.
- Sapalidis, A. A., Katsaros, F. K., and Kanellopoulos, N. K. (2011). PVA / Montmorillonite Nanocomposites: Development and Properties. **In**: Nanocomposites and Polymers with Analytical Methods. Cuppoletti, J. (Ed.), InTech.
- Sax, J., and Ottino, J. M. (1983). Modeling of transport of small molecules in polymer blends: Application of effective medium theory. *Polymer Engineering & Science*. **23**: 165-176.
- Schafer, H., Mark, A. E., and Gunsteren, W. F. v. (2000). Absolute entropies from molecular dynamics simulation trajectories. *The Journal of Chemical Physics*. **113**: 7809-7817.
- Schmidt-Rohr, K., and Spiess, H. W. (1991). Chain diffusion between crystalline and amorphous regions in polyethylene detected by 2D exchange carbon-13 NMR. *Macromolecules*. **24**: 5288-5293.
- Seta, J., Ogino, T., and Ito, T. (1984). Activation volume for the diffusion of disperse dye in nylon 6. *Sen'i Gakkaishi*. **40**: T263-T268.
- Shanklin, A. P., and Sánchez, E. R. (2005). Regulatory report: FDA's Food Contact Substance Notification Program. **In**: Food safety magazine: Building a bridge to global food safety, October/November 2005. Cianci, S. (Ed.).
- Sharpe, R. M. (2010). Is It Time to End Concerns over the Estrogenic Effects of Bisphenol A? *Toxicological Sciences*. **114**: 1-4.
- Shen, L., and Chen, Z. (2007). Critical review of the impact of tortuosity on diffusion. *Chemical Engineering Science*. **62**: 3748-3755.
- Shogren, R. (1997). Water vapor permeability of biodegradable polymers. *Journal of Environmental Polymer Degradation*. **5**: 91-95.

- Silva, A. S., García, R. S., Cooper, I., Franz, R., and Losada, P. P. (2006). Compilation of analytical methods and guidelines for the determination of selected model migrants from plastic packaging. *Trends in Food Science & Technology*. **17**: 535-546.
- Simal-Gandara, J., Damant, A. P., and Castle, L. (2002). The use of LC-MS in studies of migration from food contact materials: A review of present applications and future possibilities. *Critical Reviews in Analytical Chemistry*. **32**: 47-78.
- Simal-Gandara, J., Sarria-Vidal, M., Koorevaar, A., and Rijk, R. (2000). Tests of potential functional barriers for laminated multilayer food packages. Part I: Low molecular weight permeants. *Food Additives and Contaminants*. **17**: 703-711.
- Simha, R., and Boyer, R. F. (1962). On a General Relation Involving the Glass Temperature and Coefficients of Expansion of Polymers. *The Journal of Chemical Physics*. **37**: 1003-1007.
- Singh, S., Gupta, R. K., Ghosh, A. K., Maiti, S. N., and Bhattacharya, S. N. (2010). Poly(L-Lactic acid)/layered silicate nanocomposite blown film for packaging application : thermal, mechanical and barrier properties. *Journal of Polymer Engineering*. **30**: 361-375.
- Sinha Ray, S., Okamoto, K., and Okamoto, M. (2003a). Structure–Property Relationship in Biodegradable Poly(butylene succinate)/Layered Silicate Nanocomposites. *Macromolecules*. **36**: 2355-2367.
- Sinha Ray, S., and Okamoto, M. (2003). Polymer/layered silicate nanocomposites: a review from preparation to processing. *Progress in Polymer Science*. **28**: 1539-1641.
- Sinha Ray, S., Yamada, K., Okamoto, M., Fujimoto, Y., Ogami, A., and Ueda, K. (2003b). New polylactide/layered silicate nanocomposites. 5. Designing of materials with desired properties. *Polymer*. **44**: 6633-6646.
- Siracusa, V. (2012). Food Packaging Permeability Behaviour: A Report. *International Journal of Polymer Science*. **2012**: 11.
- Siva, N. (2012). Controversy continues over safety of bisphenol A. *The Lancet*. **379**: 1186.
- Skolnick, J., Yaris, R., and Kolinski, A. (1988). Phenomenological theory of the dynamics of polymer melts. I. Analytic treatment of self-diffusion. *The Journal of Chemical Physics*. **88**: 1407-1417.
- Smirnova, V. V., Krasnoiarova, O. V., Pridvorova, S. M., Zherdev, A. V., Gmoshinskii, I. V., Kazydub, G. V., Popov, K. I., and Khotimchenko, S. A. (2012). Characterization of silver nanoparticles migration from package materials destined for contact with foods. *Voprosy pitaniia*. **81**: 34-39.
- Solovyov, S., and Goldman, A. (2007). Mass Transport and Reactive Barriers in Packaging: Theory, Applications And Design. DEStech Pub.
- Solovyov, S., and Goldman, A. (2008). Mass Transport and Reactive Barriers in Packaging: Theory, Applications And Design. Destech Publications Incorporated.
- Solunov, C. A. (2002). The apparent activation energy and relaxation volume from the point of view of Adam–Gibbs theory. *Journal of Physics: Condensed Matter*. **14**: 7297.
- Spearot, D. E., Sudibjo, A., Ullal, V., and Huang, A. (2012). Molecular Dynamics Simulations of Diffusion of O₂ and N₂ Penetrants in Polydimethylsiloxane-Based Nanocomposites. *Journal of Engineering Materials and Technology*. **134**: 021013.
- Sperling, L. H. (2006). Introduction to physical polymer science: concentrated solutions, phase separation behavior, and diffusion. Wiley-Interscience.
- Stachel, J. (2005). Einstein's Miraculous Year: Five Papers That Changed The Face Of Physics. Princeton University Press.
- Starikov, E. B., and Nordén, B. (2007). Enthalpy–Entropy Compensation: A Phantom or Something Useful? *The Journal of Physical Chemistry B*. **111**: 14431-14435.
- Stastna, J., and De Kee, D. (1995). Transport Properties in Polymers. Technomic Publishing Company.

- Störmer, A. (2010). Final activity report: Research programme on migration from adhesives in food packaging materials in support of European Legislation and Standardisation. MIGRESIVES.
- Strawhecker, K. E., and Manias, E. (2000). Structure and Properties of Poly(vinyl alcohol)/Na⁺ Montmorillonite Nanocomposites. *Chemistry of Materials*. **12**: 2943-2949.
- Strobl, G. R. (1997). *The Physics of Polymers: Concepts for Understanding Their Structures and Behavior*. Springer-Verlag.
- Sun, H. (1998). COMPASS: An ab Initio Force-Field Optimized for Condensed-Phase Applications Overview with Details on Alkane and Benzene Compounds. *The Journal of Physical Chemistry B*. **102**: 7338-7364.
- Sunderrajan, S., Hall, C. K., and Freeman, B. D. (1996). Estimation of mutual diffusion coefficients in polymer/penetrant systems using nonequilibrium molecular dynamics simulations. *The Journal of Chemical Physics*. **105**: 1621-1632.
- Svagan, A. J., Akesson, A., Cardenas, M., Bulut, S., Knudsen, J. C., Risbo, J., and Plackett, D. (2012). Transparent Films Based on PLA and Montmorillonite with Tunable Oxygen Barrier Properties. *Biomacromolecules*. **13**: 397-405.
- Tacker, M. (2011). Endocrine disrupting components and packaging. *Ernahrung*. **35**: 308-313.
- Tan, W., Zhang, Y., Szeto, Y.-s., and Liao, L. (2008). A novel method to prepare chitosan/montmorillonite nanocomposites in the presence of hydroxy-aluminum oligomeric cations. *Composites Science and Technology*. **68**: 2917-2921.
- Tehrany, E. A., and Desobry, S. (2004). Partition coefficients in food/packaging systems: a review. *Food Additives and Contaminants Part a-Chemistry Analysis Control Exposure & Risk Assessment*. **21**: 1186-1202.
- Teraoka, I. (2002). *Polymer Solutions: An Introduction to Physical Properties*. Wiley.
- Till, D., Schwoppe, A. D., Ehntholt, D. J., Sidman, K. R., Whelan, R. H., Schwartz, P. S., and Reid, R. C. (1987). Indirect food additive migration from polymeric food packaging materials. *Crit Rev Toxicol*. **18**: 215-243.
- Tiwari, R. R., Khilar, K. C., and Natarajan, U. (2008). Synthesis and characterization of novel organo-montmorillonites. *Applied Clay Science*. **38**: 203-208.
- Tonge, M. P., and Gilbert, R. G. (2001a). Testing free volume theory for penetrant diffusion in rubbery polymers. *Polymer*. **42**: 1393-1405.
- Tonge, M. P., and Gilbert, R. G. (2001b). Testing models for penetrant diffusion in glassy polymers. *Polymer*. **42**: 501-513.
- Tosa, V., Kovacs, K., Mercea, P., and Piringer, O. (2008). A Finite Difference Method for Modeling Migration of Impurities in Multilayer Systems. *Numerical Analysis and Applied Mathematics*. **1048**: 802-805.
- Triantafyllou, V. I., Karamani, A. G., Akrida-Demertzi, K., and Demertzis, P. G. (2002). Studies on the usability of recycled PET for food packaging applications. *European Food Research and Technology*. **215**: 243-248.
- Trier, X., Granby, K., and Christensen, J. H. (2011). Polyfluorinated surfactants (PFS) in paper and board coatings for food packaging. *Environmental Science and Pollution Research*. **18**: 1108-1120.
- Trier, X., Okholm, B., Foverskov, A., Binderup, M. L., and Petersen, J. H. (2010). Primary aromatic amines (PAAs) in black nylon and other food-contact materials, 2004-2009. *Food Additives and Contaminants Part a-Chemistry Analysis Control Exposure & Risk Assessment*. **27**: 1325-1335.
- Tsipursky, S. I., and Drits, V. A. (1984). The distribution of octahedral cations in the 2:1 layers of dioctahedral smectites studied by oblique-texture electron diffraction. *Clay Minerals*. **19**: 177-193.

- Van Alsten, J. G., Lustig, S. R., and Hsiao, B. (1995). Polymer Diffusion in Semicrystalline Polymers. 2. Atactic Polystyrene-d Transport into Atactic and Isotactic Polystyrene. *Macromolecules*. **28**: 3672-3680.
- van Krevelen, D. W., and te Nijenhuis, K. (2009). *Properties of Polymers: Their Correlation with Chemical Structure; their Numerical Estimation and Prediction from Additive Group Contributions*. Elsevier Science.
- van Leeuwen, C. J., and Vermeire, T. G. (2007). *Risk Assessment of Chemicals: An Introduction*. Springer.
- Vandenberg, L. N., Maffini, M. V., Sonnenschein, C., Rubin, B. S., and Soto, A. M. (2009). Bisphenol-A and the Great Divide: A Review of Controversies in the Field of Endocrine Disruption. *Endocrine Reviews*. **30**: 75-95.
- Vartiainen, J., Tuominen, M., and Nattinen, K. (2010). Bio-Hybrid Nanocomposite Coatings from Sonicated Chitosan and Nanoclay. *Journal of Applied Polymer Science*. **116**: 3638-3647.
- Veniaminov, A. V., and Sillescu, H. (1999). Polymer and Dye Probe Diffusion in Poly(methyl methacrylate) below the Glass Transition Studied by Forced Rayleigh Scattering. *Macromolecules*. **32**: 1828-1837.
- Vera, P., Aznar, M., Mercea, P., and Nerin, C. (2011). Study of hotmelt adhesives used in food packaging multilayer laminates. Evaluation of the main factors affecting migration to food. *Journal of Materials Chemistry*. **21**: 420-431.
- Vergnaud, J. M. (1998). Problems encountered for food safety with polymer packages: chemical exchange, recycling. *Advances in Colloid and Interface Science*. **78**: 267-297.
- Vergnaud, J. M., and Rosca, I. D. (2006). *Assessing Food Safety of Polymer Packaging*. Rapra Technology.
- Vettorel, T., Meyer, H., Baschnagel, J., and Fuchs, M. (2007). Structural properties of crystallizable polymer melts: Intrachain and interchain correlation functions. *Physical Review E*. **75**.
- Vieth, W. R. (1991). *Diffusion in and Through Polymers: Principles and Applications*. Carl Hanser GmbH.
- Vignes, A. (1966). Diffusion in Binary Solutions. Variation of Diffusion Coefficient with Composition. *Industrial & Engineering Chemistry Fundamentals*. **5**: 189-199.
- Vilgis, T. A., and Heinrich, G. (2009). *Reinforcement of Polymer Nano-Composites: Theory, Experiments and Applications*. Cambridge University Press.
- Vitrac, O. (2011). FMECA engine: software developed in the framework of the project SafeFoodPack Design
- Vitrac, O. (2012). FMECAENGINE: a seamless tool to chain migration simulations and perform related sensitivity analysis. <https://github.com/ovitrac/FMECAengine>.
- Vitrac, O., Challe, B., Leblanc, J. C., and Feigenbaum, A. (2007a). Contamination of packaged food by substances migrating from a direct-contact plastic layer: Assessment using a generic quantitative household scale methodology. *Food Addit Contam.* **24**: 75-94.
- Vitrac, O., and Gillet, G. (2010). An Off-Lattice Flory-Huggins Approach of the Partitioning of Bulky Solutes between Polymers and Interacting Liquids. *International Journal of Chemical Reactor Engineering*. **8**.
- Vitrac, O., and Hayert, M. (2005). Risk assessment of migration from packaging materials into foodstuffs. *Aiche Journal*. **51**: 1080-1095.
- Vitrac, O., and Hayert, M. (2006). Identification of diffusion transport properties from desorption/sorption kinetics: An analysis based on a new approximation of fick equation during solid-liquid contact. *Industrial & Engineering Chemistry Research*. **45**: 7941-7956.

- Vitrac, O., and Hayert, M. (2007a). Design of safe food packaging under uncertainty. **In:** New trends in chemical engineering research, pp. 251-292. Berton, P. (Ed.), Nova Science Publishers, New York.
- Vitrac, O., and Hayert, M. (2007b). Effect of the distribution of sorption sites on transport diffusivities: A contribution to the transport of medium-weight-molecules in polymeric materials. *Chemical Engineering Science*. **62**: 2503-2521.
- Vitrac, O., and Leblanc, J.-C. (2007). Consumer exposure to substances in plastic packaging. I. Assessment of the contribution of styrene from yogurt pots. *Food Additives and Contaminants*. **24**.
- Vitrac, O., Lezervant, J., and Feigenbaum, A. (2006). Decision trees as applied to the robust estimation of diffusion coefficients in polyolefins. *Journal of Applied Polymer Science*. **101**: 2167-2186.
- Vitrac, O., Mougharbel, A., and Feigenbaum, A. (2007b). Interfacial mass transport properties which control the migration of packaging constituents into foodstuffs. *Journal of Food Engineering*. **79**: 1048-1064.
- Vitrac, O. a. G., Guillaume (2010). An Off-Lattice Flory-Huggins Approach of the Partitioning of Bulky Solutes between Polymers and Interacting Liquids. *International Journal of Chemical Reactor Engineering*. **8**.
- Vollmer, A., Biedermann, M., Grundboeck, F., Ingenhoff, J.-E., Biedermann-Brem, S., Altkofer, W., and Grob, K. (2011). Migration of mineral oil from printed paperboard into dry foods: survey of the German market. *European Food Research and Technology*. **232**: 175-182.
- von Goetz, N., Fabricius, L., Glaus, R., Weitbrecht, V., Gunther, D., and Hungerbuhler, K. (2013). Migration of silver from commercial plastic food containers and implications for consumer exposure assessment. *Food additives & contaminants. Part A, Chemistry, analysis, control, exposure & risk assessment*. **30**: 612-620.
- von Meerwall, E., Beckman, S., Jang, J., and Mattice, W. L. (1998). Diffusion of liquid n-alkanes: Free-volume and density effects. *The Journal of Chemical Physics*. **108**: 4299-4304.
- Von Meerwall, E., and Ferguson, R. D. (1979). Diffusion of hydrocarbons in rubber, measured by the pulsed gradient NMR method. *Journal of Applied Polymer Science*. **23**: 3657-3669.
- von Meerwall, E. D., Lin, H., and Mattice, W. L. (2007). Trace Diffusion of Alkanes in Polyethylene: Spin-Echo Experiment and Monte Carlo Simulation. *Macromolecules*. **40**: 2002-2007.
- von Smoluchowski, M. (1906). Zur kinetischen Theorie der Brownschen Molekularbewegung und der Suspensionen. *Annalen der Physik*. **326**: 756-780.
- Vrentas, J. S., and Duda, J. L. (1977). Diffusion in polymer—solvent systems. I. Reexamination of the free-volume theory. *Journal of Polymer Science: Polymer Physics Edition*. **15**: 403-416.
- Vrentas, J. S., Duda, J. L., and Huang, W. J. (1986). Regions of Fickian diffusion in polymer-solvent systems. *Macromolecules*. **19**: 1718-1724.
- Vrentas, J. S., Duda, J. L., and Ling, H. C. (1985a). Free-volume theories for self-diffusion in polymer—solvent systems. I. Conceptual differences in theories. *Journal of Polymer Science: Polymer Physics Edition*. **23**: 275-288.
- Vrentas, J. S., Duda, J. L., Ling, H. C., and Hou, A. C. (1985b). Free-volume theories for self-diffusion in polymer—solvent systems. II. Predictive capabilities. *Journal of Polymer Science: Polymer Physics Edition*. **23**: 289-304.
- Vrentas, J. S., and Vrentas, C. M. (1993). Evaluation of free-volume theories for solvent self-diffusion in polymer—solvent systems. *Journal of Polymer Science Part B: Polymer Physics*. **31**: 69-76.
- Vrentas, J. S., and Vrentas, C. M. (1994). Solvent Self-Diffusion in Rubbery Polymer-Solvent Systems. *Macromolecules*. **27**: 4684-4690.

- Vrentas, J. S., and Vrentas, C. M. (1995). Determination of Free-Volume Parameters for Solvent Self-Diffusion in Polymer-Solvent Systems. *Macromolecules*. **28**: 4740-4741.
- Vrentas, J. S., and Vrentas, C. M. (1998). Predictive methods for self-diffusion and mutual diffusion coefficients in polymer-solvent systems. *European Polymer Journal*. **34**: 797-803.
- Vrentas, J. S., Vrentas, C. M., and Faridi, N. (1996). Effect of Solvent Size on Solvent Self-Diffusion in Polymer-Solvent Systems. *Macromolecules*. **29**: 3272-3276.
- Waheed, N., Ko, M., and Rutledge, G. (2007). Atomistic Simulation of Polymer Melt Crystallization by Molecular Dynamics. In: Progress in Understanding of Polymer Crystallization, pp. 457-480. Reiter, G., and Strobl, G. (Eds.), Springer, Berlin, Heidelberg.
- Walsh, B. (2010). How dangerous is Plastic? . *Time*: 7.
- Wang, H., Keum, J. K., Hiltner, A., and Baer, E. (2009). Confined Crystallization of PEO in Nanolayered Films Impacting Structure and Oxygen Permeability. *Macromolecules*. **42**: 7055-7066.
- Wang, Z. F., Wang, B., Qi, N., Zhang, H. F., and Zhang, L. Q. (2005). Influence of fillers on free volume and gas barrier properties in styrene-butadiene rubber studied by positrons. *Polymer*. **46**: 719-724.
- Watanabe, H. (1978). Escape probability of a random walker on a lattice doped with absorbers. *The Journal of Chemical Physics*. **69**: 4872-4875.
- Welle, F., and Franz, R. (2010). Migration of antimony from PET bottles into beverages: determination of the activation energy of diffusion and migration modelling compared with literature data. *Food Additives & Contaminants: Part A*. **28**: 115-126.
- Wesselingh, J. A., and Krishna, R. (2006). Mass Transfer in Multicomponent Mixtures. VSSD.
- Widen, H. (1998). Recycled plastics for food packaging - a literature review. *SIK Rapport*: 60pp.-60pp.
- Widom, B. (1963). Some Topics in the Theory of Fluids. *The Journal of Chemical Physics*. **39**: 2808-2812.
- Wijmans, J. G., and Baker, R. W. (1995). The solution-diffusion model: a review. *Journal of Membrane Science*. **107**: 1-21.
- Williams, M. L., Landel, R. F., and Ferry, J. D. (1955). The Temperature Dependence of Relaxation Mechanisms in Amorphous Polymers and Other Glass-forming Liquids. *Journal of the American Chemical Society*. **77**: 3701-3707.
- Wirtz, A. C., Hofmann, C., and Groenen, E. J. J. (2011). Stretched Polyethylene Films Probed by Single Molecules. *ChemPhysChem*. **12**: 1519-1528.
- Wittassek, M., and Angerer, J. (2008). Phthalates: metabolism and exposure. *Int J Androl*. **31**: 131-138.
- Wolfgang, P., and Grant, D. S. (2004). Structure and dynamics of amorphous polymers: computer simulations compared to experiment and theory. *Reports on Progress in Physics*. **67**: 1117.
- Wong, C.-P., Schrag, J. L., and Ferry, J. D. (1970). Diffusion of radioactively tagged 1,1-diphenylethane and n-hexadecane through rubbery polymers: Dependence on temperature and dilution with solvent. *Journal of Polymer Science Part A-2: Polymer Physics*. **8**: 991-998.
- Wunderlich, B. (1980). Macromolecular physics. Academic Press.
- Wypych, F., and Satyanarayana, K. G. (2004). Clay Surfaces: Fundamentals and Applications. Elsevier Science.
- Xiao, J., Huang, Y., and Manke, C. W. (2010). Computational Design of Polymer Nanocomposite Coatings: A Multiscale Hierarchical Approach for Barrier Property Prediction. *Industrial & Engineering Chemistry Research*. **49**: 7718-7727.
- Xie, W., Gao, Z., Pan, W.-P., Hunter, D., Singh, A., and Vaia, R. (2001). Thermal Degradation Chemistry of Alkyl Quaternary Ammonium Montmorillonite. *Chemistry of Materials*. **13**: 2979-2990.

- Xu, R., Mead, J. L., Orroth, S. A., Stacer, R. G., and Truong, Q. T. (2001). Barrier properties of thermoplastic elastomer films. *Rubber Chemistry and Technology*. **74**: 701-714.
- Yamakawa, H. (1971). Modern theory of polymer solutions. Harper & Row.
- Yampolskii, Y., Pinnau, I., and Freeman, B. D. (2006). Materials science of membranes for gas and vapor separation: prediction of gas permeation parameters of polymers. Wiley.
- Yang, C., and Cussler, E. L. (2001). Oxygen barriers that use free radical chemistry. *Aiche Journal*. **47**: 2725-2732.
- Yang, C., Nuxoll, E. E., and Cussler, E. L. (2001). Reactive barrier films. *Aiche Journal*. **47**: 295-302.
- Yang, L., Chen, X., and Jing, X. (2008a). Stabilization of poly(lactic acid) by polycarbodiimide. *Polymer Degradation and Stability*. **93**: 1923-1929.
- Yang, S.-l., Wu, Z.-H., Yang, W., and Yang, M.-B. (2008b). Thermal and mechanical properties of chemical crosslinked polylactide (PLA). *Polymer Testing*. **27**: 957-963.
- Yu, L., Dean, K., and Li, L. (2006). Polymer blends and composites from renewable resources. *Progress in Polymer Science*. **31**: 576-602.
- Zeliger, H. (2011). Human Toxicology of Chemical Mixtures. Elsevier Science.
- Zhang, J., and Wang, C. H. (1987). Application of the laser-induced holographic relaxation technique to the study of physical aging of an amorphous polymer. *Macromolecules*. **20**: 683-685.
- Zhu, J., Chen, L.-Q., Shen, J., and Tikare, V. (2001). Microstructure dependence of diffusional transport. *Computational Materials Science*. **20**: 37-47.
- Zielinski, J. M. (1996). An Alternate Interpretation of Polymer/Solvent Jump Size Units for Free-Volume Diffusion Models. *Macromolecules*. **29**: 6044-6047.

Abstract

A material is defined as “barrier” when it is able to delay the diffusion of a penetrant. There are few possibilities to modulate the barrier properties of a prescribed material (e.g. packaging material). Most of conventional technological strategies aim at increasing the tortuosity path of the penetrant by adding obstacles. Such obstacles could be obtained either by creating a crystalline morphology or by adding of nano-fillers. The gain in diffusion barrier depends on the shape factor of obstacles, their concentration and orientation according to the main direction of transfer. In this PhD work, a novel direction to improve the barrier property has been studied; its principles have been early formalized independently from theoretical considerations on random walk on heterogeneous energy surfaces and from modeling of reactivity in heterogeneous catalysis. The central idea relies on increasing retention times instead of diffusion path lengths by incorporating nano-adsorbents (i.e. active obstacles) in the material. In this case, the considered material becomes a barrier specific to one or a family of solutes. This new concept has been tested on organic solutes to develop new barrier materials (e.g. biobased food packaging, materials for fuel tank...). The results brought out the engineering principles of such materials and experimental evidences to support the concepts. In particular, an extended free-volume theory has been developed to separate interactions with active surfaces (i.e. montmorillonites (MMT) in this work) from free-volume related effects in the polymer. Sorption properties of pristine MMT and organo-modified ones have been characterized experimentally and by molecular simulation to derive conditions where the partition coefficient $K_{contrast}$ between the surface of MMT and tested polymers (i.e. polycaprolactone (PCL), polyvinyl alcohol (PVA)) could be much greater than unity. PVA materials containing pristine MMT exhibited the most promising barrier properties to studied model solutes, which can be activated by decreasing temperature and whose selectivity can be controlled by varying the relative humidity. The blocking effects were in good agreement with the proposed description of “trapping” of organic solutes by intercalation in MMT galleries and on its enthalpic and entropic control.

Keywords: *nanocomposite, polymer, diffusion, molecular modeling, thermodynamics*

Résumé

Un matériau est dit « barrière » quand il induit un retard à la diffusion de la molécule « pénétrante ». Il existe peu de possibilités pour moduler les propriétés barrière d'un matériau donné (ex. emballage). La possibilité technologique la plus utilisée consiste à augmenter la tortuosité du chemin du pénétrant par l'addition d'obstacles. Ces obstacles peuvent être obtenus par la création d'une morphologie cristalline particulière ou par l'addition de nano-charges. L'efficacité ainsi obtenue dépend du facteur de forme des obstacles, de leur densité et orientation par rapport à la direction principale des transferts. Les travaux de thèse ont exploré une voie différente, dont les principes ont été formalisés précédemment à partir de considérations théoriques de la diffusion sur des surfaces d'énergie hétérogènes ou d'une description de la réactivité en catalyse hétérogène. L'idée directrice repose sur une augmentation du temps de parcours en lieu et place d'une augmentation du chemin de diffusion en incorporant dans le matériau de nano-adsorbants (obstacles actifs). Dans ce cas, le matériau devient une barrière spécifique à un ou une famille de solutés. En particulier, une théorie étendue des volumes libres a été développée pour séparer les interactions avec la surface active (montmorillonites dans cette étude) des effets des volumes-libres dans le polymère. Les propriétés de sorption des argiles pures et modifiées ont été caractérisées expérimentalement et par modélisation moléculaire pour déterminer les conditions pour lesquelles le coefficient de partage $K_{contrast}$ entre la surface des argiles et les polymères testés (polycaprolactone=PCL, alcool polyvinylique=PVA) seraient plus grand que l'unité. Les systèmes PVA+argiles natives ont présenté les meilleures propriétés barrières aux solutés modèles étudiés, avec une activation par les températures basses et une sélectivité modulable par l'humidité relative. Les effets bloquants ont été en bon accord avec la description du piégeage des solutés organiques dans entre les claies empilées des argiles sous contrôle à la fois entropique et enthalpique.

Mots clés : *nanocomposites, polymères, diffusion, modélisation moléculaire, thermodynamique*